Structures of Fluids

Tetsuo Kaneko[a)]

East Katsushika Institute, Kogane Kazusacho 16-1, Matsudo-shi, Chiba-ken, 270-0015, Japan

(Dated: 12 January 2022)

[a)]Electronic mail: kanekous@mac.com

A. Contents

B. Preface

The feature of a fluid in the gas state is not the same as its feature in the liquid state. The difference between them can be determined intuitively and easily. The gas phase of a fluid and the liquid phase of the fluid can coexist with the formation of the clear interface. Then, there must be a cause that makes the fluid in the gas state differ from that in the liquid state. As a mutual attractive force acts between particles comprising each particle pair, the mutually attractive force can inhibit the particles of each pair from moving freely. In a classical fluid system, particles having small relative momenta cannot homogeneously mix with particles having large relative momenta. Even in a Bose fluid system, particles having small and large relative momenta cannot homogeneously mix.

The inhibition of movements of particles owing to mutually attractive force can cause physical clusters of particles to form in the fluid. The formation of physical clusters can contribute to the changing features of the fluid. Hence, analyzing the formation of physical clusters in the fluid is extremely necessary. The formation of physical clusters should allow the fluid in the gas state to differ from that in the liquid state. The fluid in the liquid state has the capability to form the interface between the gas phase and the liquid phase; in other words, the fluid in the liquid state should be characterized by the existence of physical clusters. Fundamentally, the development of physical clusters in the fluid should influence the features of the fluid. The structure of the fluid, as a specific pattern of the particle distribution, should be characterized by the formation of physical clusters. Their formation is influenced by the features of attractive forces between the particles. In the case of a Coulomb fluid, it is influenced by both the features of an attractive force between the particles of a pair and the features of a repulsive force between the particles of another pair. A characteristic structure maintained in a fluid is caused by the features of an interparticle force between the particles of each pair.

Particles with hard cores interacting with each other through attractive forces in a Bose fluid system can form a specific pattern of the particle distribution that depends on their momenta. Even if the particles are made to have sufficiently small momenta, the thermal excitation can allow particles of small momenta and those of no small momenta to coexist. Then, the former particles cannot homogeneously mix with the latter particles. This can allow the particle distribution to have a specific pattern. The formation of the interface

between the gas phase and the liquid phase in the Bose fluid system requires a specific structure, as the pattern of the particle distribution, to be linked to the features of the fluid. At the minimum, the presence of mutually attractive forces, which make particles with hard cores interact with each other, can influence the thermodynamic features of the fluid. If the effects of attractive forces acting on a single particle, from other particles surrounding it, are treated as the mean effect, then the quasiclassical expressions of a partition function enables discussion of the thermodynamics of the system that accompanies a structural situation where particles of small momenta cannot homogeneously mix with particles of no small momenta.

The physical cluster formation in various situations, including astronomical situations, and the specific pattern formation of the particle distribution depending on the momenta of particles must be further studied. A study on linking the limitation of the appearance of the liquid phase and the features of interactions between particles also must be further developed. These indicate that the descriptions and explanations in this book must continue to be updated with progress in this field, where the principal efforts of the author have been made so far.

The publication of this book was aided by the director John Pellan, the BWW Society, the Institute of Positive Global Solutions. The author gratefully acknowledges his aid. For editing and for valuable comments, the author thanks Editage (www.editage.com).

June 2021 T. Kaneko

I. INTRODUCTION

In an ensemble of simple particles exemplifying the atoms or molecules that form a fluid, inhomogeneities can exist, because the particles interact with each other through attractive forces and repulsive forces. If a particle ensemble can preserve a state of fluid at extremely low temperatures, then the particles can move even coherently. Under the condition that a particle ensemble that preserves a state of fluid is homogeneous, the following two relations are satisfied:

(1) The distribution of particles in a microscopic volume δV located at $\mathbf{r}_a$ cannot differ from the distribution of particles in microscopic volume δV located at $\mathbf{r}_b$ ($\neq \mathbf{r}_a$).

(2) The distribution of the momenta of particles in a microscopic volume δV located at $\mathbf{r}_a$ cannot differ from the distribution of the momenta of particles in microscopic volume δV located at $\mathbf{r}_b$ ($\neq \mathbf{r}_a$).

If factors that prevent the ensemble from becoming homogeneous are generated, then the occurrence of interesting phenomena can be observed. These factors can affect the behaviors of fluids and the configurations of particles. One of these factors is the formation of physical clusters.

For an ensemble of particles exemplifying atoms or molecules, the liquid phase coexists with the gas phase at the temperatures between the triple point and the critical point. At these temperatures, the density of particles in the liquid phase is much higher than that in the gas phase, even if each portion in the liquid phase near the interface and each portion in the gas phase near the interface are in equilibrium. This requires the compressibility in the liquid phase to be much smaller than that in the gas phase. Thus, we must consider the contribution of something that generates the difference between each portion in the liquid phase and each portion in the gas phase. The contribution of the formation of physical clusters should be considered as a factor that allows features of a fluid in the liquid phase to become different from the features of the fluid in the gas phase.

Physical clusters can be formed even in the gas phase if the temperature of a system is near the liquid-vapor critical point. Particles that constitute the system interact with each other via the attractive forces between them. The system includes particles that can freely and individually move because the contribution of the relative kinetic energy between the particles of each pair exceeds the contribution of an attractive force acting between

them. The system includes other particles that cannot perform their movements being free from each other because the contribution of the attractive force acting between the particles of each pair exceeds the contribution of the relative kinetic energy between them. The particles that cannot perform their movements being free from each other can contribute to the formation of physical clusters.

At the minimum, the attractive forces between particles enable the particles to be located near each other. Repulsive forces between particles enable the particles to become far from each other. The strength of each attractive force and that of each repulsive force both depend on the mean interparticle distance. The formation of physical clusters depends on four principal factors: the attractive forces between particles, the repulsive forces between them, the mean interparticle distance, and the momenta of particles. The formation of physical clusters can influence the features of a fluid system. If the contributions of attractive forces between particles are so small that a particle ensemble maintains the liquid state, then, partial ensembles of particles that are located near each other and moving coherently can be generated as specific excitation states.[1] The formation of ensembles of particles moving coherently causes the thermodynamic properties of a quantum fluid system to change.

For a classical fluid system, a basic idea for estimating the formation of physical clusters was given by Hill[2]. A useful method for analyzing the formation of physical clusters via an integral equation was established by Coniglio et al.[3] The method allows the Ornstein–Zernike equation to be split into two integral equations and the pair correlation function to be split into two correlation functions. One of the two correlation functions is called the pair connectedness. One of the two integral equations is the integral equation for the pair connectedness. The integral equation for the pair connectedness is used to analyze the formation of physical clusters. This has enabled many studies on the off-lattice percolation of physical clusters.[4–7]

The mathematical structure of the integral equation is the same as that of the Ornstein–Zernike equation. Hence, it is necessary to solve the integral equation using a specific closure. The closure can be extracted from the Percus–Yevick (PY) approximation.[3] The relation between the PY approximation and the mean spherical approximation (MSA) yields a simple closure.[8] The use of the simple closure allows the pair connectedness and the formation of physical clusters to be estimated easily. Its use aids in revealing a specific relationship between particles belonging to physical clusters and other particles no belonging them. The

relationship can contribute to the generation of the liquid state. Use of the simple closure allows us to understand the contribution of physical cluster formation to thermodynamic properties. If the distribution of galaxies in the universe is regarded as physical clusters of galaxies, then the physical clusters have a fractal structure. Similarly, the distribution of charged particles in a specific medium has a fractal structure. The use of the simple closure and an estimate of the pair connectedness aid in revealing the fractal structure of physical clusters.

II. SINGLE-COMPONENT FLUIDS INCLUDING PHYSICAL CLUSTERS

A. Classical Fluid System of N Particles

For a classical fluid system of N particles with volume V, partition function Q_N is defined as

$$Q_N = \frac{1}{N!(2\pi\hbar)^{3N}} \int_V \mathrm{d}\mathbf{r}_1 \int_V \mathrm{d}\mathbf{r}_2 \cdots \int_V \mathrm{d}\mathbf{r}_N \times \int_{-\infty}^{\infty} \mathrm{d}\mathbf{p}_1 \int_{-\infty}^{\infty} \mathrm{d}\mathbf{p}_2 \cdots \int_{-\infty}^{\infty} \mathrm{d}\mathbf{p}_N \exp[-\beta\mathcal{H}_N], \tag{1}$$

where a coefficient $\hbar$ is the ratio of Planck's constant to 2π, and another coefficient β is defined as $\beta \equiv 1/k_B T$ with Boltzmann's constant k_B and temperature T of the system. In Eq. (1), $\mathcal{H}_N$ is given by

$$\mathcal{H}_N = \sum_{i=1}^{N} \frac{p_i^2}{2m} + V_N(\mathbf{r}_1, \mathbf{r}_2, \cdots, \mathbf{r}_N), \tag{2}$$

where m is the particle mass, and p_i is defined by $p_i \equiv |\mathbf{p}_i|$, with momentum $\mathbf{p}_i$ of the i particle. For a fluid, $V_N(\mathbf{r}_1, \mathbf{r}_2, \cdots, \mathbf{r}_N)$ in Eq. (2) can be expressed using a pair potential $u_{ij}(r_{ij})$, which includes both the contribution of the attractive force between i particle located at $\mathbf{r}_i$ and j particle located at $\mathbf{r}_j$ and the contribution of the repulsive force between them, and it is given as follows:

$$V_N(\mathbf{r}_1, \mathbf{r}_2, \cdots, \mathbf{r}_N) = \sum_{i<j}^{N} u_{ij}(r_{ij}), \tag{3}$$

where r_{ij} expresses the three-dimensional distance between i particle and j particle as follows:

$$r_{ij} = |\mathbf{r}_i - \mathbf{r}_j|. \tag{4}$$

Partition function Q_N allows the Helmholtz free energy, F, to be given as

$$F = -k_B \ln Q_N. \tag{5}$$

For a classical fluid system, Q_N can be estimated as

$$Q_N = \frac{1}{N!} \left(\frac{m}{2\pi\hbar^2\beta} \right)^{3N/2} Z_N, \tag{6}$$

where

$$Z_N = \int_V \mathrm{d}\mathbf{r}_1 \int_V \mathrm{d}\mathbf{r}_2 \cdots \int_V \mathrm{d}\mathbf{r}_N \exp[-\beta V_N(\mathbf{r}_1, \mathbf{r}_2, \cdots, \mathbf{r}_N)]. \tag{7}$$

With using Z_N, the probability density, under the condition that particle 1, particle 2, $\cdots$, and particle N are located at $\mathbf{r}_1$, $\mathbf{r}_2$, $\cdots$, and $\mathbf{r}_N$, respectively, can be estimated as

$$\frac{1}{Z_N} \exp[-\beta V_N(\mathbf{r}_1, \mathbf{r}_2, \cdots, \mathbf{r}_N)].$$

The possible ways for choosing one particle from N particles is given by $N!/(N-1)!1!$. If $n^{(1)}(\mathbf{r}_1)\mathrm{d}\mathbf{r}_1$ denotes the probability that one of the N particles is located in a volume element $\mathrm{d}\mathbf{r}_1$ at $\mathbf{r}_1$, then the probability is given as

$$n^{(1)}(\mathbf{r}_1)\mathrm{d}\mathbf{r}_1 = \left(\frac{N!}{(N-1)!1!}\right) \frac{\mathrm{d}\mathbf{r}_1}{Z_N} \int_V \mathrm{d}\mathbf{r}_2 \int_V \mathrm{d}\mathbf{r}_3 \cdots \int_V \mathrm{d}\mathbf{r}_N \exp[-\beta V_N(\mathbf{r}_1, \mathbf{r}_2, \cdots, \mathbf{r}_N)]. \tag{8}$$

The distribution of particles in a volume element cannot depend on the locations of the volume element. If this is satisfied for a fluid

$$n^{(1)}(\mathbf{r}_1) = \frac{N}{V} = \rho. \tag{9}$$

Similarly, if $n^{(2)}(\mathbf{r}_1, \mathbf{r}_2)\mathrm{d}\mathbf{r}_1\mathrm{d}\mathbf{r}_2$ denotes the probability that a particle is located in a volume element $\mathrm{d}\mathbf{r}_1$ at $\mathbf{r}_1$ and another particle is located in a volume element $\mathrm{d}\mathbf{r}_2$ at $\mathbf{r}_2$, then the probability is given as

$$\begin{aligned} n^{(2)}(\mathbf{r}_1, \mathbf{r}_2)\mathrm{d}\mathbf{r}_1\mathrm{d}\mathbf{r}_2 =& \left(\frac{N!}{(N-2)!2!}\right) \frac{\mathrm{d}\mathbf{r}_1\mathrm{d}\mathbf{r}_2}{Z_N} \\ & \times \int_V \mathrm{d}\mathbf{r}_3 \int_V \mathrm{d}\mathbf{r}_4 \cdots \int_V \mathrm{d}\mathbf{r}_N \exp[-\beta V_N(\mathbf{r}_1, \mathbf{r}_2, \cdots, \mathbf{r}_N)]. \end{aligned} \tag{10}$$

The distribution of particles in a volume element can maintain independence of locations of the volume element on average. If this is satisfied for a fluid,

$$n^{(2)}(\mathbf{r}_1, \mathbf{r}_2) = n^{(2)}(r_{12}). \tag{11}$$

Quantity $n^{(2)}(r_{12})$ corresponds to the radial distribution function for a fluid system. Pair correlation function $g(r_{12})$, which is related to $h(r_{12}) = g(r_{12}) - 1$ with correlation function $h(r_{12})$ that satisfies the Ornstein–Zernike equation, is related to the radial distribution function as follows:

$$n^{(2)}(r_{12}) = n^{(1)} n^{(1)} g(r_{12}). \tag{12}$$

Z_N can be rewritten using the Mayer f-function, which is useful for analyzing a fluid based on an aspect that allows a fluid to be considered to be an ensemble of pairs of particles. Then, Z_N is given by

$$\begin{aligned}
Z_N =& \int_V \mathrm{d}\mathbf{r}_1 \int_V \mathrm{d}\mathbf{r}_2 \cdots \int_V \mathrm{d}\mathbf{r}_N \prod_{i<j}^{N} (1 + f_{ij}) \\
=& \int_V \mathrm{d}\mathbf{r}_1 \int_V \mathrm{d}\mathbf{r}_2 \cdots \int_V \mathrm{d}\mathbf{r}_N \Big[1 + (f_{12} + f_{13} + \cdots + f_{1N}) \\
& + (f_{12}f_{13} + f_{12}f_{14} + \cdots + f_{12}f_{1N}) + \cdots \\
& + (f_{23}f_{12} + f_{23}f_{13} + \cdots + f_{23}f_{1N}) + \cdots \\
& + (f_{23}f_{12}f_{13} + f_{23}f_{12}f_{14} + \cdots + f_{23}f_{12}f_{1N}) + \cdots \\
& + (f_{34}f_{24}f_{12} + f_{34}f_{24}f_{13} + f_{34}f_{24}f_{14} + \cdots + f_{34}f_{24}f_{1N}) + \cdots \\
& + (f_{34}f_{23}f_{24}f_{12} + f_{34}f_{23}f_{24}f_{13} + f_{34}f_{23}f_{24}f_{14} + \cdots + f_{34}f_{23}f_{24}f_{1N}) + \cdots \Big],
\end{aligned} \tag{13}$$

where Mayer f-function f_{ij} is defined as

$$f_{ij}(r_{ij}) \equiv e^{-\beta u_{ij}(r_{ij})} - 1. \tag{14}$$

Hence, the f-function f_{ij} satisfies

$$\begin{aligned}
f_{ij}(r_{ij}) &= f_{ji}(r_{ji}), \\
\lim_{r_{ij}\to 0} f_{ij}(r_{ij}) &= -1, \\
\lim_{r_{ij}\to \infty} f_{ij}(r_{ij}) &= 0.
\end{aligned}$$

The minimum of $f_{ij}(r_{ij})$ is -1. If the i and j particles have hard cores, then $f_{ij}(r_{ij}) = -1$ is satisfied in the region where the hard cores contribute to their interaction, which is characterized by $u_{ij}(r_{ij}) = \infty$. However, function $f_{ij}(r_{ij})$ is positive within the range where the attractive force retains effective strength, and it expresses the strength of the attractive interaction in this range. The value of $f_{ij}(r_{ij})$ becomes zero outside this range in which an attractive force between the i particle and j particle retains effective strength. If an ensemble of particles maintains a fluid, a specific situation $-u_{ij}(r_{ij}) \gg k_B T$, i.e., $1 \ll -\beta u_{ij}(r_{ij})$, does not occur. Thus, the maximum of $f_{ij}(r_{ij})$ is not a large value.

Eq. (13) indicates that Z_N is the sum of the integrals of the products of the f-functions. This means that pair correlation function $g(r_{ij})$ also can be given as the sum of the integrals of the products of the f-functions, even though the two coordinates specified for $g(r_{ij})$ by r_{ij} are not integrated.

In Eq. (13), the integrals of the products of the f-functions have typical features. The integrals of f_{ij} for i and j, satisfying $i < j$, are identical. The integrals of $f_{12}f_{1j}$ for j, satisfying $3 < j$, are identical. The integrals of $f_{12}f_{1j}$ for j, satisfying $3 < j$, are identical. However, the integral of $f_{23}f_{13}$ is not identical to each integral of $f_{23}f_{1j}$ for j, except for $j = 2\text{and}3$. Cases similar to the above can be obtained from integrals of other products of the f-functions.

The integrals of the products of f-functions yield a specific image that illustrated that two particles specified by each f-function are linked mathematically by the f-function. This image enables an ensemble of particles to be considered clusters that are formed from particle pairs linked mathematically by f-functions. Then, each f-function forms a f-bond that mathematically links two particles.

In Eq. (13), $f_{23}f_{13}$, $f_{23}f_{12}f_{13}$, $f_{34}f_{24}f_{13}$, and $f_{34}f_{23}f_{24}f_{13}$, are found as specific products of f-functions. The first product, $f_{23}f_{13}$, denotes that two f-bonds link particle 1 and particle 2 via particle 3, as shown by a diagram symbolized by

$$1 \leftrightarrow 3 \leftrightarrow 2$$

The third product, $f_{34}f_{24}f_{13}$, denotes that particle 1 and particle 2 are linked via particle 3 and particle 4, as shown by a diagram symbolized by

$$1 \leftrightarrow 3 \leftrightarrow 4 \leftrightarrow 2,$$

which forms one path of f-bonds. The second product, $f_{23}f_{12}f_{13}$, denotes that particle 1 and particle 2 are linked through two paths of f-bonds, as shown by a diagram symbolized by

$$\begin{cases} 1 \leftrightarrow 2 \\ 1 \leftrightarrow 3 \leftrightarrow 2, \end{cases}$$

which forms two paths of f-bonds. The fourth, $f_{34}f_{23}f_{24}f_{13}$, denotes that particle 1 and particle 2 are linked through special two paths of f-bonds that form a diagram symbolized by

$$\begin{cases} 1 \leftrightarrow 3 \leftrightarrow 2 \\ 1 \leftrightarrow 3 \leftrightarrow 4 \leftrightarrow 2, \end{cases}$$

which forms two paths of f-bonds. Thus, all the paths of f-bonds that connect particle 1 to particle 2 include particle 3 as a common particle.

In the case of pair correlation function $g(r_{12})$, which is expressed for the use of f-functions, the two coordinates labeled as 1 and 2 are not integrated. Coordinates $\mathbf{r}_1$ and $\mathbf{r}_2$, which are not integrated, are called the root points. The other coordinates that are integrated are called the field points, and they are labeled as 3, 4, $\cdots$ to distinguish them from the root points. Both the root points and the field points correspond to the particle coordinates.

Pair correlation function $g(r_{12})$ includes the integrals of the products of the f-functions exemplified by the paths of f-bonds corresponding to $f_{23}f_{13}$, $f_{34}f_{24}f_{13}$, and $f_{34}f_{23}f_{24}f_{13}$; however, the two coordinates labeled as 1 and 2 are not integrated. All the paths of f-bonds given as $f_{34}f_{23}f_{24}f_{13}$ form a diagram, which comprises the two paths between 1 and 2, and the two paths include the coordinate corresponding to particle 3. The path of f-bonds given as $f_{23}f_{13}$ forms a diagram, and the path of f-bonds given as $f_{34}f_{24}f_{13}$ forms another diagram. Then, each path that forms each diagram includes the coordinate corresponding to particle 3. Thus, there are diagrams in which at least one coordinate corresponding to a particle is shared as a common coordinate by each path of f-bonds that connect particle 1 to particle 2. Each of the diagrams is called a nodal diagram, and the common coordinate is a nodal point.

Pair correlation function $g(r_{12})$ also includes the integrals of the products of the f-functions, exemplified by the paths of f-bonds corresponding to $f_{23}f_{12}f_{13}$; however, the coordinates 1 and 2 are not integrated. In a diagram that is formed by all the paths of f-bonds given as $f_{23}f_{12}f_{13}$, there is no nodal point. As exemplified by this case, there are diagrams that do not include nodal points. Each diagram that does not include nodal points is a non-nodal diagram.

Pair correlation function $g(r_{12})$ can be expressed in the form of a density expansion.[9,10] Each term found in the form of the density expansion of $g(r_{12})$ is formed by the integrals of a product of the f-functions; however, the two coordinates 1 and 2, corresponding to the root points, are not integrated in each term. The other coordinates are integrated in each term. A diagram of the f-bonds that forms each term in the density expansion corresponds to either a nodal diagram or a non-nodal diagram. According to the density expansion, $g(r_{12})$ can be given by the sum of the contribution of all the nodal diagrams and the contribution of all the non-nodal diagrams.[9,10] This demonstrates that the Ornstein–Zernike equation,

as an integral equation, should be satisfied by $g(r_{12})$ and is expressed as the sum of the contribution $N(r_{12})$ of all the nodal diagrams and the contribution $c(r_{12})$ of all the non-nodal diagrams. Thus, the use of direct correlation function $c(r_{12})$ as the contribution of all the non-nodal diagrams allows the Ornstein–Zernike equation to be expressed as

$$h(r_{12}) = c(r_{12}) + N(r_{12}), \tag{15}$$

where the contribution of all the nodal diagrams can be estimated by

$$N(r_{12}) = \rho \int_V c(r_{13})h(r_{32})\mathrm{d}\mathbf{r}_3 \tag{16}$$

with

$$h(r_{12}) = g(r_{12}) - 1. \tag{17}$$

An ensemble of the particle pairs that are specified by the f-functions, forming a product in the density expansion, is regarded as an ensemble of particle pairs linked by f-bonds. The paths of the f-bonds forming each nodal diagrams and the paths of the f- bonds forming each non-nodal diagrams allow the behavior of a particle corresponding to a root point to be propagated to the other particle corresponding to the other root point. However, a ensemble of particle pairs linked by the f-bonds cannot simply correspond to a physical cluster, even though the ensemble corresponds to a mathematical cluster.[10]

B. Contributions of physical clusters

1. Phenomena dependent on the formation of physical clusters

A fluid system can include special particle pairs. Then, each particle pair is specified as a pair formed by two particles interacting in a bound state wherein the contribution of the mutually attractive force between them exceeds the contribution of their relative kinetic energy. Each physical cluster is formed by such particle pairs.[2] Particles constituting a physical cluster can transiently stay near each other because of the mutually attractive force. The formation of physical clusters can transform the properties of a fluid system. Various phenomena involving phase behavior can be caused by the formation of physical clusters.

In a fluid system consisting of particles exemplifying atoms or molecules, inhomogeneity is generated as the density fluctuates.[12,13] The inhomogeneity is developed near the liquid-vapor critical points. The formation of physical clusters can cause density fluctuations in a fluid that is in the gas state. The degree of density fluctuations reaches its maximum at the liquid-vapor critical point of the fluid. This allows the compressibility to diverge to infinity at the liquid-vapor critical point. The compressibility equation allows pair correlation function $g(r)$ to be related to pressure P of a single component fluid as follows:

$$\left[\beta\left(\frac{\partial P}{\partial \rho}\right)_{V,T}\right]^{-1} = 1 + \lim_{V\to\infty} \rho \int_V [g(r) - 1]\mathrm{d}\mathbf{r} \quad (r \equiv |\mathbf{r}|). \tag{18}$$

Even at the critical point, $g(r)$ maintains finite values in the range of $0 \leq r < \infty$. The behavior of $g(r)$ denotes that the correlation between two particles disappears with an increase in the three-dimensional distance, r, separating one of the two particles from the other.[14] Based on these features, Eq. (18) requires that divergence of the compressibility be caused by the fact that the long-range behavior of $g(r)$ is characterized near the critical point as follows:

$$g(r) - 1 \sim r^{-\mu} \quad (0 < \mu \leq 3). \tag{19}$$

In fact, the long-range feature of $g(r)$ can be expressed in several particular conditions as the product of factor r^{D-3} $(D = 2)$ and a particular function $\phi(r)$, which is given as a Taylor series with respect to powers of r.[15,16]

$$g(r) - 1 \approx r^{D-3}\phi(r) \quad (D = 2). \tag{20}$$

Despite this, the dependence of $g(r)$ on distance r between two particles[17] deviates near the liquid-vapor critical point. Its dependence on r cannot be expressed by the product of a negative power r^{-1} and a particular function $\phi(r)$.[13,18] The density fluctuations makes the dependence of $g(r)$ on r near the liquid-vapor critical point[13,18] differ from that in the gas state when it is far from the critical point.

(a) *Anomalies near liquid-vapor critical points*

The density fluctuations can result in anomalies[19–23] with respect to various properties of the fluids near their liquid-vapor critical points. Inhomogeneity, which is generated in fluids consisting of metallic atoms near their liquid-vapor critical points,[24] can cause anomalies in the electrical properties,[19] optical reflectivity,[20] and optical absorption.[20,21] The electrical conductivity of liquid mercury maintained at a temperature near the critical point decreases with a rather steep gradient as the density of the mercury atoms decreases.[19] The real part of the dielectric constant, determined using optical reflectivity and absorption measurements, for a mercury fluid near the critical point increases sharply at a particular density as the density of the mercury atoms increases.[20] Inhomogeneities that lead to the occurrence of the anomalies can be caused by the physical cluster formation.[24]

The viscosities of fluids can become anomalous near the liquid-vapor critical points.[22,23] The viscosities of fluids exhibit asymptotic divergence near the liquid-vapor critical points. Measurements of the viscosities of carbon dioxide and xenon near their critical points yield the critical exponent that can characterize the asymptotic divergence.[22] Physical cluster formation can result in a characteristic increase in the viscosities of fluids near the critical points.[23]

When the temperature of a fluid system is reduced toward the liquid-vapor critical point, the number of specific particle pairs is increased. Then, each of the particle pairs is specified as two particles interacting in a bound state wherein the contribution of the mutually attractive force between them exceeds the contribution of their relative kinetic energy. An increase in the number of such particle pairs allows physical clusters to grow. This denotes that various critical phenomena observed in fluids are caused by the formation of physical clusters. Physical cluster formation allows the features generated in the liquid state of a fluid to differ from the features found in the gas state of the fluid. Various critical phenomena imply that physical cluster formation causes a gas-liquid phase transition. The development

of physical clusters, which are formed by attractive forces between colloidal particles, allows a colloidal solution to generate a gel state.[25] According to an analogy with the occurrence of the gel state, the contribution of the physical cluster formation induces the transition of a fluid from the liquid state to the solid state.

(b) *Contribution of the physical cluster formation*

The contribution of physical cluster formation to the gas-liquid phase transition is suggested because the liquid-vapor interface become macroscopically smooth for a fluid in which the liquid phase and the gas phase coexist. At a temperature slightly beyond the liquid-vapor critical point of the fluid, the interface disappears. To form a smooth liquid-vapor interface, particles constituting the liquid phase must have the capability to maintain their density; however, particles constituting the gas phase do not have the capability.

The high-density part maintains the liquid phase and it must generate a macroscopic force, which contributes to the minimization of the interface. The macroscopic force causes the liquid-vapor interface to become smooth. The macroscopic force is not caused by each particle pair that is specified to be two particles interacting in an unbound state wherein the contribution of their relative kinetic energy exceeds that of the mutually attractive force between them. Hence, the macroscopic force must be caused by the presence of each particle pair that is specified to be two particles interacting in a bound state wherein the contribution of the mutually attractive force between them exceeds that of their relative kinetic energy. The formation of the liquid phase must be aided by the formation of physical clusters.

The low-density part maintains the gas phase and it principally includes particle pairs that are specified to be two particles interacting in an unbound state wherein the contribution of their relative kinetic energy exceeds that of the mutually attractive force between them. The high-density part in the liquid phase also includes such particle pairs. The particles forming these particle pairs must be confined between the branches of physical clusters to generate a macroscopically smooth interface. The confinement of these particles between the branches of physical clusters allows the interface to become smooth. This confinement can aid in transforming the fluid of the liquid phase into the solid state.

The formation of physical clusters in multicomponent fluids is an interesting subject that should be considered. Physical clusters must influence the microscopic distribution pattern of particular atoms or molecules that are dissolved as solute particles in a fluid in the liquid

state. In a fluid in the gas state, an effect of the physical cluster formation is not expected. A fluid in the gas state microscopically homogeneously mixes with another fluid in the gas state.

Solute particles that cannot actively contribute to the physical cluster formation have a tendency to become distributed among the branches of physical clusters. Solute particles that can actively contribute to the physical cluster formation participate in the physical cluster formation and are distributed as portions of the physical clusters. Thus, physical clusters can make a microscopic distribution pattern of solute particles become inhomogeneous in a fluid mixture such as a liquid of metallic alloy and solute-solvent mixtures.

A specific effect of such a microscopically inhomogeneous distribution pattern of solute particles can be found as a macroscopic phenomenon called the osmotic pressure. The osmotic pressure occurs when solute particles are distributed in a fluid. The osmotic pressure depends on whether solute particles can actively contribute to the physical cluster formation. Moreover, the osmotic pressure depends on whether the stability of the physical clusters is high or low.

Under the condition that the stability of the physical clusters is low, the formation of physical clusters and the decomposition of physical clusters can occur as very sensitive responses to slight variations in the temperature. The anomalous behavior of the thermal conductivity of a fluid should be determined in such a specific situation.[26] Physical clusters formed in the fluid do not have the capability to stably confine particles that do not belong to the physical cluster, thereby allowing both the confinement of the particles and their release to occur easily. This effect enables the fluid to be stirred. Thus, the thermal conductivity of the fluid should be enhanced under the condition that the stability of the physical clusters varies sensitively.

Physical cluster formation can contribute to the occurrence of various phenomena. Indeed, the magnitude of the pair correlation function should involve an effect of the physical cluster formation. The pair correlation function is determined by X-ray scattering measurements and neutron scattering measurements. Despite this, the fraction of the contribution of the physical cluster formation to the pair correlation function is not be sufficiently clear. Therefore, a method for estimating the contribution of the physical cluster formation to the pair correlation function should be established as a readily treatment.

(c) *To estimate physical cluster formation*

Effects of physical cluster formation can appear in various phenomena. A procedure for simply estimating the physical cluster formation should be useful for examining its effects on the features of a fluid. Each physical cluster that is formed in a fluid system is an ensemble of particles that are linked to each other by bonds. Based on Hill's concept,[2] each bond is defined as a bound state in which a contribution of mutually attractive forces between pair particles exceeds a contribution of their relative kinetic energy. A useful procedure for estimating the physical cluster formation owing to such bonds can be found according to a concept of Coniglio et al.,[3] and results in an integral equation.

The use of the integral equation makes it possible to examine the physical cluster formation caused by a contribution of an extremely short-range attractive force[4] and to examine the physical cluster formation caused by the Yukawa potential.[8,27] A procedure for making corrections to the PY approximation[28] enables improvement in an estimation of the physical cluster formation as the integral equation is applied.[7] Although the integral equation enables the physical cluster formation to be examined, it is not equivalent to the Ornstein–Zernike equation with respect to their physical meanings.

The use of the Ornstein–Zernike equation has been successful for examining fluids in the gas and liquid states. The behavior of particles that is described by the Ornstein–Zernike equation indirectly involves the contribution of the physical cluster formation. The Ornstein–Zernike equation includes the contribution of the integral equation, which enables the formation of the physical clusters to be examined. This means that subtracting the contribution of the integral equation from the Ornstein–Zernike equation yields an additional integral equation, which is equivalent to both an integral equation derived by Stell[28] and another one derived by Chiew and co-workers.[6] If this additional integral equation is coupled to the integral equation that enables the physical cluster formation to be examined, then the two integral equations provides an integral equation system that is equivalent to the Ornstein–Zernike equation. An effect of the physical cluster formation on a feature of a fluid can be estimated using the integral equation system.

2. Pair connectedness for estimating physical cluster formation

(**a**) *Correlation functions*

Three-dimensional coordinates for the positions of particles in a fluid system are denoted by $\mathbf{r}_i$ for i particle and $\mathbf{r}_j$ for j particle. A situation where these particles are included in the same physical cluster is allowed. A correlation function that can play a role instead of the pair correlation function is necessary to estimate the mean size of physical clusters. The pair connectedness $\mathcal{P}(|\mathbf{r}_i - \mathbf{r}_j|)$ is an important correlation function[3] when calculating the mean size. The probability that i particle and j particle are located in the volume elements $\mathrm{d}\mathbf{r}_i$ at $\mathbf{r}_i$ and $\mathrm{d}\mathbf{r}_j$ at $\mathbf{r}_j$, respectively, is $\rho\rho g(r_{ij})\mathrm{d}\mathbf{r}_i\mathrm{d}\mathbf{r}_j$. The probability increases when particles in the fluid system are prevented from moving easily. Here, r_{ij} is the distance $|\mathbf{r}_i - \mathbf{r}_j|$, and ρ is the density of particles for a uniform distribution. Thus, the mean number of particles within a macroscopic volume V equals $V\rho$.

The magnitude of $g(r_{ij})$ is proportional to the probability that i particle in a volume element $\mathrm{d}\mathbf{r}_i$ is located at a distance r_{ij} far from j particle in a volume element $\mathrm{d}\mathbf{r}_j$. Hence, maximum values of $g(r_{ij})$ should become larger when particles in a fluid system are prevented from moving easily. The pair correlation function $g(r_{ij})$ is useful for knowing whether particles in the fluid system can move easily or can be prevented from moving easily. The use of $g(r_{ij})$ allows for estimating the density fluctuations for a fluid system even near the liquid-vapor critical point. A feature of the fluid near the liquid-vapor critical point appears to be a characteristic behavior of $g(r_{ij})$, which can express the degree to which particles in the fluid system are prevented from moving easily.[13,14,18]

Nevertheless, the pair correlation function, $g(r_{ij})$, cannot simply aid in examining the physical cluster formation. Even if a fluid is a particle system consisting of hard cores, between which mutually attractive forces do not exist, pair correlation function $g(r_{ij})$ $(i \neq j)$ can express the degree of preventing particles from moving easily because the increasing ρ increases the probability $\rho\rho g(r_{ij})\mathrm{d}\mathbf{r}_i\mathrm{d}\mathbf{r}_j$. Physical clusters are, however, not formed in the fluid.

If physical clusters are formed, then the magnitude of $g(r_{ij})$ is affected by the physical cluster formation. The magnitude of $g(r_{ij})$ includes the contribution of physical cluster formation. If the contribution of physical cluster formation is divided from the magnitude of $g(r_{ij})$, then the effects of physical cluster formation can be clearly estimated.

An f-function defined by $f(r_{ij}) \equiv e^{-\beta u(r_{ij})} - 1$ specifies a particle pair that consists of i particle at $\mathbf{r}_i$ and j particle at $\mathbf{r}_j$. The use of f-functions allows the pair correlation function $g(r_{ij})$ to be expressed in the form of a density expansion.[9,10] For an N particle fluid system, specific features of $g(r_{ij})$ are determined by $N(N-1)/2$ particle pairs. Then, the relation between two particles constituting each pair maintains one of two possibilities. One possibility is the case that the two particles are bound to each other. The other possibility is the case that the two particles are not bound to each other.

i) *Probability that two particles interact with each other in a bound state*

The Hamiltonian for describing the movements of two particles specified as a pair is given as

$$H_2 = \frac{p_i^2}{2m_i} + \frac{p_j^2}{2m_j} + u(r_{ij}), \tag{21}$$

where the mass of i particle and that of j particle are m_i and m_j, respectively. r_{ij} corresponds to the relative position between i particle and j particle. The center of mass $\mathbf{R}$ is given by

$$\mathbf{R} = (m_i\mathbf{r}_i + m_j\mathbf{r}_j)/(m_i + m_j).$$

The total momentum $\mathbf{P}$ carried by the center of mass is given by

$$\mathbf{P} = \mathbf{p}_i + \mathbf{p}_j.$$

The relative velocity between i particle and j particle is given by dividing $\mathbf{p}_{\rm rel}$ by the reduced mass $\bar{m}$. $\mathbf{p}_{\rm rel}$ and $\bar{m}$ are given by

$$\begin{cases} \mathbf{p}_{\rm rel} = (m_j\mathbf{p}_i - m_i\mathbf{p}_j)/M, \\ \bar{m} = m_i m_j/M, \end{cases}$$

where the total mass M is defined as

$$M \equiv m_i + m_j.$$

The Hamiltonian is expressed using the kinetic energy of the center of mass $P^2/2M$ and relative kinetic energy $p_{\rm rel}^2/2\bar{m}$ as follows:

$$H_2 = \frac{P^2}{2M} + \frac{p_{\rm rel}^2}{2\bar{m}} + u(r_{ij}), \tag{22}$$

where $P = |\mathbf{P}|$ and $p_{\rm rel} = |\mathbf{p}_{\rm rel}|$. Then, Eq. (22) means that the Hamiltonian is described as $H_2 = \bar{H}_2(\mathbf{P}, \mathbf{p}_{\rm rel}, \mathbf{r}_i, \mathbf{r}_j)$. Based on the assumption that particle i is located at the origin of a coordinate, the use of the relative kinetic energy that is expressed in the polar coordinate denoted by the parameters r, θ, ϕ allows H_2 to be given as

$$H_2 = \frac{P^2}{2M} + \frac{1}{2\bar{m}}\left(p_r^2 + \frac{p_\theta^2}{r^2} + \frac{p_\phi^2}{r^2\sin^2\theta}\right) + u(r), \tag{23}$$

Eq. (23) indicates that the Hamiltonian is described as $H_2 = \hat{H}_2(\mathbf{P}, p_r, p_\theta, p_\phi, r, \theta, \phi)$. In Eq. (23), the second term on the right-hand side of the equation is the contribution of the relative kinetic energy of the two particles, and the third term is the contribution of the interactions between them. For the Hamiltonian given by Eq. (23), Q_2 is denoted as

$$Q_2 = \frac{1}{2!(2\pi\hbar)^6} V \int_V {\rm d}r{\rm d}\theta{\rm d}\phi \int_{-\infty}^{\infty} {\rm d}p_r{\rm d}p_\theta{\rm d}p_\phi \int_{-\infty}^{\infty} {\rm d}\mathbf{P} \exp[-\beta\hat{H}_2]. \tag{24}$$

If parameters $\bar{p}_r$, $\bar{p}_\theta$, and $\bar{p}_\phi$ are defined as $\bar{p}_r \equiv p_r(\beta/2\bar{m})^{1/2}$, $\bar{p}_\theta \equiv (p_\theta/r)(\beta/2\bar{m})^{1/2}$ $\bar{p}_\phi \equiv (p_\phi/r\sin\theta)(\beta/2\bar{m})^{1/2}$, βH_2 is expressed as

$$\beta H_2 = \beta\frac{P^2}{2M} + \bar{p}_r^2 + \bar{p}_\theta^2 + \bar{p}_\phi^2 + \beta u(r). \tag{25}$$

The use of Eq. (25) with the parameters $\bar{p}_r$, $\bar{p}_\theta$, and $\bar{p}_\phi$ allows Eq. (24) to be rewritten as follows

$$Q_2 = \frac{V}{2\pi^{3/2}}\left(\frac{2\pi\sqrt{M\bar{m}}}{(2\pi\hbar)^2\beta}\right)^{3/2} \int_0^\infty 4\pi r^2 {\rm d}r e^{-\beta u(r)} \int_{-\infty}^{\infty} {\rm d}\bar{p}_r{\rm d}\bar{p}_\theta{\rm d}\bar{p}_\phi e^{-(\bar{p}_r^2+\bar{p}_\theta^2+\bar{p}_\phi^2)}, \tag{26}$$

According to Eq. (25), the contribution $\mathcal{E}(p)$ of the relative kinetic energy of the two particles is given as

$$\mathcal{E}(p) = \bar{p}_r^2 + \bar{p}_\theta^2 + \bar{p}_\phi^2. \tag{27}$$

$\beta u(r)$ denotes the contribution of the interactions between them at each r. At each r that allows $u(r)$ to be negative, the situation wherein the two particles are bound to each other by the mutually attractive force requires

$$\bar{p}_r^2 + \bar{p}_\theta^2 + \bar{p}_\phi^2 \leq -\beta u(r). \tag{28}$$

The probability $p(r)$ that the two particles are found in a bound state $\mathcal{E}(p) + \beta u(r) \leq 0$ is estimated from the integration of $\exp[-(\bar{p}_r^2 + \bar{p}_\theta^2 + \bar{p}_\phi^2)]$ included in Eq. (26) as follows:

$$p(r) = \frac{1}{\pi^{3/2}} \int_{\bar{p}_r^2+\bar{p}_\theta^2+\bar{p}_\phi^2 \leq -\beta u(r)} {\rm d}\bar{p}_r{\rm d}\bar{p}_\theta{\rm d}\bar{p}_\phi e^{-(\bar{p}_r^2+\bar{p}_\theta^2+\bar{p}_\phi^2)}. \tag{29}$$

Then, the integration of $\exp[-(\bar{p}_r^2+\bar{p}_\theta^2+\bar{p}_\phi^2)]$ is limited by $\bar{p}_r$, $\bar{p}_\theta$, and $\bar{p}_\phi$ that satisfy Eq. (28). If Eq. (29) is rewritten through the use of $\mathcal{E}(p)$, then the following equation is obtained for $p(r)$

$$\begin{aligned} p(r) =& \frac{2}{\pi^{1/2}} \int_0^{-\beta u(r)} e^{-\mathcal{E}} \mathcal{E}^{1/2} \mathrm{d}\mathcal{E} \\ =& \frac{2}{\pi^{1/2}} \left[\Gamma\left(\frac{3}{2}\right) - \Gamma\left(\frac{3}{2}, -\beta u(r)\right) \right], \end{aligned} \tag{30}$$

where $\Gamma(\tau, t)$ is the incomplete gamma function expressed by $\Gamma(\tau,t) = \int_t^\infty e^{-y} y^{\tau-1} \mathrm{d}y$.[2]

At each r that allows $u(r)$ to be negative, the situation wherein the two particles are not bound requires

$$\bar{p}_r^2 + \bar{p}_\theta^2 + \bar{p}_\phi^2 > -\beta u(r). \tag{31}$$

The probability $\bar{p}(r)$ that the two particles are found in an unbound state $\mathcal{E}(p) + \beta u(r) > 0$ is estimated as follows:

$$\bar{p}(r) = \frac{1}{\pi^{3/2}} \int_{\bar{p}_r^2+\bar{p}_\theta^2+\bar{p}_\phi^2 > -\beta u(r)} \mathrm{d}\bar{p}_r \mathrm{d}\bar{p}_\theta \mathrm{d}\bar{p}_\phi e^{-(\bar{p}_r^2+\bar{p}_\theta^2+\bar{p}_\phi^2)} \tag{32}$$

$$\begin{aligned} =& \frac{2}{\pi^{1/2}} \Gamma\left(\frac{3}{2}, -\beta u(r)\right) \\ =& 1 - p(r). \end{aligned} \tag{33}$$

At each r that allows $u(r)$ to be positive, Eq. (31) is always satisfied for arbitrary values of three parameters $\bar{p}_r$, $\bar{p}_\theta$, and $\bar{p}_\phi$. The two particles are not bound at each r that allows $u(r)$ to be positive. Then, the following relations is satisfied:

$$\begin{cases} \bar{p}(r) = 1, & (\text{at each } r \text{ satisfying } 0 < u(r)) \\ p(r) = 0, & (\text{at each } r \text{ satisfying } 0 < u(r)) \end{cases} \tag{34}$$

ii) *Physical cluster formed as an ensemble of particles linked with each other by f^+ bonds*

An f-function $f(r_{ij})$ specifies i particle at $\mathbf{r}_i$ and j particle at $\mathbf{r}_j$. Then, $p(r)\big|_{r=r_{ij}}$, which is obtained from Eq. (30), denotes the probability that i particle and j particle, which are specified by $f(r_{ij})$, are bound to each other. The use of the probability $p(r_{ij})$ allows f-function $f(r_{ij})$ to be given as the sum of the f^+-function and the f^*-function:

$$f(r_{ij}) = f^+(r_{ij}) + f^*(r_{ij}), \tag{35}$$

where $f^+(r_{ij})$ and $f^*(r_{ij})$ are expressed as

$$f^+(r_{ij}) \equiv p(r_{ij}) e^{-\beta u(r_{ij})} \tag{36}$$

$$f^*(r_{ij}) \equiv [1 - p(r_{ij})] e^{-\beta u(r_{ij})} - 1. \tag{37}$$

In each of diagrams found from the density expansion of $g(r_{12})$, an f-bond corresponds to an f-function. Each of the f- functions in its density expansion is substituted with the sum of an f^+-function and an f^*-function, which is exemplified by $f(r_{ij}) = f^+(r_{ij}) + f^*(r_{ij})$. As a result, each diagram is expressed as the sum of diagrams that are formed by f^+ bonds specified by f^+-functions and f^* bonds specified by f^*-functions. The sum includes specific diagrams. In each of these diagrams, one root point $\mathbf{r}_1$ is connected to the other root point $\mathbf{r}_2$ through at least one path of all f^+-bonds given as a product of f^+-functions. The diagrams denote that the two particles corresponding to the two root points are part of the same physical cluster.[2] Substituting each f-function with each sum $f^+ + f^*$ allows a correlation function corresponding to pair connectedness $\mathcal{P}(r_{12})$ to be extracted from $g(r_{12})$ expressed by the density expansion.[3] Thus, the pair connectedness $\mathcal{P}(r_{12})$ enables us to directly analyze the physical cluster formation.

iii) *Relation of pair connectedness $\mathcal{P}(r_{12})$ with pair correlation function $g(r_{12})$*

Pair connectedness $\mathcal{P}(r_{12})$ is given by the sum of the contributions obtained from every diagram that has at least one path of all f^+-bonds between the root points labeled as 1 and 2. The use of $\mathcal{P}(r_{12})$ allows $\rho\rho\mathcal{P}(r_{12})\mathrm{d}\mathbf{r}_1\mathrm{d}\mathbf{r}_2$ to express the probability that particle 1 in $\mathrm{d}\mathbf{r}_1$ located at $\mathbf{r}_1$ and particle 2 in $\mathrm{d}\mathbf{r}_2$ located at $\mathbf{r}_2$ belong to the same physical cluster.[3] If the probability that particle 1 and particle 2 belong to different physical clusters is expressed as $\rho\rho\mathcal{D}(r_{12})\mathrm{d}\mathbf{r}_1\mathrm{d}\mathbf{r}_2$,[3] then the pair connectedness $\mathcal{P}(r_{12})$ is related to $g(r_{12})$ as follows:

$$g(r_{12}) = \mathcal{P}(r_{12}) + \mathcal{D}(r_{12}), \quad (r_{12} \equiv |\mathbf{r}_1 - \mathbf{r}_2|). \tag{38}$$

According to $g(r_{12})$, the probability that particle 1 in a volume element $\mathrm{d}\mathbf{r}_1$ at $\mathbf{r}_1$ is located at a distance r_{12} from particle 2 located in a volume element $\mathrm{d}\mathbf{r}_2$ at $\mathbf{r}_2$ is given by $\rho\rho g(r_{12})\mathrm{d}\mathbf{r}_1\mathrm{d}\mathbf{r}_2$ for a uniform fluid in which $\rho\delta V$ at $\mathbf{r}_1$ is equal to $\rho\delta V$ at $\mathbf{r}_2$ on average for a microscopic volume δV. Then, the probability that particle 1 and particle 2 are in $\mathrm{d}\mathbf{r}_1$ at $\mathbf{r}_1$ and in $\mathrm{d}\mathbf{r}_2$ at $\mathbf{r}_2$, respectively, is the sum of two contributions. One of the two contributions corresponds to the probability that both particle 1 in volume element $\mathrm{d}\mathbf{r}_1$ at $\mathbf{r}_1$ and particle 2 in volume

element $d\mathbf{r}_2$ at $\mathbf{r}_2$ belong to the same physical cluster. The other contribution corresponds to the probability that particle 1 in volume element $d\mathbf{r}_1$ at $\mathbf{r}_1$ and particle 2 in volume element $d\mathbf{r}_2$ at $\mathbf{r}_2$ do not belong to the same physical cluster. The former is given by $\rho\rho\mathcal{P}(r_{12})d\mathbf{r}_1d\mathbf{r}_2$, and the latter is given by $\rho\rho\mathcal{D}(r_{12})d\mathbf{r}_1d\mathbf{r}_2$. Therefore, $\rho\rho g(r_{12})d\mathbf{r}_1d\mathbf{r}_2$ must satisfy the following relation:

$$\rho\rho g(r_{12})d\mathbf{r}_1d\mathbf{r}_2 = \rho\rho\mathcal{P}(r_{12})d\mathbf{r}_1d\mathbf{r}_2 + \rho\rho\mathcal{D}(r_{12})d\mathbf{r}_1d\mathbf{r}_2.$$

This formula indicates that variations in the thermodynamic behavior of a fluid system owing to variations in the temperature are dominated by variations in the magnitude of $\mathcal{D}(r_{12})$ if a high-temperature condition prevents the formation of physical clusters. The magnitude of $\mathcal{D}(r_{12})$ depends on the number of particles that are categorized as particles linked through each path that includes f^*-bonds. Particles linked through each path that includes f^*-bonds are either particles that do not participate in the physical cluster formation or particles that do not belong to the same physical cluster. By contrast, the magnitude of $\mathcal{P}(r_{12})$ depends on the number of particles that participate in the physical cluster formation and are linked by paths of f^+-bonds.

iv) *Features of* $\mathcal{P}(r_{12})$

Near or below the liquid-vapor critical point, effects of the physical cluster formation on the thermodynamic behavior should not be ignored. Then, unless particles contributing to the magnitude of $\mathcal{P}(r_{12})$ can microscopically and homogeneously mix with particles contributing to the magnitude of $\mathcal{D}(r_{12})$, a correlation between the behaviors of the former and latter particle groups must occur. Phenomena similar to the above correlation can be found from computer simulations of supercooled liquids. According to the computer simulations, particles having low mobility cannot microscopically and homogeneously mix with those having high mobility; hence, the particles participate in cooperative motion in structural relaxation.[29] Such cooperative motion can also be observed in colloidal suspensions.[30–32]

In every hard-sphere fluid system, cooperative motion similar to the above examples should not exist. Because of Eq. (34), every hard-sphere fluid system is characterized by a pair correlation function expressed as

$$\begin{cases} g(r_{12}) = \mathcal{D}(r_{12}) \\ \mathcal{P}(r_{12}) = 0 \quad \text{for} \quad 0 \le u(r_{12}). \end{cases} \tag{39}$$

The density fluctuations in a hard-sphere fluid system are only simply reduced as the density of hard spheres increases. This fact can be confirmed even using the equation of state obtained from the PY approximation.[9,10] An increase in the density of hard spheres limits the motion of hard spheres. This effect causes the above behavior.

If the contribution of mutually attractive forces between particles on the formation of specific particle configurations is not ignored, then a fluid system should be characterized by the pair correlation function expressed by

$$\begin{cases} g(r_{12}) = \mathcal{P}(r_{12}) + \mathcal{D}(r_{12}) \\ \mathcal{P}(r_{12}) \neq 0 \quad \text{for} \quad u(r_{12}) < 0. \end{cases} \tag{40}$$

When this fluid system is maintained near the critical point, mutually attractive forces between particles cause the density fluctuations to reach a maximum value with an increase in the density of particles. After reaching the maximum value, the density fluctuations are gradually reduced as the density of particles increases.[12,13] In a fluid system where mutually attractive forces between particles is not ignored, the magnitude of $\mathcal{P}(r_{12})$ should not be ignored near the critical point. Then, the behavior of $g(r_{12})$ is revealed via the sum $\mathcal{P}(r_{12}) + \mathcal{D}(r_{12})$.

(**b**) *Mean size $\mathcal{S}$ of physical clusters*

Physical clusters contributing to the gas-liquid phase transition naturally contribute to the transition from the liquid state of a fluid to its solid state as one of phenomena caused by the growth of physical clusters. Every physical cluster is formed from particle pairs characterized as follows: each particle pair consists of two particles interacting with each other in a bound state in which the contribution of mutually attractive forces between them exceeds the contribution of their relative kinetic energy. An increase in the number of particles interacting in unbound states increases the magnitude of $\mathcal{D}$. The correlation function $\mathcal{D}$ is that characterized by pairs of particles having a large relative momentum. An increase in the number of particle pairs interacting in bound states increases the magnitude of $\mathcal{P}$. The pair connectedness $\mathcal{P}$ is a correlation function characterized by pairs of particles having a small relative momentum. The use of $\mathcal{P}$ enables the mean size $\mathcal{S}$ of physical clusters to be estimated.

In accordance with Kirkwood and Buff,[33] pair correlation function $g(r)$ has a normaliza-

tion given as

$$\frac{1}{V}\int_V g(r)\mathrm{d}\mathbf{r} = \frac{\langle N\rangle - 1}{V\rho} + \frac{1}{V^2}\frac{1}{\rho^2}\Big[\langle NN\rangle - \langle N\rangle\langle N\rangle\Big], \tag{41}$$

where $\langle N\rangle$ is the mean number of particles within volume V. The dependence of $g(r)$ on V is negligible for macroscopic V, and the dependence of $\langle N\rangle/V$ on V and the dependence of $(\langle NN\rangle - \langle N\rangle\langle N\rangle)/V$ on V are also negligible. Thus, Eq. (41) in the limit $V \to \infty$ results in

$$\int_V g(r)\mathrm{d}\mathbf{r}/V = 1.$$

This relation, along with Eq. (38), requires the normalization for the pair correlation function to be expressed as

$$\lim_{V\to\infty}\left[\frac{1}{V}\int_V \mathcal{P}(r)\mathrm{d}\mathbf{r} + \frac{1}{V}\int_V \mathcal{D}(r)\mathrm{d}\mathbf{r}\right] = 1. \tag{42}$$

Mean size $\mathcal{S}$ of physical clusters can be estimated using $\mathcal{P}(r_{12})$. Equilibrium number n_s of physical clusters consisting of s particles can be related to the pair connectedness $\mathcal{P}$. According to the formula given by Coniglio et al.,[3] the relation between n_s and $\mathcal{P}$ is given as

$$\sum_{1\le s} s(s-1)n_s = \rho\rho\int_V\int_V \mathcal{P}(|\mathbf{r}_1 - \mathbf{r}_2|)\mathrm{d}\mathbf{r}_1\mathrm{d}\mathbf{r}_2. \tag{43}$$

Factor $\sum_s sn_s$ found in Eq. (43) can be related to the density ρ of particles in the volume V as

$$\rho = [1/V]\sum_s sn_s.$$

The mean physical cluster size $\mathcal{S}$ is given as

$$\begin{aligned}\mathcal{S} =& \sum_s s\left(\frac{sn_s}{\sum_s sn_s}\right)\\ =& \left(\sum_s s^2 n_s\right)\left(\sum_s sn_s\right)^{-1}.\end{aligned}$$

This formula and $\sum_s sn_s = V\rho$ allow Eq. (43) to be rewritten as

$$\mathcal{S} = 1 + \rho\int_V \mathcal{P}(r)\mathrm{d}\mathbf{r}. \tag{44}$$

The percolation of physical clusters occurs in a fluid system at the percolation threshold. The use of Eq. (44) allows for the examination of whether physical clusters in the fluid system

are in the percolation state. The critical condition at which the mean physical cluster size $\mathcal{S}$ given by Eq. (44) reaches infinity corresponds to the percolation threshold. The percolation of physical clusters in a macroscopic V maintained by a fluid system affects the dependence of $\mathcal{S}$ on V. If the percolation of physical clusters does not occur in V, then $\mathcal{S}$ should be sufficiently independent of V. When percolated physical clusters exist in macroscopic sizes in V, $\mathcal{S}$ should depend on V.

3. Effects of the physical cluster growth

(**a**) *Occurrence of macroscopically sized physical clusters*

The integral of $\mathcal{P}(r)$ found in Eq. (42) is related to the mean size $\mathcal{S}$ of physical clusters based on Eq. (44). If the percolation of physical clusters does not occur in a macroscopic V maintained by a fluid system, then $\mathcal{S}$ [which is estimated for the fluid system by Eq. (44)] should be sufficiently independent of V. Hence, the limit $V \to \infty$ does not affect $\mathcal{S}$. Eq. (44) can be rewritten as follows:

$$\frac{\mathcal{S}-1}{V} = \rho \frac{1}{V} \int_V \mathcal{P}(r) \mathrm{d}\mathbf{r}. \tag{45}$$

Thus, the limit $V \to \infty$ requires that the right-hand side of Eq. (45) satisfy $(\mathcal{S}-1)/V = 0$. Therefore, Eq. (45) allows $\lim_{V\to\infty}(\rho/V)\int_V \mathcal{P}(r)\mathrm{d}\mathbf{r} = 0$ to be satisfied. Moreover, Eq. (42) requires $(1/V)\int_V \mathcal{D}(r)\mathrm{d}\mathbf{r} = 1$ to be satisfied in the limit $V \to \infty$. Based on these consequences, the normalization conditions that are given in the limit $V \to \infty$ are described as

$$\begin{cases} \lim_{V\to\infty}(1/V)\int_V \mathcal{P}(r)\mathrm{d}\mathbf{r} = 0, \\ \lim_{V\to\infty}(1/V)\int_V \mathcal{D}(r)\mathrm{d}\mathbf{r} = 1. \end{cases}$$

If the percolation of physical clusters occurs in a macroscopic V maintained by the fluid system, then the mean size $\mathcal{S}$ that is estimated for the fluid system from the use of Eq. (44) should be dependent on V. Then, the magnitude of $[(\mathcal{S}-1)/V]$ can have a finite nonzero value. Eq. (42) requires conditions given as

$$\begin{cases} 0 < \lim_{V\to\infty}(1/V)\int_V \mathcal{P}(r)\mathrm{d}\mathbf{r} \le 1, \\ 0 \le \lim_{V\to\infty}(1/V)\int_V \mathcal{D}(r)\mathrm{d}\mathbf{r} < 1, \\ \lim_{V\to\infty}(1/V)\int_V \mathcal{P}(r)\mathrm{d}\mathbf{r} + \lim_{V\to\infty}(1/V)\int_V \mathcal{D}(r)\mathrm{d}\mathbf{r} = 1. \end{cases}$$

If a state of the fluid is in the immediate vicinity of the liquid-solid transition point where relation $0 < (\rho^{sd} - \rho^{lq})/\rho^{sd} \ll 1$ (ρ^{sd} denotes ρ in a solid state, and ρ^{lq} denotes ρ in a liquid state) is satisfied, then almost all physical clusters should hold macroscopic sizes in V. The dependence of $\mathcal{S}$ on V should be characterized by $\mathcal{S}/V \approx \rho^{sd}$, which corresponds to the case that the growth of physical clusters reaches the limit. Eq. (45) results in $(1/V)\rho\int_V \mathcal{P}(r)\mathrm{d}\mathbf{r} \approx \rho^{sd}$ in the limit $V \to \infty$. According to this case, Eq. (42)

allows $(1/V)\int_V \mathcal{D}(r)\mathrm{d}\mathbf{r} \approx 0$ to be satisfied in the limit $V \to \infty$. Based on these consequences, the normalization conditions that are given in the limit $V \to \infty$ are described as

$$\begin{cases} \lim_{V\to\infty}(1/V)\int_V \mathcal{P}(r)\mathrm{d}\mathbf{r} \approx 1, \\ \lim_{V\to\infty}(1/V)\int_V \mathcal{D}(r)\mathrm{d}\mathbf{r} \approx 0. \end{cases}$$

In a state specified by $(1/V)\int_V \mathcal{D}(r)\mathrm{d}\mathbf{r} = 0$, the fluid does not include particle pairs specified by each pair characterized as two particles interacting in an unbound state wherein the contribution of the relative kinetic energy of the pair particles exceeds the contribution of a mutually attractive force between them. A state specified by $(1/V)\int_V \mathcal{D}(r)\mathrm{d}\mathbf{r} \approx 0$ means that the fluid does not have features found in the liquid state. The growth of physical clusters that proceeds in macroscopic V beyond the percolation threshold can contribute to compelling the phase transition from the liquid state of the fluid to the solid state. A specific state wherein $(1/V)\int_V \mathcal{D}(r)\mathrm{d}\mathbf{r} \approx 0$ is satisfied should be found at least near the triple point.

(**b**) *Behavior of correlation functions*

The pair correlation function behaves as $g(|\mathbf{r}_1 - \mathbf{r}_2|) \approx 1$ for a large $|\mathbf{r}_1 - \mathbf{r}_2|$, which corresponds to the case that one of two particles corresponding to the location at $\mathbf{r}_1$ in a fluid system is widely separated from the other corresponding to the location at $\mathbf{r}_2$. In the limit $V \to \infty$ and $r \to \infty$, it behaves as $g(r) = 1$.[2] This requires the behaviors of the two correlation functions to be restricted by the following relation:

$$\mathcal{P}(r) + \mathcal{D}(r) \approx 1, \quad (1 \ll r/\sigma), \tag{46}$$

Then, the value of σ is restricted by the relation $r < \sigma$, which is satisfied at each r where the contribution of the repulsive force between two particles exceeds the contribution of the mutually attractive force between them. If σ is the hard-core diameter of each particle, then the following relation is satisfied:

$$\begin{cases} \mathcal{P}(r) = 0, \quad (r < \sigma), \\ \mathcal{D}(r) = 0, \quad (r < \sigma), \\ g(r) = 0, \quad (r < \sigma). \end{cases} \tag{47}$$

For a large r (satisfying $1 \ll r/\sigma$), the behaviors of $\mathcal{P}(r)$ and $\mathcal{D}(r)$ are restricted based on Eq. (46). Under the condition that no percolation of physical clusters occurs, the physical

meanings of the two correlation functions and their behavior given by Eq. (46) require the behaviors of $\mathcal{P}(r)$ and $\mathcal{D}(r)$ at a large r to be expressed by

$$\begin{cases} \lim_{r\to\infty} \mathcal{P}(r) = 0, \\ \lim_{r\to\infty} \mathcal{D}(r) = 1 \\ \lim_{r\to\infty} g(r) = \lim_{r\to\infty} \mathcal{D}(r). \end{cases} \tag{48}$$

The relations given by Eq. (48) should be satisfied even at the percolation threshold, although they are not correct beyond that point.

The above relations must be modified correctly if macroscopically sized physical clusters in the fluid can increase beyond the percolation threshold. Then, the magnitude of $\mathcal{P}(r)$ should have a nonzero finite value even for a large r. Hence, in a specific condition that allows macroscopically sized physical clusters to increase, the restriction given by Eq. (46) should require $\mathcal{P}(r)$ and $\mathcal{D}(r)$ to behave as

$$\begin{cases} 0 < \lim_{r\to\infty} \mathcal{P}(r) \leq 1, \\ 0 \leq \lim_{r\to\infty} \mathcal{D}(r) < 1, \\ \lim_{r\to\infty} [\mathcal{P}(r) + \mathcal{D}(r)] = 1. \end{cases}$$

If macroscopically sized physical clusters in the fluid can continue to grow beyond the percolation threshold, then particles that contribute to the magnitude of $\mathcal{D}(r)$ should decrease toward zero. At the final stage of the physical cluster growth, the existence of many macroscopically sized physical clusters requires the two correlation functions to behave as follows:

$$\begin{cases} \lim_{r\to\infty} \mathcal{P}(r) \approx 1, \\ \lim_{r\to\infty} \mathcal{D}(r) \approx 0, \\ \lim_{r\to\infty} g(r) \approx \lim_{r\to\infty} \mathcal{P}(r). \end{cases}$$

The above relations should be satisfied at least near the triple point where relation $(1/V)\int_V \mathcal{D}(r)\mathrm{d}\mathbf{r} \approx 0$. The transition from the liquid state of the fluid to the solid state at least at the triple point should be aided by the enhancement and development of macroscopically sized physical clusters in macroscopic V.

(**c**) *Integral equations for correlation functions including the pair connectedness*

Pair connectedness $\mathcal{P}(r_{ij})$ ($r_{ij} \equiv |\mathbf{r}_i - \mathbf{r}_j|$) is given as the sum of the contributions obtained from every diagram that has at least one path of all f^+ bonds between the root points corresponding to the two coordinates, $\mathbf{r}_i$ and $\mathbf{r}_j$. Pair correlation function $g(r_{ij})$ is given as the sum of contributions obtained from every diagram formed by paths of f-bonds between the root points, according to the density expansion of $g(r_{ij})$.[9,10] Moreover, Eq. (15) with Eq. (17) and (16) requires $g(r_{ij})$ to be given the sum of the two contributions that correspond to the contribution of the nodal diagrams having nodal points and the other contribution of the non-nodal diagrams having no nodal point. A nodal point is a specific field point in a diagram, and missing the field point in the diagram means that the diagram is separated into two groups, i.e., one group including a root point and the other group including the other root point.

Based on the example of $g(r_{ij})$, the diagrams contributing to $\mathcal{P}(r_{ij})$ are separated into two groups. One consists of the nodal diagrams of f^+-bonds and the other is the remaining group consisting of the non-nodal diagrams of f^+-bonds. This means that $\mathcal{P}(r_{ij})$ is expressed as

$$\mathcal{P}(r_{ij}) = N^+(r_{ij}) + C^+(r_{ij}),$$

where $N^+(r_{ij})$ is the contribution of all nodal diagrams having at least one path of all f^+-bonds between the two root points, and $C^+(r_{ij})$ is the contribution of all non-nodal diagrams having at least one path of all f^+-bonds between the two root points.

In the Ornstein–Zernike equation,[9] the contribution of all the non-nodal diagrams consisting of paths of f-bonds between the two root points corresponds to direct correlation function $c(r_{ij})$. According to the Ornstein–Zernike equation, $g(r_{ij}) - 1$ is equal to $N(r_{ij}) + c(r_{ij})$, in which $N(r_{ij})$ represents the contribution of all the nodal diagrams consisting of paths of f-bonds between the two root points, and $N(r_{ij})$ is given as the convolution integral $\rho \int c(r_{ik})[g(r_{kj}) - 1]\mathrm{d}\mathbf{r}_k$, which is simplified using $r_{ik} \equiv |\mathbf{r}_i - \mathbf{r}_k|$ and $r_{kj} \equiv |\mathbf{r}_k - \mathbf{r}_j|$.

If an analogy with the Ornstein–Zernike equation is assumed, then the convolution integral of the product of $C^+(r_{ik})$ and $\mathcal{P}(r_{kj})$ should yield $N^+(r_{ij}) = \rho \int C^+(r_{ik})\mathcal{P}(r_{kj})\mathrm{d}\mathbf{r}_k$. This consequence and $\mathcal{P}(r_{ij}) = C^+(r_{ij}) + N^+(r_{ij})$ result in an integral equation that is required to estimate $\mathcal{P}(r_{ij})$.[3] Hence, the pair connectedness $\mathcal{P}(r_{ij})$ is given as a solution of the integral equation expressed as

$$\mathcal{P}(r_{ij}) = C^+(r_{ij}) + \rho \int_V C^+(r_{ik})\mathcal{P}(r_{kj})\mathrm{d}\mathbf{r}_k, \tag{49}$$

where $C^+(r_{ij})$ is an unknown function. Eq. (49) has the same mathematical structure as the Ornstein–Zernike equation, and it is used in the limit $V \to \infty$,

An integral equation for the correlation function $\mathcal{D}(r_{ij})$ can be obtained by considering the Ornstein–Zernike equation. Equation (38) allows the Ornstein–Zernike equation to be expressed as

$$\begin{aligned}\mathcal{P}(r_{ij}) + \mathcal{D}(r_{ij}) - 1 = c(r_{ij}) &+ \rho \int_V c(r_{ik})\mathcal{P}(r_{kj})\mathrm{d}\mathbf{r}_k \\ &+ \rho \int_V c(r_{ik})[\mathcal{D}(r_{kj}) - 1]\mathrm{d}\mathbf{r}_k. \end{aligned} \tag{50}$$

This equation must involve the contribution of the pair connectedness $\mathcal{P}$, which should be estimated by Eq. (49). If the contribution of non-nodal diagrams that do not include the paths of all f^+-bonds between i and j particles is expressed as $C^*(r_{ij})$, then direct correlation function $c(r_{ij})$, which represents the contribution of all non-nodal diagrams consisting of paths of f-bonds between the two root points, must be equal to the sum of $C^*(r_{ij})$ and $C^+(r_{ij})$. Thus, $c(r_{ij})$ is expressed as

$$c(r_{ij}) = C^+(r_{ij}) + C^*(r_{ij}). \tag{51}$$

Then, $C^+(r_{ij})$ is the contribution of all non-nodal diagrams having at least one path of all f^+-bonds between the two root points. The ensemble of particle pairs that contribute to the magnitude of $C^+(r)$ is the same as that contributing to $\mathcal{P}(r)$. Similarly, the ensemble of particle pairs that contribute to the magnitude of $C^*(r)$ is the same as that contributing to $\mathcal{D}(r)$.

If Eq. (49) is considered, then the substitution of Eq. (51) into Eq. (50) results in an integral equation that is equivalent to both an integral equation derived by Stell[28] and another one derived by Chiew et al.[6] This integral equation is expressed as

$$\begin{aligned}\mathcal{H}(r_{ij}) =& C^*(r_{ij}) + \rho \int_V C^*(r_{ik})\mathcal{P}(r_{kj})\mathrm{d}\mathbf{r}_k \\ &+\rho \int_V C^+(r_{ik})\mathcal{H}(r_{kj})\mathrm{d}\mathbf{r}_k + \rho \int_V C^*(r_{ik})\mathcal{H}(r_{kj})\mathrm{d}\mathbf{r}_k, \end{aligned} \tag{52}$$

where

$$\mathcal{H}(r_{ij}) \equiv \mathcal{D}(r_{ij}) - 1. \tag{53}$$

In Eq. (52), $C^*(r_{ij})$ is an unknown function. The integral equation system composed of Eqs. (49) and (52) is equivalent to the Ornstein–Zernike equation, which has been successful for examining a fluid in both the gas and liquid states.

According to Eq. (51), an integral equation system consisting of Eqs. (49) and (52) is equivalent to the Ornstein–Zernike equation. Equation (49) contributes to estimating the formation of physical clusters, and Eq. (52) contributes to estimating an effect of the physical cluster formation. In fact, the second term and the third term on its right-hand side in Eq. (52) represent a way to induce an effect of the formation of physical clusters on the correlation function $\mathcal{H}$. An effect of these terms should play a role in explaining phenomena owing to the formation of physical clusters.

For a specific fluid system in which no physical cluster formation is expected, Eq. (52) is simplified as

$$\mathcal{H}(r_{ij}) = C^*(r_{ij}) + \rho \int_V C^*(r_{ik})\mathcal{H}(r_{kj})\mathrm{d}\mathbf{r}_k. \tag{54}$$

When the gas phase of a fluid and the liquid phase of the fluid are in equilibrium, Eq. (54) is applicable to examining the behavior of this gas phase, and Eq. (52) is applicable to examining the behavior of that liquid phase. In addition, when $\left|\mathcal{P}(r)/\mathcal{D}(r)\right| \ll 1$ is satisfied, the following relation can occur:

$$\left|\rho \int_V C^*(r_{ik})\mathcal{P}(r_{kj})\mathrm{d}\mathbf{r}_k + \rho \int_V C^+(r_{ik})\mathcal{H}(r_{kj})\mathrm{d}\mathbf{r}_k\right| \ll \left|\mathcal{H}(r_{ij})\right|. \tag{55}$$

Eq. (54) can be an appropriate approximation even for a fluid involving the formation of physical clusters if the condition $|\mathcal{P}(r)/\mathcal{D}(r)| \ll 1$ is satisfied for the fluid.

4. Each closure scheme for solving each integral equation

(**a**) *Two closure schemes*

According to the PY approximation, an approximate relation between $\mathcal{P}(r_{ij})$ and $C^{+}(r_{ij})$ can be given within the effective range, where the contribution of $u(r_{ij})$ to a mutually attractive force, which makes particle i interact with particle j, cannot be neglected.[3] An approximate relation between $\mathcal{D}(r_{ij})$ and $C^{*}(r_{ij})$ can also be given within the effective range. As a result, an aid of the PY approximation allows for the characterization of $\mathcal{P}(r_{ij})$ owing to a pair potential. Moreover, it allows for the characterization of $\mathcal{D}(r_{ij})$ owing to a pair potential.

The pair correlation function $g^{\rm PY}(r_{ij})$ owing to the PY approximation is expressed as $g^{\rm PY}(r_{ij})e^{\beta u(r_{ij})} = 1 + N(r_{ij})$. If relations $e^{-\beta u(r_{ij})} = f^{+}(r_{ij}) + f^{*}(r_{ij}) + 1$ and $N(r_{ij}) = N^{+}(r_{ij}) + N^{*}(r_{ij})$ are both considered, the the PY approximation is rewritten as

$$\begin{aligned} g^{\rm PY}(r_{ij}) =& f^{+}(r_{ij})\Big[1 + N^{+}(r_{ij}) + N^{*}(r_{ij})\Big] + \Big[f^{*}(r_{ij}) + 1\Big]N^{+}(r_{ij}) \\ &+ \Big[f^{*}(r_{ij}) + 1\Big]\Big[1 + N^{*}(r_{ij})\Big]. \end{aligned} \tag{56}$$

Equation (38) requires that the right-hand side of Eq. (56) be formed by the sum of the terms contributing to $\mathcal{P}(r_{ij})$ and the terms contributing to $\mathcal{D}(r_{ij})$. If three relations such as $\mathcal{P}(r_{ij}) + \mathcal{D}(r_{ij}) \approx g^{\rm PY}(r_{ij})$, $\mathcal{P}(r_{ij}) = C^{+}(r_{ij}) + N^{+}(r_{ij})$, and an expression of the PY approximation $g^{\rm PY}(r_{ij})e^{\beta u(r_{ij})} = 1 + N(r_{ij})$ with $N(r_{ij}) = N^{+}(r_{ij}) + N^{*}(r_{ij})$ are considered, then Eq. (56) is allowed to be divided into two formulae. Thus, one of the two formulae is

$$\mathcal{P}(r_{ij}) = f^{+}(r_{ij})g^{\rm PY}(r_{ij})e^{\beta u(r_{ij})} + [f^{*}(r_{ij}) + 1][\mathcal{P}(r_{ij}) - C^{+}(r_{ij})], \tag{57}$$

and the other is

$$\mathcal{D}(r_{ij}) = [f^{*}(r_{ij}) + 1][g^{\rm PY}(r_{ij}) - c^{\rm PY}(r_{ij}) - \mathcal{P}(r_{ij}) + C^{+}(r_{ij})], \tag{58}$$

where $c^{\rm PY}(r_{ij})$ is the direct correlation function owing to the PY approximation and is given as $c^{\rm PY}(r_{ij})/(1 - e^{\beta u(r_{ij})}) = g^{\rm PY}(r_{ij})$.

If Eqs. (36) and (37) are considered with Eq. (30), then Eq. (57) can be rewritten as

$$\begin{aligned} &\mathcal{P}(r_{ij}) + \frac{2\Gamma[3/2, w(r_{ij})]}{\pi^{1/2}e^{\beta u(r_{ij})} - 2\Gamma[3/2, w(r_{ij})]}C^{+}(r_{ij}) \\ &\quad = \frac{2\{\Gamma(3/2) - \Gamma[3/2, w(r_{ij})]\}e^{\beta u(r_{ij})}}{\pi^{1/2}e^{\beta u(r_{ij})} - 2\Gamma[3/2, w(r_{ij})]}\frac{c^{\rm PY}(r_{ij})}{1 - e^{\beta u(r_{ij})}}, \end{aligned} \tag{59}$$

where $w(r_{ij}) \equiv -\beta u(r_{ij})\theta[-\beta u(r_{ij})]$ ($\theta[x] = 1$ $(0 \leq x)$, $\theta[x] = 0$ $(0 > x)$). Eq. (59) can be used as a closure scheme for Eq. (49) if $c_{ij}^{\rm PY}(r)$ is given.

If Eqs. (38) and (51) are considered, then Eq. (58) can be rewritten as

$$\mathcal{D}(r_{ij}) = \frac{2\Gamma[3/2, w(r_{ij})]}{2\Gamma[3/2, w(r_{ij})] - \pi^{1/2} e^{\beta u(r_{ij})}} C^*(r_{ij}). \tag{60}$$

An estimate of $\mathcal{D}(r_{ij})$ is allowed from considering Eq. (60) as a closure scheme for Eq. (52) if $\mathcal{P}_{ij}(r)$ is estimated with the use of Eq. (49). Although Eqs. (59) and (60) can be used when either $\beta u(r_{ij}) < 0$ or $\beta u(r_{ij}) > 0$, $\beta u(r_{ij}) > 0$ requires $\mathcal{P}_{ij}(r) = 0$, $C^+(r_{ij}) = 0$, $\mathcal{D}(r_{ij}) \neq 0$, and $C^*(r_{ij}) \neq 0$.

Eqs. (59) and (60) enable $\mathcal{P}(r_{ij})$ and $\mathcal{D}(r_{ij})$ to be characterized by a pair potential if $c^{\rm PY}(r_{ij})$, $C^+(r_{ij})$, and $C^*(r_{ij})$ are given. Moreover, Eqs. (59) and (60) suggest that separating $\mathcal{P}(r_{ij})$ from $g(r_{ij})$ allows a pair potential characterizing $\mathcal{P}(r_{ij})$ to be made different from a pair potential characterizing $\mathcal{D}(r_{ij})$. Even if a pair potential controlling the behavior of pair particles can depend on relative momenta of particles, the use of Eqs. (59) and (60) enables $\mathcal{P}(r_{ij})$ and $\mathcal{D}(r_{ij})$ to be estimated. A pair potential in a situation (I) where the contribution of a mutually attractive force between pair particles exceeds the contribution of the relative kinetic energy between them can differ from that in a situation (II) where the contribution of the relative kinetic energy between them exceeds the contribution of the mutually attractive force between them. The difference between a pair potential in situation (I) and that in situation (II) may occur in a fluid system consisting of molecules that can form hydrogen bonds between them.

(**b**) *Necessity of distinguishing between u^+ and u^**

When the integral equation system given by Eqs. (49) and (52) is solved, the characteristics of attractive forces that act between particles contributing to the magnitude of $\mathcal{P}(r_{ij})$ are permitted to differ from the characteristics of attractive forces that act between particles contributing to the magnitude of $\mathcal{D}(r_{ij})$. A pair potential $u^+(r_{ij})$ that can characterize the former attractive forces can differ from a pair potential $u^*(r_{ij})$ that can characterize the latter attractive forces.

Attractive forces among particles can depend on bond angles, torsional angles, and the coordination number of particles.[34,35] Many-body effects are generated as the dependence of attractive forces on bond angles, torsional angles, and the coordination number of particles.

If pair potentials are made to function as a model for simulating effects of the attractive forces, then the features of the pair potentials must be affected by the many-body effects. The simplest model is one that allows the mean features of the many-body effects to be treated as spherically symmetric contributions such as $u^{+}(r_{ij})$ and $u^{*}(r_{ij})$. Such pair potentials that should be derived as the model must characterize the mean features of attractive forces acting among particles.

At a specific temperature that cannot allow a fluid to maintain a locally and transiently ordered microscopic structure, the many-body effects should be ignored even in a dense gas state. If a locally and transiently ordered microscopic structure is found even in the gas state of a fluid, then the many-body effects should not be ignored. The many-body effects can depend on the degree of the kinetic energies of particles because attractive forces can be affected by bond angles, torsional angles and the coordination number of particles. Then, the simplest model for examining effects of such attractive forces is one that allows $u^{+}(r_{ij})$ to differ from $u^{*}(r_{ij})$.

(**c**) *Simple closure scheme in the MSA*

The use of the closure scheme given by Eq. (59) is not practical as a way to solve Eq. (49) analytically. Fortunately, Eq. (49) has the same mathematical structure as the Ornstein–Zernike equation. The Ornstein–Zernike equation can be solved analytically for some fluids if the MSA[36] is used. In the MSA, the direct correlation function $c(r)$ is given as the sum of the short-range contribution $c^{0}(r)$ and the long- range contribution $-\beta u(r)$. This means that $c(r)$ is expressed as

$$c(r) = c^{0}(r) - \beta u(r) \tag{61}$$

$$c^{0}(r) = 0, \qquad \text{for } r > \sigma, \tag{62}$$

where σ is the diameter of the hard core of a particle. If $C^{+}(r)$ is given in the same form as $c(r)$ given in the MSA, then the procedure for solving Eq. (49) can be simplified, as found in the procedures for solving the Ornstein–Zernike equation in the MSA.

i) *Recursive solution for the Ornstein–Zernike*

According to the MSA,[10,36] the direct correlation function, $c(r)$, outside of the range in which the contribution of the hard-core interaction is effective, remains effective within the

range where the magnitude of $u(r)$ cannot be neglected. $c(r)$ decays to zero as rapidly as $-\beta u(r)$, which retains a microscopic feature. This means that the ranges within which the correlation functions $C^+(r)$ and $C^*(r)$ are not zero remain microscopic sizes because of Eq. (51). The correlation function $g(r)-1$ decays to zero much more slowly than $c(r)$.[13,18] Thus, the behavior of $g(r)-1$ is different from the behavior of $c(r)$, which has a tendency to maintain the microscopic feature.

This is demonstrated by the solution that is obtained by solving the Ornstein–Zernike equation recursively. The solution is given as a function of r as the distance between particle 1 and particle 2. This is expressed by

$$\begin{aligned} g(r)-1 =& c(r)+\rho\int_V c(r_{13})c(r_{32})\mathrm{d}\mathbf{r}_3 \\ &+\rho\rho\int_V\int_V c(r_{13})c(r_{34})c(r_{42})\mathrm{d}\mathbf{r}_3\mathrm{d}\mathbf{r}_4+\cdots, \end{aligned} \tag{63}$$

where the convolution integrals denote contributions from particle 3, particle 4, $\cdots$, which are distributed around particle 1 and particle 2 that exist away from each other at a distance r. Contributions from particle 3, particle 4, $\cdots$, make the behavior of $g(r)-1$ differ from the behavior of $c(r)$.

Pair correlation function $g(r)$, which must satisfy the Ornstein–Zernike equation, involves the contributions of many particles, which are expressed as the convolution integrals of $c(r_{13})c(r_{34})\cdots c(r_{m2})$ $(m=3,4,5,\cdots)$ found in Eq. (63). This means that the pair correlation function $g(r)$, derived from the use of an approximate $c(r)$, involves contributions of many particles, even when the approximate $c(r)$ is obtained from the contributions of limited principal particles. Even without the use of an accurate $c(r)$ obtained from the contributions of all the particles that should be considered, the mathematical procedure for making $g(r)$ satisfy the Ornstein–Zernike equation makes it possible to address the necessity of considering the contributions of many particles.

ii) *Concept for the MSA*

When the relation between the distance r and the hard-core diameter σ of each particle satisfies $r\le\sigma$, relation $g(r)-1=-1$ should be satisfied. Hence, Eq. (63) requires $c(r)$ to be negative even for $r/\sigma\approx 1$ if $0<r/\sigma<1$ is satisfied. Every convolution integral in Eq. (63) cannot always positively contribute to the magnitude of $g(r)-1$. Nevertheless, the magnitude of $g(r)-1$ can remain a positive finite value at a large r that is out of

the effective range where $c(r) \neq 0$. This means that convolution integrals that positively contribute to the magnitude of $g(r)-1$ are dominant in Eq. (63) at a large r, where $c(r) \approx 0$ is satisfied. Thus, the manner in which the direct correlation function $c(r)$ contributes to the magnitude of $g(r)-1$ denotes that the long-range contribution characterized for $\sigma < r$ differs from the short-range contribution characterized for $r \leq \sigma$. This behavior agrees with the concept for the MSA, i.e., that $c(r)$ is given as the sum of the short-range contribution and the long-range contribution.

iii) *Relations of* $C^+(r)$ *and* $C^*(r)$ *with* $c(r)$

The direct correlation function $c(r)$ is the contribution of all non-nodal diagrams consisting of paths of f-bonds between the two root points. Similarly, $C^+(r)$ is the contribution of all non-nodal diagrams having at least one path of all f^+-bonds between the two root points. $C^*(r)$ is the contribution of non-nodal diagrams that do not include paths of all f^+-bonds between the two root points. The similarity among these diagram structures suggests that both the behavior of $C^+(r)$ and the behavior of $C^*(r)$ should be similar to the behavior of $c(r)$. According to the MSA,[36] direct correlation function $c(r)$ is given by Eqs. (61) and (62), and outside the effective range of the hard-core potential, $c(r)$ behaves as the sum of the long-range contribution $c(r)/(-\beta u(r)) = 1$ and the short-range contribution $c^0(r) = 0$. According to the similarity between $c(r)$ and $C^+(r)$ with respect to the diagram structures, the behavior of $C^+(r)$ is given as the sum of the short-range contribution expressed as $C^{0+}(r)$ and the long-range contribution to $C^+(r)$. According to the similarity between $c(r)$ and $C^*(r)$ with respect to the diagram structures, the behavior of $C^*(r)$ is given as the sum of the short-range contribution expressed as $C^{0*}(r)$ and the long-range contribution to $C^*(r)$.

(**d**) *Behavior of* $C^+(r)$ *found for* $0 < -\beta u(r) \ll 1$ *at a large* r.

The behavior of $C^+(r)$ at a large r can be readily determined. If the distance r between particle 1 and particle 2 is sufficiently large, then $|\beta u(r)|$ should be sufficiently small. Equation (30) can then be approximated as

$$p(r) = \frac{4}{3\sqrt{\pi}} \left(-\beta u(r)\right)^{3/2} - \frac{4}{5\sqrt{\pi}} \left(-\beta u(r)\right)^{5/2} + \frac{2}{7\sqrt{\pi}} \left(-\beta u(r)\right)^{7/2} + \cdots . \tag{64}$$

If $p(r)$ given by Eq. (64) is substituted into Eq. (59), then the following formula is obtained:

$$C^{+}(r) = \frac{c^{\mathrm{PY}}(r)}{-\beta u(r)}\Big[\frac{4}{3\sqrt{\pi}}(-\beta u(r))^{3/2} - \frac{22}{15\sqrt{\pi}}(-\beta u(r))^{5/2} + \cdots\Big]$$
$$+\mathcal{P}(r)\Big[-\beta u(r) - \frac{4}{3\sqrt{\pi}}(-\beta u(r))^{3/2} - \frac{1}{2}(-\beta u(r))^{2} + \frac{32}{15\sqrt{\pi}}(-\beta u(r))^{5/2} + \cdots\Big]. \quad (65)$$

A long-range contribution to $C^{+}(r)$ is obtained from Eq. (65) by considering an assumption that is made for $1 < r/\sigma$ as

$$\begin{cases} \mathcal{P}(r) \sim [-\beta u(r)]^{\nu} \quad \text{with} \quad 1 \le \nu, \\ 0 < -\beta u(r) \ll 1. \end{cases}$$

Here, σ is the diameter of the hard-core of each particle. At the minimum, relation $\mathcal{P}(r)/[g(r)-1] \le 1$ is always satisfied because of $g(r)-1 = \mathcal{P}(r)+\mathcal{D}(r)-1$ and $0 \le \mathcal{D}(r)-1$. This relation is consistent with Eq. (48) that is satisfied without the percolation of physical clusters. Thus, the magnitude of $\mathcal{P}(r)$ for $0 < -\beta u(r) \ll 1$ should satisfy

$$\frac{g(r)-1}{-\beta u(r)} \ge \frac{\mathcal{P}(r)}{-\beta u(r)}.$$

The MSA yields $c^{\mathrm{PY}}(r)/[-\beta u(r)] = 1$ for $1 < r/\sigma$. Then, a general assumption $\lim_{r\to\infty} u(r) = 0$ allows $g^{\mathrm{PY}}(r) = c^{\mathrm{PY}}(r)/\{1 - \exp[\beta u(r)]\}$ owing to the PY approximation to result in

$$\lim_{r\to\infty} \frac{g(r)-1}{-\beta u(r)} = \lim_{r\to\infty} \frac{1}{-\beta u(r)}\Big[\frac{c^{\mathrm{PY}}(r)}{1-\exp(\beta u(r))} - 1\Big] = \frac{1}{2}.$$

Therefore, the above general assumption allows the following relation to be derived

$$\frac{1}{2} \ge \lim_{r\to\infty} \frac{\mathcal{P}(r)}{-\beta u(r)} \ge 0.$$

This result denotes that the behavior of $\mathcal{P}(r)$ for $1 < r/\sigma$ and $0 < -\beta u(r) \ll 1$ is expressed as $\mathcal{P}(r) \sim [-\beta u(r)]^{\nu}$ with $1 \le \nu$. Owing to this behavior of $\mathcal{P}(r)$, a long-range contribution[37] to $C^{+}(r)$ is found from Eq. (65) as

$$C^{+}(r) \approx \frac{4}{3\sqrt{\pi}}\big[-\beta u(r)\big]^{3/2}, \quad (\text{for } 1 < r/\sigma \text{ and } 0 < -\beta u(r) \ll 1). \quad (66)$$

(**e**) *Behavior of* $\mathcal{P}(r)$ *found for* $0 < -\beta u(r) \ll 1$.

The expansion of Eq. (59), which is obtained in powers of $-\beta u(r)$ for $|\beta u(r)| \ll 1$ based on the substitution of $p(r)$ expressed by Eq. (64), can be given instead of Eq. (65) as follows

$$\mathcal{P}(r) = -\frac{c^{\mathrm{PY}}(r)}{-\beta u(r)}\Big[\frac{4}{3\sqrt{\pi}}(-\beta u(r))^{1/2} + \frac{16}{9\pi}(-\beta u(r)) + \Big(\frac{64}{27\pi^{3/2}} - \frac{4}{5\sqrt{\pi}}\Big)(-\beta u(r))^{3/2} + \cdots\Big]$$
$$+\frac{C^{+}(r)}{-\beta u(r)}\Big[1 + \frac{4}{3\sqrt{\pi}}(-\beta u(r))^{1/2} + \Big(\frac{1}{2} + \frac{16}{9\pi}\Big)(-\beta u(r)) + \cdots\Big]. \quad (67)$$

The use of Eq. (66), which is obtained under the condition that no percolation of physical clusters occurs, enables Eq. (67) to yield an approximate behavior of $\mathcal{P}(r)$ for $|\beta u(r)| \ll 1$. If relation $c^{\mathrm{PY}}(r)/(-\beta u(r)) = 1$ given for the MSA is considered at each r satisfying $1 < r/\sigma$, then Eq. (67) allows the approximate behavior of $\mathcal{P}(r)$ to be expressed as

$$\mathcal{P}(r) = \frac{22}{15\sqrt{\pi}}(-\beta u(r))^{3/2} \quad \text{for} \quad 0 < -\beta u(r) \ll 1. \tag{68}$$

$\mathcal{P}(r)$ given by Eq. (68) directly depends on the feature of $\beta u(r)$. Then, the effective range within which $\beta u(r)$ remains nonzero finite values can be microscopic. Hence, the magnitude of $\mathcal{P}(r)$ given by Eq. (68) involves contributions from only limited particles. Despite this, if each physical cluster formed in a fluid where no percolation occurs has a fractal structure, $\mathcal{P}(r)$ given by Eq. (68) should represent the characteristics of the fractal structure within the rang where $\beta u(r)$ remains nonzero finite values.[37] Physical clusters can grow beyond the range that depends directly on the feature of $\beta u(r)$. The physical clusters can hold a fractal structure as discussed in II B 8.

(**f**) *Simple closure scheme for Eq. (49)*

i) *Simple closure scheme for estimating* $\mathcal{P}(r)$

The similarity between the behavior of $c(r)$ and the behavior of $C^{+}(r)$ with respect to the diagram structures should allow the behavior of $C^{+}(r)$ to be given as the sum of the short-range contribution expressed as $C^{0+}(r)$ and the long-range contribution to $C^{+}(r)$. An approximate $C^{+}(r)$ given by the sum becomes a simple closure scheme for the integral equation given by Eq. (49). The long-range contribution to $C^{+}(r)$ is given by Eq. (66). Thus, a simple closure scheme similar to the MSA is expressed as

$$C^{+}(r) = C^{0+}(r) + \frac{4}{3\sqrt{\pi}}(-\beta u(r))^{3/2} \quad \text{for} \quad \beta u(r) < 0, \tag{69}$$

where for the short-range contribution $C^{0+}(r)$ the behavior similar to $c^{0}(r)$ is required according to an analogy with the MSA. Thus, $C^{0+}(r)$ should be given as

$$C^{0+}(r) = 0, \qquad \text{for} \ \ \sigma \le r. \tag{70}$$

The most completely short-range interaction between pair particles must be attributed to a hard-core potential. For diameter σ of the hard core of each particle, the hard-core potential does not directly contribute to the interaction between the pair particles for $\sigma \le r$. Thus, Eq. (70) should be justified as an approximate expression, according to the MSA.

ii) *Recursive solution for* $\mathcal{P}(r)$

According to the MSA, $c(r)$ decay to zero as rapidly as $-\beta u(r)$, which retains a microscopic feature. Eq. (69) demonstrates that $C^+(r)$ behaves in a way similar to $c(r)$; however, Eq. (69) requires it to decay to zero more rapidly than $-\beta u(r)$. Then, the effective range of $-\beta u(r)$ can remain a microscopic size. Despite this fact, $\mathcal{P}(r)$ can still have a finite value that is nonzero even out of the effective range. This can be explained via a recursive solution. The solution is obtained from solving Eq. (49) recursively in the same manner as the mathematical procedure for solving the Ornstein–Zernike equation. Thus, the integral equation expressed by Eq. (49) has a recursive solution given as

$$\begin{aligned}\mathcal{P}(r) =& C^+(r) + \rho \int_V C^+(r_{13}) C^+(r_{32}) \mathrm{d}\mathbf{r}_3 \\ &+ \rho\rho \int_V \int_V C^+(r_{13}) C^+(r_{34}) C^+(r_{42}) \mathrm{d}\mathbf{r}_3 \mathrm{d}\mathbf{r}_4 + \cdots . \end{aligned} \tag{71}$$

According to Eq. (71), if particle 2 is located at a distance r from particle 1, then the probability that both particle 1 and particle 2 belong to the same physical cluster can be increased by the contribution of other particles $(3, 4, \cdots)$. Each term on the right-hand side of Eq. (71) has a magnitude proportional to the above probability while depending on the contribution of other particular particles $(3, 4, \cdots)$. Although the first term $C^+(r)$ without the contribution of other particular particles is the exception, the first term is also proportional to the probability that both particle 1 and particle 2 belong to the same physical cluster. If the contributions of particles $(3, 4, \cdots)$ distributed around particle 1 and particle 2 are nonnegligible, then it is possible for $\mathcal{P}(r)$ to remain nonzero, even out of the effective range in which $C^+(r) \neq 0$.

iii) *Convolution integrals synthesizing recursive solution*

Each convolution integral on the right-hand side of Eq. (71) is positive because $0 \leq C^+(r)$ is satisfied everywhere because of $0 \leq \mathcal{P}(r) \quad (0 < r)$. In Eq. (63), the convolution integrals must not always be positive as $c(r)$ is negative for $0 < r/\sigma \leq 1$ because $g(r) - 1 \approx -1$ $(0 < r/\sigma \leq 1)$ is satisfied. The contributions of particles $(3, 4, \cdots)$ distributed around particle 1 and particle 2 to $\mathcal{P}(r)$ seem different from their contributions to $g(r)$. Despite this, Eq. (63) corresponds to the sum of the contribution from $\mathcal{D}$ and the contribution from $\mathcal{P}$, according to Eq. (38). The contribution of Eq. (71) to $g(r)$ is hidden in the expression of Eq.

(63), although Eq. (63) is obtained from the Ornstein–Zernike equation. The contribution of Eq. (71) to $g(r)$ should be considered the contribution of the physical cluster formation to $g(r)$.

In addition, the pair connectedness $\mathcal{P}(r)$, which must satisfy the integral equation given by Eq. (49), involves the contributions of many particles, which are expressed as convolution integrals found in Eq. (71). This means that the pair connectedness $\mathcal{P}(r)$ derived from the use of an approximate $C^+(r)$ involves the contributions of many particles, even when the approximate $C^+(r)$ results from contributions of limited principal particles. Even without the use of an accurate $C^+(r)$ obtained from the contributions of all the particles that should be considered, making $\mathcal{P}(r)$ satisfy the integral equation given by Eq. (49) enable us to address the necessity of considering the contributions of many particles.

(**g**) *Simple closure scheme for Eq. (52).*

i) *Simple closure scheme for estimating* $\mathcal{H}(r)$

If $\beta u(r)$ is positive, there is no particle pair that contributes to the magnitude of $C^+(r)$ and then every particle pair contributes to the magnitude of $C^*(r)$. Even if $\beta u(r)$ is negative, then particle pairs contributing to the magnitude of $C^*(r)$ exist. The magnitude of $C^*(r)$ results from the contribution of non-nodal diagrams that do not include paths of all f^+-bonds between the two root points 1 and 2. Particle pairs contributing to the magnitude include particular pairs. Then, each of the particular pairs is formed by two particles interacting in an unbound state where the contribution of the relative kinetic energy of the pair particles exceeds the contribution of the mutually attractive force between them.

If the MSA and the behavior of $\mathcal{P}(r)$ given by Eq. (68) are considered, then Eq. (38) and the PY approximation $g^{\rm PY}(r) = c^{\rm PY}(r)/\{1 - \exp[\beta u(r)]\}$ result in

$$\mathcal{D}(r) - 1 \approx -\frac{1}{2}\beta u(r) \quad \text{for} \quad 1 \ll r/\sigma. \tag{72}$$

Eq. (72) denotes the behavior of $\mathcal{D}(r)$ found for $0 < |-\beta u(r)| \ll 1$ at a large r. Then, particles contributing to this behavior are very limited.

The behavior of $\mathcal{D}(r) - 1$ at a large r allows Eq. (60) to lead to

$$C^*(r) \approx -\beta u(r) \quad \text{for} \quad 1 \ll r/\sigma. \tag{73}$$

This is the long-range contribution to $C^*(r)$. Thus, the use of Eq. (73) allows the behavior of $C^*(r)$ to be approximately expressed as the sum of the short-range contribution expressed

as $C^{0*}(r)$ and the long-range contribution to $C^*(r)$ according to an analogy with the MSA. This means that an approximation of $C^*(r)$ is given for either $\beta u(r) < 0$ or $\beta u(r) > 0$ by

$$C^*(r) = C^{0*}(r) - \beta u(r), \tag{74}$$

$$C^{0*}(r) = 0, \qquad \text{for } r > \sigma. \tag{75}$$

The hard-core potential does not directly contribute to the interaction between them for $r \geq \sigma$. Thus, Eq. (75) should be justified as an approximate expression, according to the MSA.

ii) *Recursive solution for* $\mathcal{H}(r)$

Eq. (75) demonstrates that $C^*(r)$ behaves in a way similar to $c(r)$ and decays to zero as rapidly as $-\beta u(r)$. Then, the effective range of $-\beta u(r)$ can remain a microscopic size. Despite this fact, $\mathcal{H}(r)$ can still have a finite value being nonzero even out of the effective range. This can be explained via the solution that is obtained from solving Eq. (52) recursively. The integral equation expressed by Eq. (52) has the recursive solution given as

$$\begin{aligned}\mathcal{H}(r) =& C^*(r) + \rho \int_V c(r_{13}) C^*(r_{32}) \mathrm{d}\mathbf{r}_3 + \rho\rho \int_V \int_V c(r_{13}) c(r_{34}) C^*(r_{42}) \mathrm{d}\mathbf{r}_3 \mathrm{d}\mathbf{r}_4 + \\ &+ \rho \int C^*(r_{13}) \mathcal{P}(r_{32}) \mathrm{d}\mathbf{r}_3 + \rho\rho \int_V \int_V c(r_{13}) C^*(r_{34}) \mathcal{P}(r_{42}) \mathrm{d}\mathbf{r}_3 \mathrm{d}\mathbf{r}_4 \\ &+ \rho\rho\rho \int_V \int_V \int_V c(r_{13}) c(r_{34}) C^*(r_{45}) \mathcal{P}(r_{52}) \mathrm{d}\mathbf{r}_3 \mathrm{d}\mathbf{r}_4 \mathrm{d}\mathbf{r}_5 + \cdots . \end{aligned} \tag{76}$$

In Eq. (76), the convolution integrals denote the contributions from particle 3, particle 4, $\cdots$, which are distributed around particle 1 and particle 2 that exist away from each other at a distance r. The contributions from particle 3, particle 4, $\cdots$, make the behavior of $\mathcal{H}(r)$ differ from the behavior of $C^*(r)$. The magnitude of $\mathcal{H}(r)$ can retain a nonzero finite value at a large r out of the effective range in which $C^*(r) \neq 0$.

Correlation function $\mathcal{H}(r)$ that satisfies Eq. (76) involves the contributions of many particles that participate in the convolution integrals. The correlation function $\mathcal{H}(r)$ derived from the use of an approximate $C^*(r)$ involves the contributions of many particles, even when the approximate is obtained from the contributions of limited principal particles. Even without the use of an accurate $C^*(r)$ obtained from the contributions of all the particles that should be considered, the mathematical procedure for making $\mathcal{H}(r)$ satisfy Eq. (52) enables us to address the necessity of considering the contributions of many particles.

5. Percolation of physical clusters in Yukawa fluid specified by κ^{-1}

(a) *Percolation phenomena*

In a fluid system, each physical cluster of particles is formed via bonds between the particles. A bond occurring for particle pair is defined as a bound state in which relation $\mathcal{E}(p) + \beta u(r) \leq 0$ corresponding to Eq. (28) is satisfied for the particle pair. The bond denotes the situation where the contribution $\beta u(r)$ of the attractive interaction between two particles exceeds the contribution $\mathcal{E}(p)$ of their relative kinetic energy. An ensemble of particles linked with each other via bonds corresponds to a physical cluster.

The fluid system involves the smallest clusters formed by only a single particle, the second smallest clusters formed by two particles, ..., and the largest clusters formed by a number of particles. Percolation of the physical clusters corresponds to the case that the mean size of the physical clusters becomes comparable to the number of particles contained in the fluid system. The percolation of physical clusters can be estimated using the pair connectedness. A Yukawa fluid is a fluid system used to analytically estimate the percolation of physical clusters.

An alternative definition concerning a bond formed between two particles is given as Hill's idea[2], and the formation of a bond depends on distance r between a particle and another particle. According to the idea, a bond is formed between the two particles if r satisfies $r \leq r_s$, for r_s having a special value. A situation where $\mathcal{E}(p) > -\beta u(r)$ is satisfied for $r \leq r_s$ should be distinguished from another situation where $\mathcal{E}(p) \leq -\beta u(r)$ is satisfied for $r \leq r_s$. However, the definition, depending on distance r does not allow us to distinguish between the two situations. If this difficulty is avoided using a definition subjected to the relation $\mathcal{E}(p) + \beta u(r) \leq 0$ for a fluid consisting of atoms or molecules, then the temperature dependence of percolation can be satisfactory.

A Yukawa fluid system can allow particular attention to be paid to the dependence of the liquid-phase stability on the effective range of the attractive force, which occurs for a Yukawa potential working as a pair potential between two particles forming each pair.[38] Such a Yukawa fluid system also should allow us to obtain the dependence of the generation of the percolation state on the effective range of the attractive force. In fact, the dependence of the generation of the percolation state on the effective range can be dertermined for Yukawa fluid systems with an adjustable parameter.[27] The dependence can also be determined for other

fluid systems composed of core-soft-shell spheres with an attractive square-well potential.[39]

Structures of physical clusters are influenced depending on whether dominant one is the particle-cluster aggregation or the cluster–cluster aggregation as the formation process of physical clusters. A specific fractal structure of physical clusters is obtained from a formation process in which the cluster–cluster aggregation is dominant.[40] The fractal dimension that specifies the structure can depend on the formation process of the physical clusters. Examining the pair connectedness should yield the fractal dimension that can characterize the physical clusters formed in a fluid system.

The use of the pair connectedness is meaningful for analyzing phenomena that involve the physical cluster formation. Many phenomena can be found as those depending on the sizes of physical clusters. The electrical conductivity of liquid mercury maintained at a low density at a temperature near the critical point T_c decreases at a rather steep gradient as the density of mercury, ρ_{H_g}, decreases.[19] The difference between the absorption of infrared at a particular density ρ'_{H_g} and that at a density below ρ'_{H_g} increases as the temperature decreases. This difference at temperatures lower than T_c is much larger than that near T_c.[21] For a H_g fluid near T_c, the real part of the dielectric constant determined using optical reflectivity and absorption measurements increases sharply at a particular density as ρ_{H_g} increases.[20] To induce these phenomena, the formation of physical clusters of H_g-atoms in each H_g-fluid can play a role. The lowest energy required for exciting an electron of each metallic atom constituting a physical cluster decreases toward zero as the number of metallic atoms forming the physical cluster increases. The distribution of physical cluster sizes in a fluid consisting of metallic atoms is a factor that determines the dependence of optical absorption on the frequency of light.[24]

Near liquid-vapor critical points, the viscosities of fluids exhibit an asymptotic divergence. Berg and Moldover[22] determined the critical exponent that can characterize the asymptotic divergence by measuring the viscosities of carbon dioxide and xenon near their critical points. In these fluids, the distribution of particles can never be uniform owing to the large density fluctuations caused by the formation of physical clusters. Such fluctuations can result in a characteristic increase in the viscosities of fluids near the critical points.[41]

An mutually attractive force between the particles for each particle pair can drive the phase separation, and it is assisted by the physical cluster formation. The mean size of the physical clusters can be affected by the effective range of the attractive force. Therefore,

the dependence of the liquid phase stability on the effective range of the attractive force[38] should be related to the sizes of physical clusters.

(b) *Practical closure scheme for Yukawa fluid*

In a Yukawa fluid, motion of each particle is subject to a Yukawa potential being a pair potential that contribute to the mutually attractive force between two particles consisting of each pair. Moreover, each particle carries the hard core of diameter σ. The Yukawa potential can, then, be described by

$$\beta u_{\rm Y}(r) = -k_0 dd \frac{e^{-\kappa r}}{r}, \tag{77}$$

where $k_0 dd$ is defined by

$$k_0 dd \equiv \beta K e^{\kappa\sigma}, \tag{78}$$

In Eq. (78), a parameter K corresponds to the maximum depth of the Yukawa potential. In Eq. (77), the magnitude of κ^{-1} denotes the effective range in which the pair potential can effectively contribute to the interaction between two particles.

Then, the long-range contribution to $C^+(r)$ is caused by the Yukawa potential. This allows Eq. (69) to yield a closure scheme corresponding to the MSA. With accompanying Eq. (70), this closure scheme is expressed as follows:

$$\begin{cases} C^+(r) = C^{0+}(r) + \frac{4}{3\sqrt{\pi}}\Big(-\beta u_{\rm Y}(r)\Big)^{3/2} \\ C^{0+}(r) = 0 \quad (1 < r/\sigma). \end{cases} \tag{79}$$

Here, mathematical procedures for analytically solving the integral equation given by Eq. (49) require the long-range contribution to $C^+(r)$ in Eq. (79) to be modified. The modification allows a practical closure scheme to be given as

$$\begin{cases} C^+(r) = C^{0+}(r) + \breve{k}\breve{d}\breve{d}e^{-\breve{z}r}/r \\ C^{0+}(r) = 0 \quad (1 < r/\sigma), \end{cases} \tag{80}$$

where

$$\begin{cases} \breve{k}/\sigma \equiv [4/(3\sqrt{\pi})](k_0/\sigma)^{3/2}\exp[f_\nu] \\ \breve{d} \equiv d^{3/2} \\ \breve{z}\sigma \equiv (3/2)\kappa\sigma + f_\nu. \end{cases} \tag{81}$$

In Eq. (81), a coefficient f_ν is defined by

$$f_\nu \equiv \Big(\frac{\hat{n}}{2}-1\Big)\frac{\ln\nu}{\nu-1} \quad (1 \le \nu < \infty;\ \ \hat{n}=3). \tag{82}$$

Hence, the use of the practical closure scheme given by Eq. (80) allows physical quantities obtained from a solution of Eq. (49) to depend on a parameter ν.

The practical closure scheme given by Eq. (80) means that $1/r^{\hat{n}/2}$ ($\hat{n} = 3, 5, \cdots$) is approximately expressed as

$$\begin{cases} \frac{1}{r^{\hat{n}/2}} \approx (\sigma^{-\hat{n}/2+1})\exp[\hat{n}/2-1]\exp[-(\hat{n}/2-1)r/\sigma]/r, & (\nu=1,\ \ \hat{n}=3,5,\cdots), \\ \frac{1}{r^{\hat{n}/2}} \approx (\sigma^{-\hat{n}/2+1})\exp[f_\nu]\exp[-f_\nu r/\sigma]/r, & (1 \le \nu < \infty,\ \ \hat{n}=3,5,\cdots), \\ \frac{1}{r^{\hat{n}/2}} \approx \frac{\sigma^{-\hat{n}/2+1}}{r}, & (\nu=\infty,\ \ \hat{n}=3,5,\cdots), \end{cases} \tag{83}$$

where f_ν is defined by Eq. (82). In the case of $\nu = 1$ and $\hat{n} = 3$, the approximation given by Eq. (83) somewhat underestimates the long-ranged contribution of $C^+(r)$. In the case of $\nu = \infty$ and $\hat{n} = 3$, the approximation given by Eq. (83) somewhat overestimates the long-ranged contribution of $C^+(r)$. On applying the Yukawa potential to Eq. (79), the contribution of the factor $(e^{-\kappa r})^{3/2}$ to the decay of $C^+(r)$ can be much more dominant than the contribution of the factor $(1/r)^{3/2}$ as r increases. Considering this, the contribution of the factor $(1/r)^{3/2}$ can be approximated by the contribution of $1/r$ in Eq. (79). This corresponds to the case of $\nu = \infty$, which can become a reasonable approximation for a large κ. For an extremely small κ, the decay of $C^+(r)$ cannot strongly depend on the factor $(e^{-\kappa r})^{3/2}$. Then, the decay of $C^+(r)$ deviates from the decay given for $\nu = \infty$ by Eq. (80). However, the decay of $C^+(r)$ is located between the decay given for $\nu = \infty$ by Eq. (80) and that given for $\nu = 1$ by Eq. (80).

If Eq. (49) can be exactly solved with the closure scheme given by Eq. (79), then it is expected that the value of $\mathcal{P}(r)$ that is assessed from a solution obtained in a specific condition can be found between two values. In this condition, one of the two values is assessed from a solution of the integral equation system formed by Eqs. (49) and (80) when specified by $\nu = \infty$. Under the same condition, the other is assessed from the solution when specified by $\nu = 1$. The expectation mentioned here is caused by the practical closure given by Eq. (80). If the value of ν satisfies $1 < \nu < \infty$, then the approximation given by Eq. (83) can allow the value of $\mathcal{P}(r)$ estimated with the use of Eq. (80) to fall between the value of $\mathcal{P}(r)$ given in the case of $\nu = 1$ and the different value of $\mathcal{P}(r)$ given in the case of $\nu = \infty$.

All physical quantities that are estimated from a solution $\mathcal{P}(r)$ obtained from Eqs. (49) and (80) depend on the value of ν, as demonstrated by the phase diagrams given in Fig. 35. Therefore, the coefficients $\widehat{C}^{+(0)}$ and $\widehat{C}^{+(2)}$, which are defined by the integration being given by Eq. (116), depend on the value of ν when the practical closure given by Eq. (80) is used. Indeed, the internal energy and the pressure that are estimated from the use of the solution $\mathcal{P}$ obtained from Eqs. (49) and (80) depend on the value of ν.[42]

(c) *Determining reasonable value of* f_ν

It is necessary to determine a reasonable value of f_ν, which makes Eq. (80) become a suitable approximation of Eq. (79). Equation (80) requires that $\pi(r)$ defined as

$$\pi(\hat{n}/2; r) \equiv 1/r^{\hat{n}/2}, \quad (\hat{n} = 3, 5, \cdots)$$

be approximated by $\pi_{\rm a}(\hat{n}/2; r)$ defined as

$$\pi_{\rm a}(\hat{n}/2; r, f_\nu) \equiv \sigma^{-\hat{n}/2+1} e^{f_\nu} \exp[-(f_\nu/\sigma)r]/r.$$

For arbitrary f_ν that is not restricted by Eq. (82), the functions π and $\pi_{\rm a}$ satisfies at $r = \sigma$

$$\pi(\hat{n}/2; \sigma) = \pi_{\rm a}(\hat{n}/2; \sigma, f_\nu).$$

Despite this, the decay of $\pi_{\rm a}(\hat{n}/2; r, f_\nu)$ toward zero is faster than that of $\pi(\hat{n}/2; r)$ toward zero for a large r. Then, a way to reasonably determine the value of f_ν is necessary.

There is a particular value of f_ν for which the integral of $\pi_{\rm a}(\hat{n}/2; r, f_\nu)$ for the interval $\sigma \le r < \infty$ is equated with the integral of $\pi(\hat{n}/2; r)$ for the interval $\sigma \le r < \infty$. At the value of f_ν, the following relation is satisfied:

$$\int_\sigma^\infty \pi(\hat{n}/2; r) {\rm d}r = \int_\sigma^\infty \pi_{\rm a}(\hat{n}/2; r, f_\nu) {\rm d}r. \tag{84}$$

Equation (84) results in

$$(\hat{n}/2 - 1)^{-1} = -e^{f_\nu} {\rm Ei}(-f_\nu), \quad (\hat{n} = 3, 5, \cdots), \tag{85}$$

where the exponential integral ${\rm Ei}(x)$ is defined as ${\rm Ei}(-x) \equiv -\int_x^\infty e^{-t} t^{-1} {\rm d}t$ $(x > 0)$. In Eq. (85), Ei is estimated as

$${\rm Ei}(-f_\nu) = \ln f_\nu + \gamma + \sum_{m=1}^{\infty} (-1)^m \frac{(f_\nu)^m}{m m!}.$$

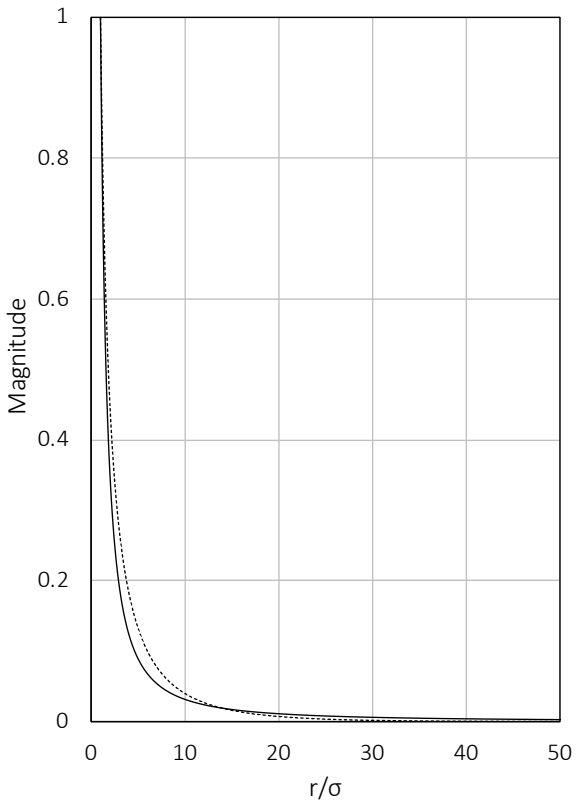

FIG. 1. Comparison between $\tau\pi_{\rm a}(\hat{n}/2; r, f_\nu)$ and $\tau\pi(\hat{n}/2; r)$; $(\tau \equiv \sigma^{\hat{n}/2})$ for $\hat{n} = 3$. Dashed curve corresponds to $\tau\pi_{\rm a}(\hat{n}/2; r, f_\nu)$. Thick curve corresponds to $\tau\pi(\hat{n}/2; r)$.

In the above, γ is Euler's constant given as

$$\gamma = \lim_{m\to\infty}\left[\sum_{k=1}^{m} - \ln m\right] = 0.5772156649\cdots .$$

Equation (85) specified for $\hat{n} = 3$ is satisfied for $f_\nu = 0.1018532115\cdots$ (corresponding to $\nu = 13.93091523\cdots$).

In Fig. 1, a comparison between the decay of $\tau\pi(\hat{n}/2; r)$ and the decay of $\tau\pi_{\rm a}(\hat{n}/2; r, f_\nu)$ can be confirmed for $f_\nu = f_{\nu_{\hat{n}/2}}$ specified by $\hat{n} = 3$. Then, τ is defined as $\tau \equiv \sigma^{\hat{n}/2}$, and $f_{\nu_{\hat{n}/2}}$

is given for $\hat{n} = 3$ as

$$f_{\nu_{3/2}} = 0.1018532115. \tag{86}$$

(d) *Solution of integral equation*

The use of Baxter's Q function[43] has allowed several analytical calculations for the Ornstein–Zernike equation.[43,83] The use of Baxter's Q function enables Eq. (49) also to be solved analytically.[27] Then, it is useful to consider the closure scheme given by Eq. (80). The Fourier transform of the integral equation given by Eq. (49) is a useful and mathematical treatment.

A Fourier transform of a correlation function symbolized by $F(r)$ is expressed as $\widetilde{F}(k)$. Then, $\widetilde{F}(k)$ is defined by

$$\begin{cases} \widetilde{F}(k) \equiv \lim_{V\to\infty} \rho \int_V F(r) \exp[i\mathbf{k}\cdot\mathbf{r}]\mathrm{d}\mathbf{r}, \quad (r \equiv |\mathbf{r}|, \quad k \equiv |\mathbf{k}|), \\ \widetilde{F}(0) = \lim_{V\to\infty} \rho \int_V F(r)\mathrm{d}\mathbf{r}. \end{cases} \tag{87}$$

For use of the above notation, the Fourier transform allows Eq. (49) to be expressed as

$$\left[1 + \widetilde{\mathcal{P}}(k)\right]\left[1 - \widetilde{C}^{+}(k)\right] = 1. \tag{88}$$

The use of Baxter's Q function[43] enables Eq. (88) to be divided into two equations as follows:

$$\begin{cases} 1 - \widetilde{C}^{+}(k) = \widetilde{Q}^{+}(k)\widetilde{Q}^{+}(-k), \\ \left[1 + \widetilde{\mathcal{P}}(k)\right]\widetilde{Q}^{+}(k) = \left[\widetilde{Q}^{+}(-k)\right]^{-1}, \end{cases} \tag{89}$$

where $\widetilde{Q}^{+}(k)$ corresponds to Baxter's Q function,[43] which is defined by

$$\begin{cases} \widetilde{Q}^{+}(k) \equiv 1 - \rho\widehat{Q}^{+}(-ik) \\ \widehat{Q}^{+}(s) \equiv \int_0^\infty Q^{+}(t)e^{-st}\mathrm{d}t \\ \int_{-\infty}^{\infty}\left[\widetilde{Q}^{+}(-k)\right]^{-1} e^{-ikr}\mathrm{d}k = 0. \end{cases} \tag{90}$$

For $k = 0$, Eq. (89) allows an important relation for estimation of percolation of physical clusters to be obtained because of Eq. (90) as follows:

$$\left[1 - \rho\widehat{Q}^{+}(0)\right]^{-2} = 1 + \rho\int_V \mathcal{P}(r)\mathrm{d}\mathbf{r}, \tag{91}$$

where

$$\lim_{k\to 0}\widetilde{\mathcal{P}}(k)=\rho\int_V \mathcal{P}(r)\mathrm{d}\mathbf{r}. \tag{92}$$

Thus, the substitution of Eq. (91) into Eq. (44) allows the mean physical cluster size to be estimated as

$$\mathcal{S}=\left[1-\rho\widehat{Q}^{+}(0)\right]^{-2}. \tag{93}$$

Then, the percolation threshold of physical clusters corresponds to the condition specified by $1-\rho\widehat{Q}^{+}(0)=0$. If $Q^{+}(r)$ is determined, then the percolation threshold is estimated from relation $1-\rho\widehat{Q}^{+}(0)=0$.

Baxter's Q function allows an equation concerning $\mathcal{P}(r)$ and the other equation concerning $C^{+}(r)$ to be separated from the integral equation formed by Eq. (49) as seen in Eq. (89). Moreover, two equations are obtained from the substitution of Eq. (90) into Eq. (89). If the integration of the product of each of the two equations and e^{-ikr} is performed with respect to k in the range $-\infty<k<\infty$, then two inverse transforms are obtained from Eq. (89).[43] One of the two inverse transforms expresses a formula concerning $\mathcal{P}(r)$, which satisfies Eq. (49). The other expresses a formula concerning $C^{+}(r)$, which satisfies Eq. (49). Thus, the two formulae are given as follows:

$$2\pi r\mathcal{P}(r)=-\frac{d}{dr}Q^{+}(r)+2\pi\rho\int_0^{\infty}Q^{+}(t)(r-t)\mathcal{P}(|r-t|)\mathrm{d}t,\quad(0<r<\infty), \tag{94}$$

and

$$2\pi rC^{+}(r)=-\frac{d}{dr}Q^{+}(r)+\rho\int_0^{\infty}Q^{+}(t)\frac{d}{dr}Q^{+}(r+t)\mathrm{d}t,\quad(0<r<\infty). \tag{95}$$

The use of these two equations allows $Q(r)$ to be determined.

A relation $\mathcal{P}(r)=0$ given by Eq. (39) for $r<\sigma$ and the requirements of $C^{+}(r)$ given by Eq. (80) require the function $Q^{+}(r)$ in Eqs. (94) and (95) to be of limited forms. The limited form should be given as

$$Q^{+}(r)=Q_0^{+}(r)+\breve{D}e^{-\breve{z}r}, \tag{96}$$

where

$$\begin{cases} Q_0^{+}(r)=(r-\sigma)\acute{q}+\breve{C}(e^{-\breve{z}r}-e^{-\breve{z}\sigma}) & (r<\sigma)\\ Q_0^{+}(r)=0 & (\sigma\le r). \end{cases} \tag{97}$$

In Eqs. (96) and (97), the unknown coefficients $\breve{C}$, $\breve{D}$, and $\acute{q}$ can be determined via the use of Eqs. (94) and (95). As a result, the function $Q^{+}(r)$ is determined. Therefore, the pair connectedness $\mathcal{P}(r)$ is determined via Eq. (94).

If $\lim_{u(r)\to\infty}\mathcal{P}(r)=0$ owing to the hard-core potential contributing for $r<\sigma$ is considered according to Eq. (39), then the substitution of Eq. (96) into Eq. (94) allows a relation for $r<\sigma$ to be obtained as

$$-\acute{q}+\breve{z}\breve{C}e^{-\breve{z}r}+\breve{z}\breve{D}e^{-\breve{z}r}-2\pi\rho\breve{D}e^{-\breve{z}r}\int_{0}^{\infty}\mathcal{P}(t)e^{-\breve{z}t}t\mathrm{d}t=0,\quad(r<\sigma). \tag{98}$$

If the left-hand sides in Eq. (98) is compared with the right-hand sides, then the restrictions for the coefficients are yielded as follows:

$$\acute{q}=0, \tag{99}$$

and

$$\breve{C}=-(1-\widehat{\mathcal{P}}(\breve{z}))\breve{D}, \tag{100}$$

where

$$\widehat{\mathcal{P}}(\breve{z})\equiv 2\pi\frac{\rho}{\breve{z}}\int_{0}^{\infty}\mathcal{P}(t)e^{-\breve{z}t}t\mathrm{d}t=2\pi\frac{\rho}{\breve{z}}\int_{\sigma}^{\infty}\mathcal{P}(t)e^{-\breve{z}t}t\mathrm{d}t. \tag{101}$$

Under the condition that $\sigma\le r$ is satisfied, the substitution of Eqs. (97) and (80) into Eq. (95) allows the following relation to be obtained:

$$2\pi\breve{k}\breve{d}\breve{d}=\breve{z}\breve{D}-\breve{z}\rho\breve{D}\widehat{Q}^{+}(\breve{z}), \tag{102}$$

where

$$\begin{aligned}\widehat{Q}^{+}(s)\equiv&\int_{0}^{\infty}Q^{+}(t)e^{-st}\mathrm{d}t\\&=\breve{C}e^{-\breve{z}\sigma}\Big(\frac{e^{\breve{z}\sigma}-e^{-s\sigma}}{s+\breve{z}}-\frac{1-e^{-s\sigma}}{s}\Big)+\breve{D}\frac{1}{s+\breve{z}}.\end{aligned} \tag{103}$$

The expression given by Eq. (103) can be obtained by substituting Eq. (96) into the integral for defining $\widehat{Q}^{+}(s)$ in Eq. (90).

For $r<\sigma$, Eqs. (96) and (97) allow Eq. (94) to be modified as

$$0=\breve{z}\breve{C}e^{-\breve{z}r}+\breve{z}\breve{D}e^{-\breve{z}r}+2\pi\rho\int_{r}^{\infty}Q^{+}(t)(r-t)\mathcal{P}(|r-t|)\mathrm{d}t. \tag{104}$$

Equation (104) is equivalent to Eq. (98) which has no singularity for $0 < r < \infty$; hence, Eq. (104) is satisfied for $0 < r < \infty$. If each factor given by Eq. (104) is subtracted from each factor given by Eq. (94), then a formula for $\sigma \le r$ can be obtained as

$$2\pi r\mathcal{P}(r) = -\breve{z}\breve{C}e^{-\breve{z}r} + 2\pi\rho\int_0^r Q^+(t)(r-t)\mathcal{P}(r-t)\mathrm{d}t. \tag{105}$$

A relation between $\widehat{\mathcal{P}}(\breve{z})$ and $\widehat{Q}^+(\breve{z})$ is estimated from the Laplace transformation corresponding to performing the integration of the product of $\exp(-\breve{z}r)$ and Eq. (105) with respect to r within the range $\sigma \le r < \infty$. This is given as

$$\frac{\breve{z}}{\rho}\widehat{\mathcal{P}}(\breve{z})[1-\rho\widehat{Q}^+(\breve{z})] = -\frac{1}{2}\breve{C}e^{-2\breve{z}\sigma}. \tag{106}$$

A relation between $\widehat{\mathcal{P}}(\breve{z})$ and $\breve{D}$ is obtained if $\widehat{Q}^+(\breve{z})$ obtained from the substitution of Eq. (100) into Eq. (103) is substituted into Eq. (102). This is given as

$$\frac{\breve{D}}{\sigma^2} = \frac{\pi\breve{z}\sigma}{6\phi}\frac{1-\left[1-\frac{24\phi}{(\breve{z}\sigma)^2}\frac{\breve{k}\breve{d}\breve{d}}{\sigma}\Big(1-(1-e^{-\breve{z}\sigma})^2(1-\widehat{\mathcal{P}}(\breve{z}))\Big)\right]^{1/2}}{1-(1-e^{-\breve{z}\sigma})^2(1-\widehat{\mathcal{P}}(\breve{z}))}, \tag{107}$$

where ϕ is the volume fraction defined as

$$\phi \equiv \frac{\pi}{6}\rho\sigma^3. \tag{108}$$

Another relation between $\widehat{\mathcal{P}}(\breve{z})$ and $\breve{D}$ is obtained if Eq. (100) is substituted into the formula obtained from the substitution of Eq. (103) into Eq. (106). This is given as

$$\widehat{\mathcal{P}}(\breve{z}) = \frac{3\phi}{\pi\breve{z}\sigma}\Big[e^{-\breve{z}\sigma} + \widehat{\mathcal{P}}(\breve{z})(1-e^{-\breve{z}\sigma})\Big]^2\frac{\breve{D}}{\sigma^2}. \tag{109}$$

Using Eqs. (107) and (109), the unknown coefficients $\breve{D}$ and $\widehat{\mathcal{P}}(\breve{z})$ can then be determined. The coefficients $\breve{D}$ and $\widehat{\mathcal{P}}(\breve{z})$ must depend on the value of ν ($1 \le \nu < \infty$) according to Eq. (81).

(e) *Estimation of percolation threshold for single-component Yukawa fluid*

The mean cluster size $\mathcal{S}$ given by Eq. (93) can be estimated via the use of $\widehat{Q}^+(0)$. $\widehat{Q}^+(0)$ is determined from the use of Eqs. (100) and (103) as

$$z\widehat{Q}^+(0) = -e^{-\breve{z}\sigma}(e^{\breve{z}\sigma} - 1 - \breve{z}\sigma)(1-\widehat{\mathcal{P}}(\breve{z}))\breve{D} + \breve{D}. \tag{110}$$

The substitution of Eq. (110) into Eq. (93) allows the mean cluster size $\mathcal{S}$ to be given as

$$\mathcal{S} = \left\{1 - \frac{6\phi}{\pi\breve{z}\sigma}\frac{\breve{D}}{\sigma^2}\Big[(1+\breve{z}\sigma)e^{-\breve{z}\sigma} + [1-(1+\breve{z}\sigma)e^{-\breve{z}\sigma}]\widehat{\mathcal{P}}(\breve{z})\Big]\right\}^{-2}. \tag{111}$$

According to Eq. (111), the percolation threshold at which $1-\rho\widehat{Q}^{+}(0)=0$ should hold can be estimated using the following equation:

$$\Big[\frac{6\phi}{\pi\check{z}\sigma}\frac{\check{D}}{\sigma^2}\Big]^{-1}-(1+\check{z}\sigma)e^{-\check{z}\sigma}-[1-(1+\check{z}\sigma)e^{-\check{z}\sigma}]\widehat{\mathcal{P}}(\check{z})=0. \tag{112}$$

The value of $\widehat{\mathcal{P}}(\check{z})$ at the percolation threshold is obtained by substituting Eq. (109) into Eq. (112) as

$$\widehat{\mathcal{P}}^{\rm P}=e^{-\check{z}\sigma}\Big\{\check{z}\sigma+e^{-\check{z}\sigma}-\Big[(\check{z}\sigma)^2+1\Big]^{1/2}\Big\}\Big[e^{-2\check{z}\sigma}-1+2\check{z}\sigma e^{-\check{z}\sigma}\Big]^{-1}, \tag{113}$$

where $\widehat{\mathcal{P}}^{\rm P}$ is the value of $\widehat{\mathcal{P}}(\check{z})$ at the percolation threshold. If the value of $\check{k}\check{d}\check{d}$ at the percolation threshold is expressed as $(\check{k}\check{d}\check{d})^{\rm P}$, then the value of $(\check{k}\check{d}\check{d})^{\rm P}$ can be obtained by modifying Eq. (107) as

$$\frac{(\check{k}\check{d}\check{d})^{\rm P}}{\sigma}=\frac{\check{z}\sigma}{2\pi}\cdot\frac{\check{D}^{\rm P}}{\sigma^2}-\frac{3\phi}{2\pi^2}\Big[1-(1-e^{-\check{z}\sigma})^2(1-\widehat{\mathcal{P}}^{\rm P})\Big]\Big(\frac{\check{D}^{\rm P}}{\sigma^2}\Big)^2, \tag{114}$$

where $\check{D}^{\rm P}$ is the value of $\check{D}$ evaluated from Eq. (109) for $\widehat{\mathcal{P}}(\check{z})=\widehat{\mathcal{P}}^{\rm P}$. The value of $K^{\rm P}/\sigma$ being the value of K/σ at the percolation threshold can be estimated through relation $(\check{k}\check{d}\check{d})^{\rm P}/\sigma=[4/(3\sqrt{\pi})](\beta K^{\rm P}/\sigma)^{3/2}\exp[f_\nu]\exp[(3/2)\kappa\sigma]$ obtained from Eqs. (78) and (81). The substitution of Eq. (109) into Eq. (114) results in a relation expressed as $1/K^{\rm P}\propto\phi^\alpha$ with $\alpha=2/3$. Relation $1/K^{\rm P}\propto\phi^\alpha$ with $\alpha=1$ corresponds to that given by Xu and Stell.[27]

(f) *Solution for Ornstein–Zernike equation for single-component Yukawa fluid*

To analyze the behavior of a single-component fluid, coefficients $\widehat{C}^{+(0)}$, $\widehat{C}^{+(2)}$, $\widehat{C}^{*(0)}$, $\widehat{C}^{*(2)}$, $\widehat{c}^{(0)}$, and $\widehat{c}^{(2)}$ must be derived from correlation functions $\widehat{C}^{+}(r)$, $\widehat{C}^{*}(r)$, and $\widehat{c}(r)$. Then, a way to differentiate a Fourier transform $\widetilde{F}(k)$ of a correlation function $F(r)$ is useful for estimating coefficients $\widehat{C}^{+(2)}$, $\widehat{C}^{*(2)}$, and $\widehat{c}^{(2)}$. If a differential operator with respect to $\mathbf{k}$ is defined as $\nabla_k\equiv(\partial/\partial k_x,\partial/\partial k_y,\partial/\partial k_z)$ owing to the use of the three-dimensional elements of $\mathbf{k}$ denoted by (k_x,k_y,k_z), then the use of this operator allows derivatives of $\widetilde{F}(k)$ to satisfy

$$\lim_{k\to0}\lim_{V\to\infty}\rho(\mathrm{d}^2/\mathrm{d}k^2)\int_V F(r)\exp[i\mathbf{k}\cdot\mathbf{r}]\mathrm{d}\mathbf{r}=(11/6)\lim_{k\to0}\nabla_k\cdot\nabla_k\widetilde{F}(k),$$

where $\nabla_k\cdot\nabla_k\widetilde{F}(k)=-\lim_{V\to\infty}\rho\int_V F(r)r^2\exp[i\mathbf{k}\cdot\mathbf{r}]\mathrm{d}\mathbf{r}$. Therefore, the following relation is found for macroscopic V:

$$\rho\int_V F(r)r^2\mathrm{d}\mathbf{r}=-(6/11)\lim_{k\to0}(\mathrm{d}^2/\mathrm{d}k^2)\widetilde{F}(k). \tag{115}$$

If $\widehat{F}^{(\alpha)}$ is defined as

$$\widehat{F}^{(\alpha)} \equiv \left(\frac{1}{6}\right)^{\alpha/2} \int_V F(r) r^\alpha \mathrm{d}\mathbf{r} \quad (\alpha = 0, 2, 4), \tag{116}$$

then, $\widehat{F}^{(0)}$ satisfies the following relation:

$$\rho \widehat{F}^{(0)} = \lim_{k \to 0} \widetilde{F}(k). \tag{117}$$

Moreover, Eq. (115) is expressed as

$$\rho \widehat{F}^{(2)} = -(1/11) \lim_{k \to 0} (\mathrm{d}^2/\mathrm{d}k^2) \widetilde{F}(k). \tag{118}$$

i) *Estimate of coefficients* $\widehat{C}^{+(0)}$ *and* $\widehat{C}^{+(2)}$

Based on Eq. (117), a coefficient $\widehat{C}^{+(0)}$ is given by the following relation:

$$\rho \widehat{C}^{+(0)} = \lim_{k \to 0} \widetilde{C}^{+}(k). \tag{119}$$

Eqs. (89) and (90) require $\widehat{C}^{+(0)}$ to satisfy

$$\rho \widehat{C}^{+(0)} = 1 - \lim_{k \to 0} \Big[1 - \rho \widehat{Q}^{+}(-ik)\Big] \Big[1 - \rho \widehat{Q}^{+}(ik)\Big]. \tag{120}$$

Moreover, if Eqs. (115) is used with Eqs. (89) and (90), $\widehat{C}^{+(2)}$ can be estimated as

$$\rho \widehat{C}^{+(2)} = -\frac{2}{11} \lim_{s \to 0} \left[\Big(-1 + \rho \widetilde{Q}^{+}(s)\Big) \rho \frac{\mathrm{d}^2}{\mathrm{d}s^2} \widehat{Q}^{+}(s) - \left(\rho \frac{\mathrm{d}}{\mathrm{d}s} \widetilde{Q}^{+}(s) \right)^2 \right]. \tag{121}$$

Therefore, Eqs. (120) and (121) allow $\widehat{C}^{+(0)}$ and $\widehat{C}^{+(2)}$ to be assessed with the use of Eqs. (90) and (103). Then, the use of Eq. (80) makes the value of $\widehat{C}^{+(0)}$ for $f_\nu = 0$ ($\nu = \infty$) differ from that for $f_\nu = 1/2$ ($\nu = 1$) and makes the value of $\widehat{C}^{+(2)}$ for $f_\infty = 0$ differ from that for $f_1 = 1/2$. This is exemplified by Figs. 2 and 3. In these figures, $\rho C \dagger 0$ and $\rho C \dagger 2/\sigma\sigma$ correspond to $\rho \widehat{C}^{+(0)}$ and $\rho \widehat{C}^{+(2)}$, respectively.

ii) *Estimate of* $\widehat{C}^{*(0)}$ *and* $\widehat{C}^{*(2)}$ *based on solution of Ornstein–Zernike equation*

Coefficients $\widehat{C}^{*(0)}$ and $\widehat{C}^{*(2)}$ can be estimated as $\widehat{C}^{*(0)} = \widehat{c}^{(0)} - \widehat{C}^{+(0)}$, and $\widehat{C}^{*(2)} = \widehat{c}^{(2)} - \widehat{C}^{+(2)}$ based on Eq. (51). Coefficients $\widehat{C}^{+(0)}$ and $\widehat{C}^{+(2)}$ are estimated by Eqs. (120) and (121). If the pair potential $u(r)$ contributing to the mutually attractive force between pair particles is independent of the momenta of the particles, then the pair potential used when solving the

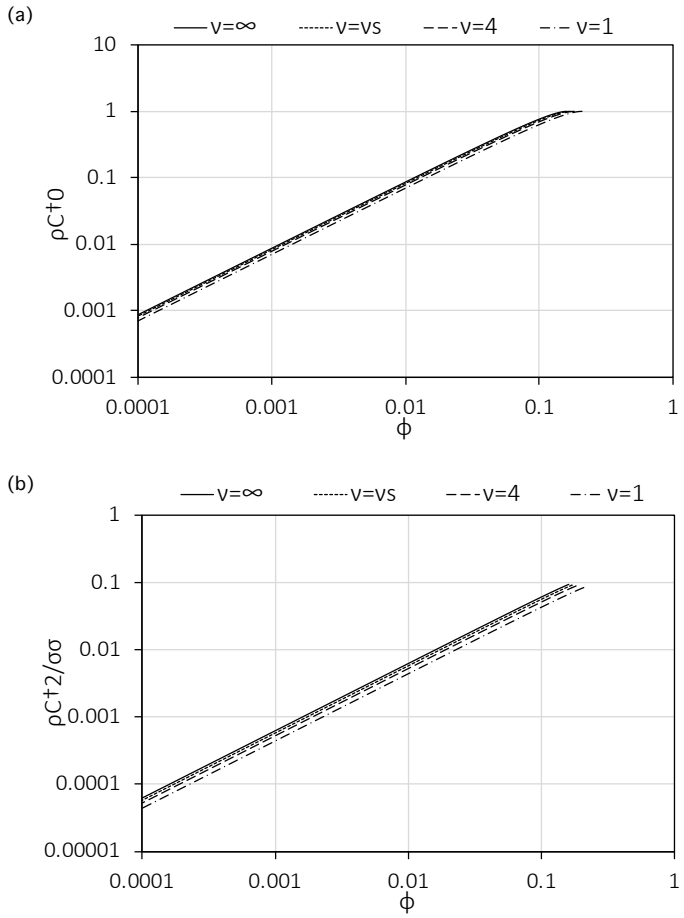

FIG. 2. Dependence of $\rho\widehat{C}^{+(0)}$ on ϕ and dependence of $\rho\widehat{C}^{+(2)}/\sigma^2$ on ϕ at $\kappa\sigma = 1.8$ and $\sigma/\beta K = 1.0315$ (corresponding to temperature near the critical point). ν_s is given as $\nu_s = 13.9309$, and $\nu = \nu_s$ is a relation for which Eq. (85) obtained from Eq.(84) is approximately satisfied. $\rho C \dagger 0$ and $\rho C \dagger 2/\sigma\sigma$ correspond to $\rho\widehat{C}^{+(0)}$ and $\rho\widehat{C}^{+(2)}/\sigma^2$, respectively.

integral equation given by Eq. (49) is not distinguished from that being used when solving the integral equation given by Eq. (52). Then, the pair potential used to solve the integral equation given by Eq. (49) can be used for solving the Ornstein–Zernike equation. From a solution of the Ornstein–Zernike equation, coefficients $\widehat{c}^{(0)}$ and $\widehat{c}^{(2)}$ can be estimated. Thus, coefficients $\widehat{C}^{*(0)}$ and $\widehat{C}^{*(2)}$ can be estimated without solving the integral equation given by

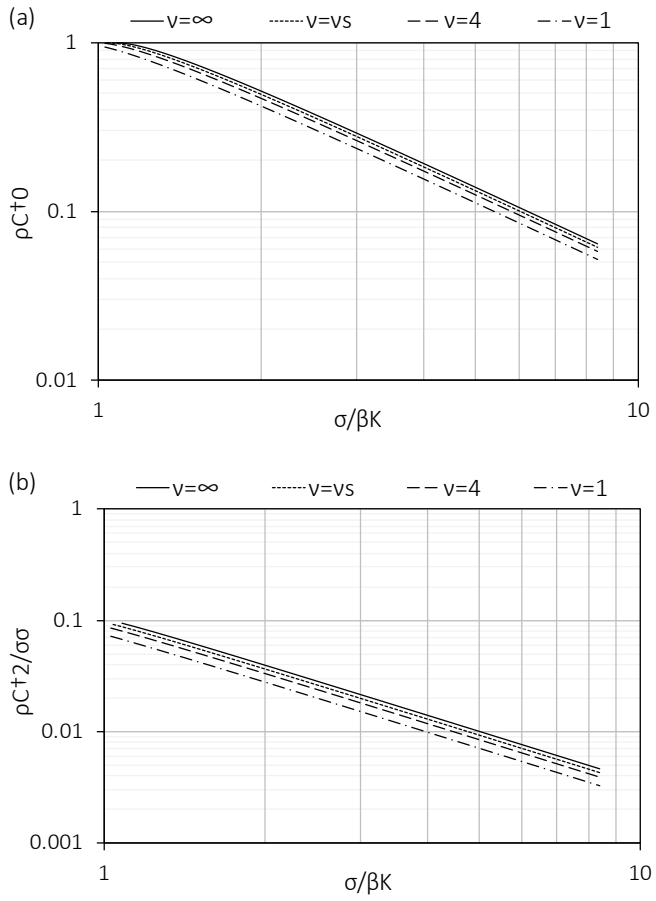

FIG. 3. Dependence of $\rho\widehat{C}^{+(0)}$ on $\sigma/\beta K$ (corresponding to reduced temperature) and dependence of $\rho\widehat{C}^{+(2)}/\sigma^2$ on $\sigma/\beta K$ at $\kappa\sigma = 1.8$ and $\phi = 0.172$ (corresponding to density near the critical point). ν_s is given as $\nu_s = 13.9309$, and $\nu = \nu_s$ is a relation for which Eq. (85) obtained from Eq.(84) is approximately satisfied. $\rho C \dagger 0$ and $\rho C \dagger 2/\sigma\sigma$ correspond to $\rho\widehat{C}^{+(0)}$ and $\rho\widehat{C}^{+(2)}/\sigma^2$, respectively.

Eq. (52).

Eq. (15) with Eqs. (16) and (17) yields the Ornstein–Zernike equation. The use of Baxter's Q function[43] allows the Fourier transform of the Ornstein–Zernike equation to be expressed

as

$$\begin{cases} [1+\widetilde{h}(k)]\widetilde{Q}(k) = \widetilde{Q}^{-1}(-k) \\ 1-\widetilde{c}(k) = \widetilde{Q}(k)\widetilde{Q}(-k), \end{cases} \tag{122}$$

where

$$\begin{cases} \widetilde{h}(k) \equiv \lim_{V\to\infty} \rho \int_V (g(r)-1)\exp[i\mathbf{k}\cdot\mathbf{r}]\mathrm{d}\mathbf{r} \\ \widetilde{Q}(k) \equiv 1-\rho\widehat{Q}(-ik) \\ \widehat{Q}(s) \equiv \int_0^\infty Q(t)e^{-st}\mathrm{d}t \\ Q(t) = Q^0(t) + dAe^{-\kappa t} \\ Q^0(t) = \frac{1}{2}q^{(2)}(t-\sigma)^2 + q^{(1)}(t-\sigma) + B(e^{-\kappa t} - e^{-\kappa\sigma}) \quad (0<t<\sigma) \\ Q^0(t) = 0 \quad (\sigma \le t) \\ B \equiv -dA\left[1 - \frac{12\phi}{\kappa\sigma}\frac{1}{\sigma^2}\int_0^\infty \tau g(\tau)e^{-\kappa\tau}\mathrm{d}\tau\right] \\ \int_{-\infty}^{\infty}\left[\widetilde{Q}(-k)\right]^{-1}e^{-ikr}\mathrm{d}k = 0. \end{cases} \tag{123}$$

In Eq. (123), A, $q^{(1)}$, and $q^{(2)}$ are unknown coefficients.

To solve the Ornstein–Zernike equation analytically, the closure scheme based on the MSA is given as

$$\begin{cases} c(r) = c^0(r) - \beta u(r) \\ c^0(r) = 0 \quad (r/\sigma > 1) \\ \beta u(r) = -k_0 dd e^{-\kappa r}/r. \end{cases} \tag{124}$$

Then, a solution for the Ornstein–Zernike equation is given according to a known procedure[46], and as a result, a coefficient $\widehat{Q}(s)$ can be given as

$$\begin{aligned} \widehat{Q}(s) =& \frac{1}{2}q^{(2)}\left[-\frac{2e^{-s\sigma}}{s^3} + \frac{1}{s}\left(\sigma^2 - \frac{2\sigma}{s} + \frac{2}{s^2}\right)\right] + q^{(1)}\left[-\frac{e^{-s\sigma}}{s^2} + \frac{1}{s}\left(-\sigma + \frac{1}{s}\right)\right] \\ & -dA[1-g^{(\kappa)}]e^{\kappa\sigma}\left[\frac{-e^{-s\sigma}+e^{\kappa\sigma}}{\kappa+s} + \frac{e^{-s\sigma}-1}{s}\right] + \frac{dA}{\kappa+s} \end{aligned} \tag{125}$$

where $q^{(1)}$ and $q^{(2)}$ are given as

$$\begin{aligned} \frac{q^{(1)}}{\sigma} =& 2\pi\frac{1+\phi/2}{(1-\phi)^2} + \frac{12\phi}{(\kappa\sigma)^2}\frac{1}{(1-\phi)^2}\left\{(1-g^{(\kappa)})e^{-\kappa\sigma}\left[(1+2\phi)\varphi_2(-\kappa)\right.\right. \\ & \left.\left. -\left(1+\frac{\phi}{2}\right)\kappa\sigma\varphi_1(-\kappa)\right] + 1 + 2\phi - \left(1+\frac{\phi}{2}\right)\kappa\sigma\right\}\frac{dA}{\sigma^2} \end{aligned} \tag{126}$$

and

$$q^{(2)} =2\pi\frac{1+2\phi}{(1-\phi)^2} - \frac{12\phi}{(\kappa\sigma)^2}\frac{1}{(1-\phi)^2}\Bigg\{(1-g^{(\kappa)})e^{-\kappa\sigma}\Bigg[(1+2\phi)\kappa\sigma\varphi_1(-\kappa) \\ -6\phi\varphi_2(-\kappa)\Bigg] + (1+2\phi)\kappa\sigma - 6\phi\Bigg\}\frac{dA}{\sigma^2} \tag{127}$$

with

$$\begin{cases}\varphi_1(\kappa) \equiv 1-\kappa\sigma-e^{-\kappa\sigma} \\ \varphi_2(\kappa) \equiv 1-\kappa+(\kappa\sigma)^2/2-e^{-\kappa\sigma}.\end{cases} \tag{128}$$

In Eq. (125), a coefficient $g^{(\kappa)}$ is defined as

$$g^{(\kappa)} \equiv 12\frac{\phi}{\kappa\sigma}\frac{1}{\sigma^2}\int_0^\infty tg(t)e^{-\kappa t}\mathrm{d}t. \tag{129}$$

Two unknown coefficients A and $g^{(\kappa)}$ found in Eqs. (125), (126), and (127) must be estimated from an equation system given as

$$g^{(\kappa)}[1-\rho\widehat{Q}(\kappa)] = \frac{6}{\pi}\frac{\phi}{(\kappa\sigma)^3}e^{-\kappa\sigma}\left(q^{(2)}+\kappa\sigma\frac{q^{(1)}}{\sigma}\right) + \frac{3}{\pi}\frac{\phi}{\kappa\sigma}e^{-2\kappa\sigma}\frac{dA}{\sigma^2}(1-g^{(\kappa)}) \tag{130}$$

$$2\pi\frac{k_0dd}{\sigma} = \frac{dA}{\sigma^2}\kappa\sigma\Bigg\{1-\frac{6\phi}{\pi}\Bigg[\frac{\varphi_2(\kappa)}{(\kappa\sigma)^3}q^{(2)}+\frac{\varphi_1(\kappa)}{(\kappa\sigma)^2}\frac{q^{(1)}}{\sigma} \\ -\varphi_3(\kappa)\frac{dA}{\sigma^2}(1-g^{(\kappa)}) + \frac{1}{2}\frac{1}{\kappa\sigma}\frac{dA}{\sigma^2}\Bigg]\Bigg\}, \tag{131}$$

where

$$\varphi_3(\kappa) \equiv e^{-\kappa\sigma}\left(\frac{e^{\kappa\sigma}-e^{-\kappa\sigma}}{2\kappa\sigma} - \frac{1-e^{-\kappa\sigma}}{\kappa\sigma}\right). \tag{132}$$

A factor $\rho\widehat{Q}(\kappa)$ in Eq. (130) can be given, according to Eq. (125), as follows:

$$\rho\widehat{Q}(\kappa) = \frac{6\phi}{\pi}\frac{\varphi_2(\kappa)}{(\kappa\sigma)^3}q^{(2)} + \frac{6\phi}{\pi}\frac{\varphi_1(\kappa)}{(\kappa\sigma)^2}\frac{q^{(1)}}{\sigma} - \frac{6\phi}{\pi}\varphi_3(\kappa)\frac{dA}{\kappa^2}\left(1-g^{(\kappa)}\right) + \frac{3\phi}{\pi}\frac{1}{\kappa\sigma}\frac{dA}{\kappa^2}. \tag{133}$$

After the substitution of Eq. (133) into Eq. (130), if coefficients $q^{(1)}$ and $q^{(2)}$ in the obtained equation are substituted with $q^{(1)}$ given by Eq. (126) and $q^{(2)}$ given by Eq. (127), respectively, then the following equation is obtained:

$$\frac{\pi(\kappa\sigma)^5}{72}\frac{(1-\phi)^2}{\phi^2}g^{(\kappa)} = \frac{\pi(\kappa\sigma)^2}{6}\frac{1+2\phi}{\phi}\left(\varphi_2(\kappa)g^{(\kappa)}+e^{-\kappa\sigma}\right) + \frac{\pi(\kappa\sigma)^3}{6}\frac{1+\phi/2}{\phi}\left(\varphi_1(\kappa)g^{(\kappa)}+e^{-\kappa\sigma}\right) \\ -\Bigg\{\left(\varphi_2(\kappa)g^{(\kappa)}+e^{-\kappa\sigma}\right)\Bigg[(1-g^{(\kappa)})e^{-\kappa\sigma}\Big((1+2\phi)\kappa\sigma\varphi_1(-\kappa)-6\phi\varphi_2(-\kappa)\Big)+(1+2\phi)\kappa\sigma-6\phi\Bigg] \\ +\kappa\sigma\left(\varphi_1(\kappa)g^{(\kappa)}+e^{-\kappa\sigma}\right)\Bigg[(1-g^{(\kappa)})e^{-\kappa\sigma}\Bigg(\Big(1+\frac{\phi}{2}\Big)\kappa\sigma\varphi_1(-\kappa)-(1+2\phi)\varphi_2(-\kappa)\Bigg)-1-2\phi \\ +\Big(1+\frac{\phi}{2}\Big)\kappa\sigma\Bigg]+(\kappa\sigma)^4\frac{(1-\phi)^2}{12\phi}\Bigg[\Big(\kappa\sigma\varphi_3(\kappa)g^{(\kappa)}-\frac{e^{-2\kappa\sigma}}{2}\Big)(1-g^{(\kappa)})-\frac{1}{2}g^{(\kappa)}\Bigg]\Bigg\}\frac{dA}{\sigma^2}. \tag{134}$$

The coefficients $g^{(\kappa)}$ and dA/σ^2 are evaluated from Eqs. (134) and (131).

Obtained values of A and $g^{(\kappa)}$ allow $\widehat{Q}(s)$ to be determined with $q^{(1)}/\sigma$ and $q^{(2)}$. Therefore, $\lim_{s\to 0}\widehat{Q}(s)$ can be estimated from the definition of $\widehat{Q}(s)$ given by Eq. (123) as follows:

$$\begin{aligned}\lim_{s\to 0}\widehat{Q}(s) =& \int_0^\infty Q(t)\mathrm{d}t \\ =& \sigma^3\left\{\frac{1}{6}q^{(2)} - \frac{1}{2}\frac{q^{(1)}}{\sigma} - \frac{dA}{\sigma^2}\left(1-g^{(\kappa)}\right)\frac{e^{-\kappa\sigma}}{\kappa\sigma}(-1-\kappa\sigma+e^{-\kappa\sigma}) + \frac{dA}{\sigma^2}\frac{1}{\kappa\sigma}\right\}. \end{aligned} \tag{135}$$

Similarly, the derivatives $\lim_{s\to 0}\mathrm{d}\widehat{Q}(s)/\mathrm{d}s$ and $\lim_{s\to 0}\mathrm{d}^2\widehat{Q}(s)/\mathrm{d}s^2$ can be estimated from the definition of $\widehat{Q}(s)$ given by Eq. (123) as follows:

$$\begin{aligned}-\lim_{s\to 0}\frac{\mathrm{d}\widehat{Q}(s)}{\mathrm{d}s} =& \int_0^\infty Q(t)t\mathrm{d}t \\ =& \sigma^4\left\{\frac{1}{24}q^{(2)} - \frac{1}{6}\frac{q^{(1)}}{\sigma} - \frac{dA}{\sigma^2}\left(1-g^{(\kappa)}\right)\frac{e^{-\kappa\sigma}}{(\kappa\sigma)^2}\left[-1-\kappa\sigma-\frac{1}{2}(\kappa\sigma)^2+e^{-\kappa\sigma}\right]\right. \\ &\left. + \frac{dA}{\sigma^2}\frac{1}{(\kappa\sigma)^2}\right\} \end{aligned} \tag{136}$$

and

$$\begin{aligned}\lim_{s\to 0}\frac{\mathrm{d}^2\widehat{Q}(s)}{\mathrm{d}s^2} =& \int_0^\infty Q(t)t^2\mathrm{d}t \\ =& \sigma^5\left\{\frac{1}{60}q^{(2)} - \frac{1}{12}\frac{q^{(1)}}{\sigma} + \frac{dA}{\sigma^2}\left(1-g^{(\kappa)}\right)\frac{e^{-\kappa\sigma}}{(\kappa\sigma)^3}\left[2+2\kappa\sigma+(\kappa\sigma)^2+\frac{1}{3}(\kappa\sigma)^3-2e^{-\kappa\sigma}\right]\right. \\ &\left. + 2\frac{dA}{\sigma^2}\frac{1}{(\kappa\sigma)^3}\right\}. \end{aligned} \tag{137}$$

iii) *Coefficients* $\widehat{c}^{(0)}$ *and* $\widehat{c}^{(2)}$

Based on Eq. (117), a coefficient $\widehat{c}^{(0)}$ is given by the following relation:

$$\rho\widehat{c}^{(0)} = \lim_{k\to 0}\widetilde{c}(k). \tag{138}$$

Hence, the Fourier transform of the Ornstein–Zernike equation given by Eq. (122) allows a coefficient $\widehat{c}^{(0)}$ to be given because of Eq. (123) as follows:

$$\rho\widehat{c}^{(0)} = 1 - \lim_{k\to 0}\Big[1-\rho\widehat{Q}(-ik)\Big]\Big[1-\rho\widehat{Q}(ik)\Big]. \tag{139}$$

Moreover, if Eq. (115) is used with Eqs. (123) and (122), then $\widehat{c}^{(2)}$ can be estimated as

$$\rho\widehat{c}^{(2)} = -\frac{2}{11}\lim_{s\to 0}\left[\Big(-1+\rho\widetilde{Q}(s)\Big)\rho\frac{\mathrm{d}^2}{\mathrm{d}s^2}\widehat{Q}(s) - \left(\rho\frac{\mathrm{d}}{\mathrm{d}s}\widetilde{Q}(s)\right)^2\right]. \tag{140}$$

Therefore, Eqs. (139) and (140) allow $\widehat{c}^{(0)}$ and $\widehat{c}^{(2)}$ to be assessed with the use of Eqs. (123) and (125).

(g) *Evaluation of percolation thresholds for Yukawa fluids*

In a fluid system, physical cluster formation and physical cluster growth affect the distribution pattern of particles and can affect phase behavior. If the effects of the physical cluster formation on properties of the fluid system cannot be ignored, they should be maximized at the percolation threshold related to the physical clusters. Thermodynamic properties of the fluid system can have characteristic dependences on temperature T at least around the value that T has at the critical point or another point on the spinodal line. In the phase diagram of the fluid system, the curved line on which $1 - \rho\widehat{c}(0) = 0$ is satisfied corresponds to the spinodal line. Thus, it is important to know the relation between the locus of the percolation threshold and the locus of the spinodal line in the phase diagram. Knowing the relation corresponds to the understanding of the links between the distribution pattern of particles and the features of the fluid system.

i) *Percolation thresholds for Yukawa fluids*

Evaluations of the percolation thresholds are achieved by the use of Eq. (114) while considering Eqs. (78), (81), and (82). The evaluations for each Yukawa fluid exemplified by $\kappa\sigma = 0.1, 0.5, 1.8, 3.6, 7.5$ allow the loci of the percolation thresholds to depend on f_ν as found in Figs. 4, 6, and 7. An overestimate for the long-ranged contribution of $C^+(r)$ is characterized by $1/r^{3/2} \approx 1/(\sigma^{1/2}r)$ for $f_\nu = 0$ ($\nu = \infty$), and this leads to an overestimate of $[\beta K^{\rm P}/\sigma]^{-1}$. An overestimate of the decay of $C^+(r)$ is characterized by $1/r^{3/2} \approx e^{1/2}e^{-r/2\sigma}/(\sigma^{1/2}r)$ for $f_\nu = 1/2$ ($\nu = 1$). This leads to an underestimate of $[\beta K^{\rm P}/\sigma]^{-1}$.

For a large $\kappa\sigma$, exemplified by $\kappa\sigma = 7.5$ and $\kappa\sigma = 3.6$, the difference between the locus of the percolation threshold for f_∞ and that for f_1 is small. However, the difference between the locus of the percolation threshold for f_∞ and that for f_1 becomes large for a small $\kappa\sigma$ exemplified by $\kappa\sigma = 0.1$. When $\kappa\sigma$ is small, a way to determine a reasonable $f_{\nu_{3/2}}$ via Eq.(84) should become useful. In Fig. 4, 6, and 7, the value of f_ν for $\nu = \nu_s$ being $\nu_s = 13.9309$ is given as $f_{\nu_{3/2}} = 0.101853$. For the f_ν assessed from $\nu = \nu_s$, Eq. (85) obtained from Eq.(84)

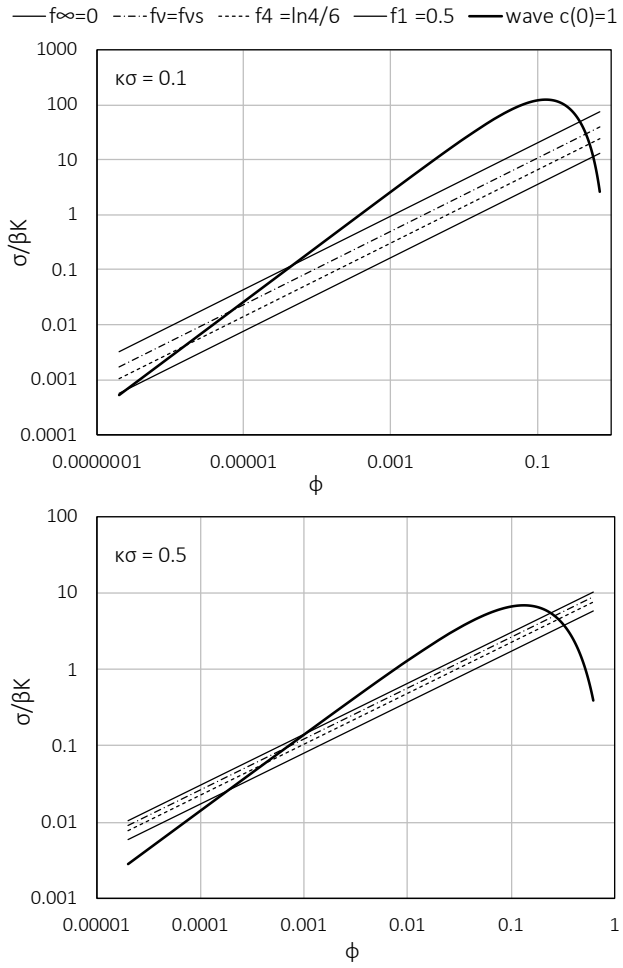

FIG. 4. Relation between percolation thresholds and curved line satisfying $\widetilde{c}(0) = 1$ for each Yukawa fluid. Curved line satisfying $\widetilde{c}(0) = 1$ corresponds to the spinodal line. Each straight line corresponds to percolation threshold. f_4 and $f_{\nu_{3/2}}$ are given as $f_4 = (1/6)\ln 4$ and $f_{\nu_{3/2}} = 0.101853$. Upper straight line, broken line, dotted line, and lower straight line correspond to percolation threshold given for f_∞, that for $f_{\nu_{3/2}}$, that for f_4, and that for f_1. $\widetilde{c}(0)$ $(= \rho\widehat{c}^{(0)})$ is expressed as "wave $c(0)$". (Continued in Figs. 6 and 7.)

is approximately satisfied.

At the temperature of a fluid that is sufficiently low in comparison with the strength of each mutually attractive force between particles, the formation of physical clusters is

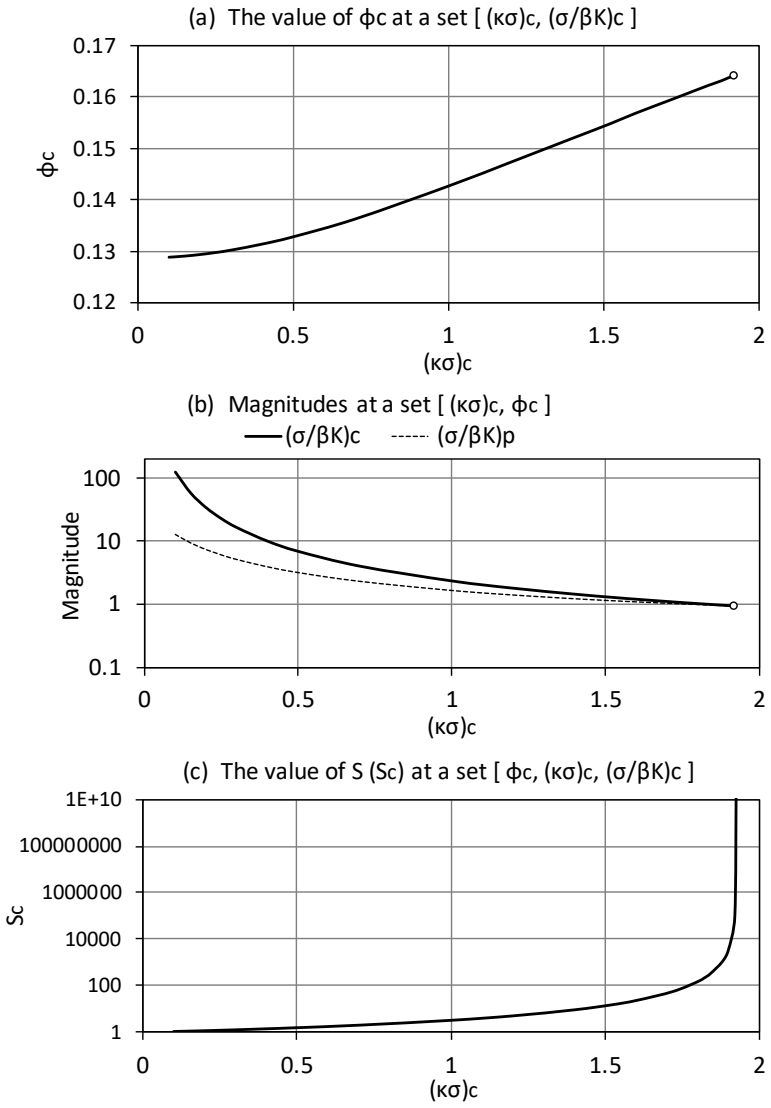

FIG. 5. Dependence of ϕ_c and $(\sigma/\beta K)_c$ on $\kappa\sigma$ for $f_\nu = f_{\nu_{3/2}} = 0.101853$. ϕ_c corresponds to value of ϕ at critical point of Yukawa fluid characterized by $\kappa\sigma$. $(\sigma/\beta K)_c$ corresponds to value of $\sigma/\beta K$ at critical point. In (b), $(\sigma/\beta K)_p$ corresponds to value of $\sigma/\beta K$ at percolation threshold specified by magnitude of ϕ_c and magnitude of $\kappa\sigma$. Circles in (a) and (b) both correspond to specific point satisfying relation $(\sigma/\beta K)_p = (\sigma/\beta K)_c$ (≈ 0.94379), which is evaluated for $\kappa\sigma = (\kappa\sigma)_s$ ($(\kappa\sigma)_s \equiv 1.924601$) and $\phi_c = 0.164275$. For $\kappa\sigma > (\kappa\sigma)_s$, relation $(\sigma/\beta K)_p < (\sigma/\beta K)_c$ is always satisfied.

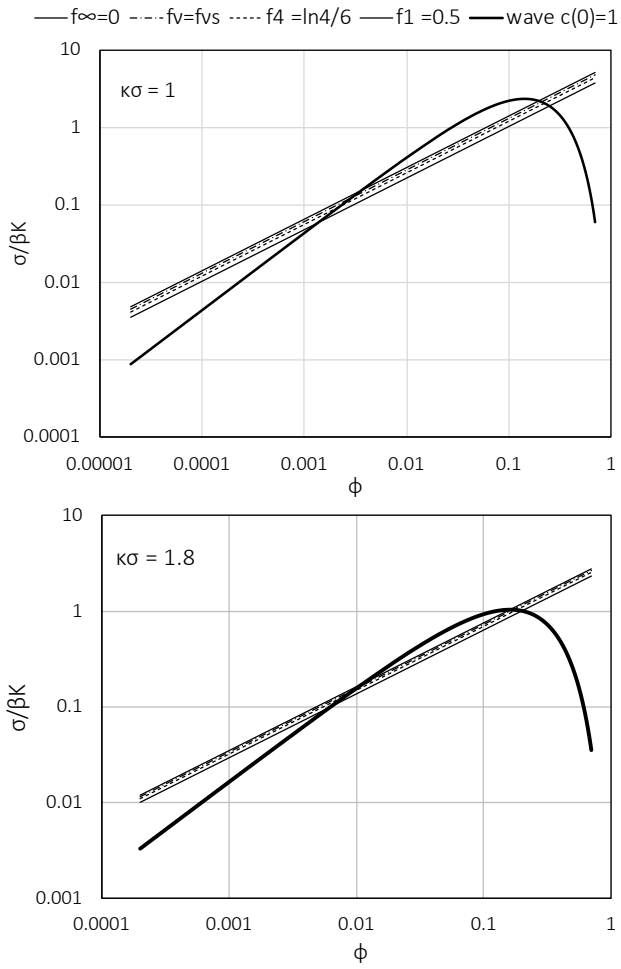

FIG. 6. Relation between percolation thresholds and curved line satisfying $\widetilde{c}(0) = 1$ for each Yukawa fluid. Details are same as those in Fig. 4. When percolation threshold that is evaluated for $f_{\nu_{3/2}} = 0.101853$ agrees with the critical point, $\kappa\sigma \approx 1.924601$ must be satisfied. When relation $\kappa\sigma < 1.924601$ is satisfied, critical point specified at $\phi = \phi_c$ is located in upper position of percolation threshold specified at $\phi = \phi_c$.

possible, even in the low-density side. This should contribute even to the distribution of astronomical matters. The evaluations for each Yukawa fluid denote that the percolation threshold for a sufficiently small $\kappa\sigma$ can be located on the low-density side as that located above the curved line obtained from relation $\beta(\partial P/\partial\rho) = 0$, which corresponds to $\rho\widehat{c}^{(0)} = 1$.

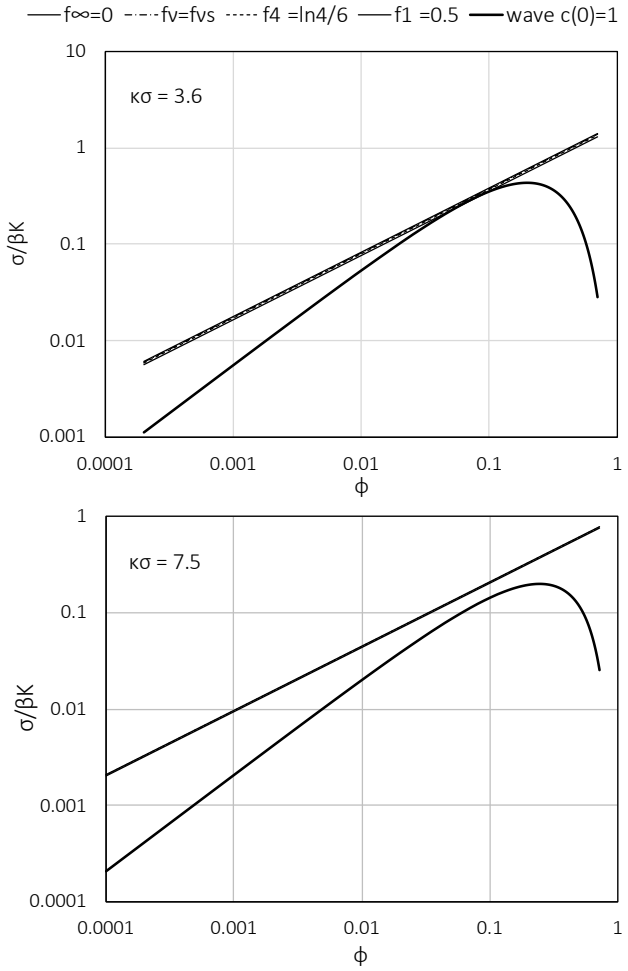

FIG. 7. Relation between percolation thresholds and curved line satisfying $\widetilde{c}(0) = 1$ for each Yukawa fluid. Details are same as those in Fig. 4. For $\kappa\sigma = 7.5$, percolation threshold estimated for f_∞ somewhat completely overlaps that estimated for f_1. When percolation threshold that is evaluated for $f_{\nu_{3/2}} = 0.101853$ agrees with critical point, $\kappa\sigma \approx 1.924601$ must be satisfied. When relation $\kappa\sigma > 1.924601$ is satisfied, percolation threshold specified at $\phi = \phi_c$ is located in upper position of critical point specified at $\phi = \phi_c$.

In the area located under the curved line consisting of the points at which $\rho\widehat{c}^{(0)} = 1$ is satisfied, the gas state of each fluid allows the phase stability to disappear. Then, the aggregation of particles allows the phase transition to occur while accompanying the phase

separation. If the phase transition occurs in the specific area that is located under the curved line and above the percolation threshold, then the liquid phase induced by the phase transition can maintain a state of no percolation of physical clusters. This phenomenon is exemplified by the phase diagrams for $\kappa\sigma = 1.8$, $\kappa\sigma = 1$, $\kappa\sigma = 0.5$, and $\kappa\sigma = 0.1$, and is similar to that found in the phase diagram in Reference.[3] This phenomenon suggests that a fluid in the liquid phase can change from a state of low viscosity to another state of high viscosity as ϕ increases. Even if the fluid maintains a state of low viscosity owing to the lack of percolation, the percolation that occurs as ϕ increases can allow the state to change to another state of high viscosity.

The percolation of physical clusters is induced even in a fluid characterized by the mutually attractive force between particles of which the effective range κ^{-1} is narrow. Then, the mean interparticle distance must be short. If the contribution of the mutually attractive force generates the liquid phase for a small κ^{-1}, then particles in the liquid phase should be located near each other. The generation of the liquid phase should require dense parts to be formed in the fluid. These dense parts should include extremely large physical clusters in the percolation state. If the liquid phase is generated even at a small κ^{-1}, then the fluid in the liquid phase should always maintain the percolation state. This is demonstrated by the diagrams given for $\kappa\sigma = 3.6$ and 7.5 in Fig. 7. Under the condition that extremely large physical clusters are included, the liquid phase should maintain a high viscosity. In addition, if the linear scale is applied, then the diagrams in Fig. 7 are represented by Fig. 8.

If the liquid phase is generated in a fluid consisting of particles interacting with a short-ranged attractive force, then the liquid phase contains extremely large physical clusters. If κ^{-1} is not small, then the mutually attractive force between particles constituting a fluid contributes over a long range. The liquid phase that is generated in the fluid cannot include physical clusters that have extremely large sizes. Without the formation of physical clusters of extremely large size, the long-ranged attractive force can allow particles to be retained in the liquid phase.

The volume fraction ϕ at the percolation threshold specified for a particular value of K decreases as the effective range κ^{-1} is extended. This behavior is readily confirmed by Fig. 8. Similar behavior has been found in a percolating system composed of core-soft-shell spheres with an attractive square-well potential.[39]

If the effective range κ^{-1} is extended, then overlaps of the effective range depending on

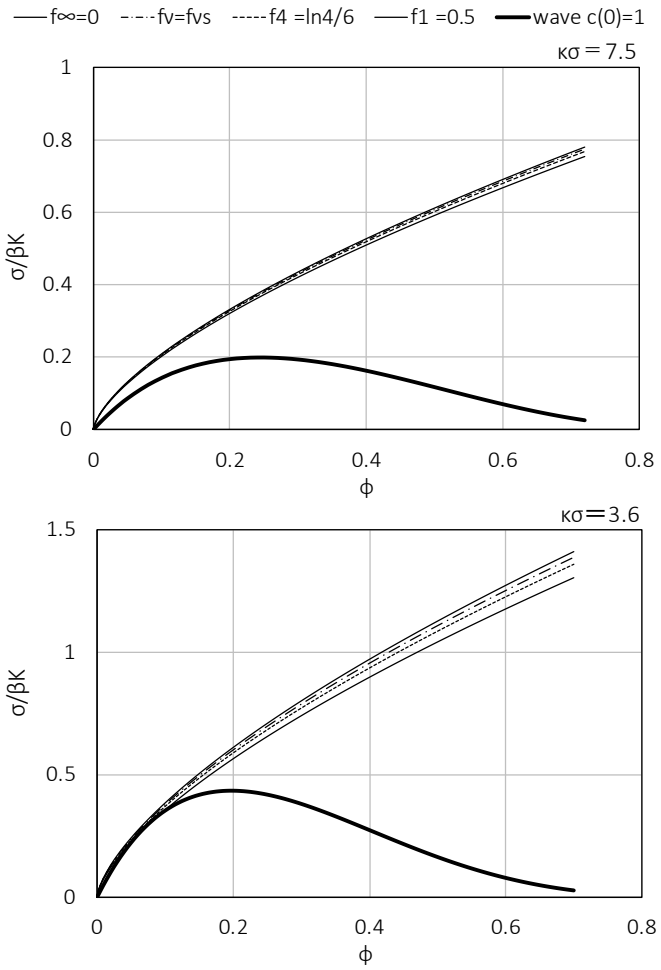

FIG. 8. Phase diagrams represented by use of linear scale for $\kappa\sigma = 3.6$ and $\kappa\sigma = 7.5$.

the distribution of particles increase. Indeed, the number of particles with which a particle interacts increases as the overlaps of the effective range increase. Thus, an increase in κ^{-1} can enhance a cooperative effect that contributes to the formation of a nonuniform particle distribution. The threshold of the phase separation is expressed by $\beta(\partial P/\partial\rho) = 0$, and the curved line on which $\beta(\partial P/\partial\rho) = 0$ is satisfied has the maximum point. The maximum point shifts to an upper position as $(\kappa\sigma)^{-1}$ increases. This can be confirmed by a comparison between phase diagrams.

When a decrease in the temperature of a fluid or an increase in the density of particles occurs, either the aggregation of particles resulting in the phase separation can be dominated

or the generation of the percolation can be dominated, depending on the distance at which the attractive forces between the particles remain effective. Either the generation of the percolation or the aggregation of particles resulting in the phase separation is enhanced as κ^{-1} increases. Nevertheless, an increase in the value of κ^{-1} cannot allow the particles that satisfy the criterion $\mathcal{E}(p) + \beta u(r) \leq 0$ with contribution $\mathcal{E}(p)$ of the relative kinetic energy to considerably increase in the distribution of particles surrounding each particle. At a large ϕ, which allows large numbers of particles to be included in their distribution, the tendency toward the aggregation that results in phase separation is more dominant than that toward the generation of the percolation. At a small ϕ, which does not allow large numbers of particles to be included in the distribution, the tendency toward the generation of the percolation can be more dominant than that toward the aggregation that results in phase separation. According to the tendency found in Fig. 4, the generation of percolation without phase separation is possible, even for an extremely large κ^{-1}, if ϕ is sufficiently small.

ii) *Two possible values of $g^{(k)}$ in each condition*

Making the assumption that the pair potential contributing to the mutually attractive force between pair particles corresponds to the Yukawa potential allows for an analytical solution formed as an algebraic equation system composed of Eqs. (131) and (130). This algebraic equation system allows at least two values to be given for $g^{(k)}$ in a condition related to the parameters: ϕ, $\kappa\sigma$, and $\sigma/\beta K$. If two values for $g^{(k)}$ are expressed as $g_S^{(k)}$ and $g_L^{(k)}$, relation $g_S^{(k)} < g_L^{(k)}$ is always satisfied. For a small $\kappa\sigma$, the difference $(g_L^{(k)} - g_S^{(k)})/g_L^{(k)}$ becomes small. For a smaller $\kappa\sigma$, the difference can more approach a situation satisfying $0 < (g_L^{(k)} - g_S^{(k)})/g_L^{(k)} \ll 1$ in each condition.

Under the condition satisfying $1 - \rho\widehat{c}^{(0)} = 0$, even $g_S^{(k)} \approx g_L^{(k)}$ is satisfied. Then, it is possible to find the value of $g_S^{(k)}$ that satisfies $1 - \rho\widehat{c}^{(0)} = 0$. Although the value of $g_L^{(k)}$ satisfying $1 - \rho\widehat{c}^{(0)} \approx 0$ can be found, finding the value of $g_L^{(k)}$ that exactly satisfies $1 - \rho\widehat{c}^{(0)} = 0$ is difficult. Moreover, quantities evaluated from the use of $g^{(k)} = g_L^{(k)}$ can deviate from those obtained from the use of $g^{(k)} = g_S^{(k)}$. Curved patterns expressed by small circles in Fig. 10 correspond to $\mathcal{P}(\sigma)/g(\sigma)$ evaluated from the use of $g^{(k)} = g_L^{(k)}$. Curved dotted lines expressed in Fig. 11 correspond to $\mathcal{D}(\sigma)$ evaluated from the use of $g^{(k)} = g_L^{(k)}$. Thus, $g^{(k)} = g_S^{(k)}$ is applied for estimating all quantities.

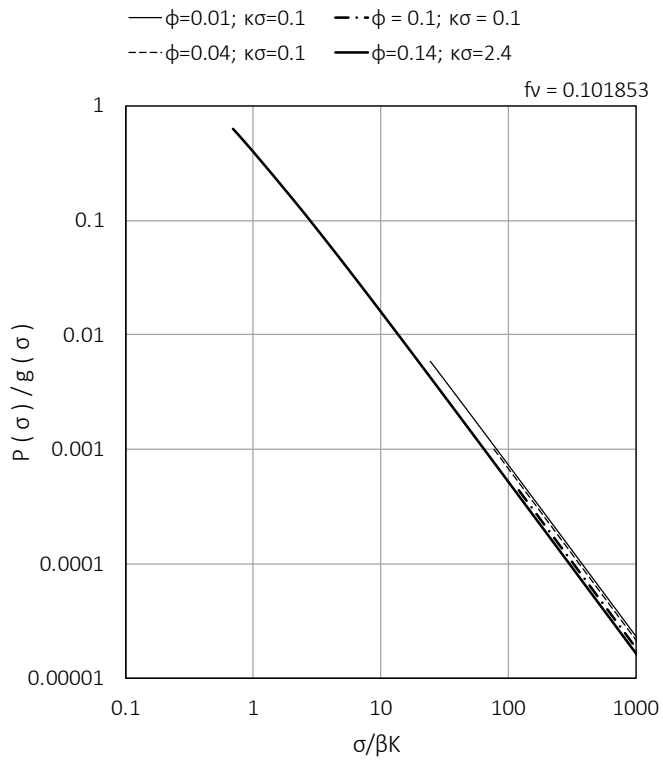

FIG. 9. Dependence of $\mathcal{P}(\sigma)/g(\sigma)$ on $\sigma/\beta K$. Both ϕ and $\kappa\sigma$ are constant. Then, $\mathcal{P}(\sigma)/g(\sigma)$ behaves as $\mathcal{P}(\sigma)/g(\sigma) \sim (\sigma/\beta K)^{\alpha}$, $(\alpha = -1.4997\cdots)$. At maximum point of each line, $1 - \rho\widehat{c}^{(0)} = 0$ is satisfied. $\mathcal{P}(\sigma)$ corresponds to $\mathcal{P}(\sigma^{+})$ estimated from Eq. (142), and $g(\sigma)$ corresponds to $g(\sigma^{+})$ estimated from Eq. (143).

Nevertheless, a physical meaning carried by $g^{(k)} = g_L^{(k)}$ cannot be simply ignored. The existence of $g_S^{(k)}$ and $g_L^{(k)}$ suggests that a structure of a fluid satisfying $1 - \rho\widehat{c}^{(0)} = 0$ and another structure of the fluid satisfying $1 - \rho\widehat{c}^{(0)} \approx 0$ are possible. The relation $g_S^{(k)} \neq g_L^{(k)}$ may allow phase separation to occur under the condition specified by $1 - \rho\widehat{c}^{(0)} = 0$. Eqs. (131) and (130) are satisfied for both $g^{(k)} = g_S^{(k)}$ and $g^{(k)} = g_L^{(k)}$. There can exist phenomena

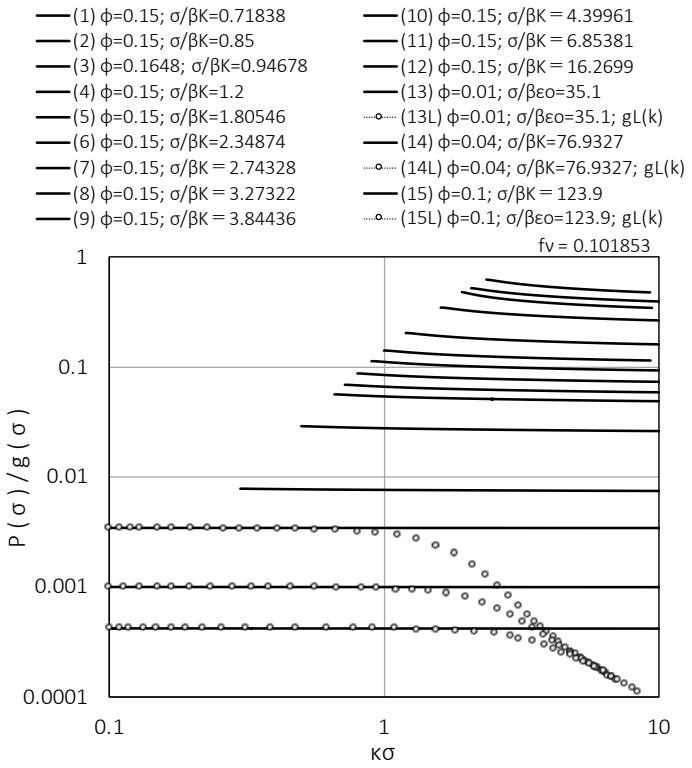

FIG. 10. Dependence of $\mathcal{P}(\sigma)/g(\sigma)$ on $\kappa\sigma$. Both ϕ and $\sigma/\beta K$ are constant. Then, behavior of $\mathcal{P}(\sigma)/g(\sigma)$ remains nearly constant. Small circles, which deviate from straight lines, denote value of $\mathcal{P}(\sigma^+)/g(\sigma^+)$ evaluated for $g^{(k)} = g_L^{(k)}$. At the endpoint of each curved line on the small side of $\kappa\sigma$, $1 - \rho\widehat{c}^{(0)} \approx 0$ is satisfied. $\mathcal{P}(\sigma)$ corresponds to $\mathcal{P}(\sigma^+)$, and $g(\sigma)$ corresponds to $g(\sigma^+)$. $gL(k)$ corresponds to $g_L^{(k)}$. Lines (1), (2), ..., and (15) correspond to top, second, ..., and bottom.

exemplified by liquid-liquid transitions.[44] According to physical intuition, $g_L^{(k)}$ should not be simply ignored.

iii) *Three parameters affecting correlation functions*

The number $n_{\rm pair}$ of particle pairs constituted by each pair satisfying the bound condition $\mathcal{E}(p) \leq -\beta u_{\rm Y}(r)$ increases as K increases. Moreover, $n_{\rm pair}$ can increase both as κ^{-1} increases and as ϕ increases. The variations in K, κ^{-1}, and ϕ can result in variations in $\mathcal{P}(r)$ and $g(r)$ owing to the change in $n_{\rm pair}$. Then, the behavior of $\mathcal{P}(r)$ and $g(r)$ owing to the variation in K can differ from that owing to the variation in κ^{-1}. The increase in K enhances the magnitude of $-u_{\rm Y}(r)$ in the range $0 < (r-\sigma)/\sigma \ll 1$, while the variation in κ^{-1} cannot change it in this range. The behavior of $\mathcal{P}(r)$ and $g(r)$ owing to the variation in K can also differ from that owing to the variation in ϕ. Without changes in the magnitude of $-u_{\rm Y}(\sigma)$, increases in κ^{-1} as well as in ϕ lead to an increase in the number of particles with which a particle interacts. Thus, the behavior of $\mathcal{P}(r)$ and $g(r)$ owing to the increases in either κ^{-1} or ϕ may differ from that owing to the increase in K.

Figure 9 shows the behavior of the ratio $\mathcal{P}(r)/g(r)$ in the range $0 < (r-\sigma)/\sigma \ll 1$. The ratio $\lim_{\delta\to 0}\mathcal{P}(\sigma+\delta)/g(\sigma+\delta)$, which is described as $\mathcal{P}(\sigma^+)/g(\sigma^+)$, is sensitive to the variations in the value of $\sigma/\beta K$, and the ratio increases as K increases. In Fig. 9, $\mathcal{P}(\sigma)$ corresponds to $\mathcal{P}(\sigma^+)$ estimated from Eq. (142), and $g(\sigma)$ corresponds to $g(\sigma^+)$ estimated from Eq. (143).

The ratio $\mathcal{P}(\sigma^+)/g(\sigma^+)$ is weakly increased with an increase in the effective range κ^{-1}, although the ratio remains nearly constant for a large $\sigma/\beta K$. This behavior is confirmed by Fig. 10. Basically, the behavior of $\mathcal{P}(\sigma^+)$ and the behavior of $\mathcal{D}(\sigma^+)$ are both insensitive to variations of $\kappa\sigma$ when $\sigma/\beta K$ is large. These behaviors are seen in Fig. 11 as well as in Fig. 12. For a small $\sigma/\beta K$, $\mathcal{P}(\sigma^+)$ is, however, increased weakly with an increase in the value of κ^{-1}, as found in Fig. 12. According to Fig. 12, $\mathcal{D}(\sigma^+)$ is then decreased with an increase in the value of κ^{-1}.

According to Fig. 13, the behavior of $\mathcal{P}(\sigma)/g(\sigma)$ remains nearly constant for variations in the value of ϕ. Then, both $\kappa\sigma$ and $\sigma/\beta K$ are constant. The ratio $\mathcal{P}(\sigma^+)/g(\sigma^+)$ can be considerably insensitive to the variations in ϕ. The value of $\mathcal{P}(\sigma^+)/g(\sigma^+)$ resists a decrease in ϕ. The behavior of $\mathcal{P}(\sigma)/g(\sigma)$ found in Fig. 13 does not mean that $\mathcal{P}(\sigma)$ and $\mathcal{D}(\sigma)$ are both insensitive to variations in the value of ϕ. In fact, an increase in $\mathcal{P}(\sigma)$ for an increase in ϕ is confirmed from Fig. 14, and an increase in $\mathcal{D}(\sigma)$ for an increase in ϕ is confirmed from Fig. 15. These features of $\mathcal{P}(\sigma)$ and $\mathcal{D}(\sigma)$ denote that $\mathcal{P}(\sigma^+)$ and $g(\sigma^+)$ can behave as $\mathcal{P}(\sigma^+) \sim \phi^{\hat{\alpha}}$ and $g(\sigma^+) \sim \phi^{\hat{\alpha}}$, respectively.

The ratio $\mathcal{P}(\sigma^+)/g(\sigma^+)$ is given as $\mathcal{P}(\sigma^+)/g(\sigma^+) = [1 + \mathcal{D}(\sigma^+)/\mathcal{P}(\sigma^+)]^{-1}$ because of

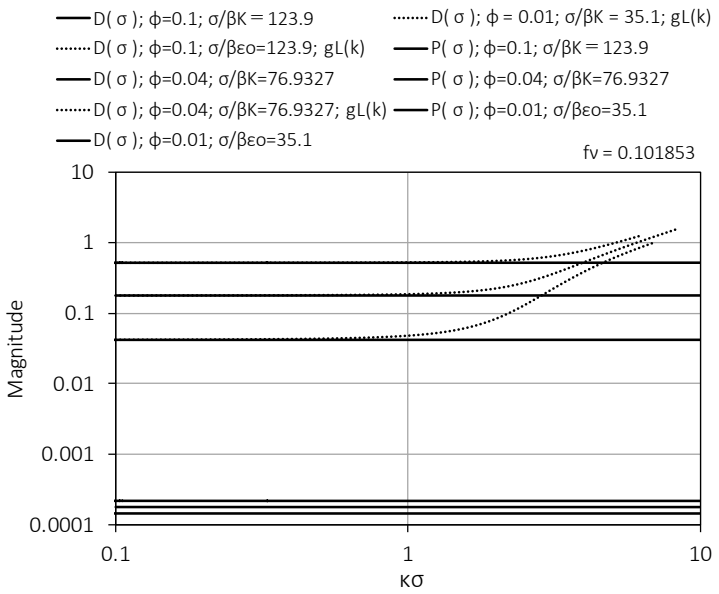

FIG. 11. Dependences of $\mathcal{P}(\sigma)$ and $\mathcal{D}(\sigma)$ on $\kappa\sigma$ for a large $\sigma/\beta K$. Both ϕ and $\sigma/\beta K$ are constant. Then, behaviors of $\mathcal{P}(\sigma)$ and $\mathcal{D}(\sigma)$ remain nearly constant. Curved dotted lines, which deviate from straight lines, denotes value of $\mathcal{D}(\sigma^+)$ evaluated for $g^{(k)} = g_L^{(k)}$. $\mathcal{P}(\sigma)$ corresponds to $\mathcal{P}(\sigma^+)$, and $\mathcal{D}(\sigma)$ corresponds to $\mathcal{D}(\sigma^+)$. $gL(k)$ corresponds to $g_L^{(k)}$. Top three lines, i.e., top, second, and bottom correspond to $\mathcal{D}(\sigma)$, $\phi = 0.1$, $\phi = 0.04$, and $\phi = 0.01$, respectively. Bottom three lines, i.e., top, second, and bottom correspond to $\mathcal{P}(\sigma)$, $\phi = 0.1$, $\phi = 0.04$, and $\phi = 0.01$, respectively.

Eq. (38). The probability that two particles are accidentally located in the range $0 < (r - \sigma)/\sigma \ll 1$ is equal to the sum of the probability that a bound state is formed between the particles located in the range $0 < (r - \sigma)/\sigma \ll 1$ and the probability that the particles

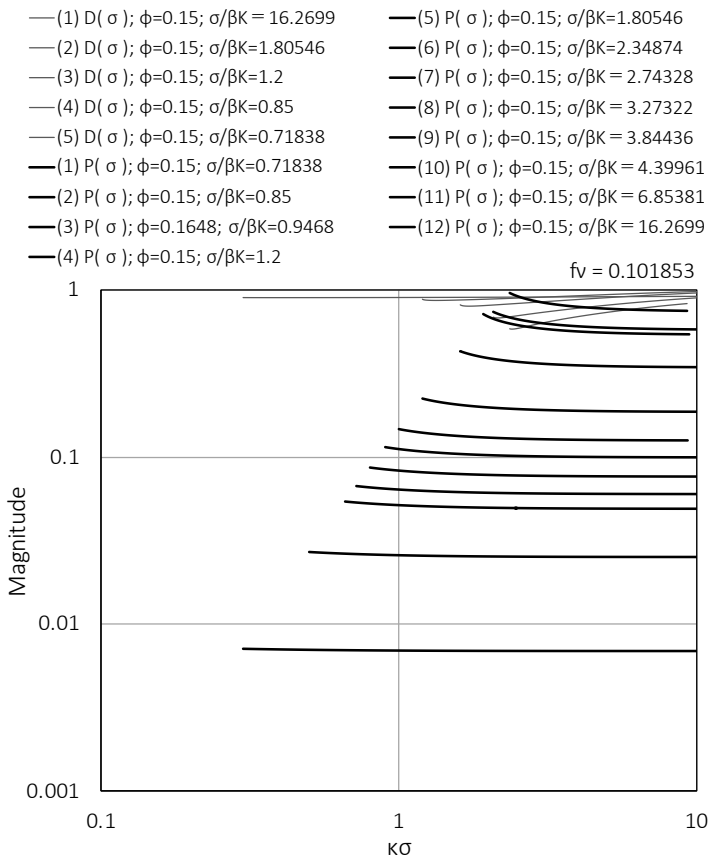

FIG. 12. Dependences of $\mathcal{P}(\sigma)$ and $\mathcal{D}(\sigma)$ on $\kappa\sigma$ for a small $\sigma/\beta K$. Both ϕ and $\sigma/\beta K$ are constant. Then, $\mathcal{P}(\sigma)$ is increased weakly, and $\mathcal{D}(\sigma)$ is decreased weakly. $\mathcal{P}(\sigma)$ corresponds to $\mathcal{P}(\sigma^+)$, and $\mathcal{D}(\sigma)$ corresponds to $\mathcal{D}(\sigma^+)$. At the endpoint of each curved line on the small side of $\kappa\sigma$, $1-\rho\widehat{c}^{(0)} \approx 0$ is satisfied. Thin lines from the top to bottom correspond to lines from (1) $\mathcal{D}(\sigma)$ to (5) $\mathcal{D}(\sigma)$. Thick lines from top to bottom correspond to lines from (1) $\mathcal{P}(\sigma)$ to (12) $\mathcal{P}(\sigma)$.

are located in the range $0 < (r-\sigma)/\sigma \ll 1$ without forming the bound state. Then, $\mathcal{P}(\sigma^+)$ is proportional to the probability that they form the bound state, and $\mathcal{D}(\sigma^+)$ is proportional to the probability that they are located in the range $0 < (r-\sigma)/\sigma \ll 1$ without forming the bound state. Figures 14 and 15 denote that $\mathcal{P}(\sigma^+)$ and $\mathcal{D}(\sigma^+)$ behave as $\mathcal{P}(\sigma^+) \sim \phi^{\hat{\alpha}}$

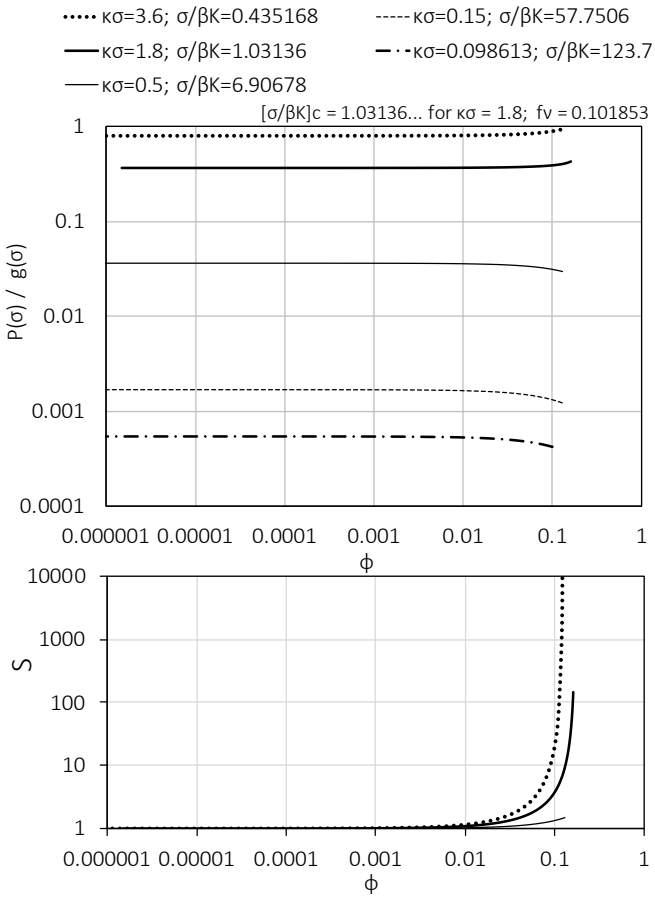

FIG. 13. Dependence of $\mathcal{P}(\sigma)/g(\sigma)$ on ϕ. The endpoint of each curved line on the side of a large ϕ corresponds to the point at which $1 - \rho\widehat{c}^{(0)} \approx 0$ is satisfied, except the uppermost dotted line on which endpoint is percolation threshold. $\mathcal{P}(\sigma)$ corresponds to $\mathcal{P}(\sigma^+)$ estimated from Eq. (142), and $g(\sigma)$ corresponds to $g(\sigma^+)$ estimated from Eq. (143). S is the mean size of physical clusters. $[\sigma/\beta K]_c$ denotes the value of $\sigma/\beta K$ at the critical point.

and $\mathcal{D}(\sigma^+) \sim \phi^{\hat{\alpha}}$. This demonstrates that $g(\sigma^+)$ behaves as $g(\sigma^+) \sim \phi^{\hat{\alpha}}$.

As the density of particles approaches zero, the probability characterized by $\mathcal{P}(\sigma^+)$ approaches zero more rapidly than the probability characterized by $\mathcal{D}(\sigma^+)$. If this is correct, then the procedure for making the density approach zero should allow the distribution of

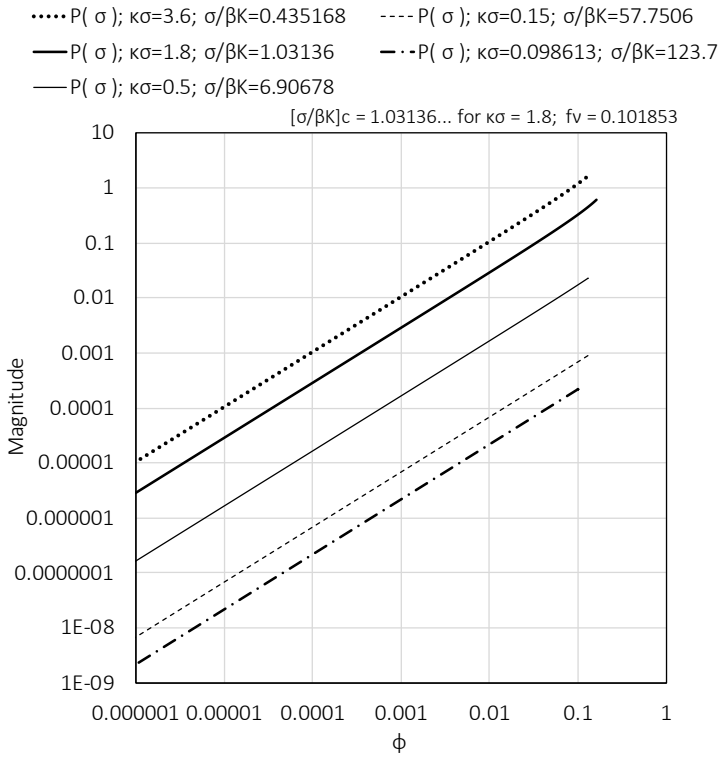

FIG. 14. Dependence of $\mathcal{P}(\sigma)$ on ϕ. Both $\sigma/\beta K$ and $\kappa\sigma$ are constant. Then, $\mathcal{P}(\sigma)$ can behave as $\mathcal{P}(\sigma) \sim \phi^{\hat{\alpha}}$ ($\hat{\alpha} = 1.0010\cdots$). Endpoint of each curve on side of large ϕ corresponds to the point at which $1 - \rho\widehat{C}^{+}(0) \approx 0$ is satisfied. $\mathcal{P}(\sigma)$ corresponds to $\mathcal{P}(\sigma^{+})$. $[\sigma/\beta K]_c$ denotes the value of $\sigma/\beta K$ at the critical point.

particles to become homogeneous, independently of attractive interactions between particles. However, this is not correct. The probability characterized by $\mathcal{P}(\sigma^{+})$ becomes proportional to the probability characterized by $\mathcal{P}(\sigma^{+}) + \mathcal{D}(\sigma^{+})$ when the density is sufficiently low. The behavior of $\mathcal{P}(\sigma^{+})/g(\sigma^{+})$ revealed in Fig. 13 requires that the following relation is satisfied:

$$\lim_{\phi \to 0} \mathcal{P}(\sigma^{+})/g(\sigma^{+}) \neq 0. \tag{141}$$

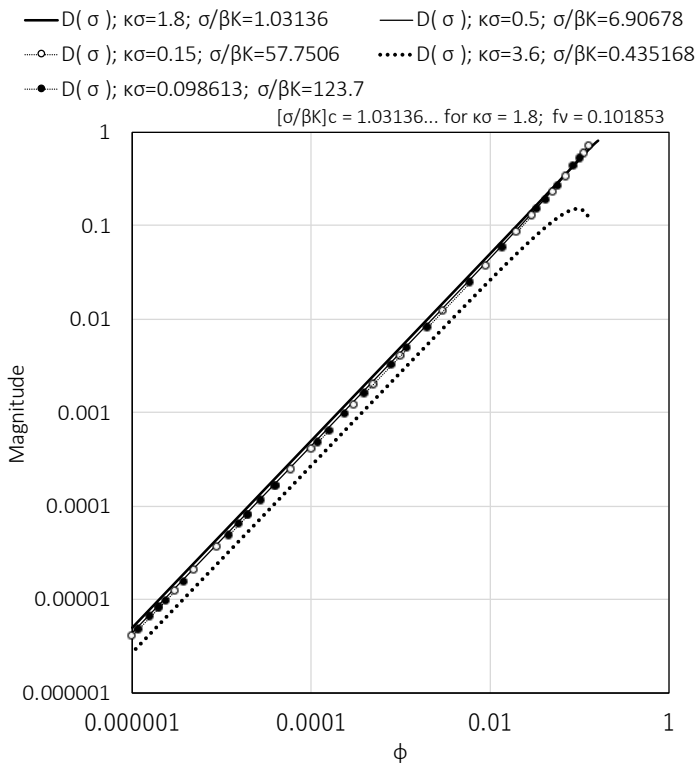

FIG. 15. Dependence of $\mathcal{D}(\sigma)$ on ϕ. Both $\sigma/\beta K$ and $\kappa\sigma$ are constant. Then, $\mathcal{D}(\sigma)$ both can behave as $\mathcal{D}(\sigma) \sim \phi^{\hat{\alpha}}$, ($\hat{\alpha} = 1.0010\cdots$). Endpoint of each curve on the side of large ϕ corresponds to the point at which $1 - \rho\widehat{C}^{+}(0) \approx 0$ is satisfied. $\mathcal{D}(\sigma)$ corresponds to $\mathcal{D}(\sigma^{+})$ estimated from $\mathcal{D}(\sigma^{+}) = g(\sigma^{+}) - \mathcal{P}(\sigma^{+})$. $[\sigma/\beta K]_c$ denotes value of $\sigma/\beta K$ at the critical point.

The feature of $\mathcal{P}(\sigma^{+})/g(\sigma^{+})$ resisting a decrease in ϕ demonstrates that attractive forces between particles allow the particle distribution to remain inhomogeneous no matter how low the particle density is. A typical example of this can be found as the distribution of astronomical matter.

iv) *Estimations of* $\mathcal{P}(\sigma^+)$ *and* $\mathcal{D}(\sigma^+)$

In the range $0 < (r-\sigma)/\sigma \ll 1$, $\mathcal{P}(r)$ can be estimated readily. If Eqs. (100) and (105) are used with $\lim_{u(r)\to\infty}\mathcal{P}(r) = 0$ owing to a relation given by Eq. (39), then it is given as

$$2\pi\sigma\mathcal{P}(\sigma^+) = ze^{-z\sigma}(1-\widehat{\mathcal{P}}(z))\breve{D}. \tag{142}$$

In the range $0 < (r-\sigma)/\sigma \ll 1$, the pair correlation function $g(r)$ can be given on the basis of references[83] as

$$g(\sigma^+) = g^{\rm HS} + \frac{\beta K}{\sigma}[F_0(\kappa\sigma,\phi) + \kappa\sigma X F_1(\kappa\sigma,\phi)]^{-2}, \tag{143}$$

where

$$g^{\rm HS} \equiv \frac{1}{1-\phi}\Big(1+\frac{2}{3}\cdot\frac{3\phi}{1-\phi}\Big),$$

$$F_0(\kappa\sigma,\phi) \equiv 1 + \frac{1}{\kappa\sigma}(1-e^{-\kappa\sigma})\frac{3\phi}{1-\phi} - \frac{4}{(\kappa\sigma)^3}\Big[1-\frac{\kappa\sigma}{2}-\Big(1+\frac{\kappa\sigma}{2}\Big)e^{-\kappa\sigma}\Big] \times\frac{3\phi}{1-\phi}\Big(1+\frac{\kappa\sigma}{2}+\frac{3\phi}{1-\phi}\Big),$$

and

$$F_1(\kappa\sigma,\phi) \equiv \frac{1}{\kappa\sigma}(1-e^{-\kappa\sigma}) - \frac{4}{(\kappa\sigma)^3}\Big[1-\frac{\kappa\sigma}{2}-\Big(1+\frac{\kappa\sigma}{2}\Big)e^{-\kappa\sigma}\Big]\frac{3\phi}{1-\phi}.$$

An unknown coefficient X in the above equation is determined from the following equation:

$$X(X+1)\Big[X+\frac{F_0(\kappa\sigma,\phi)}{\kappa\sigma F_1(\kappa\sigma,\phi)}\Big]^2 = -\frac{\beta K}{\sigma}\frac{6\phi}{[(\kappa\sigma)^2F_1(\kappa\sigma,\phi)]^2}.$$

The behavior of $\mathcal{P}(\sigma^+)$ can represent features accompanied by the probability that a particle located at $r=0$ and another particle located in the range $0 < (r-\sigma)/\sigma \ll 1$ form a bound state. The behavior of $\mathcal{D}(\sigma^+)$ can represent features accompanied by the probability that the two particles are located at the same positions without forming the bound state. Although $\mathcal{P}(\sigma^+)$ depends sensitively on $\sigma/\beta K$, for constant ϕ and constant $\kappa\sigma$, $\mathcal{D}(\sigma^+)$ can remain constant with resisting variations in $\sigma/\beta K$. This is confirmed by Fig. 16.

If ϕ and $\sigma/\beta K$ are constant, then the value of $\mathcal{P}(\sigma^+)$ can remain nearly constant with resisting variations in $\kappa\sigma$ as confirmed from Fig. 11 and 12. In addition, the value of $\mathcal{D}(\sigma^+)$ can remain nearly constant. For a small $\sigma/\beta K$, the value of $\mathcal{D}(\sigma^+)$ is weakly increased with an increase in the value of $\kappa\sigma$, although $\mathcal{P}(\sigma^+)$ is weakly decreased. As the effective range κ^{-1} is shortened, the probability that a particle located at $r=0$ and another particle

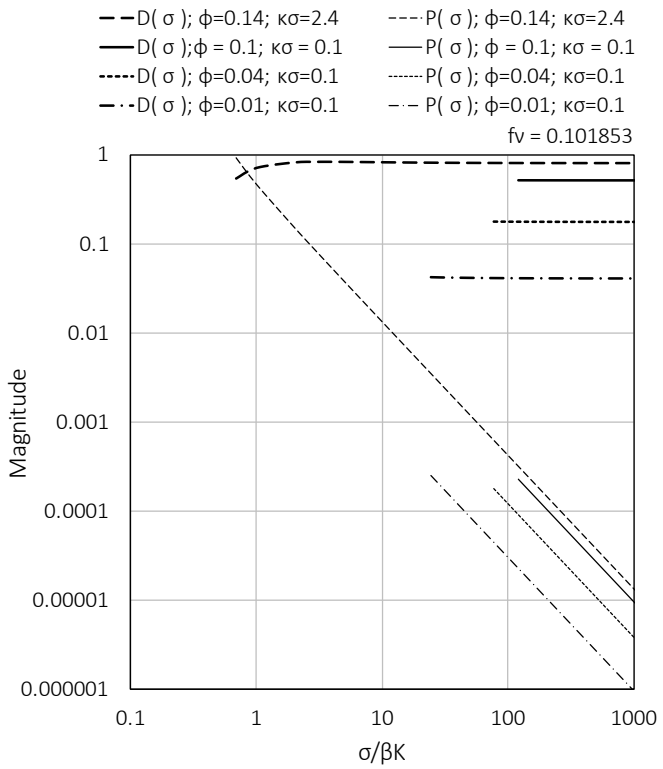

FIG. 16. Dependence of $\mathcal{P}(\sigma)$ on $\sigma/\beta K$ and the dependence of $\mathcal{D}(\sigma)$ on $\sigma/\beta K$. Both ϕ and $\kappa\sigma$ are constant. Then, $\mathcal{P}(\sigma)$ can behave as $\mathcal{P}(\sigma) \sim (\sigma/\beta K)^{\hat{\alpha}}$, $(\hat{\alpha} = -1.5010\cdots)$. $\mathcal{D}(\sigma)$ can remain nearly constant. At left endpoint of each line, $1 - \rho\widehat{c}^{(0)} = 0$ is satisfied. $\mathcal{P}(\sigma)$ corresponds to $\mathcal{P}(\sigma^+)$. $\mathcal{D}(\sigma)$ corresponds to $\mathcal{D}(\sigma^+)$ estimated from $\mathcal{D}(\sigma^+) = g(\sigma^+) - \mathcal{P}(\sigma^+)$.

located in the range $0 < (r-\sigma)/\sigma \ll 1$ do not form a bound state are increased. An increase in the probability corresponds to an increase in the number of particles that do not form bound states. When the effective range κ^{-1} is further shortened, unless the value of $\sigma/\beta K$ is further decreased, a Yukawa fluid specified by κ^{-1} cannot undergo phase separation as known from a comparison between Figs. 7 and 6.

If κ^{-1} is sufficiently large, then sizes of the physical clusters in the fluid remain small while the fluid falls into a state where it can undergo phase separation. Thus, an increase in κ^{-1} allows the tendency toward the generation of percolation to be less dominant than that toward aggregation, resulting in only phase separation. If the effective range κ^{-1} is narrow, then the number of particles should be large near each particle to induce the percolation. Thus, the dependence of $\mathcal{P}(\sigma^+)/g(\sigma^+)$ on $\sigma/\beta K$ is strong, although its dependences on $\kappa\sigma$ and ϕ are not strong.

6. Differential equations for correlation functions

(**a**) *Maclaurin series expansions*

The magnitude of the direct correlation function $c(r)$ tends to decay to zero within a microscopic range, and both $C^+(r)$ and $C^*(r)$ also have a tendency to decay to zero within microscopic ranges according to $c(r) = C^+(r) + C^*(r)$. By contrast, the correlation function $g(r) - 1$ can decay to zero much more slowly out of the ranges where $c(r) \neq 0$.[13,18] Further, $\mathcal{P}(r)$ and $\mathcal{H}(r)$ can decay to zero much more slowly out of the ranges where $C^+(r) \neq 0$ and $C^*(r) \neq 0$ according to $g(r) - 1 = \mathcal{P}(r) + \mathcal{H}(r)$. Thus, the particular ranges for which $c(r)$, $C^+(r)$, and $C^*(r)$ decay to zero remain much smaller than those for which $\mathcal{P}(r)$ and $\mathcal{H}(r)$ decay to zero. This allows $\mathcal{P}(r)$ and $\mathcal{H}(r)$ in the convolution integrals of Eqs. (49) and (52) to be expressed as Maclaurin series expansions.

If a polar coordinate system with a point $\mathbf{r}_1$ located at the origin and another point $\mathbf{r}_2$ located on the z axis is applied, then Eq. (49) can be rewritten as

$$\mathcal{P}(r) = C^+(r) + \rho \int_0^\infty \int_0^\pi C^+(r_3)\mathcal{P}(|\mathbf{r}_3 - \mathbf{r}_2|)2\pi(r_3)^2 \sin\theta \mathrm{d}r_3 \mathrm{d}\theta_3, \tag{144}$$

where $r \equiv |\mathbf{r}_1 - \mathbf{r}_2| = |\mathbf{r}_2|$, $r_3 \equiv |\mathbf{r}_1 - \mathbf{r}_3| = |\mathbf{r}_3|$, and $\theta_3 = \cos^{-1}[\mathbf{r}_2 \cdot \mathbf{r}_3/(rr_3)]$. In Eq. (144), the short-range feature of $C^+(r_3)$ allows relation $0 < r_3/r \ll 1$ to be maintained for a large r. Thus, the Maclaurin series expansion for $\mathcal{P}(|\mathbf{r}_3 - \mathbf{r}_2|)$ found in Eq. (144) is effective for representing the behavior of $\mathcal{P}(r)$ at a large r. Then, the Maclaurin series expansion corresponds to

$$\mathcal{P}(|\mathbf{r}_3 - \mathbf{r}_2|) = \sum_{m=0}^{\infty} \frac{1}{m!} \frac{\partial^m}{\partial r_3^m} \mathcal{P}(r_{32})\Big|_{r_3=0} (r_3)^m, \tag{145}$$

where $r_{32} \equiv |\mathbf{r}_3 - \mathbf{r}_2| = [(r_3)^2 - 2r_3 r\cos\theta_3 + r^2]^{1/2} = r[(r_3/r)^2 - 2(r_3/r)\cos\theta_3 + 1]^{1/2}$.

The substitution of the Maclaurin series expansion given by Eq. (145) allows Eq. (144) to be given as

$$\left[1 - \rho\widehat{C}^{+(0)}\right]\mathcal{P}(r) = C^+(r) + \rho\widehat{C}^{+(2)}\nabla^2\mathcal{P}(r) + \frac{9}{4}\rho\widehat{C}^{+(4)}\Delta_r\mathcal{P}(r) + \cdots, \tag{146}$$

where

$$\Delta_r \equiv \frac{8}{15}\frac{1}{r}\frac{\partial^3}{\partial r^3} + \frac{2}{15}\frac{\partial^4}{\partial r^4}.$$

The coefficient $\widehat{C}^{+(\alpha)}$ $(\alpha = 0, 2, 4)$ is defined by Eq. (116), and it is given as follows:

$$\widehat{C}^{+(\alpha)} = \left(\frac{1}{6}\right)^{\alpha/2} \int_V C^+(|\mathbf{r}_3|)|\mathbf{r}_3|^\alpha \mathrm{d}\mathbf{r}_3, \quad (\alpha = 0, 2, 4). \tag{147}$$

In Eq. (146), the factor $\frac{9}{4}\rho\widehat{C}^{+(4)}\Delta_r\mathcal{P}(r)$ corresponds to a correction term under the condition that the value of r is not large, although its value is out of the microscopic range in which $C^+(r) \neq 0$ is satisfied.

If the polar coordinate system with a point $\mathbf{r}_1$ located at the origin and another point $\mathbf{r}_2$ located on the z axis is applied, then Eq. (52) can be rewritten as

$$\begin{aligned}\mathcal{H}(r) =& C^*(r) + \rho \int_0^\infty \int_0^\pi C^*(r_3)\mathcal{P}(|\mathbf{r}_3 - \mathbf{r}_2|)2\pi(r_3)^2 \sin\theta_3 \mathrm{d}r_3\mathrm{d}\theta_3 \\ &+\rho \int_0^\infty \int_0^\pi C^+(r_3)\mathcal{H}(|\mathbf{r}_3 - \mathbf{r}_2|)2\pi(r_3)^2 \sin\theta_3 \mathrm{d}r_3\mathrm{d}\theta_3 \\ &+\rho \int_0^\infty \int_0^\pi C^*(r_3)\mathcal{H}(|\mathbf{r}_3 - \mathbf{r}_2|)2\pi(r_3)^2 \sin\theta_3 \mathrm{d}r_3\mathrm{d}\theta_3,\end{aligned} \tag{148}$$

The Maclaurin series expansion for $\mathcal{H}(|\mathbf{r}_3 - \mathbf{r}_2|)$ corresponds to

$$\mathcal{H}(|\mathbf{r}_3 - \mathbf{r}_2|) = \sum_{m=0}^\infty \frac{1}{m!}\frac{\partial^m}{\partial r_3^m}\mathcal{H}(r_{32})\Big|_{r_3=0}(r_3)^m. \tag{149}$$

The substitution of the Maclaurin series expansions given by Eqs. (145) and (149) allows Eq. (148) to be given as

$$\begin{aligned}\left[1 - \rho\widehat{c}^{(0)}\right]\mathcal{H}(r) =& C^*(r) + \rho\widehat{C}^{*(0)}\mathcal{P}(r) \\ &+\rho\widehat{C}^{*(2)}\nabla^2\mathcal{P}(r) + \rho\widehat{c}^{(2)}\nabla^2\mathcal{H}(r) \\ &+\frac{9}{4}\rho\widehat{C}^{*(4)}\Delta_r\mathcal{P}(r) + \frac{9}{4}\rho\widehat{c}^{(4)}\Delta_r\mathcal{H}(r) + \cdots,\end{aligned} \tag{150}$$

where the coefficients $\widehat{C}^{*(\alpha)}$ and $\widehat{c}^{(\alpha)}$ $(\alpha = 0, 2, 4)$ are given by Eq. (116) as follows:

$$\widehat{C}^{*(\alpha)} = \left(\frac{1}{6}\right)^{\alpha/2} \int_V C^*(|\mathbf{r}_3|)|\mathbf{r}_3|^\alpha \mathrm{d}\mathbf{r}_3, \quad (\alpha = 0, 2, 4), \tag{151}$$

and

$$\widehat{c}^{(\alpha)} \equiv \left(\frac{1}{6}\right)^{\alpha/2} \int_V c(|\mathbf{r}_3|)|\mathbf{r}_3|^\alpha \mathrm{d}\mathbf{r}_3, \quad (\alpha = 0, 2, 4). \tag{152}$$

Then, the following relation is satisfied:

$$\widehat{c}^{(\alpha)} = \widehat{C}^{+(\alpha)} + \widehat{C}^{*(\alpha)}, \quad (\alpha = 0, 2, 4) \tag{153}$$

In Eq. (150), factors $\frac{9}{4}\rho_k \widehat{C}^{*(4)} \Delta_r \mathcal{P}(r)$ and $\frac{9}{4}\rho \widehat{c}^{(4)} \Delta_r \mathcal{H}(r)$ correspond to correction terms under the condition that the value of r is not large, although its value is out of the microscopic range in which $C^+(r) \neq 0$ and $C^*(r) \neq 0$ are satisfied.

(**b**) *Differential equations for two correlation functions*

If the correction terms in Eqs. (146) and (150) are ignored, then simple differential equations for $\mathcal{P}(r)$ and $\mathcal{H}(r)$ are given for a single-component fluid[47]. The differential equations are expressed as

$$\mathcal{P}(r) = \Big[1 - \rho \widehat{C}^{+(0)}\Big]^{-1} \Big[C^+(r) + \rho \widehat{C}^{+(2)} \nabla^2 \mathcal{P}(r)\Big] \tag{154}$$

and

$$\mathcal{H}(r) = \Big[1 - \rho \widehat{c}^{(0)}\Big]^{-1} \Big[C^*(r) + \rho \widehat{C}^{*(0)} \mathcal{P}(r) + \rho \widehat{C}^{*(2)} \nabla^2 \mathcal{P}(r) + \rho \widehat{c}^{(2)} \nabla^2 \mathcal{H}(r)\Big]. \tag{155}$$

In the two above differential equations, the behavior of the two differentiated correlation functions should be noted. Unless the condition of the fluid goes beyond the percolation threshold, the behavior of $\mathcal{P}(r)$, which satisfies a relation given by Eq. (48), allows $\nabla^2 \mathcal{P}(r)$ to satisfy

$$\lim_{V \to \infty} \rho \int_V \nabla^2 \mathcal{P}(r) \mathrm{d}\mathbf{r} = 0, \tag{156}$$

because of Gauss' theorem. Similarly, the behavior of $\mathcal{D}(r)$ $(= \mathcal{H}(r) + 1)$, which satisfies another relation given by Eq. (48), allows $\nabla^2 \mathcal{H}(r)$ to satisfy

$$\lim_{V \to \infty} \rho \int_V \nabla^2 \mathcal{H}(r) \mathrm{d}\mathbf{r} = 0. \tag{157}$$

Equations (156) and (157) should be satisfied, even at the percolation threshold. The relation should, however, result in failure if a fluid includes extremely large physical clusters developed under conditions beyond the percolation threshold.

If Eqs. (156) and (157) are satisfied, Fourier transforms of Eqs. (154) and (155) result in

$$\lim_{k \to 0} \widetilde{\mathcal{P}}(k) = \Big[1 - \rho \widehat{C}^{+(0)}\Big]^{-1} \lim_{k \to 0} \widetilde{C}^+(k) \tag{158}$$

and

$$\lim_{k \to 0} \widetilde{\mathcal{H}}(k) = \Big[1 - \rho \widehat{c}^{(0)}\Big]^{-1} \lim_{k \to 0} \Big[\widetilde{C}^*(k) + \rho \widehat{C}^{*(0)} \widetilde{\mathcal{P}}(k)\Big]. \tag{159}$$

Here, a Fourier transform of each correlation function is expressed as the form symbolized by Eq. (87). If a fluid does not include extremely large physical clusters developed under conditions beyond the percolation threshold, then the solutions obtained from Eqs. (154) and (155) satisfy Eqs. (158) and (159).

Fourier transforms of the integral equations given by Eqs. (49) and (52) should be compared with Eqs. (158) and (159), respectively. Their Fourier transforms allow Eqs. (49) and (52) to be rewritten as follows:

$$\lim_{k\to 0}\widetilde{\mathcal{P}}(k)=\lim_{k\to 0}\Big[1-\widetilde{C}^{+}(k)\Big]^{-1}\widetilde{C}^{+}(k), \tag{160}$$

and

$$\lim_{k\to 0}\widetilde{\mathcal{H}}(k)=\lim_{k\to 0}\Big[1-\widetilde{C}^{+}(k)-\widetilde{C}^{*}(k)\Big]^{-1}\Big[\widetilde{C}^{*}(k)+\widetilde{C}^{*}(k)\widetilde{\mathcal{P}}(k)\Big]. \tag{161}$$

These results denote that Eqs. (160) and (161) are equivalent to Eqs. (158) and (159), respectively, because $\widetilde{C}^{+}(0)=\rho\widehat{C}^{+(0)}$ and $\widetilde{C}^{*}(0)=\rho\widehat{C}^{*(0)}$ are satisfied.

A Fourier transform of the Ornstein–Zernike equation, given by Eq. (15) with Eqs. (16) and (17), allows a formula for a single-component fluid to be obtained as follows:

$$\lim_{k\to 0}\widetilde{h}(k)=\lim_{k\to 0}\Big[1-\widetilde{c}(k)\Big]^{-1}\widetilde{c}(k). \tag{162}$$

Here, an equation system formed by Eqs. (160) and (161) is equivalent to Eq. (162) because of relations $\widetilde{c}(k)=\widetilde{C}^{+}(k)+\widetilde{C}^{*}(k)$ and $\widetilde{h}(k)=\widetilde{\mathcal{P}}(k)+\widetilde{\mathcal{H}}(k)$.

This demonstrates that the compressibility that is estimated from $\mathcal{P}(r)$ and $\mathcal{H}(r)$ derived from Eqs. (154) and (155) is equivalent to that estimated from $\mathcal{P}(r)$ and $\mathcal{H}(r)$ derived from the two integral equations corresponding to Eqs. (49) and (52) unless a fluid includes extremely large physical clusters developed under conditions beyond the percolation threshold. The sum of two factors $\widetilde{\mathcal{P}}(0)+\widetilde{\mathcal{H}}(0)$ is expressed as

$$\widetilde{\mathcal{P}}(0)+\widetilde{\mathcal{H}}(0)\equiv\lim_{V\to\infty}\rho\int_{V}[g(r)-1]\mathrm{d}\mathbf{r}\quad(r\equiv|\mathbf{r}|).$$

Then, Eq. (18) allows the compressibility $(1/\beta)\big(\partial\rho/\partial P\big)_{V,T}$ of a single-component fluid to be given as follows:

$$\left[\beta\left(\frac{\partial P}{\partial\rho}\right)_{V,T}\right]^{-1}=\lim_{k\to 0}\Big[\widetilde{\mathcal{P}}(k)+\widetilde{\mathcal{H}}(k)\Big]+1. \tag{163}$$

Based on Eq. (163), the compressibility estimated from the two differential equations Eqs. (154) and (155) is equal to that estimated from the two integral equations Eqs. (49) and (52)

unless a fluid includes extremely large physical clusters developed under conditions beyond the percolation threshold.

When the compressibility is estimated from the use of Eq. (163), $\mathcal{P}(r)$ and $\mathcal{H}(r)$ estimated from Eqs. (154) and (155), respectively can be equivalent to $\mathcal{P}(r)$ and $\mathcal{H}(r)$ estimated from Eqs. (49) and (52), respectively. In this case, $\mathcal{P}(r)$ and $\mathcal{H}(r)$ given as solutions satisfying Eqs. (154) and (155) are adequate approximations for examining the cooperation between particles contributing to the magnitude of $\mathcal{P}(r)$ and particles contributing to the magnitude of $\mathcal{H}(r)$. Eqs (158) and (159), which are derived from the two differential equations given by Eqs. (154) and (155), allow the compressibility to be given by $(1/\beta)\big(\partial\rho/\partial P\big)_{V,T} = \big[1 - \rho\widehat{c}^{(0)}\big]^{-1}$. In addition, Eqs (160) and (161), which are derived from the two integral equations, allow the compressibility to be given by $(1/\beta)\big(\partial\rho/\partial P\big)_{V,T} = \big[1-\rho\widehat{c}(0)\big]^{-1}$ with $\rho\widehat{c}(0) = \rho\widehat{c}^{(0)}$. These estimates of the compressibility demonstrate that correlation functions $\mathcal{P}(r)$ and $\mathcal{H}(r)$ satisfying the two differential equations are equivalent to those which satisfy the two integral equations corresponding to Eqs. (49) and (52) unless a fluid includes extremely large physical clusters developed beyond the percolation threshold.

In addition, if Eqs. (160) and (161) are considered with $\widetilde{c}(0) = \widetilde{C}^{+}(0) + \widetilde{C}^{*}(0)$, Eq. (163) is rewritten as

$$\left[\beta\left(\frac{\partial P}{\partial \rho}\right)_{V,T}\right]^{-1} = \frac{\widetilde{C}^{+}(0)}{1-\widetilde{C}^{+}(0)} + \frac{\widetilde{C}^{*}(0) + \widetilde{C}^{*}(0)\widetilde{\mathcal{P}}(0)}{1-\widetilde{C}^{+}(0)-\widetilde{C}^{*}(0)} + 1 \tag{164}$$

$$= \frac{1}{1-\widetilde{C}^{+}(0)-\widetilde{C}^{*}(0)} \tag{165}$$

$$= \frac{1}{1-\rho\widehat{c}^{(0)}}. \tag{166}$$

The compressibility diverges to infinity at the liquid-vapor critical point. This denotes that relation $1 - \rho\widehat{c}^{(0)} = 0$ is then satisfied.

(**c**) *Solutions for differential equations*[48]

i) *Differential equations without terms including* $C^{+}(r)$, $C^{*}(r)$, $\rho\widehat{C}^{*(0)}$, *and* $\rho\widehat{C}^{*(2)}$

A solution $\mathcal{P}_0(r)$ that is obtained from Eq. (154) described without $C^{+}(r)$ must satisfy the following relation:

$$\Big[\nabla^2 - (\xi^{+})^2\Big]\mathcal{P}_0(r) = 0, \tag{167}$$

where the coefficient ξ^+ is defined as

$$\xi^+ \equiv \left(\frac{1 - \rho \widehat{C}^{+(0)}}{\rho \widehat{C}^{+(2)}} \right)^{1/2}. \tag{168}$$

The solution $\mathcal{P}_0(r)$ should satisfy a relation $\lim_{r\to\infty} \mathcal{P}_0(r) = 0$. Hence,

$$\mathcal{P}_0(r) = \mathcal{P}(\sigma^+) \frac{e^{-\xi^+(r-\sigma)}}{r/\sigma}, \tag{169}$$

$\mathcal{P}_0(r)$ satisfies the boundary condition $\lim_{\delta\to 0} \mathcal{P}_0(r)\big|_{r=\sigma+\delta} = \mathcal{P}(\sigma^+)$.

A solution $\mathcal{H}_0(r)$ that is obtained from Eq. (155) described without the three terms including $C^*(r)$, $\rho\widehat{C}^{*(0)}$, and $\rho\widehat{C}^{*(2)}$ must satisfy the following relation:

$$\Big[\nabla^2 - \xi^2\Big] \mathcal{H}_0(r) = 0, \tag{170}$$

where the coefficient ξ is defined as

$$\xi \equiv \left(\frac{1 - \rho \widehat{c}^{(0)}}{\rho \widehat{c}^{(2)}} \right)^{1/2}. \tag{171}$$

The solution $\mathcal{H}_0(r)$ should satisfy a relation $\lim_{r\to\infty} \mathcal{H}_0(r) = 0$. Hence,

$$\mathcal{H}_0(r) = \mathcal{H}(\sigma^+) \frac{e^{-\xi(r-\sigma)}}{r/\sigma}, \tag{172}$$

$\mathcal{H}_0(r)$ satisfies the boundary condition $\lim_{\delta\to 0} \mathcal{H}_0(r)\big|_{r=\sigma+\delta} = \mathcal{H}(\sigma^+)$.

ii) *Simple forms of Eqs. (154) and (155)*

If Eqs. (154) and (155) are rewritten, then simple forms of the differential equations are found. For Eq. (154),

$$\Big[\nabla^2 - (\xi^+)^2\Big] \mathcal{P}(r) = \breve{C}^+(r), \tag{173}$$

where

$$\breve{C}^+(r) \equiv \frac{1}{\rho \widehat{C}^{+(2)}} C^+(r). \tag{174}$$

For Eq. (155),

$$\Big[\nabla^2 - \xi^2\Big] \mathcal{H}(r) = \breve{C}^*(r), \tag{175}$$

where

$$\breve{C}^*(r) \equiv \frac{1}{\rho \widehat{c}^{(2)}} \Big\{ C^*(r) + \Big[\rho \widehat{C}^{*(0)} + \xi^{+2} \rho \widehat{C}^{*(2)}\Big] \mathcal{P}(r) - \frac{\widehat{C}^{*(2)}}{\widehat{C}^{+(2)}} C^+(r) \Big\}. \tag{176}$$

Then, coefficients $\rho\widehat{c}^{(0)}$ and $\rho\widehat{c}^{(2)}$ are obained from solving the Ornstein–Zernike equation. Coefficients $\widehat{C}^{*(0)}$ and $\rho\widehat{C}^{*(2)}$ are determined owing to Eq. (51) without solving integral equation Eq. (52). Coefficients $\rho\widehat{C}^{+(0)}$ and $\rho\widehat{C}^{+(2)}$ are estimated from solving integral equation Eq. (49). In addition, the above coefficients are estimated based on assuming that the characteristic of the pair potential contributing to the mutual attractive force between two particles is independent of the relative momentum of the two particles.

iii) *Solution for Eq. (173) with* $C^+(r) \neq 0$

In order to obtain exact solutions satisfying the differential equation Eq. (173), the fluid system should be imaginarily divided into the internal area of a spherical region of radius r and the external area of the spherical region. Then, the center of the spherical region is located at the origin $t = 0$ of a spherical coordinate.

A bound state where the contribution of the mutually attractive force between two particles exceeds the contribution of the relative kinetic energy is specified by an f^+-bond. The correlation that is generated between a particle at $t = 0$ and another particle at $t = r$ via at least one path of particles linked by only f^+-bonds is given by the sum of two partial contributions. One of the two partial contributions results from particles distributed inside a spherical region of radius r. This is estimated from the differential equation given by Eq. (173), and it is given by

$$\mathcal{P}_{\rm in}(r) = -\frac{\xi^+\sigma}{\rho\widehat{C}^{+(2)}/\sigma^2} h_0^{(1)}(i\xi^+ r) \int_\sigma^r \mathcal{G}(\xi^+;t) C^+(t) \left(\frac{t}{\sigma}\right)^2 \frac{1}{\sigma} {\rm d}t, \quad (t < r), \tag{177}$$

where $\mathcal{G}(\xi^+;t)$ is defined using the spherical Bessel function $j_0(\tau)$ and the spherical Hankel function of the first kind $h_0^{(1)}(\tau)$. The function $\mathcal{G}(\xi^+;t)$ is expressed as

$$\mathcal{G}(\xi^+;t) \equiv j_0(i\xi^+ t) - \frac{j_0(i\xi^+\sigma)}{h_0^{(1)}(i\xi^+\sigma)} h_0^{(1)}(i\xi^+ t), \tag{178}$$

where

$$j_0(\tau) = \tau^{-1}\sin\tau$$

and

$$h_0^{(1)}(\tau) = i\tau^{-1}e^{-i\tau}.$$

The remainder of the two partial contributions results from particles distributed outside the spherical region. This is estimated from the differential equation given by Eq. (173), and it is given by

$$\mathcal{P}_{\rm ex}(r) = -\frac{\xi^+\sigma}{\rho\widehat{C}^{+(2)}/\sigma^2}\mathcal{G}(\xi^+;r)\int_r^\infty h_0^{(1)}(i\xi^+t)C^+(t)\left(\frac{t}{\sigma}\right)^2\frac{1}{\sigma}{\rm d}t, \quad (r<t). \tag{179}$$

In Eqs. (177) and (179), the product $h_0^{(1)}\mathcal{G}$ can be expressed as follows:

$$h_0^{(1)}(i\xi^+r)\mathcal{G}(\xi^+;t) = -\frac{e^{-\xi^+(r-t)}}{2\xi^+r\xi^+t} + \left(1+\frac{2\sinh\xi^+\sigma}{e^{-\xi^+\sigma}}\right)\frac{e^{-\xi^+(r+t)}}{2\xi^+r\xi^+t}, \tag{180}$$

$$\mathcal{G}(\xi^+;r)h_0^{(1)}(i\xi^+t) = -\frac{e^{-\xi^+(t-r)}}{2\xi^+t\xi^+r} + \left(1+\frac{2\sinh\xi^+\sigma}{e^{-\xi^+\sigma}}\right)\frac{e^{-\xi^+(t+r)}}{2\xi^+t\xi^+r}. \tag{181}$$

The pair connectedness $\mathcal{P}(r)$ given as an exact solution satisfying Eq. (173) is expressed by the sum of Eqs. (169), (177) and (179), i.e.,

$$\mathcal{P}(r) = \mathcal{P}_0(r) + \mathcal{P}_{\rm in}(r) + \mathcal{P}_{\rm ex}(r). \tag{182}$$

Ultimately, Eq. (182) results in

$$\mathcal{P}(r) = \mathcal{P}_0(r) - \mathcal{M}^+\frac{e^{-\xi^+r}}{2\xi^+r} + \frac{e^{-\xi^+r}}{2\xi^+r}\int_\sigma^r e^{\xi^+t}\breve{C}^+(t)t{\rm d}t + \frac{e^{\xi^+r}}{2\xi^+r}\int_r^\infty e^{-\xi^+t}\breve{C}^+(t)t{\rm d}t, \tag{183}$$

where

$$\mathcal{M}^+ \equiv e^{2\xi^+\sigma}\int_\sigma^\infty \breve{C}^+(t)e^{-\xi^+t}t{\rm d}t. \tag{184}$$

If Eqs. (77), (78), (79), and (169) are considered, Eqs. (183) and (184) are estimated as follows:

$$\mathcal{P}(r) = -\widehat{\mathcal{M}}^+\frac{e^{-\xi^+r}}{2\xi^+r} + \frac{1}{2\xi^+r}\left[I^{(-)}(\sigma,r) + I^{(+)}(r,\infty)\right], \tag{185}$$

where

$$\widehat{\mathcal{M}}^+ \equiv -2\xi^+\sigma e^{-\xi^+\sigma}\mathcal{P}(\sigma^+) + \mathcal{M}^+, \tag{186}$$

$$\mathcal{M}^+ = \frac{\Xi_0}{(z^{(+)}\sigma)^{1/2}}e^{2\xi^+\sigma}\Gamma(1/2, z^{(+)}\sigma), \tag{187}$$

$$I^{(+)}(r,\infty) \equiv \Xi_0 e^{\xi^+r}\frac{1}{\sigma^{1/2}}\int_r^\infty e^{-z^{(+)}t}t^{-1/2}{\rm d}t, \tag{188}$$

$$I^{(-)}(\sigma, r) \equiv \Xi_0 e^{-\xi^+ r} \frac{1}{\sigma^{1/2}} \int_\sigma^r e^{-z^{(-)}t} t^{-1/2} \mathrm{d}t, \tag{189}$$

$$\Xi_0 \equiv \frac{4}{3\sqrt{\pi}} \frac{(\beta K e^{\kappa\sigma}/\sigma)^{3/2}}{\rho \widehat{C}^{+(2)}/\sigma^2}, \tag{190}$$

and

$$z^{(\pm)} \equiv \frac{3}{2}\kappa \pm \xi^+. \tag{191}$$

The integration expressed by Eq. (188) is performed as follows:

$$I^{(+)}(r, \infty) = \Xi_0 \frac{e^{-\xi^+ r}}{(z^{(+)}\sigma)^{1/2}} \left[\Gamma(1/2) - \gamma(1/2, z^{(+)}r)\right]. \tag{192}$$

Similarly, the integration expressed by Eq. (189) is performed. For $0 < z^{(-)}$,

$$I^{(-)}(\sigma, r) = \Xi_0 \frac{e^{-\xi^+ r}}{(z^{(-)}\sigma)^{1/2}} \left[\gamma(1/2, z^{(-)}r) - \gamma(1/2, z^{(-)}\sigma)\right], \tag{193}$$

and for $z^{(-)} \leq 0$,

$$\begin{aligned} I^{(-)}(\sigma, r) = \Xi_0 \Bigg[& \frac{e^{-(3/2)\kappa r}}{(-z^{(-)}\sigma)^{1/2}(-z^{(-)}r)^{1/2}} \Phi(-z^{(-)}r) \\ & - \frac{e^{-\xi^+ r} e^{-z^{(-)}\sigma}}{(-z^{(-)}\sigma)^{1/2}(-z^{(-)}\sigma)^{1/2}} \Phi(-z^{(-)}\sigma) \Bigg], \end{aligned} \tag{194}$$

where

$$\Phi(-\zeta r) \equiv \sum_{k=1}^{\infty} (-1)^{k-1} \frac{(-2\zeta r)^k}{(2k-1)!!}, \quad (\zeta \leq 0). \tag{195}$$

In addition, Ξ_0 is a dimensionless coefficient. Coefficients $\widehat{C}^{+(0)}$ and $\widehat{C}^{+(2)}$ are estimated by using Eqs. (120) and (121), respectively.

iv) *Solution for Eq. (175) with* $\breve{C}^*(r) \neq 0$

In order to obtain exact solutions satisfying differential equation Eq. (175), the fluid system should be imaginarily divided into the internal area of a spherical region of radius r and the external area of the spherical region. Then, the center of the spherical region is located at the origin $t = 0$ of a spherical coordinate.

An unbound state where the contribution of the relative kinetic energy of two particles exceeds the contribution of the mutually attractive force is specified by an f^*-bond. The

correlation that is generated between a particle at $t = 0$ and another particle at $t = r$ via particles linked through each path that includes f^*-bonds is given by the sum of two partial contributions. One of the two partial contributions comes from particles distributed within a spherical region of radius r with its center located at the origin, $t = 0$. This is estimated from the differential equation given by Eq. (175), and it can be divided into two parts as $\breve{C}^*(r)$ is defined by Eq. (176). One part involves the effects of physical cluster formation and is given by

$$\begin{aligned}\mathcal{H}_{\rm in}^{(+)}(r) =& -\frac{\xi\sigma}{\rho\widehat{C}^{(2)}/\sigma^2}h_0^{(1)}(i\xi r)\int_\sigma^r \mathcal{G}(\xi;t) \\ &\times\left\{\left[\rho\widehat{C}^{*(0)}+\xi^{+2}\rho\widehat{C}^{*(2)}\right]\mathcal{P}(t)-\frac{\widehat{C}^{*(2)}}{\widehat{C}^{+(2)}}C^+(t)\right\}\left(\frac{t}{\sigma}\right)^2\frac{1}{\sigma}{\rm d}t, \quad (t<r). \end{aligned} \tag{196}$$

The other part is non-zero even if physical clusters do not exist, and it is given by

$$\mathcal{H}_{\rm in}^{(*)}(r) = -\frac{\xi\sigma}{\rho\widehat{C}^{(2)}/\sigma^2}h_0^{(1)}(i\xi r)\int_\sigma^r \mathcal{G}(\xi;t)C^*(t)\left(\frac{t}{\sigma}\right)^2\frac{1}{\sigma}{\rm d}t, \quad (t<r). \tag{197}$$

The remainder of the two partial contributions results from particles distributed outside the spherical region. This is estimated from the differential equation given by Eq. (175), and it can be divided into two parts as $\breve{C}^*(r)$ is defined by Eq. (176). One part involves effects of the physical cluster formation and is given by

$$\begin{aligned}\mathcal{H}_{\rm ex}^{(+)}(r) =& -\frac{\xi\sigma}{\rho\widehat{C}^{(2)}/\sigma^2}\mathcal{G}(\xi;r)\int_r^\infty h_0^{(1)}(i\xi t) \\ &\times\left\{\left[\rho\widehat{C}^{*(0)}+\xi^{+2}\rho\widehat{C}^{*(2)}\right]\mathcal{P}(t)-\frac{\widehat{C}^{*(2)}}{\widehat{C}^{+(2)}}C^+(t)\right\}\left(\frac{t}{\sigma}\right)^2\frac{1}{\sigma}{\rm d}t, \quad (r<t). \end{aligned} \tag{198}$$

The other part is nonzero even if physical clusters do not exist, and it is given by

$$\mathcal{H}_{\rm ex}^{(*)}(r) = -\frac{\xi\sigma}{\rho\widehat{C}^{(2)}/\sigma^2}\mathcal{G}(\xi;r)\int_r^\infty h_0^{(1)}(i\xi t)C^*(t)\left(\frac{t}{\sigma}\right)^2\frac{1}{\sigma}{\rm d}t, \quad (r<t). \tag{199}$$

In Eqs. (196), (197), (198), and (199), the product $h_0^{(1)}\mathcal{G}$ has the same form as that expressed by Eqs. (180) and (181).

The correlation function $\mathcal{H}(r)$ given as an exact solution satisfying Eq. (155) is expressed as the sum of Eqs. (172), (196), (197), (198), and (199), i.e.,

$$\mathcal{H}(r) = \mathcal{H}_0(r) + \mathcal{H}_{\rm in}^{(+)}(r) + \mathcal{H}_{\rm ex}^{(+)}(r) + \mathcal{H}_{\rm in}^{(*)}(r) + \mathcal{H}_{\rm ex}^{(*)}(r). \tag{200}$$

Thus, if relation given by Eq. (176) is considered, Eq. (200) allows the correlation function $\mathcal{H}(r)$ to be given as follows:

$$\mathcal{H}(r) = \mathcal{H}_0(r) - \mathcal{M}^*\frac{e^{-\xi r}}{2\xi r} + \frac{e^{-\xi r}}{2\xi r}\int_\sigma^r e^{\xi t}\breve{C}^*(t)t{\rm d}t + \frac{e^{\xi r}}{2\xi r}\int_r^\infty e^{-\xi t}\breve{C}^*(t)t{\rm d}t, \tag{201}$$

where

$$\mathcal{M}^* \equiv e^{2\xi\sigma} \int_{\sigma}^{\infty} \breve{C}^{*}(t) e^{-\xi t} t \mathrm{d}t. \tag{202}$$

In addition, the coefficients $\widehat{c}^{(0)}$, $\widehat{C}^{*(0)}$, $\widehat{c}^{(2)}$, and $\widehat{C}^{*(2)}$ are estimated from using Eqs. (120), (121), (139), and (140) with Eq. (153).

If the physical cluster formation is ignored, then correlation functions satisfy $\mathcal{P}(r) = 0$, $C^{+}(r) = 0$, and $\breve{C}^{*}(r) = C^{*}(r)/(\rho\widehat{c}^{(2)})$ for $0 < r$. The pair correlation function $g(r)$ is related to $\mathcal{H}(r)$ as $g(r) = \mathcal{P}(r) + \mathcal{H}(r) + 1$. When the physical cluster formation is ignored with a requirement $\xi = 0$, the relationship between $g(r)$ and $\mathcal{H}(r)$ allows Eq. (201) to result in

$$\begin{aligned} g_0(r) - 1 &= \mathcal{H}(r) \\ &= \mathcal{H}(\sigma^{+})\frac{\sigma}{r} + \left(\frac{\beta K e^{\kappa\sigma}/\sigma}{\kappa\sigma\rho\widehat{c}^{(2)}/\sigma^2}\right)\frac{e^{-\kappa\sigma} - e^{-\kappa r}}{\kappa r}, \quad (\text{for } 1 \ll r/\sigma), \end{aligned} \tag{203}$$

where $g_0(r)$ denotes $g(r)$ satisfying the requirement formed by both $\xi = 0$ and no contribution of physical clusters. Equation (203) obtained from the requirement formed by no physical clusters and $\xi = 0$ allows the behavior of $g_0(r) - 1$ for a large r to be approximately expressed by $g_0(r) - 1 \sim r^{-1}$.

7. Features of correlation functions near critical point[48]

(a) *Effects of physical cluster formation on behavior of correlation functions*

When the compressibility given as $(1/\beta)\big(\partial\rho/\partial P\big)_{V,T} = 1/(1-\rho\widehat{c}^{(0)})$ diverges to infinity, the coefficient ξ becomes zero. This does not mean that the coefficient ξ^+ becomes zero because the critical point does not generally coincide with the percolation threshold that results in $\xi^+ = 0$. Hence, the coefficient ξ^+ can have a finite value that is nonzero even when ξ becomes zero. Considering this, estimation of Eq. (201) must be performed in the general conditions that $\xi \neq 0$ is satisfied and the contributions of physical clusters are involved.

Equation (201) includes many terms of integration because $\breve{C}^*(t)$ is defined by Eq. (176) with $\mathcal{P}(t)$ given by Eq. (185). To express Eq. (201) in a simple manner, a function $\Delta_{(\zeta)}(a,b)$, which is dimensionless, is defined as follows:

$$\Delta_{(\zeta)}(a,b) \equiv \frac{1}{\sigma^{1/2}}\int_a^b e^{-\zeta t}t^{-1/2}\mathrm{d}t \tag{204}$$

For $0 < \zeta$,

$$\Delta_{(\zeta)}(a,b) = \frac{1}{(\zeta\sigma)^{1/2}}\Big[\gamma\left(1/2,\zeta b\right) - \gamma\left(1/2,\zeta a\right)\Big]. \tag{205}$$

For $0 < \zeta$ and large ζa, $\lim_{b\to\infty}\Delta_{(\zeta)}(a,b)$ behaves as follows:

$$\lim_{b\to\infty}\Delta_{(\zeta)}(a,b) \approx \frac{1}{\sqrt{\zeta\sigma}}\frac{1}{\sqrt{\zeta a}}e^{-\zeta a}. \tag{206}$$

For $\zeta \leq 0$,

$$\Delta_{(\zeta)}(a,b) = \frac{1}{-\zeta\sigma}\left[\left(\frac{\sigma}{b}\right)^{1/2}e^{-\zeta b}\Phi(-\zeta b) - \left(\frac{\sigma}{a}\right)^{1/2}e^{-\zeta a}\Phi(-\zeta a)\right], \tag{207}$$

where $\Phi(-\zeta r)$ is defined by Eq. (195).

Eq. (201) includes integration expressed in a specific form. If the integral is expressed as $I_{(\pm\xi)}(\breve{C}^*;a,b)$, then it is dimensionless and is given as

$$I_{(\mp\xi)}(\breve{C}^*;a,b) \equiv \int_a^b e^{-(\mp\xi)t}\breve{C}^*(t)t\mathrm{d}t. \tag{208}$$

Then, the use of $\Delta_{(\zeta)}(a,b)$ allows the substitution of Eq. (176) into Eq. (208) to result in

$$\begin{aligned} I_{(\mp\xi)}(\breve{C}^*;a,b) = \frac{\sigma^2}{\rho\widehat{C}^{(2)}}\Bigg\{ & \frac{\beta K e^{\kappa\sigma}/\sigma}{-z_\kappa^{(\mp\xi)}\sigma}\left[\exp(-z_\kappa^{(\mp\xi)}b) - \exp(-z_\kappa^{(\mp\xi)}a)\right] \\ & -\frac{4}{3\sqrt{\pi}}(\beta K e^{\kappa\sigma}/\sigma)^{3/2}\frac{\widehat{C}^{*(2)}}{\widehat{C}^{+(2)}}\Delta_{(z_{3/2}^{(\mp\xi)})}(a,b) + [\rho\widehat{C}^{*(0)} + (\xi^+\sigma)^2\rho\widehat{C}^{*(2)}/\sigma^2] \\ & \times\Big[-\mathcal{J}_{\widehat{\mathcal{M}}^+}^{(\mp\xi)}(a,b) + \mathcal{J}_{I^-}^{(\mp\xi)}(a,b) + \mathcal{J}_{I^+}^{(\mp\xi)}(a,b)\Big]\Bigg\}, \end{aligned} \tag{209}$$

where

$$\mathcal{J}^{(\mp\xi)}_{\widehat{\mathcal{M}}^+}(a,b)\equiv \frac{\widehat{\mathcal{M}}^+}{2\xi^+\sigma^2}\int_a^b \exp(-z^{(\mp\xi)}t)\mathrm{d}t$$
$$= \frac{\widehat{\mathcal{M}}^+}{2\xi^+\sigma}\frac{1}{(-z^{(\mp\xi)}\sigma)}\left[\exp(-z^{(\mp\xi)}b)-\exp(-z^{(\mp\xi)}a)\right], \tag{210}$$

$$\mathcal{J}^{(\mp\xi)}_{I^-}(a,b) \equiv \frac{1}{2\xi^+\sigma^2}\int_a^b \exp[-(\mp\xi)t]I^-(\sigma,t)\mathrm{d}t$$
$$=\frac{\Xi_0}{2\xi^+\sigma}\frac{1}{(-z^{(\mp\xi)}\sigma)}\left[\exp(-z^{(\mp\xi)}b)\Delta_{(z^{(-)})}(\sigma,b)-\exp(-z^{(\mp\xi)}a)\Delta_{(z^{(-)})}(\sigma,a)\right]$$
$$-\frac{\Xi_0}{2\xi^+\sigma}\frac{1}{(-z^{(\mp\xi)}\sigma)}\Delta_{(z^{(\mp\xi)}_{3/2})}(a,b), \tag{211}$$

and

$$\mathcal{J}^{(\mp\xi)}_{I^+}(a,b) \equiv \frac{1}{2\xi^+\sigma^2}\int_a^b \exp[-(\mp\xi t)]I^+(t,\infty)\mathrm{d}t$$
$$=\frac{\Xi_0}{2\xi^+\sigma}\frac{1}{z^{(\pm\xi)}\sigma}\left[\exp(z^{(\pm\xi)}b)\Delta_{(z^{(+)})}(b,\infty)-\exp(z^{(\pm\xi)}a)\Delta_{(z^{(+)})}(a,\infty)\right]$$
$$+\frac{\Xi_0}{2\xi^+\sigma}\frac{1}{z^{(\pm\xi)}\sigma}\Delta_{(z^{(\mp\xi)}_{3/2})}(a,b), \tag{212}$$

with

$$z^{(\pm\xi)}_{3/2}\equiv \frac{3}{2}\kappa\pm\xi, \tag{213}$$
$$z^{(\pm\xi)}_{\kappa}\equiv \kappa\pm\xi, \tag{214}$$
$$z^{(\pm\xi)}\equiv \xi^+\pm\xi. \tag{215}$$

$z^{(\pm)}$ is defined by Eq. (191). If $I_{(\pm\xi)}(\breve{C}^*;a,b)$ given by Eq. (209) is used, then Eq. (201) is exactly estimated as follows:

$$\mathcal{H}(r)=\mathcal{H}_0(r)-e^{2\xi\sigma}\frac{e^{-\xi r}}{2\xi r}I_{(+\xi)}(\breve{C}^*;\sigma,\infty)+\frac{e^{-\xi r}}{2\xi r}I_{(-\xi)}(\breve{C}^*;\sigma,r)+\frac{e^{\xi r}}{2\xi r}I_{(+\xi)}(\breve{C}^*;r,\infty), \tag{216}$$

where $\mathcal{H}_0(r)$ is given by Eq. (172).

The behavior of a correlation function $g(r)-1$ is expressed by the sum of Eq. (185) and Eq. (216). The sum is given as follows:

$$g(r)-1 =\mathcal{H}(\sigma^+)\frac{e^{-\xi(r-\sigma)}}{r/\sigma}-\widehat{\mathcal{M}}^+\frac{e^{-\xi^+ r}}{2\xi^+ r}+\frac{1}{2\xi^+ r}\left[I^{(-)}(\sigma,r)+I^{(+)}(r,\infty)\right]$$
$$-e^{2\xi\sigma}\frac{e^{-\xi r}}{2\xi r}I_{(+\xi)}(\breve{C}^*;\sigma,\infty)+\frac{e^{-\xi r}}{2\xi r}I_{(-\xi)}(\breve{C}^*;\sigma,r)+\frac{e^{\xi r}}{2\xi r}I_{(+\xi)}(\breve{C}^*;r,\infty). \tag{217}$$

Equation (217) is adequate even when $0 \leq \xi$ and $0 \leq \xi^+$ are both satisfied. A point on the spinodal curve where $\xi\sigma = 0$ ($\sigma > 0$) is satisfied corresponds a critical condition before the occurrence of a phase separation. At the critical point corresponding to the maximum point on the spinodal curve, $\xi\sigma = 0$ is satisfied. The condition where $\xi^+\sigma = 0$ is specified corresponds to the percolation threshold; hence, the mean size of physical clusters at $\xi^+\sigma = 0$ reaches the maximum infinity.

(b) *Dependence of behavior of correlation functions on physical cluster formation*

Even in a specific condition where $\xi\sigma = 0$ and $0 \leq \xi^+\sigma$ are satisfied, Eq. (217) is adequate. In this condition, Eq. (217) allows the estimation of $g(r)-1$. Hence, the behavior of $g(r)-1$ for a large r satisfying $1 \ll (r-\sigma)/\sigma$ can be expressed even at the critical point by Eq. (217).

Because $\beta\big(\partial P/\partial\rho\big)_{V,T} = 0$ is satisfied at every point on the spinodal curve specified in the phase diagram of a fluid, $\xi\sigma$ given by Eqs. (166) and (171) equals zero ($\sigma \neq 0$) on the spinodal curve. If the maximum point of the spinodal curve is a point specified by $T = T_{\rm c}$ and $\phi = \phi_{\rm c}$, the liquid–vapor critical point correspond to a point represented by $[T_{\rm c},\, \phi_{\rm c}]$. Here, ϕ represents the volume fraction defined as $\phi \equiv (\pi/6)\rho\sigma^3$.

The relation $\xi^+\sigma = 0$ ($\sigma \neq 0$) is satisfied at every point on the curved line that expresses the percolation threshold in the phase diagram. The mean physical cluster size $\mathcal{S}$ given by Eq. (93) is related to ξ^+ because of Eqs. (120) and (168) as

$$\xi^+ = \Big(\mathcal{S}\rho\widehat{C}^{+(2)}\Big)^{-1/2}. \tag{218}$$

Hence, every specific condition where $\xi^+\sigma = 0$ is satisfied corresponds to the percolation threshold.

If physical clusters do not exist at the critical point, i.e., $[T_{\rm c},\, \phi_{\rm c}]$, then $g(r)$ given by Eq. (217) becomes equivalent to $g_0(r)$ given by Eq. (203). If $\mathcal{P}(r) = 0$ and $C^+(r) = 0$ are satisfied independently of r, then $g(r)$ expressed for $\xi\sigma = 0$ by Eq. (217) becomes equivalent to $g_0(r)$ expressed by Eq. (203). When $\mathcal{P}(r) = 0$ and $C^+(r) = 0$ are satisfied independently of r, the fluid system includes no physical clusters. Thus, the behavior of $g(r)$ that is equivalent to $g_0(r)$ is characterized by $g(r) - 1 \sim r^{-1}$ for a large r satisfying $1 \ll (r-\sigma)/\sigma$.

For a Yukawa fluid characterized by a specific value of $\kappa\sigma$, the spinodal curve coincides at two points with the curved line. If one of them is specified by $[T_{\rm p}, \phi_{\rm p}]$, the other is

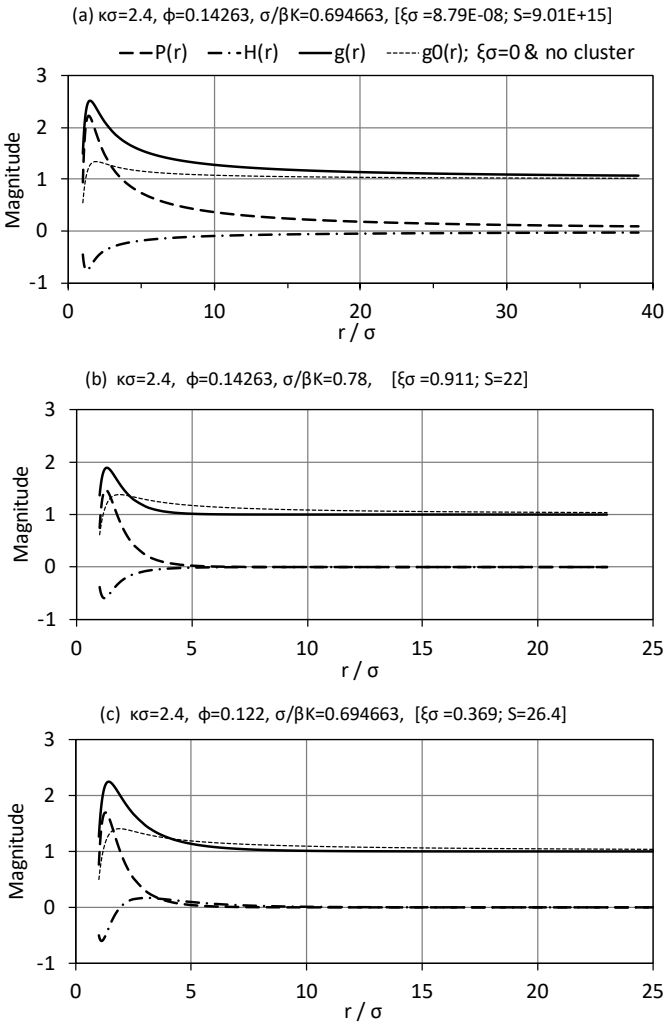

FIG. 17. Dependences of $\mathcal{P}(r)$, $\mathcal{H}(r)$, $g(r)$, and $g_0(r)$ on r for $\kappa\sigma = 2.4$ $(f_\nu = 0.101853)$. Each curved line is evaluated according to Eqs. (185), (216), (217), and (203). A point at which the percolation threshold coincide with the spinodal curve is located at $[T_\mathrm{p}, \phi_\mathrm{p}]$; the critical point is the locus specified by $T_\mathrm{c} \approx T_\mathrm{p}$, and $\phi_\mathrm{c} \approx \phi_\mathrm{p} + 0.032$. In (a), each curved line is obtained for $\sigma/\beta K = 0.694663$ and $\phi = 0.14263$ which correspond to $T \approx T_\mathrm{p}$ and $\phi \approx \phi_\mathrm{p}$; the fluid is characterized by $[\mathcal{S} = 9.01 \times 10^{15}, \xi\sigma = 8.79 \times 10^{-8}]$. In (b), each curved line is obtained for $\sigma/\beta K = 0.78$ and $\phi = 0.14263$ whcih corresponds to $T > T_\mathrm{p}$ and $\phi \approx \phi_\mathrm{p}$; the fluid is characterized by $[\mathcal{S} = 22$, $\xi\sigma = 0.911]$. In (c), each curved line is obtained for $\sigma/\beta K = 0.694663$ and $\phi = 0.122$ which corresponds to $T \approx T_\mathrm{p}$ and $\phi \approx \phi_\mathrm{p} - 0.206$; the fluid is characterized by $[\mathcal{S} = 26.4$, $\xi\sigma = 0.369]$.

specified by $[T_{\rm p}', \phi_{\rm p}']$, and the relationship between them satisfy $T_{\rm p}' < T_{\rm p}$ and $\phi_{\rm p}' < \phi_{\rm p}$. For $\kappa\sigma = 1.6$ characterizing a mutual attractive force with a more long-ranged feature than that for $\kappa\sigma = 1.8$, $T_{\rm p} \approx T_{\rm c}$ and $(\phi_{\rm p} - \phi_{\rm c})/\phi_{\rm c} \approx 0.14$ are satisfied. For $\kappa\sigma = 1.8$ characterizing a mutual attractive force with a less long-ranged feature than that for $\kappa\sigma = 1.6$, $T_{\rm p} \approx T_{\rm c}$ and $(\phi_{\rm p} - \phi_{\rm c})/\phi_{\rm c} \approx 0.05$ are satisfied. For $\kappa\sigma = 2.4$ characterizing a mutual attractive force with a less long-ranged feature than that for $\kappa\sigma = 1.8$, $T_{\rm p} \approx T_{\rm c}$ and $(\phi_{\rm p} - \phi_{\rm c})/\phi_{\rm c} \approx -0.18$ are satisfied.

If physical clusters exist at the critical point, then the behavior of the pair correlation function for a large r must deviate from $g(r) - 1 \sim r^{-1}$. Then, the relationship between $g(r)$ given by Eq. (217) and $g_0(r)$ given by Eq. (203) is characterized by $g(r) \neq g_0(r)$. The behavior of $g(r)$ expressed by subfigure (a) in Figs. 17, 18, and 19 demonstrates that relation $g(r) > g_0(r)$ is satisfied at a point near the spinodal curve where $0 < \xi\sigma \ll 1$ is satisfied. Even in a fluid system including only small sizes of physical clusters, relation $g(r) > g_0(r)$ is satisfied near such a point ($\xi\sigma \approx 0$) over a wide range of r as exemplified by subfigure (a) in Fig. 19. Thus, the formation of physical clusters at the critical point of a fluid can allow $g(r)$ to become more long-ranged than $g_0(r)$.

If values of parameters for a fluid system deviate from their values that yield $\xi \approx 0$ near the critical point, then $g_0(r)$ that is equivalent to $g(r)$ evaluated for $\xi\sigma = 0$ with no contribution of physical clusters can decay at a slower rate than $g(r)$ decays. As a consequence, relation $g(r) < g_0(r)$ for a large r can be found. This can be confirmed by each figure of (b) in Figs. 17, 18, and 19. Unless $\xi\sigma$ is sufficiently small, relation $g(r) < g_0(r)$ for a large r can occur even for a small $\xi\sigma$ as exemplified by figure (b) in Fig. 19.

Unless $\xi\sigma$ is sufficiently small, relation $g(r) < g_0(r)$ for a large r can occur even for a fluid system that includes extremely large physical clusters. This is confirmed from each figure (a) in Figs. 20 and 21. The value of $\xi\sigma$ that is not sufficiently small aids in making $g(r)$ decay rapidly. Even if values of parameters characterizing the fluid system allow $\xi^+\sigma \approx 0$, their values cannot allow the value of $\xi\sigma$ to be sufficiently small. Hence, relation $g(r) < g_0(r)$ occurs as demonstrated by each figure (a) in Figs. 20 and 21 although large physical clusters are included in the fluids.

Ultimately, a fluid system that allows relation $g_0(r) < g(r)$ to occur requires that values of parameters characterizing the fluid system cause $0 \leq \xi\sigma \ll 1$, i.e., a sufficiently small magnitude and cause $1/(\xi^+\sigma) \neq 0$. The mean physical cluster size $\mathcal{S}$ given by Eq. (93) is

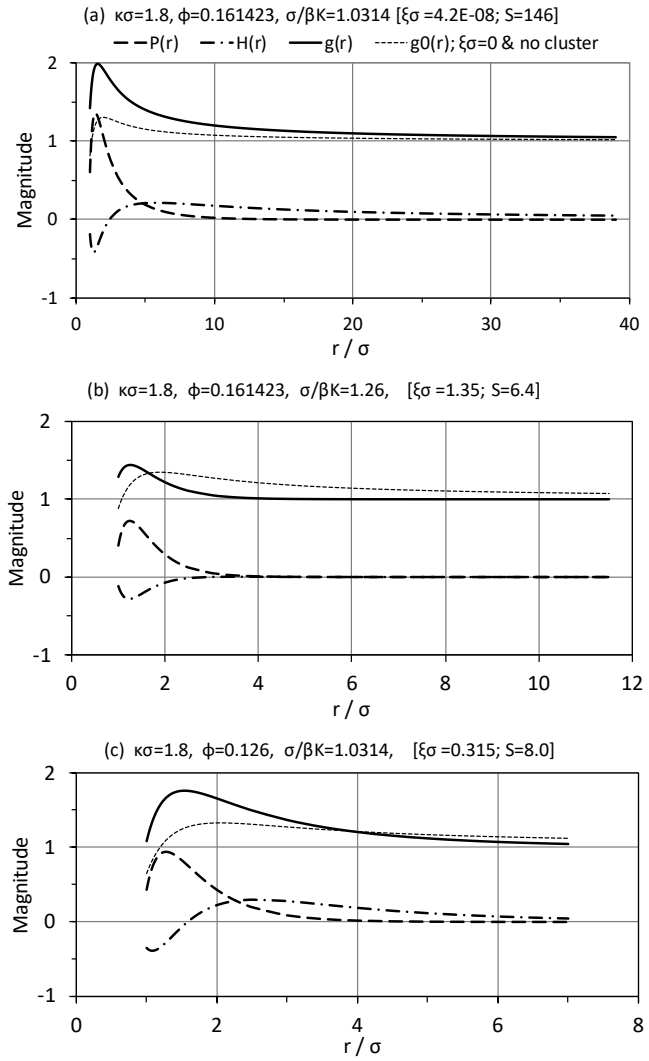

FIG. 18. Dependences of $\mathcal{P}(r)$, $\mathcal{H}(r)$, $g(r)$, and $g_0(r)$ on r for $\kappa\sigma = 1.8$ $(f_\nu = 0.101853)$. Each curved line is evaluated on basis of Eqs. (185), (216), (217), and Eq. (203). The critical point is the locus specified by $T_{\rm c} \approx T_{\rm p}$, and $\phi_{\rm c} \approx \phi_{\rm p} - 0.008$. In (a), each curved line is obtained for $\sigma/\beta K = 1.0314$ and $\phi = 0.161423$ which correspond to $T \approx T_{\rm p}$ and $\phi \approx \phi_{\rm p} - 0.008$; the fluid is characterized by $[\mathcal{S} = 146, \xi\sigma = 4.2 \times 10^{-8}]$. In (b), each curved line is obtained for $\sigma/\beta K = 1.26$ and $\phi = 0.161423$ which corresponds to $T > T_{\rm p}$ and $\phi \approx \phi_{\rm p} - 0.008$; the fluid is characterized by $[\mathcal{S} = 6.4, \xi\sigma = 1.35]$. In (c), each curved line is obtained for $\sigma/\beta K = 1.0314$ and $\phi = 0.126$ which corresponds to $T \approx T_{\rm p}$ and $\phi \approx \phi_{\rm p} - 0.035$; the fluid is characterized by $[\mathcal{S} = 6.4, \xi\sigma = 1.35]$.

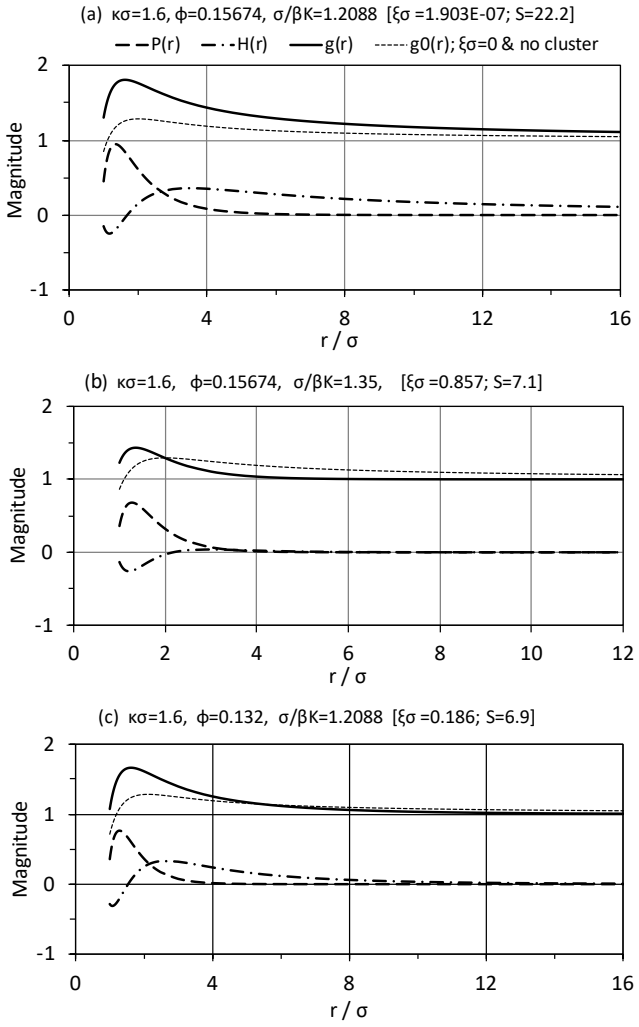

FIG. 19. Behaviors of $\mathcal{P}(r)$, $\mathcal{H}(r)$, $g(r)$, and $g_0(r)$ for $\kappa\sigma = 1.6$ $(f_\nu = 0.101853)$. Each curved line is evaluated on basis of Eqs. (185), (216), (217), and Eq. (203). In (a), each curved line is obtained for $\sigma/\beta K = 1.2088$ and $\phi = 0.15674$ which correspond to $T > T_{\rm p}$ and $\phi \approx \phi_{\rm p} - 0.02$; the critical point is the locus specified by $T_{\rm c} \approx T$ and $\phi_{\rm c} \approx \phi$; the fluid is characterized by $[\mathcal{S} = 22.2,\, \xi\sigma = 1.903\times 10^{-7}]$. In (b), each curved line is obtained for $\sigma/\beta K = 1.35$ and $\phi = 0.15674$ which corresponds to $T > T_{\rm p}$, $T > T_{\rm c}$, and $\phi \approx \phi_{\rm p} - 0.02$; the fluid is characterized by $[\mathcal{S} = 7.1,\, \xi\sigma = 0.857]$. In (c), each curved line is obtained for $\sigma/\beta K = 1.2088$ and $\phi = 0.132$ which corresponds to $T > T_{\rm p}$, $T \approx T_{\rm c}$, and $\phi \approx \phi_{\rm p} - 0.046$; the fluid is characterized by $[\mathcal{S} = 7.1,\, \xi\sigma = 0.857]$.

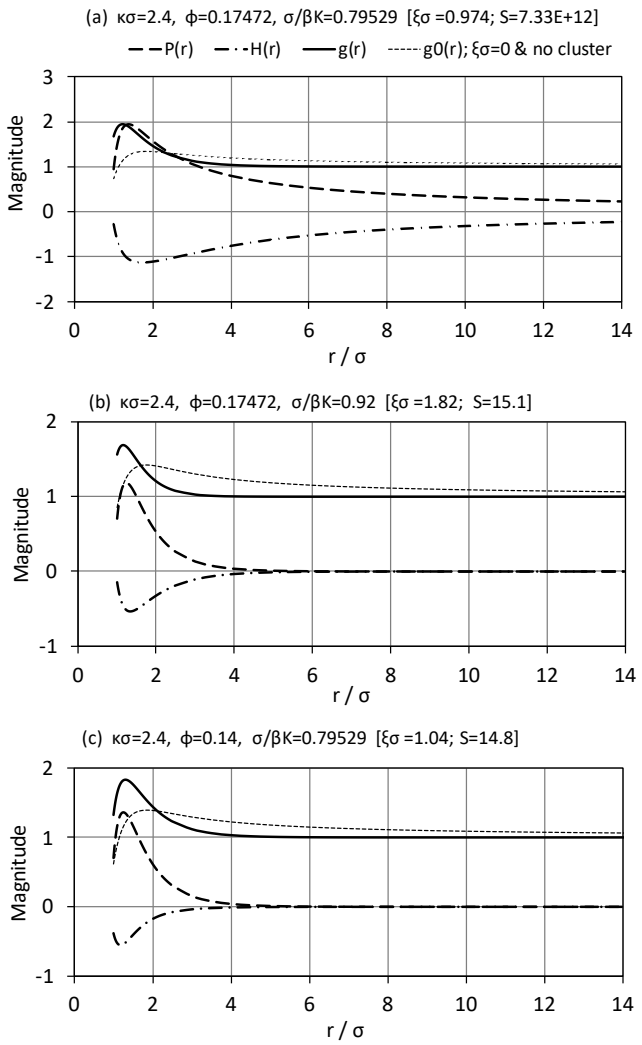

FIG. 20. Dependences of $\mathcal{P}(r)$, $\mathcal{H}(r)$, $g(r)$, and $g_0(r)$ on r for $\kappa\sigma = 2.4$ $(f_\nu = 0.101853)$ in loci far from critical point. Evaluations are based on Eqs. (185), (216), (217), and Eq. (203). In (a), each curved line is obtained for $\sigma/\beta K = 0.79529$ and $\phi = 0.17472$; the fluid condition is characterized as $T \approx T_{\rm p}$, $\phi \approx \phi_{\rm p}$, $T_{\rm c} < T$, and $\phi_{\rm c} \approx \phi$; features of the fluid are $[\mathcal{S} = 7.33 \times 10^{12}, \xi\sigma = 0.974]$. In (b), each curved line is obtained for $\sigma/\beta K = 0.92$ and $\phi = 0.17472$; the fluid condition is characterized as $T > T_{\rm p}$, $\phi \approx \phi_{\rm p}$, $T_{\rm c} < T$, and $\phi \approx \phi_{\rm c}$; features of the fluid are $[\mathcal{S} = 15.1, \xi\sigma = 1.82]$. In (c), each curved line is obtained for $\sigma/\beta K = 0.79529$ and $\phi = 0.14$; the fluid condition is characterized as $T \approx T_{\rm p}$, $\phi \approx \phi_{\rm p} - 0.026$, $T_{\rm c} < T$, and $\phi \approx \phi_{\rm c} - 0.026$; features of the fluid are $[\mathcal{S} = 14.8, \xi\sigma = 1.04]$.

related to ξ^+ by Eq. (218). This demonstrates that the occurrence of relation $g_0(r) < g(r)$ for a large r requires $\mathcal{S} \neq 0$ and $\xi\sigma \ll 1$. A condition specified by $\mathcal{S} \neq 0$ and $\xi\sigma \ll 1$ causes the behavior of $g(r)$ that cannot be expressed as the product of r^{-1} and a particular function given by a series with respect to positive powers of r.

Even if physical clusters formed in a fluid system is small, their formation causes the dependence of the pair correlation function on r to deviate from the dependence that is expressed by $g_0(r)$. To explain the deviation from its behavior expressed as $g(r) - 1 \sim r^{-1}$,[18] the contribution of the presence of physical clusters to $g(r)$ should not be ignored. Representing the pair correlation function as the sum of two correlation functions contributes to explaining critical phenomena if the presence of physical clusters is not ignored. In addition, effects yielded by a decrease in ϕ and effects yielded by a decrease in $(\sigma/\beta K)^{-1}$ can have similarities. This fact is exemplified by the behaviors of the correlation functions seen in Figs. 17, 20 and 21.

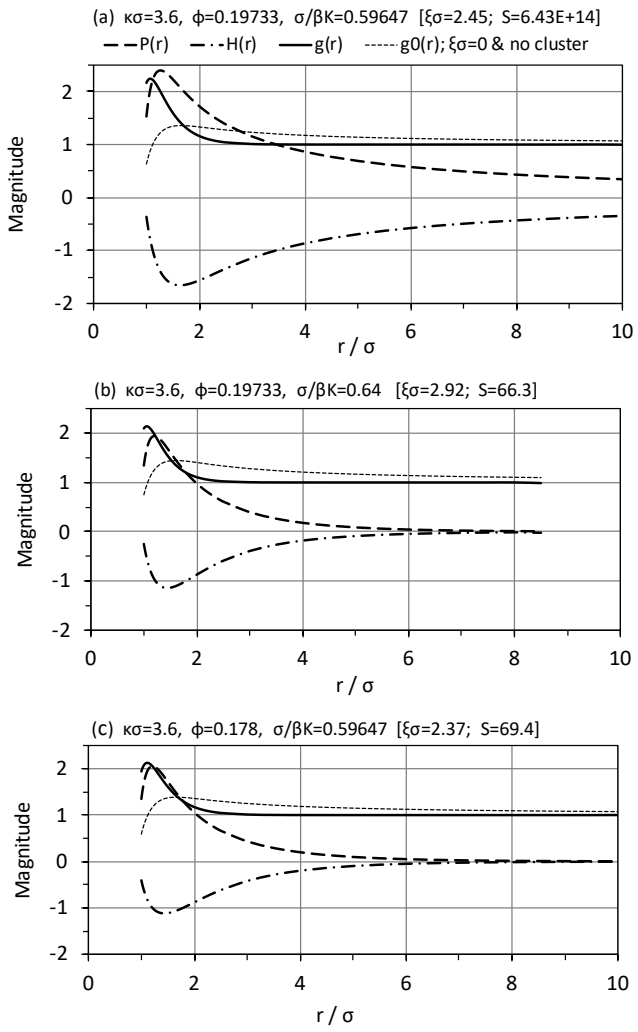

FIG. 21. Dependences of $\mathcal{P}(r)$, $\mathcal{H}(r)$, and $g(r)$ on r for $\kappa\sigma = 3.6$ $(f_\nu = 0.101853)$. Evaluations are based on Eqs. (185), (216), (217), and Eq. (203). In (a), each curved line is obtained for $\sigma/\beta K = 0.59647$ and $\phi = 0.19733$; the fluid condition is characterized as $T \approx T_{\rm p}$, $\phi \approx \phi_{\rm p}$, $T_{\rm c} < T$, and $\phi_{\rm c} \approx \phi$; features of the fluid are $[\mathcal{S} = 6.43 \times 10^{14}$, $\xi\sigma = 2.45]$. In (b), each curved line is obtained for $\sigma/\beta K = 0.64$ and $\phi = 0.19733$; the fluid condition is characterized as $T > T_{\rm p}$, $\phi \approx \phi_{\rm p}$, $T_{\rm c} < T$, and $\phi \approx \phi_{\rm c}$; features of the fluid are $[\mathcal{S} = 66.3$, $\xi\sigma = 2.92]$. In (c), each curved line is obtained for $\sigma/\beta K = 0.59647$ and $\phi = 0.178$; the fluid condition is characterized as $T \approx T_{\rm p}$, $\phi \approx \phi_{\rm p} - 0.019$, $T_{\rm c} < T$, and $\phi \approx \phi_{\rm c} - 0.019$; features of the fluid are $[\mathcal{S} = 69.4$, $\xi\sigma = 2.37]$.

8. Fractal structures of physical clusters at percolation threshold[48]

(a) *Fractal dimensions of physical clusters*

The dependence of $\mathcal{P}(r)$ on a large r is given by Eq. (185). However, the form of the dependence is not clear. It is possible to derive a suitable form from the dependence expressed by by Eq. (185). The form is expressed as a special product, which is obtained by multiplying a factor $(r/\sigma)^{-(3-d_f)}$ by the remainder. The product is expressed as

$$\mathcal{P}(r) = C_f \left(\frac{r}{\sigma}\right)^{-(3-d_f)}, \tag{219}$$

where coefficients C_f and d_f are not constant in general. Under the condition that a fluid system includes extremely large physical clusters having a fractal structure, C_f and d_f can be constant. Then, d_f represents the fractal dimension of the fractal structure.[40] This is understood from the behavior of the curved line of $\mathcal{P}(r)$ specified by $\mathcal{S} = 9.01 \times 10^{15}$ in Fig. 22.

According to the assumption that C_f and d_f behave as constant values for variations in the value of r satisfying $|r_0 - r|/r_0 \ll 1 \quad (r_0 > \sigma)$, C_f and d_f are easily estimated. Then, the derivative $\mathrm{d}\mathcal{P}(r)/\mathrm{d}r$ at $r = r_0$ is given as $\mathrm{d}\mathcal{P}(r)/\mathrm{d}r\Big|_{r=r_0} = -(3-d_f)(r/\sigma)^{-1}\mathcal{P}(r)/\sigma\Big|_{r=r_0}$. Hence, the use of $\mathcal{P}(r_0) = C_f\,(r_0/\sigma)^{-(3-d_f)}$ and $\mathrm{d}\mathcal{P}(r)/\mathrm{d}r\Big|_{r=r_0}$ allows C_f to be estimated as

$$C_f = \left[\left(\frac{r_0}{\sigma}\right)^{-1}\left(-\frac{1}{3}r_0\frac{\mathrm{d}\mathcal{P}(r)}{\mathrm{d}r}\Big|_{r=r_0}\right)^{-\ln r_0/\sigma}\left(\mathcal{P}(r_0)\right)^{-\frac{1}{3}+\ln r_0/\sigma}\right]^{-1/3}. \tag{220}$$

Similarly, the use of $\mathcal{P}(r_0) = C_f\,(r_0/\sigma)^{-(3-d_f)}$ and $\mathrm{d}\mathcal{P}(r)/\mathrm{d}r\Big|_{r=r_0}$ allows d_f to be estimated as

$$d_f = \left[-\frac{r_0}{3\mathcal{P}(r_0)}\frac{\mathrm{d}\mathcal{P}(r)}{\mathrm{d}r}\Big|_{r=r_0}\right]^{-1/3}. \tag{221}$$

Thus, the two unknown coefficients C_f and d_f are expressed by the above formulae. Evaluations of C_f and d_f are achieved if $\mathcal{P}(r)$ given by Eq. (185) is substituted into Eqs. (220) and (221). Then, the derivative $\mathrm{d}\mathcal{P}(r)/\mathrm{d}r$ is obtained from the use of Eq. (185) as follows:

$$\begin{aligned}\frac{\mathrm{d}\mathcal{P}(r)}{\mathrm{d}r} =& \widehat{\mathcal{M}}^{+}\frac{e^{-\xi^{+}r}}{2\xi^{+}r^2}(1+\xi^{+}r) - \frac{1}{2\xi^{+}r^2}(1+\xi^{+}r)I^{(-)}(\sigma,r) \\ & -\frac{1}{2\xi^{+}r^2}(1-\xi^{+}r)I^{(+)}(r,\infty) \\ =& -(1+\xi^{+}r)\frac{\mathcal{P}(r)}{r} + \frac{1}{r}I^{(+)}(r,\infty).\end{aligned} \tag{222}$$

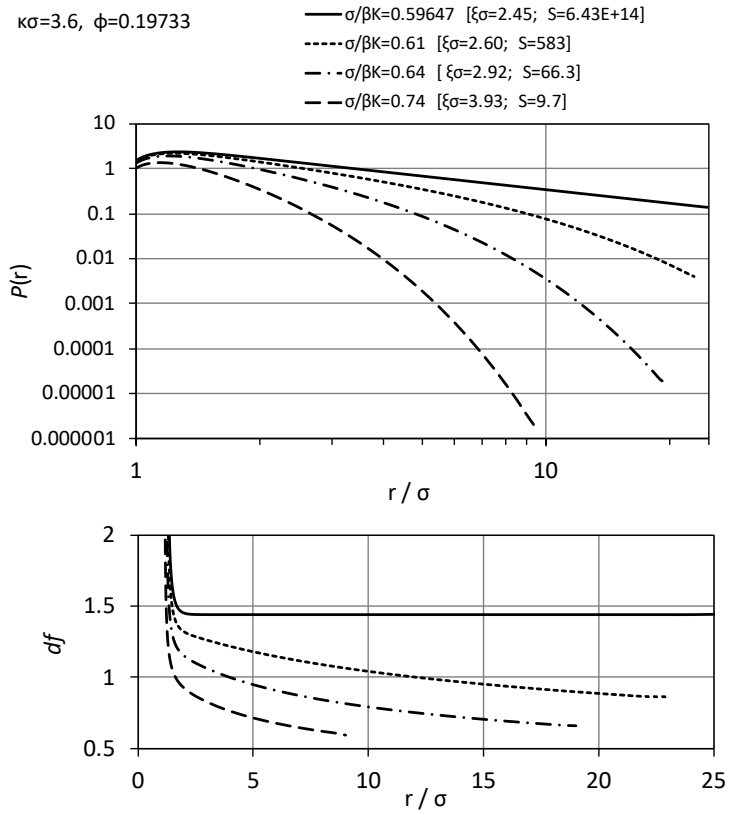

FIG. 22. Dependences of $\mathcal{P}(r)$ and d_f on r ($f_\nu = 0.101853$). Each curved line is evaluated for $\kappa\sigma = 3.6$ and $\phi = 0.19733 \approx \phi_{\rm p}$. Two thick solid curved lines are characterized by a set [$\mathcal{S} = 6.43 \times 10^{14}$, $\xi\sigma = 2.45$] because $\sigma/\beta K = 0.59647$ corresponds to $T \approx T_{\rm p}$ near percolation threshold. Dotted curved line is characterized by [$\mathcal{S} = 583$, $\xi\sigma = 2.60$] linked to $\sigma/\beta K = 0.61$ ($T > T_{\rm p}$); dashed and single-dotted curved line by [$\mathcal{S} = 66.3$, $\xi\sigma = 2.92$] linked to $\sigma/\beta K = 0.64$ ($T > T_{\rm p}$); dashed curved line by [$\mathcal{S} = 9.7$, $\xi\sigma = 3.93$] linked to $\sigma/\beta K = 0.74$ ($T > T_{\rm p}$). $\mathcal{P}(r)$ is evaluated from Eq. (185). d_f is evaluated from Eq. (221) for $r_0 \approx r$.

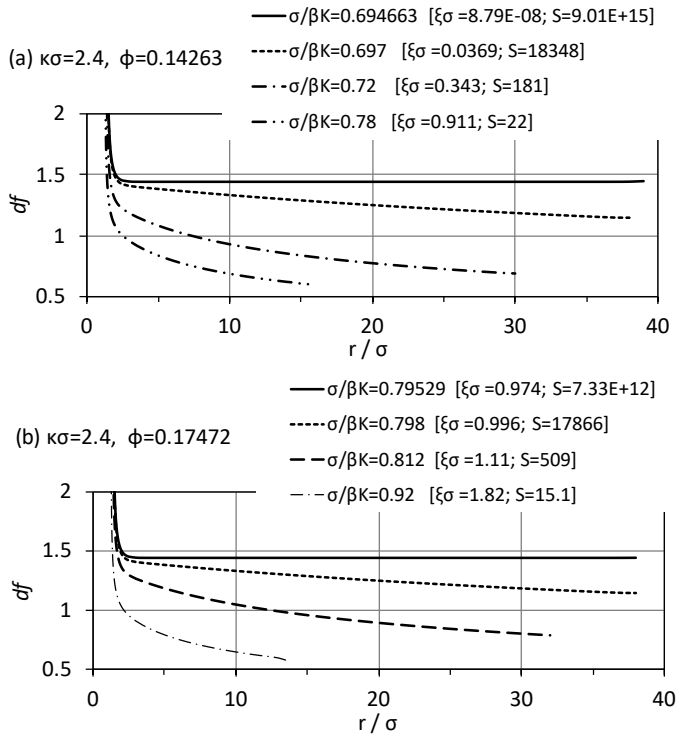

FIG. 23. Dependence of d_f on r for $\kappa\sigma = 2.4$ $(f_\nu = 0.101853)$. d_f for $r_0 \approx r$ is evaluated from Eq. (221) for $\phi = 0.14263 \approx \phi_{\rm p}$ in (a) and $\phi = 0.17472 \approx \phi_{\rm c}$ in (b). In (a), thick solid curved line is characterized by a set $[\mathcal{S} = 9.01 \times 10^{15}, \xi\sigma = 8.79 \times 10^{-8}]$ because $\sigma/\beta K = 0.694663$ corresponds to $T \approx T_{\rm p}$ near a percolation threshold on the spinodal line. Other curved lines are characterized by $[\mathcal{S} = 18348, \xi\sigma = 0.0369]$ linked to $\sigma/\beta K = 0.697$ ($T > T_{\rm p}$); $[\mathcal{S} = 181, \xi\sigma = 0.343]$ linked to $\sigma/\beta K = 0.72$ ($T > T_{\rm p}$); $[\mathcal{S} = 22, \xi\sigma = 0.911]$ linked to $\sigma/\beta K = 0.78$ ($T > T_{\rm p}$). In (b), thick solid curved line is characterized by $[\mathcal{S} = 7.33 \times 10^{12}, \xi\sigma = 0.974]$ because $\sigma/\beta K = 0.79529$ corresponds to a relation near a percolation threshold satisfying $T > T_{\rm c}$ above the spinodal line. Other curved lines are characterized by $[\mathcal{S} = 17866, \xi\sigma = 0.996]$ linked to $\sigma/\beta K = 0.798$ ($T > T_{\rm c}$); $[\mathcal{S} = 509, \xi\sigma = 1.11]$ linked to $\sigma/\beta K = 0.812$ ($T > T_{\rm c}$); and $[\mathcal{S} = 15.1, \xi\sigma = 1.82]$ linked to $\sigma/\beta K = 0.92$ ($T > T_{\rm c}$).

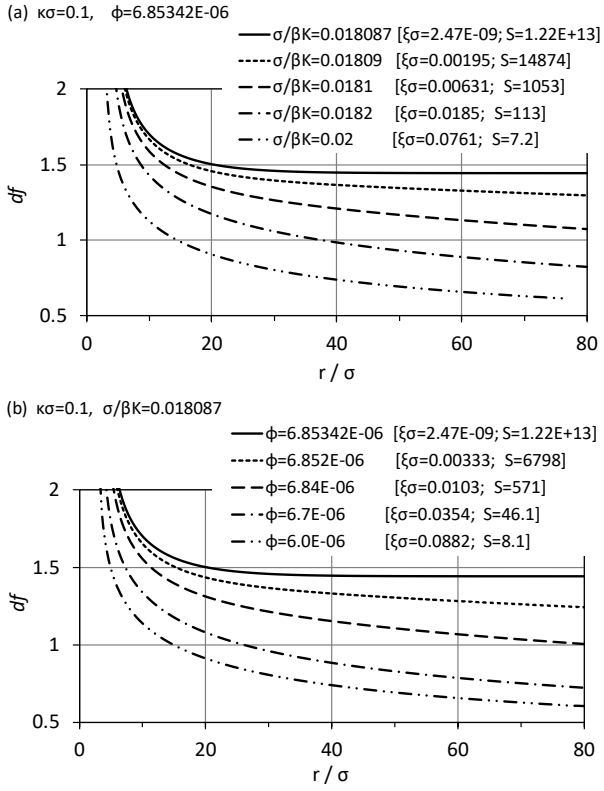

FIG. 24. Dependence of d_f on r for a small $\kappa\sigma$ ($\kappa\sigma = 0.1$) ($f_\nu = 0.101853$). d_f for $r_0 \approx r$ is evaluated from Eq. (221). In (a) evaluated for $\phi = 6.85342 \times 10^{-6} \approx \phi'_{\rm p}$, thick solid curved line is characterized by a set [$\mathcal{S} = 1.22 \times 10^{13}$, $\xi\sigma = 2.47 \times 10^{-9}$] because $\sigma/\beta K = 0.018087$ corresponds to $T \approx T'_{\rm p}$ near a percolation threshold on the spinodal line. Other curved lines are characterized by [$\mathcal{S} = 14874$, $\xi\sigma = 0.00195$] linked to $\sigma/\beta K = 0.01809$ ($T > T'_{\rm p}$); [$\mathcal{S} = 1053$, $\xi\sigma = 0.00631$] linked to $\sigma/\beta K = 0.0181$ ($T > T'_{\rm p}$); [$\mathcal{S} = 113$, $\xi\sigma = 0.0185$] linked to $\sigma/\beta K = 0.0182$ ($T > T'_{\rm p}$); and [$\mathcal{S} = 7.2$, $\xi\sigma = 0.0761$] linked to $\sigma/\beta K = 0.02$ ($T > T'_{\rm p}$). In (b) evaluated for $\sigma/\beta K = 0.018087$ ($T \approx T'_{\rm p}$), thick solid curved line for $\phi = 6.85342 \times 10^{-6}$ is the same as that shown for $\sigma/\beta K = 0.018087$ in (a). Other curved lines are characterized by [$\mathcal{S} = 6798$, $\xi\sigma = 0.00333$] linked to $\phi = 6.852 \times 10^{-6}$ ($\phi < \phi'_{\rm p}$); [$\mathcal{S} = 571$, $\xi\sigma = 0.0103$] linked to $\phi = 6.84 \times 10^{-6}$ ($\phi < \phi'_{\rm p}$); [$\mathcal{S} = 46.1$, $\xi\sigma = 0.0354$] linked to $\phi = 6.7 \times 10^{-6}$ ($\phi < \phi'_{\rm p}$); and [$\mathcal{S} = 8.1$, $\xi\sigma = 0.0882$] linked to $\phi = 6.0 \times 10^{-6}$ ($\phi < \phi'_{\rm p}$).

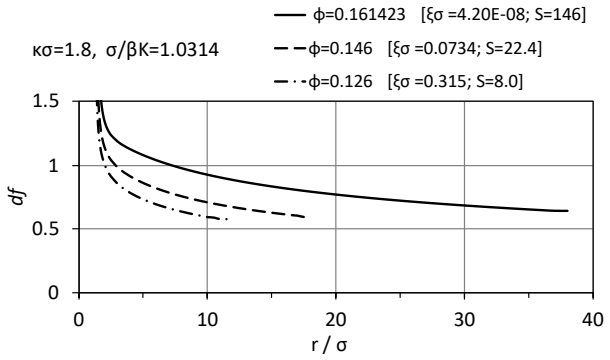

FIG. 25. Dependence of d_f on r for $\kappa\sigma = 1.8$ $(f_\nu = 0.101853)$. d_f for $r_0 \approx r$ is evaluated from Eq. (221) for $\sigma/\beta K \approx 1.0314$ linked to $T \approx T_{\rm c}$. Thick solid curved line is characterized by a set $[\mathcal{S} = 146, \xi\sigma = 4.20 \times 10^{-8}]$ because $\phi = 0.161423$ is linked to $\phi \approx \phi_{\rm c} \approx \phi_{\rm p} - 0.008$. Other curved lines are characterized by $[\mathcal{S} = 22.4, \xi\sigma = 0.0734]$ linked to $\phi = 0.146$ ($\phi < \phi_{\rm c}$); and $[\mathcal{S} = 8.0, \xi\sigma = 0.315]$ linked to $\phi = 0.126$ ($\phi < \phi_{\rm c}$).

The behavior of $\mathcal{P}(r)$ is characterized by the form of Eq. (219) at r satisfying $|r_0 - r|/r_0 \ll 1$ with $1 \ll r_0/\sigma$. If physical clusters formed in a fluid system by a mutually attractive force between two particles, which is characterized by a Yukawa potential $u_{\rm Y}(r)$, have a fractal structure, then the fractal dimension d_f of the physical clusters is evaluated by the use of Eq. (221). When the fluid system includes sufficiently large physical clusters, the physical clusters maintain a fractal structure with the fractal dimension approximated as $d_f \approx 1.4$.

This fact is confirmed in Figs. 22, 23, and 24. Moreover, Fig. 24 indicates that the physical clusters can maintain a fractal structure characterized by $d_f \approx 1.4$ if the percolation of physical clusters occurs even under a condition $0 < \kappa\sigma \ll 1$. This example denotes that even astronomical physical clusters formed by the contribution of a long-ranged attractive force such as gravitation should exhibit a fractal structure characterized by $d_f \approx 1.4$.

(b) *Structure resulting from mixing inhomogeneously*

The representation of d_f introduced by Eq. (219) is not complete for physical cluster elements formed in a fluid system unless the aggregation of physical cluster elements with each other enhances the long-range feature of $\mathcal{P}(r)$ sufficiently. The pair connectedness $\mathcal{P}(r)$ described by Eq. (68) via the Percus–Yevick (PY) approximation[8] implies that each small element of physical clusters formed in a Yukawa fluid can have a structure that is characterized as a fractal structure. If a condition of the fluid system deviates slightly from the percolation threshold, physical clusters cannot be developed towards large sizes as shown in Figs. 22, 23, 24, and 25. Even under the condition, each physical cluster element should maintain a fractal feature.

Growth of a physical cluster in a fluid can proceed via either particle–cluster aggregation or cluster–cluster aggregation.[40] Then, each physical cluster of particles grows in shapes that are similar to branches and does not form a block of aggregated particles. Physical cluster growth yielded by the cluster–cluster aggregation allows each physical cluster to maintain a structure characterized by branches. The cluster–cluster aggregation allows large physical clusters to have the structure with a fractal dimension near 1.5.[40]

The representation of $\mathcal{P}(r)$ given by Eq. (68) implies that large physical clusters formed via cluster–cluster aggregation in a Yukawa fluid have a structure that is characterized as a fractal structure. This indicates that the aggregation of physical cluster elements with each other allows large physical clusters with the fractal structure to be formed. Physical clusters with a fractal structure can be formed under the condition of a fluid system that is located far from the percolation threshold even if the behavior of d_f given by Eq. (221) is not constant for variations in r.

In a fluid, physical clusters are formed by particle pairs contributing to the magnitude of $\mathcal{P}(r)$. The physical clusters can grow infinitely without disappearing, and the formation of large physical clusters causes the behavior of d_f given by Eq. (221) to become constant.

This indicates that the particle pairs do not homogeneously mix in each microscopic volume with other particle pairs contributing to the magnitude of $\mathcal{D}(r)$. Such inhomogeneity in a fluid system is a state shown from the behavior of d_f given by Eq. (221). At the liquid–vapor critical point, the inhomogeneity causes the deviation from behavior of $g(r)$ expressed as $g(r) - 1 \sim r^{-1}$.

C. Phase behaviors influenced by physical clusters

1. Specific behaviors of correlation functions

(**a**) *Reduction of density fluctuations owing to exclusion effect caused by hard core of each particle*

The degree of the density fluctuations is linked to the compressibility because Eq. (18) can be modified with the use of Eq. (41) as follows:

$$\lim_{V\to\infty}\frac{V}{\rho}\left[\left\langle\left(\frac{N}{V}\right)^2\right\rangle-\left\langle\left(\frac{N}{V}\right)\right\rangle^2\right]=\left[\beta\left(\frac{\partial P}{\partial\rho}\right)_{V,T}\right]^{-1}. \tag{223}$$

Based on Eq. (223), it is easy to confirm the degree of the density fluctuations for a hard-sphere fluid system. The equation of state of a hard-sphere fluid can be given as a simple formula that more precise than that obtained from the PY approximation,[9,10] and it is expressed as[10,11]

$$\frac{\beta P}{\rho}=\frac{1+\phi+\phi^2-\phi^3}{(1-\phi)^3}. \tag{224}$$

The differentiation of Eq. (224) with respect to ρ allows the compressibility equation to be expressed as

$$\left[\beta\left(\frac{\partial P}{\partial\rho}\right)_{V,T}\right]^{-1}=(1-\phi)^4(1+6\phi+6\phi^2-14\phi^3+7\phi^4)^{-1}. \tag{225}$$

According to the magnitude of $\beta^{-1}(\partial\rho/\partial P)_{V,T}$ evaluated from Eq. (225), the density fluctuations in a hard-sphere fluid system are simply reduced as the density of the hard spheres increases. This is confirmed by Fig. 26. For a hard-sphere fluid system, $\widetilde{\mathcal{P}}(0)=0$ is satisfied. Hence, a comparison of Eq. (225) with Eq. (163) allows the following relation to be obtained:

$$\widetilde{\mathcal{H}}(0)=(1-\phi)^4(1+6\phi+6\phi^2-14\phi^3+7\phi^4)^{-1}-1. \tag{226}$$

A comparison of Eq. (226) with Eq. (225) requires the behavior of $\widetilde{\mathcal{H}}(0)$ to be equivalent to the behavior of $\beta^{-1}(\partial\rho/\partial P)_{V,T}$ shown in Fig. 26. The exclusion effect caused by the hard core of each particle allows the degree of the density fluctuations to be reduced as the density of particles is increased. If Eq. (165) is considered, then for a hard-sphere fluid system, $\left[\beta\big(\partial P/\partial\rho\big)_{V,T}\right]^{-1}=\widetilde{\mathcal{H}}(0)+1=1/[1-\widetilde{C}^*(0)]$, $\widetilde{\mathcal{P}}(0)=0$, and $\widetilde{C}^+(0)=0$ must be satisfied. Therefore, the exclusion effect owing to the hard core of each particle requires

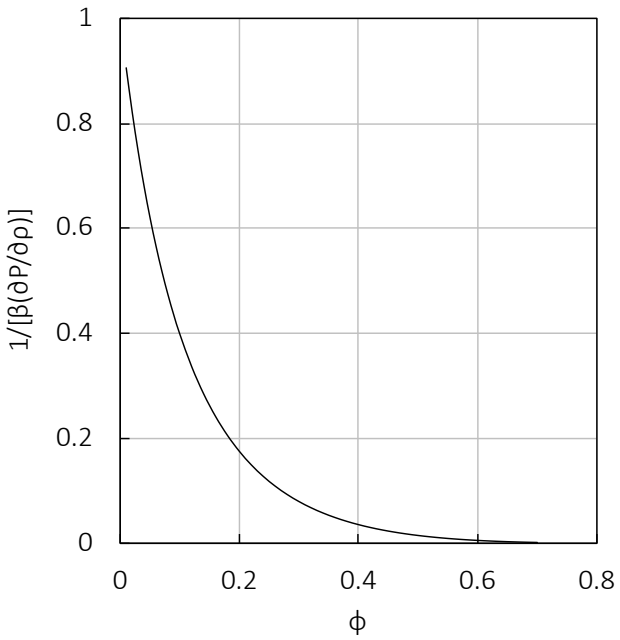

FIG. 26. Degree of density fluctuations of hard-sphere fluid. This fluid is a typical system where contribution of formation of physical clusters does not exist, but the exclusion effect owing to the hard-core potential of each particle exists. The degree of density fluctuations is denoted by $\left[\beta\left(\partial P/\partial\rho\right)_{V,T}\right]^{-1}$, which is evaluated based on Eq. (225).

relations $0 \geq \widetilde{C}^*(0) < -\infty$ and $0 \leq \widetilde{\mathcal{H}}(0) \leq 1$ to be satisfied. This indicates that $\widetilde{C}^*(0)$ and $\widetilde{\mathcal{H}}(0)$ have negative values if the exclusion effect owing to the hard core of each particle becomes dominant for a large ϕ, i.e., for a large ρ, in a fluid system where a mutually attractive force acts between particles of each pair. Then, $\widetilde{C}^*(0)$ can become even a large

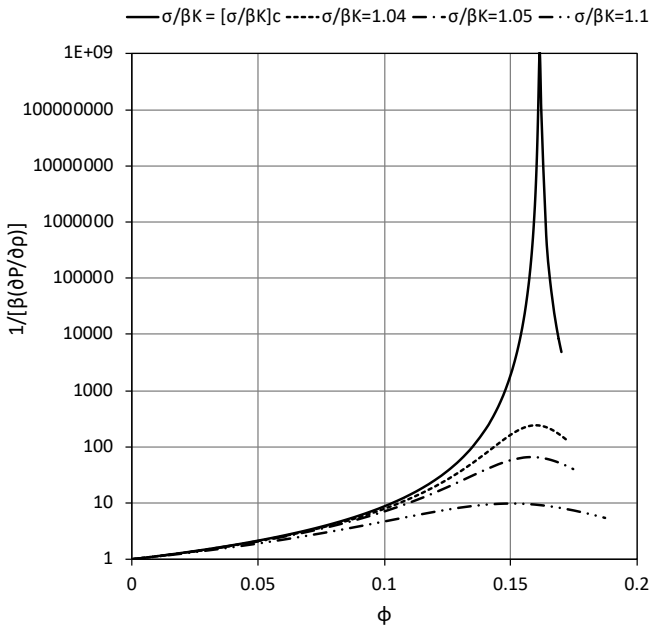

FIG. 27. Degree of density fluctuations of Yukawa fluid $\kappa\sigma = 1.8$ ($f_\nu = 0.101853$). Degree of density fluctuations denotes $\left[\beta\left(\partial P/\partial\rho\right)_{V,T}\right]^{-1}$ evaluated based on Eq. (166) that is formed from $\rho\widehat{c}^{(0)}$ given by Eq. (139). Then, $\left[\beta\left(\partial P/\partial\rho\right)_{V,T}\right]^{-1} = \widetilde{\mathcal{P}}(0) + \widetilde{\mathcal{H}}(0) + 1$ and $\widetilde{\mathcal{P}}(0) \neq 0$ are satisfied. $[\sigma/\beta K]_c$ is given as $[\sigma/\beta K]_c \approx 1.0314$.

negative value.

(**b**) *Resistance to phase separation of particles belonging to physical clusters*

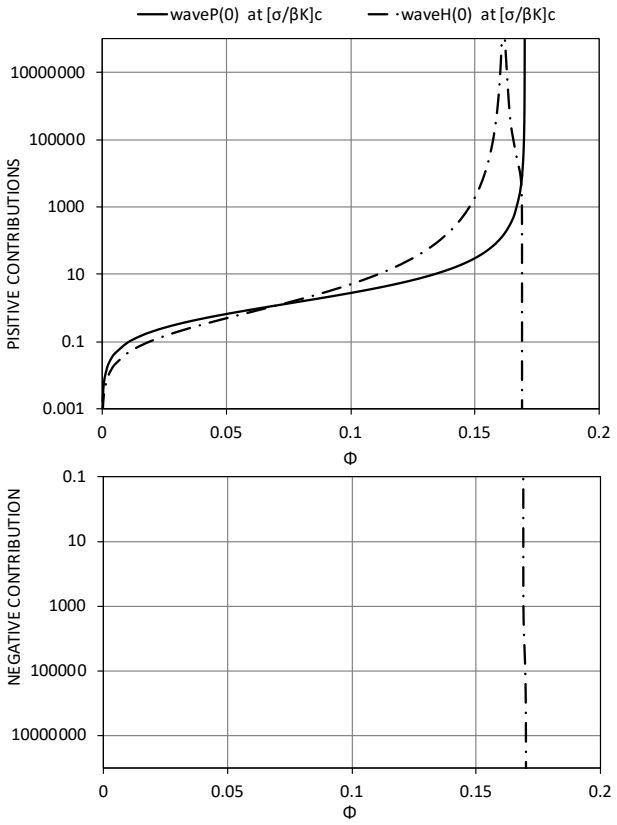

FIG. 28. Behaviors of $\widetilde{\mathcal{P}}(0)$ and $\widetilde{\mathcal{H}}(0)$ for condition satisfying $\kappa\sigma = 1.8$ and $\sigma/\beta K = [\sigma/\beta K]_c$ ($f_\nu = 0.101853$). Large negative values of $\widetilde{\mathcal{H}}(0)$ near percolation threshold is compensated for large positive values of $\widetilde{\mathcal{P}}(0)$ near percolation threshold in summation $\widetilde{\mathcal{P}}(0) + \widetilde{\mathcal{H}}(0) + 1$ that is equivalent to $\left[\beta\left(\partial P/\partial\rho\right)_{V,T}\right]^{-1}$. In figure, "wave $P(0)$" means $\widetilde{\mathcal{P}}(0)$, and "wave $H(0)$" means $\widetilde{\mathcal{H}}(0)$. $[\sigma/\beta K]_c$ is given as $[\sigma/\beta K]_c \approx 1.0314$.

The presence of a mutually attractive force between hard-core particles of each pair makes the behavior of $\left[\beta\left(\partial P/\partial\rho\right)_{V,T}\right]^{-1}$ for a fluid system become different from that seen in Fig. 26. The presence of the mutually attractive force enables the density fluctuations to become extremely large as ρ increases toward the critical point. Then, even the existence of

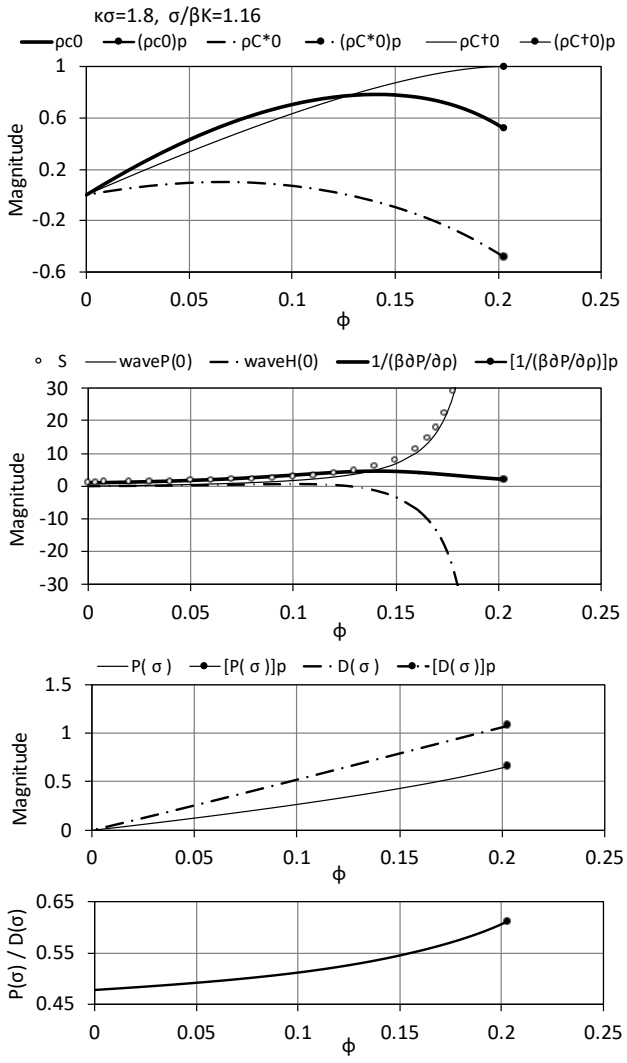

FIG. 29. Behaviors of $\widetilde{C}^{+}(0)$ and $\widetilde{C}^{*}(0)$, $\widetilde{c}(0)$, $\widetilde{\mathcal{P}}(0)$, $\widetilde{\mathcal{H}}(0)$, $\mathcal{S}$, $[\beta\partial P/\partial\rho]^{-1}$, $\mathcal{P}(\sigma)$, and $\mathcal{D}(\sigma)$ for $\kappa\sigma = 1.8$ and $\sigma/\beta K = 1.16$ ($f_\nu = 0.101853$). $\rho C\dagger 0 \equiv \widetilde{C}^{+}(0)$, $\rho C^{*}0 \equiv \widetilde{C}^{*}(0)$, $\rho c0 \equiv \widetilde{c}(0)$, wave$P(0) \equiv \widetilde{\mathcal{P}}(0)$, and wave$H(0) \equiv \widetilde{\mathcal{H}}(0)$. $\left[\beta\left(\partial P/\partial\rho\right)\right]^{-1} = \widetilde{\mathcal{P}}(0) + \widetilde{\mathcal{H}}(0) + 1$. $P(\sigma) \equiv \mathcal{P}(\sigma)$ and $D(\sigma) \equiv \mathcal{D}(\sigma)$. Each dot "•" corresponds to a point given at percolation threshold.

small physical clusters can influence the phase behavior at the critical point, as confirmed by Figs. 18 (a) and 19 (a). When the temperature of a fluid decreases or the density of particles increases, either the aggregation of particles that results in phase separation can be domi-

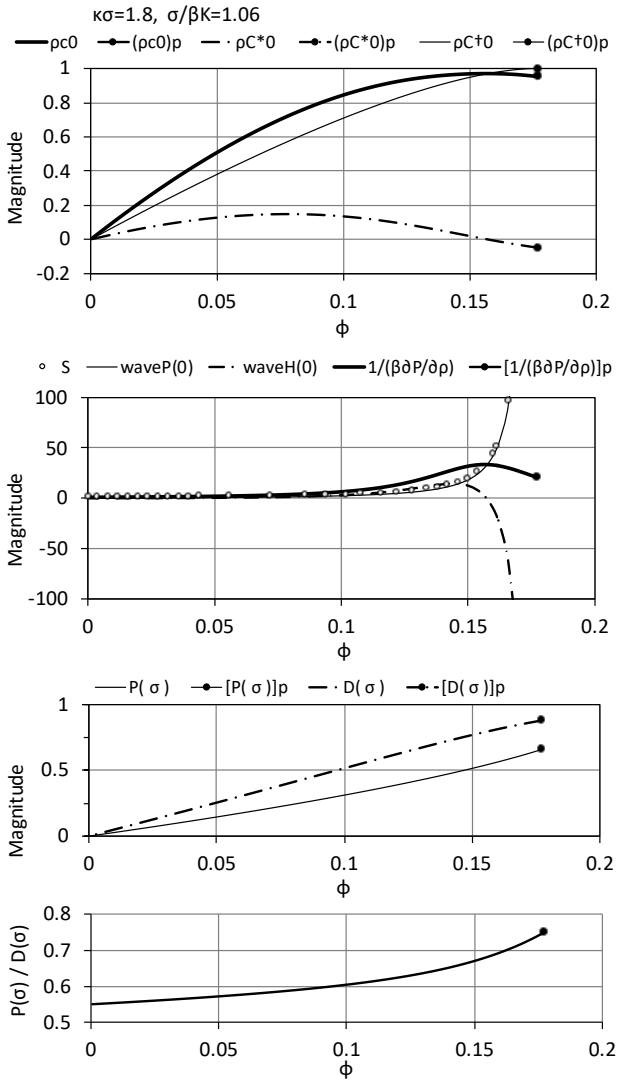

FIG. 30. Behaviors of $\widetilde{C}^{+}(0)$ and $\widetilde{C}^{*}(0)$, $\widetilde{c}(0)$, $\widetilde{\mathcal{P}}(0)$, $\widetilde{\mathcal{H}}(0)$, $\mathcal{S}$, $[\beta\partial P/\partial\rho]^{-1}$, $\mathcal{P}(\sigma)$, and $\mathcal{D}(\sigma)$ for $\kappa\sigma = 1.8$ and $\sigma/\beta K = 1.06$ $(f_\nu = 0.101853)$. Detail is same as that in Fig. 29.

nated or the generation of the percolation can be dominated, depending on the distance at which the attractive forces between the particles remain effective. Phase separation in a fluid before reaching the percolation threshold or percolation before inducing phase separation occurs depending on the distance at which the attractive forces between the particles remain effective. Similarly, a critical behavior at the critical point before reaching the percolation

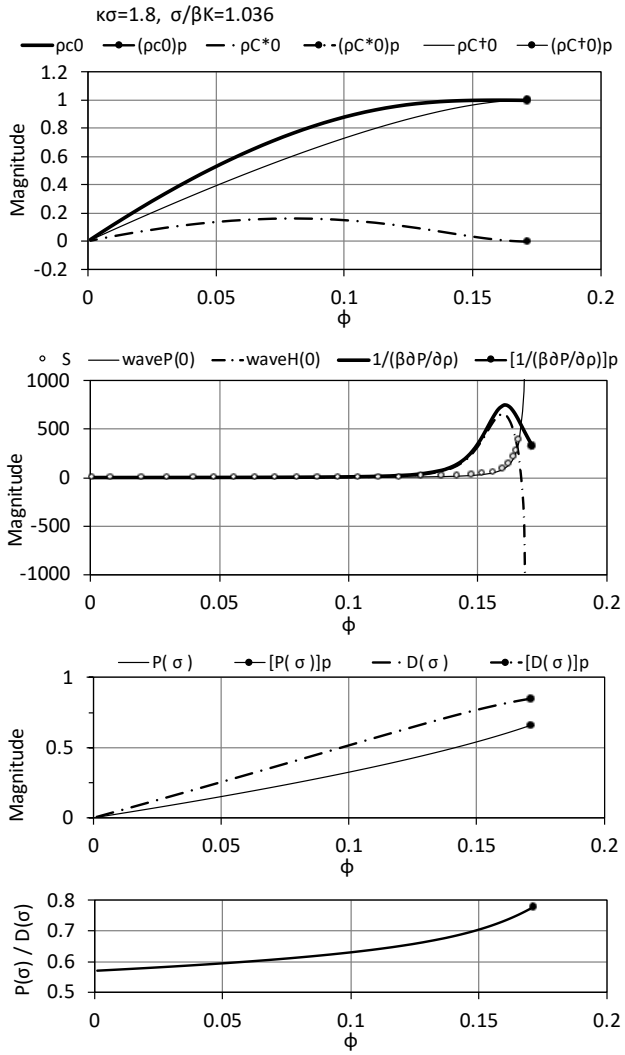

FIG. 31. Behaviors of $\widetilde{C}^{+}(0)$ and $\widetilde{C}^{*}(0)$, $\widetilde{c}(0)$, $\widetilde{\mathcal{P}}(0)$, $\widetilde{\mathcal{H}}(0)$, $\mathcal{S}$, $[\beta\partial P/\partial\rho]^{-1}$, $\mathcal{P}(\sigma)$, and $\mathcal{D}(\sigma)$ for $\kappa\sigma = 1.8$ and $\sigma/\beta K = 1.036 > [\sigma/\beta K]_c$ $(f_\nu = 0.101853)$. Critical point is specified by $\sigma/\beta K = [\sigma/\beta K]_c$ and $\phi = \phi_c$ with $[\sigma/\beta K]_c \approx 1.0314$ and $\phi_c \approx 0.161423$. Detail is same as that in Fig. 29.

threshold or percolation before reaching the critical point are observed depending on the effective length to which the influence of each attractive force reaches. Thus, the two cases are possible, depending on whether the effective length is short or long. In the case that the effective length is long, *critical phenomena in a fluid occurs before a condition of a fluid*

reaches the percolation threshold of physical clusters; the spinodal line is located above the percolation threshold in the phase diagram. In the case that the effective length is short, *the percolation occurs before a condition of a fluid reaches the critical point; the percolation threshold is located above the spinodal line in the phase diagram.* These facts should imply that the appearance of the liquid phase of a fluid depends on the effective length to which the influence of each attractive force reaches.

According to Fig. 6, a fluid system that is specified for $\kappa\sigma = 1.8$ and ρ satisfying $0.0099792 < \phi < 0.16432$ corresponds to a system under the condition that the spinodal line is located above the percolation threshold. If $\sigma/\beta K = [\sigma/\beta K]_c$ is maintained with $[\sigma/\beta K]_c \approx 1.03136$ given at the critical point of the fluid system, then an increase in the density of the fluid system can allow the occurrence of a critical behavior at the critical point to appear before reaching the percolation threshold. The critical behavior appears at the set specified by $\phi = \phi_c$ ($\phi_c \approx 0.161423$) and $\sigma/\beta K = [\sigma/\beta K]_c$, and the percolation threshold is located at the set specified by $\phi = \phi_p$ ($\phi_p \approx 0.170034$) and $\sigma/\beta K = [\sigma/\beta K]_c$ ($[\sigma/\beta K]_c \approx 1.0314$). This fact enables phase behavior near the critical point to be linked to variations in structures of particle distribution that are characterized by $\widetilde{\mathcal{P}}(0)$ and $\widetilde{\mathcal{H}}(0)$.

In the fluid system, the growth of physical clusters is linked to an increase in the number of particle pairs contributing to the magnitude of $\widetilde{\mathcal{P}}(0)$. As an increase in the value of ϕ corresponds to a decrease in the mean distance between particles, this increase allows the strength of the mutually attractive force between the particles of each pair to be increased on average. An increase in the mutually attractive force makes the particles stay more stably near each other. As a result, the magnitude of $\mathcal{D}(\sigma)$ $(= \mathcal{H}(\sigma) + 1)$ and the magnitude of $\mathcal{P}(\sigma)$ both should be increased. According to Figs. 29, 30, and 31, the ratio $\mathcal{P}(\sigma)/\mathcal{D}(\sigma)$ is also increased by an increase in the value of ϕ. The contraction of the mean distance between particles owing to the increase in the value of ϕ allows the effect of the mutually attractive force to be strengthened. However, the magnitude of $\mathcal{P}(\sigma)$ remains small even at the percolation threshold. If it is possible to induce a phenomenon in which only particles belonging to the physical clusters are aggregated in the vicinity of each other, then the magnitude of $\mathcal{P}(\sigma)$ should become large as the condition of the fluid approaches the percolation threshold. Further, this phenomenon should allow the particles belonging to the physical clusters to be separated from the phase of the fluid. These are negated by the behavior of $\mathcal{P}(\sigma)$ remaining small even at the percolation threshold.

The fluid system has a capability to resist the phase separation of particles belonging to the physical clusters. The magnitude of $\widetilde{\mathcal{H}}(0)$ includes the contribution of particle pairs characterized by the fact that two particles of each pair interact in an unbound state where the contribution of the relative kinetic energy of the pair particles exceeds the contribution of the attractive force between them. The particles that form the physical clusters coexist with particles specified as particle pairs contributing to the magnitude of $\widetilde{\mathcal{H}}(0)$. The latter particles have a tendency to be confined among branches of physical clusters.[52] Thus, the particles contributing to the magnitude of $\widetilde{\mathcal{H}}(0)$ prevent the occurrence of the phase separation of particles belonging to the physical clusters. Resistance to the occurrence of the phase separation of particles that form the physical clusters is assisted by the particles contributing to the magnitude of $\widetilde{\mathcal{H}}(0)$.

2. Maximization of density fluctuations near critical point

When a condition of a fluid is not in the vicinity of the critical point, evaluations based on Eqs. (203) and (217) do not allow relation $g_0(r) < g(r)$ to be found for a large r even if $\mathcal{S}$ is sufficiently large. The case of (a) found in Fig. 21 denotes that a fluid system includes physical clusters of which the mean size is given as $\mathcal{S} = 6.43 \times 10^{14}$. In this case, $g_0(r) > g(r)$ is found for a large r. The case of (a) found in Fig. 20 denotes that a fluid system includes physical clusters for which the mean size is given as $\mathcal{S} = 7.33 \times 10^{12}$. In this case, $g_0(r) > g(r)$ is found for a large r. For a fluid maintained in the vicinity of both the critical point and the percolation threshold, finding $g_0(r) < g(r)$ for a large r is necessary based on the contribution of $\mathcal{P}(r)$ to $g(r)$. This is confirmed from (a) in Fig. 17. Nevertheless, relation $g_0(r) < g(r)$ for a large r can be found even if the mean size of physical clusters $\mathcal{S}$ is not sufficiently large when a condition of a fluid is maintained in the vicinity of the critical point. The case of (a) found in Fig. 18 denotes that the fluid includes physical clusters of which the mean size is given as $\mathcal{S} = 146$. The case of (a) found in Fig. 19 denotes that the fluid includes physical clusters of which the mean size is given as $\mathcal{S} = 22.2$. These indicate that the existence of physical clusters contributes to the maximization of the density fluctuations at the critical point even if $\mathcal{S}$ is not large.

The percolation of physical clusters occurs at the percolation threshold corresponding to the condition given as $1 - \widetilde{C}^{+}(0) = 0$. Despite this fact, the magnitude of $\beta^{-1}(\partial\rho/\partial P)_{V,T}$ given as Eq. (164) is prevented from diverging to infinity at the condition $1 - \widetilde{C}^{+}(0) = 0$. This is demonstrated by the form given by Eq. (165). Thus, the extremely large density fluctuations that are specified through Eq. (166) at the condition $1 - \widetilde{c}(0) = 0$ occur owing to the second term on the right-hand side of Eq. (164). This term is equivalent to $\widetilde{\mathcal{H}}(0)$, i.e.,

$$\widetilde{\mathcal{H}}(0) = \frac{\widetilde{C}^{*}(0) + \widetilde{C}^{*}(0)\widetilde{\mathcal{P}}(0)}{1 - \widetilde{C}^{+}(0) - \widetilde{C}^{*}(0)}, \tag{227}$$

where neither $\widetilde{\mathcal{P}}(0)$ nor $\widetilde{C}^{+}(0)$ are zero if a fluid system includes physical clusters. Examples showing $\widetilde{\mathcal{P}}(0) \neq 0$ and $\widetilde{C}^{+}(0) \neq 0$ for $\phi > 0$ are confirmed from Figs. 29, 30, and 31. Equation (227) implies that the extremely large density fluctuations occur because particles belonging to physical clusters restrict the behavior of particles contributing to the magnitude of $\widetilde{\mathcal{H}}(0)$.

If particles specified as particle pairs contributing to the magnitude of $\widetilde{\mathcal{H}}(0)$ are confined among branches of physical clusters formed in a fluid system, the movements of the particles

are restricted. According to the behaviors of $\mathcal{H}(r)$ and $\mathcal{P}(r)$ found from Figs. 17, 18, 19, 20, and 21, the minimum of $\mathcal{H}(r)$ occurs near the value of r at which $\mathcal{P}(r)$ is maximized. This demonstrates that particles contributing to the magnitude of $\mathcal{H}(r)$ have a tendency to be excluded from particles contributing to the magnitude of $\mathcal{P}(r)$. The magnitude of $\mathcal{H}(r)$ includes the contribution of particle pairs characterized by the fact that two particles of each pair interact in an unbound state where the contribution of the relative kinetic energy of the pair particles exceeds the contribution of the attractive force between them. Unless particles contributing to the magnitude of $\mathcal{H}(r)$ prevent physical clusters from contracting, particles belonging to the physical clusters must undergo phase separation from the fluid system. Particles contributing to the magnitude of $\mathcal{H}(r)$ are confined among branches of physical clusters. Hence, these particles prevent phase separation. Then, the movements of the particles are restricted by particles belonging to physical clusters.

A contribution of the exclusion effect owing to each hard core allows the degree of the density fluctuations $[\beta(\partial P/\partial\rho)_{V,T}]^{-1}$ to be decreased as the density ρ of particles is increased. Moreover, an increase in the density ρ, i.e., the volume fraction ϕ decreases the mean distance between particles; hence, the increase strengthens the effects of attractive forces between particles. Then, physical clusters can be stabilized even if the physical clusters are small. Ultimately, at least the number of physical clusters is increased by the increase in the value of ϕ.

Simultaneously, the increase in the value of ϕ should raise the probability that particle pairs contributing to the magnitude of $\widetilde{\mathcal{H}}(0)$ are exchanged for particle pairs contributing to the magnitude of $\widetilde{\mathcal{P}}(0)$. An increase in the number of physical clusters means that the particle pairs contributing to the magnitude of $\widetilde{\mathcal{H}}(0)$ are confined in larger number among the branches of physical clusters. Thus, the effect of increasing the probability should enhance the instability of physical clusters.

An increase in the volume fraction ϕ can lead to at least three different types of effects, i.e., *a*) the enhancement of the exclusion effect reducing $[\beta(\partial P/\partial\rho)_{V,T}]^{-1}$, *b*) the stabilization of physical clusters owing to the contraction of the mean interparticle distance, and *c*) the enhancement of the instability of physical clusters owing to confinement of particles contributing to the magnitude of $\widetilde{\mathcal{H}}(0)$. Then, the effect of *b*) competes with the effect of *c*). This competitive phenomenon should have the ability to enhance the density fluctuations.

The behavior of $\widetilde{\mathcal{H}}(0)$ is changed when ϕ exceeds ϕ_c that is the value of ϕ at the critical

point. The effect of a) becomes dominant. Moreover, the effect of b) becomes more dominant than the effect of c). Thus, the maximized density fluctuations are reduced as ϕ is increased beyond the value of ϕ_c. According to Eq. (227), $0 < \widetilde{C}^*(0) < 1$, $0 < \widetilde{C}^+(0) < 1$, $0 < \widetilde{\mathcal{P}}(0)$, and $0 < 1 - \widetilde{C}^+(0) - \widetilde{C}^*(0) \ll 1$ must be satisfied when $0 < (\phi - \phi_c)/\phi \ll 1$ is satisfied. As ϕ increases, the magnitude of $\widetilde{C}^*(0)$ decreases toward zero. Then, the magnitude of $\widetilde{\mathcal{P}}(0)$ is increased. The magnitude of $\widetilde{\mathcal{H}}(0)$ decreases and reaches zero at $\widetilde{C}^*(0) = 0$. As ϕ is increased more, $\widetilde{C}^*(0)$ becomes negative although its absolute value is not large. Then, $\widetilde{\mathcal{P}}(0)$ reaches a large value toward the percolation threshold. Thus, $\widetilde{\mathcal{H}}(0)$ has a large negative value near the percolation threshold, as confirmed by Fig. 28.

3. Magnitude of $\mathcal{D}(r)$ vanishing at triple point

According to the compressibility equation expressed by Eq.(165), the pressure P of a single-component fluid satisfies relation $[\beta(\partial P/\partial\rho)_{V,T}]^{-1} = 1/(1 - \widetilde{C}^{+}(0) + \widetilde{C}^{*}(0))$. The behavior of the pressure P at the triple point enables specific features of correlation functions to be revealed.

According to Eqs. (44) and (169), the mean physical cluster size S is given as $S = 1+\widetilde{\mathcal{P}}(0)$, in which relation $0 < \widetilde{\mathcal{P}}(0)$ is always satisfied. If a relation given by Eq. (88) is considered, then it is expressed as $S = 1/(1 - \widetilde{C}^{+}(0))$. As the relation $1 \leq S$ is always satisfied, the value of $\widetilde{C}^{+}(0)$ must satisfy

$$0 \leq \widetilde{C}^{+}(0) \leq 1. \tag{228}$$

If $(\partial\rho/\partial P)_{V,T} \approx 0$ is generally satisfied at the triple point, then Eq. (165) requires $\widetilde{C}^{*}(0)$ to satisfy the following relation at the triple point:

$$0 < 1/(-\widetilde{C}^{*}(0)) \ll 1, \tag{229}$$

because the magnitude of $\widetilde{C}^{+}(0)$ is limited by Eq. (228). This denotes that the exclusion effect owing to the hard core of each particle becomes sufficiently dominant at the triple point.

According to Eqs. (163) and (223), the density fluctuations are expressed as

$$\langle (N/V)^2 \rangle - \langle N/V \rangle^2 = (\langle N/V \rangle/V)(\widetilde{\mathcal{P}}(0) + \widetilde{\mathcal{H}}(0) + 1),$$

where the mean number of particles included in a fluid system of volume V is expressed as $\langle N \rangle$. Hence, requiring relation $(\partial\rho/\partial P)_{V,T} \approx 0$ at the triple point corresponds to requiring relation $\langle (N/V)^2 \rangle - \langle N/V \rangle^2 \approx 0$. At the triple point, the density fluctuations are prevented.

This suggests the occurrence of two phenomena. One of the two phenomena indicates that particular particle pairs contributing to the magnitude of $\mathcal{D}(r)$ are confined among branches of physical clusters. The other represents that almost all physical clusters are in the state of the percolation at least near the triple point. In the state of the percolation of physical clusters, relation $1 \ll \widetilde{\mathcal{P}}(0)$ is satisfied according to Eq. (44). The state of percolation at the triple point requires relation $1 \ll \widetilde{\mathcal{P}}(0)$ and $1 \ll -\widetilde{\mathcal{H}}(0)$. Relation $1 \ll -\widetilde{\mathcal{H}}(0)$ is equivalent to $(1/V)\int_V \mathcal{D}(r)\mathrm{d}\mathbf{r} \approx 0$ owing to $\mathcal{D}(r) = \mathcal{H}(r) + 1$. Decreasing the magnitude of $\mathcal{D}(r)$ toward zero means that the magnitude of $-\widetilde{\mathcal{H}}(0)$ is made diverge. Particle pairs that

contribute to the magnitude of $\mathcal{D}(r)$ includes specific particle pairs characterized by the fact that two particles of each particle pair interact in an unbound state where the contribution of the relative kinetic energy of the pair particles exceeds the contribution of the attractive force acting between them. The particle pairs should contribute to maintaining the density fluctuations near the triple point. This fact suggests the assumption that particle pairs that contribute to the magnitude of $\mathcal{D}(r)$ are confined among branches of physical clusters formed by particle pairs that contribute to the magnitude of $\mathcal{P}(r)$. The more densely branches of physical clusters are developed, the more frequently particle pairs that contribute to the magnitude of $\mathcal{D}(r)$ and which are confined among the branches of physical clusters can be exchanged for particle pairs that contribute to the magnitude of $\mathcal{P}(r)$. The development of branches of physical clusters allows for a decrease in the magnitude of $\mathcal{D}(r)$ and allows $1 \ll -\widetilde{\mathcal{H}}(0)$, which leads to $(1/V)\int_V \mathcal{D}(r)\mathrm{d}\mathbf{r} \approx 0$. This is consistent with a consequence obtained from the discussion in Sec.II B 3 as it shows that $(1/V)\int_V \mathcal{D}(r)\mathrm{d}\mathbf{r} \approx 0$ is satisfied near a liquid-solid transition point. The fluid system is allowed to be transformed from the liquid state into the solid state when $(1/V)\int_V \mathcal{D}(r)\mathrm{d}\mathbf{r} \approx 0$ is satisfied.

If the percolation of physical clusters does not occur even at the triple point, then the magnitude of $\widetilde{\mathcal{P}}(0)$ is not large according to Eq. (44). Then, the magnitude of $-\widetilde{\mathcal{H}}(0)$ is also not large as relation $(\partial\rho/\partial P)_{V,T} \approx 0$ requires $\widetilde{\mathcal{H}}(0) \approx -1 - \widetilde{\mathcal{P}}(0)$. This means that the magnitude of $\mathcal{D}(r)$ does not reach zero when an increase in the value of ρ allows the value to reach a specific value given at the triple point. It is somewhat unreasonable to allow a fluid system to be transformed from the liquid state into the solid state under the condition that the magnitude of $\mathcal{D}(r)$ does not become sufficiently small.

Therefore, the condition $1 \ll \widetilde{\mathcal{P}}(0)$ denoting the state of the percolation should be satisfied near the triple point. The occurrence of $1 \ll \widetilde{\mathcal{P}}(0)$ means that branches of physical clusters that develop densely over the entirety of V can confine particle pairs contributing to the magnitude of $\mathcal{D}(r)$ among them. The occurrence of $1 \ll \widetilde{\mathcal{P}}(0)$ near the triple point is effective for explaining why the density fluctuations decease toward vanishing as ρ increases toward a specific value being given at the triple point.

D. Effects on thermodynamic properties of classical fluids

1. Effects of physical cluster formation on features of various fluids

(**a**) *Pressure equation*

In the gas state, the fluid should be characterized as an ensemble of particle pairs consisting of only particles having large relative momenta. Then, each particle pair is characterized as pair particles interacting in an unbound state in which a contribution of their relative kinetic energy exceeds a contribution of the mutually attractive force characterized by a specific pair potential $u(r)$. By contrast, each particle pair forming an ensemble of particles having small relative momenta is characterized as pair particles interacting in a bound state in which a contribution of the mutually attractive force characterized by a specific pair potential exceeds a contribution of their relative kinetic energy. A physical cluster is an ensemble of particles that are linked to each other via bonds defined by such bound states. Particles that participate in the physical cluster formation contribute to the magnitude of the pair connectedness $\mathcal{P}(r)$. These particles have small relative momenta; hence, they cannot actively contribute to the pressure P.

According to the pressure equation, the pressure P for a single-component fluid involves an effect of the physical cluster formation owing to $g(r) = \mathcal{P}(r) + \mathcal{D}(r)$ and is given as follows:

$$\beta P = \rho - (\rho^2/6)\beta \int_V r[\mathrm{d}u(r)/\mathrm{d}r][\mathcal{P}(r) + \mathcal{D}(r)]\mathrm{d}\mathbf{r}.$$

In the pressure equation, particles that contribute to the magnitude of a correlation function $\mathcal{D}(r)$ can have large relative momenta. This can principally contribute to the pressure P. A fluid must consist of particles contributing to $\mathcal{P}(r)$ and particles contributing to $\mathcal{D}(r)$. According to a macroscopic aspect of the fluid, the expectation is that a group of particles contributing to $\mathcal{P}(r)$ homogeneously mix with a group of particles contributing to $\mathcal{D}(r)$. According to microscopic aspect, effects of the physical cluster formation on the fluid do not allow the two groups to homogeneously mix with each other. Moreover, particles having large relative momenta can be confined among branches of physical clusters. Thus, effects of the physical cluster formation on the pressure should be observed. Features of the fluid at a temperature at least below the liquid-vapor critical point should be generated via the cooperation between a group of particles having large relative momenta and another group

of particles having small relative momenta.

Based on Eq. (163), the compressibility estimated from the two differential equations Eqs. (154) and (155) is equal to that estimated from the two integral equations Eqs. (49) and (52), unless a fluid includes extremely large physical clusters developed under conditions beyond the percolation threshold. The two correlation functions $\mathcal{P}(r)$ and $\mathcal{D}(r)$ that are estimated as exact solutions from the two differential equations Eqs. (154) and (155) should be adequate approximations that allow the pressure P to be expressed as the sum of contributions of the physical cluster formation and the other contributions.[42]

(**b**) *Confinement of particles caused by branches of each physical cluster*

Attractive forces between particles constituting each physical cluster must make the branches of each physical cluster contract, and particles having small relative momenta should not be allowed to microscopically homogeneously mix with particles having large relative momenta. Despite this fact, the solid state cannot be found even in a specific fluid being maintained near the freezing point. Hence, particles having large relative momenta must be confined among branches of physical clusters and must prevent physical clusters from contracting. The formation of a structure that prevents the phase separation between a group of particles having highly kinetic abilities and another group of particles having small relative momenta is consistent with the *law of the increase of entropy*. Moreover, the fact that branches of physical clusters confine particles having large relative momenta should allow the liquid-vapor interface to become macroscopically clear and smooth in a fluid system being maintained below the critical point. A capability to allow a fluid to maintain the liquid state[55] should be a result of the physical cluster formation, which allows particles of large relative momenta to be confined, and the physical cluster formation should make the liquid state differ from the gas state.

(**c**) *Features of fluids generated by physical cluster formation*

A microscopic fluid structure induced by the physical cluster formation should allow some features of a fluid in a liquid phase to be interpreted. No matter how high the density of particles becomes, a fluid in the gas state where the effect of the physical cluster formation is not expected can microscopically homogeneously mix with another fluid in the gas state

where the effect of the physical cluster formation is also not expected. However, a fluid in the liquid state cannot homogeneously mix in each microscopic element of volume with another fluid in the liquid state. This phenomenon is caused by an effect of the physical cluster formation.

Physical clusters can contribute to forming a microscopic distribution pattern of particular particles (atoms or molecules) that are dissolved as solute particles in a fluid in the liquid state. Solute particles that cannot actively participate in the physical cluster formation have a tendency to be distributed among branches of physical clusters. Solute particles that can actively participate in the physical cluster formation have a tendency to be distributed as a portion of the particle group that consists of particles forming physical clusters. Thus, physical clusters can make a microscopic distribution pattern of solute particles inhomogeneous in a fluid mixture, such as a liquid of metallic alloy or another solute-solvent mixture. A microscopic fluid structure, resulting in a microscopic distribution pattern of solute particles, might aid in interpreting even the anomaly of the specific heat that can be obtained from a fluid mixture near the consolute point[54] as the stability of physical clusters depends on the temperature.

The formation of a microscopic inhomogeneous distribution pattern of solute particles characterizes a macroscopic phenomenon called the osmotic pressure. The behavior of the osmotic pressure when dissolving solute particles that cannot actively participate in the physical cluster formation differs from that when dissolving solute particles that can actively participate in the physical cluster formation. The difference between microscopic inhomogeneous distribution patterns can allow the temperature dependence of the osmotic pressure for a fluid mixture to differ from that for another different fluid mixture.

Under the condition that the stability of physical clusters is low, both the formation of physical clusters and the decomposition of physical clusters can occur as very sensitive responses to slight variations in temperature. Such highly sensitive responses should allow the thermal conductivity of a fluid to behave anomalously[26]. A microscopic fluid structure induced by the physical cluster formation should influence various phenomena found from a fluid.

At the temperatures of a fluid that is beyond the liquid-vapor critical point although is near this point, the physical cluster formation can cause inhomogeneity as the density fluctuations[12]. As physical clusters that are formed in a fluid in the gas state restricts the

motion of particles, the fluid should gain a specific structure[14]. After the density fluctuations reaches the maximum at the critical point, they are reduced as the density of particles increases[12].

The degree of the density fluctuations can be confirmed from the compressibility as known from Eq. (223). In a hard-sphere fluid system, the density fluctuations are only simply reduced as the density of hard spheres increases according to the equation of state[55]. No existence of attractive forces between particles causes the phase behavior to be simple. The presence of attractive forces between particles can cause complexity of the phase behavior, which depends on features of the attractive forces[56]. Various characteristic phenomena[19–24] can be influenced by the physical cluster formation depending on features of attractive forces acting between particles.

The dependence of the heat capacity of a fluid on temperature behaves characteristically near the critical points.[57,58] According to relation $g(r) = \mathcal{P}(r) + \mathcal{D}(r)$, the internal energy U for a single component fluid involves an effect of the physical cluster formation and is given as follows:

$$U = \frac{3\rho V}{2\beta} + \frac{1}{2}\rho^2 V \int_V u(r)\big[\mathcal{P}(r) + \mathcal{D}(r)\big]\,\mathrm{d}\mathbf{r}.$$

The dependence of the heat capacities of liquids on temperature[54,59] should involve the influence of the stability of physical clusters. Although extremely large physical clusters occur at the percolation threshold, the dependence of the heat capacity of a fluid on temperature can be affected by physical clusters that do not reach a percolation state near the critical point.[42,57,58]

2. Pressure affected by physical cluster growth

Under the condition that Eqs. (156) and (157) are satisfied, two correlation functions $\mathcal{P}(r)$ and $\mathcal{H}(r)$ that are given as exact solutions satisfying the two differential equations expressed by Eqs. (154) and (155) should allow the pressure P maintained by a single-component fluid to be adequately estimated. This is supported by the fact that the compressibility is given by Eq. (163). Moreover, it is supported by the fact that a requirement for making the use of the pressure equation $\beta P = \rho - (\rho^2/6)\beta \int_V r[\mathrm{d}u(r)/\mathrm{d}r][\mathcal{P}(r) + \mathcal{D}(r)]\mathrm{d}\mathbf{r}$ become effective requires approximations for $\mathcal{P}(r)$ and $\mathcal{H}(r)$ to be adequate only in a microscopic range in which $|\mathrm{d}u(r)/\mathrm{d}r|$ retains an effective magnitude. Hence, the pressure P that is estimated from the two correlation functions given as the exact solutions should be an adequate approximation for the pressure that should be estimated from two correlation functions derived from the two integral equations corresponding to Eqs. (49) and (52).

(**a**) *Correlation functions for describing fluid*

The correlation functions $\mathcal{P}(r)$ and $\mathcal{H}(r)$ are given as exact solutions of the two differential equations. According to Eq. (182), $\mathcal{P}(r)$ is expressed by

$$\mathcal{P}(r) = \mathcal{P}_0(r) + \mathcal{P}_{\mathrm{in}}(r) + \mathcal{P}_{\mathrm{ex}}(r),$$

where $\mathcal{P}_0(r)$ expresses the direct contribution of the particle located at the origin, i.e., $r = 0$, and it decreases steeply as $\xi^+ r$ is increased because it depends on an exponential factor $e^{-\xi^+(r-\sigma)}$ $(\sigma \leq r)$. If a condition of the fluid is not in the vicinity of the percolation threshold where $0 \leq \xi^+\sigma \ll 1$ is satisfied, then the contribution of $\mathcal{P}_0(r)$ can become sufficiently small. According to Eq. (200), $\mathcal{H}(r)$ is expressed by

$$\mathcal{H}(r) + 1 = \mathcal{H}_0(r) + \mathcal{H}_{\mathrm{in}}^{(+)}(r) + \mathcal{H}_{\mathrm{ex}}^{(+)}(r) + \mathcal{H}_{\mathrm{in}}^{(*)}(r) + \mathcal{H}_{\mathrm{ex}}^{(*)}(r) + 1,$$

where $\mathcal{H}_0(r)$ expresses the direct contribution of the particle located at the origin, i.e., $r = 0$, and it decreases steeply as ξr is increased because it depends on an exponential factor $e^{-\xi(r-\sigma)}$ $(\sigma \leq r)$. If a condition of the fluid is not in the vicinity of the critical point where $0 \leq \xi^+\sigma \ll 1$ is satisfied, then the contribution of $\mathcal{H}_0(r)$ can become sufficiently small.

According to the dependence of $\mathcal{H}(r)$ on ϕ in cases of $\mathcal{P}(r) \neq 0$, an increase in the value of ϕ can allow the absolute value of the negative magnitude of $\mathcal{H}(r)$ to be increased. This is confirmed by a comparison between (a) and (c) in Fig. 20 and another comparison between

(a) and (c) in Fig. 21. The behaviors mentioned here can be caused by the exclusion effect owing to the hard-core potential of each particle.

(**b**) *Estimate of pressure*

To consider the exclusion effect owing to the hard-core potential of each particle, the pressure equation should be rewritten as

$$P = \frac{\rho}{\beta}\left[1 - 4\phi\int_0^{\sigma}\sigma\frac{\mathrm{d}\beta u_{\mathrm{r}}(r)}{\mathrm{d}r}g(r)\left(\frac{r}{\sigma}\right)^3\frac{1}{\sigma}\mathrm{d}r - 4\phi\int_{\sigma}^{\infty}\sigma\frac{\mathrm{d}\beta u_{\mathrm{a}}(r)}{\mathrm{d}r}g(r)\left(\frac{r}{\sigma}\right)^3\frac{1}{\sigma}\mathrm{d}r\right] \quad (230)$$

Here, the pair potential contributing to the interaction of a particle with another particle is expressed as $u(r) = u_{\mathrm{r}}(r)$ for $0 \le r \le \sigma$ and $u(r) = u_{\mathrm{a}}(r)$ for $\sigma \le r < \infty$. $u_{\mathrm{r}}(r)$ is a repulsive pair potential owing to the hard core, and $u_{\mathrm{a}}(r)$ is an attractive pair potential. Then, $\lim_{\delta\to 0} u(\sigma - \delta) \neq \lim_{\delta\to 0} u(\sigma + \delta)$ appears. For $0 \le r \le \sigma$, $u(r) = \infty$ is satisfied. For $\sigma < r < \infty$, $-\infty < u(r) < 0$ is satisfied, and $-u(r)$ has a finite positive value.

i) *Direct effect of the hard-core potential on the pressure*

To assess the second factor on the right-hand side of Eq. (230), the PY approximation can be expressed as

$$c(r) = \eta(r)f(r), \quad (231)$$

where $f(r)$ is the Mayer f-function given as $f(r) = e^{-\beta u_{\mathrm{r}}(r)} - 1$, and $\eta(r)$ is defined by

$$\eta(r) \equiv g(r)e^{\beta u_{\mathrm{r}}(r)}, \quad (232)$$

According to Eq. (231), the hard-core potential $u_{\mathrm{r}}(r) = \infty$ functioning for $0 < r \le \sigma$ requires

$$c(\sigma - \delta) = \eta(\sigma - \delta)f(\sigma - \delta) = -\eta(\sigma - \delta), \quad (0 < \delta \ll 1). \quad (233)$$

The MSA requires Eq. (231) to satisfy

$$c(\sigma + \delta) = \eta(\sigma + \delta)f(\sigma + \delta) = -\beta u_{\mathrm{r}}(\sigma + \delta), \quad (0 < \delta \ll 1). \quad (234)$$

Then,

$$c(\sigma + \delta) \neq c(\sigma - \delta), \quad (0 < \delta \ll 1). \quad (235)$$

However, Eqs. (233) and (233) require $c(\sigma+\delta)$ and $c(\sigma-\delta)$ to remain finite values for $0<\delta\ll 1$. Therefore, $\eta(\sigma+\delta)$ and $\eta(\sigma-\delta)$ are finite values for $0<\delta\ll 1$, and it is acceptable to assume that

$$\lim_{\delta\to 0}\eta(\sigma+\delta)=\lim_{\delta\to 0}\eta(\sigma-\delta). \tag{236}$$

Thus, the use of Eq. (232) allows the second factor on the right-hand side of Eq. (230) to be rewritten as

$$\begin{aligned}4\phi\int_0^{\sigma}\sigma\frac{\mathrm{d}\beta u_{\mathrm{r}}(r)}{\mathrm{d}r}g(r)\left(\frac{r}{\sigma}\right)^3\frac{1}{\sigma}\mathrm{d}r=&4\phi\lim_{\delta\to 0}\int_0^{\sigma+\delta}\sigma\frac{\mathrm{d}\beta u_{\mathrm{r}}(r)}{\mathrm{d}r}\eta(r)e^{-\beta u_{\mathrm{r}}(r)}\left(\frac{r}{\sigma}\right)^3\frac{1}{\sigma}\mathrm{d}r\\ =&-4\phi\lim_{\delta\to 0}\int_0^{\sigma+\delta}\sigma\eta(r)\left(\frac{\mathrm{d}}{\mathrm{d}r}e^{-\beta u_{\mathrm{r}}(r)}\right)\left(\frac{r}{\sigma}\right)^3\frac{1}{\sigma}\mathrm{d}r.\end{aligned} \tag{237}$$

Then, the hard-core potential requires $u_{\mathrm{r}}(r)=\infty$ for $0\le r\le\sigma$ and $u_{\mathrm{r}}(r)=0$ for $\sigma\le r$ to be satisfied, and the direct effect owing to the hard-core potential corresponds to the impact occurring at $r=\sigma$. Hence, a factor $e^{-\beta u_{\mathrm{r}}(r)}$ for expressing the direct effect is equivalent to the Heaviside step function $\theta(r-\sigma)$. Thus, the derivative in Eq. (237) is expressed as $\frac{\mathrm{d}}{\mathrm{d}r}e^{-\beta u_{\mathrm{r}}(r)}=\frac{\mathrm{d}}{\mathrm{d}r}\theta(r-\sigma)=\delta(r-\sigma)$. Ultimately, Eq. (236) requires Eq. (237) to be estimated as

$$\begin{aligned}4\phi\int_0^{\sigma}\sigma\frac{\mathrm{d}\beta u_{\mathrm{r}}(r)}{\mathrm{d}r}g(r)\left(\frac{r}{\sigma}\right)^3\frac{1}{\sigma}\mathrm{d}r=&-4\phi\lim_{\delta\to 0}\int_0^{\sigma+\delta}\sigma\eta(r)\delta(r-\sigma)\left(\frac{r}{\sigma}\right)^3\frac{1}{\sigma}\mathrm{d}r\\ =&-4\phi\lim_{\delta\to 0}\eta(\sigma+\delta)\left(\frac{\sigma+\delta}{\sigma}\right)^3\\ =&-4\phi g(\sigma).\end{aligned} \tag{238}$$

ii) *Pressure given by Eq. (230)*

The use of $\mathcal{P}(r)$ and $\mathcal{H}(r)$ given as the exact solutions allows the pressure P of the fluid to be expressed by the following formula:

$$P=\frac{\rho}{\beta}\left[1+4\phi g(\sigma)-\frac{\beta}{\rho}P_{\mathrm{c}}(\mathcal{P})-\frac{\beta}{\rho}P_{\mathrm{c}}(\mathcal{D})\right], \tag{239}$$

where $\mathcal{D}(r)=\mathcal{H}(r)+1$.

On the right-hand side of Eq. (239), a factor $(\beta/\rho)P_{\mathrm{c}}(\mathcal{P})$ is given by

$$\frac{\beta}{\rho}P_{\mathrm{c}}(\mathcal{P})\equiv\frac{\beta}{\rho}P_{\mathrm{c}}(\mathcal{P}_0)+4\phi\int_{\sigma}^{\infty}\sigma\frac{\mathrm{d}\beta u_{\mathrm{a}}(r)}{\mathrm{d}r}[\mathcal{P}_{\mathrm{in}}(r)+\mathcal{P}_{\mathrm{ex}}(r)]\left(\frac{r}{\sigma}\right)^3\frac{1}{\sigma}\mathrm{d}r, \tag{240}$$

where

$$\frac{\beta}{\rho}P_{\rm c}(\mathcal{P}_0) \equiv 4\phi\int_{\sigma}^{\infty}\sigma\frac{{\rm d}\beta u_{\rm a}(r)}{{\rm d}r}\mathcal{P}_0(r)\left(\frac{r}{\sigma}\right)^3\frac{1}{\sigma}{\rm d}r. \tag{241}$$

If a condition of the fluid is far from the percolation threshold, then the expectation is that the contribution of $(\beta/\rho)P_{\rm c}(\mathcal{P}_0)$ is sufficiently smaller than the other factor.

Moreover, Eq. (239) includes a factor $(\beta/\rho)P_{\rm c}(\mathcal{D})$ that is given by

$$\frac{\beta}{\rho}P_{\rm c}(\mathcal{D}) = \frac{\beta}{\rho}P_{\rm c}(\mathcal{H}_0) + \frac{\beta}{\rho}P_{\rm c}(\mathcal{H}^{(+)}) + \frac{\beta}{\rho}P_{\rm c}(\mathcal{H}^{(*)}+1), \tag{242}$$

where

$$\frac{\beta}{\rho}P_{\rm c}(\mathcal{H}_0) \equiv 4\phi\int_{\sigma}^{\infty}\sigma\frac{{\rm d}\beta u_{\rm a}(r)}{{\rm d}r}\mathcal{H}_0(r)\left(\frac{r}{\sigma}\right)^3\frac{1}{\sigma}{\rm d}r, \tag{243}$$

$$\frac{\beta}{\rho}P_{\rm c}(\mathcal{H}^{(+)}) \equiv 4\phi\int_{\sigma}^{\infty}\sigma\frac{{\rm d}\beta u_{\rm a}(r)}{{\rm d}r}[\mathcal{H}_{\rm in}^{(+)}(r)+\mathcal{H}_{\rm ex}^{(+)}(r)]\left(\frac{r}{\sigma}\right)^3\frac{1}{\sigma}{\rm d}r, \tag{244}$$

and

$$\frac{\beta}{\rho}P_{\rm c}(\mathcal{H}^{(*)}+1) \equiv 4\phi\int_{\sigma}^{\infty}\sigma\frac{{\rm d}\beta u_{\rm a}(r)}{{\rm d}r}[\mathcal{H}_{\rm in}^{(*)}(r)+\mathcal{H}_{\rm ex}^{(*)}(r)+1]\left(\frac{r}{\sigma}\right)^3\frac{1}{\sigma}{\rm d}r. \tag{245}$$

If a condition of the fluid is far from the critical point, then the expectation is that the contribution of $(\beta/\rho)P_{\rm c}(\mathcal{H}_0)$ is sufficiently smaller than that of the other factors.

(**c**) *Effects of physical cluster formation on pressure*

In Eq. (239), the contribution of $(\beta/\rho)P_{\rm c}(\mathcal{P})$ to the magnitude of P corresponds to an effect from the particles participating in the physical cluster formation. A requirement $-{\rm d}\beta u(r)/{\rm d}r < 0$ for considering the mutually attractive force and another requirement $\mathcal{P}(r) \geq 0$ for considering a feature of the pair connectedness allow a relation $(\beta/\rho)P_{\rm c}(\mathcal{P}) > 0$ to always be satisfied according to Eqs. (240) and (241). Thus, recognition obtained from Eq. (239) denotes that the contribution of $(\beta/\rho)P_{\rm c}(\mathcal{P})$ plays a role in decreasing the magnitude of P. This demonstrates that the physical cluster formation plays a role in reducing the pressure of the fluid. This effect can allow each fluid in the liquid state to maintain its volume without being confined, and it can allow each fluid in the liquid state to maintain its surface without a container. Simultaneously, this can allow surface tension to be generated.

A factor $(\beta/\rho)P_{\rm c}(\mathcal{H}^{(+)})$, which is given by Eq. (244), represents an effect induced in the case that the physical clusters confine particles contributing to the magnitude of $\mathcal{H}(r)$. If

the contributions of the physical cluster formation to the pressure are ignored, then the factor $(\beta/\rho)P_{\rm c}(\mathcal{H}^{(+)})$ should be zero with $(\beta/\rho)P_{\rm c}(\mathcal{P})$. Then, Eqs. (239) and (242) require the pressure to be expressed by

$$P = \frac{\rho}{\beta}\left[1 + 4\phi g(\sigma) - \frac{\beta}{\rho}P_{\rm c}(\mathcal{H}_0) - \frac{\beta}{\rho}P_{\rm c}(\mathcal{H}^{(*)} + 1)\right]. \tag{246}$$

The magnitude of P that is estimated from Eq. (246) should be larger than that estimated form Eq. (239) in which the contributions of the two factors $(\beta/\rho)P_{\rm c}(\mathcal{P})$ and $(\beta/\rho)P_{\rm c}(\mathcal{H}^{(+)})$ are not ignored. If the contributions of the two factors for P are not ignored, then the physical cluster formation plays a role in reducing the pressure. Then, particles having large relative momenta are confined among branches of physical clusters.[42]

3. Internal energy affected by physical cluster growth

(a) *Estimate of internal energy U for single-component fluid*

The two correlation functions $\mathcal{P}(r)$ and $\mathcal{H}(r)$ are given as the exact solutions satisfying Eqs. (154) and (155) under the condition that Eqs. (156) and (157) are satisfied. The internal energy can be sufficiently accurately estimated from the use of a specific equation if approximations for $\mathcal{P}(r)$ and $\mathcal{H}(r)$ are adequate within a domain where a pair potential causing the interaction of a particle with another remains effective. Then, this domain retains a microscopic extent. On the contrary, the domain within which $\mathcal{P}(r)$ and $\mathcal{H}(r)$ are estimated reaches a macroscopic extent. On the surface of the domain, the requirements expressed by Eqs. (156) and (157) are satisfied.

The features of the pair potential require the equation for an estimate of the internal energy U to be expressed by

$$U = \frac{3\rho V}{2\beta}\left[1 + 8\phi\int_0^\sigma \beta u_{\rm r}(r)g(r)\left(\frac{r}{\sigma}\right)^2\frac{1}{\sigma}{\rm d}r + 8\phi\int_\sigma^\infty \beta u_{\rm a}(r)g(r)\left(\frac{r}{\sigma}\right)^2\frac{1}{\sigma}{\rm d}r\right]. \tag{247}$$

The continuity given by Eq. (236) with Eq. (232) can be expressed as follows:

$$0 < \lim_{\delta\to 0} g(\sigma-\delta)e^{\beta u_{\rm r}(\sigma-\delta)} = \lim_{\delta\to 0} g(\sigma+\delta)e^{\beta u_{\rm a}(\sigma+\delta)} < \infty. \tag{248}$$

Thus, Eq. (248) requires

$$0 \le \lim_{\delta\to 0} g(\sigma-\delta)\beta u_{\rm r}(\sigma-\delta) \ll \lim_{\delta\to 0} g(\sigma-\delta)e^{\beta u_{\rm r}(\sigma-\delta)}. \tag{249}$$

Then, Eq. (249) means that the following relation is satisfied:

$$\lim_{\delta\to 0} g(\sigma-\delta)\beta u_{\rm r}(\sigma-\delta)=0. \tag{250}$$

Therefore, the contribution of the second factor on the right-hand side of Eq. (247) disappears, and the internal energy is estimated as

$$U=\frac{3\rho V}{2\beta}\left[1+8\phi\int_{\sigma}^{\infty}\beta u_{\rm a}(r)g(r)\left(\frac{r}{\sigma}\right)^2\frac{1}{\sigma}{\rm d}r\right], \tag{251}$$

where $g(r)=\mathcal{P}(r)+\mathcal{D}(r)$ with $\mathcal{D}(r)=\mathcal{H}(r)+1$.

If the approximations for $\mathcal{P}(r)$ and $\mathcal{H}(r)$ are adequate in the effective range in which $|u(r)|\neq 0$ is satisfied, then the approximations allow U to be estimated in a sufficiently accurate fashion. Hence, the internal energy U that is estimated from the exact solutions should be an adequate approximation for the internal energy that should be estimated from two correlation functions derived from the two integral equations corresponding to Eqs. (49) and (52).

The use of the exact solutions given by $\mathcal{P}(r)=\mathcal{P}_0(r)+\mathcal{P}_{\rm in}(r)+\mathcal{P}_{\rm ex}(r)$ and $\mathcal{D}(r)=\mathcal{H}_0(r)+\mathcal{H}_{\rm in}^{(+)}(r)+\mathcal{H}_{\rm ex}^{(+)}(r)+\mathcal{H}_{\rm in}^{(*)}(r)+\mathcal{H}_{\rm ex}^{(*)}(r)+1$ allows the internal energy U for the single-component fluid to be given as

$$U=\frac{3\rho V}{2\beta}\left[1+\frac{2\beta}{3\rho V}U_{\rm c}(\mathcal{P})+\frac{2\beta}{3\rho V}U_{\rm c}(\mathcal{D})\right]. \tag{252}$$

On the right-hand side of Eq. (252), a factor $(2\beta/3\rho V)U_{\rm c}(\mathcal{P})$ is given by

$$\frac{2\beta}{3\rho V}U_{\rm c}(\mathcal{P})\equiv\frac{2\beta}{3\rho V}U_{\rm c}(\mathcal{P}_0)+8\phi\int_{\sigma}^{\infty}\beta u_{\rm a}(r)\left[\mathcal{P}_{\rm in}(r)+\mathcal{P}_{\rm ex}(r)\right]\left(\frac{r}{\sigma}\right)^2\frac{1}{\sigma}{\rm d}r, \tag{253}$$

where

$$\frac{2\beta}{3\rho V}U_{\rm c}(\mathcal{P}_0)\equiv 8\phi\int_{\sigma}^{\infty}\beta u_{\rm a}(r)\mathcal{P}_0(r)\left(\frac{r}{\sigma}\right)^2\frac{1}{\sigma}{\rm d}r. \tag{254}$$

If a condition of the fluid is far from the percolation threshold, then the expectation is that the contribution of $(2\beta/3\rho V)U_{\rm c}(\mathcal{P}_0)$ is sufficiently smaller than the other factor. In Eq. (252), relation $(2\beta/3\rho V)U_{\rm c}(\mathcal{P})<0$ is satisfied because $u(r)<0$ and $\mathcal{P}(r)>0$ are satisfied. The factor $(2\beta/3\rho V)U_{\rm c}(\mathcal{P})$ plays a role in reducing the magnitude of the internal energy. The physical cluster formation contributes to reducing the value of U. The internal energy as a thermodynamic property of a classical fluid system is affected by the formation of a specific structure generated in the fluid.

Moreover, Eq. (252) includes a factor $(2\beta/3\rho V)U_{\rm c}(\mathcal{D})$, which is given by

$$\frac{2\beta}{3\rho V}U_{\rm c}(\mathcal{D}) \equiv \frac{2\beta}{3\rho V}U_{\rm c}(\mathcal{H}_0) + \frac{2\beta}{3\rho V}U_{\rm c}(\mathcal{H}^{(+)}) + \frac{2\beta}{3\rho V}U_{\rm c}(\mathcal{H}^{(*)}+1), \tag{255}$$

where

$$\frac{2\beta}{3\rho V}U_{\rm c}(\mathcal{H}_0) \equiv 8\phi\int_\sigma^\infty \beta u_{\rm a}(r)\mathcal{H}_0(r)\left(\frac{r}{\sigma}\right)^2\frac{1}{\sigma}{\rm d}r, \tag{256}$$

$$\frac{2\beta}{3\rho V}U_{\rm c}(\mathcal{H}^{(+)}) \equiv 8\phi\int_\sigma^\infty \beta u_{\rm a}(r)\left[\mathcal{H}_{\rm in}^{(+)}(r)+\mathcal{H}_{\rm ex}^{(+)}(r)\right]\left(\frac{r}{\sigma}\right)^2\frac{1}{\sigma}{\rm d}r, \tag{257}$$

and

$$\frac{2\beta}{3\rho V}U_{\rm c}(\mathcal{H}^{(*)}+1) \equiv 8\phi\int_\sigma^\infty \beta u_{\rm a}(r)\left[\mathcal{H}_{\rm in}^{(*)}(r)+\mathcal{H}_{\rm ex}^{(*)}(r)+1\right]\left(\frac{r}{\sigma}\right)^2\frac{1}{\sigma}{\rm d}r. \tag{258}$$

If a condition of the fluid is far from the critical point, then the expectation is that the contribution of $(2\beta/3\rho V)U_{\rm c}(\mathcal{H}_0)$ is sufficiently smaller than the other factors.

The exact solutions given by $\mathcal{P}(r) = \mathcal{P}_0(r) + \mathcal{P}_{\rm in}(r) + \mathcal{P}_{\rm ex}(r)$ and $\mathcal{H}(r)+1 = \mathcal{H}_0(r) + \mathcal{H}_{\rm in}^{(+)}(r) + \mathcal{H}_{\rm ex}^{(+)}(r) + \mathcal{H}_{\rm in}^{(*)}(r) + \mathcal{H}_{\rm ex}^{(*)}(r) + 1$ satisfy Eqs. (156) and (157) as requirements before reaching the percolation threshold. Hence, the internal energy that is obtained from the substitution of the exact solutions $\mathcal{P}(r)$ and $\mathcal{H}(r)$ into Eq. (252) corresponds to that which should be estimated in a condition before reaching the percolation threshold. The internal energy obtained from the use of the exact solutions cannot be allowed to express the internal energy that should be estimated under the condition that a fluid includes extremely large physical clusters developed beyond the percolation threshold. Despite this fact, the internal energy estimated from Eq. (252) should preserve an adequate approximation even near the percolation threshold.

By contrast, if the contributions of the physical cluster formation to the internal energy are ignored, then $(2\beta/3\rho V)U_{\rm c}(\mathcal{P}) = 0$ and $(2\beta/3\rho V)U_{\rm c}(\mathcal{H}^{(+)}) = 0$ should be satisfied. This becomes adequately real at least at high temperatures. Then, Eqs. (252) and (255) require the internal energy to be given as

$$U = \frac{3\rho V}{2\beta}\left[1 + \frac{2\beta}{3\rho V}U_{\rm c}(\mathcal{H}_0) + \frac{2\beta}{3\rho V}U_{\rm c}(\mathcal{H}^{(*)}+1)\right]. \tag{259}$$

If a fluid is the ideal gas, then the internal energy satisfies $(2/3)\beta U/\rho V = 1$, which is independent of temperature. When ignoring the formation of physical clusters is acceptable for a fluid, the exclusion effect owing to the hard-core potential of each particle becomes a dominant factor that makes $(2/3)\beta U/\rho V$ depend on temperature. This is confirmed according

to the form of the above equation for a fluid that does not have a specific structure owing to the physical cluster formation.

(b) *Relations of internal energy U with structures of fluid*

A fluid in the gas state should be characterized as a specific ensemble of particle pairs consisting of particles having large relative momenta. Then, each particle pair is characterized as pair particles interacting in an unbound state in which a contribution of their relative kinetic energy exceeds a contribution of the mutually attractive force characterized by a specific pair potential $u(r)$. Even in the fluid in the liquid state, such particle pairs having large relative momenta are included. Indeed, the contribution of their large relative momenta to the internal energy U should be dominant in comparison with that of small relative momenta carried by particle pairs forming physical clusters. Each particle pair formed by pair particles having small relative momenta is characterized as pair particles interacting in a bound state in which a contribution of the mutually attractive force characterized by the pair potential exceeds a contribution of their relative kinetic energy. Each physical cluster mentioned here is an ensemble of particles that are linked with each other via bonds defined by such bound states.

Particles that participate in physical cluster formation contribute to the magnitude of $\mathcal{P}(r)$. These particles have small relative momenta; hence, they cannot actively contribute to U. Particles that contribute to the magnitude of $\mathcal{D}(r)$ have large relative momenta. These particles can principally contribute to U. Thus, particles are classified into two groups. According to the microscopic aspect, effects of the physical cluster formation on the fluid do not allow particles belonging to the two groups homogeneously to mix with each other. Particles having large relative momenta can be confined among branches of physical clusters. Thus, an effect of the physical cluster formation must influence the internal energy. The internal energy of the fluid at a temperature at least below the liquid-vapor critical point should involve effects caused by the cooperation between a group of particles having large relative momenta and another group of particles having small relative momenta.

The internal energy U given by Eq. (252) includes a contribution $U_{\rm c}(\mathcal{P})$ of physical clusters and another contribution $U_{\rm c}(\mathcal{D})$. Movements of particles participating in the physical cluster formation have a tendency to be inhibited by mutually attractive forces making the particles interact with each other. The effect of the inhibition of kinetic abilities of

the particles on the internal energy is given as $(2/3)\beta U_{\rm c}(\mathcal{P})/\rho V$ in Eq. (252). If a fluid includes physical clusters, then the magnitude of $(2/3)\beta U_{\rm c}(\mathcal{D})/\rho V$ involves a confinement effect that is generated by confining particles of large relative momenta among branches of physical clusters. If a fluid include no physical cluster, then the temperature dependence of $(2/3)\beta U_{\rm c}(\mathcal{D})/\rho V$ is characterized by a contribution caused by the exclusion effect owing to the hard-core potential of each particle.

Even if a contribution of the formation of extremely large physical clusters may not be required, the dependence of the specific heat on temperature T near a special temperature T_0, at which a property of a fluid varies anomalously, can be characterized by $(1 - T/T_0)^{-\alpha}$ $(0 < \alpha)$. This can be expected at least for the measurements of heat capacity for argon and oxygen.[57] It is impossible to find the above dependence for a hard-sphere fluid system without the formation of physical clusters.

For a fluid in the liquid state, the dependence of $(2/3)\beta U/\rho V$ on the temperature of the fluid is not simple.[59] A confinement effect that results from confining particles of large relative momenta among branches of physical clusters can affect the temperature dependence of $(2/3)\beta U/\rho V$. Indeed, the temperature dependence in a region of high temperature should be different from that in a region of low temperature because the mean size of physical clusters depends sharply on the temperature. When variations in the temperature of the fluid occurs, even variations in the magnitude of $(2/3)\beta U_{\rm c}(\mathcal{D})/\rho V$ can become more sensitive in the region of lower temperature where physical clusters should be more stabilized.

The mean size of physical clusters is steeply decreased if the temperature of the fluid is slightly increased from that at the percolation threshold. Hence, when variations in temperature occur, variations in the magnitude of $(2/3)\beta U_{\rm c}(\mathcal{P})/\rho V$ should be ignored in the temperature region that is higher than that at the percolation threshold. By contrast, when variations in temperature occur, the magnitude of $(2/3)\beta U_{\rm c}(\mathcal{D})/\rho V$ can sensitively vary even when the temperature is much higher than that at the percolation threshold because particles that contribute to the magnitude of $\mathcal{D}(r)$ increase in number as the temperature is increased. When the temperature approaches that at the percolation threshold, physical clusters grow steeply in the vicinity of the percolation threshold. A steep growth of physical clusters in the vicinity of the percolation threshold should allow for the contribution of $(2/3)\beta U_{\rm c}(\mathcal{P})/\rho V$ to the internal energy to be considerably enhanced. As exemplified by the internal energy, thermodynamic properties of a classical fluid system can be affected via

the formation of a specific structure generated for the physical cluster formation and the confinement of particles having large relative momenta.

III. PHYSICAL CLUSTER FORMATION IN MULTICOMPONENT FLUIDS

Phase behavior of a multicomponent fluid mixture system is complicated by the contribution of physical cluster growth that involves several constituents of the system. It is useful to establish an equation system corresponding to that composed of Eqs. (49) and (52) to analyze the effects of the physical cluster formation on the properties of the multicomponent fluid mixture system. Each physical cluster is formed as an ensemble of pair particles that interact with each other in a bound state.

Two particles can interact with each other in a bound state or in an unbound state in the multicomponent fluid mixture system. If the two particles are particle 1 of species i and particle 2 of species j, the three-dimensional coordinates for the particles of species i and j can be denoted by $\mathbf{r}_1^{(i)}$ and $\mathbf{r}_2^{(j)}$, respectively. Then, a bound state, i.e., $\mathcal{E}_{(1,2)}^{ij} + \beta u_{ij}(|\mathbf{r}_1^{(i)} - \mathbf{r}_2^{(j)}|) \leq 0$ corresponds to a specific state where the contribution $\beta u_{ij}(|\mathbf{r}_1^{(i)} - \mathbf{r}_2^{(j)}|)$ of a mutually attractive force between the particles 1 and 2 exceeds the contribution $\mathcal{E}_{(1,2)}^{ij}$ of relative kinetic energy between the two particles because their relative momentum is small. An unbound state, i.e., $\mathcal{E}_{(1,2)}^{ij} + \beta u_{ij}(|\mathbf{r}_1^{(i)} - \mathbf{r}_2^{(j)}|) > 0$ corresponds to a specific state where the contribution $\mathcal{E}_{(1,2)}^{ij}$ of the relative kinetic energy between the particles 1 and 2 exceeds the contribution $\beta u_{ij}(|\mathbf{r}_1^{(i)} - \mathbf{r}_2^{(j)}|)$ of the mutually attractive force between the two particles because their relative momentum is large.

Unless phase separation occurs in a multicomponent fluid mixture system, the macroscopic picture of the system allows particles that have large and small relative momenta to be homogeneously mixed. However, these particles cannot be microscopically homogeneously mixed. Branches of physical clusters can confine particles that have large relative momenta. Thus, the physical cluster growth wherein particles that have small relative momenta participate can affect various properties of the multicomponent fluid mixture system.

A. Two integral equations for describing an $\mathcal{L}$-component fluid mixture system

The probability that one particle each of species i and j are located in a volume element $\mathrm{d}\mathbf{r}_1^{(i)}$ at $\mathbf{r}_1^{(i)}$ and in volume element $\mathrm{d}\mathbf{r}_2^{(j)}$ at $\mathbf{r}_2^{(j)}$ respectively is expressed using the pair correlation function g_{ij}. Then, a three-dimensional coordinate $\mathbf{r}_h^{(i)}$ denotes the location of an h particle of species i ($i = 1,\ 2,\ \cdots,\ \mathcal{L}$). If the two root points are labeled 1 and 2, one of two particles occupying the two root point is located at $\mathbf{r}_1^{(i)}$ and the other at $\mathbf{r}_2^{(i')}$. The three-dimensional coordinates of field points labeled 3, 4, $\cdots$ are expressed as $\mathbf{r}_3^{(i'')}$, $\mathbf{r}_4^{(i''')}$, $\cdots$, respectively.

The above probability is given as $\rho_i\rho_j g_{ij}(r)\mathrm{d}\mathbf{r}_1^{(i)}\mathrm{d}\mathbf{r}_2^{(j)}$, wherein ρ_i and ρ_j represent the particle densities of species i and j for a uniform distribution in a fluid mixture system of $\mathcal{L}$ constituents, respectively. Parameter r is the distance between the two root points and it is given as $r = |\mathbf{r}|$ and $\mathbf{r} = \mathbf{r}_1^{(i)} - \mathbf{r}_2^{(j)}$.

The relationship between a particle of species i in $\mathrm{d}\mathbf{r}_1^{(i)}$ at $\mathbf{r}_1^{(i)}$ and a particle of species j in $\mathrm{d}\mathbf{r}_2^{(j)}$ at $\mathbf{r}_2^{(j)}$ is characterized by two possibilities: Both of them belong to the same physical cluster or each of them belongs to different physical clusters.

The probability that both of the two particles belong to the same physical cluster is expressed using the pair connectedness $\mathcal{P}_{ij}$. Then, the probability is given by $\rho_i\rho_j\mathcal{P}_{ij}(r)\mathrm{d}\mathbf{r}_1^{(i)}\mathrm{d}\mathbf{r}_2^{(j)}$. The pair connectedness $\mathcal{P}_{ij}(r)$ allows estimating the mean size of the physical clusters.[3]

The probability that the particle of i in $\mathrm{d}\mathbf{r}_1^{(i)}$ at $\mathbf{r}_1^{(i)}$ and the particle of j in $\mathrm{d}\mathbf{r}_2^{(j)}$ at $\mathbf{r}_2^{(j)}$ belong to a physical cluster and another physical cluster respectively is expressed using a correlation function $\mathcal{D}_{ij}$. Then, the probability is given by $\rho_i\rho_j\mathcal{D}_{ij}(r)\mathrm{d}\mathbf{r}_1^{(i)}\mathrm{d}\mathbf{r}_2^{(j)}$. Ultimately, the probability that the particles of i and j are located in $\mathrm{d}\mathbf{r}_1^{(i)}$ at $\mathbf{r}_1^{(i)}$ and in $\mathrm{d}\mathbf{r}_2^{(j)}$ at $\mathbf{r}_2^{(j)}$ respectively is represented as the sum $\rho_i\rho_j\mathcal{P}_{ij}(r)\mathrm{d}\mathbf{r}_1^{(i)}\mathrm{d}\mathbf{r}_2^{(j)} + \rho_i\rho_j\mathcal{D}_{ij}(r)\mathrm{d}\mathbf{r}_1^{(i)}\mathrm{d}\mathbf{r}_2^{(j)}$. Thus, the pair connectedness $\mathcal{P}_{ij}(r)$ for the fluid mixture system of $\mathcal{L}$ constituents is related to $g_{ij}(r)$ as

$$g_{ij}(r) = \mathcal{P}_{ij}(r) + \mathcal{D}_{ij}(r). \tag{260}$$

This relationship holds the same meaning as that maintained by Eq. (38) for a single-component fluid system.

1. Probability that two particles interact with each other in the bound state

(a) *Probability* $p_{ij}(r)$

A mutually attractive force can make a particle interact with another. Hence, the relationship between pair particles specified by an f-function have two possibilities. If the pair particles are an h_i particles of species i and an h_j particles of j, one possibility suggests that the contribution of a mutually attractive force between the h_i and h_j particles exceeds the contribution $\mathcal{E}^{ij}_{(h_i,h_j)}$ of the relative kinetic energy between them. The other possibility suggests that $\mathcal{E}^{ij}_{(h_i,h_j)}$ exceeds the contribution of the mutually attractive forces. When one particle each of species i and j are located at $\mathbf{r}^{(i)}_{h_i}$ and $\mathbf{r}^{(j)}_{h_j}$ respectively, the distance between them is $r_{ij} = |\mathbf{r}^{(i)}_{h_i} - \mathbf{r}^{(j)}_{h_j}|$. Then, the contribution of a mutually attractive force between the two particles is given by $\beta u_{ij}(r_{ij})$. This allows Eq. (30) to express the probability $p_{ij}(r_{ij})$ that the pair particles satisfy the condition $\mathcal{E}^{ij}_{(h_i,h_j)} + u_{ij}(r_{ij}) \leq 0$. The probability $p_{ij}(r_{ij})$ is given by

$$p_{ij}(r_{ij}) = 2\pi^{-1/2}\Big[\Gamma(3/2) - \Gamma(3/2, -\beta u_{ij}(r_{ij}))\Big]. \tag{261}$$

Indeed, this probability should behave as $p_{ij}(r_{ij}) = 0$ if $u_{ij}(r_{ij})$ is a repulsive potential, i.e., $\beta u_{ij}(r_{ij}) > 0$. If the particles are located outside the effective ranges within which mutually attractive forces make the particles interact with each other, $p_{ij}(r_{ij}) = 0$ should also be satisfied. Further, the use of the Heaviside step function $\theta(\tau) = 1\ (\tau > 0),\ 0\ (\tau < 0)$ allows Eq. (261) to be rewritten as

$$p_{ij}(r_{ij}) = 2\pi^{-1/2}\Big[\Gamma(3/2) - \Gamma(3/2, w_{ij}(r_{ij}))\Big], \tag{262}$$

where w_{ij} is defined as

$$w_{ij}(r_{ij}) \equiv -\beta u_{ij}(r_{ij})\theta[-\beta u_{ij}(r_{ij})]. \tag{263}$$

(b) f^+*-function and* f^**-function*

An ensemble of particle pairs specified by f-functions forming a product in each term of the density expansion of g_{ij} can be symbolized as a diagram with a structure formed from particle pairs linked by f-bonds defined as the f-functions. Every diagram found in the density expansion of g_{ij} has the same pair of root points; the density expansion corresponds to the sum of all diagrams with structures that form f-bonds' paths joining a root point

to the other root point. Then, the paths of f-bonds found in the density expansion allow effects of the behavior of a particle at a root point to be propagated to the other particle at the other root point.

Pair particles specified by an f-function $f_{ij}(r_{ij})$ interact with each other in a bound state or in an unbound state. The use of $p_{ij}(r_{ij})$ enables $f_{ij}(r_{ij})$ to be divided into two contributions. One contribution is expressed as $f_{ij}^{+}(r_{ij})$, which is linked to the case that the pair particles interact with each other in a bound state $\mathcal{E}_{(h_i,h_j)}^{ij} + u_{ij}(r_{ij}) \leq 0$. The other is expressed as $f_{ij}^{*}(r_{ij})$, which is linked to the case that the pair particles interact with each other in an unbound state $\mathcal{E}_{(h_i,h_j)}^{ij} + u_{ij}(r_{ij}) > 0$. Thus, $f_{ij}(r_{ij})$ are expressed as the sum of the f^{+}- and f^{*}-functions, i.e.,

$$f_{ij}(r_{ij}) = f_{ij}^{+}(r_{ij}) + f_{ij}^{*}(r_{ij}). \tag{264}$$

Then, the f^{+}-function and f^{*}-function are given by

$$\begin{cases} f_{ij}^{+}(r_{ij}) \equiv p_{ij}(r_{ij}) e^{-\beta u_{ij}(r_{ij})}, \\ f_{ij}^{*}(r_{ij}) \equiv [1 - p_{ij}(r_{ij})] e^{-\beta u_{ij}(r_{ij})} - 1. \end{cases} \tag{265}$$

2. Physical clusters

The use of Eq. (264) allows each f-bond in a diagram found in the density expansion of $g_{ij}(r_{ij})$ to be expressed as the sum of the f^{+}-bond defined by the contribution from the interaction in a bound state and the f^{*}-bond defined by the contribution from the interaction in an unbound state. Thus, the use of Eq. (264) makes it be possible to find a diagram wherein the root point is connected to the other root point through at least one path of all f^{+}-bonds given as a product of f^{+}- functions. Particles that participate in forming such a diagram constitute a portion of a physical cluster. Indeed, the two particles corresponding to the two root points are two particles constituting the physical cluster. This fact allows $\mathcal{P}_{ij}(r_{ij})$ to be given as the sum of contributions obtained from every diagram with at least one path of all f^{+} bonds between the root points.

The second simplest diagram found in the density expansion of $g_{ij}(r_{ij}) - 1$ comprises three particles linked by two f-bonds. The three particles occupy a root point $\mathbf{r}_1^{(i)}$, the other root point $\mathbf{r}_2^{(j)}$, and one field point $\mathbf{r}_3^{(k)}$, respectively. The field point corresponds to a coordinate

of a particle of species k. If the three particles participate in the formation of a physical cluster, the three particles are retained via the f-bonds in the bound states characterized as the conditions $\mathcal{E}^{ik}_{(1,3)} + u_{ik}(|\mathbf{r}_1^{(i)} - \mathbf{r}_3^{(k)}|) \leq 0$ and $\mathcal{E}^{kj}_{(3,2)} + u_{kj}(|\mathbf{r}_3^{(k)} - \mathbf{r}_2^{(j)}|) \leq 0$. The three particles in these bound states correspond to those participating in a diagram in which a root point is connected to the other root point through at least one path of all f^+-bonds given as a product of f^+-functions. The two particles corresponding to the two root points are two of particles that constitute the same physical cluster.

The above fact allows $\mathcal{P}_{ij}(r_{ij})$ to be given as the sum of contributions obtained from every diagram that has at least one path of all f^+ bonds between the root points. Particle pairs contributing to the magnitude of $\mathcal{P}_{ij}(r_{ij})$ should not have large relative momenta. Particle pairs that have large relative momenta should principally contribute to the magnitude of $\mathcal{D}_{ij}(r_{ij})$, and those that have small relative momenta should principally contribute to the magnitude of $\mathcal{P}_{ij}(r_{ij})$. In a fluid mixture system, particle pairs contributing to the magnitude of $\mathcal{P}_{ij}(r_{ij})$ cannot be homogeneously mixed with particle pairs contributing to the magnitude of $\mathcal{D}_{ij}(r_{ij})$. This fact allows the fluid mixture system to exhibit various properties.

3. Integral equations for analyzing physical cluster formation

According to the similarity to a single-component fluid system, each diagram found in the density expansion of $g_{ij}(r_{ij}) - 1$ is a diagram that comprises paths of f-bonds between the two root points. The diagrams found in the density expansion of $g_{ij}(r_{ij}) - 1$ are divided into two groups: One comprises the nodal diagrams with nodal points, and the other comprises the non-nodal diagrams that have no nodal point. A nodal point is a specific field point in a diagram. Missing the field point in the diagram implies that the diagram is separated into a group including a root point and the other group including the other root point. Thus, if the contribution of the nodal diagrams is expressed as $N_{ij}(r_{ij})$ and that of the non-nodal diagrams as $c_{ij}(r_{ij})$, then the density expansion of $g_{ij}(r_{ij}) - 1$ requires $g_{ij}(r_{ij}) - 1$ to be given as

$$g_{ij}(r) - 1 = c_{ij}(r) + N_{ij}(r), \tag{266}$$

where $r = r_{ij} \equiv |\mathbf{r}_1^{(i)} - \mathbf{r}_2^{(j)}|$. This equation is equivalent to the Ornstein–Zernike equation,[9] and $c_{ij}(r)$ corresponds to the direct correlation function. $N_{ij}(r)$ is given as the convolution

integral, i.e.,

$$N_{ij}(r) = \sum_{k=1}^{\mathcal{L}} \rho_k \int_V c_{ik}(r_{ik}) \Big[g_{kj}(r_{kj}) - 1 \Big] \mathrm{d}\mathbf{r}_3^{(k)},$$

where $r_{ik} \equiv |\mathbf{r}_1^{(i)} - \mathbf{r}_3^{(k)}|$ and $r_{kj} \equiv |\mathbf{r}_3^{(k)} - \mathbf{r}_2^{(j)}|$. In the above equation, $\mathcal{L}$ is the number of constituents .

Similarly, the diagrams contributing to $\mathcal{P}_{ij}(r)$ comprise the nodal diagrams and the non-nodal diagrams. Hence, $\mathcal{P}_{ij}(r)$ is given as the sum of the contribution of all the nodal diagrams and that of all the non-nodal diagrams.[3] This implies that $\mathcal{P}_{ij}(r)$ is expressed as

$$\mathcal{P}_{ij}(r) = N_{ij}^{+}(r) + C_{ij}^{+}(r). \tag{267}$$

Here, $C_{ij}^{+}(r)$ denotes the contribution of all the non-nodal diagrams, and each non-nodal diagram has at least one path of all f^{+}-bonds between the two root points. $N_{ij}^{+}(r)$ is the contribution of all the nodal diagrams, and each nodal diagram has at least one path of all f^{+}-bonds between the two root points.

The direct correlation function $c_{ij}(r)$ represents the contribution of all non-nodal diagrams that comprise paths of f-bonds between the two root points. A correlation function $C_{ij}^{*}(r)$ that is similar to $c_{ij}(r)$ with respect to the behavior at a large r is obtained from the subtraction of $C_{ij}^{+}(r)$ from $c_{ij}(r)$. It satisfies the following formula:

$$c_{ij}(r) = C_{ij}^{+}(r) + C_{ij}^{*}(r). \tag{268}$$

Equation (268) requires the correlation function $C_{ij}^{*}(r)$ to represents the contribution of all non-nodal diagrams which do not include any paths formed by all f^{+}-bonds between the two root points $\mathbf{r}_1^{(i)}$ and $\mathbf{r}_2^{(j)}$.

Then, subtracting Eq. (267) from Eq. (266) allows useful relations to be found because of Eq. (260). The relations are summarized as

$$\begin{cases} g_{ij} = \mathcal{P}_{ij} + \mathcal{D}_{ij} \\ g_{ij} - 1 = c_{ij} + N_{ij} \\ \mathcal{P}_{ij} = C_{ij}^{+} + N_{ij}^{+} \\ \mathcal{D}_{ij} - 1 = C_{ij}^{*} + N_{ij}^{*} \\ C_{ij}^{*} \equiv c_{ij} - C_{ij}^{+} \quad (\textit{all non-nodal diagrams}) \\ N_{ij}^{*} \equiv N_{ij} - N_{ij}^{+} \quad (\textit{all nodal diagrams}). \end{cases} \tag{269}$$

The difference $N_{ij}-N_{ij}^{+}$ represents the contribution of all nodal diagrams that do not include any paths formed by all f^{+}- bonds between the two root points $\mathbf{r}_1^{(i)}$ and $\mathbf{r}_2^{(j)}$.

Moreover, $N_{ij}^{+}(r)$ is provided as the convolution integral of the product of $C_{ik}^{+}(r)$ and $\mathcal{P}_{kj}(r)$, i.e.,

$$N_{ij}^{+}(r)=\sum_{k=1}^{\mathcal{L}}\rho_k\int_V C_{ik}^{+}(r_{ik})\mathcal{P}_{kj}(r_{kj})\mathrm{d}\mathbf{r}_3^{(k)}.$$

Therefore, Eq. (267) allows the pair connectedness $\mathcal{P}_{ij}(r)$ to be provided as a solution of the integral equation expressed as

$$\mathcal{P}_{ij}(r)=C_{ij}^{+}(r)+\sum_{k=1}^{\mathcal{L}}\rho_k\int_V C_{ik}^{+}(r_{ik})\mathcal{P}_{kj}(r_{kj})\mathrm{d}\mathbf{r}_3^{(k)}, \tag{270}$$

where $r=r_{ij}\equiv|\mathbf{r}_1^{(i)}-\mathbf{r}_2^{(j)}|$.

The integral equation given by Eq. (270), which is used in the limit $V\to\infty$, has the same mathematical structure as the Ornstein–Zernike equation. The correlation function C_{ij}^{+}, which is an unknown function in Eq. (270), is composed of only non-nodal diagrams of f^{+}-bonds. The direct correlation function c_{ij} is composed of only non-nodal diagrams of f-bonds. This fact guarantees that the use of a mathematical procedure similar to that for solving the Ornstein–Zernike equation enables Eq. (270) to be solved.

An integral equation for the correlation function $\mathcal{D}_{ij}(r)$ can be extracted from the Ornstein–Zernike equation. Owing to Eq. (260), the Ornstein–Zernike equation is expressed as

$$\begin{aligned}\mathcal{P}_{ij}(r_{ij})+\mathcal{D}_{ij}(r_{ij})-1=c_{ij}(r_{ij})&+\sum_{k=1}^{\mathcal{L}}\rho_k\int_V c_{ik}(r_{ik})\mathcal{P}_{kj}(r_{kj})\mathrm{d}\mathbf{r}_3^{(k)}\\&+\sum_{k=1}^{\mathcal{L}}\rho_k\int_V c_{ik}(r_{ik})[\mathcal{D}_{kj}(r_{kj})-1]\mathrm{d}\mathbf{r}_3^{(k)}.\end{aligned} \tag{271}$$

To obtain an integral equation for $\mathcal{D}_{ij}(r)$, the contribution of $\mathcal{P}_{ij}(r)$ expressed by Eq. (270) must be subtracted from Eq. (271). Then, the direct correlation function c_{ij} expressed by Eq. (268) must be substituted for c_{ij} in Eq. (271). Thus, the obtained integral equation is equivalent to both an integral equation derived by Stell[28] and the other one derived by

Chiew et al.[6] The integral equation is expressed as

$$\begin{aligned}\mathcal{H}_{ij}(r) =& C^*_{ij}(r) + \sum_{k=1}^{\mathcal{L}} \rho_k \int_V C^*_{ik}(r_{ik}) \mathcal{P}_{kj}(r_{kj}) \mathrm{d}\mathbf{r}_3^{(k)} \\ &+ \sum_{k=1}^{\mathcal{L}} \rho_k \int_V C^+_{ik}(r_{ik}) \mathcal{H}_{kj}(r_{kj}) \mathrm{d}\mathbf{r}_3^{(k)} + \sum_{k=1}^{\mathcal{L}} \rho_k \int_V C^*_{ik}(r_{ik}) \mathcal{H}_{kj}(r_{kj}) \mathrm{d}\mathbf{r}_3^{(k)}, \end{aligned} \tag{272}$$

where $r = r_{ij} \equiv |\mathbf{r}_1^{(i)} - \mathbf{r}_2^{(j)}|$ and

$$\mathcal{H}_{ij}(r) \equiv \mathcal{D}_{ij}(r) - 1. \tag{273}$$

Then, Eq. (272) requires N^*_{ij} in Eq. (269) to satisfy

$$N^*_{ij}(r_{ij}) = \sum_{k=1}^{\mathcal{L}} \rho_k \int_V C^*_{ik}(r_{ik}) \mathcal{P}^+_{kj}(r_{kj}) \mathrm{d}\mathbf{r}_3^{(k)} + \sum_{k=1}^{\mathcal{L}} \rho_k \int_V c_{ik}(r_{ik}) \Big(\mathcal{D}_{kj}(r_{kj}) - 1 \Big) \mathrm{d}\mathbf{r}_3^{(k)}. \tag{274}$$

Although Eqs. (270) and Eq. (272) are not equivalent to the Ornstein–Zernike equation, an integral equation system composed of Eqs. (270) and (272) becomes equivalent to the Ornstein–Zernike equation because of Eq. (268). Equation (270) contributes to estimating the formation of physical clusters. Equation (272) contributes to estimating effects of the physical cluster formation. In fact, the second and third terms on the right-hand side of Eq. (272) represent the reason that the formation of the physical clusters affect the correlation function $\mathcal{H}_{ij}$. The existence of these terms play roles in explaining various phenomena caused by physical cluster formation and physical cluster growth.

4. Appendix: Rewrite of integration equation Eq. (272)

With respect to mathematical structure, Eq. (272) is different from the Ornstein–Zernike equation. Despite this fact, it is possible to rewrite Eq. (272) as an integral equation that has the same mathematical structure as the Ornstein–Zernike equation. Then, the relation given by Eq. (270) must be considered. Thus, a formal rewrite of Eq. (272) results in

$$\overline{\mathcal{H}}_{ij}(r_{ij}) = \overline{C}^*_{ij}(r_{ij}) + \sum_{k=1}^{\mathcal{L}} \rho_k \int_V \overline{C}^*_{ik}(r_{ik}) \overline{\mathcal{H}}_{kj}(r_{kj}) \mathrm{d}\mathbf{r}_k, \tag{275}$$

where

$$\overline{\mathcal{H}}_{ij}(r_{ij}) \equiv \mathcal{H}_{ij}(r_{ij}) - \sum_{k=1}^{\mathcal{L}} \rho_k \int_V C^+_{ik}(r_{ik}) \mathcal{H}_{kj}(r_{kj}) \mathrm{d}\mathbf{r}_k \tag{276}$$

and

$$\overline{\mathcal{C}}^{*}_{ij}(r_{ij}) \equiv C^{*}_{ij}(r_{ij}) + \sum_{k=1}^{\mathcal{L}} \rho_k \int_V C^{*}_{ik}(r_{ik}) \mathcal{P}_{kj}(r_{kj}) \mathrm{d}\mathbf{r}_k. \tag{277}$$

The correlation function $\overline{\mathcal{C}}^{*}_{ij}$ includes both non-nodal diagrams and nodal diagrams because of the second term on the right-hand side of Eq. (277). The correlation functions C^{+}_{ij}, C^{*}_{ij}, and c_{ij} are composed of only non-nodal diagrams. Only in the case that the contribution of the second term on the right-hand side of Eq. (277) cannot be considered important, it is possible to solve Eq. (275) using a mathematical procedure similar to that for the Ornstein–Zernike equation.

Further, a correlation function $\overline{\mathcal{H}}_{ij}(r_{ij})$ is affected via $C^{+}_{ik}(r_{ik})$ by the physical cluster formation. In addition, the correlation function $\overline{\mathcal{C}}^{*}_{ij}(r_{ij})$ is affected via $\mathcal{P}_{kj}(r_{kj})$ by the physical cluster formation. Particles contributing to the magnitude of $\overline{\mathcal{H}}_{ij}(r_{ij})$ are not prevented from behaving independently of particles contributing to the magnitude of $\mathcal{P}_{ij}(r_{ij})$. The particles contributing to the magnitude of $\mathcal{H}_{ij}(r_{ij})$ are not homogeneously mixed with particles contributing to the magnitude of $\mathcal{P}_{ij}(r_{ij})$. Therefore, a formal equation style of Eq. (275) accompanying Eqs. (276) and (277) demonstrates that particles with large relative momenta cannot be homogeneously mixed with particles that have small relative momenta.

B. Features of correlation functions for multicomponent fluid mixture system

According to Kirkwood and Buff,[33] the pair correlation function $g_{ij}(r)$ for the multicomponent fluid mixture system[2] has the normalization given as

$$\frac{1}{V}\int_V g_{ij}(r)\mathrm{d}\mathbf{r} = \frac{\langle N_i\rangle - \delta_{ij}}{V\rho_i} + \frac{1}{V^2}\frac{1}{\rho_i\rho_j}\Big[\langle N_iN_j\rangle - \langle N_i\rangle\langle N_j\rangle\Big], \tag{278}$$

where $\langle N_i\rangle$ represents the mean number of particles of species i within volume V. The dependence of $g_{ij}(r)$ on V is negligible for macroscopic V. The dependence of $\langle N_i\rangle/V$ on V and that of $(\langle N_iN_j\rangle - \langle N_i\rangle\langle N_j\rangle)/V$ on V are also negligible. Thus, Eq. (278) results in

$$\lim_{V\to\infty}\frac{1}{V}\int_V g_{ij}(r)\mathrm{d}\mathbf{r} = 1.$$

This relation and Eq. (260) require $\mathcal{P}_{ij}(r)$ and $\mathcal{D}_{ij}(r)$ to satisfy

$$\lim_{V\to\infty}\left[\frac{1}{V}\int_V \mathcal{P}_{ij}(r)\mathrm{d}\mathbf{r} + \frac{1}{V}\int_V \mathcal{D}_{ij}(r)\mathrm{d}\mathbf{r}\right] = 1. \tag{279}$$

Moreover, the pair correlation function behaves as $g_{ij}(|\mathbf{r}_1^{(i)} - \mathbf{r}_2^{(j)}|) \approx 1$ when two particles located at $\mathbf{r}_1^{(i)}$ and $\mathbf{r}_2^{(j)}$ in the fluid system are widely separated. In the limit $V \to \infty$ and $r \to \infty$, it behaves as $g_{ij}(r) = 1$.[2] Thus, Eq. (260) allows the physical meanings of $\mathcal{P}_{ij}(r)$ and $\mathcal{D}_{ij}(r)$ to result in

$$\begin{cases} \lim_{r\to\infty}\mathcal{P}_{ij}(r) = 0 \\ \lim_{r\to\infty}\mathcal{D}_{ij}(r) = 1. \end{cases}$$

1. Mean size $\mathcal{S}$ of physical clusters for multicomponent fluid mixture system

The mean size $\mathcal{S}$ of physical clusters can be estimated from the use of $\mathcal{P}_{ij}(r)$. The equilibrium number n_s of physical clusters comprising s particles can be related to the pair connectedness $\mathcal{P}_{ij}$. According to the formula given by Coniglio et al.,[3] the relationship between n_s and $\mathcal{P}_{ij}$ is given as

$$\sum_{2\le s} s(s-1)n_s = \sum_{i=1}^{\mathcal{L}}\sum_{j=1}^{\mathcal{L}}\rho_i\rho_j\int_V\int_V \mathcal{P}_{ij}(|\mathbf{r}_1^{(i)} - \mathbf{r}_2^{(j)}|)\mathrm{d}\mathbf{r}_1^{(i)}\mathrm{d}\mathbf{r}_2^{(j)}. \tag{280}$$

If probability $p^{(i)}$ that a particle of i species exists in a cluster is independent of s, then the factor $\sum_s sn_s$ included in Eq. (280) can be related to the density ρ_i of particles of i species in the volume V as

$$\rho_i = \frac{p^{(i)}}{V} \sum_s sn_s.$$

If $\sum_{i=1}^{\mathcal{L}} p^{(i)} = 1$ is considered, the sum $\sum_s sn_s$ is estimated as

$$\sum_s sn_s = V \sum_{i=1}^{\mathcal{L}} \rho_i.$$

The mean physical cluster size $\mathcal{S}$ is given as $\mathcal{S} = (\sum_s s^2 n_s)/(\sum_s sn_s)$. Hence,

$$\mathcal{S} = \left(V \sum_{i=1}^{\mathcal{L}} \rho_i \right)^{-1} \sum_s s^2 n_s.$$

This formula allows Eq. (280) to be rewritten as

$$\mathcal{S} = 1 + \left(\sum_{k=1}^{\mathcal{L}} \rho_k \right)^{-1} \sum_{i=1}^{\mathcal{L}} \sum_{j=1}^{\mathcal{L}} \rho_i \rho_j \int_V \mathcal{P}_{ij}(r) \mathrm{d}\mathbf{r}. \tag{281}$$

2. Percolation of physical clusters

(a) *System without percolation of physical clusters*

If the percolation of physical clusters does not occur in macroscopic V found in the fluid mixture system of $\mathcal{L}$ constituents, $\mathcal{S}$ estimated for the fluid mixture system using Eq. (281) should be sufficiently independent of V. The limit $V \to \infty$ does not influence $\mathcal{S}$. Thus, the limit $V \to \infty$ allows Eq. (281) to result in

$$\begin{cases} \lim_{V\to\infty} [(\mathcal{S} - 1)/V] \sum_{k=1}^{\mathcal{L}} \rho_k = 0 \\ \lim_{V\to\infty} (1/V) \int_V \mathcal{P}_{ij}(r) \mathrm{d}\mathbf{r} = 0. \end{cases} \tag{282}$$

Eq. (282) allows Eq. (279) to result in the normalization condition given in the limit $V \to \infty$ as

$$\lim_{V\to\infty} (1/V) \int_V \mathcal{D}_{ij}(r) \mathrm{d}\mathbf{r} = 1. \tag{283}$$

(b) *System involving percolation of physical clusters*

If the percolation of physical clusters occurs in macroscopic V found in the fluid mixture system, $\mathcal{S}$ estimated for the fluid system using Eq. (281) should be dependent on V. Then, the magnitude of $[(\mathcal{S}-1)/V]\sum_{k=1}^{\mathcal{L}}\rho_k$ can have a finite value different from zero, i.e.,

$$\begin{cases} \lim_{V\to\infty}[(\mathcal{S}-1)/V]\sum_{k=1}^{\mathcal{L}}\rho_k \neq 0 \\ \lim_{V\to\infty}(1/V)\int_V \mathcal{P}_{ij}(r)\mathrm{d}\mathbf{r} \neq 0. \end{cases} \tag{284}$$

If a state of the fluid is in the immediate vicinity of the liquid–solid transition point where $0 < \rho_i^{sd} - \rho_i^{lq} \ll 1$ (ρ_i^{sd} denotes ρ_i in a solid state, and ρ_i^{lq} denotes ρ_i in a liquid state that can be transformed into the solid state) is satisfied, the dependence of $\mathcal{S}$ on V may be estimated as $\mathcal{S}/V \approx \sum_{i=1}^{\mathcal{L}}\rho_i^{sd}$, which corresponds to the case that the growth of the physical clusters reaches the limit. If this estimate for $\mathcal{S}/V$ is considered, in the limit $V\to\infty$, Eq. (281) should have the meaning expressed as

$$(1/V)\sum_{i=1}^{\mathcal{L}}\sum_{j=1}^{\mathcal{L}}\rho_i\rho_j\int_V \mathcal{P}_{ij}(r)\mathrm{d}\mathbf{r} \approx \sum_{i=1}^{\mathcal{L}}\rho_i^{sd}\sum_{k=1}^{\mathcal{L}}\rho_k. \tag{285}$$

Thus, Eq. (285) allows Eq. (279) to result in

$$(1/V)\int_V \mathcal{D}_{ij}(r)\mathrm{d}\mathbf{r} \approx 0. \tag{286}$$

A state specified by $(1/V)\int_V \mathcal{D}_{ij}(r)\mathrm{d}\mathbf{r} = 0$ means there are no particle pairs that comprise particles interacting with each other in unbound states. In a fluid mixture system characterized by $(1/V)\int_V \mathcal{D}_{ij}(r)\mathrm{d}\mathbf{r} \approx 0$, it is extremely impossible to observe an unbound state where the contribution of the relative kinetic energy between pair particles exceeds the contribution of a mutually attractive force between them, for each particle pair. This implies that the fluid mixture system loses a feature found as liquid. Thus, the growth of physical clusters can contribute the phase transition from the liquid state of the fluid mixture system to the solid state.

C. Effects depending on physical cluster formation in multicomponent fluids

1. Classification of constituents

In a multicomponent fluid mixture system, an ensemble of particles linked with each other as each pair of particles interacting in a bound state cannot be microscopically homogeneously mixed with an ensemble of particles that is formed by each pair of particles interacting in an unbound state. However, it is possible to prevent the former and latter ensembles from separating from the mixed condition that seems macroscopically homogeneous in the multicomponent fluid mixture system. Branches of each physical cluster corresponding to the former ensemble have a tendency to microscopically confine particles that belong to a latter ensemble to prevent the phase separation. Then, the constituents of the multicomponent fluid mixture can be classified into $\mathcal{A}$ and $\mathcal{B}$. Particles belonging to constituents $\mathcal{A}$ have a tendency to participate in the former ensemble, and those belonging to the other constituents $\mathcal{B}$ have a tendency to participate in the latter ensemble. Particles belonging to constituents $\mathcal{A}$ have a strong tendency to participate in the formation of physical clusters, and those belonging to constituents $\mathcal{B}$ have a strong tendency to be confined among branches of the physical clusters. As a result, the relationships between the physical cluster formation and features of constituents can affect phase behaviors of the multicomponent fluid mixture.

2. Various phenomena and interpretations

For multicomponent fluid mixtures in their liquid phase, the contributions of the physical cluster formation to their features are not ignored in comparison with multicomponent fluid mixtures in their gas phase. The results of the Monte Carlo simulations indicate that the statistics of cluster size diversity can contribute to the statistical description of a complex system.[88] The phase behaviors of a multicomponent fluid mixture should be complicated[87] when the contribution of the formation of physical clusters is not ignored.

(a) *Occurrence of microscopic nonuniformity known from the behavior of colloidal particles*

For temperatures beyond the consolute point, a binary fluid mixture composed of two constituents L_1 and L_2 should be macroscopically homogeneous. For temperatures being

below the consolute point, the binary mixture is separated into an L_1-rich phase and an L_2-rich phase. Then, the binary mixture forms a boundary between the two phases. If the temperature is raised near the consolute point, the dense areas of L_2 particles in the L_1-rich phase should be microscopically developed near the boundary, whereas the dense areas of L_1 particles in the L_2-rich phase should be microscopically developed near the boundary. If colloidal particles are distributed in this complex medium, colloidal particles that prefer the L_2-rich phase should be aggregated close to the boundary in the L_2-rich phase near the consolute point. Further, colloidal particles preferring the L_1-rich phase should be aggregated close to the boundary in the L_1-rich phase near the consolute point. Such phenomena were experimentally demonstrated for the binary fluid mixtures of 2,6-lutidine plus water.[63] Either the aggregation of colloidal particles[85] or the contraction of a flexible linear polymer[86] in binary fluid mixtures can be induced by developing the nonuniform distribution of each constituent.

(b) *Density fluctuations induced in multicomponent fluid mixture*

Density fluctuations for a specific constituent in a multicomponent fluid mixture can induce density fluctuations for other constituents as predicted from the aggregation of colloidal particles described above. This phenomenon can be a factor complicating a phase diagram for a multicomponent fluid mixture. Monte Carlo simulation revealed the complicated phase diagrams for a binary fluid mixture composed of particles interacting with the attractive force caused by a square-well potential.[87] Furthermore, the complexity in the multicomponent fluid mixture is characterized by the extent of density fluctuations. According to the results demonstrated by the Monte Carlo simulations,[88] the diversity of dense areas for a constituent can be considered a measurement of the complexity.

(c) *Physical cluster formation in multicomponent fluid mixture*

In a multicomponent fluid mixture, particles that interact with each other via mutually attractive forces that are strong can effectively contribute to the formation of physical clusters. These particles should belong to the group of $\mathcal{A}$. Further, particles that cannot interact both with each other and with other particles via mutually attractive forces that are strong cannot effectively contribute to the formation of physical clusters. These particles should belong to the group of $\mathcal{B}$. Particles within regions surrounded by branches of physical clus-

ters interact with each other in unbound states. Particles belonging to $\mathcal{B}$ can be surrounded by branches of physical clusters.

Particles belonging to $\mathcal{B}$ should receive passively attractive forces generated from the cooperation between the exclusion of the particles caused by the hard-core potential and each mutually attractive force between particles belonging to $\mathcal{A}$. Passively attractive forces need to contribute to driving the phase separation of particles belonging to $\mathcal{B}$; however, features of forces cannot be simple because they can depend on the stability of physical clusters. The phase separation of particles that belong to $\mathcal{A}$ can be driven by the strength of each mutually attractive force that interacts between particles belonging to $\mathcal{A}$. The stability of a phase should be influenced via the growth of physical clusters caused by an increase in particles belonging to $\mathcal{A}$.

(d) *Effects caused by bismuth atoms added in mercury fluid*

If particles added into a fluid interact with a sufficiently strongly attractive force between one of them and another particle composed of the fluid, the addition of the particles should stabilize the physical clusters in the fluid. Bismuth atoms migrating into physical clusters of mercury atoms will further stabilize physical clusters if an interaction similar to that caused by the added particles is achieved when atoms of bismuth are added into a mercury fluid maintained at a low density at a temperature near the critical point. The stabilization of the physical clusters achieved by the addition of bismuth atoms will enhance the electrical conductivity of the mercury fluid because the physical clusters are electrical paths that help electrons to migrate. Furthermore, their stabilization reduces the pressure of the mercury fluid because branches of the stabilized physical clusters can confine unbound mercury atoms. These phenomena caused by the addition of bismuth atoms has already been experimentally demonstrated.[60]

(e) *Viscosity anomaly near consolute point*

The stability of physical clusters in a fluid mixture should be reduced if the temperature of the fluid mixture rises. Then, it can become difficult for branches of the physical clusters stably to confine particles belonging to the group $\mathcal{B}$ stably, within regions surrounded by their branches. This phenomenon can disturb a macroscopically homogeneous phase of the fluid mixture. The physical clusters can not only contribute to prohibiting a transition from a

liquid phase of a fluid to its gas phase, but also prohibit the transition from a macroscopically homogeneous phase of a multicomponent fluid mixture to its macroscopically inhomogeneous phase. Therefore, a multicomponent fluid mixture can be considered a good medium for examining the contribution of physical clusters to phase behavior; however, the mathematical procedures for examining the mixture becomes complicated.

Hydrodynamical transport phenomena need to be influenced by generating the nonuniform distribution of particles in a fluid mixture. The nonuniform distribution of particular particles can be a significant factor for inducing the viscosity anomaly. The nonuniform distribution can be developed near the consolute point.

The formation of physical clusters allows a specific distribution structure of particles to be formed; unbound particles do not homogeneously mix with particles that form the physical clusters, and they are surrounded by branches of the physical clusters. It is expected that the distribution structure can play a role in microscopically interpreting phenomena found for a specific fluid mixture. For a binary fluid mixture, the viscosity anomaly[61] can be induced near the consolute point that corresponds to the critical transition point for demixing the two constituents macroscopically. It is considered for the distribution structure caused by the formation of physical clusters to contribute to the viscosity anomaly.

(f) *Binary fluid mixture composed of 2,6-lutidine and water*

Particles belonging to a group $\mathcal{B}$ can be stably confined within regions surrounded by branches of physical clusters if their particle sizes are small. If particles have larger sizes than those of the regions, the stable confinement of these particles will become more difficult than that of the small particles. Such size effects can contribute to the phase behavior of a binary fluid mixture.[62] This size effect can contribute to the phase behavior of a binary fluid mixture of 2,6-lutidine plus water near the consolute point because the size of the 2,6-lutidine molecule is considerably larger than that of the water molecule.

2,6-lutidine molecules should be considered molecules belonging to the group $\mathcal{A}$ with water molecules. Either the attractive force between 2,6-lutidine molecules or that between a 2,6-lutidine molecule and a water molecule cannot be ignored, although these attractive forces are weaker than the attractive force between water molecules. Thus, it is possible for two types of physical clusters to be generated in a binary fluid mixture of 2,6-lutidine plus water; these include water molecule clusters that are principally composed of water

molecules and 2,6-lutidine molecule clusters that are principally composed of 2,6-lutidine molecules. However, a partial amount of 2,6-lutidine molecules should have a tendency to enter regions surrounded by branches of water molecule clusters. The size effect mentioned above can induce the phase separation of 2,6-lutidine molecules when 2,6-lutidine molecules in the binary fluid mixture exceed a specific amount.

2,6-lutidine molecules participating in the formation of a water molecule cluster with water molecules can contribute to cutting branches of the water molecule cluster because the attractive force between 2,6-lutidine molecules is weaker than that between a water molecule and a 2,6-lutidine molecule. Therefore, 2,6-lutidine molecules participating in the formation of water molecule clusters can contribute to expanding the sizes of regions surrounded by branches of the water molecule clusters in cooperation with the temperature effect. If regions surrounded by branches of the water molecule clusters expand, 2,6-lutidine molecules can be confined within the regions. Then, even 2,6-lutidine molecule clusters should be found within the regions if the regions are sufficiently large. The contribution of 2,6-lutidine molecules to the cutting branches of the water molecule cluster can decrease the average extent of water molecule clusters. Therefore, declining water molecule clusters should allow 2,6-lutidine molecule clusters to exist among them. Thus, it is expected that a macroscopically homogeneous mixture of 2,6-lutidine plus water should be generated, although the microscopic distribution of water molecules and 2,6-lutidine molecules is nonuniform.

Further, the microscopically nonuniform distribution of 2,6-lutidine molecules can be developed in binary fluid mixtures of 2,6-lutidine plus water near the consolute point. The microscopically nonuniform distribution can be realized through the aggregation phenomena of colloidal particles.[63] Density fluctuations in a specific constituent in a multicomponent fluid mixture can induce density fluctuations for other constituents as predicted from the aggregation of colloidal particles. This phenomenon can be a factor that complicates a phase diagram for a multicomponent fluid mixture. The Monte Carlo simulation revealed such complicated phase diagrams even for a binary fluid mixture composed of particles interacting with the attractive force caused by a square-well potential.[87]

(g) *Specific phenomenon appearing near consolute point of fluid mixture*

When colloidal particles have mesoscopic sizes as hard-core spheres in the absence of attractive forces, it is possible for passively attractive forces to be generated between the

colloidal particles immersed in a molecular fluid mixture. At a temperature near the consolute point of the fluid mixture, a distribution structure that is formed by branches of physical clusters and unbound molecules surrounded by them can vary considerably. If the average extent of physical clusters increases beyond that comparable with the diameter of a colloidal particle, passively attractive forces between the colloidal particles should be strengthened because the surface of a colloidal particle cannot contribute to the growth of a physical cluster. Thus, it is expected that such attractive forces can contribute to Casimir forces, which can act between colloidal particles (or between parallel plates) immersed within a binary fluid mixture near the consolute point (or a single-component fluid near the liquid-vapor critical transition point).[64]

(h) *Pair connectedness for multicomponent fluid mixture*

Particles belonging to group $\mathcal{A}$ should effectively contribute to the magnitude of $\mathcal{P}_{ij}(r)$; those belonging to group $\mathcal{B}$ can be a principal portion of particles that contribute to the magnitude of $\mathcal{D}_{ij}(r)$. These particles should have a tendency to be distributed within regions surrounded by branches of physical clusters. Thus, the distribution structure of particles characterized by $\mathcal{P}_{ij}(r)$ and $\mathcal{D}_{ij}(r)$ should play a role for describing several features of a multicomponent fluid mixture. The percolation concerning physical clusters of particles belonging to $\mathcal{A}$ is estimated using $\mathcal{P}_{ij}(r)$.

In a binary component fluid mixture of constituents L_1 and L_2, the mutually attractive force between an L_1 particle and an L_2 particle is considerably smaller than that between L_1 particles. Further, the mutually attractive force between L_2 particles is much smaller than that between L_1 particles. Then, physical clusters of L_1 particles can be principally developed under certain conditions. If L_2 particles are added into the mixture, then it is expected that the addition of L_2 particles raises the probability that an L_1 particle is located near another L_1 particle. However, the percolation concerning physical clusters of L_1 particles can hardly be perturbed by the addition of L_2 particles into the mixture.

D. Closure schemes for two integral equations

1. *Formal closure schemes for estimating correlation functions $\mathcal{P}_{ij}$ and $\mathcal{D}_{ij}$*

An approximate relation between $\mathcal{P}_{ij}(r)$ and $C_{ij}^{+}(r)$ is obtained from a formula representing the PY approximation.[3] The procedure for obtaining the approximate relation is the same as that for a single-component fluid system discussed in II B 4. The procedure can be summarized as follows.

(a) *Approximate expressions of $\mathcal{P}_{ij}$ and $\mathcal{D}_{ij}$*

For an $\mathcal{L}$-component fluid mixture system, Eq. (269) and $e^{-\beta u_{ij}(r)} = f_{ij}^{+}(r) + f_{ij}^{*}(r) + 1$ allow a formula $g_{ij}^{\rm PY}(r)e^{\beta u_{ij}} = 1 + N_{ij}(r)$ representing the PY approximation to be rewritten as

$$\begin{aligned} g_{ij}^{\rm PY}(r) =& f_{ij}^{+}(r)\Big[1 + N_{ij}^{+}(r) + N_{ij}^{*}(r)\Big] + \Big[f_{ij}^{*}(r) + 1\Big]N_{ij}^{+}(r) \\ &+ \Big[f_{ij}^{*}(r) + 1\Big]\Big[1 + N_{ij}^{*}(r)\Big]. \end{aligned} \tag{287}$$

Eq. (287) is divided into terms contributing to $\mathcal{P}_{ij}(r)$ and those contributing to $\mathcal{D}_{ij}(r)$. Thus,

$$\mathcal{P}_{ij}(r) = f_{ij}^{+}(r)g_{ij}^{\rm PY}(r)e^{\beta u_{ij}(r)} + [f_{ij}^{*}(r) + 1][\mathcal{P}_{ij}(r) - C_{ij}^{+}(r)], \tag{288}$$

and

$$\mathcal{D}_{ij}(r) = [f_{ij}^{*}(r) + 1][g_{ij}^{\rm PY}(r) - c_{ij}^{\rm PY}(r) - \mathcal{P}_{ij}(r) + C_{ij}^{+}(r)], \tag{289}$$

where $c_{ij}^{\rm PY}(r)/(1 - e^{\beta u_{ij}(r)}) = g_{ij}^{\rm PY}(r)$.

Because of Eqs. (262), (264), (265), and (269), Eq. (288) is rewritten as

$$\begin{aligned} &\mathcal{P}_{ij}(r) + \frac{2\Gamma[3/2, w_{ij}(r)]}{\pi^{1/2}e^{\beta u_{ij}(r)} - 2\Gamma[3/2, w_{ij}(r)]}C_{ij}^{+}(r) \\ &\quad = \frac{2\{\Gamma(3/2) - \Gamma[3/2, w_{ij}(r)]\}e^{\beta u_{ij}(r)}}{\pi^{1/2}e^{\beta u_{ij}(r)} - 2\Gamma[3/2, w_{ij}(r)]}\frac{c_{ij}^{\rm PY}(r)}{1 - e^{\beta u_{ij}(r)}}, \end{aligned} \tag{290}$$

where $w_{ij}(r)$ is defined by Eq. (263). Similarly, Eq. (289) is rewritten as

$$\mathcal{D}_{ij}(r) = \frac{2\Gamma[3/2, w_{ij}(r)]}{2\Gamma[3/2, w_{ij}(r)] - \pi^{1/2}e^{\beta u_{ij}(r)}}C_{ij}^{*}(r). \tag{291}$$

According to Eq. (290), the symmetry $C_{ij}^{+} = C_{ji}^{+}$ is maintained because of the symmetry $\mathcal{P}_{ij} = \mathcal{P}_{ji}$. Similarly, Eq. (291) allows the symmetry $C_{ij}^{*} = C_{ji}^{*}$ to be maintained due to

the symmetry $\mathcal{D}_{ij} = \mathcal{D}_{ji}$. Equations (290) and (291) can be used when either $\beta u_{ij} < 0$ or $\beta u_{ij} > 0$. Eqs. (290) and (291) enable $\mathcal{P}_{ij}(r)$ and $\mathcal{D}_{ij}(r)$ to be characterized by a pair potential if $c_{ij}^{\rm PY}(r)$, $C_{ij}^{+}(r)$, and $C_{ij}^{*}(r)$ are given. For solving Eq. (270), Eq. (290) becomes a closure scheme if $c_{ij}^{\rm PY}(r)$ is given. If $\mathcal{P}_{ij}(r)$ is estimated, $\mathcal{H}_{ij}(r)$ can be obtained by solving Eq. (272) with the use of Eq. (291).

(b) *Advanced interpretation on Eqs. (290) and (291)*

Eqs. (290) and (291) implies that separating $\mathcal{P}_{ij}(r)$ from $g_{ij}(r)$ allows a pair potential characterizing $\mathcal{P}_{ij}(r)$ to be made different from a pair potential characterizing $\mathcal{D}_{ij}(r)$. A pair potential controlling the behavior of pair particles can depend on their relative momentum when the behavior of each particle is affected by many-body effects. A pair potential controlling the behavior of pair particles can be specified when a contribution of an attractive force between them exceeds a contribution of their relative kinetic energy. If many-body effects are not ignored, then the pair potential can differ from that controlling the behavior of pair particles under a condition that a contribution of their relative kinetic energy exceeds a contribution of the attractive force between them. Then, the use of Eqs. (290) and (291) enables $\mathcal{P}_{ij}(r)$ and $\mathcal{D}_{ij}(r)$ to be estimated.

2. Behavior of correlation functions at large r

(a) *Behavior of* C_{ij}^{+} *for* $\beta u_{ij} < 0$ *and* $1 \ll r/\sigma_{ij}$.

The use of the closure scheme given by Eq. (290) does not allow Eq. (270) to solved analytically. It is necessary to find a practical method of solving Eq. (270) analytically. The integral equation given by Eq. (270) has the same mathematical structure as the Ornstein–Zernike equation. With the use of the mean spherical approximation (MSA),[36] the Ornstein–Zernike equation can be solved analytically for some fluids. In the MSA, the direct correlation function c_{ij} is given as the sum of short-range contribution $c_{ij}^{0}(r)$ and long-range contribution $-\beta u_{ij}(r)$. The MSA indicates that $c_{ij}(r)$ behaves as $c_{ij}(r)/(-\beta u_{ij}(r)) = 1$ and $c_{ij}^{0}(r) = 0$ outside the effective range of the hard-core potential. According to the analysis of diagrams of f-bonds, $c_{ij}(r)$ represents the contribution of all the non-nodal diagrams of f-bonds. $C_{ij}^{+}(r)$ represents the contribution of all the non-nodal diagrams of f^{+}-bonds. This implies

that C_{ij}^{+} has the form given by the sum of the short-range and long-range contributions. Therefore, a procedure similar to that for the MSA is available for solving Eq. (270).

When the distance ($r = r_{ij}$) between i and j is sufficiently large, $|\beta u_{ij}|$ should be small. Equation (262) can then be approximated as

$$\begin{aligned} p_{ij}(r) =& \frac{4}{3\sqrt{\pi}}(-\beta u_{ij})^{3/2} - \frac{4}{5\sqrt{\pi}}(-\beta u_{ij})^{5/2} \\ &+ \frac{2}{7\sqrt{\pi}}(-\beta u_{ij})^{7/2} + \cdots . \end{aligned} \tag{292}$$

The substitution of Eq. (292) into Eq. (290) results in

$$\begin{aligned} C_{ij}^{+} =& \frac{c_{ij}^{\mathrm{PY}}}{-\beta u_{ij}}\Big[\frac{4}{3\sqrt{\pi}}(-\beta u_{ij})^{3/2} - \frac{22}{15\sqrt{\pi}}(-\beta u_{ij})^{5/2} + \cdots\Big] \\ &+ \mathcal{P}_{ij}\Big[-\beta u_{ij} - \frac{4}{3\sqrt{\pi}}(-\beta u_{ij})^{3/2} - \frac{1}{2}(-\beta u_{ij})^{2} + \frac{32}{15\sqrt{\pi}}(-\beta u_{ij})^{5/2} + \cdots\Big]. \end{aligned} \tag{293}$$

Therefore, if $c_{ij}^{\mathrm{PY}}/(-\beta u_{ij}) = 1$ for the MSA is substituted into Eq. (293), the behavior of C_{ij}^{+} for $1 \ll r/\sigma_{ij}$ is expressed as

$$C_{ij}^{+} \approx 4/(3\sqrt{\pi})(-\beta u_{ij})^{3/2}. \tag{294}$$

To derive Eq. (294) from Eq. (293), the condition $(-\beta u_{ij})\mathcal{P}_{ij} \ll 4/(3\sqrt{\pi})(-\beta u_{ij})^{3/2}$ is assumed for $1 \ll r/\sigma_{ij}$.

The MSA results in $\lim_{r\to\infty} \frac{g_{ij}-1}{-\beta u_{ij}} = \frac{1}{2}$ with a general assumption $\lim_{r\to\infty} u_{ij}(r) = 0$, since the PY approximation is given as $g_{ij}^{\mathrm{PY}} = \frac{c_{ij}^{\mathrm{PY}}}{1-\exp(\beta u_{ij})}$. The condition $\mathcal{P}_{ij}/(g_{ij}-1) \le 1$ is always satisfied. Thus, $\mathcal{P}_{ij}$ for $1 \ll r$ satisfies $\frac{g_{ij}-1}{-\beta u_{ij}} \ge \frac{\mathcal{P}_{ij}}{-\beta u_{ij}}$. This implies that $\mathcal{P}_{ij} \sim [-\beta u_{ij}]^{\nu}$ and $1 \le \nu$ are satisfied. Therefore, $\lim_{r\to\infty} \frac{\mathcal{P}_{ij}}{(-\beta u_{ij})^{1/2}} = 0$ is derived. Thus, the above assumption is validated.

(b) *Behavior of* $\mathcal{P}_{ij}$ *for* $|\beta u_{ij}| \ll 1$ *and* $1 \ll r/\sigma_{ij}$

Using Eq. (292), the expansion of Eq. (290) in powers of $-\beta u_{ij}$ can be performed as

$$\begin{aligned} \mathcal{P}_{ij} =& -\frac{c_{ij}^{\mathrm{PY}}}{-\beta u_{ij}}\Big[\frac{4}{3\sqrt{\pi}}(-\beta u_{ij})^{1/2} + \frac{16}{9\pi}(-\beta u_{ij}) + \Big(\frac{64}{27\pi^{3/2}} - \frac{4}{5\sqrt{\pi}}\Big)(-\beta u_{ij})^{3/2} + \cdots\Big] \\ &+ \frac{C_{ij}^{+}}{-\beta u_{ij}}\Big[1 + \frac{4}{3\sqrt{\pi}}(-\beta u_{ij})^{1/2} + \Big(\frac{1}{2} + \frac{16}{9\pi}\Big)(-\beta u_{ij}) + \cdots\Big]. \end{aligned} \tag{295}$$

If the approximation given by Eq. (294) and $c_{ij}^{\mathrm{PY}}/(-\beta u_{ij}) = 1$ caused by the MSA are considered in Eq. (295), the result can be expressed as

$$\mathcal{P}_{ij} \approx \frac{22}{15\sqrt{\pi}}(-\beta u_{ij})^{3/2} \quad \text{for} \quad u_{ij} < 0. \tag{296}$$

If a physical cluster in the fluid mixture has a fractal structure, then $\mathcal{P}_{ij}(r)$ given by Eq. (296) represents the characteristics of the fractal structure.

(c) *Behavior of C^*_{ij} for $|\beta u_{ij}| \ll 1$ and $1 \ll r/\sigma_{ij}$*

Equation (260), relation $c^{\rm PY}_{ij}/(-\beta u_{ij}) = 1$ caused by the MSA , and behavior of $\mathcal{P}_{ij}(r)$ given by Eq. (296) allow the relation $g^{\rm PY}_{ij}(r) = c^{\rm PY}_{ij}(r)/\{1 - \exp[\beta u_{ij}(r)]\}$ to result in

$$\mathcal{D}_{ij}(r) - 1 \approx -(1/2)\beta u_{ij}(r) \quad \text{for} \quad 1 \ll r/\sigma_{ij}. \tag{297}$$

Because of Eq. (297), Eqs. (262) and (292) allow Eq. (291) to result in

$$C^*_{ij}(r) \approx -\beta u_{ij}(r) \quad \text{for} \quad 1 \ll r/\sigma_{ij}. \tag{298}$$

3. Simple closure schemes similar to MSA

(a) *Expression of simple closure schemes similar to MSA*

The direct correlation function $c_{ij}(r)$ formed by the contribution of all non-nodal diagrams comprising paths of f-bonds between the two root points is given as the sum of the short-range and long-range contributions. A correlation function $C^+_{ij}(r)$ is formed by the contribution of all non-nodal diagrams that have at least one path of all f^+-bonds between the two root points. Thus, C^+_{ij} can be given as the sum of the short-range and long-range contributions.[37] Further, a correlation function C^*_{ij} can be given as the sum of the short-range and long-range contributions because of $C^*_{ij} = c_{ij} - C^+_{ij}$.

Owing to the consequence given by Eq. (294), an analogy with the MSA allows C^+_{ij} to be expressed as

$$C^+_{ij} = C^{0+}_{ij} + \frac{4}{3\sqrt{\pi}}(-\beta u_{ij})^{3/2} \quad \text{for} \quad \beta u_{ij} < 0, \tag{299}$$

where C^{0+}_{ij} is the short-range contribution, i.e.,

$$C^{0+}_{ij}(r) = 0, \qquad \text{for} \ r \geq \sigma_{ij}. \tag{300}$$

Here, σ_{ij} is defined as

$$\sigma_{ij} \equiv \frac{1}{2}(\sigma_i + \sigma_j), \tag{301}$$

where σ_i and σ_j denote the diameters of the hard cores of i and j particles (i.e., particles of species i and j), respectively. Thus, Eq. (270) can be solved using the closure scheme given as Eq. (299).

Owing to the consequence given by Eq. (298), an analogy with the MSA allows C_{ij}^{*} to be expressed as

$$C_{ij}^{*} = C_{ij}^{0*} + (-\beta u_{ij}) \quad \text{for} \quad \beta u_{ij} < 0, \tag{302}$$

where C_{ij}^{0*} denotes the short-range contribution, i.e.,

$$C_{ij}^{0*}(r) = 0, \qquad \text{for } r \geq \sigma_{ij}. \tag{303}$$

The formula given by Eq. (302) is available for either $\beta u_{ij} < 0$ or $\beta u_{ij} > 0$. Thus, Eq. (272) can be solved using the closure scheme given by Eq. (302).

(b) *Effective range in which* $\mathcal{P}_{ij}(r) \neq 0$

The consequence obtained from recursively solving Eq. (270) indicates that particles (i.e., species $k_1, k_2, \cdots$) distributed around i and j particles (i.e., particles of species i and j) allow the correlation function $\mathcal{P}_{ij}(r)$ to decay to zero more slowly than $C_{ij}^{+}(r)$ decays. $C_{ij}^{+}(r)$ can decay to zero more rapidly than $-\beta u_{ij}(r)$, which represents a microscopic feature. The effective range in which $C_{ij}^{+}(r) \neq 0$ is satisfied remains microscopic according to Eq. (299). Yet, $\mathcal{P}_{ij}(r) \neq 0$ can be satisfied for a large r at which $C_{ij}^{+}(r) \approx 0$ is satisfied.

The recursive solution of Eq. (270) guarantees that a feature of $\mathcal{P}_{ij}(r)$ estimated with the use of Eq. (299) can become macroscopic. The recursive solution for $\mathcal{P}_{ij}$ is given as

$$\begin{aligned} \mathcal{P}_{ij} =& C_{ij}^{+} + \sum_{k_1=1}^{\mathcal{L}} \rho_{k_1} \int C_{ik_1}^{+} C_{k_1 j}^{+} \mathrm{d}\mathbf{r}_3^{(k_1)} \\ &+ \sum_{k_1=1}^{\mathcal{L}} \sum_{k_2=1}^{\mathcal{L}} \rho_{k_1} \rho_{k_2} \int \int C_{ik_1}^{+} C_{k_1 k_2}^{+} C_{k_2 j}^{+} \mathrm{d}\mathbf{r}_3^{(k_1)} \mathrm{d}\mathbf{r}_4^{(k_2)} + \cdots . \end{aligned} \tag{304}$$

If a fluid mixture system includes extremely large physical clusters, $\mathcal{P}_{ij}(r)$ should have a long-range feature on the macroscopic scale even if $C_{ij}^{+}(r)$ retains a microscopic feature. The long-range feature is formed by convolution integrals found in Eq. (304).

If contributions of particles $(k_1, k_2, \cdots)$ distributed around the i and j particles are not negligible in Eq. (304), it is possible for $\mathcal{P}_{ij}(r)$ to remain nonzero even out of the effective range where $C_{ij}^{+}(r) \neq 0$is satisfied. The pair connectedness $\mathcal{P}_{ij}(r)$ that must satisfy the

integral equation given by Eq. (270) involves contributions of many particles expressed as convolution integrals found in Eq. (304). This implies that the pair connectedness $\mathcal{P}_{ij}(r)$ derived from the use of an approximate $C_{ij}^{+}(r)$ involves the contributions of many particles, even when the approximate $C_{ij}^{+}(r)$ results from the contributions of limited principal particles. Even without the use of an accurate $C_{ij}^{+}(r)$ obtained from the contributions of all particles that should be considered, it possible to succeed in replying to the necessity of considering the contributions of many particles if $\mathcal{P}_{ij}(r)$ satisfy the integral equation formed by Eq. (270) and the approximate $C_{ij}^{+}(r)$.

$\mathcal{P}_{ij}$ is proportional to the probability that both i and j particles belong to the same physical cluster. Indeed, each term on the right-hand side of Eq. (304) is proportional to the probability that both the i and j particles belong to the same physical cluster via the contribution of other particular particles $(k_1, k_2, \cdots)$. The first term C_{ij}^{+} without the contribution of other particular particles $(k_1, k_2, \cdots)$ is proportional to the probability. The first term C_{ij}^{+} has a simpler bonding structure compared to that of the other terms.

(c) *Effective range in which* $\mathcal{H}_{ij}(r) \neq 0$

The effective range in which $C_{ij}^{*}(r) \neq 0$ remains microscopic according to Eq. (302). The recursive solution of Eq. (272) guarantees that a feature of $\mathcal{H}_{ij}(r)$ estimated with the use of Eq. (302) can become macroscopic.

i) *Basis of usefulness of MSA*

The MSA allows the direct correlation function $c_{ij}(r)$ to decay to zero as rapidly as $-\beta u_{ij}(r)$. Then, the effective range in which $u_{ij}(r) \neq 0$ is satisfied retains a microscopic feature. The correlation function $g_{ij}(r) - 1$ can decay to zero much slower than $c_{ij}(r)$.[13,18] The recursive solution of the Ornstein–Zernike equation is given by

$$\begin{aligned} g_{ij} - 1 =& c_{ij} + \sum_{k_1=1}^{\mathcal{L}} \rho_{k_1} \int_V c_{ik_1} c_{k_1 j} \mathrm{d}\mathbf{r}_3^{(k_1)} \\ &+ \sum_{k_1=1}^{\mathcal{L}} \sum_{k_2=1}^{\mathcal{L}} \rho_{k_1} \rho_{k_2} \int_V \int_V c_{ik_1} c_{k_1 k_2} c_{k_2 j} \mathrm{d}\mathbf{r}_3^{(k_1)} \mathrm{d}\mathbf{r}_4^{(k_2)} + \cdots . \end{aligned} \tag{305}$$

Convolution integrals found in Eq. (305) denote contributions from particles $(k_1, k_2, \cdots)$, which are distributed around i and j particles. These contributions cause the behavior of

$g_{ij}-1$ to differ from the behavior of c_{ij}. The recursive solution indicates that the pair correlation function $g_{ij}(r)$ that satisfies requirements based on the Ornstein–Zernike equation involves the contributions of many particles. This allows the pair correlation function $g_{ij}(r)$ derived from the use of an approximate $c_{ij}(r)$ to involve contributions of many particles, even when the approximate $c_{ij}(r)$ results from the contributions of limited principal particles. Without the use of an accurate $c_{ij}(r)$ obtained from the contributions of all particles which should be considered, $g_{ij}(r)$ estimated from the Ornstein–Zernike equation and the approximate $c_{ij}(r)$ replies to the necessity of considering the contributions of many particles.

ii) *Usefulness of approximate* $C^*_{ij}(r)$

As known from the case of $g_{ij}(r)-1$, particles $(k_1, k_2, \cdots)$ distributed around i and j particles enable the correlation function $\mathcal{H}_{ij}(r)$ to decay to zero considerably slower than $C^*_{ij}(r)$ decays. $C^*_{ij}(r)$ can decay to zero as rapidly as $-\beta u_{ij}(r)$, which expresses a microscopic feature. $\mathcal{H}_{ij}(r)\neq 0$ is satisfied at a large r where $C^*_{ij}(r)\approx 0$ is satisfied. This can be known through a solution obtained by recursively solving Eq. (272) for $\mathcal{H}_{ij}$. The recursive solution for $\mathcal{H}_{ij}$ is given as

$$\begin{aligned}\mathcal{H}_{ij} =& C^*_{ij}+\sum_{k_1=1}^{\mathcal{L}}\rho_{k_1}\int_V c_{ik_1}C^*_{k_1j}\mathrm{d}\mathbf{r}_3^{(k_1)}+\sum_{k_1=1}^{\mathcal{L}}\sum_{k_2=1}^{\mathcal{L}}\rho_{k_1}\rho_{k_2}\int_V\int_V c_{ik_1}c_{k_1k_2}C^*_{k_2j}\mathrm{d}\mathbf{r}_3^{(k_1)}\mathrm{d}\mathbf{r}_4^{(k_2)}+\\ &+\sum_{k_1=1}^{\mathcal{L}}\rho_{k_1}\int C^*_{ik_1}\mathcal{P}_{k_1j}\mathrm{d}\mathbf{r}_3^{(k_1)}+\sum_{k_1=1}^{\mathcal{L}}\sum_{k_2=1}^{\mathcal{L}}\rho_{k_1}\rho_{k_2}\int_V\int_V c_{ik_1}C^*_{k_1k_2}\mathcal{P}_{k_2j}\mathrm{d}\mathbf{r}_3^{(k_1)}\mathrm{d}\mathbf{r}_4^{(k_2)}\\ &+\sum_{k_1=1}^{\mathcal{L}}\sum_{k_2=1}^{\mathcal{L}}\sum_{k_3=1}^{\mathcal{L}}\rho_{k_1}\rho_{k_2}\rho_{k_3}\int_V\int_V\int_V c_{ik_1}c_{k_1k_2}C^*_{k_2k_3}\mathcal{P}_{k_3j}\mathrm{d}\mathbf{r}_3^{(k_1)}\mathrm{d}\mathbf{r}_4^{(k_2)}\mathbf{r}_5^{(k_3)}+\cdots. \end{aligned}\tag{306}$$

The magnitude of $\mathcal{H}_{ij}(r)$ at a large r, where $C^*_{ij}(r)\approx 0$ is satisfied, remains a finite value that is not zero because of the convolution integrals. The correlation function $\mathcal{H}_{ij}(r)$, which satisfies the integral equation given by Eq. (272), involves the contributions of many particles that are expressed as convolution integrals found in Eq. (306). The correlation function $\mathcal{H}_{ij}(r)$ satisfying Eq. (272) with the use of an approximate $C^*_{ij}(r)$ involves the contributions of many particles, even when the approximate $C^*_{ij}(r)$ results from the contributions of limited principal particles. Without the use of an accurate $C^*_{ij}(r)$ obtained from the contributions of all particles that should be considered, $\mathcal{H}_{ij}(r)$ that satisfies the integral equation formed by Eq. (272) and the approximate $C^*_{ij}(r)$ replies to the necessity of considering the contributions of many particles.

(d) *Expression of practical closure scheme similar to MSA*

A mutually attractive force between particles must be characterized by a pair potential for analyzing an $\mathcal{L}$-component fluid mixture system. Hence, the contribution βu_{ij} of the pair potential must characterize the interaction between a particle of species i (an i particle) and a particle of species j (a j particle). Thus, it is assumed that βu_{ij} is given by a potential formed as the sum of $\mathcal{N}$ terms to analyze the $\mathcal{L}$-component fluid mixture system. The potential is expressed as

$$-\beta u_{ij}(r) = \sum_{n=1}^{\mathcal{N}} k_0^{(n)} d_i^{(n)} d_j^{(n)} \frac{\exp(-z_n r)}{r} \quad \text{for} \quad r \geq \sigma_{ij}. \tag{307}$$

Then, the closure scheme given by Eq. (299) is expressed as

$$C_{ij}^{+}(r) = C_{ij}^{0+}(r) + \frac{4}{3\sqrt{\pi}} \left[\sum_{n=1}^{\mathcal{N}} k_0^{(n)} d_i^{(n)} d_j^{(n)} \exp(-z_n r) \right]^{3/2} \frac{1}{r^{3/2}}. \tag{308}$$

Here, z_n and $k_0^{(n)}$ are independent of the species of the particle. A factor $k_0^{(n)}$ is proportional to $1/k_B T$, and it is proportional to the strength of a common effect that contributes to each mutually attractive force that causes two particles to interact with each other. $1/z_n$ represents a feature that corresponds to the effective range of the mutually attractive force between the two particles. A factor $d_i^{(n)}$ represents the feature of an i particle, and it represents the strength of a common effect contributing to each interaction that occurs between the i particle and another particle. Further, the feature of the i particle is independent of the magnitude of $k_0^{(n)}$.

The decrease in $C_{ij}^{+}(r)$ caused by each term of the exponential function can be considerably more dominant than that caused by the factor $(1/r)^{3/2}$, as r increases. Hence, significant terms that contributes to the long-range contribution of the closure scheme need to be extracted from the terms included in the factor $\left[\sum_n k_0^{(n)} d_i^{(n)} d_j^{(n)} \exp(-z_n r)\right]^{3/2}$ in Eq. (308) by considering an assumption made as

$$0 < z_1 \leq z_2 \leq \cdots \leq z_{\mathcal{N}} < \infty. \tag{309}$$

Based on this assumption, the above factor should be modified as

$$\left[\sum_{n=1}^{\mathcal{N}} k_0^{(n)} d_i^{(n)} d_j^{(n)} \exp(-z_n r) \right]^{3/2} \approx \left[k_0^{(1)} d_i^{(1)} d_j^{(1)} \exp(-z_1 r) \right]^{3/2} \times \left[1 + \frac{3}{2} \frac{\exp(z_1 r)}{k_0^{(1)} d_i^{(1)} d_j^{(1)}} \sum_{n=2}^{\mathcal{N}} k_0^{(n)} d_i^{(n)} d_j^{(n)} \exp(-z_n r) \right]. \tag{310}$$

Then, the terms on the right-hand side of Eq. (310) correspond to significant terms that should be considered in the long-range contribution of the closure scheme

An approximate expression for the factor $(1/r)^{3/2}$ in Eq. (308) can be given by Eq. (83). The approximate expression help avoid the mathematical difficulty caused by $(1/r)^{3/2}$ when solving Eq. (270) analytically. According to Eq. (83), the approximate expression is expressed as

$$\frac{1}{r^{3/2}} \approx \sigma_{ij}^{-1/2} \exp[f_\nu] \exp[-(f_\nu/\sigma_{ij})r] \frac{1}{r}. \tag{311}$$

In this expression, the value of f_ν need to satisfy the relation $0 < f_\nu \leq 1/2$. Despite this, Eq. (84) allows the value of f_ν to be reasonably determined without the restriction given by Eq. (82). Thus, a reasonable value of f_ν can be obtained as a solution of Eq. (85) for $\hat{n} = 3$. This value is expressed as $f_\nu \approx f_{\nu_{3/2}}$ with $f_{\nu_{3/2}} = 0.1018532115$.

Equations (311) and (310) yield an approximate expression for a long-range contribution of the closure scheme; thus, the approximate expression for Eq. (308) is derived. The approximate expression is characterized by the parameter f_ν, and expressed as

$$C_{ij}^{+}(r) = C_{ij}^{0+}(r) + \sum_{n=1}^{\mathcal{N}} \breve{k}_0^n \breve{d}_i^n \breve{d}_j^n \frac{\exp(-\breve{z}_n r)}{r}, \tag{312}$$

where

$$0 < \breve{z}_1 \leq \breve{z}_2 \leq \breve{z}_3 \leq \cdots, \tag{313}$$

$$\breve{z}_1 = z_1 + \frac{f_\nu}{a}, \tag{314}$$

$$\breve{z}_n = z_n + \frac{1}{2} z_1 + \frac{f_\nu}{a}, \quad (n = 2, 3, \cdots, \mathcal{N}), \tag{315}$$

$$\breve{k}_0^1 \breve{d}_i^1 \breve{d}_j^1 = \frac{4 \exp(f_\nu)}{3\sqrt{\pi}\sqrt{a}} (k_0^{(1)})^{3/2} (d_i^{(1)})^{3/2} (d_j^{(1)})^{3/2}, \tag{316}$$

and

$$\breve{k}_0^n \breve{d}_i^n \breve{d}_j^n = \frac{2 \exp(f_\nu)}{\sqrt{\pi}\sqrt{a}} (k_0^{(1)})^{1/2} k_0^{(n)} (d_i^{(1)})^{1/2} d_i^{(n)} (d_j^{(1)})^{1/2} d_j^{(n)}, \quad (n = 2, 3, \cdots, \mathcal{N}), \tag{317}$$

with

$$\begin{cases} a = \sigma_{ij}, \\ 0 < f_\nu \leq 1/2 \\ \text{or} \quad f_\nu \approx f_{\nu_{3/2}} \quad \text{with} \quad f_{\nu_{3/2}} = 0.1018532115. \end{cases} \tag{318}$$

If the closure expressed as Eq. (312) is used, then the integral equation system given by Eqs. (270) and (312) can be solved based on the method for exactly solving the Orstein-Zernike equation system[82,84] that has the Yukawa closure for the MSA.

Further, the approximation given by Eq. (312) for $f_\nu = 0$ overestimates the long-range contribution of $C_{ij}^{+}(r)$. This is because the approximation specified for $f_\nu = 0$ implies that the long-range contribution described by the factor $(1/r)^{3/2}$ in Eq. (308) is approximated as $(1/\sqrt{a})(1/r)$. The alternative approximation given by Eq. (312) for $f_\nu = 1/2$ overestimates the decay of $C_{ij}^{+}(r)$ dependent on r because the long-range contribution described by the factor $(1/r)^{3/2}$ in Eq. (308) is approximated as $(e^{1/2}/\sqrt{a})(1/r)\exp[-r/(2a)]$.

According to a previous study on Yukawa fluids[8], overestimation of the long-range contribution of $C_{ij}^{+}(r)$ can lead to an overestimation of $1/(\breve{k}_0^n \breve{d}_i^n \breve{d}_j^n)$ at the percolation threshold. However, the diagram of the percolation threshold for overestimating the long-range contribution has the same pattern as that for overestimating the decay of $C_{ij}^{+}(r)$.

E. Solution of integral equation for $\mathcal{P}_{ij}(r)$

Equation (270) and the practical closure scheme given by Eq. (312) result in an integral equation system that can be solved analytically without an additional approximation. Then, a mathematical procedure similar to that used for solving the Orstein-Zernike equation[43,83,84] is used. The use of Baxter's Q function[43] enables $\mathcal{P}_{ij}(r)$ and $C^{+}_{ij}(r)$ to be estimated from Eq. (270) for the $\mathcal{L}$-component fluid mixture.[37,52]

1. Fourier transforms of integral equations

If each correlation function is expressed as $F_{ij}(r)$ that satisfies $\lim_{r\to 0} rF_{ij}(r) = 0$, then a Fourier transform of $F_{ij}(r)$ is given as

$$\begin{aligned}\widetilde{F}_{ij}(k) \equiv & \lim_{V\to\infty} (\rho_i\rho_j)^{1/2} \int_V F_{ij}(r) \exp[i\mathbf{k}\cdot\mathbf{r}]\mathrm{d}\mathbf{r} \\ =& 4\pi(\rho_i\rho_j)^{1/2} \int_0^\infty \cos kr\mathrm{d}r \int_r^\infty t\mathrm{d}tF_{ij}(t) \quad (r \equiv |\mathbf{r}|,\ \ k \equiv |\mathbf{k}|).\end{aligned} \tag{319}$$

If V is macroscopic, the integral $\sqrt{\rho_i\rho_j}\int_V F_{ij}(r)e^{i\mathbf{k}\cdot\mathbf{r}}\mathrm{d}\mathbf{r}$ can be expressed as $\widetilde{F}_{ij}(k)$, which is given by Eq. (319). According to the expression of Eq. (319), the Fourier transform of Eq. (270) is given as

$$\sum_{k=1}^{\mathcal{L}} \left[\delta_{ik} - \widetilde{C}^{+}_{ik}(k)\right] \widetilde{\mathcal{P}}_{kj}(k) = \widetilde{C}^{+}_{ij}(k). \tag{320}$$

The Fourier transform of Eq. (272) is given as

$$\sum_{k=1}^{\mathcal{L}} \left[\delta_{ik} - \widetilde{C}^{*}_{ik}(k) - \widetilde{C}^{+}_{ik}(k)\right] \widetilde{\mathcal{H}}_{kj}(k) = \widetilde{C}^{*}_{ij}(k) + \sum_{k=1}^{\mathcal{L}} \widetilde{C}^{*}_{ik}(k)\widetilde{\mathcal{P}}_{kj}(k). \tag{321}$$

The Fourier transform of the Ornstein–Zernike equation expressed as Eq. (271) is given as

$$\sum_{k=1}^{\mathcal{L}} \left[\delta_{ik} - \widetilde{c}_{ik}(k)\right] \left[\widetilde{\mathcal{P}}_{kj}(k) + \widetilde{\mathcal{H}}_{kj}(k)\right] = \widetilde{c}_{ij}(k), \tag{322}$$

where

$$\widetilde{c}_{ij}(k) = \widetilde{C}^{+}_{ij}(k) + \widetilde{C}^{*}_{ij}(k) \tag{323}$$

because of Eq. (268).

The use of Baxter's Q function[43] allows the equation given by Eq. (320) to be expressed as

$$\begin{cases} \sum_{k=1}^{\mathcal{L}}[\delta_{ik}+\widetilde{\mathcal{P}}_{ik}(k)]\widetilde{Q}_{kj}^{+}(k)=\widetilde{Q}_{ij}^{+(-1)}(-k) \\ \delta_{ij}-\widetilde{C}_{ij}^{+}(k)=\sum_{k=1}^{\mathcal{L}}\widetilde{Q}_{ik}^{+}(k)\widetilde{Q}_{jk}^{+}(-k), \\ \sum_{k=1}^{\mathcal{L}}\widetilde{Q}_{ki}^{+(-1)}(-k)\widetilde{Q}_{jk}^{+}(-k)=\delta_{ij}\ \ \delta_{ii}=1;\ \ \delta_{ij}=0\ \ (i\neq j). \end{cases} \tag{324}$$

If an inverse Fourier transform is applied to the first and second equations included in Eq. (324), the following equations can be obtained as

$$\begin{aligned} 2\pi r\mathcal{P}_{ij}(r) =& -\frac{\mathrm{d}}{\mathrm{d}r}Q_{ij}(r) \\ & +2\pi\sum_{k=1}^{\mathcal{L}}\rho_k\int_{\lambda_{jk}}^{\infty}Q_{kj}(t)(r-t)\mathcal{P}_{ik}(|r-t|)\mathrm{d}t, \\ & \quad \text{for}\ \ \lambda_{ji}\leq r<\infty, \end{aligned} \tag{325}$$

and

$$\begin{aligned} 2\pi r C_{ij}^{+}(r) =& -\frac{\mathrm{d}}{\mathrm{d}r}Q_{ij}(r) \\ & +\sum_{k=1}^{\mathcal{L}}\rho_k\int_{sup[\lambda_{kj},\lambda_{ki}-r]}^{\infty}Q_{jk}(t)\frac{\mathrm{d}}{\mathrm{d}r}Q_{ik}(r+t)\mathrm{d}t, \\ & \quad \text{for}\ \ \lambda_{ji}\leq r<\infty, \end{aligned} \tag{326}$$

where λ_{ji} is defined as $\lambda_{ji}\equiv\frac{1}{2}(\sigma_j-\sigma_i)$. The function $Q_{ij}(r)$ in Eqs. (325) and (326) is introduced as

$$\widetilde{Q}_{ij}(k)=\delta_{ij}-(\rho_i\rho_j)^{1/2}\int_{\lambda_{ji}}^{\infty}e^{ikr}Q_{ij}(r)\mathrm{d}r, \tag{327}$$

where $\delta_{ij}=0\ \ (i\neq j)$ and $\delta_{ii}=1$.

The short-range contribution to $C_{ij}^{+}(r)$ is expressed as $C_{ij}^{0+}(r)$ in Eq. (300). The correlation function $C_{ij}^{+}(r)$ is related to $Q_{ij}(r)$ via Eq. (326). Hence, the characteristic of the short-range contribution $C_{ij}^{0+}(r)$ is provided by $Q_{ij}(r)$. Similarly, the characteristic of the long-range contribution to $C_{ij}^{+}(r)$ is related to a form of $Q_{ij}(r)$. Therefore, $Q_{ij}(r)$ must be expressed as

$$Q_{ij}(r)=Q_{ij}^{0}(r)+\sum_{n=1}^{\mathcal{N}}D_{ij}^{n}e^{-\check{z}_n r}\ \ (\lambda_{ji}<r<\sigma_{ji}), \tag{328}$$

$$Q_{ij}(r) = \sum_{n=1}^{\mathcal{N}} D_{ij}^n e^{-\breve{z}_n r} \quad (\sigma_{ji} \le r), \tag{329}$$

and

$$Q_{ij}^0(r) = 0 \quad (\sigma_{ji} \le r). \tag{330}$$

In the above, D_{ij} $(i, j = 1, 2, \cdots, \mathcal{L})$ are unknown coefficients, and these coefficients must be determined via the use of Eqs. (325) and (326).

Hard-core potentials that are characterized by $u_{ij}(r) = \infty$ at $r = \sigma_{ij}$ allow $\lim_{\delta \to 0} g_{ij}(\sigma_{ij} + \delta) = 0$ $(\delta > 0)$ to be satisfied. Similarly, $\lim_{\delta \to 0} \mathcal{P}_{ij}(\sigma_{ij} + \delta) = 0$ $(\delta > 0)$ is satisfied because of Eqs. (265) and (288); hence, $\mathcal{P}_{ij}(r) = 0$ for $\lambda_{ji} < r < \sigma_{ji}$ is derived. This feature maintained by $\mathcal{P}_{ij}(r)$ requires the function $Q_{ij}(r)$ derived from Eq. (325) for $|\rho_k| \ll 1$ to not include the powers of r in the range $\lambda_{ji} < r < \sigma_{ji}$. If this fact is considered with the behavior of $Q_{ij}(r)$ expressed by Eq. (328), the feature of $Q_{ij}^0(r)$ given by Eq. (330) requires $Q_{ij}^0(r)$ to have a specific form, i.e.,

$$Q_{ij}^0(r) = \sum_{n=1}^{\mathcal{N}} \left[-D_{ij}^n + 2\pi \sum_{k=1}^{\mathcal{L}} \frac{\rho_k}{\breve{z}_n} \widehat{\mathcal{P}}_{ik}(\breve{z}_n) D_{kj}^n \right] (e^{-\breve{z}_n r} - e^{-\breve{z}_n \sigma_{ij}}) \quad (\lambda_{ji} < r < \sigma_{ji}), \tag{331}$$

where

$$\widehat{\mathcal{P}}_{ik}(\breve{z}_n) \equiv \int_0^\infty \mathcal{P}_{ik}(t) e^{-\breve{z}_n t} t \mathrm{d}t. \tag{332}$$

Because of Eq. (313), the quantities $\widehat{\mathcal{P}}_{ik}(\breve{z}_n)$ should satisfy

$$\widehat{\mathcal{P}}_{ik}(\breve{z}_1) \ge \widehat{\mathcal{P}}_{ik}(\breve{z}_2) \ge \cdots \quad (0 < \breve{z}_1 \le \breve{z}_2 \le \cdots). \tag{333}$$

Thus, the quantity $\widehat{\mathcal{P}}_{ik}(\breve{z}_n)$ is small, if the effective range of the attractive force between pair particles i and k is short. The effective range of the attractive force between the pair particles is characterized by the coefficient $\breve{z}_n$ given by Eq. (314).

2. *Formulas for determining coefficients* $\widehat{\mathcal{P}}_{ij}(\breve{z}_n)$ *and* D_{ij}^n

(a) *Formula for determining* $\widehat{\mathcal{P}}_{ij}(\breve{z}_n)$ *and* D_{ij}^n

Equations (328)–(330) and $\mathcal{P}_{ij}(r) = 0$ should be satisfied over the range $\lambda_{ji} < r < \sigma_{ji}$; hence, Eq. (325) for $r < \sigma_{ji}$ yields the following formula because of Eq. (331):

$$\sum_{n=1}^{\mathcal{N}} \breve{z}_n \Big[-D_{ij}^n + 2\pi \sum_{k=1}^{\mathcal{L}} \frac{\rho_k}{\breve{z}_n} \widehat{\mathcal{P}}_{ik}(\breve{z}_n) D_{kj}^n \Big] e^{-\breve{z}_n r} + \sum_{n=1}^{\mathcal{N}} \breve{z}_n D_{ij}^n e^{-\breve{z}_n r}$$
$$- 2\pi \sum_{k=1}^{\mathcal{L}} \sum_{n=1}^{\mathcal{N}} \rho_k D_{kj}^n e^{-\breve{z}_n r} \int_0^\infty \mathcal{P}_{ik}(t) e^{-\breve{z}_n t} t \mathrm{d}t = 0. \tag{334}$$

If Eq. (329) is considered, then Eq. (326) can be rewritten as

$$2\pi r C_{ij}^+(r) = \sum_{n=1}^{\mathcal{N}} \breve{z}_n D_{ij}^n e^{-\breve{z}_n r} - \sum_{n=1}^{\mathcal{N}} \breve{z}_n e^{-\breve{z}_n r} \sum_{k=1}^{\mathcal{L}} \rho_k D_{ik}^n \widehat{Q}_{jk}(\breve{z}_n), \qquad \text{for} \quad \sigma_{ji} < r, \tag{335}$$

where

$$\widehat{Q}_{jk}(s) \equiv \int_{\lambda_{kj}}^\infty Q_{jk}(t) e^{-st} \mathrm{d}t$$
$$= \sum_{m=1}^{\mathcal{N}} \Bigg[\Big[-D_{jk}^m + 2\pi \sum_{l=1}^{\mathcal{L}} \frac{\rho_l}{\breve{z}_m} \widehat{\mathcal{P}}_{jl}(\breve{z}_m) D_{lk}^m \Big] e^{-s\lambda_{kj}} e^{-\breve{z}_m \sigma_{kj}}$$
$$\times \Big(\frac{e^{\breve{z}_m \sigma_j} - e^{-s\sigma_j}}{s + \breve{z}_m} - \frac{1 - e^{-s\sigma_j}}{s} \Big) + \frac{1}{s + \breve{z}_m} D_{jk}^m e^{-\breve{z}_m \lambda_{kj}} e^{-s\lambda_{kj}} \Bigg]. \tag{336}$$

Here, Eq. (336) can be derived using Eqs. (328)–(331). The relation between $\widehat{\mathcal{P}}_{jk}(\breve{z}_n)$ and $\widehat{Q}_{jk}(\breve{z}_n)$ can be obtained from Eq. (336) as

$$\widehat{Q}_{jk}(\breve{z}_n) = e^{-\breve{z}_n \lambda_{kj}} \sum_{m=1}^{\mathcal{N}} \Bigg\{ e^{-\breve{z}_m \sigma_{kj}} D_{jk}^m \Big(\frac{e^{-\breve{z}_n \sigma_j}}{\breve{z}_n + \breve{z}_m} + \frac{1 - e^{-\breve{z}_n \sigma_j}}{\breve{z}_n} \Big)$$
$$+ \sum_{l=1}^{\mathcal{L}} \frac{2\pi \rho_l}{\breve{z}_m} \widehat{\mathcal{P}}_{jl}(\breve{z}_m) D_{lk}^m \Big[\frac{e^{-\breve{z}_m \lambda_{kj}}}{\breve{z}_n + \breve{z}_m} - e^{-\breve{z}_m \sigma_{kj}} \Big(\frac{e^{-\breve{z}_n \sigma_j}}{\breve{z}_n + \breve{z}_m} + \frac{1 - e^{-\breve{z}_n \sigma_j}}{\breve{z}_n} \Big) \Big] \Bigg\}. \tag{337}$$

By considering Eqs. (328) and (331), Eq. (325) for $r < \sigma_{ji}$ can be rewritten as

$$0 = \sum_{n=1}^{\mathcal{N}} \breve{z}_n \Big[-D_{ij}^n + 2\pi \sum_{k=1}^{\mathcal{L}} \frac{\rho_k}{\breve{z}_n} \widehat{\mathcal{P}}_{ik}(\breve{z}_n) D_{kj}^n \Big] e^{-\breve{z}_n r} + \sum_{n=1}^{\mathcal{N}} \breve{z}_n D_{ij}^n e^{-\breve{z}_n r}$$
$$+ 2\pi \sum_{k=1}^{\mathcal{L}} \rho_k \int_r^\infty Q_{kj}(t)(r - t) \mathcal{P}_{ik}(|r - t|) \mathrm{d}t. \tag{338}$$

Equation (338) is equivalent to Eq. (334), which has no singularity for $0 < r < \infty$; hence, Eq. (338) is satisfied for $0 < r < \infty$. If the terms in Eq. (338) are then subtracted from those in Eq. (325) for $\sigma_{ji} \le r$, a formula can be derived as

$$2\pi r \mathcal{P}_{ij}(r) = - \sum_{m=1}^{\mathcal{N}} \breve{z}_m \Big[-D_{ij}^m + 2\pi \sum_{k=1}^{\mathcal{L}} \frac{\rho_k}{\breve{z}_m} \widehat{\mathcal{P}}_{ik}(\breve{z}_m) D_{kj}^m \Big] e^{-\breve{z}_m r}$$
$$+ 2\pi \sum_{k=1}^{\mathcal{L}} \rho_k \int_{\lambda_{jk}}^r Q_{kj}(t)(r - t) \mathcal{P}_{ik}(r - t) \mathrm{d}t. \tag{339}$$

The Laplace transformation of Eq. (339) results in

$$2\pi\widehat{\mathcal{P}}_{ij}(s) = -\sum_{m=1}^{\mathcal{N}} \frac{\breve{z}_m}{s+\breve{z}_m} e^{-(s+\breve{z}_m)\sigma_{ij}} \left[-D_{ij}^m + 2\pi \sum_{k=1}^{\mathcal{L}} \frac{\rho_k}{\breve{z}_m} \widehat{\mathcal{P}}_{ik}(\breve{z}_m) D_{kj}^m \right] + 2\pi \sum_{k=1}^{\mathcal{L}} \rho_k \widehat{\mathcal{P}}_{ik}(s) \widehat{Q}_{kj}(s). \tag{340}$$

Ultimately, substituting Eq. (337) into Eq. (340) for $s = \breve{z}_n$ alows the relation between $\widehat{\mathcal{P}}_{ij}(\breve{z}_n)$ and $\breve{D}_{ij}^n$ to be determined by

$$\begin{aligned} 2\pi\widehat{\mathcal{P}}_{ij}(\breve{z}_n) =& \sum_{m=1}^{\mathcal{N}} \frac{\breve{z}_m}{\breve{z}_n+\breve{z}_m} e^{-(\breve{z}_n+\breve{z}_m)\sigma_{ij}} \left(D_{ij}^m - 2\pi \sum_{k=1}^{\mathcal{L}} \frac{\rho_k}{\breve{z}_m} \widehat{\mathcal{P}}_{ik}(\breve{z}_m) D_{kj}^m \right) \\ &+ 2\pi \sum_{k=1}^{\mathcal{L}} \rho_k \widehat{\mathcal{P}}_{ik}(\breve{z}_n) e^{-\breve{z}_n\lambda_{jk}} \sum_{m=1}^{\mathcal{N}} \Bigg\{ e^{-\breve{z}_m\sigma_{jk}} D_{kj}^m \left(\frac{e^{-\breve{z}_n\sigma_k}}{\breve{z}_n+\breve{z}_m} + \frac{1-e^{-\breve{z}_n\sigma_k}}{\breve{z}_n} \right) \\ &+ \sum_{l=1}^{\mathcal{L}} \frac{2\pi\rho_l}{\breve{z}_m} \widehat{\mathcal{P}}_{kl}(\breve{z}_m) D_{lj}^m \left[\frac{e^{-\breve{z}_m\lambda_{jk}}}{\breve{z}_n+\breve{z}_m} - e^{-\breve{z}_m\sigma_{jk}} \left(\frac{e^{-\breve{z}_n\sigma_k}}{\breve{z}_n+\breve{z}_m} + \frac{1-e^{-\breve{z}_n\sigma_k}}{\breve{z}_n} \right) \right] \Bigg\}. \end{aligned} \tag{341}$$

(b) *Another formula for determining* $\widehat{\mathcal{P}}_{ij}(\breve{z}_n)$ *and* D_{ij}^n

If Eq. (300) is considered, the substitution of Eq. (312) into Eq. (335) results in

$$2\pi\breve{k}_0^n \breve{d}_i^n \breve{d}_j^n = \breve{z}_n D_{ij}^n - \sum_{k=1}^{\mathcal{L}} \breve{z}_n \rho_k D_{ik}^n \widehat{Q}_{jk}(\breve{z}_n). \tag{342}$$

Further, substituting Eq. (337) into Eq. (342) yields another formula to determine the relation between $\widehat{\mathcal{P}}_{ij}(\breve{z}_n)$ and D_{ij}^n as follows:

$$\begin{aligned} 2\pi\breve{k}_0^n \breve{d}_i^m \breve{d}_j^n = \breve{z}_n D_{ij}^n &- \sum_{m=1}^{\mathcal{N}} \sum_{k=1}^{\mathcal{L}} \rho_k D_{ik}^n D_{jk}^m e^{-\breve{z}_n\lambda_{kj}} e^{-\breve{z}_m\sigma_{kj}} \frac{\breve{z}_n+\breve{z}_m-\breve{z}_m e^{-\breve{z}_n\sigma_j}}{\breve{z}_n+\breve{z}_m} \\ &- \sum_{m=1}^{\mathcal{N}} \sum_{k=1}^{\mathcal{L}} \sum_{l=1}^{\mathcal{L}} \rho_k D_{ik}^n D_{lk}^m \frac{2\pi\rho_l}{\breve{z}_m} \widehat{\mathcal{P}}_{jl}(\breve{z}_m) e^{-\breve{z}_n\lambda_{kj}} e^{-\breve{z}_m\sigma_{kj}} \\ &\times \frac{-\breve{z}_n-\breve{z}_m+\breve{z}_m e^{-\breve{z}_n\sigma_j}+\breve{z}_n e^{\breve{z}_m\sigma_j}}{\breve{z}_n+\breve{z}_m}. \end{aligned} \tag{343}$$

(c) *Simplification of two formulas*

Each term on the right-hand side of Eq. (341) includes coefficients D_{ij}^n with suffix j. Each term on the right- hand side of Eq. (343) includes coefficients D_{ij}^n with suffix i. The term

on the left-hand side of Eq. (343) is formed by a product composed of a factor related to suffix i and that related to suffix j. This implies that a coefficient D_{ij}^n can be divided into factors related to suffixes i and j. Thus, coefficient D_{ij}^n is given as

$$D_{ij}^n = -\breve{d}_i^n a_j^n exp(\breve{z}_n \sigma_j/2), \tag{344}$$

where a_j^n is an unknown coefficient.

Further, to simplify Eq. (341), a coefficient $\mathcal{P}_j^n$ is defined as

$$\mathcal{P}_j^n \equiv 12 \sum_{l=1}^{\mathcal{L}} \phi_l \frac{\breve{d}_l^n}{\sigma_l} \frac{\widehat{\mathcal{P}}_{lj}(\breve{z}_n)}{\sigma_l^2} \tag{345}$$

where ϕ_l is the volume fraction of species l given as

$$\phi_l \equiv \frac{\pi}{6} \rho_l \sigma_l^3. \tag{346}$$

The coefficient $\mathcal{P}_j^n$ defined by Eq. (345) must always be positive because $\breve{d}_j^n/\sigma_j$ should be positive for each value of j and each value of n. According to Eq. (333), the coefficient $\mathcal{P}_j^n$ should be small if the effective range characterized by $\breve{z}_n$ is short.

The use of Eqs. (344), (345), and (346) simplifies Eq. (341) as

$$-\mathcal{P}_j^n = \sum_{m=1}^{\mathcal{N}} x_j^n x^{nm} \frac{a_j^m}{\sigma_j} \tag{347}$$

where

$$x_j^n \equiv \frac{6}{\pi} \breve{z}_n \sigma_j e^{-\breve{z}_n \sigma_j/2} \tag{348}$$

$$\begin{aligned} x^{nm} \equiv & \sum_{l=1}^{\mathcal{L}} \frac{e^{\breve{z}_n \sigma_l/2} e^{-\breve{z}_m \sigma_l/2}}{\breve{z}_n \sigma_l (\breve{z}_n + \breve{z}_m) \sigma_l} \left[\breve{z}_m \sigma_l e^{-\breve{z}_n \sigma_l} \frac{\breve{d}_l^n}{\sigma_l} \left(\frac{\breve{d}_l^m}{\sigma_l} - \frac{1}{\breve{z}_m \sigma_l} \mathcal{P}_l^m \right) \right. \\ & \left. + \mathcal{P}_l^n \left(\frac{\breve{d}_l^m}{\sigma_l} Y_{ll}^{mn} + \mathcal{P}_l^m Z_{ll}^{mn} \right) \right] \phi_l \end{aligned} \tag{349}$$

$$Y_{jl}^{mn} \equiv \frac{1}{\breve{z}_n \sigma_l} \left[(\breve{z}_n + \breve{z}_m) \sigma_l - \breve{z}_m \sigma_l e^{-\breve{z}_n \sigma_j} \right] \tag{350}$$

$$Z_{jl}^{mn} \equiv \frac{1}{\breve{z}_m \sigma_j \breve{z}_n \sigma_l} \left[\breve{z}_n \sigma_l e^{\breve{z}_m \sigma_j} - (\breve{z}_n + \breve{z}_m) \sigma_l + \breve{z}_m \sigma_l e^{-\breve{z}_n \sigma_j} \right] \tag{351}$$

Further, the use of Eqs. (344), (345), and (346) simplifies Eq. (343) as

$$2\pi \frac{\breve{k}_0^n}{\breve{z}_n} \frac{\breve{d}_j^n}{\sigma_j} e^{-\breve{z}_n \sigma_j/2} = -\frac{a_j^n}{\sigma_j} - \frac{6}{\pi} \sum_{m=1}^{\mathcal{N}} \sum_{l=1}^{\mathcal{L}} \phi_l \frac{a_l^n}{\sigma_l} \frac{a_l^m}{\sigma_l} \frac{e^{-\breve{z}_m \sigma_j/2}}{(\breve{z}_n + \breve{z}_m) \sigma_l} \left[\frac{\breve{d}_j^m}{\sigma_j} Y_{jl}^{mn} + \mathcal{P}_j^m Z_{jl}^{mn} \right]. \tag{352}$$

3. Coefficients estimated for two terms' potential ($\mathcal{N} = 2$)

The potentials composed of the two terms are remarkable for describing the simplest fluid mixture, and are expressed by Eq. (307) for $\mathcal{N} = 2$. Further, the fluid mixture can involve two species of particles: one includes particles interacting with each other via a mutually attractive force contributing only within a short range, and the other includes particles interacting with each other via a mutually attractive force contributing over a long range.

For $\mathcal{N} = 2$, coefficients a_j/σ_j can be readily derived from Eq. (347) as

$$\frac{a_j^n}{\sigma_j} = -\frac{1}{x}\sum_{m=1}^{2} X_j^{nm}\mathcal{P}_j^m, \tag{353}$$

where

$$\begin{pmatrix} X_j^{11} & X_j^{12} \\ X_j^{21} & X_j^{22} \end{pmatrix} \equiv \begin{pmatrix} \frac{1}{x_j^1}x^{22} & -\frac{1}{x_j^2}x^{12} \\ -\frac{1}{x_j^1}x^{21} & \frac{1}{x_j^2}x^{11} \end{pmatrix}, \tag{354}$$

and

$$x \equiv x^{11}x^{22} - x^{12}x^{21}. \tag{355}$$

To derive an equation to determine unknown coefficients $\mathcal{P}_j^m$, Eq. (353) is substituted into Eq. (352), which results in

$$\begin{aligned} &2\pi e^{-\breve{z}_n\sigma_j/2}\frac{\breve{k}_0^n}{\breve{z}_n}\frac{\breve{d}_j^n}{\sigma_j}x^2 - x\sum_{r=1}^{2} X_j^{nr}\mathcal{P}_j^r \\ &+\frac{6}{\pi}\sum_{m=1}^{2}\sum_{r=1}^{2}\sum_{s=1}^{2}\sum_{l=1}^{\mathcal{L}}\left[\phi_l X_l^{nr}X_l^{ms}\mathcal{P}_l^r\mathcal{P}_l^s\frac{e^{-\breve{z}_m\sigma_j/2}}{(\breve{z}_n+\breve{z}_m)\sigma_l}\left(\frac{\breve{d}_j^m}{\sigma_j}Y_{jl}^{mn} + \mathcal{P}_j^m Z_{jl}^{mn}\right)\right] = 0, \end{aligned} \tag{356}$$

where X_j^{nm} and x include $\mathcal{P}_j^m$ because of Eq. (349).

4. Value of $\mathcal{P}_{ij}(\sigma_{ij})$ estimated for $\mathcal{N} = 2$

The behavior of the pair connectedness $\mathcal{P}_{ij}(r)$ can be readily estimated for $r = \sigma_{ij}$ with the particular distance at which hard spheres of i and j particles contact each other. The second term on the right-hand side of Eq. (325) is a continuous function of r at $r = \sigma_{ij}$. Thus, the pair connectedness $\mathcal{P}_{ij}(r)$ given by Eq. (325) must satisfy

$$\begin{aligned}\lim_{\epsilon\to 0} 2\pi\sigma_{ij}\Big[\mathcal{P}_{ij}(\sigma_{ij}+\epsilon) - \mathcal{P}_{ij}(\sigma_{ij}-\epsilon)\Big] \\ = -\lim_{\epsilon\to 0}\Big\{\Big[\frac{\mathrm{d}}{\mathrm{d}r}Q_{ij}(r)\Big]_{r=\sigma_{ij}+\epsilon} - \Big[\frac{\mathrm{d}}{\mathrm{d}r}Q_{ij}(r)\Big]_{r=\sigma_{ij}-\epsilon}\Big\}.\end{aligned} \tag{357}$$

If Eqs. (330), (331), (344), and (345) are considered with $\mathcal{P}_{ij}(r) = 0 \quad (r < \sigma_{ij})$ after substituting Eq. (328) into Eq. (357), the pair connectedness $\mathcal{P}_{ij}(r)$ at $r = \sigma_{ij}$ can be found as

$$\mathcal{P}_{ij}(\sigma_{ij}) = -\frac{1}{2\pi}\frac{\sigma_j}{\sigma_{ij}}\sum_{n=1}^{\mathcal{N}}\left(\breve{z}_n\sigma_i\frac{\breve{d}_i^n}{\sigma_i} + \mathcal{P}_i^n\right)e^{-\breve{z}_n\sigma_i/2}\frac{a_j^n}{\sigma_j}. \tag{358}$$

For $\mathcal{N} = 2$, the use of Eq. (353) allows Eq. (358) to be expressed as

$$\mathcal{P}_{ij}(\sigma_{ij}) = \frac{1}{2\pi}\frac{\sigma_j}{\sigma_{ij}}\frac{1}{x}\sum_{m=1}^{2}\sum_{n=1}^{2}\left(\breve{z}_n\sigma_i\frac{\breve{d}_i^n}{\sigma_i} - \mathcal{P}_i^n\right)e^{-\breve{z}_n\sigma_i/2}X_j^{nm}\mathcal{P}_j^m. \tag{359}$$

The probability that a particle of i species exists in the immediate vicinity of a particle of j species can be known because the magnitude of $\mathcal{P}_{ij}(\sigma_{ij})$ is proportional to the probability.

F. Mean size S of physical clusters

1. *Estimate of of S for an $\mathcal{L}$-component fluid mixture*

The mean physical cluster size S can be related to the pair connectedness $\mathcal{P}_{ij}$ because of Eq. (281). The relation between the pair connectedness $\mathcal{P}_{ij}$ and Baxter's Q function can be expressed by Eq. (324). A specific relation is derived from the first equation in Eq. (324) as

$$\begin{aligned}\lim_{k\to 0}\widetilde{\mathcal{P}}_{ij}(k) =&(\rho_i\rho_j)^{1/2}\int \mathcal{P}_{ij}(r)\mathrm{d}\mathbf{r}\\ =&\lim_{k\to 0}\sum_{h=1}^{\mathcal{L}}\widetilde{Q}_{hi}^{-1}(-k)\widetilde{Q}_{hj}^{-1}(k)-\delta_{ij}.\end{aligned}\tag{360}$$

Ultimately, substituting Eq. (360) into Eq. (281) allows the mean physical cluster size S to results in

$$S=\sum_{i=1}^{\mathcal{L}}\left\{\sum_{j=1}^{\mathcal{L}}\left[\sum_{k=1}^{\mathcal{L}}\frac{\phi_k}{\phi_i}\left(\frac{\sigma_i}{\sigma_k}\right)^3\right]^{-1/2}\widetilde{Q}_{ij}^{-1}(0)\right\}^2.\tag{361}$$

Equation (361) denotes that the mean physical cluster size diverges to infinity if $\widetilde{Q}_{ij}^{-1}(0)$ reaches infinity. $\widetilde{Q}_{ij}^{-1}(0)=\infty$ indicates the occurrence of the percolation of physical clusters.

The comparison between Eqs. (327) and (336) allows the relation between $\widetilde{Q}_{ij}(0)$ and $\widehat{Q}_{ij}(0)$ to be found. Thus, $\widetilde{Q}_{ij}(0)$ is given as

$$\widetilde{Q}_{ij}(0)=\delta_{ij}-\frac{6}{\pi}\left(\frac{\phi_i}{\sigma_i^3}\frac{\phi_j}{\sigma_j^3}\right)^{1/2}\widehat{Q}_{ij}(0).\tag{362}$$

If Eq. (336) for $s=0$ is used with Eqs. (344)–(346), an expression for $\widehat{Q}_{ij}(0)$ can be derived as

$$\frac{6}{\pi}\left(\frac{\phi_i}{\sigma_i^3}\frac{\phi_j}{\sigma_j^3}\right)^{1/2}\widehat{Q}_{ij}(0)=\sum_{m=1}^{\mathcal{N}}\left(\frac{6}{\pi}\phi_i\sigma_i\right)^{1/2}Q_i^m\left(\frac{6}{\pi}\phi_j\frac{1}{\sigma_j}\right)^{1/2}\frac{a_j^m}{\sigma_j},\tag{363}$$

where

$$\begin{aligned}Q_i^m\equiv&\frac{e^{-\breve{z}_m\sigma_i/2}}{\breve{z}_m\sigma_i}\left\{-\frac{e^{z_m\sigma_i}-1-\breve{z}_m\sigma_i}{\breve{z}_m\sigma_i}\mathcal{P}_i^m-\frac{\breve{d}_i^m}{\sigma_i}(\breve{z}_m\sigma_i+1)\right\}\\ =&\frac{e^{\breve{z}_m\sigma_i/2}}{(\breve{z}_m\sigma_i)^2}\overline{Q}_i^m,\end{aligned}\tag{364}$$

with

$$\overline{Q}_i^m\equiv-\left[1-(1+\breve{z}_m\sigma_i)e^{-\breve{z}_m\sigma_i}\right]\mathcal{P}_i^m-\frac{\breve{d}_i^m}{\sigma_i}\breve{z}_m\sigma_i(\breve{z}_m\sigma_i+1)e^{-\breve{z}_m\sigma_i}.\tag{365}$$

If $\mathcal{N}$ is restricted as $\mathcal{N}=2$, then $\widetilde{Q}_{ij}(0)$ can be given as

$$\widetilde{Q}_{ij}(0)=\delta_{ij}+\frac{1}{x}\sum_{m=1}^{2}\sum_{n=1}^{2}\left(\frac{6}{\pi}\phi_i\sigma_i\right)^{1/2}Q_i^n\left(\frac{6}{\pi}\phi_j\frac{1}{\sigma_j}\right)^{1/2}X_j^{nm}\mathcal{P}_j^m. \tag{366}$$

2. Percolation requirements

(a) *Percolation requirement for two-component mixture ($\mathcal{L}=2$, $\mathcal{N}=\mathcal{N}$)*

The inverse $\widetilde{Q}_{ij}^{-1}(0)$ can be readily estimated for a two-component mixture comprising particles interacting with each other via mutually attractive forces described by $\mathcal{N}$ terms' potentials. Thus, the use of Eq. (362) results in $\widetilde{Q}_{ij}^{-1}(0)$ expressed as

$$\begin{pmatrix}\widetilde{Q}_{11}^{-1}(0) & \widetilde{Q}_{12}^{-1}(0)\\ \widetilde{Q}_{21}^{-1}(0) & \widetilde{Q}_{22}^{-1}(0)\end{pmatrix}=\frac{1}{\det|\widetilde{Q}_{ij}(0)|}\begin{pmatrix}1-\frac{6}{\pi}\frac{\phi_2}{\sigma_2^3}\widehat{Q}_{22}(0) & \frac{6}{\pi}\left[\frac{\phi_1}{\sigma_1^3}\frac{\phi_2}{\sigma_2^3}\right]^{1/2}\widehat{Q}_{12}(0)\\ \frac{6}{\pi}\left[\frac{\phi_2}{\sigma_2^3}\frac{\phi_1}{\sigma_1^3}\right]^{1/2}\widehat{Q}_{21}(0) & 1-\frac{6}{\pi}\frac{\phi_1}{\sigma_1^3}\widehat{Q}_{11}(0)\end{pmatrix}, \tag{367}$$

where

$$\begin{aligned}\det|\widetilde{Q}_{ij}(0)|\equiv&1-\frac{6}{\pi}\frac{\phi_1}{\sigma_1^3}\widehat{Q}_{11}(0)-\frac{6}{\pi}\frac{\phi_2}{\sigma_2^3}\widehat{Q}_{22}(0)+\left(\frac{6}{\pi}\right)^2\frac{\phi_1}{\sigma_1^3}\frac{\phi_2}{\sigma_2^3}\widehat{Q}_{11}(0)\widehat{Q}_{22}(0)\\&-\left(\frac{6}{\pi}\right)^2\frac{\phi_1}{\sigma_1^3}\frac{\phi_2}{\sigma_2^3}\widehat{Q}_{12}(0)\widehat{Q}_{21}(0)\\=&1-\frac{6}{\pi}\sum_{m=1}^{2}\sum_{l=1}^{2}\phi_l Q_l^m\frac{a_l^m}{\sigma_l}+\left(\frac{6}{\pi}\right)^2\phi_1\phi_2\Big(Q_1^1Q_2^2-Q_1^2Q_2^1\Big)\left(\frac{a_1^1}{\sigma_1}\frac{a_2^2}{\sigma_2}-\frac{a_2^1}{\sigma_2}\frac{a_1^2}{\sigma_1}\right).\end{aligned} \tag{368}$$

The final line in the above equation is obtained using the relation given by Eq. (363).

If $\det|\widetilde{Q}_{ij}(0)|$ reaches zero under a certain condition, then $\widetilde{Q}_{ij}^{-1}(0)$ diverges to infinity. This implies that the mean physical cluster size S given by Eq. (361) diverges to infinity. Therefore, the percolation threshold concerning the percolation of the physical clusters can be estimated as particular states satisfying

$$\det|\widetilde{Q}_{ij}(0)|=0. \tag{369}$$

(b) *Percolation requirement for two-component mixture ($\mathcal{L}=2$, $\mathcal{N}=2$)*

The percolation threshold can be readily estimated for a two-component fluid mixture ($\mathcal{L}=2$) composed of particles interacting with each other via mutually attractive forces

caused by two terms' potentials ($\mathcal{N}=2$). After substituting Eqs. (353) into Eq. (368), Eq. (369) result in

$$x+\frac{6}{\pi}\sum_{l=1}^{2}\phi_l\left[Q_l^1\left(\frac{x^{22}}{x_l^1}\mathcal{P}_l^1-\frac{x^{12}}{x_l^2}\mathcal{P}_l^2\right)+Q_l^2\left(-\frac{x^{21}}{x_l^1}\mathcal{P}_l^1+\frac{x^{11}}{x_l^2}\mathcal{P}_l^2\right)\right]$$
$$+\left(\frac{6}{\pi}\right)^2\phi_1\phi_2\big(Q_1^1Q_2^2-Q_1^2Q_2^1\big)\left(\frac{1}{x_1^1x_2^2}\mathcal{P}_1^1\mathcal{P}_2^2-\frac{1}{x_2^1x_1^2}\mathcal{P}_1^2\mathcal{P}_2^1\right)=0. \tag{370}$$

To derive Eq. (370), Eq. (354) must be considered. Thus, a particular state satisfying Eq. (370) allows the physical clusters of macroscopic sizes induced at the percolation threshold to be found within the two-component fluid mixture.

Furhter, the two terms' potential ($\mathcal{N}=2$) enables a mutually attractive force between particles of species 1 to be distinguished from a mutually attractive force between a particle of species 1 and a particle of species 2, and it allows the mutually attractive force between particles of species 1 to be distinguished from a mutually attractive force between particles of species 2. Hence, the estimations of the percolation threshold described by Eq. (370) can contribute to identifying the variations of percolation behaviors caused by the distinctions among these attractive forces.

3. Estimate of S for two-component fluid mixture

The mean size of physical clusters S can be estimated for a two-component mixture system ($\mathcal{L}=2$) composed of particles interacting with each other via mutually attractive forces caused by two-term potentials ($\mathcal{N}=2$). For a two-component mixture ($\mathcal{L}=2$), the use of Eqs. (353), (363), and (367) allows Eq. (361) to result in

$$S=\left[1+\frac{\phi_2}{\phi_1}\left(\frac{\sigma_1}{\sigma_2}\right)^3\right]^{-1}\Big(\det|\widetilde{Q}_{ij}(0)|\Big)^{-1}$$
$$\times\Bigg\{\Bigg[1-\frac{6}{\pi}\frac{1}{x}\sum_{m=1}^{2}\sum_{r=1}^{2}\Bigg(\left(\phi_1\phi_2\frac{\breve{z}_m\sigma_1}{\breve{z}_m\sigma_2}\right)^{1/2}e^{\breve{z}_m\sigma_1/2}Q_1^me^{-\breve{z}_m\lambda_{12}}-\phi_2e^{\breve{z}_m\sigma_2/2}Q_2^m\Bigg)$$
$$\times e^{-\breve{z}_m\sigma_2/2}X_2^{mr}\mathcal{P}_2^r\Bigg]^2+\left(\frac{\sigma_1}{\sigma_2}\right)^2\Bigg[\left(\frac{\phi_2}{\phi_1}\frac{\sigma_1}{\sigma_2}\right)^{1/2}+\frac{6}{\pi}\frac{1}{x}\sum_{m=1}^{2}\sum_{r=1}^{2}\Bigg(\left(\phi_1\phi_2\frac{\breve{z}_m\sigma_1}{\breve{z}_m\sigma_2}\right)^{1/2}$$
$$\times e^{\breve{z}_m\sigma_1/2}Q_1^m-\phi_2e^{\breve{z}_m\sigma_2/2}Q_2^me^{-\breve{z}_m\lambda_{21}}\Bigg)e^{-\breve{z}_m\sigma_1/2}X_1^{mr}\mathcal{P}_1^r\Bigg]^2\Bigg\}. \tag{371}$$

G. Pair correlation function

1. *Pair correlation function for $\mathcal{L}$-component fluid mixture*

For the potential given as Eq. (307), the Ornstein–Zernike equation can be solved analytically.[82,84] If the solutions[82,84] given for the potential are modified, the correlation function $g_{ij}(r)$ can be expressed as

$$\begin{aligned} g_{ij}(\sigma_{ij}) =& \Delta^{-1} + \frac{3}{2}\Delta^{-2}\sum_{l=1}^{\mathcal{L}}\phi_l\frac{\sigma_i\sigma_j}{\sigma_l\sigma_{ij}} + \frac{1}{2\pi}\sum_{n=1}^{\mathcal{N}}\Bigg\{-\frac{12}{z_n\sigma_{ij}}\left[3\Delta^{-1}\sum_{l=1}^{\mathcal{L}}\phi_l\frac{1}{z_n\sigma_l} - \frac{1}{2} + \frac{1}{z_n\sigma_i}\right] \\ &\times\Delta^{-1}\sum_{l=1}^{\mathcal{L}}\phi_l\frac{z_n\sigma_i}{z_n\sigma_l}\left[\Psi_1(z_n\sigma_l)z_n\sigma_l e^{z_n\sigma_l}B_l^{(n)} + \frac{d_l^{(n)}}{\sigma_l}\left(\frac{1}{2}+\frac{1}{z_n\sigma_l}\right)\right]e^{-z_n\lambda_{lj}} \\ &+\frac{3}{z_n\sigma_{ij}}\Delta^{-1}\sum_{l=1}^{\mathcal{L}}\phi_l\frac{z_n\sigma_i}{z_n\sigma_l}\left(\frac{d_l^{(n)}}{\sigma_l} + \frac{\Phi_0(z_n\sigma_l)}{z_n\sigma_l}z_n\sigma_l e^{z_n\sigma_l}B_l^{(n)}\right)e^{-z_n\lambda_{lj}} \\ &-\left(\frac{d_i^{(n)}}{\sigma_i} - \frac{e^{-z_n\sigma_i}}{(z_n\sigma_i)^2}z_n\sigma_i e^{z_n\sigma_i}B_i^{(n)}\right)\frac{z_n\sigma_i}{z_n\sigma_{ij}}e^{-z_n\lambda_{ij}}\Bigg\}z_n\sigma_j e^{-z_n\sigma_j/2}\frac{a_j^{(n)}}{\sigma_j}, \end{aligned} \tag{372}$$

where

$$\begin{aligned} \Delta \equiv& 1 - \sum_{l=1}^{\mathcal{L}}\phi_l, \\ \Psi_1(z_n\sigma_l) \equiv& (z_n\sigma_l)^{-3}[1 - z_n\sigma_l/2 - (1+z_n\sigma_l/2)e^{-z_n\sigma_l}], \\ \text{and}\qquad \Phi_0(z_n\sigma_l) \equiv& (z_n\sigma_l)^{-1}(1-e^{-z_n\sigma_l}). \end{aligned} \tag{373}$$

A coefficient expressed as $B_i^{(n)}$ in Eq. (372) is defined as

$$z_n\sigma_i e^{z_n\sigma_i}B_i^{(n)} \equiv 12\sum_{l=1}^{\mathcal{L}}\phi_l\frac{d_l^{(n)}}{\sigma_l}\frac{z_n\sigma_i}{(z_n\sigma_l)^2}e^{2z_n\lambda_{il}}e^{z_n\sigma_l}\left[\int_0^\infty e^{-\tau}g_{il}(\tau/s)\tau d\tau\right]_{s=z_n}. \tag{374}$$

Then, the values of $B_i^{(n)}$ should satisfy

$$\begin{aligned} 0 =& 2\pi z_n\sigma_i\frac{k_0^{(n)}}{z_n}\frac{d_i^{(n)}}{\sigma_i}\frac{d_j^{(n)}}{\sigma_j}e^{-z_n\sigma_j} + \sum_{l=1}^{\mathcal{L}}\frac{z_n\sigma_i}{z_n\sigma_l}\frac{d_i^{(n)}/\sigma_i}{d_l^{(n)}/\sigma_l}\left(\frac{d_l^{(n)}}{\sigma_l}z_n\sigma_l e^{-z_n\sigma_l}\frac{a_l^{(n)}}{\sigma_l}\right)e^{-z_n\lambda_{jl}}\left[\frac{z_n\sigma_l}{z_n\sigma_j}\delta_{lj}\right. \\ &\left.+\frac{3}{\Delta}\frac{z_n\sigma_j}{z_n\sigma_l}\phi_l\Phi_0(z_n\sigma_j) - \frac{12}{\Delta}\left(\frac{z_n\sigma_j}{z_n\sigma_l}\right)^2\phi_l\Psi_1(z_n\sigma_j)\left(1+\frac{3}{\Delta}\sum_{h=1}^{\mathcal{L}}\phi_h\frac{z_n\sigma_l}{z_n\sigma_h}+\frac{1}{2}z_n\sigma_l\right)\right] \\ &-\frac{6}{\pi}\sum_{m=1}^{N}\sum_{k=1}^{\mathcal{L}}\sum_{l=1}^{\mathcal{L}}\frac{z_n\sigma_i}{z_n\sigma_k}\frac{d_i^{(n)}/\sigma_i}{d_k^{(n)}/\sigma_k}\phi_k\left(\frac{d_k^{(n)}}{\sigma_k}z_n\sigma_k e^{-z_n\sigma_k}\frac{a_k^{(n)}}{\sigma_k}\right) \\ &\times\left(\frac{d_k^{(m)}}{\sigma_k}z_m\sigma_k e^{-z_m\sigma_k}\frac{a_k^{(m)}}{\sigma_k}\right)\mathcal{M}_{jkl}^{mn}, \end{aligned} \tag{375}$$

where the coefficient $\mathcal{M}_{jkl}^{mn}$ in Eq. (375) are defined as

$$\begin{aligned}
\mathcal{M}_{jkl}^{mn} \equiv & \frac{1}{(z_n+z_m)\sigma_j}\frac{1}{z_m\sigma_k}\frac{1}{z_m\sigma_l}e^{-z_n\lambda_{jk}}e^{-z_m\lambda_{lk}}\frac{z_n\sigma_l}{z_n\sigma_k}\Bigg\{\left[\Phi_0(z_n\sigma_j)\delta_{lj}-\frac{12}{\Delta}\phi_l\left(\frac{z_n\sigma_j}{z_n\sigma_l}\right)^3\Psi_1(z_n\sigma_j)\right] \\
& \times\Bigg[\frac{d_l^{(m)}/\sigma_l}{d_k^{(m)}/\sigma_k}\frac{z_m\sigma_l e^{z_m\sigma_l}B_l^{(m)}}{d_l^{(m)}/\sigma_l}-z_m\sigma_l\frac{12}{\Delta}\left(1+\frac{1}{2}z_m\sigma_l+\frac{3}{\Delta}\sum_{h=1}^{\mathcal{L}}\phi_h\frac{z_m\sigma_l}{z_m\sigma_h}\right) \\
& \times\sum_{t=1}^{\mathcal{L}}\phi_t\frac{1+z_m\sigma_t/2}{(z_m\sigma_t)^2}\frac{d_t^{(m)}/\sigma_t}{d_k^{(m)}/\sigma_k}e^{-z_m\lambda_{tl}}+\frac{3}{\Delta}\sum_{h=1}^{\mathcal{L}}\phi_h z_m\sigma_l\frac{z_m\sigma_l}{z_m\sigma_h}\frac{d_h^{(m)}/\sigma_h}{d_k^{(m)}/\sigma_k}e^{-z_m\lambda_{hl}} \\
& -\left(1+\frac{1}{2}z_m\sigma_l+\frac{3}{\Delta}\sum_{h=1}^{\mathcal{L}}\phi_h\frac{z_m\sigma_l}{z_m\sigma_h}\right)\frac{12}{\Delta}\sum_{h=1}^{\mathcal{L}}\phi_h\Psi_1(z_m\sigma_h)\frac{d_h^{(m)}/\sigma_h}{d_k^{(m)}/\sigma_k}\frac{z_m\sigma_l}{z_m\sigma_h} \\
& \times z_m\sigma_h\frac{e^{z_m\sigma_h}B_h^{(m)}}{d_h^{(m)}/\sigma_h}e^{-z_m\lambda_{hl}}+\frac{3}{\Delta}\sum_{h=1}^{\mathcal{L}}\phi_h\frac{z_m\sigma_l}{z_m\sigma_h}\Phi_0(z_m\sigma_h)\frac{d_h^{(m)}/\sigma_h}{d_k^{(m)}/\sigma_k}\frac{z_m\sigma_l}{z_m\sigma_h}z_m\sigma_h\frac{e^{z_m\sigma_h}B_h^{(m)}}{d_h^{(m)}/\sigma_h}e^{-z_m\lambda_{hl}} \\
& -(z_m\sigma_l)^2\sum_{h=1}^{\mathcal{L}}\left(\delta_{lh}-\frac{12}{\Delta}\phi_h\frac{1+z_m\sigma_h/2}{(z_m\sigma_h)^2}\right)\frac{d_h^{(m)}/\sigma_h}{d_k^{(m)}/\sigma_k}e^{-z_m\lambda_{hl}}-z_m\sigma_l\sum_{h=1}^{\mathcal{L}}(\Phi_0(z_m\sigma_l)\delta_{lh} \\
& -\frac{12}{\Delta}\phi_h\Psi_1(z_m\sigma_h))\frac{d_h^{(m)}/\sigma_h}{d_k^{(m)}/\sigma_k}\frac{z_m\sigma_l}{z_m\sigma_h}z_m\sigma_h\frac{e^{z_m\sigma_h}B_h^{(m)}}{d_h^{(m)}/\sigma_h}e^{-z_m\lambda_{hl}}\Bigg] \\
& -\Bigg[z_m\sigma_l\sum_{h=1}^{\mathcal{L}}\left(\delta_{lh}-\frac{12}{\Delta}\phi_h\frac{1+z_m\sigma_h/2}{(z_m\sigma_h)^2}\right)\frac{d_h^{(m)}/\sigma_h}{d_k^{(m)}/\sigma_k}e^{-z_m\lambda_{hl}}+\sum_{h=1}^{\mathcal{L}}(\Phi_0(z_m\sigma_l)\delta_{lh} \\
& -\frac{12}{\Delta}\phi_h\Psi_1(z_m\sigma_h))\frac{d_h^{(m)}/\sigma_h}{d_k^{(m)}/\sigma_k}\frac{z_m\sigma_l}{z_m\sigma_h}z_m\sigma_h\frac{e^{z_m\sigma_h}B_h^{(m)}}{d_h^{(m)}/\sigma_h}e^{-z_m\lambda_{hl}}\Bigg] \\
& \times\Bigg[\delta_{lj}+\frac{3}{\Delta}\left(\frac{z_n\sigma_j}{z_n\sigma_l}\right)^2\phi_l\Phi_0(z_n\sigma_j)-\frac{12}{\Delta}\left(\frac{z_n\sigma_j}{z_n\sigma_l}\right)^3\phi_l\Psi_1(z_n\sigma_j) \\
& \times\left(1+\frac{3}{\Delta}\sum_{h=1}^{\mathcal{L}}\phi_h\frac{z_n\sigma_l}{z_n\sigma_h}+\frac{1}{2}z_n\sigma_l\right)\Bigg]\Bigg\}. \qquad (376)
\end{aligned}$$

2. Estimation for two-component fluid mixture

For $\mathcal{N}=2$, the factor $z_n\sigma_j e^{-z_n\sigma_j/2}a_j^{(n)}/\sigma_j$ in Eq. (375) can be given as

$$z_n\sigma_j e^{-z_n\sigma_j/2}\frac{a_j^{(n)}}{\sigma_j}=\frac{1}{Y}\sum_{m=1}^{2}(-1)^{n+m}Y_j^{3-m,3-n}\mathcal{V}_j^m, \qquad (377)$$

where

$$Y\equiv Y_j^{1,1}Y_j^{2,2}-Y_j^{1,2}Y_j^{2,1}. \qquad (378)$$

$$
\begin{aligned}
Y_j^{n,m} \equiv & \frac{6}{\pi}\frac{z_n\sigma_j}{z_m\sigma_j}\sum_{l=1}^{2}\phi_l\frac{z_m\sigma_j}{(z_n+z_m)\sigma_l}e^{-(z_n+z_m)\lambda_{lj}}\left[\sum_{k=1}^{2}e^{-z_n\lambda_{kl}}\left(\delta_{lk}-\frac{12}{\Delta}\phi_k\frac{1+z_n\sigma_k/2}{(z_n\sigma_k)^2}\right)\frac{d_k^{(n)}}{\sigma_k}\right. \\
& \left.+\sum_{k=1}^{2}e^{-z_n\lambda_{kl}}\left(\Phi_0(z_n\sigma_l)\delta_{lk}-\frac{12}{\Delta}\phi_k\Psi_1(z_n\sigma_k)\right)e^{z_n\sigma_k}B_k^{(n)}\right]\left[\frac{\mathcal{V}_l^m}{(z_m\sigma_l)^2}\right. \\
& +\sum_{h=1}^{2}e^{-z_m\lambda_{hl}}\left(\delta_{lh}-\frac{12}{\Delta}\phi_h\frac{1+z_m\sigma_h/2}{(z_m\sigma_h)^2}\right)\frac{d_h^{(m)}}{\sigma_h} \\
& \left.+\sum_{h=1}^{2}e^{-z_m\lambda_{hl}}\left(\Phi_0(z_m\sigma_l)\delta_{lh}-\frac{12}{\Delta}\phi_h\Psi_1(z_m\sigma_h)\right)e^{z_m\sigma_h}B_h^{(m)}\right] \\
& -\frac{6}{\pi}\frac{z_n\sigma_j}{z_m\sigma_j}\sum_{l=1}^{2}\phi_l\frac{z_n\sigma_j}{(z_n+z_m)\sigma_l}e^{-(z_n+z_m)\lambda_{lj}}\left[\sum_{k=1}^{2}e^{-z_m\lambda_{kl}}\left(\delta_{lk}-\frac{12}{\Delta}\phi_k\frac{1+z_m\sigma_k/2}{(z_m\sigma_k)^2}\right)\frac{d_k^{(m)}}{\sigma_k}\right. \\
& \left.+\sum_{k=1}^{2}e^{-z_m\lambda_{kl}}\left(\Phi_0(z_m\sigma_l)\delta_{lk}-\frac{12}{\Delta}\phi_k\Psi_1(z_m\sigma_k)\right)e^{z_m\sigma_k}B_k^{(m)}\right]\frac{\mathcal{V}_l^n}{(z_n\sigma_l)^2}. \qquad (379)
\end{aligned}
$$

$$
\begin{aligned}
\mathcal{V}_j^n \equiv & \frac{3}{\Delta}\sum_{l=1}^{2}\left[4\left(1+\frac{3}{\Delta}\sum_{k=1}^{2}\phi_k\frac{z_n\sigma_j}{z_n\sigma_k}+\frac{1}{2}z_n\sigma_j\right)\frac{1+z_n\sigma_l/2}{z_n\sigma_l}-z_n\sigma_j\right]\phi_l\frac{z_n\sigma_j}{z_n\sigma_l}\frac{d_l^{(n)}}{\sigma_l}e^{-z_n\lambda_{lj}} \\
& -\frac{3}{\Delta}\sum_{l=1}^{2}\left[\left(\frac{3}{\Delta}\frac{z_n\sigma_j}{z_n\sigma_l}e^{-z_n\lambda_{lj}}\right)^{-1}\delta_{lj}-4\left(1+\frac{3}{\Delta}\sum_{k=1}^{2}\phi_k\frac{z_n\sigma_j}{z_n\sigma_k}+\frac{1}{2}z_n\sigma_j\right)\phi_l\Psi_1(z_n\sigma_l)\right. \\
& \left.+\phi_l\frac{z_n\sigma_j}{z_n\sigma_l}\Phi_0(z_n\sigma_l)\right]\frac{z_n\sigma_j}{z_n\sigma_l}e^{-z_n\lambda_{lj}}z_n\sigma_l e^{z_n\sigma_l}B_l^{(n)}. \qquad (380)
\end{aligned}
$$

H. Two-component specific fluid mixture system

1. Formulae for evaluating correlation functions

(a) *Specific fluid mixture*

All coefficients expressed as $\mathcal{P}_j^n$ in Eq. (356) must be assessed to evaluate the percolation threshold for a fluid mixture composed of particles interacting with each other through a two-term potential ($\mathcal{N} = 2$). The evaluation of the coefficients can be simplified for a two-component specific fluid mixture. This fluid mixture is specified as

$$\sigma_1 = \sigma_2 = \sigma, \tag{381}$$

$$z_1 = z, \quad 0 < z\sigma < z_2\sigma, \quad 1 \ll z_2\sigma, \tag{382}$$

$$\frac{d_1^{(1)}}{\sigma} = \frac{d}{\sigma}, \qquad 0 \le \frac{d_2^{(1)}}{\sigma}\left[\frac{d}{\sigma}\right]^{-1} \ll 1, \tag{383}$$

$$\frac{d_1^{(2)}}{\sigma} = \frac{d_2^{(2)}}{\sigma} = \frac{\delta}{\sigma}, \qquad 0 \le \frac{\delta}{\sigma} \ll 1, \tag{384}$$

$$k_0^{(1)} = k, \quad \text{and} \quad 0 \le k_0^{(2)} \ll 1. \tag{385}$$

Then, Eqs. (314)–(317) result in

$$\breve{z}_1\sigma = \frac{3}{2}z_1\sigma + f_\nu, \tag{386}$$

$$\breve{z}_2\sigma = z_2\sigma + \frac{1}{2}z_1\sigma + f_\nu, \tag{387}$$

$$\frac{\breve{z}_1}{z_1}\frac{\breve{k}_0^1}{\breve{z}_1}\frac{\breve{d}_i^1}{\sigma}\frac{\breve{d}_j^1}{\sigma} = \frac{4}{3\sqrt{\pi}}\exp(f_\nu)\sqrt{z_1\sigma}\left(\frac{k_0^{(1)}}{z_1}\frac{d_i^{(1)}}{\sigma}\frac{d_j^{(1)}}{\sigma}\right)^{3/2}. \tag{388}$$

$$\frac{\breve{z}_2}{z_2}\frac{\breve{k}_0^2}{\breve{z}_2}\frac{\breve{d}_i^2}{\sigma}\frac{\breve{d}_j^2}{\sigma} = \frac{2}{\sqrt{\pi}}\exp(f_\nu)\sqrt{z_1\sigma}\left(\frac{k_0^{(1)}}{z_1}\frac{d_i^{(1)}}{\sigma}\frac{d_j^{(1)}}{\sigma}\right)^{1/2}\frac{k_0^{(2)}}{z_2}\frac{d_i^{(2)}}{\sigma}\frac{d_j^{(2)}}{\sigma}. \tag{389}$$

Thus, Eqs. (388) and (389) lead to the simplest assumption made as

$$\frac{\breve{d}_i^1}{\sigma} = \left(\frac{d_i^{(1)}}{\sigma}\right)^{3/2}. \tag{390}$$

and

$$\frac{\breve{d}_i^2}{\sigma} = \left(\frac{d_i^{(1)}}{\sigma}\right)^{1/2} \frac{d_i^{(2)}}{\sigma}. \tag{391}$$

Therefore, according to Eqs. (386)–(389) and Eqs. (390)–(391), Eqs. (381)–(385) require that the parameters for estimating the pair connectedness be expressed as

$$\breve{z}_1 \equiv \breve{z}, \quad 0 < \breve{z}\sigma < \breve{z}_2\sigma, \quad \breve{z}\sigma/\breve{z}_2\sigma \ll 1, \tag{392}$$

$$\frac{\breve{d}_1^1}{\sigma_1} = \frac{\breve{d}}{\sigma}, \quad 0 \leq \frac{\breve{d}_2^1}{\sigma_2} \ll 1, \tag{393}$$

$$\frac{\breve{d}_1^2}{\sigma_1} = \frac{\breve{d}_2^2}{\sigma_2} = \frac{\breve{\delta}}{\sigma}, \quad 0 \leq \frac{\breve{\delta}}{\sigma} \ll 1, \tag{394}$$

$$\breve{k}_0^1 = \breve{k}, \text{ and } \quad 0 \leq \breve{k}_0^2 \ll 1. \tag{395}$$

For $\sigma_1 = \sigma_2 = \sigma$, Eq. (352) can be rewritten as

$$\begin{aligned} 2\pi \frac{\breve{k}_0^n}{\breve{z}_n} \frac{\breve{d}_j^n}{\sigma} e^{-\breve{z}_n\sigma/2} =& -\frac{a_j^n}{\sigma} - \frac{6}{\pi} \sum_{m=1}^{2} \left(\phi_1 \frac{a_1^n}{\sigma}\frac{a_1^m}{\sigma} + \phi_2 \frac{a_2^n}{\sigma}\frac{a_2^m}{\sigma}\right) \\ & \times \frac{e^{\breve{z}_m\sigma/2}}{\breve{z}_m\sigma(\breve{z}_n + \breve{z}_m)\sigma} \left[\frac{\breve{d}_j^m}{\sigma}(\breve{z}_m\sigma)^2 e^{-\breve{z}_m\sigma/2}\overline{Y}^{mn} + \mathcal{P}_j^m \overline{Z}^{mn}\right], \end{aligned} \tag{396}$$

where $\overline{Y}^{mn}$ and $\overline{Z}^{mn}$ are defined as

$$Y_{jl}^{mn}\big|_{\sigma_j=\sigma_l=\sigma} \equiv \breve{z}_m\sigma\overline{Y}^{mn} \tag{397}$$

$$Z_{jl}^{mn}\big|_{\sigma_j=\sigma_l=\sigma} \equiv \frac{e^{\breve{z}_m\sigma}}{\breve{z}_m\sigma}\overline{Z}^{mn}. \tag{398}$$

The above two coefficients behave as $\lim_{\breve{z}_m\sigma\to\infty} \overline{Y}^{mn} < \infty$ and $\lim_{\breve{z}_m\sigma\to\infty} \overline{Z}^{mn} < \infty$.

For an extremely large $\breve{z}_2\sigma$ satisfying $0 < \breve{z}/\breve{z}_2 \ll 1$, coefficients a_j^n given by Eq. (353) are required to satisfy $a_j^1 \neq 0$ and $a_j^2 \approx 0$ (which are known from Eqs. (427) and (428)). Hence, this allows Eq. (396) to be simplified as

$$\begin{aligned} 2\pi \frac{\breve{k}_0^1}{\breve{z}} \frac{\breve{d}_j^1}{\sigma} e^{-\breve{z}\sigma/2} \approx& -\frac{a_j^1}{\sigma} - \frac{3}{\pi} \left(\phi_1 \frac{a_1^1}{\sigma}\frac{a_1^1}{\sigma} + \phi_2 \frac{a_2^1}{\sigma}\frac{a_2^1}{\sigma}\right) \\ & \times \frac{e^{\breve{z}\sigma}}{(\breve{z}\sigma)^2} \left[\frac{\breve{d}_j^1}{\sigma}(\breve{z}\sigma)^2 e^{-\breve{z}\sigma/2}\overline{Y}^{11} + \mathcal{P}_j^1 \overline{Z}^{11}\right], \end{aligned} \tag{399}$$

A specific fluid mixture described by Eqs. (381)–(385) is a two-component fluid mixture that comprises particles of species $i = 1$ and the other particles of species $i = 2$. Particles specified by $i = 1$ interact with each other through the contributions of the hard-core potential and mutually attractive force. Particles specified by $i = 2$ interact with each other only through the contribution of the hard-core potential. Within the fluid mixture, the hard-core spheres interacting with each other via the contribution of the mutually attractive force are mixed with the hard-core spheres interacting with each other in the absence of mutually attractive forces.

Further, it is easy to assess the pair connectedness $\mathcal{P}_{ij}(\sigma)$ and the pair correlation function $g_{ij}(\sigma)$, if $\breve{d}/\sigma = 1$ is selected. For this condition, the relation $d/\sigma = 1$ is satisfied because of Eq. (390). Then, Eqs. (386) and (388) results in

$$\frac{\breve{k}}{\breve{z}} = \frac{8}{9\sqrt{\pi}} \exp(f_\nu) \left[z\sigma + \frac{2}{3} f_\nu \right]^{-1} \left(\frac{kd^2}{\sigma} \right)^{3/2}, \quad (0 < f_\nu \leq 1/2). \tag{400}$$

(b) *Pair connectedness* $\mathcal{P}_{ij}(\sigma)$

A mutual attractive force acts between particles of species 1. No mutual attractive force acts between particle of species 1 and that of species 2. Moreover, no mutual attractive force acts between particles of species 2. Then, the three types of pair connectedness are required to satisfy $\mathcal{P}_{11}(r) \neq 0$, $\mathcal{P}_{12}(r) = \mathcal{P}_{21}(r) = 0$, and $\mathcal{P}_{22}(r) = 0$. Equation (358) allows the three types of pair connectedness to be estimated for the fluid mixture characterized by Eqs. (392)–(395). They are given as

$$\mathcal{P}_{11}(\sigma) = -\frac{1}{2\pi} \left(\breve{z}\sigma \frac{\breve{d}}{\sigma} + \mathcal{P}_1^1 \right) e^{-\breve{z}\sigma/2} \frac{a_1^1}{\sigma}, \tag{401}$$

$$\mathcal{P}_{12}(\sigma) \approx 0, \quad \mathcal{P}_{21}(\sigma) \approx 0, \quad \text{and} \quad \mathcal{P}_{22}(\sigma) \approx 0. \tag{402}$$

A coefficient a_1^1 for the fluid mixture is given by Eq. (440) in the appendix of this chapter (III H 4), i.e.,

$$\frac{a_1^1}{\sigma} \approx -\frac{1}{x_1^1 x^{11}} \mathcal{P}_1^1.$$

Then, another coefficient a_2^1 is required to satisfy $a_2^1/\sigma \approx 0$. Coefficients x_1^1 and x^{11} for the fluid mixture are expressed as Eqs. (415) and (442) in the appendix of this chapter (III H 4). The product $x_1^1 x^{11}$ is independent of ϕ_2. Therefore, $\mathcal{P}_{11}(\sigma)$ estimated for the fluid mixture

is independent of ϕ_2, although $\phi_2 \neq 0$ is satisfied. This effect is caused by the behavior of $\mathcal{P}_2^1$ that satisfies $0 < \mathcal{P}_2^1 \ll 1$ for $0 < \breve{d}_2^1/\sigma \ll 1$.

If $a_1^1/\sigma \neq 0$ and $a_2^1/\sigma \approx 0$ are considered with Eqs. (401) and (402), then Eq. (399) is rewritten as

$$2\pi \frac{\breve{k}_0^1}{\breve{z}} \frac{\breve{d}}{\sigma} e^{-\breve{z}\sigma/2} \approx -\frac{1}{x_1^1 x^{11}} \mathcal{P}_1^1 - \frac{3}{\pi}\phi_1 \left(\frac{1}{x_1^1 x^{11}} \mathcal{P}_1^1 \right)^2 \times \frac{e^{\breve{z}\sigma}}{(\breve{z}\sigma)^2} \left[\frac{\breve{d}}{\sigma} (\breve{z}\sigma)^2 e^{-\breve{z}\sigma/2} \overline{Y}^{11} + \mathcal{P}_1^1 \overline{Z}^{11} \right]. \tag{403}$$

Coefficient $\mathcal{P}_1^1$, which is nonzero, is estimated from Eq. (403). Other coefficients must satisfy $\mathcal{P}_2^1 \approx 0$, $\mathcal{P}_1^2 \approx 0$, and $\mathcal{P}_2^2 \approx 0$. In addition, Eq. (403) implies that $\mathcal{P}_1^1$ is independent of ϕ_2.

(c) *Percolation threshold*

The percolation threshold for the fluid mixture characterized by Eqs. (392)–(395) is determined as a particular state wherein the mean physical cluster size S expressed by Eq. (371) diverges to infinity. The magnitude of $\mathcal{P}_1^1$ at the percolation threshold can be assessed from formulae that are given in the appendix of this chapter (III H 4).

Substituting x^{11} and $\overline{Q}_1^1$ with those given by Eqs. (442) and (448) allows Eq. (447) to yield an approximate formula, which does not include ϕ_1. If $\mathcal{P}_1^1$ at the percolation threshold is denoted by $(\mathcal{P}_1^1)^p$, then the approximate formula is expressed as

$$\left[-\frac{3}{2} + (2 + \breve{z}\sigma) e^{-\breve{z}\sigma} - \frac{1}{2} e^{-2\breve{z}\sigma} \right] (\mathcal{P}_1^1)^p (\mathcal{P}_1^1)^p - \frac{\breve{d}}{\sigma} e^{-\breve{z}\sigma} \left[\breve{z}\sigma(\breve{z}\sigma + 1) + 1 + e^{-\breve{z}\sigma} \right] (\mathcal{P}_1^1)^p + \frac{1}{2} \left(\frac{\breve{d}}{\sigma} \right)^2 \breve{z}\sigma e^{-2\breve{z}\sigma} \approx 0. \tag{404}$$

Equation (404) does not include both ϕ_1 and ϕ_2. However, the percolation threshold can depend on ϕ_1 in the phase diagram because $\mathcal{P}_1^1$ depends on ϕ_1. Then, the percolation threshold is independent of ϕ_2, because $\mathcal{P}_1^1$ is independent of ϕ_2.

(d) *Pair correlation function* $g_{ij}(\sigma)$

For a two-component fluid mixture specified by Eqs. (381)–(385), Eq. (372) can be sim-

plified as

$$
\begin{aligned}
g_{ij}(\sigma)\approx & \frac{1}{\Delta}+\frac{3}{2}\frac{\phi_1+\phi_2}{\Delta^2}-\frac{1}{6}\Bigg\{-\frac{12}{\Delta}\left[\frac{3}{\Delta}(\phi_1+\phi_2)\frac{1}{z\sigma}+\frac{1}{z\sigma}-\frac{1}{2}\right] \\
& \times\left[\frac{1}{z\sigma}\left(-\frac{1}{2}+\frac{1}{z\sigma}-\frac{e^{-z\sigma}}{2}-\frac{e^{-z\sigma}}{z\sigma}\right)\sum_{k=1}^{2}\phi_k e^{z\sigma}B_k^{(1)}+\left(\frac{1}{2}+\frac{1}{z\sigma}\right)\frac{d}{\sigma}\phi_1\right] \\
& +\frac{3}{\Delta}\Phi_0(z\sigma)\sum_{k=1}^{2}\phi_k e^{z\sigma}B_k^{(1)}+\frac{3}{\Delta}\phi_1\frac{d}{\sigma}-\left(\frac{d_i^{(1)}}{\sigma}-\frac{e^{-z\sigma}}{z\sigma}e^{z\sigma}B_i^{(1)}\right)z\sigma\Bigg\} \\
& \times\Bigg\{e^{z\sigma}B_j^{(1)}-\frac{12}{\Delta}\left(1+\frac{1}{2}z\sigma+\frac{3}{\Delta}(\phi_1+\phi_2)\right)\frac{1+z\sigma/2}{(z\sigma)^2}\phi_1\frac{d}{\sigma}+\frac{3}{\Delta}\phi_1\frac{d}{\sigma} \\
& -\frac{3}{\Delta}\left[4\left(1+\frac{1}{2}z\sigma+\frac{3}{\Delta}(\phi_1+\phi_2)\right)\Psi_1(z\sigma)+\Phi_0(z\sigma)\right]\sum_{k=1}^{2}\phi_k e^{z\sigma}B_k^{(1)}\Bigg\} \\
& \times\Bigg\{\sum_{l=1}^{2}\phi_l\left[\frac{d_l^{(1)}}{\sigma}-\frac{12(1+z\sigma/2)}{\Delta(z\sigma)^2}\phi_1\frac{d}{\sigma}+\Phi_0(z\sigma)e^{z\sigma}B_l^{(1)}\right. \\
& \left.-\frac{12}{\Delta}\Psi_1(z\sigma)\sum_{k=1}^{2}\phi_k e^{z\sigma}B_k^{(1)}\right]^2\Bigg\}^{-1}, \qquad (405)
\end{aligned}
$$

where

$$
\begin{aligned}
\Delta \equiv & 1-\sum_{l=1}^{\mathcal{L}}\phi_l,\ \ (\mathcal{L}=2), \\
\Psi_1(z\sigma) \equiv & (z\sigma)^{-3}[1-z\sigma/2-(1+z\sigma/2)e^{-z\sigma}], \\
\text{and} \qquad \Phi_0(z\sigma) \equiv & (z\sigma)^{-1}(1-e^{-z\sigma}).
\end{aligned}
$$

A coefficient expressed as $B_i^{(n)}$ in Eq. (405) is defined by Eq. (374); it must always be positive because $d_i^{(n)}/\sigma_i$ should be positive for arbitrary values of i and n.

According to Eq. (374), this coefficient should be small if the effective range characterized by $1/z_n$ is short. In fact, Eqs. (375) and (377) for $n=2$ results in

$$
\lim_{z_2\to\infty} e^{z_2\sigma}B_j^{(2)}=0. \qquad (406)
$$

Thus, the coefficients $B_1^{(2)}$ and $B_2^{(2)}$ are not included in Eq. (405). The above relation helps derive Eq. (405) from Eq. (372). In addition, even a product $z_2\sigma e^{z_2\sigma}B_j^{(2)}$ has a finite value as $\lim_{z_2\sigma\to\infty}[z_2\sigma e^{z_2\sigma}B_j^{(2)}]<\infty$, according to Eqs. (375) and (377).

Equation (375) for $n=1$ and $j=1$ results in a formula given as

$$0\approx 6\frac{k}{z}\frac{d}{\sigma}e^{-z\sigma}\Bigg[\sum_{l=1}^{2}\phi_l\Bigg(\frac{d_l^{(1)}}{\sigma}-\frac{12(1+z\sigma/2)}{\Delta(z\sigma)^2}\phi_1\frac{d}{\sigma}+\Phi_0(z\sigma)e^{z\sigma}B_l^{(1)}-\frac{12}{\Delta}\Psi_1(z\sigma)$$
$$\times\sum_{k=1}^{2}\phi_k e^{z\sigma}B_k^{(1)}\Bigg)^2\Bigg]^2+\sum_{h=1}^{2}(-1)^h e^{z\sigma}B_h^{(1)}\sum_{l=1}^{2}\phi_l\Bigg(\frac{d_l^{(1)}}{\sigma}-\frac{12(1+z\sigma/2)}{\Delta(z\sigma)^2}\phi_1\frac{d}{\sigma}+\Phi_0(z\sigma)e^{z\sigma}B_l^{(1)}$$
$$-\frac{12}{\Delta}\Psi_1(z\sigma)\sum_{k=1}^{2}\phi_k e^{z\sigma}B_k^{(1)}\Bigg)^2+\frac{1}{z\sigma}\sum_{l=1}^{2}\phi_l\Bigg\{e^{z\sigma}B_l^{(1)}-\frac{12}{\Delta}\Bigg(1+\frac{1}{2}z\sigma+\frac{3}{\Delta}(\phi_1+\phi_2)\Bigg)$$
$$\times\frac{1+z\sigma/2}{(z\sigma)^2}\phi_1\frac{d}{\sigma}+\frac{3}{\Delta}\phi_1\frac{d}{\sigma}-\frac{3}{\Delta}\Bigg[4\Bigg(1+\frac{1}{2}z\sigma+\frac{3}{\Delta}(\phi_1+\phi_2)\Bigg)\Psi_1(z\sigma)+\Phi_0(z\sigma)\Bigg]$$
$$\times\sum_{k=1}^{2}\phi_k e^{z\sigma}B_k^{(1)}\Bigg\}^2\Bigg\{\frac{d}{\sigma}+z\sigma\Phi_0(z\sigma)\frac{d}{\sigma}-z\sigma\big[\Phi_0(z\sigma)\big]^2\sum_{h=1}^{2}(-1)^h e^{z\sigma}B_h^{(1)}\Bigg\}. \tag{407}$$

Equation (375) for $n=1$ and $j=2$ results in a formula given as

$$0\approx\sum_{k=1}^{2}\phi_k\Bigg(\frac{d_k^{(1)}}{\sigma}-\frac{12(1+z\sigma/2)}{\Delta(z\sigma)^2}\phi_1\frac{d}{\sigma}+\Phi_0(z\sigma)e^{z\sigma}B_k^{(1)}-\frac{12}{\Delta}\Psi_1(z\sigma)\sum_{h=1}^{2}\phi_h e^{z\sigma}B_h^{(1)}\Bigg)^2$$
$$\times\sum_{l=1}^{2}\Bigg[\delta_{l2}+\frac{3}{\Delta}\phi_l\Phi_0(z\sigma)-\frac{12}{\Delta}\phi_l\Psi_1(z\sigma)\Bigg(1+\frac{1}{2}z\sigma+\frac{3}{\Delta}(\phi_1+\phi_2)\Bigg)\Bigg]\Bigg\{e^{z\sigma}B_l^{(1)}-\frac{12}{\Delta}$$
$$\times\Bigg(1+\frac{1}{2}z\sigma+\frac{3}{\Delta}(\phi_1+\phi_2)\Bigg)\frac{1+z\sigma/2}{(z\sigma)^2}\phi_1\frac{d}{\sigma}+\frac{3}{\Delta}\phi_1\frac{d}{\sigma}-\frac{3}{\Delta}\Bigg[4\Bigg(1+\frac{1}{2}z\sigma+\frac{3}{\Delta}(\phi_1+\phi_2)\Bigg)$$
$$\times\Psi_1(z\sigma)+\Phi_0(z\sigma)\Bigg]\sum_{h=1}^{2}\phi_h e^{z\sigma}B_h^{(1)}\Bigg\}+\frac{1}{z\sigma}\sum_{k=1}^{2}\phi_k\Bigg\{e^{z\sigma}B_k^{(1)}-\frac{12}{\Delta}\Bigg(1+\frac{1}{2}z\sigma+\frac{3}{\Delta}(\phi_1+\phi_2)\Bigg)$$
$$\times\frac{1+z\sigma/2}{(z\sigma)^2}\phi_1\frac{d}{\sigma}+\frac{3}{\Delta}\phi_1\frac{d}{\sigma}-\frac{3}{\Delta}\Bigg[4\Bigg(1+\frac{1}{2}z\sigma+\frac{3}{\Delta}(\phi_1+\phi_2)\Bigg)\Psi_1(z\sigma)+\Phi_0(z\sigma)\Bigg]$$
$$\times\sum_{h=1}^{2}\phi_h e^{z\sigma}B_h^{(1)}\Bigg\}^2\Bigg\{\sum_{l=1}^{2}\Bigg(\frac{12}{\Delta}\Psi_1(z\sigma)\phi_l-\Phi_0(z\sigma)\delta_{l2}\Bigg)\Bigg\{e^{z\sigma}B_l^{(1)}-z\sigma\frac{d}{\sigma}\delta_{l1}$$
$$+\frac{3}{\Delta}\frac{d}{\sigma}\phi_1\Bigg(3+\frac{4}{z\sigma}\Bigg)-\frac{12}{\Delta}\Bigg(1+\frac{1}{2}z\sigma+\frac{3}{\Delta}(\phi_1+\phi_2)\Bigg)\Bigg(\frac{2+z\sigma}{2(z\sigma)^2}\phi_1\frac{d}{\sigma}+\Psi_1(z\sigma)\sum_{h=1}^{2}\phi_h e^{z\sigma}B_h^{(1)}\Bigg)$$
$$+\sum_{h=1}^{2}\Bigg[-z\sigma\Phi_0(z\sigma)\delta_{lh}+\frac{3}{\Delta}\Big(\Phi_0(z\sigma)+4z\sigma\Psi_1(z\sigma)\Big)\phi_h\Bigg]e^{z\sigma}B_h^{(1)}\Bigg\}+\sum_{l=1}^{2}\Bigg[\Bigg(\delta_{l1}$$
$$-\frac{12}{\Delta}\phi_1\frac{2+z\sigma}{2(z\sigma)^2}\Bigg)\frac{d}{\sigma}+\sum_{h=1}^{2}\Bigg(\Phi_0(z\sigma)\delta_{lh}-\frac{12}{\Delta}\phi_h\Psi_1(z\sigma)\Bigg)e^{z\sigma}B_h^{(1)}\Bigg]\Bigg[\delta_{l2}+\frac{3}{\Delta}\phi_l\Phi_0(z\sigma)$$
$$-\frac{12}{\Delta}\phi_l\Psi_1(z\sigma)\Bigg(1+\frac{1}{2}z\sigma+\frac{3}{\Delta}(\phi_1+\phi_2)\Bigg)\Bigg]\Bigg\}. \tag{408}$$

$g_{ij}(\sigma) = g_{ji}(\sigma)$ imposes a restriction on the coefficients $B_1^{(1)}$ and $B_2^{(1)}$, and it is given as

$$
\begin{aligned}
0 \approx & -\left(4 - 2z\sigma + \frac{12}{\Delta}(\phi_1 + \phi_2)\right) \sum_{l=1}^{2} (-1)^l e^{z\sigma} B_l^{(1)} \left[-(z\sigma)^2 \Psi_1(z\sigma) \sum_{l=1}^{2} \phi_l e^{z\sigma} B_l^{(1)} \right. \\
& \left. -\left(1 + \frac{1}{2} z\sigma\right) \frac{d}{\sigma} \phi_1 \right] + \left(4 + 2z\sigma + \frac{12}{\Delta}(\phi_1 + \phi_2)\right) \left(\sum_{l=1}^{2} (-1)^l B_l^{(1)} + z\sigma \frac{d}{\sigma} \right) \\
& \times \left[\left(\frac{2}{z\sigma} - (z\sigma)^2 \Psi_1(z\sigma) \right) \sum_{l=1}^{2} \phi_l e^{z\sigma} B_l^{(1)} - \left(1 + \frac{1}{2} z\sigma\right) \frac{d}{\sigma} \phi_1 \right] \\
& + \left(-(1 - e^{-z\sigma}) \sum_{l=1}^{2} (-1)^l e^{z\sigma} B_l^{(1)} + z\sigma \frac{d}{\sigma} \right) \left[(1 - e^{-z\sigma}) \sum_{l=1}^{2} \phi_l e^{z\sigma} B_l^{(1)} + z\sigma \frac{d}{\sigma} \phi_1 \right] z\sigma \\
& + (z\sigma)^3 \frac{\Delta}{3} \frac{d}{\sigma} e^{z\sigma} B_2^{(1)}. \qquad (409)
\end{aligned}
$$

Thus, the use of Eqs. (407), (408), and (409) allows coefficients $B_1^{(1)}$ and $B_2^{(1)}$ in Eq. (405) to be assessed.

For the two-component fluid mixture specified by Eqs. (381)–(385), Equation (377) can be simplified as

$$
\begin{aligned}
e^{-z\sigma/2} \frac{a_j^{(1)}}{\sigma} \approx & -\frac{\pi}{3} \left\{ e^{z\sigma} B_j^{(1)} - \frac{12}{\Delta} \left(1 + \frac{1}{2} z\sigma + \frac{3}{\Delta}(\phi_1 + \phi_2)\right) \frac{1 + z\sigma/2}{(z\sigma)^2} \phi_1 \frac{d}{\sigma} + \frac{3}{\Delta} \phi_1 \frac{d}{\sigma} \right. \\
& \left. - \frac{3}{\Delta} \left[4 \left(1 + \frac{1}{2} z\sigma + \frac{3}{\Delta}(\phi_1 + \phi_2)\right) \Psi_1(z\sigma) + \Phi_0(z\sigma) \right] \sum_{h=1}^{2} \phi_h e^{z\sigma} B_h^{(1)} \right\} \\
& \times \left\{ \sum_{h=1}^{2} \phi_h \left[\frac{d_h^{(1)}}{\sigma} - \frac{12(1 + z\sigma/2)}{\Delta (z\sigma)^2} \phi_1 \frac{d}{\sigma} + \Phi_0(z\sigma) e^{z\sigma} B_h^{(1)} \right. \right. \\
& \left. \left. - \frac{12}{\Delta} \Psi_1(z\sigma) \sum_{k=1}^{2} \phi_k e^{z\sigma} B_k^{(1)} \right]^2 \right\}^{-1} \qquad (410)
\end{aligned}
$$

and

$$
e^{-z_2\sigma/2} \frac{a_j^{(2)}}{\sigma} \approx 0. \qquad (411)
$$

(e) *Adequate relation between* $B_1^{(1)}$ *and* $B_2^{(1)}$

Correlation function $g_{12}(r)$ should be proportional to the probability that an $i = 2$ particle exists in a volume element $\mathrm{d}\mathbf{r}_2$ located at a particular place specified by a distance r from an

$i = 1$ particle. Hence, $g_{12}(r)$ should become zero, when $i = 2$ particles separate from a phase in which the particles are macroscopically homogeneously mixed with $i = 1$ particles. Near a specific point at which this phase separation occurs, $g_{12}(r)$ should extremely rapidly decay to zero as r increases. The coefficient $B_2^{(1)}$ is an integral involving $g_{12}(r)$ as an integrand, as shown in Eq. (374) with coefficients given by Eq. (384). The coefficient $B_1^{(1)}$ is an integral involving $g_{11}(r)$ as an integrand, as shown in Eq. (374) with coefficients given by Eq. (384). Therefore, $B_2^{(1)}$ should be considerably smaller than $B_1^{(1)}$ when the phase separation of $i = 2$ particles occurs. Numerical pairs of $B_1^{(1)}$ and $B_2^{(1)}$ that satisfy Eqs. (407)–(409) depend on a parameter such as k given by Eq. (395). When the value of k is close to the value at which the phase separation of $i = 2$ particles occurs, adequately numerical pairs of $B_1^{(1)}$ and $B_2^{(1)}$ should satisfy $B_2^{(1)}/B_1^{(1)} \ll 1$.

2. Evaluations of correlation functions

(a) *Pair connectedness evaluated from Eq. (401)*

The pair connectedness $\mathcal{P}_{11}(\sigma)$ at the percolation threshold can be assessed from Eqs. (401) and (404). For an arbitrary value of k and an arbitrary value of ϕ_1, the pair connectedness $\mathcal{P}_{11}(\sigma)$ must be assessed from Eqs. (401), (403), and (404). Then, the pair connectedness $\mathcal{P}_{11}(\sigma)$ depends on a parameter f_ν that expresses the characteristics of the closure represented by Eq. (312) with Eqs. (314) and (316).

When the closure represented by Eq. (312) is specified for $f_\nu = 0$, the closure overestimates the long-range contribution of $C_{11}^+(r)$ given by Eq. (308). When the closure is specified for $f_\nu = 1/2$, it overestimates the decay of $C_{11}^+(r)$ dependent on r. Fortunately, the values of $\mathcal{P}_{11}(\sigma)$ assessed from Eqs. (401), (403), and (404) for $f_\nu = 0$ hardly differ from those for $f_\nu = 1/2$, unless ϕ_1 or $z\sigma$ is too small. Therefore, the pair connectedness $\mathcal{P}_{11}(\sigma)$ derived from the use of the closure represented by Eq. (312) can well approximate that derived from that given by Eq. (308), unless ϕ_1 or $z\sigma$ is too small. When ϕ_1 or $z\sigma$ is too small, it is possible to select a specific value of f_ν as $f_\nu = f_{\nu_{3/2}}$, which is expressed by Eq. (86). If both Eqs. (403) and (404) are satisfied for $\phi_1 = (\phi_1)_p$, $kd^2/\sigma = (kd^2/\sigma)_p$, and $z\sigma = (z\sigma)_p$, these values correspond to the values of ϕ_1, kd^2/σ, and $z\sigma$ at the percolation threshold.

(b) *Contribution of physical clusters to phase behavior*

A physical cluster as an ensemble of particles that interact with each other in a bound state should form a dense region of $i = 1$ particles. Then, there is a possibility that branches of the physical cluster has a fractal structure because the approximate behavior of $\mathcal{P}_{11}(r)$ at a large r, where $0 < -\beta u_{11}(r) \ll 1$ is satisfied, can be expressed as $\mathcal{P}_{11}(r) \sim [-\beta u_{11}(r)]^{3/2}$. This structure is hardly perturbed by the addition of $i = 2$ particles because the added $i = 2$ particles are not allowed to participate in the physical cluster formation of $i = 1$ particles. Further, a considerably different model from that treating physical clusters formed by mutually attractive forces between particles was used to demonstrate that the fractal dimensions found from the clusters aggregated in the binary mixtures can be insensitive to molar fractions within the range of the high molar fraction.[89]

Unbound particles must comprise $i = 1$ particles with large momenta and $i = 2$ particles both. With the growth of the branches of physical clusters, the branches confine unbounded particles within regions surrounded by the branches. This is predicted based on the use of Eqs. (401) and (403).

Values of $\mathcal{P}_1^1$ evaluated from Eq. (403) can satisfy $0 < \mathcal{P}_1^1 \ll 1$ under various conditions. This relation allows Eq. (403) to yield an approximate $\mathcal{P}_1^1$, which is given as

$$\mathcal{P}_1^1 \approx \left[2(\breve{z}\sigma)^2 \frac{\breve{d}}{\sigma}\overline{Y}^{11}\right]^{-1} \left[1 - \sqrt{1 - 24\frac{\breve{k}}{\breve{z}}\left(\frac{\breve{d}}{\sigma}\right)^2 \overline{Y}^{11}\phi_1}\right]. \tag{412}$$

Moreover, if $0 < \mathcal{P}_1^1 \ll 1$ is considered with Eq. (412), then Eq. (401) allows an approximate $\mathcal{P}_{11}(\sigma)$ to be obtained from the substitution of coefficient a_1^1 that is given by Eq. (440) in the appendix of this chapter (III H 4). It is expressed as

$$\mathcal{P}_{11}(\sigma) \approx \frac{1}{12} e^{\breve{z}\sigma} \left[\left(\frac{\breve{d}}{\sigma}\right)^2 \overline{Y}^{11}\right]^{-1} \left[1 - \sqrt{1 - 24\frac{\breve{k}}{\breve{z}}\left(\frac{\breve{d}}{\sigma}\right)^2 \overline{Y}^{11}\phi_1}\right] \frac{1}{\phi_1}. \tag{413}$$

The mean physical cluster size increases as ϕ_1 increases, and it diverges to infinity at $\phi_1 = (\phi_1)^p$, which denotes the value of ϕ_1 at the percolation threshold. If $\mathcal{P}_1^1$ in Eq. (412) is substituted by $(\mathcal{P}_1^1)^p$ obtained from Eq. (404), then conditions $0 < \mathcal{P}_1^1 \ll 1$ and $1 \ll z\sigma$ allow the magnitude of $(\phi_1)_p$ to be approximately estimated. It is expressed as

$$(\phi_1)_p \approx \frac{1}{12}(\breve{z}\sigma)^3 e^{-\breve{z}\sigma}[\breve{z}\sigma(\breve{z}\sigma + 1) + 1 + e^{-\breve{z}\sigma}]^{-1}. \tag{414}$$

Although the mean physical cluster size increases as ϕ_1 increases, the pair connectedness $\mathcal{P}_{11}(\sigma)$ hardly varies as ϕ_1 increases.[52] In fact, if $0 < 24(\breve{k}/\breve{z})(\breve{d}/\sigma)^2\overline{Y}^{11} \ll 1$ is satisfied, then

the numerator on the right hand side of Eq. (413) is proportional to ϕ_1. This indicates that $\mathcal{P}_{11}(\sigma)$ is insensitive to variations in the value of ϕ_1. Therefore, each physical cluster grows toward that with a larger span as ϕ_1 increases. Such growth of physical clusters implies that an increase in ϕ_1 enhances the number of unbound particles confined by the branches of the physical clusters.

Unbound $i = 1$ particles within regions surrounded by branches of physical clusters should become denser than those outside of the regions, if their branches prohibit the boundaries of the regions from expanding freely. This implies that the densities of unbound $i = 1$ particles in the regions should be enhanced, and therefore, their densities outside of the regions should be reduced. If a contribution of the latter to a decrease in $g_{11}(\sigma)$ is more dominant than that of the former to an increase in $g_{11}(\sigma)$, the value of $g_{11}(\sigma)$ should decrease as ϕ_1 increases. There is a possibility that the branches of physical clusters prohibit the boundaries of the regions from expanding freely.

Parameter f_ν found in Eq. (413) specifies the characteristics of the closure given as Eq. (312). The closure specified for $f_\nu = 0$ overestimates the long-range contribution of $C_{11}^{+}(r)$ given by Eq. (308), and the closure specified for $f_\nu = 1/2$ overestimates the decay of $C_{11}^{+}(r)$ dependent on r. Nevertheless, Eq. (413) shows that $\mathcal{P}_{11}(\sigma)$ cannot be insensitive to ϕ_1. This means that the pair connectedness $\mathcal{P}_{ij}(\sigma)$ derived from the use of the closure represented by Eq. (312) leads to the same behavior as that derived using Eq. (308). Therefore, it should be inferred that the growth of physical clusters caused by an increase in ϕ_1 enhances the number of unbound particles confined by the branches of the physical clusters.

(c) *Behavior of $i = 2$ particles*

i) *Separation of rich $i = 2$ particle phase*

The formation of physical clusters cannot directly be helped by $i = 2$ particles. There is no mutually attractive force between two of the $i = 2$ particles, and they behave as hard cores in the absence of an attractive force between an $i = 1$ particle and an $i = 2$ particle. Hence, the $i = 2$ particles should be distributed with unbound $i = 1$ particles among branches of physical clusters. The $i = 2$ particles can then be confined with the unbound $i = 1$ particles within regions surrounded by their branches. Then, their distribution contributes to the magnitude of $\mathcal{D}_{ij}(r)$.

If a state of a fluid mixture allows physical clusters to be small and their stability to

be low, $i = 1$ particles should be mixed with $i = 2$ particles because $i = 2$ particles can be distributed with unbound $i = 1$ particles among small physical clusters. The separation between $i = 1$ and $i = 2$ particle rich phases cannot occur in the fluid mixture because physical clusters that do not have a sufficient stability allow $i = 2$ particles to be distributed among branches of physical clusters. The stability of physical clusters is enhanced with an increase in the value of (ϕ_1). Then, $i = 2$ particles can be stably confined among branches of physical clusters. This implies that the number of $i = 2$ particles that are allowed to be confined among branches of physical clusters is limited. Thus, stabilized physical clusters allow the separation between $i = 1$ and $i = 2$ particle rich phases to occur.

ii) *Passively attractive force between $i = 2$ particles*

In a fluid mixture, $i = 2$ particles can receive a passively attractive force generated from the cooperation between the exclusion of $i = 2$ particles caused by the hard-core potential and mutually attractive forces between $i = 1$ particles. Such a passively attractive force contributes to stuffing many $i = 2$ particles within a region surrounded by branches of physical clusters. Then, $i = 2$ particles in the region should have larger relative momenta than those of $i = 1$ particles in the region. Hence, the probability that a large number of $i = 2$ particles are stably retained in the region is low; the $i = 2$ particles can be redistributed.

A passively attractive force generated from the cooperation between the exclusion of $i = 2$ particles caused by the hard-core potential and mutually attractive forces between $i = 1$ particles should depend at least on both the diameter of the hard core of an $i = 2$ particle and the effective range of the mutually attractive force between the pair particles. Hence, particles of a constituent contributing principally to the magnitude of $\mathcal{D}_{ij}(r)$ can contribute to the phase behavior of a fluid mixture through their particle sizes. If the particles are small, they can be confined relatively stably within regions surrounded by the branches of physical clusters. If the particles have larger sizes than those of the regions, the addition of these particles into the fluid mixture can more strongly disturb the stability of the phase that seems macroscopically homogeneous.

The probability that these particles are stably retained in the regions is low if the particles interacting through only their hard-core potentials are considerably larger than regions surrounded by branches of physical clusters. Yet, it is expected that the particles can be diffused into areas among the physical clusters, if the average extent of the physical clusters

is sufficiently smaller than the sizes of the particles. When colloidal particles are considered hard-core spheres that do not interact with each other via attractive forces, the colloidal particles can be distributed into a molecular fluid mixture wherein the physical clusters hold only sufficiently small extents. If the physical clusters develop near a specific temperature, then passively attractive forces generated between colloidal particles should be strengthened. The attractive forces may contribute to special forces that act between colloidal particles immersed within a binary fluid mixture near the consolute point[64].

3. General perception found from effects of physical cluster formation

A fluid mixture comprising $i = 1$ particles and $i = 2$ particles cannot become homogeneous if physical clusters of $i = 1$ particles are formed. In a fluid mixture wherein mutually attractive forces make particles interact with each other, particles that have small relative momenta are prevented from being homogeneously mixed with particles that have large relative momenta. If the formation of physical clusters is ignored, the dependence of $g_{ij}(r)$ on r can be characterized by the product of r^{-1} and a particular function which can be given as the Taylor series with respect to r. Nevertheless, particles that have small relative momenta can contribute to physical cluster growth, which allows particles to be distributed in a a characteristic structure. The distribution of particles allows the dependence of $g(r)$ on r to deviate from the behavior characterized by the product of the factor r^{-1} and a particular function that can be given as the Taylor series with respect to r.[47] The distribution of particles allows the fluid system to acquire various features. Therefore, particles contributing to the magnitude of $\mathcal{D}_{ij}(r)$ are confined in local small areas surrounded by particles that contribute to the magnitude of $\mathcal{P}_{ij}(r)$.[52] Particles contributing to the magnitude of $\mathcal{D}_{ij}(r)$ lead to a structure that prevents physical clusters from contracting.

4. *Appendix: Formulae for evaluating $\mathcal{P}_j^n$ for specific fluid mixture*

A specific fluid mixture that is specified by Eqs. (381)–(385) requires that the parameters for estimating pair connectedness be expressed by Eqs. (392)–(395). Unknown coefficients $\mathcal{P}_j^n$ depend on $\breve{z}_n$. Modifying Eq. (345) allows the dependence of $\mathcal{P}_j^n$ on $\breve{z}_n$ to be known as

$$\mathcal{P}_j^n \equiv 12\sum_{l=1}^{2}\phi_l\frac{\breve{d}_l^n}{\sigma_l}\frac{1}{(\breve{z}_n\sigma_l)^2}\left[\int_0^\infty \mathcal{P}_{lj}(\tau/s)e^{-\tau}\tau\mathrm{d}\tau\right]_{s=\breve{z}_n}.$$

Thus, $0<\mathcal{P}_j^2\ll\mathcal{P}_j^1$ is satisfied for the specific fluid mixture because of $0<\breve{z}_1/\breve{z}_2\ll 1$.

(a) *Estimations of coefficients*

i) *Estimations for large $\breve{z}_2\sigma$ satisfying $1\ll\breve{z}_2/\breve{z}$*

For the specific fluid mixture, each coefficient x_j^n given by Eq. (348) is represented as

$$x_1^1 = x_2^1 = \frac{6}{\pi}\breve{z}\sigma e^{-\breve{z}\sigma/2}, \tag{415}$$

$$x_1^2 = x_2^2 = \frac{6}{\pi}\breve{z}_2\sigma e^{-\breve{z}_2\sigma/2}, \tag{416}$$

Each coefficient x^{mn} given by Eq. (349) is represented for the specific fluid mixture as follows:

$$\begin{aligned}x^{11} =&\frac{e^{\breve{z}\sigma}}{2(\breve{z}\sigma)^3}\left\{\frac{\breve{d}}{\sigma}e^{-\breve{z}\sigma}\left[\frac{\breve{d}}{\sigma}\breve{z}\sigma e^{-\breve{z}\sigma}+2(1+e^{-\breve{z}\sigma})\mathcal{P}_1^1\right]\phi_1+\frac{\breve{d}_2^1}{\sigma}e^{-\breve{z}\sigma}\left[\frac{\breve{d}_2^1}{\sigma}\breve{z}\sigma e^{-\breve{z}\sigma}\right.\right.\\ &\left.\left.+2(1+e^{-\breve{z}\sigma})\mathcal{P}_2^1\right]\phi_2+(1-e^{-\breve{z}\sigma})^2(\phi_1\mathcal{P}_1^1\mathcal{P}_1^1+\phi_2\mathcal{P}_2^1\mathcal{P}_2^1)\right\},\end{aligned} \tag{417}$$

$$x^{22} \approx \frac{e^{\breve{z}_2\sigma}}{2(\breve{z}_2\sigma)^3}\overline{x}^{22}, \tag{418}$$

$$\overline{x}^{22} \equiv \phi_1\mathcal{P}_1^2\mathcal{P}_1^2+\phi_2\mathcal{P}_2^2\mathcal{P}_2^2, \tag{419}$$

$$x^{12} \approx \frac{e^{\breve{z}\sigma}}{\breve{z}\sigma}\frac{e^{\breve{z}_2\sigma/2}}{(\breve{z}_2\sigma)^2}\overline{x}^{12}, \tag{420}$$

$$\overline{x}^{12} \equiv \phi_1\mathcal{P}_1^1\mathcal{P}_1^2+\phi_2\mathcal{P}_2^1\mathcal{P}_2^2, \tag{421}$$

$$x^{21} \approx \frac{e^{\breve{z}_2\sigma/2}e^{-\breve{z}\sigma}}{(\breve{z}_2\sigma)^2}\overline{x}^{21}, \tag{422}$$

$$\overline{x}^{21} \equiv \frac{\breve{d}}{\sigma}\mathcal{P}_1^2\phi_1+\frac{\breve{d}_2^1}{\sigma}\mathcal{P}_2^2\phi_2+\frac{e^{-\breve{z}\sigma}-1}{\breve{z}\sigma}(\phi_1\mathcal{P}_1^1\mathcal{P}_1^2+\phi_2\mathcal{P}_2^1\mathcal{P}_2^2). \tag{423}$$

Then,

$$\begin{aligned} x =& x^{11}x^{22} - x^{12}x^{21} \\ \approx& \frac{e^{\breve{z}_2\sigma}}{2(\breve{z}_2\sigma)^3} x^{11}\overline{x}^{22}. \end{aligned} \tag{424}$$

Thus,

$$\frac{1}{x}\begin{pmatrix} \frac{1}{x_j^1}x^{22} & -\frac{1}{x_j^2}x^{12} \\ -\frac{1}{x_j^1}x^{21} & \frac{1}{x_j^2}x^{11} \end{pmatrix} \approx \begin{pmatrix} \frac{1}{x_j^1}\frac{1}{x^{11}} & -\frac{2}{x_j^1}\frac{\overline{x}^{12}}{x^{11}\overline{x}^{22}} \\ -\frac{\pi}{3}\frac{\breve{z}_2\sigma/\breve{z}\sigma}{\exp(\breve{z}_2\sigma/2)}\frac{\overline{x}^{21}}{x^{11}\overline{x}^{22}} & \frac{\pi}{3}\frac{(\breve{z}_2\sigma)^2}{\exp(\breve{z}_2\sigma/2)}\frac{1}{\overline{x}^{22}} \end{pmatrix}. \tag{425}$$

Therefore, for an extremely large $\breve{z}_2\sigma$ satisfying $0 < \breve{z}/\breve{z}_2 \ll 1$, Eq. (354) yields an approximation given by

$$\begin{pmatrix} \frac{1}{x}X_j^{11} & \frac{1}{x}X_j^{12} \\ \frac{1}{x}X_j^{21} & \frac{1}{x}X_j^{22} \end{pmatrix} \approx \begin{pmatrix} \frac{1}{x_j^1}\frac{1}{x^{11}} & -\frac{2}{x_j^1}\frac{\overline{x}^{12}}{x^{11}\overline{x}^{22}} \\ -\frac{\pi}{3}\frac{\breve{z}_2\sigma/\breve{z}\sigma}{\exp(\breve{z}_2\sigma/2)}\frac{\overline{x}^{21}}{x^{11}\overline{x}^{22}} & \frac{\pi}{3}\frac{(\breve{z}_2\sigma)^2}{\exp(\breve{z}_2\sigma/2)}\frac{1}{\overline{x}^{22}} \end{pmatrix}. \tag{426}$$

Eq. (426) allows coefficients a_j^n given by Eq. (353) to be estimated for an extremely large $\breve{z}_2\sigma$ satisfying $0 < \breve{z}/\breve{z}_2 \ll 1$. Then, the coefficients are expressed as

$$\frac{a_j^1}{\sigma} \approx -\frac{1}{x_j^1}\frac{1}{x^{11}}\left(\mathcal{P}_j^1 - 2\frac{\overline{x}^{12}}{\overline{x}^{22}}\mathcal{P}_j^2\right) \tag{427}$$

and

$$\frac{a_j^2}{\sigma} \approx (\breve{z}_2\sigma)^2 e^{-\breve{z}_2\sigma/2}\frac{\overline{a}_j^2}{\sigma}, \tag{428}$$

where

$$\frac{\overline{a}_j^2}{\sigma} \equiv \frac{\pi}{3}\frac{1}{\overline{x}^{22}}\left(\frac{1}{\breve{z}\sigma\breve{z}_2\sigma}\frac{\overline{x}^{21}}{x^{11}}\mathcal{P}_j^1 - \mathcal{P}_j^2\right). \tag{429}$$

If Eq. (429) is used, then Eq. (396) multiplied by $(\breve{z}_2\sigma)^2 e^{-\breve{z}_2\sigma/2}$ can be rewritten for $n = 2$ as

$$\begin{aligned} \frac{2\pi}{(\breve{z}_2\sigma)^2}\frac{\breve{k}_0^2}{\breve{z}_2}\frac{\breve{d}_j^2}{\sigma} \approx& -\frac{\overline{a}_j^2}{\sigma} - \frac{6}{\pi}\Bigg\{\left(\phi_1\frac{\overline{a}_1^2}{\sigma}\frac{a_1^1}{\sigma} + \phi_2\frac{\overline{a}_2^2}{\sigma}\frac{a_2^1}{\sigma}\right)\frac{e^{\breve{z}\sigma/2}}{\breve{z}\sigma(\breve{z}_2+\breve{z})\sigma}\Bigg[\frac{\breve{d}_j^1}{\sigma}(\breve{z}\sigma)^2 e^{-\breve{z}\sigma/2}\overline{Y}^{12} \\ &+\mathcal{P}_j^1\overline{Z}^{12}\Bigg] + \left(\phi_1\frac{\overline{a}_1^2}{\sigma}\frac{\overline{a}_1^2}{\sigma} + \phi_2\frac{\overline{a}_2^2}{\sigma}\frac{\overline{a}_2^2}{\sigma}\right)\frac{1}{2\breve{z}_2\sigma}\left[\frac{\breve{d}_j^2}{\sigma}(\breve{z}_2\sigma)^2 e^{-\breve{z}_2\sigma/2}\overline{Y}^{22} + \mathcal{P}_j^2\overline{Z}^{22}\right]\Bigg\}. \end{aligned} \tag{430}$$

Because of $\lim_{\breve{z}_2\sigma\to\infty}\overline{a}_j^2/\sigma < \infty$, Eq. (430) requires $\overline{a}_j^2/\sigma \approx 0$ to be satisfied for an extremely large $\breve{z}_2\sigma$. Then, Eq. (429) yields

$$\mathcal{P}_j^2 \approx \frac{1}{\breve{z}\sigma\breve{z}_2\sigma}\frac{\overline{x}^{21}}{x^{11}}\mathcal{P}_j^1. \tag{431}$$

Eq. (431) requires $\mathcal{P}_2^2/\mathcal{P}_1^2$ to be given as

$$\frac{\mathcal{P}_2^2}{\mathcal{P}_1^2} \approx \frac{\mathcal{P}_2^1}{\mathcal{P}_1^1}. \tag{432}$$

Moreover, Eq. (431) requires that a factor $(\overline{x}^{12}/\overline{x}^{22})\mathcal{P}_j^2$ in Eq. (427) satisfy for an extremely large $\breve{z}_2\sigma$

$$\frac{\overline{x}^{12}}{\overline{x}^{22}}\mathcal{P}_j^2 \approx 0. \tag{433}$$

Therefore, Eq. (427) can be rewritten as

$$\frac{a_j^1}{\sigma} \approx -\frac{1}{x_j^1 x^{11}}\mathcal{P}_j^1. \tag{434}$$

Because of Eq. (428), coefficient a_j^2 for an extremely large $\breve{z}_2\sigma$ is required to satisfy

$$\frac{a_j^2}{\sigma} \approx 0. \tag{435}$$

ii) *No attraction between particle of species 1 and that of species 2*

A mutual attractive force acts between particles of species 1. No mutual attractive force acts between a particle of species 1 and that of species 2. Moreover, no mutual attractive force acts between particles of species 2. Then, the three types of pair connectedness are required to satisfy $\mathcal{P}_{11}(r) \neq 0$, $\mathcal{P}_{12}(r) = \mathcal{P}_{21}(r) = 0$, and $\mathcal{P}_{22}(r) = 0$. Hence, Eq. (345) for the fluid mixture specified by Eqs. (381)–(395) requires that the following four relations be satisfied:

$$\mathcal{P}_1^1 \neq 0 \tag{436}$$

$$\mathcal{P}_2^1 \approx 0 \tag{437}$$

$$\mathcal{P}_1^2 \approx 0 \tag{438}$$

$$\mathcal{P}_2^2 \approx 0 \tag{439}$$

These relations allow Eq. (434) to be simplified as

$$\frac{a_1^1}{\sigma} \approx -\frac{1}{x_1^1 x^{11}}\mathcal{P}_1^1, \tag{440}$$

$$\frac{a_2^1}{\sigma} \approx 0, \tag{441}$$

Then, x^{11} given by Eq. (417) can be rewritten as

$$x^{11} \approx \frac{e^{\breve{z}\sigma}}{2(\breve{z}\sigma)^3}\left\{\frac{\breve{d}}{\sigma}e^{-\breve{z}\sigma}\left[\frac{\breve{d}}{\sigma}\breve{z}\sigma e^{-\breve{z}\sigma}+2(1+e^{-\breve{z}\sigma})\mathcal{P}_1^1\right]+(1-e^{-\breve{z}\sigma})^2\mathcal{P}_1^1\mathcal{P}_1^1\right\}\phi_1. \tag{442}$$

This implies that $x_1^1 x^{11}$ is independent of ϕ_2. Therefore, coefficient a_1^1 given by Eq. (440) is independent of ϕ_2.

(b) *Requirement for percolation threshold*

i) *Requirement for large $\breve{z}_2\sigma$ satisfying $1 \ll \breve{z}_2/\breve{z}$*

The percolation threshold for the fluid mixture specified by Eqs. (381)–(395) is determined by applying the requirement given by Eq. (370). For $\sigma_1 = \sigma_2 = \sigma$ and $1 \ll \breve{z}_2\sigma$, Eq. (370) multiplied by $2(\breve{z}_2\sigma)^3 e^{-\breve{z}_2\sigma}/\overline{x}^{22}$ can be rewritten because of $x_1^1 = x_2^1$ as

$$\begin{aligned} &x^{11}+\frac{6}{\pi}\sum_{l=1}^{2}\phi_l\left[\frac{e^{\breve{z}\sigma/2}}{(\breve{z}\sigma)^2}\overline{Q}_l^1\left(\frac{1}{x_1^1}\mathcal{P}_l^1-2\frac{\overline{x}^{12}}{x_1^1\overline{x}^{22}}\mathcal{P}_l^2\right)+2\frac{\overline{Q}_l^2}{\overline{x}^{22}}\left(-\frac{e^{\breve{z}\sigma}}{\breve{z}_2\sigma}\frac{\overline{x}^{21}}{x_1^1}\mathcal{P}_l^1+\frac{\pi}{6}x^{11}\mathcal{P}_l^2\right)\right] \\ &+\left(\frac{12}{\pi x_1^1}\right)\phi_1\phi_2\frac{\mathcal{P}_1^2\mathcal{P}_1^2}{\overline{x}^{22}}\left(Q_1^1\frac{\overline{Q}_2^2}{\mathcal{P}_1^2}-\frac{\overline{Q}_1^2}{\mathcal{P}_1^2}Q_2^1\right)\left(\mathcal{P}_1^1\frac{\mathcal{P}_2^2}{\mathcal{P}_1^2}-\mathcal{P}_1^2\right)\approx 0. \end{aligned} \tag{443}$$

For $\sigma_1 = \sigma_2 = \sigma$, Eq. (365) can be rewritten as

$$\overline{Q}_l^m \equiv -\left[1-(1+\breve{z}_m\sigma)e^{-\breve{z}_m\sigma}\right]\mathcal{P}_l^m-\frac{\breve{d}_l^m}{\sigma}\breve{z}_m\sigma(\breve{z}_m\sigma+1)e^{-\breve{z}_m\sigma}. \tag{444}$$

For a large $z_2\sigma$, Eq. (444) yields an approximate relation as

$$\overline{Q}_l^2 \approx -\mathcal{P}_l^2. \tag{445}$$

If Eqs. (432) and (433) are considered with Eq. (445), then Eq. (443) multiplied by $1/\phi_1$ can be rewritten for a large $z_2\sigma$ as

$$\frac{x^{11}}{\phi_1}+\frac{6}{\pi}\left\{\frac{Q_1^1}{x_1^1}\mathcal{P}_1^1-\frac{\pi}{3}\frac{x^{11}}{\phi_1+(\mathcal{P}_2^1/\mathcal{P}_1^1)^2\phi_2}+\frac{\phi_2}{\phi_1}\left[\frac{Q_2^1}{x_1^1}\mathcal{P}_2^1-\frac{\pi}{3}\frac{x^{11}(\mathcal{P}_2^1/\mathcal{P}_1^1)^2}{\phi_1+(\mathcal{P}_2^1/\mathcal{P}_1^1)^2\phi_2}\right]\right\}\approx 0. \tag{446}$$

ii) *No attraction between particle of species 1 and that of species 2*

If Eqs. (436)–(439) are considered, then Eq. (446) can be simplified as

$$\frac{e^{\breve{z}\sigma}}{(\breve{z}\sigma)^3}\overline{Q}_1^1\mathcal{P}_1^1 - \frac{x^{11}}{\phi_1} \approx 0. \tag{447}$$

Then, Eq. (444) allows coefficient $\overline{Q}_l^1$ to be expressed as

$$\overline{Q}_1^1 \approx -\left[1-(1+\breve{z}\sigma)e^{-\breve{z}\sigma}\right]\mathcal{P}_1^1 - \frac{\breve{d}}{\sigma}\breve{z}\sigma(\breve{z}\sigma+1)e^{-\breve{z}\sigma} \tag{448}$$

$$\overline{Q}_2^1 \approx 0. \tag{449}$$

In Eq. (447), x^{11} is given by Eq. (442). Equation (447) does not include ϕ_2, and is independent of ϕ_2.

IV. PHYSICAL CLUSTER FORMATION IN IONIC FLUIDS

An ensemble of charged particles distributed in an ionic fluid system includes both charged particles that have large relative momenta and and those with small relative momenta. Charged particles that have small relative momenta have a tendency to interact with each other via attractive Coulomb forces in the bound states. The charged particles can actively contribute to the formation of physical clusters. The distribution of the charged particles is caused to become nonuniform by the attractive Coulomb forces. Then, there is a possibility that a nonuniform distribution of charged particles have a specific pattern that is characterized as a fractal. The formation of a nonuniform distribution pattern contributes to various features that appear for an ionic fluid system. Phase separation that occurs in the ionic fluid system is caused by the contributions of attractive Coulomb forces between charged particles.[71]

The same method used for analyzing the behavior of a multicomponent nonionic fluid mixture system can be used to analyze the behavior of a multicomponent ionic fluid mixture system. The equation system composed of Eqs. (270) and (272) can be employed to analyze effects of the physical cluster formation on the properties of a multicomponent ionic fluid mixture system. The equation system are equivalent to the Ornstein–Zernike equation, which is expressed by Eq. (271).

An attractive Coulomb force causes a charged particle to interact with another charged particle that has a different type. A repulsive Coulomb force causes a charged particle to interact with another charged particle of the same type. These Coulomb forces have an extremely long-range feature. Thus, such specific features of forces that cause charged particles to interact with other charged particles require additional ideas for analyzing the physical cluster formation. Even in an ionic fluid mixture, physical clusters are formed by charged particles that interact with each other in bound states that can be caused by their small relative momenta and the attractive Coulomb forces between them. In addition, unbound states are generated depending on their large relative momenta and depending on repulsive Coulomb forces between them independently of their relative momenta.

The features of Coulomb forces allows characterizing the behavior of a multicomponent ionic fluid mixture system via the physical cluster formation. However, it is possible to identify specific behaviors that are similar to those found for multicomponent nonionic fluid

mixture systems. Unless phase separation occurs in the multicomponent ionic fluid mixture system, the macroscopic picture of the system allows charged particles with large relative momenta to be homogeneously mixed with charged particles that have small relative momenta. Then, these charged particles cannot be microscopically homogeneously mixed with each other. The branches of physical clusters can confine charged particles with large relative momenta; therefore, physical cluster growth wherein charged particles that have small relative momenta participate can affect various properties of the multicomponent ionic fluid mixture system.

A. Correlation functions for describing an $\mathcal{L}$-component ionic fluid mixture system

One of the two integral equations for analyzing an $\mathcal{L}$-component ionic fluid mixture system corresponds to Eq. (270) for the pair connectedness $\mathcal{P}_{ij}$; the other corresponds to Eq. (272) for another correlation function $\mathcal{H}_{ij}$. Analyzing an $\mathcal{L}$-component nonionic fluid mixture system is enabled via the use of the two integral equations. For the $\mathcal{L}$-component ionic fluid mixture system, the electroneutrality is required as an additional requirement; it causes the features of correlation functions including $\mathcal{P}_{ij}$ and $\mathcal{H}_{ij}$ to be different from those for the $\mathcal{L}$-component nonionic fluid mixture system. The structural features of large physical clusters formed in ionic fluids can be understood via the long-range features of $\mathcal{P}_{ij}(r)$ and $\mathcal{H}_{ij}(r) + 1$.[40,67–70]

1. Requirement of Electroneutrality

(a) *Electroneutrality*

Electroneutrality indicates that the whole charge of an $\mathcal{L}$-component ionic fluid mixture system is zero. This is based on the assumption that the whole system is electrically neutral. According to the electroneutrality of an $\mathcal{L}$-component ionic fluid mixture system, the normalization of the pair correlation function $g_{ij}(r)$ for macroscopic volume V requires $\mathcal{P}_{ij}(r)$

and $\mathcal{D}_{ij}(r)$ to satisfy

$$\sum_{j=1}^{\mathcal{L}} e_j\rho_j \int_V \mathcal{P}_{ij}(r)\mathrm{d}\mathbf{r} + \sum_{j=1}^{\mathcal{L}} e_j\rho_j \int_V \mathcal{D}_{ij}(r)\mathrm{d}\mathbf{r} + e_i = 0, \tag{450}$$

where e_i denotes the charge of species i, and e_j represents the charge of species j. Equation (450) is used for an $\mathcal{L}$-component ionic fluid mixture system, instead of Eq. (279) for an $\mathcal{L}$-component nonionic fluid mixture system.

For large r at which $g_{ij}(r) - 1 \approx 0$ is satisfied, the electroneutrality expressed by Eq. (450) means

$$\begin{aligned} 0 \approx & 4\pi \sum_{k=1}^{\mathcal{L}} e_k\rho_k \int_0^{r+\delta r} [\mathcal{P}_{ik}(t) + \mathcal{D}_{ik}(t)]t^2\mathrm{d}t + e_i \\ = & 4\pi \sum_{k=1}^{\mathcal{L}} e_k\rho_k \int_0^{r} [\mathcal{P}_{ik}(t) + \mathcal{D}_{ik}(t)]t^2\mathrm{d}t + e_i + 4\pi \sum_{k=1}^{\mathcal{L}} e_k\rho_k \int_r^{r+\delta r} [\mathcal{P}_{ik}(t) + \mathcal{D}_{ik}(t)]t^2\mathrm{d}t. \end{aligned} \tag{451}$$

Then, electroneutrality requires $4\pi \sum_{k=1}^{\mathcal{L}} e_k\rho_k \int_0^r [\mathcal{P}_{ik}(t) + \mathcal{D}_{ik}(t)]t^2\mathrm{d}t + e_i = 0$. Ultimately, the electroneutrality requires Eq. (451) to result in a relation satisfied for for a large r. The relation is expressed as

$$4\pi \sum_{k=1}^{\mathcal{L}} e_k\rho_k \mathcal{P}_{ik}(r) r^2 \delta r \approx -4\pi \sum_{k=1}^{\mathcal{L}} e_k\rho_k \mathcal{D}_{ik}(r) r^2 \delta r \quad \text{for} \quad 0 < \delta r/r \ll 1. \tag{452}$$

(b) *Behavior of correlation functions at large r*

If the value of $\sum_{k=1}^{\mathcal{L}} e_k\rho_k \mathcal{P}_{ik}(r)$ is equal to q, Eq. (452) requires $\sum_{k=1}^{\mathcal{L}} e_k\rho_k \mathcal{D}_{ik}(r)$ to be equal to $-q$. This is, the absolute value of the charge carried by a group of particles contributing to the magnitude of $\mathcal{P}_{ik}$ is equal to the absolute value of the charge carried by a group of particles contributing to the magnitude of $\mathcal{D}_{ik}$. The pair connectedness $\mathcal{P}_{ik}$ represents the contribution of particle pairs characterized as pair particles that interact in bound states wherein the contribution of an attractive force between the pair particles exceeds that of their relative kinetic energy; further it represents the correlation between particles involved in the formation of physical clusters. The case that q is not zero means that physical clusters have charges on average. However, the physical clusters should maintain no charges on average, if an increase in the densities of particles allows physical clusters to grow readily. Further, causing physical cluster to grow without difficulty requires that q be

equal to zero. Therefore, Eq. (452), which represents the requirement of the electroneutrality results in an assumption is given as

$$\sum_{k=1}^{\mathcal{L}} e_k \rho_k \mathcal{P}_{ik}(r) \approx 0 \quad \text{for} \quad 1 \ll r \tag{453}$$

and

$$\sum_{k=1}^{\mathcal{L}} e_k \rho_k \mathcal{D}_{ik}(r) \approx 0 \quad \text{for} \quad 1 \ll r. \tag{454}$$

When two particles located at $\mathbf{r}_1^{(i)}$ and $\mathbf{r}_2^{(j)}$ in a fluid system are widely separated, the pair correlation function that expresses a correlation between these particles behaves[2] as $g_{ij}(|\mathbf{r}_1^{(i)} - \mathbf{r}_2^{(j)}|) \approx 1$. This fact requires the physical meanings of $\mathcal{P}_{ij}(r)$ and those of $\mathcal{D}_{ij}(r)$ to result in

$$\begin{cases} \mathcal{P}_{ij}(r) \approx 0 & \text{for} \quad 1 \ll r \\ \mathcal{D}_{ij}(r) \approx 1 & \text{for} \quad 1 \ll r, \end{cases} \tag{455}$$

because of Eq. (260). This consequence is wholly adequate if the state of an ionic fluid is far from a state wherein the percolation of physical clusters occur in a macroscopic volume.

The relations expressed by Eq. (455) allows the assumption given by Eqs. (453) and (454) to be satisfied for a large r without physical clusters inducing the percolation. If physical clusters with macroscopic sizes caused by the percolation are included in an ionic fluid, $\mathcal{P}_{ij}(r) \neq 0$ and $\mathcal{D}_{ij}(r) \neq 1$ can be satisfied for a large r despite $\mathcal{P}_{ij}(r) + \mathcal{D}_{ij}(r) \approx 1$. Yet, the assumption given as Eqs. (453) and (454) is satisfied at a large r if each physical cluster is electrically neutral.

If the growth of large charged physical clusters allows the percolation of the physical clusters to occur in a macroscopic volume, it is possible to assume

$$\begin{cases} \sum_{k=1}^{\mathcal{L}} e_k \rho_k \mathcal{P}_{ik}(r) \neq 0 \\ \sum_{k=1}^{\mathcal{L}} e_k \rho_k \mathcal{H}_{ik}(r) \neq 0. \end{cases}$$

Even if it is possible, the electrical repulsion allows charged physical clusters to be expanded. The electrical repulsion requires the charged physical clusters to be unstable, and therefore, it should be reasonable to assume Eqs. (453) and (454).

2. Features of correlation functions for multicomponent ionic fluid mixture system

(a) *System without percolation of physical clusters*

The mean size $\mathcal{S}$ of physical clusters estimated by Eq. (281) should be sufficiently independent of V, if the percolation of physical clusters does not occur in macroscopic V found in an $\mathcal{L}$-component ionic fluid mixture system. In the limit $V \to \infty$, the independence of $\mathcal{S}$ from V allows Eq. (281) to result in

$$\begin{cases} \lim_{V\to\infty}[(\mathcal{S}-1)/V]\sum_{k=1}^{\mathcal{L}}\rho_k = 0 \\ \lim_{V\to\infty}(1/V)\int_V \mathcal{P}_{ij}(r)d\mathbf{r} = 0. \end{cases}$$

This corresponds to Eq. (282).

In the limit $V \to \infty$, Eq. (282) requires Eq. (450) to result in the normalization condition for $\mathcal{D}_{ij}$. It is given as

$$\sum_{j=1}^{\mathcal{L}} e_j\rho_j \int_V \mathcal{D}_{ij}(r)\mathrm{d}\mathbf{r} = -e_i. \tag{456}$$

Instead of Eq. (283), Eq. (456) must be applied for the $\mathcal{L}$-component ionic fluid mixture system.

(b) *System involving percolation of physical clusters*

If the percolation of physical clusters occurs in macroscopic V found in an ionic fluid system, $\mathcal{S}$ estimated for the ionic fluid system by Eq. (281) should be dependent on V. Then, $[(\mathcal{S}-1)/V]\sum_{k=1}^{\mathcal{L}}\rho_k \neq 0$ should be satisfied. If a state of the ionic fluid is in the immediate vicinity of a liquid-solid transition point where $0 < \rho_i^{sd} - \rho_i^{lq} \ll 1$ (ρ_i^{sd} denotes ρ_i in a solid state, and ρ_i^{lq} denotes ρ_i in a liquid state which can be transformed into the solid state) is satisfied, the dependence of $\mathcal{S}$ on V can be estimated as

$$\mathcal{S}/V \approx \sum_{i=1}^{\mathcal{L}} \rho_i^{sd}$$

which corresponds to a state wherein the growth of physical clusters reaches the limit. Then, Eq. (281) should result in

$$(1/V)\sum_{i=1}^{\mathcal{L}}\sum_{j=1}^{\mathcal{L}}\rho_i\rho_j\int_V \mathcal{P}_{ij}(r)\mathrm{d}\mathbf{r} \approx \sum_{i=1}^{\mathcal{L}}\rho_i^{sd}\sum_{k=1}^{\mathcal{L}}\rho_k.$$

This consequence requires $(1/V)\int_V \mathcal{P}_{ij}(r)\mathrm{d}\mathbf{r} \approx 1$ to be satisfied in the limit $V \to \infty$. Therefore, it requires Eq. (450) to result in

$$\begin{cases} (1/V)\int_V \mathcal{D}_{ij}(r)\mathrm{d}\mathbf{r} \approx 0 \\ \sum_{j=1}^{\mathcal{L}} e_j\rho_j \int_V \mathcal{P}_{ij}(r)\mathrm{d}\mathbf{r} = -e_i. \end{cases}$$

A state specified by $(1/V)\int_V \mathcal{D}_{ij}(r)\mathrm{d}\mathbf{r} \approx 0$ should considerably lack particle pairs characterized as an ensemble of pair particles interacting in unbound states wherein a contribution of the relative kinetic energy of the pair particles exceeds a contribution of an attractive force between them. The lack of the particle pairs allows a feature found as a liquid to be lost from the ionic fluid system. The growth of physical clusters must allow the phase transition from the liquid state of an ionic fluid to the solid state.

B. Various phenomena depending on physical cluster formation in ionic fluids

(a) *Physical clusters of charged particles formed in ionic fluids*

The Coulomb force, which is an extremely long-range attractive force between positive and negative charged particles, can efficiently contribute to enhancing density fluctuations in an ionic fluid system. It has the capability to make the distribution of charged particles become nonuniform. The nonuniform distribution of charged particles developed by attractive Coulomb forces among them allow phase separation to occur in the ionic fluid system.[71]

In an ionic fluid system, charged particles with small relative momenta are distributed with those that have large relative momenta. The charged particles with small relative momenta can contribute to physical cluster formation because their small relative momenta enhance the possibility that the contribution of the attractive Coulomb force between a positively charged particle and a negatively charged particle exceed the contribution of their relative kinetic energy.

The Bjerrum theory based on the ion pair model[76] can allow a discussion of the critical thermodynamics of an ionic fluid to result in a satisfactory description for the ionic fluid.[18] However, the ionic cluster model beyond the ion pair model based on the Bjerrum theory need to allow the thermodynamics of ionic fluids to be estimated more precisely.[50,51] Several features of the ionic fluid should be caused by the cooperating effect of many charged particles. Hence, it is significant to consider the fact that the distribution of charged particles in an ionic fluid have the strong tendency to become nonuniform. The precise estimate of the thermodynamics of ionic fluids[51] indicates that an ionic cluster model beyond the ion pair model need to be considered.[75]

A numerical calculation allows the estimation of the mean size of ionic clusters formed in an ionic fluid.[79] The physical clusters, which can be easily formed by charged particles with small relative momenta, can grow as the densities of the charged particles increase. If the physical clusters reaches extremely large sizes, then the features of an ionic fluid are influenced by the physical clusters.[77,78] Large physical clusters of charged particles formed in an ionic fluid influence the viscosity of the ionic fluid. A viscosity anomaly is detected near the critical consolute point of an ionic ethylammonium nitrate-n-octanol mixture.[77] This is evidence of the formation of large physical clusters.

(b) *Electrical conductivity in ionic fluid*

If pair-charged particles interact with each other in the bound state, they cannot freely migrate away from each other even when an external electric field is applied. If the free charged particles that can freely migrate decrease in an ionic fluid despite the increase in the densities of the charged particles, the contribution of the free charged particles to the electrical conductivity will decrease. An increase in the densities of charged particles can make the physical clusters of charged particles grow via the process of cluster–cluster aggregation in the ionic fluid. If physical clusters of charged particles percolate,[80] physical clusters that have macroscopic sizes can effectively contribute to the electrical transport as paths for the electric current. The contribution of the physical clusters to the electric current can be generated by only a small shift in each charged particle caused by the external electric field. As the densities of charged particles increase, the percolation state is developed, and the electrical conductivity should be enhanced. As the densities of charged particles increase from a sufficiently low level, the electrical conductivity of an ionic fluid can decrease; after reaching a minimum, the electrical conductivity can increase. This behavior of electrical conductivity can be experimentally demonstrated.[78] The behavior of the electrical conductivity can become evidence of the formation of physical clusters that have macroscopic sizes.

1. Fractal structures of physical clusters formed in ionic fluids

(a) *Estimates of pair correlation functions*

The feature of an attractive Coulomb force via which a positively charged particle and negatively charged particle effectively interact with each other can differ depending on whether charged particles are distributed near the two charged particles. Within an ionic fluid system, a feature of the effective interaction between two charged particles surrounded by other charged particles is assumed to have a shorter range than that without contributions from other charged particles.

A pair correlation function exhibits the possibility that pair-charged particles are located at a specific configuration in an ionic fluid, and it involves contributions from charged particles distributed near the pair-charged particles. The estimate of pair correlation functions

can aid in examining the effects of the contributions of charged particles distributed near particular pair-charged particles in an ionic fluid; further, it can aid in examining specific configurations of charged particles on a large extent scale.[67–70,80] The magnitude of a pair correlation function is decreased with the increase in a large distance r between specific pair-charged particles. Under several conditions, the long-range features of pair correlation functions can be expressed as the product of r^{-1} and a particular function expressed by a Taylor series with respect to r.[15,16]

(b) *Fractal structures of physical clusters*

If the developed physical clusters of charged particles are formed in an ionic fluid, then there is a possibility that the structure of each physical cluster has a specific pattern characterized as a fractal. The formation of physical clusters with a fractal structure causes the dependence of a pair correlation function on r to deviate from that expressed as the product of r^{-1} and a particular function expressed by a Taylor series with respect to r. This is implied from examples in ionic fluid systems wherein charged colloidal particles are suspended.

In ionic fluid systems wherein charged colloidal particles are suspended, charged colloidal particles are not distributed homogeneously.[67–70] Electrostatic interactions between charged colloidal particles cause their nonuniform distributions to occur. According to numerical simulations, nonuniform distributions of charged particles have fractal structures.[72] The fractal structures depend on the densities of charged colloidal particles.[73] According to the experiments for ionic fluids wherein charged colloidal particles are suspended, the nonuniform distributions of charged colloidal particles have various fractal structures.[74] Further, the growth of physical clusters of charged colloidal particles can induce gelation with a fractal structure.[70]

The growth process of physical clusters caused by the contact of small physical clusters corresponds to a growth process known as cluster–cluster aggregation that results in the fractal structure with the fractal dimension d_f determined as $d_f \sim 1.75$.[40] This fact and the numerical simulations[72] support the possibility that a nonuniform distribution of charged colloidal particles in a suspension has a fractal structure with the fractal dimension d_f expressed as $d_f < 2$.[67–70]. Hence, a nonuniform distribution of charged particles, which can considerably affect the properties of an ionic fluid, should have a particular structure

characterized by pair correlation functions involving a contribution of the factor r^{d_f-3} ($d_f < 2$).[40,72]

2. Correlation functions for examining effects of physical cluster formation

Attractive Coulomb forces via which charged particles comprising an ionic fluid system interact with each other, allow the distribution of charged particles to become inhomogeneous. Charged particle pairs contributing to the magnitude of the pair connectedness $\mathcal{P}_{ij}$ belong to a group of charged particle pairs characterized by particles that have small relative momenta. Then, charged particles forming each pair interact in bound states where the contribution of an attractive Coulomb force between the pair charged particles exceeds the contribution of their relative kinetic energy. Charged particle pairs contributing to the magnitude of $\mathcal{D}_{ij}$ belong to the other group of particle pairs characterized by particles that have large relative momenta. Then, the charged particles that form each pair interact with each other in unbound states where the contribution of the relative kinetic energy of the pair charged particles exceeds the contribution of the attractive Coulomb force between them. The attractive Coulomb forces cannot allow charged particles belonging to the former group to be homogeneously mixed with those belonging to the latter group. Charged particles contributing to the magnitude of $\mathcal{D}_{ij}$ have a tendency to be confined in local areas surrounded by charged particles contributing to the magnitude of $\mathcal{P}_{ij}$.[49,80]

Equation (453) indicates that the electroneutrality is maintained for each physical cluster of charged particles. Electroneutrality enables each physical cluster to grow toward macroscopic sizes. According to the above examples of charged colloidal particles, each physical cluster of charged particles formed in an ionic fluid can have a fractal structure. Then, the dependence of a pair correlation function on r deviates from a form expressed as the product of r^{-1} and a particular function given as a Taylor series with respect to r.

The pair correlation function g_{ij} related to a charged particle of species i and another charged particle of species j is equivalent to the sum of the pair connectedness $\mathcal{P}_{ij}$ and another correlation function $\mathcal{D}_{ij}$. The structure of each physical cluster of charged particles is characterized by $\mathcal{P}_{ij}$. The dependence of $\mathcal{P}_{ij}$ on r should not have a form expressed as the product of r^{-1} and a particular function given as a Taylor series with respect to r, according to an example found from analyzing a non-ionic fluid.[47] A consequence obtained

from analyzing ionic fluids demonstrates that the dependence of $\mathcal{P}_{ij}$ on r does not have the form.[49] A differential equation for $\mathcal{P}_{ij}$ can be derived from the integral equation expressed by Eq. (270) being relevant to $\mathcal{P}_{ij}$. The differential equation corresponds to Eq. (154) for a single-component fluid. The pair connectedness $\mathcal{P}_{ij}$ obtained as a solution from the differential equation has a specific form that is different from that expressed as the product of r^{-1} and a particular function given as a Taylor series with respect to r.

C. Closure schemes for two integral equations

1. Approximate features of correlation functions due to ionic fluid mixture

(a) *Behavior of $C_{ij}^{+}(r)$ for $\beta u_{ij} < 0$ in $\mathcal{L}$-component ionic fluid mixture system*

The behavior of $C_{ij}^{+}(r)$ at $1 \ll r/\sigma_{ij}$ in an $\mathcal{L}$-component ionic fluid mixture system is equivalent to that expressed by Eq. (294) if $\beta u_{ij} < 0$. Thus, the behavior of $C_{ij}^{+}(r)$ caused by $\beta u_{ij} < 0$ allows a closure scheme for solving the integral equation given by Eq. (270) to be given by Eqs. (299) and (300). The closure scheme for solving the integral equation for the $\mathcal{L}$-component ionic fluid mixture system is given as

$$C_{ij}^{+}(r) = C_{ij}^{0+}(r) + \frac{4}{3\sqrt{\pi}}[-\beta u_{ij}(r)]^{3/2}, \quad \text{for} \quad \beta u_{ij} < 0,$$

and

$$C_{ij}^{0+}(r) = 0, \qquad \text{for} \quad r > \sigma_{ij}.$$

(b) *Behavior of $C_{il}^{+}(r)$ for $\beta u_{il} > 0$ and $1 \ll r/\sigma_{il}$*

i) *Behavior of $C_{il}^{+}(r)$ in $\mathcal{L}$-component ionic fluid mixture system*

For $\beta u_{il} > 0$, $\mathcal{P}_{il}(r)$ is equal to zero unless the contributions of both $\beta u_{il} > 0$ and $\beta u_{jl} > 0$ coexist at a large r. In an ionic fluid mixture system, a j particle that attracts both i and l particles by the Coulomb force coexists. Thus, $\mathcal{P}_{il}(r) \neq 0$ occurs for $\beta u_{il} > 0$. A physical cluster can grow via a particle corresponding to the j particle that satisfies $\beta u_{ij}(r) < 0$ $(i \neq j)$ and $\beta u_{jl}(r) < 0$ $(j \neq l)$. When the distance r between i and l is sufficiently large, Eq. (290) can be approximated as

$$\beta u_{il}\Big[\mathcal{P}_{il}(r) - C_{il}^{+}(r)\Big] + C_{il}^{+}(r) \approx 0, \quad \text{for} \quad \beta u_{il}(r) > 0.$$

For $1 \ll r/\sigma_{il}$, this relation must be satisfied. Then, the dependence of $\beta u_{il}\mathcal{P}_{il}(r)$ on r should be the same as that of $-C_{il}^{+}(r)$ on r. Thus, an approximate formula for $1 \ll r/\sigma_{il}$ can be simplified as

$$\beta u_{il}\mathcal{P}_{il}(r) \approx -C_{il}^{+}(r), \quad \text{for} \quad \beta u_{il}(r) > 0. \tag{457}$$

By substituting Eq. (457) into Eq. (453), the behavior of $C_{il}^{+}(r)$ caused by the Coulomb potential that satisfies $\beta u_{il} > 0$ is estimated as

$$\sum_{\substack{l \\ \text{for } u_{il}>0}} \frac{e_l \rho_l}{\beta u_{il}(r)} C_{il}^{+}(r) \approx \sum_{\substack{k \\ \text{for } u_{ik}<0}} e_k \rho_k \mathcal{P}_{ik}(r), \qquad \text{for } r/\sigma_{il} \gg 1. \tag{458}$$

According to Eq. (296), a long-range contribution to $\mathcal{P}_{ij}(r)$ should be expressed as $\mathcal{P}_{ij}(r) \approx [22/(15\sqrt{\pi})][-\beta u_{ij}(r)]^{3/2}$ for $\beta u_{ij} < 0$. The use of this long- range contribution allows Eq. (458) to be rewritten as

$$\sum_{\substack{l \\ \text{for } u_{il}>0}} \frac{e_l \rho_l}{\beta u_{il}(r)} C_{il}^{+}(r) \approx \sum_{\substack{k \\ \text{for } u_{ik}<0}} e_k \rho_k \frac{22}{15\sqrt{\pi}} [-\beta u_{ik}(r)]^{3/2}, \qquad \text{for } r/\sigma_{il} \gg 1. \tag{459}$$

Therefore, this result and analogy with the MSA should allow the behavior of $C_{il}^{+}(r)$ to be approximately expressed as

$$\sum_{\substack{l \\ \text{as } u_{il}>0}} \frac{e_l \rho_l}{\beta u_{il}(r)} \left[C_{il}^{+}(r) - C_{il}^{0+}(r) \right] = \sum_{\substack{k \\ \text{as } u_{ik}<0}} e_k \rho_k \frac{22}{15\sqrt{\pi}} [-\beta u_{ik}(r)]^{3/2}, \tag{460}$$

and

$$C_{il}^{0+}(r) = 0, \qquad \text{for } r > \sigma_{il}. \tag{461}$$

If the Heaviside step function $\theta(x) = 0\ (x < 0),\ 1\ (x > 0)$ is used, Eq. (460) can be rewritten as a specific form that can be mathematically readily treated, i.e.,

$$\begin{aligned} &\sum_{l=1}^{\mathcal{L}} \frac{e_l \rho_l}{\beta u_{il}(r)} \theta\left[\beta u_{il}(r)\right] \left[C_{il}^{+}(r) - C_{il}^{0+}(r) \right] \\ &\quad = \sum_{k=1}^{\mathcal{L}} e_k \rho_k \frac{22}{15\sqrt{\pi}} \left\{ 1 - \theta\left[\beta u_{ik}(r)\right] \right\} \left[-\beta u_{ik}(r)\right]^{3/2}. \end{aligned} \tag{462}$$

ii) *Behavior of $C_{il}^{+}(r)$ in two-component ionic fluid mixture system*

If an ionic fluid is a two-component mixture ($\mathcal{L} = 2$), $e_j \rho_j / (e_i \rho_i) = -1\ (i \neq j)$ is satisfied. Then, Eq. (460) is simplified as

$$C_{ii}^{+}(r) = C_{ii}^{0+}(r) - \frac{22}{15\sqrt{\pi}} \beta u_{ii}(r) [-\beta u_{ij}(r)]^{3/2}, \quad \text{for} \quad \beta u_{ij} < 0, \tag{463}$$

and

$$C_{ii}^{0+}(r) = 0, \qquad \text{for } r > \sigma_{ii}. \tag{464}$$

If this expression for $C_{ii}^{+}(r)$ is a closure scheme for the integral equation given by Eq. (270), the closure scheme allows Eq. (270) to be readily solved.

Moreover, for $\mathcal{L} = 2$, Eqs. (299) and (463) allow the long-range contribution to $C_{ij}^{+}(r)$ to be expressed as

$$C_{ij}^{+}(r) \approx K_{ij}^{+} \frac{1}{r^{5/2-|i-j|}} \quad \text{for} \quad r/\sigma_{ij} \gg 1 \quad (i = 1, 2; \;\; j = 1, 2), \tag{465}$$

where

$$K_{ij}^{+} \equiv \frac{1}{\sqrt{\pi}} \left(\frac{4}{3}\right)^{|i-j|} \left(-\frac{22}{15} \frac{\beta e_i e_i}{4\pi\epsilon}\right)^{1-|i-j|} \left(\frac{-\beta e_i e_{\mu_i}}{4\pi\epsilon}\right)^{3/2}, \quad (\mu_i = 2^{2-i}). \tag{466}$$

Here, ϵ denotes the macroscopic dielectric constant of the medium wherein charged particles are distributed. Equation (465) is applicable to both the case of $\beta u_{ij} < 0$ and the case of $\beta u_{ij} > 0$.

(c) *Behavior of C_{ij}^{*} for $1 \ll r/\sigma_{ij}$ in $\mathcal{L}$-component ionic fluid mixture system*

Features of $C_{ij}^{*}(r)$ in the case of $u_{ij} < 0 \quad (i \neq j)$ is caused by the contribution of the group of charged particles characterized as each pair of charged particles interacting with each other in unbound states wherein the contribution of their relative kinetic energy exceeds the contribution of the attractive Coulomb force between them. Further, features of $C_{ij}^{*}(r)$ in the case of $0 \leq u_{ij}$ is caused by the contribution of the group of charged particles characterized as each pair of charged particles interacting with each other via the repulsive Coulomb force between them. Then, the behavior of $C_{ij}^{*}(r)$ can be simply estimated for a large r.

According to Eq. (297), $\mathcal{D}_{ij}(r) - 1 \approx -(1/2)\beta u_{ij}(r)$ is satisfied for $1 \ll r/\sigma_{ij}$ in two cases, i.e., $0 \leq u_{ij}$ and $u_{ij} < 0$. Further, according to Eq. (298), $C_{ij}^{*}(r) \approx -\beta u_{ij}(r)$ is satisfied for $1 \ll r/\sigma_{ij}$ in the two cases, i.e., $0 \leq u_{ij}$ and $u_{ij} < 0$. Thus, Eq. (298) represents the long-range contribution of $C_{ij}^{*}(r)$ for an $\mathcal{L}$-component ionic fluid mixture system in the two cases specified by $\beta u_{ij} < 0$ and $\beta u_{ij} > 0$.

An integral equation for $\mathcal{H}_{ij}(r)$ applied to the $\mathcal{L}$-component ionic fluid mixture system is equivalent to Eq. (272) derived for an $\mathcal{L}$-component nonionic fluid mixture system. According to the above discussion, an analogy with the MSA allows Eq. (302) to become a closure scheme for solving the integral equation when $\beta u_{ij} < 0$ and $\beta u_{ij} > 0$. Thus, the closure

scheme is expressed as

$$C_{ij}^{*}(r) = C_{ij}^{0*}(r) - \beta u_{ij}(r), \qquad \text{for } \beta u_{ij} < 0 \text{ and } \beta u_{ij} > 0, \tag{467}$$

where

$$C_{ij}^{0*}(r) = 0, \qquad \text{for } r > \sigma_{ij}. \tag{468}$$

Then, the long-range contribution to $C_{ij}^{*}(r)$ in terms of $-\beta u_{ij}(r)$ can be expressed as

$$C_{ij}^{*}(r) \approx K_{ij}^{*}\frac{1}{r} \quad \text{for} \quad r/\sigma_{ij} \gg 1, \tag{469}$$

where

$$K_{ij}^{*} \equiv -\frac{\beta e_i e_j}{4\pi\epsilon}. \tag{470}$$

Moreover, relations formed by Eqs. (299), (300), (460), (461), (467), and (468) can be consistent with the MSA because $c_{ij} = C_{ij}^{+} + C_{ij}^{*}$ given in Eq. (269) behaves as $c_{ij} \approx C_{ij}^{*}$ for a large r.

2. Expression of practical closure schemes similar to MSA

(a) *Closure scheme for solving Ornstein–Zernike equation in $\mathcal{L}$-component ionic fluid mixture system*

To avoid a mathematical difficulty caused by $\kappa = 0$, the contribution of the Coulomb potential to the closure scheme is regarded as a Yukawa potential type that have the effective range expressed by $0 < \kappa^{-1} < \infty$ although κ^{-1} is sufficiently large.[82] Then, the MSA allows a closure scheme for solving the Ornstein–Zernike equation to be given as

$$\begin{cases} c_{ij}(r) = c_{ij}^{0}(r) + K_{ij}e^{-\kappa r}/r, & \text{for} \quad 0 \le \kappa \ll 1 \\ c_{ij}^{0}(r) = 0, & \text{for} \quad r/\sigma_{ij} > 1, \end{cases} \tag{471}$$

where

$$\begin{cases} K_{ij} \equiv \beta\mathcal{K}_{ij} \\ \beta\mathcal{K}_{ij} \equiv -(\alpha_0^2/4\pi)(e_i/e_0)(e_j/e_0) \\ \alpha_0^2 \equiv \beta e_0^2/\epsilon. \end{cases} \tag{472}$$

Here, e_0 represents the elementary charge and K_{ij} is equivalent to K^*_{ij}.

(b) *Closure scheme for solving Eq. (270) in two-component ionic fluid mixture system*

i) *Closure scheme for solving Eq. (270)*

Equation (471) requires the long-range contribution expressed by Eq. (465) to involve a factor $e^{-\kappa r}$. Thus, the closure scheme given for the Ornstein–Zernike equation as Eq. (471) requires a closure scheme for solving the integral equation given by Eq. (270) to be given as

$$C^{+}_{ij}(r) = C^{0+}_{ij}(r) + K^{+}_{ij}\left(\frac{e^{-\kappa r}}{r}\right)^{5/2-|i-j|}, \quad (i=1,2;\ \ j=1,2), \tag{473}$$

where

$$C^{0+}_{ij}(r) = 0, \qquad \text{for } r > \sigma_{ij}. \tag{474}$$

Instead of using the long-range contribution expressed by Eq. (465), a long-range contribution involving a factor $e^{-\kappa r}$ is applied to the closure scheme for solving Eq. (270).

ii) *Practical closure scheme for solving Eq. (270)*

An approximate expression for the factor $(1/r)^{\hat{n}/2}$ $(\hat{n}=3,5)$ in Eq. (473) can be given by Eq. (83). The approximate expression enables mathematical difficulty caused by $(1/r)^{\hat{n}/2}$ to be avoided when solving Eq. (270) analytically. According to Eq. (83), the approximate expression is given as

$$\frac{1}{r^{\hat{n}/2}} \approx (\sigma_{ij})^{-\hat{n}/2+1}\exp[f_\nu]\exp[-(f_\nu/\sigma_{ij})r]\frac{1}{r}, \quad \hat{n}\equiv 2n+1, \quad (n=1,\ 2). \tag{475}$$

In this expression, the value of f_ν should satisfy $0 < f_\nu \leq 1/2$. Despite this, Eq. (84) allows the value of f_ν to be reasonably determined. Thus, Eq. (85) allows its value for $\hat{n}=3$ to be expressed as $f_\nu \approx f_{\nu_{3/2}}$, which is given by $f_{\nu_{3/2}} = 0.1018532115$. Similarly, Eq. (85) allows its value for $\hat{n}=5$ to be expressed as $f_\nu \approx f_{\nu_{5/2}}$, which is given by $f_{\nu_{5/2}} = 0.8457924344$.

The approximate expression of Eq. (475) depends on diameters of hard cores of particles. If an approximate relation between $\phi(r) = 1/r^{\hat{n}/2}$ and $\overline{\phi}(r) = \zeta_{z_n}e^{-\alpha_{z_n}r}/r$ with two unknown coefficients (ζ_{z_n} and α_{z_n}) is formed independently of diameters of hard cores of particles, then it is easy to proceed to calculate for considering a condition $0 < \kappa\sigma_{ij} \ll 1$. Hence, the two unknown coefficients ζ_{z_n} and α_{z_n} are determined using the following relation:

(1) $\phi(r_1) = \overline{\phi}(r_1)$ and $\phi(r_2) = \overline{\phi}(r_2)$ for $r_1 < r_2$,

(2) assumption: $r_2 = 1/z_n \ \ (n = 1,\ 2)$ with $z_n = \hat{n}\kappa/2 \ \ (\hat{n} \equiv 2n + 1)$,

(3) $I(\hat{\eta} r_1) = \overline{I}(\hat{\eta} r_1) \ \ (0 < \hat{\eta} < 1)$ with $I(\hat{\eta} r_1) \equiv \int_{\hat{\eta} r_1}^{\infty} \phi(r) \mathrm{d}r$ and $\overline{I}(\hat{\eta} r_1) \equiv \int_{\hat{\eta} r_1}^{\infty} \overline{\phi}(r) \mathrm{d}r$.

The above relations allows the following formulae to be obtained:

$$0 = -1 + (\hat{n}/2 - 1)\hat{\eta}^{\hat{n}/2-1} (z_n r_1)^{z_n r_1 (\hat{n}/2-1)/(z_n r_1 - 1)} \mathrm{Ei}\left[-\hat{\eta} z_n r_1 \frac{\hat{n}/2 - 1}{z_n r_1 - 1} \ln(z_n r_1) \right], \tag{476}$$

$$\alpha_{z_n} = z_n \frac{\hat{n}/2 - 1}{z_n r_1 - 1} \ln(z_n r_1), \tag{477}$$

$$\zeta_{z_n} = (z_n)^{\hat{n}/2-1} \exp\left(\frac{\alpha_{z_n}}{z_n} \right). \tag{478}$$

If $\hat{n}$, $\hat{\eta}$, and z_n are given, then r_1, α_{z_n}, and ζ_{z_n} are assessed from the above formulae. When z_n is required to sufficiently approach zero, α_{z_n} given by Eq. (477) approaches zero, i.e., $\lim_{\kappa \to 0} \alpha_{z_n} = 0$.

Thus, a practical closure scheme is given as

$$\begin{cases} C_{ij}^{+}(r) = C_{ij}^{0+}(r) + \sum_{n=1}^{2} K_{ij}^{n} \exp(-\breve{z}_n r)/r, \quad (i = 1, 2;\ \ j = 1, 2), \\ C_{ij}^{0+}(r) = 0 \ \ (r/\sigma_{ij} > 1), \end{cases} \tag{479}$$

where

$$K_{ij}^{1} \equiv \frac{4}{3\sqrt{\pi}} (\beta \mathcal{K}_{ij})^{3/2} \zeta_{z_1}, \quad (i \neq j) \tag{480}$$

$$K_{ij}^{2} \equiv 0, \quad (i \neq j) \tag{481}$$

$$K_{ii}^{1} \equiv 0, \tag{482}$$

$$K_{ii}^{2} \equiv \frac{22}{15\sqrt{\pi}} (\beta \mathcal{K}_{ii})(\beta \mathcal{K}_{ij})^{3/2} \zeta_{z_2}, \quad (i \neq j) \tag{483}$$

$$\beta \mathcal{K}_{ij} = \beta \mathcal{K}_{ji}, \tag{484}$$

and

$$\breve{z}_1 \equiv (3/2)\kappa + \alpha_{z_1}, \quad (\lim_{\kappa \to 0} \alpha_{z_1} = 0) \tag{485}$$

$$\breve{z}_2 \equiv (5/2)\kappa + \alpha_{z_2}, \quad (\lim_{\kappa \to 0} \alpha_{z_2} = 0). \tag{486}$$

(c) *Closure scheme for solving Eq. (272) in $\mathcal{L}$-component ionic fluid mixture system*

Equation (471) requires the long-range contribution expressed by Eq. (469) to involve a factor $e^{-\kappa r}$. Thus, the closure scheme given for the Ornstein–Zernike equation as Eq. (471) requires a closure scheme for solving the integral equation given by Eq. (272) to be given as

$$C_{ij}^{*}(r) = C_{ij}^{0*}(r) + K_{ij}^{*} \frac{e^{-\kappa r}}{r}, \tag{487}$$

where

$$C_{ij}^{0*}(r) = 0, \qquad \text{for } r > \sigma_{ij}. \tag{488}$$

The closure scheme given by Eq. (487) is applicable both when $\beta u_{ij} < 0$ and when $\beta u_{ij} > 0$.

3. Solution of integral equation

Equation (270) and the practical closure scheme given by Eq. (479) result in an integral equation that can be solved analytically. If the consequences given by Eqs. (320)−(343) are used, a solution for the integral equation can be summarized as

$$\sum_{k=1}^{2} \widetilde{Q}_{ki}^{+(-1)}(-k)\widetilde{Q}_{jk}^{+}(-k) = \delta_{ij}, \quad \delta_{ii} = 1; \ \ \delta_{ij} = 0 \ \ (i \neq j), \tag{489}$$

$$\widetilde{Q}_{ij}^{+}(k) \equiv \delta_{ij} - (\rho_i \rho_j)^{1/2} \widehat{Q}_{ij}^{+}(-ik), \tag{490}$$

$$\widehat{Q}_{ij}^{+}(ik) \equiv \int_{\lambda_{ji}}^{\infty} e^{-ikr'} Q_{ij}^{+}(r') \mathrm{d}r', \tag{491}$$

$$Q_{ij}^{+}(r') = Q_{ij}^{+0}(r') + \sum_{n=1}^{2} D_{ij}^{n} e^{-\breve{z}_n r'}, \quad (\lambda_{ji} < r' < \sigma_{ji}), \tag{492}$$

$$Q_{ij}^{+}(r') = \sum_{n=1}^{2} D_{ij}^{n} e^{-\breve{z}_n r'}, \quad (\sigma_{ji} \leq r'), \tag{493}$$

$$Q_{ij}^{+0}(r') = 0, \quad (\sigma_{ji} \leq r'), \tag{494}$$

$$\widehat{Q}_{ij}^{+}(ik) = \sum_{m=1}^{2} \left[C_{ij}^{m} e^{-ik\lambda_{ji}} e^{-\breve{z}_m \sigma_{ji}} \left(\frac{e^{\breve{z}_m \sigma_j} - e^{-ik\sigma_j}}{ik + \breve{z}_m} - \frac{1 - e^{-ik\sigma_j}}{ik} \right) + \frac{1}{ik + \breve{z}_m} D_{ij}^{m} e^{-\breve{z}_m \lambda_{ji}} e^{-ik\lambda_{ji}} \right], \tag{495}$$

$$C_{ij}^{m} \equiv -D_{ij}^{n} + 2\pi \sum_{k=1}^{2} (\rho_k / \breve{z}_n) \widehat{\mathcal{P}}_{ik}(\breve{z}_n) D_{kj}^{n}, \tag{496}$$

$$\widehat{\mathcal{P}}_{ij}(\breve{z}_n) \equiv \int_{0}^{\infty} \mathcal{P}_{ij}(t) e^{-\breve{z}_n t} t \mathrm{d}t. \tag{497}$$

Here, $\lambda_{ji} \equiv \frac{1}{2}(\sigma_j - \sigma_i)$ and $\sigma_{ji} \equiv \frac{1}{2}(\sigma_j + \sigma_i)$.

Two relations need between $\widehat{\mathcal{P}}_{ij}(\breve{z}_n)$ and D^n_{ij}; one is given as

$$\begin{aligned}2\pi\widehat{\mathcal{P}}_{ij}(\breve{z}_n) =&\sum_{m=1}^{2}\frac{\breve{z}_m}{\breve{z}_n+\breve{z}_m}e^{-(\breve{z}_n+\breve{z}_m)\sigma_{ij}}\left(D^m_{ij}-2\pi\sum_{k=1}^{2}\frac{\rho_k}{\breve{z}_m}\widehat{\mathcal{P}}_{ik}(\breve{z}_m)D^m_{kj}\right)\\&+2\pi\sum_{k=1}^{2}\rho_k\widehat{\mathcal{P}}_{ik}(\breve{z}_n)e^{-\breve{z}_n\lambda_{jk}}\sum_{m=1}^{2}\Bigg\{e^{-\breve{z}_m\sigma_{jk}}D^m_{kj}\Big(\frac{e^{-\breve{z}_n\sigma_k}}{\breve{z}_n+\breve{z}_m}+\frac{1-e^{-\breve{z}_n\sigma_k}}{\breve{z}_n}\Big)\\&+\sum_{l=1}^{2}\frac{2\pi\rho_l}{\breve{z}_m}\widehat{\mathcal{P}}_{kl}(\breve{z}_m)D^m_{lj}\Bigg[\frac{e^{-\breve{z}_m\lambda_{jk}}}{\breve{z}_n+\breve{z}_m}-e^{-\breve{z}_m\sigma_{jk}}\Big(\frac{e^{-\breve{z}_n\sigma_k}}{\breve{z}_n+\breve{z}_m}+\frac{1-e^{-\breve{z}_n\sigma_k}}{\breve{z}_n}\Big)\Bigg]\Bigg\}.\end{aligned}\tag{498}$$

The other is given as

$$2\pi K^n_{ij}=\breve{z}_nD^n_{ij}-\sum_{m=1}^{2}\sum_{k=1}^{2}\rho_kD^n_{ik}D^m_{jk}\zeta^{nm}_{kj}-\sum_{m=1}^{2}\sum_{k=1}^{2}\sum_{l=1}^{2}\rho_kD^n_{ik}D^m_{lk}\frac{2\pi\rho_l}{z_m}\widehat{\mathcal{P}}_{jl}(\breve{z}_m)\xi^{nm}_{kj},\tag{499}$$

where

$$\begin{cases}\zeta^{nm}_{kj}\equiv e^{-\breve{z}_n\lambda_{kj}}e^{-\breve{z}_m\sigma_{kj}}(\breve{z}_n+\breve{z}_m-\breve{z}_me^{-\breve{z}_n\sigma_j})(\breve{z}_n+\breve{z}_m)^{-1}\\ \xi^{nm}_{kj}\equiv e^{-\breve{z}_n\lambda_{kj}}e^{-\breve{z}_m\sigma_{kj}}(-\breve{z}_n-\breve{z}_m+\breve{z}_me^{-\breve{z}_n\sigma_j}+\breve{z}_ne^{\breve{z}_m\sigma_j})(\breve{z}_n+\breve{z}_m)^{-1}.\end{cases}\tag{500}$$

Modifying Eq. (499) allows $\widehat{\mathcal{P}}_{ij}(\breve{z}_n)$ to be given as

$$\begin{aligned}2\pi\rho_i\widehat{\mathcal{P}}_{ji}(\breve{z}_n)=&\sum_{m'=1}^{2}\breve{z}_{m'}\xi^{nm'(-1)}_{jj}\frac{\breve{z}_n}{\rho_j}D^{n(-1)}_{ji}\\&-\sum_{m=1}^{2}\sum_{m'=1}^{2}\sum_{h=1}^{2}\breve{z}_nD^{n(-1)}_{hi}D^m_{hj}\xi^{nm'(-1)}_{hj}\zeta^{m'm}_{hj}\\&-2\pi\sum_{m'=1}^{2}\sum_{h=1}^{2}\sum_{k=1}^{2}\frac{\breve{z}_n}{\rho_h}D^{n(-1)}_{hi}\xi^{nm'(-1)}_{hj}D^{m'(-1)}_{hk}K^{m'}_{kj},\end{aligned}\tag{501}$$

where

$$\begin{cases}\sum_{m'=1}^{2}\xi^{nm'(-1)}_{ij}\xi^{m'm}_{ij}=\delta_{nm}\\ \sum_{k=1}^{2}D^{n(-1)}_{ik}D^n_{kj}=\delta_{ij}.\end{cases}\tag{502}$$

D. Ionic fluid structures characterized by formation of large physical clusters

If an ionic fluid mixture system includes extremely large physical clusters, $\mathcal{P}_{ij}(r)$ should have a long-range feature on a macroscopic scale even if $C^{+}_{ij}(r)$ retains the microscopic feature. The recursive solution given by Eq. (304) clearly denotes that particles $(k_1, k_2, \cdots)$ distributed around an i particle and a j particle enable the correlation function $\mathcal{P}_{ij}(r)$ to decay to zero considerably slower than $C^{+}_{ij}(r)$ decays. Further, $C^{+}_{ij}(r)$ can decay to zero more rapidly than $-\beta u_{ij}(r)$, which expresses a microscopic feature. If the contributions of particles $(k_1, k_2, \cdots)$ distributed around the particles of species i and j are not negligible, Eq. (304) demonstrates that $\mathcal{P}_{ij}(r)$ can retain a finite positive value except zero even out of the effective range where $C^{+}_{ij}(r) \neq 0$.

Convolution integrals found in the recursive solution given by Eq. (306) allow a feature of $\mathcal{H}_{ij}(r)$ to remain in a longer range than both that of $C^{*}_{ij}(r)$ and that of $c_{ij}(r)$. Eq. (306) denotes that particles $(k_1, k_2, \cdots)$ distributed around the particles of species i and j enable the absolute value $|\mathcal{H}_{ij}(r)|$ to decay to zero considerably slower than $|C^{*}_{ij}(r)|$ and $|c_{ij}(r)|$ decay.

The ranges within which the correlation functions $c_{ij}(r)$, $C^{+}_{ij}(r)$ and $C^{*}_{ij}(r)$ retain effective values different from zero, can remain microscopic sizes in comparison with other correlation functions such as $g_{ij}(r) - 1$, $\mathcal{H}_{ij}(r)$, and $\mathcal{P}_{ij}(r)$. The known assumption that the feature of $c_{ij}(r)$ is retained in the short range[13,18] restricts the features of $C^{+}_{ij}(r)$ and $C^{*}_{ij}(r)$. Thus, the features of $c_{ij}(r)$, $C^{+}_{ij}(r)$, and $C^{*}_{ij}(r)$ allow $\mathcal{P}_{ij}(r)$ and $\mathcal{H}_{ij}(r)$ in the convolution integrals found in Eqs. (270) and (272) to be approximated using the Maclaurin series expansions.

1. Maclaurin series expansions

(a) *Maclaurin series expansion of convolution integrals in Eqs. (270)*

If a polar coordinate system with the origin located at $\mathbf{r}_1^{(i)}$ and a point $\mathbf{r}_2^{(j)}$ located on the $z^{(k)}$ axis is applied, Eq. (270) can be rewritten as

$$\mathcal{P}(r) = C^{+}(r) + \sum_{k=1}^{\mathcal{L}} \rho_k \int_0^{\infty} \int_0^{\pi} C^{+}_{ik}(r_3^{(k)}) \mathcal{P}_{kj}(|\mathbf{r}_3^{(k)} - \mathbf{r}_2^{(j)}|) 2\pi (r_3^{(k)})^2 \sin\theta_3^{(k)} \mathrm{d}r_3^{(k)} \mathrm{d}\theta_3^{(k)}, \tag{503}$$

where $r \equiv |\mathbf{r}_1^{(i)} - \mathbf{r}_2^{(j)}| = |\mathbf{r}_2^{(j)}|$, $r_3^{(k)} \equiv |\mathbf{r}_1^{(i)} - \mathbf{r}_3^{(k)}| = |\mathbf{r}_3^{(k)}|$, and $\theta_3^{(k)} = \cos^{-1}[\mathbf{r}_2^{(j)} \cdot \mathbf{r}_3^{(k)} / (r r_3^{(k)})]$.

In Eq. (503), the short-range feature of $C_{ik}^{+}(r_3^{(k)})$ allows $0 < r_3^{(k)}/r \ll 1$ to be maintained for large r. Thus, a Maclaurin series expansion for $\mathcal{P}(|\mathbf{r}_3^{(k)} - \mathbf{r}_2^{(j)}|)$ found in Eq. (503) is effective for representing the behavior of $\mathcal{P}_{ij}(r)$ at large r.

Then, the Maclaurin series expansion corresponds to

$$\mathcal{P}(|\mathbf{r}_3^{(k)} - \mathbf{r}_2^{(j)}|) = \sum_{m=0}^{\infty} \frac{1}{m!} \frac{\partial^m}{\partial (r_3^{(k)})^m} \mathcal{P}(r_{32}^{(k)}) \Big|_{r_3^{(k)}=0} (r_3^{(k)})^m, \tag{504}$$

where

$$r_{32}^{(k)} \equiv |\mathbf{r}_3^{(k)} - \mathbf{r}_2^{(j)}| = r \left[(r_3^{(k)}/r)^2 - 2(r_3^{(k)}/r) \cos\theta_3^{(k)} + 1 \right]^{1/2}.$$

The substitution of the Maclaurin series expansion given by Eq. (504) allows Eqs. (503) to be given as

$$\begin{aligned} \mathcal{P}_{ij}(r) =& C_{ij}^{+}(r) + \sum_{k=1}^{\mathcal{L}} \rho_k \int_V C_{ik}^{+}(|\mathbf{r}_3^{(k)}|) \mathcal{P}_{kj}(r) \mathrm{d}\mathbf{r}_3^{(k)} + \frac{1}{6} \sum_{k=1}^{\mathcal{L}} \rho_k \int_V C_{ik}^{+}(|\mathbf{r}_3^{(k)}|) |\mathbf{r}_3^{(k)}|^2 \nabla^2 \mathcal{P}_{kj}(r) \mathrm{d}\mathbf{r}_3^{(k)} \\ &+ \frac{9}{4 \cdot 6^2} \sum_{k=1}^{\mathcal{L}} \rho_k \int_V C_{ik}^{+}(|\mathbf{r}_3^{(k)}|) |\mathbf{r}_3^{(k)}|^4 \Delta_r \mathcal{P}_{kj}(r) \mathrm{d}\mathbf{r}_3^{(k)} + \cdots, \end{aligned} \tag{505}$$

where

$$\Delta_r \equiv \frac{8}{15} \frac{1}{r} \frac{\partial^3}{\partial r^3} + \frac{2}{15} \frac{\partial^4}{\partial r^4}.$$

If the formula defined by Eq. (116) is used as the forms of coefficients, Eq. (505) is simplified as

$$\begin{aligned} \sum_{k=1}^{\mathcal{L}} \left[\delta_{ik} - \rho_k \widehat{C}_{ik}^{+(0)} \right] \mathcal{P}_{kj}(r) = C_{ij}^{+}(r) &+ \sum_{k=1}^{\mathcal{L}} \rho_k \widehat{C}_{ik}^{+(2)} \nabla^2 \mathcal{P}_{kj}(r) \\ &+ \frac{9}{4} \sum_{k=1}^{\mathcal{L}} \rho_k \widehat{C}_{ik}^{+(4)} \Delta_r \mathcal{P}_{kj}(r) + \cdots, \end{aligned} \tag{506}$$

The formula defined by Eq. (116) is expressed as $\widehat{C}_{ik}^{+(\alpha)}$ $(\alpha = 0, 2, 4)$, and it is given as

$$\widehat{C}_{ik}^{+(\alpha)} = \left(\frac{1}{6} \right)^{\alpha/2} \int_V C_{ik}^{+}(|\mathbf{r}_3^{(k)}|) |\mathbf{r}_3^{(k)}|^{\alpha} \mathrm{d}\mathbf{r}_3^{(k)}, \quad (\alpha = 0, 2, 4). \tag{507}$$

In Eq. (506), the factor $\frac{9}{4} \sum_{k=1}^{\mathcal{L}} \rho_k \widehat{C}_{ik}^{+(4)} \Delta_r \mathcal{P}_{kj}(r)$ corresponds to a correction term under the condition that the value of r is not large although its value is out of the microscopic range in which $C^{+}(r)_{ik} \neq 0$ is satisfied.

(b) *Maclaurin series expansion of convolution integrals in Eq. (272)*

If a polar coordinate system with the origin located at $\mathbf{r}_1^{(i)}$ and a point $\mathbf{r}_2^{(j)}$ located on the $z^{(k)}$ axis is applied, Eq. (272) can be rewritten as

$$\begin{aligned}\mathcal{H}_{ij}(r) =& C_{ij}^{*}(r) + \sum_{k=1}^{\mathcal{L}} \rho_k \int_0^{\infty} \int_0^{\pi} C_{ik}^{*}(r_3^{(k)}) \mathcal{P}_{kj}(|\mathbf{r}_3^{(k)} - \mathbf{r}_2^{(j)}|) 2\pi (r_3^{(k)})^2 \sin\theta_3^{(k)} \mathrm{d}r_3^{(k)} \mathrm{d}\theta_3^{(k)} \\ &+ \sum_{k=1}^{\mathcal{L}} \rho_k \int_0^{\infty} \int_0^{\pi} C_{ik}^{+}(r_3^{(k)}) \mathcal{H}(|\mathbf{r}_3^{(k)} - \mathbf{r}_2^{(j)}|) 2\pi (r_3^{(k)})^2 \sin\theta_3^{(k)} \mathrm{d}r_3^{(k)} \mathrm{d}\theta_3^{(k)} \\ &+ \sum_{k=1}^{\mathcal{L}} \rho_k \int_0^{\infty} \int_0^{\pi} C_{ik}^{*}(r_3^{(k)}) \mathcal{H}(|\mathbf{r}_3^{(k)} - \mathbf{r}_2^{(j)}|) 2\pi (r_3^{(k)})^2 \sin\theta_3^{(k)} \mathrm{d}r_3^{(k)} \mathrm{d}\theta_3^{(k)}, \end{aligned} \tag{508}$$

A Maclaurin series expansion for $\mathcal{H}(|\mathbf{r}_3^{(k)} - \mathbf{r}_2^{(j)}|)$ corresponds to

$$\mathcal{H}(|\mathbf{r}_3^{(k)} - \mathbf{r}_2^{(j)}|) = \sum_{m=0}^{\infty} \frac{1}{m!} \frac{\partial^m}{\partial (r_3^{(k)})^m} \mathcal{H}(r_{32}^{(k)}) \Big|_{r_3^{(k)}=0} (r_3^{(k)})^m. \tag{509}$$

The substitution of the Maclaurin series expansions given by Eqs. (504) and (509) allows Eqs. (508) to be given as

$$\begin{aligned}\mathcal{H}_{ij}(r) =& C_{ij}^{*}(r) + \sum_{k=1}^{\mathcal{L}} \rho_k \int_V C_{ik}^{*}(|\mathbf{r}_3^{(k)}|) \mathcal{P}_{kj}(r) \mathrm{d}\mathbf{r}_3^{(k)} + \frac{1}{6} \sum_{k=1}^{\mathcal{L}} \rho_k \int_V C_{ik}^{*}(|\mathbf{r}_3^{(k)}|) |\mathbf{r}_3^{(k)}|^2 \nabla^2 \mathcal{P}_{kj}(r) \mathrm{d}\mathbf{r}_3^{(k)} \\ &+ \frac{9}{4 \cdot 6^2} \sum_{k=1}^{\mathcal{L}} \rho_k \int_V C_{ik}^{*}(|\mathbf{r}_3^{(k)}|) |\mathbf{r}_3^{(k)}|^4 \Delta_r \mathcal{P}_{kj}(r) \mathrm{d}\mathbf{r}_3^{(k)} + \cdots \\ &+ \sum_{k=1}^{\mathcal{L}} \rho_k \int_V c_{ik}(|\mathbf{r}_3^{(k)}|) \mathcal{H}_{kj}(r) \mathrm{d}\mathbf{r}_3^{(k)} + \frac{1}{6} \sum_{k=1}^{\mathcal{L}} \rho_k \int_V c_{ik}(|\mathbf{r}_3^{(k)}|) |\mathbf{r}_3^{(k)}|^2 \nabla^2 \mathcal{H}_{kj}(r) \mathrm{d}\mathbf{r}_3^{(k)} \\ &+ \frac{9}{4 \cdot 6^2} \sum_{k=1}^{\mathcal{L}} \rho_k \int_V c_{ik}(|\mathbf{r}_3^{(k)}|) |\mathbf{r}_3^{(k)}|^4 \Delta_r \mathcal{H}_{kj}(r) \mathrm{d}\mathbf{r}_3^{(k)} + \cdots . \end{aligned} \tag{510}$$

If the formula defined by Eq. (116) is used as the forms of coefficients, Eq. (505) is simplified as

$$\begin{aligned}\sum_{k=1}^{\mathcal{L}} \left[\delta_{ik} - \rho_k \widehat{c}_{ik}^{(0)} \right] \mathcal{H}_{kj}(r) =& C_{ij}^{*}(r) + \sum_{k=1}^{\mathcal{L}} \rho_k \widehat{C}_{ik}^{*(0)} \mathcal{P}_{kj}(r) \\ &+ \sum_{k=1}^{\mathcal{L}} \rho_k \widehat{C}_{ik}^{*(2)} \nabla^2 \mathcal{P}_{kj}(r) + \sum_{k=1}^{\mathcal{L}} \rho_k \widehat{c}_{ik}^{(2)} \nabla^2 \mathcal{H}_{kj}(r) \\ &+ \frac{9}{4} \sum_{k=1}^{\mathcal{L}} \rho_k \widehat{C}_{ik}^{*(4)} \Delta_r \mathcal{P}_{kj}(r) + \frac{9}{4} \sum_{k=1}^{\mathcal{L}} \rho_k \widehat{c}_{ik}^{(4)} \Delta_r \mathcal{H}_{kj}(r) + \cdots , \end{aligned} \tag{511}$$

where the coefficients $\widehat{C}_{ik}^{*(\alpha)}$ and $\widehat{c}_{ik}^{(\alpha)}$ $(\alpha = 0, 2, 4)$ are given by Eq. (116) as

$$\widehat{C}_{ik}^{*(\alpha)} = \left(\frac{1}{6}\right)^{\alpha/2} \int_V C_{ik}^*(|\mathbf{r}_3^{(k)}|)|\mathbf{r}_3^{(k)}|^\alpha \mathrm{d}\mathbf{r}_3^{(k)}, \quad (\alpha = 0, 2, 4), \tag{512}$$

and

$$\widehat{c}_{ik}^{(\alpha)} \equiv \left(\frac{1}{6}\right)^{\alpha/2} \int_V c_{ik}(|\mathbf{r}_3^{(k)}|)|\mathbf{r}_3^{(k)}|^\alpha \mathrm{d}\mathbf{r}_3^{(k)}, \quad (\alpha = 0, 2, 4). \tag{513}$$

Then, Eq. (269) requires the following relation to be satisfied.

$$\widehat{c}_{ik}^{(\alpha)} = \widehat{C}_{ik}^{+(\alpha)} + \widehat{C}_{ik}^{*(\alpha)}, \quad (\alpha = 0, 2, 4). \tag{514}$$

In Eq. (511), factors $\frac{9}{4}\rho_k \widehat{C}_{ik}^{*(4)} \Delta_r \mathcal{P}_{kj}(r)$ and $\frac{9}{4}\rho_k \widehat{c}_{ik}^{(4)} \Delta_r \mathcal{H}_{kj}(r)$ correspond to correction terms under the condition that the value of r is not large although its value is out of the microscopic range in which $C^+(r) \neq 0$ and $C^*(r) \neq 0$ are satisfied.

2. *Estimates of* $\widehat{C}_{\alpha\beta}^{+(0)}$, $\widehat{C}_{\alpha\beta}^{+(2)}$, $\widehat{C}_{\alpha\beta}^{*(0)}$, *and* $\widehat{C}_{\alpha\beta}^{*(2)}$

Equation (324) allows a coefficient $\widehat{C}_{\alpha\beta}^{+(0)}$ to be estimated as

$$\widehat{C}_{\alpha\beta}^{+(0)} = \frac{1}{(\rho_\alpha \rho_\beta)^{1/2}} \lim_{k\to 0} \left[\delta_{\alpha\beta} - \sum_{h=1}^{2} \widetilde{Q}_{\alpha h}^+(k) \widetilde{Q}_{\beta h}^+(-k) \right]. \tag{515}$$

If the three-dimensional elements of $\mathbf{k}$ are denoted as (k_x, k_y, k_z), a differential operator with respect to $\mathbf{k}$ can be defined as $\nabla_k \equiv (\partial/\partial k_x, \partial/\partial k_y, \partial/\partial k_z)$. For a correlation function $F_{ij}(r)$ satisfying $\lim_{r\to\infty} F_{ij}(r) = 0$, the above definition results in

$$\lim_{k\to 0} \lim_{V\to\infty} (\rho_i \rho_j)^{1/2} (\mathrm{d}^2/\mathrm{d}k^2) \int_V F_{ij}(r) \exp[i\mathbf{k}\cdot\mathbf{r}] \mathrm{d}\mathbf{r} = \frac{11}{6} \lim_{k\to 0} (\nabla_k \cdot \nabla_k) \widetilde{F}_{ij}(k).$$

This relation implies

$$(\rho_i \rho_j)^{1/2} \int_V F_{ij}(r) r^2 \mathrm{d}\mathbf{r} = -(6/11) \lim_{k\to 0} (\mathrm{d}^2/\mathrm{d}k^2) \widetilde{F}_{ij}(k).$$

According to this formula, Eq. (324) allows a coefficient $\widehat{C}_{\alpha\beta}^{+(2)}$ to be estimated as

$$\begin{aligned} \widehat{C}_{\alpha\beta}^{+(2)} = \frac{1}{11} \frac{1}{(\rho_\alpha \rho_\beta)^{1/2}} \lim_{k\to 0} \sum_{h=1}^{2} \Bigg[& \frac{\mathrm{d}^2}{\mathrm{d}k^2} \widetilde{Q}_{\alpha h}^+(k) \widetilde{Q}_{\beta h}^+(-k) - \frac{\mathrm{d}}{\mathrm{d}k} \widetilde{Q}_{\alpha h}^+(k) \frac{\mathrm{d}}{\mathrm{d}(-k)} \widetilde{Q}_{\beta h}^+(-k) \\ & + \widetilde{Q}_{\alpha h}^+(k) \frac{\mathrm{d}^2}{\mathrm{d}(-k)^2} \widetilde{Q}_{\beta h}^+(-k) \Bigg]. \end{aligned} \tag{516}$$

A coefficient $\widetilde{Q}^{+}_{\alpha\beta}(k)$ in Eqs. (515) and (516) is described by Eqs. (490) and (495). According to Eq. (514), $\widehat{C}^{*(0)}_{\alpha\beta}$, and $\widehat{C}^{*(2)}_{\alpha\beta}$ can be estimated as

$$\widehat{C}^{*(0)}_{\alpha\beta} = \widehat{c}^{(0)}_{\alpha\beta} - \widehat{C}^{+(0)}_{\alpha\beta}, \tag{517}$$

$$\widehat{C}^{*(2)}_{\alpha\beta} = \widehat{c}^{(2)}_{\alpha\beta} - \widehat{C}^{+(2)}_{\alpha\beta}. \tag{518}$$

The coefficients $\widehat{c}^{(0)}_{\alpha\beta}$ and $\widehat{c}^{(2)}_{\alpha\beta}$ can be estimated by solving the Ornstein–Zernike equation. When $\widehat{C}^{+(0)}_{\alpha\beta}$ and $\widehat{C}^{+(2)}_{\alpha\beta}$ for a point charge system are be assessed, Eqs. (572), (573), (574), and (575) can be used with Eqs. (490), (495), (515) and (516).

3. Differential equations for characterizing long-range features of $\mathcal{P}_{ij}(r)$

(a) *Differential equation for* $\mathcal{L}$ *components*

The magnitude of $\mathcal{P}_{ij}(r)$ in Eqs. (506) and (511) cannot be neglected in an ionic fluid including sufficiently large physical clusters even when the particles of species i and j are located at a great distance out of the effective range in which the magnitude of $u_{ij}(r)$ cannot be neglected. Differential equations that contribute to estimating $\mathcal{P}_{ij}(r)$ and $\mathcal{H}_{ij}(r)$ for the ionic fluid can be derived from Eqs. (506) and (511).

A differential equation derived from Eq. (506) is expressed as

$$\sum_{k=1}^{\mathcal{L}} \rho_k \widehat{C}^{+(2)}_{ik} \nabla^2 \mathcal{P}_{kj}(r) - \sum_{k=1}^{\mathcal{L}} \left(\delta_{ik} - \rho_k \widehat{C}^{+(0)}_{ik} \right) \mathcal{P}_{kj}(r) \approx -C^{+}_{ij}(r). \tag{519}$$

If Eq. (519) is multiplied by $(\rho_i \rho_j)^{1/2}$,

$$\sum_{k=1}^{\mathcal{L}} \sqrt{\rho_i \rho_k} \widehat{C}^{+(2)}_{ik} \nabla^2 \overline{\mathcal{P}}_{kj}(r) - \sum_{k=1}^{\mathcal{L}} \left(\delta_{ik} - \sqrt{\rho_i \rho_k} \widehat{C}^{+(0)}_{ik} \right) \overline{\mathcal{P}}_{kj}(r) \approx -\sqrt{\rho_i \rho_j} C^{+}_{ij}(r), \tag{520}$$

where

$$\overline{\mathcal{P}}_{kj}(r) \equiv \sqrt{\rho_k \rho_j} \mathcal{P}_{kj}(r). \tag{521}$$

If the determinant of the matrix M_{hi} is expressed as $\det|M_{hi}|$, the inverse matrix of $\sqrt{\rho_\gamma \rho_\delta} \widehat{C}^{+(2)}_{\gamma\delta}$ is given as

$$(-1)^{h+i} \frac{\det|\sqrt{\rho_h \rho_i} \widehat{C}^{+(2)\epsilon}_{hi}|}{\det|\sqrt{\rho_\gamma \rho_\delta} \widehat{C}^{+(2)}_{\gamma\delta}|},$$

where matrix $\sqrt{\rho_h\rho_i}\widehat{C}_{hi}^{+(2)\epsilon}$ does not include the specific elements $\sqrt{\rho_h\rho_\delta}\widehat{C}_{h\delta}^{+(2)}$ $(\delta = 1, 2, \cdots \mathcal{L})$ and $\sqrt{\rho_\gamma\rho_i}\widehat{C}_{\gamma i}^{+(2)}$ $(\gamma = 1, 2, \cdots \mathcal{L})$.

If this inverse matrix is used, Eq. (519) can be rewritten as

$$\begin{aligned}\nabla^2\overline{\mathcal{P}}_{ij}(r) - &\sum_{h=1}^{\mathcal{L}}(-1)^{h+i}\frac{\det|\sqrt{\rho_h\rho_i}\widehat{C}_{hi}^{+(2)\epsilon}|}{\det|\sqrt{\rho_\gamma\rho_\delta}\widehat{C}_{\gamma\delta}^{+(2)}|}\sum_{k=1}^{\mathcal{L}}\left(\delta_{hk} - \sqrt{\rho_h\rho_k}\widehat{C}_{hk}^{+(0)}\right)\overline{\mathcal{P}}_{kj}(r) \\ \approx &-\sum_{h=1}^{\mathcal{L}}(-1)^{h+i}\frac{\det|\sqrt{\rho_h\rho_i}\widehat{C}_{hi}^{+(2)\epsilon}|}{\det|\sqrt{\rho_\gamma\rho_\delta}\widehat{C}_{\gamma\delta}^{+(2)}|}\sqrt{\rho_h\rho_j}C_{hj}^{+}(r), \end{aligned} \tag{522}$$

where $C_{hj}^{+}(r)$ must be given as the long-range contribution. Equations (519) and (522) allow $C_{ij}^{+}(r)$ to become a source of generating the correlation characterized by $\mathcal{P}_{ij}(r)$. Thus, Eqs. (519) and (522) enable the estimation of the long-range feature of $\mathcal{P}_{ij}(r)$ for an ionic fluid including large physical clusters.

(b) *Approximated differential equation for $\mathcal{L} = 2$ at large r*

The behavior of $\mathcal{P}_{ij}(r)$ at large r must be restricted by $\sum_{k=1}^{2} e_k\rho_k\mathcal{P}_{ik}(r) = 0$, which is given by Eq. (453). This fact denotes that Eq. (453) requires $\mathcal{P}_{ij}(r) = \mathcal{P}_{ii}(r)$ $(i \neq j)$ at large r because the electroneutrality requires $\sum_{k=1}^{2} e_k\rho_k = 0$. Thus, Eq. (522) can be approximated owing to Eq. (521) as

$$\nabla^2\mathcal{P}_{ij}(r) - \left(\xi_i^{+}\right)^2\mathcal{P}_{ij}(r) \approx \sum_{h=1}^{2}\zeta_{ij}^{(h)+}\left(\frac{e^{-\kappa r}}{r}\right)^{5/2-|h-j|}, \tag{523}$$

where

$$\xi_i^{+} \equiv \left[\sum_{h=1}^{2}(-1)^{h+i}\frac{\det|\sqrt{\rho_h\rho_i}\widehat{C}_{hi}^{+(2)\epsilon}|}{\det|\sqrt{\rho_\gamma\rho_\delta}\widehat{C}_{\gamma\delta}^{+(2)}|}\sum_{k=1}^{2}\left(\delta_{hk} - \sqrt{\rho_h\rho_k}\widehat{C}_{hk}^{+(0)}\right)\sqrt{\frac{\rho_k}{\rho_i}}\right]^{1/2}, \tag{524}$$

and

$$\zeta_{ij}^{(h)+} \equiv -(-1)^{h+i}\frac{\det|\sqrt{\rho_h\rho_i}\widehat{C}_{hi}^{+(2)\epsilon}|}{\det|\sqrt{\rho_\gamma\rho_\delta}\widehat{C}_{\gamma\delta}^{+(2)}|}\sqrt{\frac{\rho_h}{\rho_i}}K_{hj}^{+}. \tag{525}$$

The form of $C_{hj}^{+}(r)$ that should be considered for deriving Eq. (523) is given by Eq. (473) as the long-range contribution; it is expressed as $C_{hj}^{+}(r) = K_{hj}^{+}\left(e^{-\kappa r}/r\right)^{5/2-|h-j|}$ for $h = 1, 2$ and $j = 1, 2$. Further, an advantage of the above equation is that the long-range feature of $\mathcal{P}_{ij}(r)$ is estimated without knowing the contribution of $C_{ij}^{0+}(r)$, which is strongly dependent on the hard-core potential of each particle.

(c) *Solution of differential equation for* $\mathcal{L} = 2$

i) *Solution of differential equation Eq. (523)*

To form a solution satisfying the differential equation Eq. (523), the ionic fluid system should be imaginarily divided into the internal area of a spherical region of radius r and the external area of the spherical region. Then, the center of the spherical region is located at the origin, $t = 0$, of a spherical coordinate.

A bound state wherein the contribution of the mutually attractive force between two charged particles exceeds the contribution of their relative kinetic energy is specified as an f^+-bond. The correlation generated between a charged particle at $t = 0$ and another charged particle at $t = r$ via charged particles linked by only f^+-bonds is given by two partial contributions. One of the two partial contributions results from charged particles distributed inside a spherical region of radius r. This is approximately estimated from the differential equation given by Eq. (523), and it is given by

$$\mathcal{P}_{ij}^{\rm in}(r) = -\xi_i^+\sigma_{ij}\sum_{h=1}^{2}\zeta_{ij}^{(h)+}(\sigma_{ij})^2 h_0^{(1)}(i\xi_i^+ r)\int_{\sigma_{ij}}^{r}\mathcal{G}_{ij}(\xi_i^+;t)\left(\frac{e^{-\kappa t}}{t}\right)^{5/2-|h-j|}\left(\frac{t}{\sigma_{ij}}\right)^2\frac{1}{\sigma_{ij}}{\rm d}t, \quad (t<r), \tag{526}$$

where $\mathcal{G}_{ij}(\xi_i^+;t)$ is defined using the spherical Bessel function $j_0(\tau)$ and the spherical Hankel function of the first kind $h_0^{(1)}(\tau)$. The function $\mathcal{G}_{ij}(\xi_i^+;t)$ is expressed as

$$\mathcal{G}_{ij}(\xi_i^+;t) \equiv j_0(i\xi_i^+ t) - \frac{j_0(i\xi_i^+\sigma_{ij})}{h_0^{(1)}(i\xi_i^+\sigma_{ij})}h_0^{(1)}(i\xi_i^+ t), \tag{527}$$

where

$$\begin{cases} j_0(\tau) = \tau^{-1}\sin\tau \\ h_0^{(1)}(\tau) = i\tau^{-1}e^{-i\tau}. \end{cases}$$

The remainder of the two partial contributions results from charged particles distributed outside the spherical region. This is approximately estimated from the differential equation given by Eq. (523); it is given by

$$\mathcal{P}_{ij}^{\rm ex}(r) = -\xi_i^+\sigma_{ij}\sum_{h=1}^{2}\zeta_{ij}^{(h)+}(\sigma_{ij})^2\mathcal{G}_{ij}(\xi_i^+;r)\int_{r}^{\infty}h_0^{(1)}(i\xi_i^+ t)\left(\frac{e^{-\kappa t}}{t}\right)^{5/2-|h-j|}\left(\frac{t}{\sigma_{ij}}\right)^2\frac{1}{\sigma_{ij}}{\rm d}t, \quad (r<t). \tag{528}$$

The pair connectedness $\mathcal{P}_{ij}$ given as solutions that depend on the term on the right-hand side of Eq. (523) are obtained as the sum $\mathcal{P}_{ij}^{\rm in} + \mathcal{P}_{ij}^{\rm ex}$. In Eqs. (526) and (528), the product $h_0^{(1)}\mathcal{G}_{ij}$ can be expressed as

$$h_0^{(1)}(i\xi_i^+ r)\mathcal{G}_{ij}(\xi_i^+;t) = -\frac{e^{-\xi_i^+(r-t)}}{2\xi_i^+ r\xi_i^+ t} + \left(1 + \frac{2\sinh\xi_i^+\sigma_{ij}}{e^{-\xi_i^+\sigma_{ij}}}\right)\frac{e^{-\xi_i^+(r+t)}}{2\xi_i^+ r\xi_i^+ t}, \tag{529}$$

$$\mathcal{G}_{ij}(\xi_i^+;r)h_0^{(1)}(i\xi_i^+ t) = -\frac{e^{-\xi_i^+(t-r)}}{2\xi_i^+ t\xi_i^+ r} + \left(1 + \frac{2\sinh\xi_i^+\sigma_{ij}}{e^{-\xi_i^+\sigma_{ij}}}\right)\frac{e^{-\xi_i^+(t+r)}}{2\xi_i^+ t\xi_i^+ r}. \tag{530}$$

If the expressions of Eqs. (529) and (530) are considered, the sum $\mathcal{P}_{ij}^{\rm in} + \mathcal{P}_{ij}^{\rm ex}$ is given as

$$\begin{aligned}\mathcal{P}_{ij}(r) =& -\mathcal{M}_{ij}^+\frac{e^{-\xi_i^+ r}}{2\xi_i^+ r} + \sum_{h=1}^{2}\zeta_{ij}^{(h)+}(\sigma_{ij})^2\frac{1}{2\xi_i^+ r}\int_{\sigma_{ij}}^{r} e^{\xi_i^+(t-r)}\left(\frac{e^{-\kappa t}}{t}\right)^{5/2-|h-j|}\left(\frac{t}{\sigma_{ij}}\right)\frac{1}{\sigma_{ij}}{\rm d}t \\ &+ \sum_{h=1}^{2}\zeta_{ij}^{(h)+}(\sigma_{ij})^2\frac{e^{\xi_i^+ r}}{2\xi_i^+ r}\int_{r}^{\infty} e^{-\xi_i^+ t}\left(\frac{e^{-\kappa t}}{t}\right)^{5/2-|h-j|}\left(\frac{t}{\sigma_{ij}}\right)\frac{1}{\sigma_{ij}}{\rm d}t,\end{aligned} \tag{531}$$

where

$$\mathcal{M}_{ij}^+ = e^{\xi_i^+\sigma_{ij}}\sum_{h=1}^{2}\zeta_{ij}^{(h)+}(\sigma_{ij})^2\int_{\sigma_{ij}}^{\infty} e^{-\xi_i^+ t}\left(\frac{e^{-\kappa t}}{t}\right)^{5/2-|h-j|}\left(\frac{t}{\sigma_{ij}}\right)\frac{1}{\sigma_{ij}}{\rm d}t. \tag{532}$$

Further, the above solution does not include the contribution given in the case that the term on the right-hand side of Eq. (523) is equal to zero.

ii) *Behavior of $\mathcal{P}_{ij}(r)$ revealed under the condition that $\xi_i^+ = 0$ is satisfied*

According to Eq. (524), $\xi_i^+ = 0$ is satisfied if $\delta_{hk} - \sqrt{\rho_h\rho_k}\widehat{C}_{hk}^{+(0)} = 0$ is satisfied. According to Eq. (320), the following equation must be satisfied:

$$\sum_{k=1}^{\mathcal{L}}\left[\delta_{ik} - \sqrt{\rho_i\rho_k}\widehat{C}_{ik}^{+(0)}\right]\sqrt{\rho_k\rho_j}\widehat{\mathcal{P}}_{kj}(0) = \sqrt{\rho_i\rho_j}\widehat{C}_{ij}^{+(0)}. \tag{533}$$

If $\delta_{hk} - \sqrt{\rho_h\rho_k}\widehat{C}_{hk}^{+(0)} = 0$ and Eq. (533) are satisfied, then $(\rho_k\rho_j)^{1/2}\widehat{\mathcal{P}}_{kj}(0)$ must diverge toward the infinity. Then, the percolation of physical clusters must occur. This implies that the ionic fluid mixture system includes extremely large physical clusters in the condition $\xi_i^+ = 0$.

If $\xi_i^+ \ll 1$ is satisfied, Eq. (557) is approximated as

$$\mathcal{G}_{ij}(\xi_i^+;t) \approx 1 - \frac{\sigma_{ij}}{t} + \frac{\sigma_{ij}}{t}(\xi_i^+\sigma_{ij} - \xi_i^+ t). \tag{534}$$

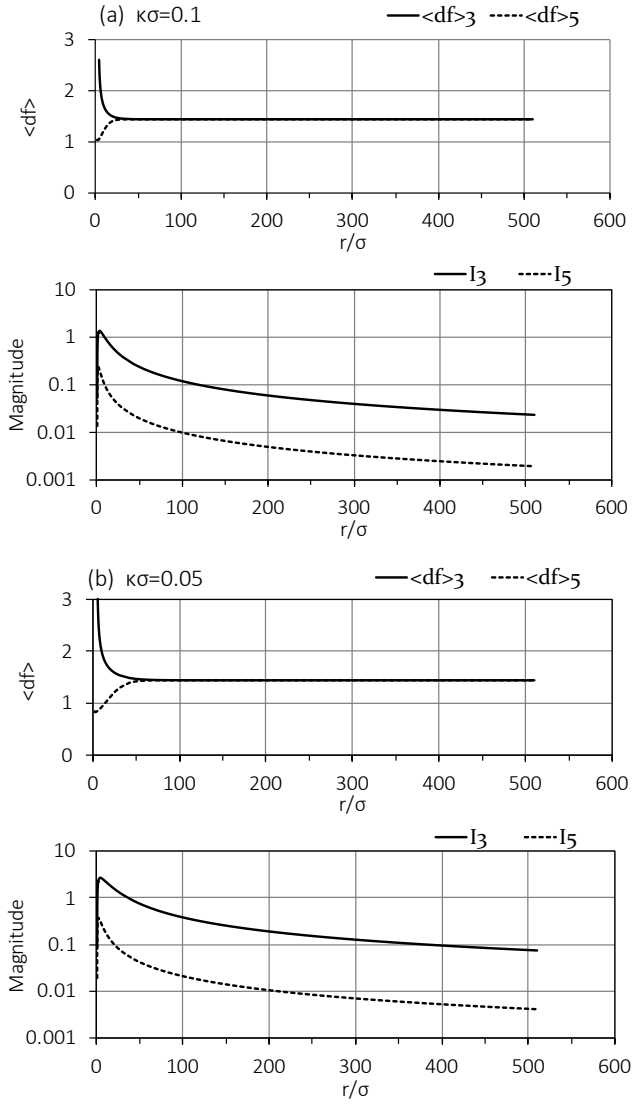

FIG. 32. Behaviors of $\mathcal{I}(\nu, \kappa\sigma; \kappa r)$ ($\nu = 3,\ 5$) for $\kappa\sigma = 0.1$ and 0.05. I_3 and I_5 correspond to $\mathcal{I}(3, \kappa\sigma; \kappa r)$ and $\mathcal{I}(5, \kappa\sigma; \kappa r)$, respectively. $\langle df \rangle_\nu$ ($\nu = 3,\ 5$) is evaluated from Eq. (545).

If $\xi_i^+ = 0$ is satisfied, then Eq. (534) allows Eq. (526) to result in

$$\mathcal{P}_{ij}^{\rm in}(r) = -\sum_{h=1}^{2} \zeta_{ij}^{(h)+} (\sigma_{ij})^2 \left(\frac{\sigma_{ij}}{r}\right) \int_{\sigma_{ij}}^{r} \left(1 - \frac{\sigma_{ij}}{t}\right) \left(\frac{e^{-\kappa t}}{t}\right)^{5/2-|h-j|} \left(\frac{t}{\sigma_{ij}}\right)^2 \frac{1}{\sigma_{ij}} {\rm d}t, \quad (t < r). \tag{535}$$

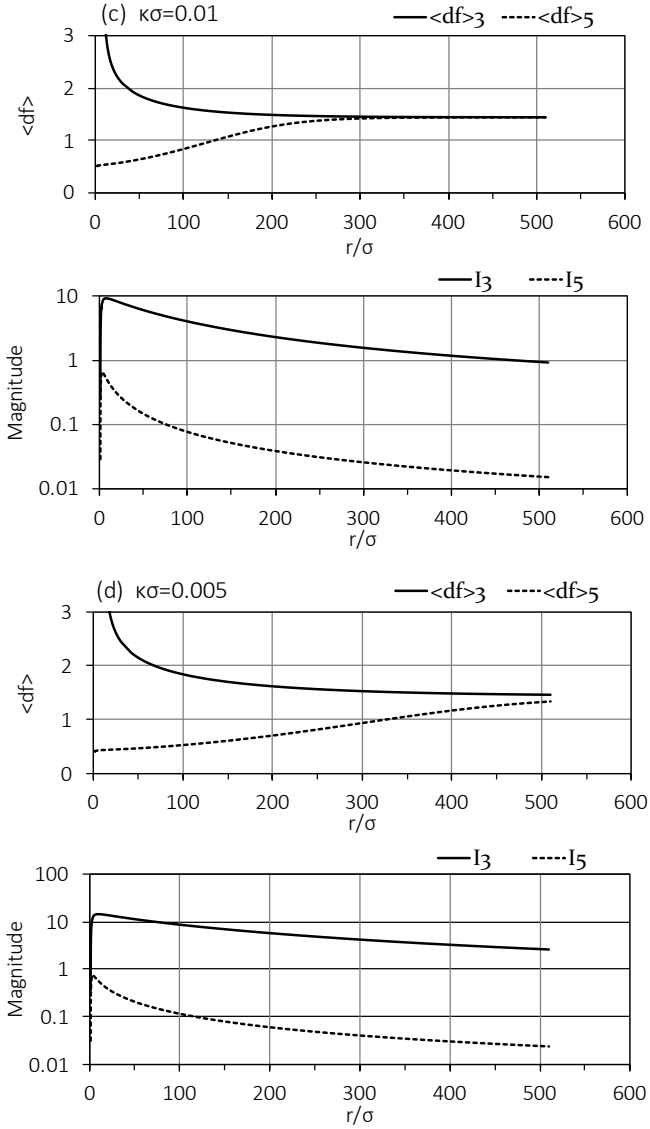

FIG. 33. Behaviors of $\mathcal{I}(\nu, \kappa\sigma; \kappa r)$ ($\nu = 3,\ 5$) for $\kappa\sigma = 0.01$ and 0.005. I_3 and I_5 correspond to $\mathcal{I}(3, \kappa\sigma; \kappa r)$ and $\mathcal{I}(5, \kappa\sigma; \kappa r)$, respectively. $\langle df \rangle_\nu$ ($\nu = 3,\ 5$) is evaluated from Eq. (545).

Further, the relation $\xi_i^+ = 0$ and Eq. (534) allow Eq. (528) to result in

$$\mathcal{P}_{ij}^{\rm ex}(r) = -\sum_{h=1}^{2} \zeta_{ij}^{(h)+} (\sigma_{ij})^2 \left(1 - \frac{\sigma_{ij}}{r}\right) \int_r^\infty \left(\frac{\sigma_{ij}}{t}\right) \left(\frac{e^{-\kappa t}}{t}\right)^{5/2-|h-j|} \left(\frac{t}{\sigma_{ij}}\right)^2 \frac{1}{\sigma_{ij}} {\rm d}t, \quad (r < t). \tag{536}$$

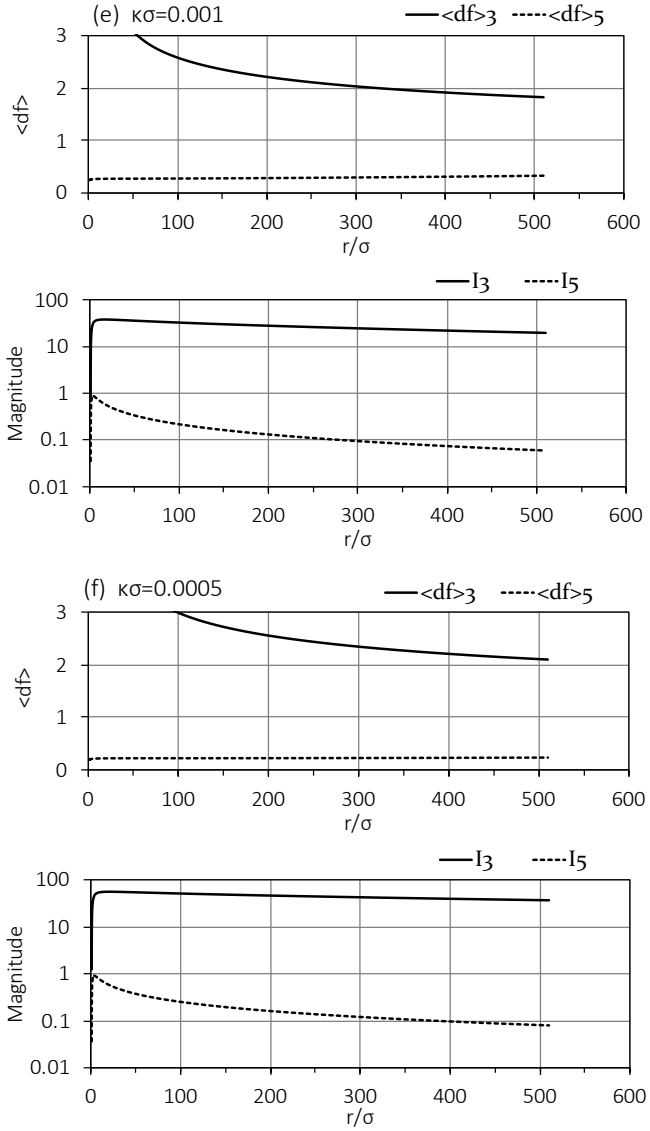

FIG. 34. Behaviors of $\mathcal{I}(\nu, \kappa\sigma; \kappa r)$ ($\nu = 3,\ 5$) for $\kappa\sigma = 0.001$ and 0.0005. I_3 and I_5 correspond to $\mathcal{I}(3, \kappa\sigma; \kappa r)$ and $\mathcal{I}(5, \kappa\sigma; \kappa r)$, respectively. $\langle df \rangle_\nu$ ($\nu = 3,\ 5$) is evaluated from Eq. (545).

The behavior of $\mathcal{P}_{ij}(r)$ found for $\xi_i^+ = 0$ is expressed by the sum of Eq. (535) and Eq. (536). If the integration in Eq. (535) is performed,

$$\mathcal{P}_{ij}^{\rm in}(r) = -\sum_{h=1}^{2} \zeta_{ij}^{(h)+} \left(\frac{1}{\sigma_{ij}}\right)^{\nu_{hj}/2-2} \frac{\sigma_{ij}}{r} \mathcal{I}^{\rm in}(\nu_{hj}, \kappa\sigma_{ij}; \kappa r), \tag{537}$$

where

$$\begin{cases} \nu_{hj} = 3, \ \ h \neq j \\ \nu_{hj} = 5, \ \ h = j. \end{cases} \tag{538}$$

and

$$\begin{aligned} \mathcal{I}^{\rm in}(\nu_{hj}, \kappa\sigma_{ij}; \kappa r) \equiv & \left[1 - \frac{\frac{\nu_{hj}}{2}\kappa\sigma_{ij}}{-\frac{\nu_{hj}}{2}+2}\right] \left(\frac{\nu_{hj}}{2}\kappa\sigma_{ij}\right)^{\nu_{hj}/2-3} \gamma\left(-\frac{\nu_{hj}}{2}+3, \frac{\nu_{hj}}{2}\kappa r\right) \\ & - \frac{1}{-\frac{\nu_{hj}}{2}+2} \left(\frac{r}{\sigma_{ij}}\right)^{-\nu_{hj}/2+2} \exp\left(-\frac{\nu_{hj}}{2}\kappa r\right) \\ & - \left[1 - \frac{\frac{\nu_{hj}}{2}\kappa\sigma_{ij}}{-\frac{\nu_{hj}}{2}+2}\right] \left(\frac{\nu_{hj}}{2}\kappa\sigma_{ij}\right)^{\nu_{hj}/2-3} \gamma\left(-\frac{\nu_{hj}}{2}+3, \frac{\nu_{hj}}{2}\kappa\sigma_{ij}\right) \\ & + \frac{1}{-\frac{\nu_{hj}}{2}+2} \exp\left(-\frac{\nu_{hj}}{2}\kappa\sigma_{ij}\right). \end{aligned} \tag{539}$$

If the integration in Eq. (536) is performed,

$$\mathcal{P}_{ij}^{\rm ex}(r) = -\sum_{h=1}^{2} \zeta_{ij}^{(h)+} \left(\frac{1}{\sigma_{ij}}\right)^{\nu_{hj}/2-2} \left(1 - \frac{\sigma_{ij}}{r}\right) \mathcal{I}^{\rm ex}(\nu_{hj}, \kappa\sigma_{ij}; \kappa r), \tag{540}$$

where

$$\begin{aligned} \mathcal{I}^{\rm ex}(\nu_{hj}, \kappa\sigma_{ij}; \kappa r) \equiv & - \frac{1}{-\frac{\nu_{hj}}{2}+2} \left(\frac{\nu_{hj}}{2}\kappa\sigma_{ij}\right)^{\nu_{hj}/2-2} \gamma\left(-\frac{\nu_{hj}}{2}+3, \frac{\nu_{hj}}{2}\kappa r\right) \\ & - \frac{1}{-\frac{\nu_{hj}}{2}+2} \left(\frac{r}{\sigma_{ij}}\right)^{-\nu_{hj}/2+2} \exp\left(-\frac{\nu_{hj}}{2}\kappa r\right) \\ & + \frac{1}{-\frac{\nu_{hj}}{2}+2} \left(\frac{\nu_{hj}}{2}\kappa\sigma_{ij}\right)^{\nu_{hj}/2-2} \Gamma\left(-\frac{\nu_{hj}}{2}+3\right). \end{aligned} \tag{541}$$

If $\sigma_{ij} = \sigma$ is satisfied independently of i and j, $\mathcal{P}_{ij}(r)$ can be simplified. Then, the sum of Eqs. (537) and (540) allows $\mathcal{P}_{ij}(r)$ to be given as

$$\begin{aligned} \mathcal{P}_{ij}(r) = -\zeta_{ij}^{(h)+} \left(\frac{1}{\sigma}\right)^{-1/2} \mathcal{I}(3, \kappa\sigma; \kappa r)\Big|_{h\neq j} - \zeta_{ij}^{(j)+} \left(\frac{1}{\sigma}\right)^{1/2} \mathcal{I}(5, \kappa\sigma; \kappa r), \\ (i = 1, \ 2; \ \ j = 1, \ 2), \end{aligned} \tag{542}$$

where

$$\begin{aligned} \mathcal{I}(\nu_{hj}, \kappa\sigma; \kappa r) \equiv & \left[\frac{\sigma}{r}\mathcal{I}^{\rm in}(\nu_{hj}, \kappa\sigma; \kappa r) + \left(1 - \frac{\sigma}{r}\right) \mathcal{I}^{\rm ex}(\nu_{hj}, \kappa\sigma; \kappa r)\right] \\ & (\nu_{hj} = 3, \ (h \neq j); \ \nu_{hj} = 5 \ (h = j)). \end{aligned} \tag{543}$$

Thus, the dependence of $\mathcal{P}_{ij}(r)$ on r is caused by $\mathcal{I}(3, \kappa\sigma; \kappa r)$ and $\mathcal{I}(5, \kappa\sigma; \kappa r)$.

If Eq. (221) is used, then the behavior of $\mathcal{I}(\nu, \kappa\sigma; \kappa r)$ ($\nu = 3,\ 5$) is expressed as

$$\mathcal{I}(\nu, \kappa\sigma; \kappa r) \sim \left(\frac{r}{\sigma}\right)^{-3+\langle df\rangle_\nu}, \quad (\nu = 3,\ 5), \tag{544}$$

where

$$\langle df\rangle_\nu \equiv \left[-\frac{r}{3\mathcal{I}(\nu, \kappa\sigma; \kappa r)}\frac{d}{dr}\mathcal{I}(\nu, \kappa\sigma; \kappa r)\right]^{-1/3}. \tag{545}$$

The behaviors of $\langle df\rangle_\nu$ ($\nu = 3,\ 5$) at least in Figs. 32 and 33 demonstrate that the dependence of $\mathcal{P}_{ij}(r)$ ($i = 1, 2;\ j = 1, 2$) on r cannot be expressed as the product of r^{-1} and a function given as a Taylor series with respect to r. According to Figs. 32, 33, and 34, the behaviors of $\langle df\rangle_\nu$ ($\nu = 3,\ 5$) depend on $\kappa\sigma$. Although the factor $\langle d_f\rangle_\nu$ is not equivalent to a fractal dimension of physical cluster, the factor can characterize a fractal structure of the distribution of charged particles. Thus, the consequences appearing in the figures indicate that fractal structures formed by physical clusters of charged particles can hold the dependence on $\kappa\sigma$.

4. Differential equations for characterizing long-range features of $\mathcal{H}_{ij}(r)$

(a) *Differential equation for $\mathcal{L}$ components*

A differential equation derived from Eq. (511) enables $\mathcal{H}_{ij}(r_{ij})$ to be estimated, and it is given as

$$\sum_{k=1}^{\mathcal{L}} \rho_k \widehat{c}_{ik}^{(2)} \nabla^2 \mathcal{H}_{kj}(r) - \sum_{k=1}^{\mathcal{L}} \Bigg(\delta_{ik} - \rho_k \widehat{c}_{ik}^{(0)} \Bigg) \mathcal{H}_{kj}(r)$$
$$\approx -C_{ij}^{*}(r) - \sum_{k=1}^{\mathcal{L}} \rho_k \widehat{C}_{ik}^{*(0)} \mathcal{P}_{kj}(r) - \sum_{k=1}^{\mathcal{L}} \rho_k \widehat{C}_{ik}^{*(2)} \nabla^2 \mathcal{P}_{kj}(r). \tag{546}$$

If Eq. (546) is multiplied by $(\rho_i \rho_j)^{1/2}$,

$$\sum_{k=1}^{\mathcal{L}} \sqrt{\rho_i \rho_k} \widehat{c}_{ik}^{(2)} \nabla^2 \overline{\mathcal{H}}_{kj}(r) - \sum_{k=1}^{\mathcal{L}} \Bigg(\delta_{ik} - \sqrt{\rho_i \rho_k} \widehat{c}_{ik}^{(0)} \Bigg) \overline{\mathcal{H}}_{kj}(r)$$
$$\approx -\sqrt{\rho_i \rho_j} C_{ij}^{*}(r) - \sum_{k=1}^{\mathcal{L}} \sqrt{\rho_i \rho_k} \widehat{C}_{ik}^{*(0)} \overline{\mathcal{P}}_{kj}(r) - \sum_{k=1}^{\mathcal{L}} \sqrt{\rho_i \rho_k} \widehat{C}_{ik}^{*(2)} \nabla^2 \overline{\mathcal{P}}_{kj}(r), \tag{547}$$

where

$$\overline{\mathcal{H}}_{kj}(r) \equiv \sqrt{\rho_k \rho_j} \mathcal{H}_{kj}(r). \tag{548}$$

If $\nabla^2 \overline{\mathcal{P}}_{ij}(r)$ given by Eq. (522) is substituted into Eq. (547), then

$$\sum_{k=1}^{\mathcal{L}} \sqrt{\rho_i \rho_k} \widehat{c}_{ik}^{(2)} \nabla^2 \overline{\mathcal{H}}_{kj}(r) - \sum_{k=1}^{\mathcal{L}} \Bigg(\delta_{ik} - \sqrt{\rho_i \rho_k} \widehat{c}_{ik}^{(0)} \Bigg) \overline{\mathcal{H}}_{kj}(r)$$
$$\approx -\sqrt{\rho_i \rho_j} C_{ij}^{*}(r) - \sum_{k=1}^{\mathcal{L}} \Bigg[\sqrt{\rho_i \rho_k} \widehat{C}_{ik}^{*(0)} + \sum_{l=1}^{\mathcal{L}} \sqrt{\rho_i \rho_l} \widehat{C}_{il}^{*(2)} \sum_{h=1}^{\mathcal{L}} (-1)^{h+l} \frac{\det |\sqrt{\rho_h \rho_l} \widehat{C}_{hl}^{+(2)\epsilon}|}{\det |\sqrt{\rho_\gamma \rho_\delta} \widehat{C}_{\gamma\delta}^{+(2)}|}$$
$$\times \Bigg(\delta_{hk} - \sqrt{\rho_h \rho_k} \widehat{C}_{hk}^{+(0)} \Bigg) \Bigg] \overline{\mathcal{P}}_{kj}(r) + \sum_{k=1}^{\mathcal{L}} \sqrt{\rho_i \rho_k} \widehat{C}_{ik}^{*(2)} \sum_{h=1}^{\mathcal{L}} (-1)^{h+k} \frac{\det |\sqrt{\rho_h \rho_k} \widehat{C}_{hk}^{+(2)\epsilon}|}{\det |\sqrt{\rho_\gamma \rho_\delta} \widehat{C}_{\gamma\delta}^{+(2)}|} \sqrt{\rho_h \rho_j} C_{hj}^{+}(r). \tag{549}$$

The inverse matrix of $\sqrt{\rho_\gamma \rho_\delta} \widehat{c}_{\gamma\delta}^{(2)}$ is given as

$$(-1)^{g+i} \frac{\det |\sqrt{\rho_g \rho_i} \widehat{c}_{gi}^{(2)\epsilon}|}{\det |\sqrt{\rho_\gamma \rho_\delta} \widehat{c}_{\gamma\delta}^{(2)}|},$$

where the matrix $\sqrt{\rho_g\rho_i}\widehat{c}_{gi}^{(2)\epsilon}$ does not include the specific elements $\sqrt{\rho_g\rho_\delta}\widehat{c}_{g\delta}^{(2)}$ $(\delta = 1, 2, \cdots \mathcal{L})$ and $\sqrt{\rho_\gamma\rho_i}\widehat{c}_{\gamma i}^{(2)}$ $(\gamma = 1, 2, \cdots \mathcal{L})$. If this inverse matrix is used, Eq. (549) can be rewritten as

$$
\begin{aligned}
&\nabla^2\overline{\mathcal{H}}_{ij}(r) - \sum_{g=1}^{\mathcal{L}}(-1)^{g+i}\frac{\det|\sqrt{\rho_g\rho_i}\widehat{c}_{gi}^{(2)\epsilon}|}{\det|\sqrt{\rho_\gamma\rho_\delta}\widehat{c}_{\gamma\delta}^{(2)}|}\sum_{k=1}^{\mathcal{L}}\left(\delta_{gk} - \sqrt{\rho_g\rho_k}\widehat{c}_{gk}^{(0)}\right)\overline{\mathcal{H}}_{kj}(r) \\
&\approx -\sum_{g=1}^{\mathcal{L}}(-1)^{g+i}\frac{\det|\sqrt{\rho_g\rho_i}\widehat{c}_{gi}^{(2)\epsilon}|}{\det|\sqrt{\rho_\gamma\rho_\delta}\widehat{c}_{\gamma\delta}^{(2)}|}\Bigg\{\sqrt{\rho_g\rho_j}C_{gj}^{*}(r) \\
&+\sum_{k=1}^{\mathcal{L}}\Bigg[\sqrt{\rho_g\rho_k}\widehat{C}_{gk}^{*(0)} + \sum_{l=1}^{\mathcal{L}}\sqrt{\rho_g\rho_l}\widehat{C}_{gl}^{*(2)}\sum_{h=1}^{\mathcal{L}}(-1)^{h+l}\frac{\det|\sqrt{\rho_h\rho_l}\widehat{C}_{hl}^{+(2)\epsilon}|}{\det|\sqrt{\rho_\gamma\rho_\delta}\widehat{C}_{\gamma\delta}^{+(2)}|} \\
&\times\left(\delta_{hk} - \sqrt{\rho_h\rho_k}\widehat{C}_{hk}^{+(0)}\right)\Bigg]\overline{\mathcal{P}}_{kj}(r) \\
&-\sum_{k=1}^{\mathcal{L}}\sqrt{\rho_g\rho_k}\widehat{C}_{gk}^{*(2)}\sum_{h=1}^{\mathcal{L}}(-1)^{h+k}\frac{\det|\sqrt{\rho_h\rho_k}\widehat{C}_{hk}^{+(2)\epsilon}|}{\det|\sqrt{\rho_\gamma\rho_\delta}\widehat{C}_{\gamma\delta}^{+(2)}|}\sqrt{\rho_h\rho_j}C_{hj}^{+}(r)\Bigg\},
\end{aligned}
\tag{550}
$$

where $C_{gj}^{*}(r)$ and $C_{hj}^{+}(r)$, as well as $\mathcal{P}_{kj}(r)$, must be given as long-range contributions.

(b) *Approximated differential equation for $\mathcal{L} = 2$ at large r*

In a ionic fluid system specified by $\mathcal{L} = 2$, the behavior of $\mathcal{H}_{ij}(r)$ at large r must be restricted by $\sum_{k=1}^{2} e_k\rho_k\mathcal{H}_{ik}(r) = 0$, which is given for $\mathcal{L} = 2$ by Eq. (454). This fact denotes that Eq. (454) requires $\mathcal{H}_{ij}(r) = \mathcal{H}_{ii}(r)$ $(i \neq j)$ to be satisfied at large r because the electroneutrality requires $\sum_{k=1}^{2} e_k\rho_k = 0$. For $\mathcal{L} = 2$, Eq. (453) requires $\mathcal{P}_{ij}(r) = \mathcal{P}_{ii}(r)$ $(i \neq j)$ at large r. Therefore, Eq. (550) and a relation Eq. (548) allow the following approximation

$$
\nabla^2\mathcal{H}_{ij}(r) - (\xi_i)^2\mathcal{H}_{ij}(r) \approx \sum_{g=1}^{2}\Theta_{ig}C_{gj}^{*}(r) + \sum_{g=1}^{2}\Theta_{ig}^{(P)}\mathcal{P}_{ij}(r) + \sum_{g=1}^{2}\Theta_{ig}^{(C^+)}C_{gj}^{+}(r), \tag{551}
$$

where the four coefficients are defined as

$$
\xi_i \equiv \left[\sum_{g=1}^{2}(-1)^{g+i}\frac{\det|\sqrt{\rho_g\rho_i}\widehat{c}_{gi}^{(2)\epsilon}|}{\det|\sqrt{\rho_\gamma\rho_\delta}\widehat{c}_{\gamma\delta}^{(2)}|}\sum_{k=1}^{2}\left(\delta_{gk} - \sqrt{\rho_g\rho_k}\widehat{c}_{gk}^{(0)}\right)\sqrt{\frac{\rho_k}{\rho_i}}\right]^{1/2}, \tag{552}
$$

$$\Theta_{ig} \equiv -(-1)^{g+i}\frac{\det|\sqrt{\rho_g\rho_i}\widehat{c}^{(2)\epsilon}_{gi}|}{\det|\sqrt{\rho_\gamma\rho_\delta}\widehat{c}^{(2)}_{\gamma\delta}|}\sqrt{\frac{\rho_g}{\rho_i}}, \tag{553}$$

$$\begin{aligned}\Theta^{(P)}_{ig} \equiv & -\sum_{k=1}^{2}(-1)^{k+i}\frac{\det|\sqrt{\rho_k\rho_i}\widehat{c}^{(2)\epsilon}_{ki}|}{\det|\sqrt{\rho_\gamma\rho_\delta}\widehat{c}^{(2)}_{\gamma\delta}|}\Bigg[\sqrt{\rho_k\rho_g}\widehat{C}^{*(0)}_{kg}+\sum_{l=1}^{2}\sqrt{\rho_k\rho_l}\widehat{C}^{*(2)}_{kl} \\ & \times\sum_{h=1}^{2}(-1)^{h+l}\frac{\det|\sqrt{\rho_h\rho_l}\widehat{C}^{+(2)\epsilon}_{hl}|}{\det|\sqrt{\rho_\gamma\rho_\delta}\widehat{C}^{+(2)}_{\gamma\delta}|}\left(\delta_{hg}-\sqrt{\rho_h\rho_g}\widehat{C}^{+(0)}_{hg}\right)\Bigg]\sqrt{\frac{\rho_g}{\rho_i}},\end{aligned} \tag{554}$$

$$\Theta^{(C^+)}_{ig} \equiv \sum_{h=1}^{2}(-1)^{h+i}\frac{\det|\sqrt{\rho_h\rho_i}\widehat{c}^{(2)\epsilon}_{hi}|}{\det|\sqrt{\rho_\gamma\rho_\delta}\widehat{c}^{(2)}_{\gamma\delta}|}\sum_{k=1}^{2}\sqrt{\rho_h\rho_k}\widehat{C}^{*(2)}_{hk}(-1)^{g+k}\frac{\det|\sqrt{\rho_g\rho_k}\widehat{C}^{+(2)\epsilon}_{gk}|}{\det|\sqrt{\rho_\gamma\rho_\delta}\widehat{C}^{+(2)}_{\gamma\delta}|}\sqrt{\frac{\rho_g}{\rho_i}}. \tag{555}$$

If physical clusters of charged particles do not exist in an ionic fluid system specified by $\mathcal{L}=2$, the correlation functions related to the formation of physical clusters should vanish, i.e., $\mathcal{P}_{ij}(r)=0$ and $C^+_{ij}(r)=0$. If an ionic fluid includes large physical clusters, the physical clusters should contribute to forming specific features of the ionic fluid. $\mathcal{H}_{ij}(r)$ for the ionic fluid can be estimated as a solution of Eq. (551) using a solution of Eq. (523). Then, the solution of Eq. (551) is not independent of $\mathcal{P}_{ij}(r)$. Thus, the formation of physical clusters of charged particles affects the behavior of $\mathcal{H}_{ij}(r)$ for the ionic fluid.

(c) *Solution of differential equation for ionic fluid system*

When an ionic fluid system includes physical clusters of charged particles, $\mathcal{P}_{ij}(r)\neq 0$ and $C^+_{ij}(r)\neq 0$ are satisfied. In order to form a solution satisfying the differential equation Eq. (551) for the ionic fluid system, the ionic fluid system should be imaginarily divided into the internal area of a spherical region of radius r and the external area of the spherical region. Then, the center of the spherical region is located at origin $t=0$ of a spherical coordinate.

An unbound state in which the contribution of the relative kinetic energy of two charged particles exceeds the contribution of the mutually attractive force is specified as an f^*-bond. The correlation specified by $\mathcal{H}_{ij}(r)$ is generated between a charged particle at $t=0$ and another charged particle at $t=r$ via charged particles linked through each path that includes f^*-bonds; it is given by the sum of two partial contributions. One of the two partial contributions comes from charged particles distributed within a spherical region of radius r with its center located at $t=0$. This is estimated from the differential equation given by

Eq. (551), and it is described as a sum $\mathcal{H}_{ij}^{(+)\mathrm{in}}(r)+\mathcal{H}_{ij}^{(*)\mathrm{in}}(r)$. The first part $\mathcal{H}_{ij}^{(+)\mathrm{in}}(r)$ involves effects of the physical cluster formation, and it is given by

$$\mathcal{H}_{ij}^{(+)\mathrm{in}}(r) = -\xi_i\sigma_{ij}h_0^{(1)}(i\xi_i r)\int_{\sigma_{ij}}^{r}\mathcal{G}_{ij}(\xi_i;t)$$
$$\times\left\{\sum_{g=1}^{2}(\sigma_{ij})^2\Theta_{ig}^{(P)}\mathcal{P}_{ij}(t)+\sum_{g=1}^{2}(\sigma_{ij})^2\Theta_{ig}^{(C^+)}C_{gj}^{+}(t)\right\}\left(\frac{t}{\sigma_{ij}}\right)^2\frac{1}{\sigma_{ij}}\mathrm{d}t,\quad(t<r),\tag{556}$$

where $\mathcal{G}_{ij}(\xi_i;t)$ is defined as

$$\mathcal{G}_{ij}(\xi_i;t)\equiv j_0(i\xi_i t)-\frac{j_0(i\xi_i\sigma_{ij})}{h_0^{(1)}(i\xi_i\sigma_{ij})}h_0^{(1)}(i\xi_i t).\tag{557}$$

Here, the spherical Bessel function $j_0(\tau)$ and spherical Hankel function of the first kind $h_0^{(1)}(\tau)$ are expressed

$$\begin{cases}j_0(\tau)=\tau^{-1}\sin\tau\\ h_0^{(1)}(\tau)=i\tau^{-1}e^{-i\tau}.\end{cases}$$

The second part $\mathcal{H}_{ij}^{(*)\mathrm{in}}(r)$ is non-zero even if physical clusters do not exist, and it is given by

$$\mathcal{H}_{ij}^{(*)\mathrm{in}}(r) = -\xi_i\sigma_{ij}h_0^{(1)}(i\xi_i r)\int_{\sigma_{ij}}^{r}\mathcal{G}_{ij}(\xi_i;t)\sum_{g=1}^{2}(\sigma_{ij})^2\Theta_{ig}C_{gj}^{*}(t)\left(\frac{t}{\sigma_{ij}}\right)^2\frac{1}{\sigma_{ij}}\mathrm{d}t,\quad(t<r).\tag{558}$$

The remainder of the two partial contributions results from charged particles distributed outside the spherical region. This is estimated from the differential equation given by Eq. (551), and it is described as a sum $\mathcal{H}_{ij}^{(+)\mathrm{ex}}(r)+\mathcal{H}_{ij}^{(*)\mathrm{ex}}(r)$. The first part $\mathcal{H}_{ij}^{(+)\mathrm{ex}}(r)$ involves effects of the physical cluster formation and it is given by

$$\mathcal{H}_{ij}^{(+)\mathrm{ex}}(r) = -\xi_i\sigma_{ij}\mathcal{G}_{ij}(\xi_i;r)\int_{r}^{\infty}h_0^{(1)}(i\xi_i t)$$
$$\times\left\{\sum_{g=1}^{2}(\sigma_{ij})^2\Theta_{ig}^{(P)}\mathcal{P}_{ij}(t)+\sum_{g=1}^{2}(\sigma_{ij})^2\Theta_{ig}^{(C^+)}C_{gj}^{+}(t)\right\}\left(\frac{t}{\sigma_{ij}}\right)^2\frac{1}{\sigma_{ij}}\mathrm{d}t,\quad(r<t).\tag{559}$$

The other part $\mathcal{H}_{ij}^{(*)\mathrm{ex}}(r)$ is non-zero even if physical clusters do not exist, and it is given by

$$\mathcal{H}_{ij}^{(*)\mathrm{ex}}(r) = -\xi_i\sigma_{ij}\mathcal{G}_{ij}(\xi_i;r)\int_{r}^{\infty}h_0^{(1)}(i\xi_i t)\sum_{g=1}^{2}(\sigma_{ij})^2\Theta_{ig}C_{gj}^{*}(t)\left(\frac{t}{\sigma_{ij}}\right)^2\frac{1}{\sigma_{ij}}\mathrm{d}t,\quad(r<t).\tag{560}$$

In Eqs. (556), (558), (559), and (560), the product $h_0^{(1)}\mathcal{G}_{ij}$ has the same form as that expressed by Eqs. (529) and (530) as

$$h_0^{(1)}(i\xi_i r)\mathcal{G}_{ij}(\xi_i;t) = -\frac{e^{-\xi_i(r-t)}}{2\xi_i r\xi_i t} + \left(1+\frac{2\sinh\xi_i\sigma_{ij}}{e^{-\xi_i\sigma_{ij}}}\right)\frac{e^{-\xi_i(r+t)}}{2\xi_i r\xi_i t}, \tag{561}$$

$$\mathcal{G}_{ij}(\xi_i;r)h_0^{(1)}(i\xi_i t) = -\frac{e^{-\xi_i(t-r)}}{2\xi_i t\xi_i r} + \left(1+\frac{2\sinh\xi_i\sigma_{ij}}{e^{-\xi_i\sigma_{ij}}}\right)\frac{e^{-\xi_i(t+r)}}{2\xi_i t\xi_i r}. \tag{562}$$

The correlation function $\mathcal{H}_{ij}(r)$ given as a solution satisfying Eq. (551) is expressed as the sum of Eqs. (556), (558), (559), and (560), i.e.,

$$\mathcal{H}_{ij}(r) = \mathcal{H}_{ij}^{(+)\text{in}}(r) + \mathcal{H}_{ij}^{(+)\text{ex}}(r) + \mathcal{H}_{ij}^{(*)\text{in}}(r) + \mathcal{H}_{ij}^{(*)\text{ex}}(r). \tag{563}$$

Thus, if Eqs. (561) and (562) are considered, Eq. (563) allows the correlation function $\mathcal{H}_{ij}(r)$ to be given as

$$\begin{aligned}\mathcal{H}_{ij}(r) =& -\mathcal{M}_{ij}^*\frac{e^{-\xi_i r}}{2\xi_i r} \\ &+\frac{1}{2\xi_i r}\int_{\sigma_{ij}}^{r} e^{\xi_i(t-r)}\left[\sum_{g=1}^{2}\Theta_{ig}C_{gj}^*(t)+\sum_{g=1}^{2}\Theta_{ig}^{(P)}\mathcal{P}_{ij}(t)+\sum_{g=1}^{2}\Theta_{ig}^{(C^+)}C_{gj}^+(t)\right]t\mathrm{d}t \\ &+\frac{e^{\xi_i r}}{2\xi_i r}\int_{r}^{\infty} e^{-\xi_i t}\left[\sum_{g=1}^{2}\Theta_{ig}C_{gj}^*(t)+\sum_{g=1}^{2}\Theta_{ig}^{(P)}\mathcal{P}_{ij}(t)+\sum_{g=1}^{2}\Theta_{ig}^{(C^+)}C_{gj}^+(t)\right]t\mathrm{d}t,\end{aligned} \tag{564}$$

where

$$\mathcal{M}_{ij}^* \equiv e^{2\xi_i\sigma}\int_{\sigma_{ij}}^{\infty}\left[\sum_{g=1}^{2}\Theta_{ig}C_{gj}^*(t)+\sum_{g=1}^{2}\Theta_{ig}^{(P)}\mathcal{P}_{ij}(t)+\sum_{g=1}^{2}\Theta_{ig}^{(C^+)}C_{gj}^+(t)\right]e^{-\xi_i t}t\mathrm{d}t. \tag{565}$$

In addition, the above solution does not include the contribution that is given independently of the term on the right-hand side of Eq. (551).

(d) *For the ionic fluid system with no existence of physical clusters of charged particles*

If the physical clusters of charged particles do not exist in an ionic fluid system, correlation functions related to the formation of physical clusters should vanish, i.e., $\mathcal{P}_{ij}(r) = 0$ and $C_{ij}^+(r) = 0$. For the ionic fluid system that does not include physical clusters of charged particles, contributions of $\mathcal{P}_{ij}(r)$ and $C_{ij}^+(r)$ to the differential equations are completely neglected. For example, Eq. (551) is simplified as

$$\nabla^2\mathcal{H}_{ij}(r) - (\xi_i)^2\mathcal{H}_{ij}(r) \approx \sum_{g=1}^{2}\Theta_{ig}C_{gj}^*(r), \tag{566}$$

where Eq. (487) requires $C^*_{gj}(r)$ in Eq. (566) to expressed as

$$C^*_{gj}(r) = K^*_{gj}\frac{e^{-\kappa r}}{r} \tag{567}$$

A solution satisfying Eq. (566) is given by Eq. (564) as

$$\begin{aligned}\mathcal{H}_{ij}(r) =& -\mathcal{M}^*_{ij}\frac{e^{-\xi_i r}}{2\xi_i r} \\ &+\sum_{g=1}^{2}\Theta_{ig}\left[\frac{1}{2\xi_i r}\int_{\sigma_{ij}}^{r} e^{\xi_i(t-r)}C^*_{gj}(t)t\mathrm{d}t + \frac{e^{\xi_i r}}{2\xi_i r}\int_{r}^{\infty} e^{-\xi_i t}C^*_{gj}(t)t\mathrm{d}t\right],\end{aligned} \tag{568}$$

where

$$\mathcal{M}^*_{ij} \equiv e^{2\xi_i\sigma}\int_{\sigma_{ij}}^{\infty}\sum_{g=1}^{2}\Theta_{ig}C^*_{gj}(t)e^{-\xi_i t}t\mathrm{d}t. \tag{569}$$

If the integration is performed in Eq. (568),

$$\begin{aligned}\mathcal{H}_{ij}(r) =& -\mathcal{M}^*_{ij}\frac{e^{-\xi_i r}}{2\xi_i r} \\ &+\frac{e^{-\kappa r}}{2\xi_i r}\sum_{g=1}^{2}\Theta_{ig}\left[\frac{K^*_{gj}}{\xi_i-\kappa}(1-e^{(\xi_i-\kappa)\sigma_{ij}}e^{-(\xi_i-\kappa)r}) + \frac{K^*_{gj}}{\xi_i+\kappa}\right].\end{aligned} \tag{570}$$

Eq. (570) denotes that the dependence of $\mathcal{H}_{ij}(r)$ on r is characterized by the product of r^{-1} and a particular function given as the Taylor series with respect to r. When physical clusters of charged particles do not exist in the ionic fluid system, the dependence of $g_{ij}(r)$ on r is characterized by the product of r^{-1} and a particular function given as the Taylor series with respect to r, because $g_{ij}(r)$ is given as the sum $\mathcal{P}_{ij}(r) + \mathcal{H}_{ij}(r) + 1$. This result is similar to both the behavior of $g_{ij}(r)$ found by Ulander and Kjellander[15] and that found by Attard[16]. However, if the magnitude of $\mathcal{P}_{ij}(r)$ cannot be ignored, contributions of the physical cluster formation predicted from Figs. 32, 33, and 34 allow the dependence of $g_{ij}(r)$ on r to deviate from the behavior characterized by the product of r^{-1} and a particular function given as the Taylor series with respect to r. This means that charged particles that have small relative momenta cannot be homogeneously mixed with charged particles that have large relative momenta below temperatures at which the formation of physical clusters are allowed.

5. Long-range features of correlation functions in ionic fluid systems

Particles with small and large relative momenta cannot be homogeneously mixed; particles with small relative momenta contribute to the physical cluster growth. The fluid system

in which the physical cluster formation is allowable has a characteristic structure.[52] Even in an ionic fluid system, charged particles that have small relative momenta cannot be homogeneously mixed with charged particles that have large relative momenta. The physical cluster formation allows the factor $\langle d_f \rangle_\nu$ to imply that the distribution of charged particles can have a fractal structure, although the factor is not equivalent to a fractal dimension of the physical cluster. Thus, the behavior of $\langle d_f \rangle_\nu$ found from Figs. 32, 33, and 34 implies that the dependence of the sum $\mathcal{P}_{ij}(r) + \mathcal{H}_{ij}(r) + 1$ on r can deviate from the behavior characterized by the product of r^{-1} and a particular function given as the Taylor series with respect to r.

If the formation of physical clusters is ignored, the dependence of $g_{ij}(r)$ on r can be characterized by the product of r^{-1} and a particular function given as the Taylor series with respect to r. Deviations from the dependence characterized by the product can be found through both experiments and numerical simulations. Some experiments allow the deviations to be demonstrated as the distribution patterns of colloidal particles which occur with fractal structures.[40,67–70] Further, the n umerical simulations allow the deviations to be demonstrated.[72] The distribution patterns of colloidal particles distributed as highly charged particles in a colloidal suspension indicates that the dependence of $g_{ij}(r)$ on r should be expressed through the sum of $\mathcal{P}_{ij}(r)$ and $\mathcal{H}_{ij}(r) + 1$.

Both an interface of an ensemble of particles contributing to the magnitude of $\mathcal{P}_{ij}(r)$ and that of an ensemble of particles contributing to the magnitude of $\mathcal{D}_{ij}(r)$ should be approximately determined by the Laplace equation. Each physical cluster should be electrically neutral because of $\sum_{k=1}^{2} e_k \rho_k \mathcal{P}_{ik}(r) = 0$, which corresponds to Eq. (453) being satisfied for large r. Further, each ensemble of particles contributing to the magnitude of $\mathcal{D}_{ij}(r)$ should be electrically neutral according to $\sum_{k=1}^{2} e_k \rho_k \mathcal{D}_{ik}(r) = 0$, which corresponds to Eq. (454) being satisfied for large r. These facts and Gauss' law imply that each interface formed by such ensembles and physical clusters can be determined by the Laplace equation. This consequence suggests the similarity of the physical cluster formation to the fact that the probability of finding a diffusing particle at a given point and the patter formation caused by the aggregation of diffusing particles are described by the Laplace equation[40,81]. The characteristic structure formation known from the charged particle distributions described by $\mathcal{P}_{ij}(r)$ and $\mathcal{D}_{ij}(r)$ can be one of phenomena related to fractal growth governed by the Laplace equation.

6. Appendix: Estimates for point charge system

(a) *Estimates depending on physical cluster formation*

Eqs. (485) and (486) allow for relation $\lim_{\kappa\to 0}\breve{z}_n = 0$. Eq. (497) allows for relation $\lim_{\kappa\to 0}(\widehat{\mathcal{P}}_{ij}(\breve{z}_n) - \widehat{\mathcal{P}}_{ij}(\breve{z}_m)) = 0$ even for $n \neq m$. Then, the use of Eq. (498) allows the relation $\lim_{\kappa\to 0}(\widehat{\mathcal{P}}_{ij}(\breve{z}_n) - \widehat{\mathcal{P}}_{ij}(\breve{z}_m))/(\breve{z}_n + \breve{z}_m) < \infty$ to be proved for $n \neq m$. This relation should be approximately satisfied for $0 < \kappa \ll 1$ and allows Eq. (498) to be modified for $0 < \kappa \ll 1$ and $0 < \kappa\sigma_i \ll 1$ as follows:

$$2\pi\widehat{\mathcal{P}}_{ij} = \frac{1}{2}\sum_{m=1}^{2} D_{ij}^{m} + 2\pi\sum_{m=1}^{2}\sum_{k=1}^{2}\rho_k\sigma_k\widehat{\mathcal{P}}_{ik}D_{kj}^{m} + 2\pi^2\sum_{m=1}^{2}\sum_{k=1}^{2}\sum_{l=1}^{2}\rho_k\rho_l\widehat{\mathcal{P}}_{ik}\widehat{\mathcal{P}}_{kl}D_{lj}^{m}\sigma_k^2, \quad (571)$$

where $\widehat{\mathcal{P}}_{ij} \equiv \widehat{\mathcal{P}}_{ij}(\breve{z}_1) \approx \widehat{\mathcal{P}}_{ij}(\breve{z}_2)$.

For a point charge system given as $\kappa\sigma_i = 0$ ($\kappa \neq 0$), Eqs. (501) and (571) can be extremely simplified as

$$2\pi\widehat{\mathcal{P}}_{ij} = \frac{1}{2}\sum_{n=1}^{2} D_{ij}^{n} \quad (572)$$

and

$$D_{ij}^{n} = \frac{\breve{z}_1 + \breve{z}_2}{\breve{z}_{\nu_n}}\left[\frac{\breve{z}_{\nu_n}}{\rho_j}\delta_{ij} - \frac{2\pi}{\rho_j}\sum_{k=1}^{2} D_{jk}^{\nu_n(-1)}K_{ki}^{\nu_n} - \frac{1}{2}D_{ij}^{\nu_n}\right], \quad (573)$$

where $\nu_n \equiv 2^{2-n}$. Then, Eq. (573) allows the dependence of D_{ij}^{n} on κ, although the dependence was neglected in the previous work.[80]

The symmetry condition $\widehat{\mathcal{P}}_{12} = \widehat{\mathcal{P}}_{21}$ allows Eq. (572) to result in

$$\sum_{n=1}^{2} D_{12}^{n} - \sum_{n=1}^{2} D_{21}^{n} = 0. \quad (574)$$

Since the requirement of a symmetry condition given as $|e_1| = |e_2|$ requires $\widehat{\mathcal{P}}_{11} = \widehat{\mathcal{P}}_{22}$, the condition $|e_1| = |e_2|$ allows Eqs. (572) and (573) to result in

$$\sum_{n=1}^{2} D_{11}^{n} - \sum_{n=1}^{2} D_{22}^{n} = 0 \quad (575)$$

and

$$D_{22}^{2} = \pm\left[\frac{\breve{z}_2 + \breve{z}_1}{\breve{z}_2 - \breve{z}_1}\left(\frac{4\pi}{\rho_1}K_{22}^{2} + \frac{\breve{z}_2 - \breve{z}_1}{\breve{z}_2 + \breve{z}_1}D_{12}^{2}D_{21}^{2}\right)\right]. \quad (576)$$

In addition, the selection of plus sign in Eq. (576) can give $\widehat{C}_{\alpha\beta}^{+(0)}$ and $\widehat{C}_{\alpha\beta}^{+(2)}$ to approximate values which lack physical meanings.

(b) *Estimates depending on Ornstein–Zernike equation*

i) *Solution of Ornstein–Zernike equation*

The coefficients $\widehat{c}_{\alpha\beta}^{(0)}$, and $\widehat{c}_{\alpha\beta}^{(2)}$ can be estimated by solving the Ornstein–Zernike equation. The Ornstein–Zernike equation can be expressed as

$$\begin{cases} \sum_{k=1}^{2}[\delta_{ik}+\widetilde{h}_{ik}(k)]\widetilde{Q}_{kj}(k)=\widetilde{Q}_{ij}^{(-1)}(-k) \\ \delta_{ij}-\widetilde{c}_{ij}(k)=\sum_{k=1}^{2}\widetilde{Q}_{ik}(k)\widetilde{Q}_{jk}(-k), \end{cases} \tag{577}$$

where

$$\begin{cases} \widetilde{h}_{ij}(k)\equiv \lim_{V\to\infty}(\rho_i\rho_j)^{1/2}\int_V (g_{ij}(r)-1)\exp[i\mathbf{k}\cdot\mathbf{r}]\mathrm{d}\mathbf{r} \\ \sum_{k=1}^{2}\widetilde{Q}_{ki}^{(-1)}(-k)\widetilde{Q}_{jk}(-k)=\delta_{ij}. \end{cases} \tag{578}$$

According to a solution of the Ornstein–Zernike equation,[82] the coefficient $\widetilde{Q}_{ij}(k)$ can be simply given for a point charge system as

$$\begin{cases} \widetilde{Q}_{ij}(k)\equiv \delta_{ij}-(\rho_i\rho_j)^{1/2}(-ik+z)^{-1}D_{ij} \\ D_{ij}\equiv -2\Gamma e_i e_j\left(\sum_l^2 \rho_l (e_l)^2\right)^{-1} \\ \Gamma=\frac{1}{2}\left[-z+\left(z^2+\alpha_0^2\sum_k^2\rho_k(e_k/e_0)^2\right)^{1/2}\right] \\ z\equiv\kappa. \end{cases} \tag{579}$$

ii) *Coefficients* $\widehat{C}_{\alpha\beta}^{*(0)}$ *and* $\widehat{C}_{\alpha\beta}^{*(2)}$

The coefficients $\widehat{C}_{\alpha\beta}^{*(0)}$, and $\widehat{C}_{\alpha\beta}^{*(2)}$ can be estimated as $\widehat{C}_{\alpha\beta}^{*(0)}=\widehat{c}_{\alpha\beta}^{(0)}-\widehat{C}_{\alpha\beta}^{+(0)}$, and $\widehat{C}_{\alpha\beta}^{*(2)}=\widehat{c}_{\alpha\beta}^{(2)}-\widehat{C}_{\alpha\beta}^{+(2)}$ according to Eq. (514).

If $(\rho_i\rho_j)^{1/2}\int_V c_{ij}(r)r^2\mathrm{d}\mathbf{r}=-(6/11)\lim_{k\to0}(\mathrm{d}^2/\mathrm{d}k^2)\widetilde{c}_{ij}(k)$ is considered with Eqs. (577) and (579), the coefficients $\widehat{c}_{\alpha\beta}^{(0)}$ and $\widehat{c}_{\alpha\beta}^{(2)}$ are estimated for a point charge system as

$$\widehat{c}_{\alpha\beta}^{(0)}=\frac{1}{z}(D_{\alpha\beta}+D_{\beta\alpha})-\frac{1}{z^2}\sum_k^2\rho_k D_{\alpha k}D_{\beta k} \tag{580}$$

and

$$\widehat{c}_{\alpha\beta}^{(2)}=\frac{2}{11z^3}(D_{\alpha\beta}+D_{\beta\alpha})-\frac{2}{11z^4}\sum_k^2\rho_k D_{\alpha k}D_{\beta k}. \tag{581}$$

V. CONTRIBUTIONS CAUSED BY STRUCTURE FORMED IN BOSE FLUID SYSTEM

The specific heat C_V of a Bose fluid system, which can be explained using quasiclassical expressions of its partition function, exhibits a discontinuity at a temperature T_c. The maximum of C_V at $T = \lim_{\delta\to 0}(T_c - \delta)$ is different from that at $T = \lim_{\delta\to 0}(T_c + \delta)$. T_c corresponds to the temperature at which the absolute value of the chemical potential becomes equivalent to the magnitude of the mean effect of attractive forces acting between a single particle and other particles surrounding it. The dependence of T_c on repulsive interactions can be found as the mean effect of exclusion caused by the hard core of each particle. Further, if the contribution of specific motions of particles having sufficiently low kinetic energies corresponds to the contribution from rotons, the contribution leads to a sharp increase in C_V near T_c.

A. Introduction

A discontinuity in the temperature dependence of the specific heat can occur at the transition temperature below which features of a Bose fluid deviate from their normal behavior. The confirmation of the discontinuity is demonstrated for an ideal Bose gas in a uniform gravitational field.[90] The possibility of the discontinuity is generally suggested in terms of energy fluctuations.[91] Thus, it should be possible to confirm the discontinuity even for a real Bose fluid system wherein the constituent particles interact with each other.

The features of a Bose fluid are affected by interactions between particles that constitute its fluid system. From analytical estimates of thermodynamic quantities,[92,93] it is possible to briefly know the behavior of a Bose fluid system, which consists of particles that interact with each other only via repulsive forces. According to a theoretical interpretation,[92] the Bose fluid system becomes unstable if attractive forces contribute to interactions between the particles. In a trapped Bose fluid system, attractive forces between particles that constitute the system can lead to phase disturbance of the system.[94,95] Decreases in the mean interparticle distance can induce a condition where the contribution of attractive interparticle interactions is dominant if the mean interparticle distance is decreased beyond a critical value. This allows the sign of the reciprocal of the isothermal compressibility κ^{-1} to change

from positive to negative.[96]

The transition temperature at which the normal behavior of a Bose fluid system disappears is affected by interactions between particles constituting a Bose fluid system. If only repulsive forces contribute to interactions between the particles, the transition temperature is increased to a value exceeding that of an ideal Bose gas.[92,97] If both a repulsive force being dominant only within a short range and an attractive force being influential over a long-range contribute to the interactions between each pair of particles, the transition temperature for a Bose fluid system consisting of the particles is decreased to a lower value than that of an ideal Bose gas.[98] This is a phenomenon confirmed numerically under the condition that the particle density ρ of the system is sufficiently low.[98] In the condition, the relation $\rho|a_s|^3 \ll 1$ is satisfied with a_s denoting the s-wave scattering length corresponding to the hard-sphere diameter.

Conversely, if the mean interparticle distance $\rho^{-1/3}$ is comparable with the diameter σ_0 of hard core of each particle, a relation $1 < \rho^{-1/3}/\sigma_0 < 1.2$ can be satisfied. Then, each of particles constituting the Bose fluid system should transiently localize around its average position owing to the hard cores of other particles surrounding it, while thermally randomly moving. An increase in the density of hard cores can affect the normal macroscopic behavior of the Bose fluid that should be characterized by the thermally random motion of particles. The increase can affect the transition temperature, which corresponds to the lowest temperature at which the Bose fluid maintains normal macroscopic behavior. In case of liquid helium, its transition temperature depends on the density of hard cores caused by helium atoms.[99]

If the temperature of liquid helium is below the transition temperature, then a phase that allows generation of quasiparticles, such as rotons and phonons,[99–102] is induced. If many microscopic portions that maintain the phase occur within liquid helium, then the normal behavior induced for the existence of the other phase is disturbed.[103]

To mathematically analyze the phase wherein particles constituting a Bose fluid system move thermally and randomly, the kinetic energy of the translational motion of each particle in the phase is treated quasiclassically.[104] This allows quasiclassical expressions of a partition function to be adequate approximations. An approximate method for treating repulsive and attractive interactions as mean-field effects aids in forming the quasiclassical expressions. The quasiclassical expressions allow the behavior of the specific heat to be confirmed near

the transition temperature. According to the quasiclassical expressions, the transition temperature depends on the repulsive force, and the discontinuity in the behavior of the specific heat is confirmed as known.[90,91,105]

B. Approximate Aspects

1. Characterizations of system

The thermodynamics of a Bose fluid system consisting of particles moving with positive energies ε_α ($\alpha = 0, 1, 2, \cdots$) at temperature T are characterized by a partition function $Q^{(\mu)} = \prod_\alpha \Big\{ 1 - \exp\big[-\beta(\varepsilon_\alpha - \mu)\big] \Big\}^{-1}$. The chemical potential μ is negative for $T > 0$, and its negative value limits the number of particles moving with lower energies. The quantity β is defined by $\beta \equiv 1/(k_B T)$, where k_B denotes the Boltzmann constant. If the average number of particles moving with an energy ε_α is denoted by $\langle n_\alpha \rangle$, the total number of particles in the system is given by $\langle N \rangle \equiv \sum_\alpha \langle n_\alpha \rangle$, where $\langle n_\alpha \rangle = \big\{ \exp[\beta(\varepsilon_\alpha - \mu)] - 1 \big\}^{-1}$. For the total number $\langle N \rangle$, the wave function for characterizing the behavior of the system is expressed as $\Psi(\mathbf{r}_1, \mathbf{r}_2, \cdots, \mathbf{r}_{\langle N \rangle})$.

When localized ensembles are formed in the system by particles with sufficiently low energies ε_{α^*}, it is difficult for the particles to move with random mutual scattering. If the hard cores of particles constituting each ensemble are located near each other, they can be allowed to move coherently. Under the condition that the existence of the particles with ε_{α^*} is not ignored, the characteristic excitation states corresponding to quasiparticles is induced.[1] At low temperatures below the transition temperature, the thermodynamic properties of the system can involve specific portions that are described in terms of the contributions of quasiparticles, namely, rotons and phonons.[1,104,106]

Given the assumption that each of $\langle N \rangle - \langle \bar{n} \rangle$ particles is subject to random motion due to scattering from other particles in the Bose fluid system of $\langle N \rangle$ particles, $\langle \bar{n} \rangle$ particles should contribute to coherent motion. The contribution from $\langle \bar{n} \rangle$ particles to the internal energy is given by $\sum_{\alpha^*} \langle n_{\alpha^*} \rangle \varepsilon_{\alpha^*}$ for α^* satisfying $\sum_{\alpha^*} \langle n_{\alpha^*} \rangle = \langle \bar{n} \rangle$. The quantity $\sum_{\alpha^*} \langle n_{\alpha^*} \rangle \varepsilon_{\alpha^*}$ should, however, be estimated as the contribution from quasiparticles to avoid difficulty in estimating ε_{α^*}.

If the temperature of the system increases toward the transition temperature, then more

particles undergo thermal scattering, and this changes the properties of the system. In this process, a loss of ensembles of particles moving coherently occurs, and simultaneously, a loss of the excitation states is exhibited. Ultimately, the number of quasiparticles decreases in the process.[100] The random thermal motion of the particles causes coherent motion to disappear. However, at temperatures near the transition temperature, particles participating in the formation of excitation states can coexist with other particles that move with random thermal scattering.[102]

For each particle in the system, the three-dimensional area in which $|\Psi(\mathbf{r}_1, \mathbf{r}_2, \cdots, \mathbf{r}_{\langle N \rangle})|^2 \neq 0$ is satisfied is not equivalent to the volume V of the system. This is caused by the exclusion effect that results from the presence of repulsive interactions between particles. It decreases in strength with increases in the degree of random motion of each hard-core particle due to scattering from other particles. Conversely, the exclusion effect becomes stronger at lower temperatures. If the effective volume V_{eff} is applied for random movements of particles, V_{eff} decreases in the aforementioned situation. Furthermore, if particles that are located near each other with small momenta move coherently without mutual scattering, the effective volume V_{eff} for random movements of particles becomes further small in comparison with the volume V of the system. The consideration of the exclusion effect is equivalent to the consideration of repulsive interactions in terms of the mean-field effect, and the use of V_{eff} facilitates the consideration of repulsive interactions.

2. Hartree approximation

In a fluid system, the motion of a particle is affected by the attractive forces due to the other particles surrounding it. When this is considered as a mean-field effect of the attractive forces, it facilitates a simple analysis of the thermodynamic behavior. In this context, a suitable approach denotes the Hartree approximation, which is applied for analyzing oscillations of a Bose–Einstein condensate fluid[107] and describing the condensate wave function[108] for N particles.

The Hartree approximation is based on an approximate expression of the form $\Psi(\mathbf{r}_1, \mathbf{r}_2, \cdots, \mathbf{r}_N) = \prod_{i=1}^{N} \phi_i(\mathbf{r}_i)$, where the state $\phi_i(\mathbf{r})$ of a single particle at location $\mathbf{r}$ in the fluid system satisfies

the equation

$$-\frac{\hbar^2}{2m}\nabla^2\phi_i(\mathbf{r}) + \sum_{j=1,(j\neq i)}^{N}\int_V \phi_j^*(\mathbf{r}_j)\breve{u}(|\mathbf{r}-\mathbf{r}_j|)\phi_j(\mathbf{r}_j)\mathrm{d}\mathbf{r}_j\phi_i(\mathbf{r}) - \varepsilon_i\phi_i(\mathbf{r}) = 0. \qquad (582)$$

In Eq. (582), m is the mass of each particle. Specifically, a single particle i belonging to the state $\phi_i(\mathbf{r})$ moves with energy ε_i, and ϕ_j satisfies $\int_V \phi_j^*(\mathbf{r}_j)\phi_j(\mathbf{r}_j)\mathrm{d}\mathbf{r}_j \equiv \langle\phi_j|\phi_j\rangle = 1$. The pair potential $\breve{u}(|\mathbf{r}-\mathbf{r}_j|)$ characterizes attractive and repulsive forces acting between a particle j at location $\mathbf{r}_j$ and another particle at location $\mathbf{r}$. Hence, it denotes $\breve{u}(|\mathbf{r}-\mathbf{r}_j|) = \breve{u}_a(|\mathbf{r}-\mathbf{r}_j|) + \breve{u}_r(|\mathbf{r}-\mathbf{r}_j|)$.

With respect to an aspect for the motion of each particle in the fluid system, it is possible to consider that a single particle moves within an imaginal cylinder with a length equal to the mean free path l_f and with a cross section equal to that of a particle, as exemplified in Fig. 35. The aforementioned aspect allows $\sum_{j=1,(j\neq i)}^{N}\int_V \phi_j^*(\mathbf{r}_j)\breve{u}_a(|\mathbf{r}-\mathbf{r}_j|)\phi_j(\mathbf{r}_j)\mathrm{d}\mathbf{r}_j$ to be expressed as the total contribution of attractive pair potentials characterizing attractive forces between the single particle within the cylinder and other particles ($j = 1, 2, \cdots$) surrounding the cylinder. An approximation of the total contribution is obtained by assuming a spherically symmetric well as a pair potential. The spherically symmetric well is given as follows:

$$\begin{cases} \breve{u}_r(|\mathbf{r}-\mathbf{r}_j|) = +\infty & (|\mathbf{r}-\mathbf{r}_j| < \sigma_0), \\ \breve{u}_r(|\mathbf{r}-\mathbf{r}_j|) = 0 & (\sigma_0 < |\mathbf{r}-\mathbf{r}_j|), \\ \breve{u}_a(|\mathbf{r}-\mathbf{r}_j|) = -u_a & (\sigma_0 \leq |\mathbf{r}-\mathbf{r}_j| \leq \sigma_1 \text{ and } u_a > 0), \\ \breve{u}_a(|\mathbf{r}-\mathbf{r}_j|) = 0 & (\sigma_1 < |\mathbf{r}-\mathbf{r}_j| < \infty). \end{cases}$$

For the features of the pair potential, ϕ_j must satisfy $\phi_j(\mathbf{r}_j) = 0$ $(0 < |\mathbf{r}_j| < \sigma_0)$ and $\phi_j(\mathbf{r}_j) \neq 0$ $(\sigma_0 < |\mathbf{r}_j| < \infty)$.

The particles ($j = 1, 2, \cdots$) surrounding the cylinder are distributed with the particle density given by $\rho = \sum_{j=1,\ (j\neq i)}^{N}\phi_j^*(\mathbf{r}_j)\phi_j(\mathbf{r}_j)$. If ρ maintains the same value in any microscopic portions of the fluid system on average, the total contribution of attractive pair potentials is constant in the cylinder on average. Therefore, the depth of the total contribution should be proportional to both $-u_a$ and ρ, i.e.,

$$\sum_{j=1,(j\neq i)}^{N}\int_V \phi_j^*(\mathbf{r}_j)\breve{u}_a(|\mathbf{r}-\mathbf{r}_j|)\phi_j(\mathbf{r}_j)\mathrm{d}\mathbf{r}_j = -\breve{V}_a\rho u_a,$$

where $\breve{V}_a$ denotes the proportionality constant.

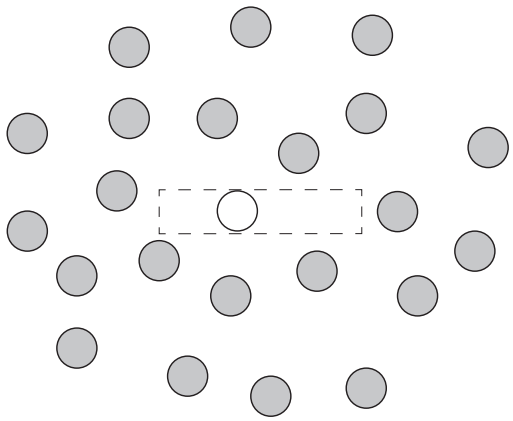

FIG. 35. Schematic image representing the distribution of particles in a fluid system. The white particle moves within an imaginal cylinder with length l_f of the mean free path.

$\sum_{j=1,(j\neq i)}^{N} \int_V \phi_j^*(\mathbf{r}_j)\breve{u}_r(|\mathbf{r}-\mathbf{r}_j|)\phi_j(\mathbf{r}_j)\mathrm{d}\mathbf{r}_j$ is expressed as the total contribution of repulsive pair potentials that appear at the end of the cylinder because only the hard core of each particle contributes to repulsion. Hence, the total contribution should be proportional to the number of particles colliding with the single particle in the cylinder. The number is given by

$\rho\breve{V}_r$ with $\breve{V}_r \equiv (1/2)[4\pi\sigma_0^3/3 - 4\pi(\sigma_0/2)^3/3]$. In an isotropic phase maintained on average, the magnitude of $\sum_{j=1,(j\neq i)}^{N}\int_V \phi_j^*(\mathbf{r}_j)\breve{u}_r(|\mathbf{r}-\mathbf{r}_j|)\phi_j(\mathbf{r}_j)\mathrm{d}\mathbf{r}_j$ is independent of the orientation of the cylinder. Thus,

$$\sum_{j=1,(j\neq i)}^{N}\int_V \phi_j^*(\mathbf{r}_j)\breve{u}_r(|\mathbf{r}-\mathbf{r}_j|)\phi_j(\mathbf{r}_j)\mathrm{d}\mathbf{r}_j = u_r\rho\breve{V}_r\theta(r-l_f),\ \ (r=|\mathbf{r}|).$$

Specifically, u_r denotes the proportionality constant although the dependence of u_r on ρ can appear for a variation in ρ. In the above equation, $\theta(r-l_f)$ denotes the Heaviside step function with the mean free path l_f.

Ultimately, the mean-field effects of the attractive and repulsive forces on the motion of the single particle at location $\mathbf{r}$ is expressed as follows:

$$\sum_{j=1,\ (j\neq i)}^{N}\int_V \phi_j^*(\mathbf{r}_j)\breve{u}(|\mathbf{r}-\mathbf{r}_j|)\phi_j(\mathbf{r}_j)\mathrm{d}\mathbf{r}_j = -\breve{V}_a\rho u_a + u_r\rho\breve{V}_r\theta(r-l_f),\quad (r=|\mathbf{r}|).$$

Given the use of the Hartree approximation and the aforementioned formalism for the mean-field effects, the energy ε_α corresponding to an approximate state ϕ_α of a single particle approximately satisfies the following simple equation:

$$(\varepsilon_\alpha-\mu)|\phi_\alpha\rangle = \left[-\frac{\hbar^2}{2m}\nabla^2 - U_a + U_r\theta(r-l_f) - \mu\right]|\phi_\alpha\rangle, \tag{583}$$

where $U_a \equiv \breve{V}_a\rho u_a$ and $U_r \equiv u_r\rho\breve{V}_r$ denote positive quantities.

Additionally, the temperature at which the equality $U_a+\mu=0$ holds is denoted by T_c in the study. The inequality $U_a+\mu<0$ always holds for $T_c<T$, and $U_a+\mu\geq 0$ holds for $T\leq T_c$.

C. Two quasiclassical expressions for $Q^{(\mu)}$

Two quasiclassical expressions are given for the partition function $Q^{(\mu)}$. One of the expressions corresponds to $Q^{(\mu)}$ for $T_c<T$, and the other expression corresponds to $Q^{(\mu)}$ for $T\leq T_c$. Each of the two quasiclassical expressions for $Q^{(\mu)}$ of a Bose fluid system is given in terms of a form corresponding to Eq. (583).

If the kinetic energy of translational motion of a particle is expressed in terms of its momentum $\mathbf{p}$, then a quasiclassical expression for Eq. (583) is given as follows:

$$\varepsilon_\alpha-\mu = p^2/(2m) - U_a + U_r\theta(r-l_f) - \mu, \tag{584}$$

where $p \equiv |\mathbf{p}|$ and $\varepsilon_\alpha - \mu > 0$.

1. *Expression for $Q^{(\mu)}$ for $T > T_c$*

For $T > T_c$, the inequality $-U_a - \mu > 0$ is satisfied, and thus $p^2/(2m) - U_a - \mu > 0$ is satisfied for p with an arbitrary value in the range $0 \leq p < \infty$. There is no restriction on the value of p. Therefore, a quasiclassical expression for $Q^{(\mu)}$ is given for $T_c < T$ by

$$\frac{1}{\beta} \ln Q^{(\mu)} = -\frac{1}{\beta} \int_V \mathrm{d}^3\mathbf{r} \int_0^\infty \frac{s\,\mathrm{d}^3\mathbf{p}}{(2\pi\hbar)^3} \ln \left\{ 1 - \wp \exp \left[-\beta \left(\frac{p^2}{2m} - U_a + U_r \theta(r - l_f) - \mu \right) \right] \right\}, \tag{585}$$

where the factor $\mathrm{d}^3\mathbf{r} s\,\mathrm{d}^3\mathbf{p}/(2\pi\hbar)^3$ denotes the number of modes existing in a volume $\mathrm{d}^3\mathbf{r}$ between $\mathbf{p}$ and $\mathbf{p} + \mathrm{d}\mathbf{p}$ with s denoting the number of possible spin states ($s = 3,\ m \neq 0$). Additionally, $\wp = 1$ must be satisfied in Eq. (585) based on the assumptions in the study.

Re-writing of Eq. (585) yields the following expression:

$$\frac{1}{\beta} \ln Q^{(\mu)} = \frac{2s}{3\beta(2\pi)^2\hbar^3} \left(\frac{\beta}{2m} \right)^{3/2} \Gamma\left(\tfrac{5}{2}\right) \sum_{k=1}^{\infty} \wp^k \frac{e^{k\bar{\mu}}}{k^{5/2}} V_k(U_r), \tag{586}$$

where $\bar{\mu}$ denotes a dimensionless quantity that is defined as follows:

$$\bar{\mu} \equiv \beta(U_a + \mu), \tag{587}$$

Additionally, V_k is defined as follows:

$$V_k(U_r) \equiv \int_V \exp\left[-k\beta U_r \theta(r - l_f)\right] 4\pi r^2\,\mathrm{d}r. \tag{588}$$

To facilitate the summation in Eq. (586), the Cauchy–Schwarz inequality should be considered. It results in the following expression:

$$\sum_{k=1}^{\infty} \wp^k \frac{e^{k\bar{\mu}}}{k^{5/2}} V_k(U_r) \leq \sum_{k=1}^{\infty} \wp^k \frac{e^{k\bar{\mu}}}{k^{5/2}} \sum_{k=1}^{\infty} V_k(U_r).$$

However, the factor $\sum_{k=1}^{\infty} V_k(U_r)$ cannot simply correspond to a quantity V_{eff} representing the effective volume because the factor diverges to infinity for $U_r = 0$. It is possible to avoid this problem. Multiplying the factor by $e^{-k\delta}$ allows its behavior to be normalized.

For $\delta = \ln 2$, the relation $\lim_{U_r \to 0} \sum_{k=1}^{\infty} V_k(U_r) e^{-k\delta} = V$ is satisfied. This allows a practical definition of $V_{\rm eff}$ as follows:

$$\begin{aligned} V_{\rm eff} &\equiv \sum_{k=1}^{\infty} V_k(U_r) e^{-2k} \\ &= v_f + \frac{V - v_f}{2e^{\beta U_r} - 1}, \end{aligned} \tag{589}$$

where v_f is defined as $v_f \equiv 4\pi l_f^3/3$. The use of $V_{\rm eff}$ can allow simple approximate forms to be given to thermodynamic quantities.

Additionally, $V_{\rm eff}$ in the normal liquid state should always significantly exceed v_f; i.e., $0 < v_f/V_{\rm eff} \ll 1$ because l_f denotes the mean free path. If atomic arrangements are locally similar to those in the solid state, then v_f is allowed to become comparable to $V_{\rm eff}$.

The dependence of U_r on ρ is revealed if the effective volume $V_{\rm eff}$ given by Eq. (589) is substituted into Eq. (B2). Additionally, assuming that the condition $0 < v_f/V \ll 1$ holds at $T = T_c$, the dependence is simplified as follows:

$$U_r = \frac{1}{\beta_c} \ln \left[\frac{1}{2} + \frac{s}{\sqrt{\pi}} \left(\frac{m}{2\pi\hbar^2 \beta_c} \right)^{3/2} \frac{\Gamma(3/2)\zeta(3/2)}{\rho} \right], \tag{590}$$

where $\beta_c \equiv 1/(k_B T_c)$. Thus, T_c depends on U_r.

2. *Expression for* $Q^{(\mu)}$ *for* $T \le T_c$

The partition function $Q^{(\mu)}$ is re-expressed as follows:

$$\frac{1}{\beta} \ln Q^{(\mu)} = \mathcal{G}_1 + \mathcal{G}_2, \tag{591}$$

where

$$\mathcal{G}_1 \equiv -\frac{1}{\beta} \sum_{\substack{\alpha^* \\ \text{for } 0 \le p < p_{\rm min}}} \ln\left[1 - e^{-\beta(\varepsilon_{\alpha^*} - \mu)}\right] \tag{592}$$

$$\mathcal{G}_2 \equiv -\frac{1}{\beta} \sum_{\substack{\alpha^* \\ \text{for } p_{\rm min} \le p < \infty}} \ln\left[1 - e^{-\beta(\varepsilon_{\alpha^*} - \mu)}\right]. \tag{593}$$

In Eq. (592), $\mathcal{G}_1$ denotes the contribution from $\langle \bar{n} \rangle$ particles that move with momenta being within the range $0 \le p < p_{\rm min}$, because the number of particle $\langle N \rangle$ in the system is given as

follows:

$$\langle N\rangle = \langle \bar{n}\rangle + \sum_{\substack{\alpha^* \\ \text{for } p_{\min}\le p<\infty}} \langle n_{\alpha^*}\rangle, \tag{594}$$

where

$$\langle \bar{n}\rangle = \sum_{\substack{\alpha^* \\ \text{for } 0\le p<p_{\min}}} \langle n_{\alpha^*}\rangle. \tag{595}$$

Then, $\mathcal{G}_2$ in Eq. (593) denotes the contribution from $\langle N\rangle - \langle \bar{n}\rangle$ particles that move with momenta being within the range $p_{\min} \le p < \infty$. In the aforementioned formulas, there is no requirement for restricting the value of $p_{\min}$.

If Eq. (593) is expressed as a quasiclassical expression, $\mathcal{G}_2$ is given as follows:

$$\mathcal{G}_2 = -\frac{1}{\beta}\int_V \mathrm{d}^3\mathbf{r}\int_{p_{\min}}^{\infty}\frac{s\,\mathrm{d}^3\mathbf{p}}{(2\pi\hbar)^3}\ln\left[1-\exp\left(-\frac{\beta p^2}{2m}+\bar{\mu}-\beta U_r\theta(r-l_f)\right)\right]. \tag{596}$$

The integral forming Eq. (596) is modified, and the following expression is obtained:

$$\begin{aligned}\mathcal{G}_2 = &-\frac{4\pi s}{3(2\pi\hbar)^3\beta}\left\{v_f p_{\min}^3\ln\left[1-\exp\left(-\frac{\beta p_{\min}^2}{2m}+\bar{\mu}\right)\right]\right.\\ &-(V-v_f)p_{\min}^3\ln\left[1-\exp\left(-\frac{\beta p_{\min}^2}{2m}+\bar{\mu}-\beta U_r\theta(r-l_f)\right)\right]\\ &\left.-\frac{\beta}{m}\sum_{k=1}^{\infty}\int_{p_{\min}}^{\infty}\mathrm{d}^3\mathbf{p}\;p^4\exp\left[-k\left(\frac{\beta p^2}{2m}-\bar{\mu}\right)\right]\int_V\mathrm{d}^3\mathbf{r}\;\exp\left(-k\beta U_r\theta(r-l_f)\right)\right\}.\end{aligned} \tag{597}$$

The final term on the right-hand side of Eq. (597) is estimated by using V_{eff}. Thus, an expression of $Q^{(\mu)}$ for $T \le T_c$ is re-expressed as the sum including $\mathcal{G}_2$ given by Eq. (597).

When T is less than T_c, the inequality $\bar{\mu} > 0$ must be satisfied. Hence, Eq. (597) requires $p_{\min}$ to satisfy the relation $-\beta p_{\min}^2/2m + \bar{\mu} < 0$. The relation $\sqrt{2m\bar{\mu}} < p_{\min}$ must be considered for Eq. (597) as a requirement for restricting the value of $p_{\min}$. When $\mathcal{G}_2$ given by Eq. (597) is used to estimate $(1/\beta)\ln Q^{(\mu)}$, $\langle \bar{n}\rangle$ particles that cause the contribution $\mathcal{G}_1$ must have small momenta restricted by $0 \le p < p_{\min}$ with $\sqrt{2m\bar{\mu}} < p_{\min}$. Conversely, $\langle N\rangle - \langle \bar{n}\rangle$ particles that cause the contribution $\mathcal{G}_2$ have large momenta satisfying $p_{\min} \le p < \infty$. Hence, it should be possible for the $\langle N\rangle - \langle \bar{n}\rangle$ particles to assume that they move individually in a random manner.

The $\langle \bar{n}\rangle$ particles should be prevented from moving individually and freely, because they carry momenta limited within the range $0 \le p < p_{\min}$ while interacting with each other via attractive forces. Nevertheless, the particles should not be prevented from moving coher-

ently, while being assisted by the effect of repulsive interactions. Excitation states accompanying the motion should allow the inequality $\varepsilon_{\alpha^*} - \mu > 0$ to be preserved in conjunction with the inequality $-U_a - \mu < 0$. Under the condition that p and μ satisfy $0 \leq p < p_{\min}$ and $-U_a - \mu < 0$, respectively, ε_{α^*} should satisfy $\varepsilon_{\alpha^*} - \mu > 0$. Thus, contributions to thermodynamic properties from the excitation states should be estimated. In the study, the contributions are estimated as the sum of the contributions from quasiparticles.

Additionally, the value of $p_{\min}$ is estimated from the following expression:

$$\frac{\beta p_{\min}^2}{2m} - \beta(U_a + \mu) = \eta \quad (\eta > 0). \tag{598}$$

η is estimated via a procedure shown in Appendix B. The basis of the procedure follows the relation

$$\lim_{\delta \to 0} \frac{\partial}{\partial \mu} \left(\frac{1}{\beta} \ln Q^{(\mu)} \right) \Bigg|_{T=T_c+\delta} = \lim_{\delta \to 0} \frac{\partial}{\partial \mu} \left(\frac{1}{\beta} \ln Q^{(\mu)} \right) \Bigg|_{T=T_c-\delta}. \tag{599}$$

The relation requires the number of particles in the system to be preserved at $T = T_c$ given $\langle N \rangle = (\partial/\partial\mu)[(1/\beta) \ln Q^{(\mu)}]$.

D. Thermodynamic quantities obtained from quasiclassical expressions

1. Internal energy

The internal energy E of the system is estimated via the relation $E = -(\partial \ln Q^{(\mu)}/\partial\beta)_\mu + \mu(\partial\beta^{-1} \ln Q^{(\mu)}/\partial\mu)_\beta$. For $T_c < T$, the use of Eq. (585) allows the estimation of E to proceed. Based on the use of a function Z^0, which is defined in Appendix A for $p_{\min} = 0$, E is given as follows:

$$E = \frac{2}{\beta \xi_T} Z_{5/2}^0 (\bar{\mu}) - \frac{2}{\beta \xi_T} \left[\beta U_a - \left(1 - \frac{v_f}{V_{\text{eff}}} \right) \beta U_r \right] Z_{3/2}^0 (\bar{\mu}), \tag{600}$$

where ξ_T denotes a dimensionless quantity that is defined as follows:

$$\xi_T \equiv \frac{\sqrt{\pi}}{s V_{\text{eff}}} \left(\frac{2\pi\hbar^2}{m k_B T} \right)^{3/2}. \tag{601}$$

Similarly, the internal energy for $T \leq T_c$ is estimated by applying Eq. (591) with Eqs. (592) and (597) to $E = -(\partial \ln Q^{(\mu)}/\partial\beta)_{\mu,p_{\min}} + \mu(\partial\beta^{-1} \ln Q^{(\mu)}/\partial\mu)_{\beta,p_{\min}}$. Based on the use of a function Z that is defined in Appendix A for $p_{\min} \neq 0$, E is given as follows:

$$E = \sum_{\substack{\alpha^* \\ \text{for } 0 \leq p < p_{\min}}} \varepsilon_{\alpha^*} \langle n_{\alpha^*} \rangle + \frac{2}{\beta \xi_T} Z_{5/2} (\bar{\mu}; \eta) - \frac{2}{\beta \xi_T} \left[\beta U_a - \left(1 - \frac{v_f}{V_{\text{eff}}} \right) \beta U_r \right] Z_{3/2} (\bar{\mu}; \eta). \tag{602}$$

The second and third terms on the right-hand side of Eq. (602) represent the sum of the contributions from the particles with momenta within the range $p_{\min} \leq p < \infty$. The first term denotes the sum of all energies carried by the specific motions of $\langle \bar{n} \rangle$ particles wherein each is limited by $0 \leq p < p_{\min}$. In the study, $\sum_{\alpha^*} \varepsilon_{\alpha^*} \langle n_{\alpha^*} \rangle$ is estimated as the contributions from quasiparticles.

2. Specific heat C_V at constant volume

For $T_c < T$, the derivative $(\partial E/\partial T)_V$ is calculated from Eq. (600). The derivative allows the specific heat C_V at constant volume for $T_c < T$ to be expressed as follows:

$$\begin{aligned} C_V = & \frac{2}{T\xi_T}\left(\frac{5}{2\beta} - \frac{1}{V_{\text{eff}}}\frac{\partial V_{\text{eff}}}{\partial \beta}\right) Z^0_{5/2}(\bar{\mu}) \\ & + \frac{1}{T}\left\{\left[\beta U_a\left(\frac{1}{V_{\text{eff}}}\frac{\partial V_{\text{eff}}}{\partial \beta} - \frac{3}{2\beta}\right) - \beta U_r \frac{1}{V_{\text{eff}}}\left(\frac{\partial V_{\text{eff}}}{\partial \beta} - \frac{\partial v_f}{\partial \beta}\right) + \frac{3}{2}U_r\left(1 - \frac{v_f}{V_{\text{eff}}}\right)\right]\langle N \rangle \right. \\ & \left. + \frac{1}{\xi_T}\left[\beta U_a - \beta U_r\left(1 - \frac{v_f}{V_{\text{eff}}}\right)\right] Z^0_{1/2}(\bar{\mu})\frac{\partial \bar{\mu}}{\partial \beta}\right\} - \frac{3}{2T}\langle N \rangle \frac{\partial \bar{\mu}}{\partial \beta}. \end{aligned} \tag{603}$$

Specifically, $\partial \bar{\mu}/\partial \beta$ is obtained by differentiating Eq. (B1) with respect to β at constant V and constant $\langle N \rangle$. Finally, $\partial \bar{\mu}/\partial \beta$ is obtained for $T_c < T$ as

$$\frac{\partial \bar{\mu}}{\partial \beta} = \frac{\xi_T}{Z^0_{1/2}(\bar{\mu})}\left(\frac{3}{2\beta} - \frac{1}{V_{\text{eff}}}\frac{\partial V_{\text{eff}}}{\partial \beta}\right)\langle N \rangle. \tag{604}$$

The use of Eq. (604) allows Eq. (603) to be somewhat simplified as follows:

$$\begin{aligned} C_V = & \frac{2}{T\xi_T}\left(\frac{5}{2\beta} - \frac{1}{V_{\text{eff}}}\frac{\partial V_{\text{eff}}}{\partial \beta}\right) Z^0_{5/2}(\bar{\mu}) + \frac{\langle N \rangle}{T}\beta U_r\left(\frac{1}{V_{\text{eff}}}\frac{\partial v_f}{\partial \beta} - \frac{v_f}{V^2_{\text{eff}}}\frac{\partial V_{\text{eff}}}{\partial \beta}\right) \\ & - \frac{3}{2T}\langle N \rangle \frac{\partial \bar{\mu}}{\partial \beta}. \end{aligned} \tag{605}$$

The formula implies that the value of C_V for $T_c < T$ cannot directly depend on U_a. Thus, C_V is related to U_a only via $\bar{\mu}$.

As $T \to T_c$, $Z^0_{1/2}(\bar{\mu})$ diverges to $+\infty$. Near T_c, the behavior of $Z^0_{1/2}$ allows $\partial \bar{\mu}/\partial \beta$ given by Eq. (604) to approach zero. Based on Appendix A, $\lim_{T \to T_c} Z^0_{5/2}(\bar{\mu}) = \Gamma(5/2)\zeta(5/2)$ because $\bar{\mu} = 0$ at $T = T_c$. Therefore, the value of C_V evaluated from Eq. (605) must reach its maximum at $T = T_c$.

To estimate C_V for $T \leq T_c$, the derivative $(\partial E/\partial T)_V$ must be calculated from Eq. (602).

Subsequently, C_V obtained for $T \leq T_c$ is expressed as follows:

$$\begin{aligned} C_V = & \frac{2}{T\xi_T}\left(\frac{5}{2\beta} - \frac{1}{V_{\rm eff}}\frac{\partial V_{\rm eff}}{\partial \beta}\right) Z_{5/2}(\bar{\mu};\eta) \\ & + \frac{1}{T}\left\{\left[\beta U_a\left(\frac{1}{V_{\rm eff}}\frac{\partial V_{\rm eff}}{\partial \beta} - \frac{3}{2\beta}\right) - \beta U_r \frac{1}{V_{\rm eff}}\left(\frac{\partial V_{\rm eff}}{\partial \beta} - \frac{\partial v_f}{\partial \beta}\right) + \frac{3}{2}U_r\left(1 - \frac{v_f}{V_{\rm eff}}\right)\right](\langle N\rangle - \langle \bar{n}\rangle)\right. \\ & \left. + \frac{1}{\xi_T}\left[\beta U_a - \beta U_r\left(1 - \frac{v_f}{V_{\rm eff}}\right)\right] Z_{1/2}(\bar{\mu};\eta)\frac{\partial \bar{\mu}}{\partial \beta}\right\} \\ & - \frac{3}{2T}(\langle N\rangle - \langle \bar{n}\rangle)\frac{\partial \bar{\mu}}{\partial \beta} - \frac{\beta}{T}\left(\frac{\partial}{\partial \beta}\sum_{\substack{\alpha^* \\ \text{for } 0\leq p<p_{\rm min}}} \varepsilon_{\alpha^*}\langle n_{\alpha^*}\rangle\right)_V . \end{aligned} \tag{606}$$

For $T \leq T_c$, $\partial\bar{\mu}/\partial\beta$ is estimated by differentiating Eq. (B4) with respect to β at constant V and constant $\langle N\rangle$, and is given as follows:

$$\frac{\partial \bar{\mu}}{\partial \beta} = \frac{\xi_T}{Z_{1/2}(\bar{\mu};\eta)}\left[(\langle N\rangle - \langle \bar{n}\rangle)\left(\frac{3}{2\beta} - \frac{1}{V_{\rm eff}}\frac{\partial V_{\rm eff}}{\partial \beta}\right) - \frac{\partial \langle \bar{n}\rangle}{\partial \beta}\right]. \tag{607}$$

The use of Eq. (607) allows Eq. (606) to be somewhat simplified as follows:

$$\begin{aligned} C_V = & \frac{2}{T\xi_T}\left(\frac{5}{2\beta} - \frac{1}{V_{\rm eff}}\frac{\partial V_{\rm eff}}{\partial \beta}\right) Z_{5/2}(\bar{\mu};\eta) \\ & + \frac{\langle N\rangle - \langle \bar{n}\rangle}{T}\beta U_r\left(\frac{1}{V_{\rm eff}}\frac{\partial v_f}{\partial \beta} - \frac{v_f}{V_{\rm eff}^2}\frac{\partial V_{\rm eff}}{\partial \beta}\right) - \frac{3}{2T}(\langle N\rangle - \langle \bar{n}\rangle)\frac{\partial \bar{\mu}}{\partial \beta} \\ & - \frac{1}{T}\left(\beta U_a - \beta U_r + \beta U_r \frac{v_f}{V_{\rm eff}}\right)\frac{\partial \langle \bar{n}\rangle}{\partial \beta} - \frac{\beta}{T}\left(\frac{\partial}{\partial \beta}\sum_{\substack{\alpha^* \\ \text{for } 0\leq p<p_{\rm min}}} \varepsilon_{\alpha^*}\langle n_{\alpha^*}\rangle\right)_V . \end{aligned} \tag{608}$$

The relationship between C_V and βU_a in Eq. (608) is different from that in Eq. (605), and the value of C_V for $T \leq T_c$ can depend directly on U_a.

When η, $\langle \bar{n}\rangle$, and $\partial\varepsilon_{\alpha^*}\langle n_{\alpha^*}\rangle/\partial\beta$ are all considered as zero in Eq. (608), the resulting value of C_V at $T = T_c$ agrees with that obtained from Eq. (605) at $T = T_c$. Based on Eq. (B7), $\eta = 0$ implies that the value of $\langle \bar{n}\rangle$ is evaluated as zero at $T = T_c$. If η is considered as a positive nonzero value, $\langle \bar{n}\rangle$ is not zero at $T = T_c$. Then, the value of C_V evaluated from Eq. (608) at $T = T_c$ is different from that evaluated from Eq. (605) at $T = T_c$. For $\eta \neq 0$, Eqs. (605) and (608) allow a discontinuity in C_V at $T = T_c$. Such a discontinuity is theoretically predicted for an ideal Bose gas in a uniform gravitational field[90], experimentally demonstrated for liquid helium[105], and theoretically predicted in terms of energy fluctuation.[91] Additionally, the occurrence of a discontinuity in C_V at $T = T_c$ is independent of the method by which the quantity $\sum_{\alpha^*}(\partial\varepsilon_{\alpha^*}\langle n_{\alpha^*}\rangle/\partial\beta)_V$ is estimated.

Equation (607) involves the quantity $Z_{1/2}(\bar{\mu};\eta)$ that is characterized by the value of η, which should be sufficiently small based on Eq. (B7). From Eq. (A4) in Appendix A, $Z_{1/2}(\bar{\mu};\eta)$ is expressed as follows:

$$Z_{1/2}(\bar{\mu};\eta) = \sum_{k=1}^{\infty} \frac{e^{k\bar{\mu}}}{k^{1/2}} \Gamma(1/2, k(\bar{\mu}+\eta)) .$$

Based on the equation, the value of $Z_{1/2}(\bar{\mu};\eta)$ is large and finite for small η, even if $\bar{\mu} = 0$ is satisfied.

3. Value of U_a and restriction on value of η

A restriction, which is expressed as $\eta \neq 0$, is determined by estimating the isothermal compressibility κ for $T \leq T_c$. A restriction on the value of U_a for which a phase transition specified by $1/\kappa = 0$ is avoided is determined from κ for $T_c < T$. For $T_c < T$ (i.e., $\bar{\mu} < 0$), $1/\kappa$ is estimated by differentiating the pressure given by $P = \beta^{-1}(\partial \ln Q^{(\mu)}/\partial V)_{\langle N\rangle} - \langle N\rangle(\partial\mu/\partial V)_{\langle N\rangle}$.

From the use of Eq. (585), P is obtained as follows:

$$P = \frac{4}{3\beta\xi_T V} Z^0_{5/2}(\bar{\mu}) + \left[\frac{\partial U_a}{\partial V} - \frac{\partial U_r}{\partial V}\left(1 - \frac{v_f}{V_{\rm eff}}\right) - \frac{v_{\rm eff}}{3V_{\rm eff}}\frac{U_r}{V}\right]\langle N\rangle, \tag{609}$$

where $v_{\rm eff} \equiv 3v_f/(2e^{\beta U_r} - 1)$. Based on the relation $1/\kappa = -V(\partial P/\partial V)_T$, differentiating Eq. (609) at constant T yields $1/\kappa$ for $T_c < T$ as follows:

$$\begin{aligned} 1/\kappa = & -\frac{4}{3\beta V_{\rm eff}} \mathcal{D}_1(\beta; V_{\rm eff}) Z^0_{5/2}(\bar{\mu}) + \frac{1}{\beta V_{\rm eff}} \langle N\rangle \mathcal{D}_2(\beta; V_{\rm eff}, U_a, U_r) \\ & + \frac{1}{\beta} \mathcal{D}_3(\beta; V_{\rm eff}, U_a, U_r) Z^0_{1/2}(\bar{\mu}) \frac{\partial\bar{\mu}}{\partial V} - \frac{1}{\beta}\langle N\rangle \frac{\partial\bar{\mu}}{\partial V}, \end{aligned} \tag{610}$$

where

$$\mathcal{D}_1(\beta; V_{\rm eff}) \equiv \frac{1}{\xi_T}\left(\frac{\partial V_{\rm eff}}{\partial V} - \frac{V_{\rm eff}}{V}\right), \tag{611}$$

$$\begin{aligned} \mathcal{D}_2(\beta; V_{\rm eff}, U_a, U_r) \equiv V \Bigg[& -\frac{\partial V_{\rm eff}}{\partial V}\beta\frac{\partial U_a}{\partial V} - V_{\rm eff}\beta\frac{\partial^2 U_a}{\partial V^2} + \beta\frac{\partial^2 U_r}{\partial V^2}(V_{\rm eff} - v_f) \\ & + \beta\frac{\partial U_r}{\partial V}\left(\frac{\partial V_{\rm eff}}{\partial V} - \frac{\partial v_f}{\partial V}\right) + \frac{1}{3V}\left(\frac{\partial v_{\rm eff}}{\partial V} - \frac{v_{\rm eff}}{V}\right)\beta U_r + \frac{v_{\rm eff}}{3V}\beta\frac{\partial U_r}{\partial V}\Bigg], \end{aligned} \tag{612}$$

$$\mathcal{D}_3(\beta; V_{\rm eff}, U_a, U_r) \equiv \frac{V}{\xi_T V_{\rm eff}}\left[-V_{\rm eff}\beta\frac{\partial U_a}{\partial V} + \beta\frac{\partial U_r}{\partial V}(V_{\rm eff} - v_f) + \frac{v_{\rm eff}}{3V}\beta U_r\right]. \tag{613}$$

Specifically, $\partial\bar{\mu}/\partial V$ is estimated by differentiating Eq. (B1) with respect to V at constant T and constant $\langle N\rangle$, and $\partial\bar{\mu}/\partial V$ is obtained for $T_c < T$ as follows:

$$\frac{\partial\bar{\mu}}{\partial V} = -2\frac{Z^0_{3/2}(\bar{\mu})}{Z^0_{1/2}(\bar{\mu})}\left(\frac{1}{V_{\rm eff}}\frac{\partial V_{\rm eff}}{\partial V}\right). \tag{614}$$

The derivative $\partial V_{\rm eff}/\partial V$ is given in Appendix C. The derivative $\partial v_{\rm eff}/\partial V$ is estimated from $v_{\rm eff}$ given in Appendix C.

The derivatives $\partial U_a/\partial V$ and $\partial^2 U_a/\partial V^2$ at constant T should satisfy $\partial U_a/\partial V = -U_a/V$ and $\partial^2 U_a/\partial V^2 = 2U_a/V^2$, respectively, because $U_a \propto \rho$. The derivatives $\partial U_r/\partial V$ and $\partial^2 U_r/\partial V^2$ are estimated at constant T from expressions given in Appendix C. The expression for $1/\kappa$ given by Eq. (610) is simplified using the expression for $V_{\rm eff}$ if all the contributions from $v_{\rm eff}$ and v_f are ignored because $0 < v_f/V \ll 1$ and $0 < v_{\rm eff}/V \ll 1$. As the result, $1/\kappa$ given at $T = T_c$ by Eq. (610) allows deriving a formula that U_a satisfies approximately. The formula is expressed as

$$U_a = \frac{4}{3}\left(1 + \frac{V^c_{\rm eff}}{V}\right)\frac{Z^0_{5/2}(0)}{Z^0_{3/2}(0)}V\frac{\partial U_r}{\partial V} + 2V^2\frac{\partial^2 U_r}{\partial V^2} - \frac{2}{\rho\kappa_c}, \tag{615}$$

where $V^c_{\rm eff}$ and κ_c denote the value of $V_{\rm eff}$ at $T = T_c$ and the value of κ at $T = T_c$, respectively, and $\left|V^2(\partial^2 U_r/\partial V^2)/V(\partial U_r/\partial V)\right| \ll 1$ is satisfied.

For $T \le T_c$ (i.e., $0 \le \bar{\mu}$), the relation $P = \beta^{-1}(\partial \ln Q^{(\mu)}/\partial V)_{\langle N\rangle, p_{\rm min}} - \langle N\rangle(\partial\mu/\partial V)_{\langle N\rangle}$ allows the pressure P to be estimated using Eq. (591) with Eqs. (592) and (597) as follows:

$$\begin{aligned} P = & -\sum_{\substack{\alpha^* \\ \text{for } 0\le p<p_{\rm min}}} \langle n_{\alpha^*}\rangle\frac{\partial\varepsilon_{\alpha^*}}{\partial V} + \frac{4}{3\beta\xi_T V_{\rm eff}}\left[\frac{v_f}{V}\ln\left(1-e^{-\eta}\right) + \left(1-\frac{v_f}{V}\right)\ln\left(1-e^{-\eta}e^{-\beta U_r}\right)\right] \\ & \times(\bar{\mu}+\eta)^{3/2} + \frac{4}{3\beta\xi_T V}Z_{5/2}\left(\bar{\mu};\eta\right) + \left(\frac{\partial U_a}{\partial V} - \frac{v_{\rm eff}}{3V_{\rm eff}}\frac{U_r}{V}\right)\frac{2}{\xi_T}Z_{3/2}\left(\bar{\mu};\eta\right). \end{aligned} \tag{616}$$

For $T \le T_c$, κ is estimated from the derivative of P, which is obtained by differentiating Eq. (616) at constant T, and the use of Eqs. (611)–(613) enables κ to be expressed as follows:

$$\begin{aligned} 1/\kappa = & -\frac{4}{3\beta V_{\rm eff}}\mathcal{D}_1(\beta; V_{\rm eff})Z_{5/2}\left(\bar{\mu};\eta\right) + \frac{1}{\beta V_{\rm eff}}\left(\langle N\rangle - \langle\bar{n}\rangle\right)\mathcal{D}_2(\beta; V_{\rm eff}, U_a, U_r) \\ & + \frac{1}{\beta}\mathcal{D}_3(\beta; V_{\rm eff}, U_a, U_r)Z_{1/2}\left(\bar{\mu};\eta\right)\frac{\partial\bar{\mu}}{\partial V} - \frac{1}{\beta}\left(\langle N\rangle - \langle\bar{n}\rangle\right)\frac{\partial\bar{\mu}}{\partial V} \\ & + V\sum_{\substack{\alpha^* \\ \text{for } 0\le p<p_{\rm min}}}\left[\frac{\partial\langle n_{\alpha^*}\rangle}{\partial V}\frac{\partial\varepsilon_{\alpha^*}}{\partial V} + \langle n_{\alpha^*}\rangle\frac{\partial^2\varepsilon_{\alpha^*}}{\partial V^2}\right] - \frac{4}{3\beta\xi_T V_{\rm eff}}\mathcal{K}(\bar{\mu},\eta), \end{aligned} \tag{617}$$

where $\mathcal{K}(\bar{\mu},\eta)$ is defined as follows:

$$\mathcal{K}(\bar{\mu},\eta) \equiv \left(\frac{\partial v_f}{\partial V} - \frac{v_f}{V}\right)(\bar{\mu}+\eta)^{3/2}\ln(1-e^{-\eta}) + \frac{3}{2}v_f\left(\frac{\partial \bar{\mu}}{\partial V} + \frac{\partial \eta}{\partial V}\right)(\bar{\mu}+\eta)^{1/2}\ln(1-e^{-\eta})$$
$$+ \frac{\partial \eta}{\partial V}\frac{Ve^{-\eta}}{1-e^{-\eta}}\left[\frac{v_f - V_{\rm eff}}{V}(\bar{\mu}+\eta)^{3/2} - \frac{3}{2}\left(V_{\rm eff}\beta\frac{\partial U_a}{\partial V} - (V_{\rm eff}-v_f)\beta\frac{\partial U_r}{\partial V} - \frac{v_{\rm eff}}{3V}\beta U_r\right)(\bar{\mu}+\eta)^{1/2}\right]$$
$$- (\bar{\mu}+\eta)^{3/2}\left(\frac{\partial v_f}{\partial V} - \frac{v_f}{V}\right)\ln(1-e^{-\eta}e^{-\beta U_r}) + (\bar{\mu}+\eta)^{3/2}\frac{V-v_f}{e^{\eta}e^{\beta U_r}-1}\left(\frac{\partial \eta}{\partial V} + \beta\frac{\partial U_r}{\partial V}\right)$$
$$+ \frac{3}{2}(V-v_f)(\bar{\mu}+\eta)^{1/2}\frac{\partial(\bar{\mu}+\eta)}{\partial V}\ln(1-e^{-\eta}e^{-\beta U_r}). \tag{618}$$

For $T \le T_c$, $\partial\bar{\mu}/\partial V$ occurring in Eq. (617) is estimated based on Eq. (B8) as follows:

$$\frac{\partial \bar{\mu}}{\partial V} = \frac{\xi_T}{Z_{1/2}(\bar{\mu};\eta)}\left[-\frac{\partial\langle\bar{n}\rangle}{\partial V} - \frac{2}{\xi_T V_{\rm eff}}Z_{3/2}(\bar{\mu};\eta)\frac{\partial V_{\rm eff}}{\partial V} + \frac{2}{\xi_T}\frac{\partial\eta}{\partial V}\frac{\sqrt{\bar{\mu}+\eta}}{e^{\eta}-1}\right]. \tag{619}$$

Eq. (619) is $\partial\bar{\mu}/\partial V$ estimated at constant $\langle N\rangle$.

If we set η, $\langle n_{\alpha^*}\rangle$, $\partial\varepsilon_{\alpha^*}/\partial V$, and $\mathcal{K}(\bar{\mu},\eta)$ equal to zero, Eq. (617) becomes equivalent to Eq. (610) at $T = T_c$ (i.e., $\bar{\mu} = 0$). However, the assumption that $\eta = 0$ is not appropriate. At $T < T_c$, the inequality $\bar{\mu} > 0$ should be satisfied. If $\eta = 0$ and $\bar{\mu} > 0$ are both satisfied, then the factor $1 - e^{-\eta}$ occurring in Eq. (618) allows the value of $1/\kappa$ to diverge. By taking $\eta \neq 0$, the problem is simply avoided. This implies that $\langle\bar{n}\rangle \neq 0$ is satisfied at $T = T_c$ given Eq. (B7) in Appendix B. Subsequently, the value of η satisfying $\eta \neq 0$ requires the value of $1/\kappa$ evaluated at $T = T_c$ from Eq. (617) to differ from that evaluated at $T = T_c$ from Eq. (610). The inequality $\eta \neq 0$ allows a discontinuity in $1/\kappa$ at $T = T_c$.

With $\eta \neq 0$, Eq. (617) requires that $\lim_{\delta\to 0} 1/\kappa|_{T_c-\delta} \neq 0$ even if Eq. (615) requires that $\lim_{\delta\to 0} 1/\kappa|_{T_c+\delta} = 0$ for the specific case in which $U_a = \bar{U}_a$ is satisfied. Specifically, $\bar{U}_a$ is defined as $\bar{U}_a \equiv (4/3)(1 + V^c_{\rm eff}/V)[Z^0_{5/2}(0)/Z^0_{3/2}(0)]V\partial U_r/\partial V + 2V^2\partial^2 U_r/\partial V^2$. Based on Eq. (615), the inequality $\lim_{\delta\to 0} 1/\kappa|_{T_c+\delta} > 0$ requires $0 < U_a < \bar{U}_a$ to be satisfied. The inequality implies that the phase transition specified by $1/\kappa = 0$ does not occur for $0 < U_a < \bar{U}_a$ at an arbitrary temperature satisfying $0 < (T - T_c)/T \ll 1$. Thus, it is possible to evaluate the specific heat C_V for the value of U_a that prevents the occurrence of the phase transition.

E. Evaluation of specific heat

Based on Eq. (B4), the value of $\bar{\mu}$ for $T \le T_c$ must satisfy the inequality $0 \le \bar{\mu} \ll 1$ at constant $\langle N\rangle$. The restriction on $\bar{\mu}$ allows the approximate relations $\bar{\mu} \approx 0$ and $\partial\bar{\mu}/\partial\beta \approx 0$ to

be satisfied for $T \leq T_c$. If these approximate relations are considered, Eq. (608) is simplified as follows:

$$C_V \approx \frac{2}{T\xi_T}\left(\frac{5}{2\beta} - \frac{1}{V_{\rm eff}}\frac{\partial V_{\rm eff}}{\partial \beta}\right) Z_{5/2}(\bar{\mu};\eta) \\ - \frac{1}{T}\left(\beta U_a - \beta U_r\right)\frac{\partial \langle \bar{n}\rangle}{\partial \beta} - \frac{\beta}{T}\left(\frac{\partial}{\partial \beta}\sum_{\substack{\alpha^* \\ \text{for } 0\leq p<p_{\rm min}}} \varepsilon_{\alpha^*}\langle n_{\alpha^*}\rangle\right)_V . \tag{620}$$

Based on the context, the contribution of the final term in Eq. (620) should be evaluated as the contribution from rotons, and this is achieved by the use of Eqs. (D24) and (D25). The derivative $\partial\langle\bar{n}\rangle/\partial\beta$ is obtained by differentiating Eq. (B4). If the approximate relations $\bar{\mu} \approx 0$ and $\partial\bar{\mu}/\partial\beta \approx 0$ are assumed, $\partial\langle\bar{n}\rangle/\partial\beta$ is expressed as

$$\frac{\partial \langle \bar{n}\rangle}{\partial \beta} \approx \frac{2}{\beta\xi_T} Z_{3/2}(\bar{\mu};\eta)\Big|_{\bar{\mu}=0}\left(\frac{3}{2} + 2\beta U_r e^{\beta U_r}\frac{V_{\rm eff}}{V}\right). \tag{621}$$

The inequality $v_f/V_{\rm eff} \ll 1$ is assumed when deriving Eq. (620). Given the same assumption, Eq. (605) for $T_c < T$ is approximated as

$$C_V \approx \frac{2}{T\xi_T}\left(\frac{5}{2\beta} - \frac{1}{V_{\rm eff}}\frac{\partial V_{\rm eff}}{\partial \beta}\right) Z^0_{5/2}\left(\bar{\mu}\right) - \frac{3}{2T}\langle N\rangle\frac{\partial \bar{\mu}}{\partial \beta}. \tag{622}$$

To evaluate C_V given by Eq. (622), it is necessary to determine the value of U_r by using Eq. (590). From the value of U_r, C_V given by Eq. (620) can also be evaluated. U_a is considered as a parameter that satisfies $0 < U_a < \bar{U}_a$, and it corresponds to a value that is given as follows:

$$U_a = a_0(4/3)(1 + V^c_{\rm eff}/V)(V\partial U_r/\partial V) Z^0_{5/2}(0)/Z^0_{3/2}(0), \quad (0 < a_0).$$

An approximate value of $\langle\bar{n}\rangle_c/\langle N\rangle$, where $\langle\bar{n}\rangle_c \equiv \langle\bar{n}\rangle|_{T=T_c}$, is estimated by the extrapolation of data reported previously[109] as follows:

$$\langle\bar{n}\rangle_c/\langle N\rangle = 0.001 \quad \text{corresponding to } \eta = 1.34 \times 10^{-6},$$

where the corresponding value of η is evaluated using Eq. (B7).

An example of the results is shown in Fig. 36, which represents a case evaluated using a specific value of U_r for which $T_c = 2.17$ K. Figure 36 reveals that C_V exhibits a singularity appearing as a discontinuity at $T = T_c$. The contribution from the $\langle\bar{n}\rangle$ particles that carry small momenta limited within the range $0 \leq p < p_{\rm min}$ is evaluated as the contribution from

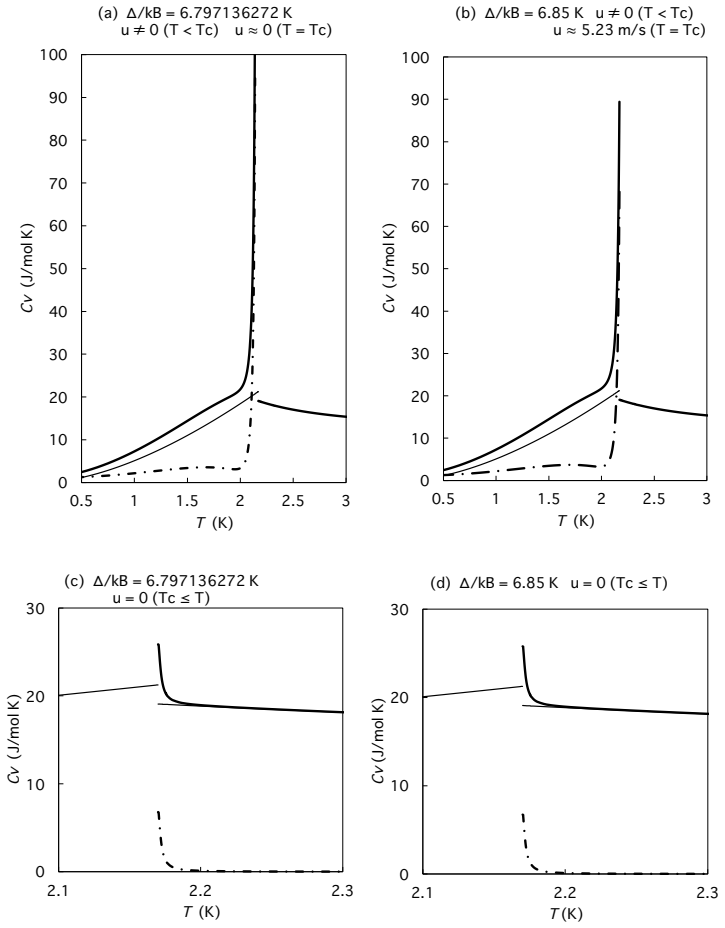

FIG. 36. Dependence of C_V on T near T_c. The dashed-dotted curves correspond to the contribution of rotons evaluated for $\langle n\rangle_c/\langle N\rangle = 0.001$. In (a) and (b), the thick curves on the left correspond to C_V evaluated for $\langle n\rangle_c/\langle N\rangle = 0.001$ and $\beta_c U_a = 0.171$ ($a_0 = 0.0644$), and then, C_V includes the roton contribution. In (a) and (b), the thick curves on the right correspond to C_V evaluated for $T_c < T$ ($T_c = 2.17$K) without the roton contribution. The thick curves in (c) and (d) for $T_c < T$ correspond to C_V including the roton contribution. In (a), (b), (c), and (d), thin curves are obtained by eliminating the roton contribution. The roton contribution is characterized with a quantity u by the three parameters $p_0/\hbar = 1.92 \times 10^{10}\mathrm{m}^{-1}$, $\hat{\mu} = 0.115 m_{\mathrm{He}}$, and $\hat{\Delta}/k_B$, which are estimated from neutron scattering at 2.17K.[110] However, for (a) and (c), $\hat{\Delta}/k_B$ is specified as $\hat{\Delta}/k_B \simeq 6.7971$K, because Eq. (D18) allows $u \approx 0$ (m/s) at $T = T_c$ for the value.

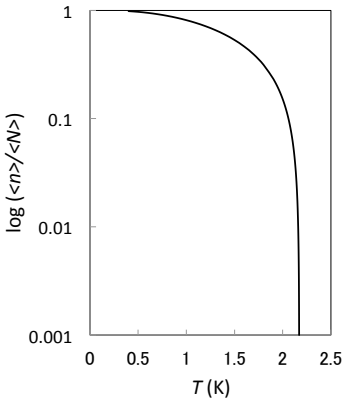

FIG. 37. Dependence of $\langle\bar{n}\rangle/\langle N\rangle$ on T. The solid curve corresponds to $\langle\bar{n}\rangle/\langle N\rangle$ that is evaluated for $\langle n\rangle_c/\langle N\rangle = 0.001$ and $\beta_c U_a = 0.171$ ($a_0 = 0.0644$) with the use of Eq. (B4).

rotons and is confirmed in Fig. 36. The dependence of $\langle\bar{n}\rangle/\langle N\rangle$ on T is confirmed in Fig. 37. The contribution from rotons increases sharply near T_c. The largest value obtained from the contribution at $T = T_c$ can sensitively decrease for a small decrease in the magnitude of $\hat{\Delta}/k_B$. The behavior determined in the range $T \leq T_c$ is different from that in the range $T_c < T$. The largest value based on the contribution from rotons can be insensitive to a decrease in the magnitude of $\hat{\Delta}/k_B$ in the range $T_c < T$.

Rotons may exist even for $T_c < T$ based on the assumption that particles that carry small momenta limited within the range $0 \leq p < p_{\min}$ contribute to the generation of rotons. The

contributions from such rotons correspond to the dashed and single dotted curves found in (c) and (d) in Fig. 36. They are evaluated via Eqs. (D34) and (D35).

The roton contribution exhibits a specific physical meaning if the final term in Eq. (620) is subject to the contribution. At temperatures near T_c, $\langle \bar{n} \rangle$ particles are extremely fewer than the $\langle N \rangle - \langle \bar{n} \rangle$ particles with large momenta satisfying $p_{\min} < p < \infty$. Despite $0 < \langle \bar{n} \rangle / (\langle N \rangle - \langle \bar{n} \rangle) \ll 1$, the $\langle \bar{n} \rangle$ particles with small momenta satisfying $0 \leq p < p_{\min}$ maintain the form of microscopic ensembles where particles are located near each other with being assisted by the attractive interparticle forces. The $\langle \bar{n} \rangle$ particles remain as the microscopic ensembles without mixing homogeneously with the $\langle N \rangle - \langle \bar{n} \rangle$ particles. The microscopic ensembles exist while being included within the body of a macroscopic ensemble of the $\langle N \rangle - \langle \bar{n} \rangle$ particles. The microscopic ensembles allow the generation of characteristic excitation states corresponding to rotons. Thus, if the contribution of the $\langle \bar{n} \rangle$ particles is exhibited by the roton contribution, the sharp increase of C_V near T_c due to the roton contribution suggests that phase separation is maintained at a microscopic level. If temperatures are near T_c, the aforementioned type of a phenomenon should be induced even above T_c. This is suggested by the behavior of the thick curves found in (c) and (d) in Fig. 36. According to results of measurements, the characteristic excitation states remain as rotons at temperatures near T_c.[102]

F. Conclusions

Two quasiclassical expressions of the partition function for a Bose fluid system indicate a dependence of the specific heat on T that exhibits a discontinuity at a temperature T_c. This implies that the maximum of the specific heat at $T = \lim_{\delta \to 0}(T_c - \delta)$ differs from that at $T = \lim_{\delta \to 0}(T_c + \delta)$. The sum of the chemical potential μ and contribution U_a of attractive forces between particles reaches zero at $T = T_c$. The dependence of T_c on repulsive interactions between particles is expressed by a simple equation. If the contribution of the motion of particles with small momenta satisfying $0 \leq p < p_{\min}$ corresponds to the contribution from rotons, the contribution sharply increases the specific heat near T_c. This means that particles with small momenta satisfying $0 \leq p < p_{\min}$ cannot homogeneously mix with particles with large momenta satisfying $p_{\min} < p < \infty$. Even in a classical fluid system, mutually attractive forces between particles cannot allow particles with small momenta to

be homogeneously mixed with particles that have large momenta. When particles with small momenta and particles with large momenta coexist without being homogeneously mixed, two different types of excitation states should be generated because of the contribution of the hard-core potential that requires particles to be excluded from each other. In the Bose fluid system, the interface that distinguishes the liquid phase from the gas phase can be formed; it is not formed without the contribution of physical cluster formation. It is necessary to adequately understand the relation between excitation states and the contribution of the physical cluster formation.

ACKNOWLEDGMENTS : The author would like to thank referees of several journals. Their useful and valuable criticisms contributed to improvement on this article.

Appendix A: Summarized mathematics for $Z^0_{\nu/2}(\bar{\mu})$ and $Z_{\nu/2}(\bar{\mu};\eta)$

$$p_{\min} = \begin{cases} 0 & (T_c < T), \\ \sqrt{2m(U_a + \mu + \eta/\beta)} & (T \le T_c). \end{cases}$$

1. When $p_{\min} = 0$ $(\bar{\mu} \le 0, \quad 0 < \nu)$

A function Z^0 involving the gamma function is defined as follows:

$$Z^0_{\nu/2}(\bar{\mu}) \equiv \sum_{k=1}^{\infty} \frac{\exp(k\bar{\mu})}{k^{\nu/2}} \Gamma(\nu/2)\,. \tag{A1}$$

When $\bar{\mu} = 0$ $(T = T_c)$,

$$Z^0_{\nu/2}(0) = \zeta(\nu/2)\Gamma(\nu/2), \tag{A2}$$

where the Riemann zeta function ζ is defined as $\zeta(\nu) \equiv \sum_{k=1}^{\infty} 1/k^{\nu}$. For $1 < \nu$, $\zeta(\nu)$ is finite. For $\nu \le 1$, $\zeta(\nu)$ diverges to $+\infty$. When $|\bar{\mu}|$ is sufficiently close to zero, $Z^0_{1/2}(\bar{\mu})$ behaves as

$$Z^0_{1/2}(\bar{\mu}) \approx \Gamma(1/2)\left\{\exp(\bar{\mu}) + |\bar{\mu}|^{-1/2}\Big[\Gamma(1/2) - \gamma(1/2, 3|\bar{\mu}|/2)\Big]\right\}. \tag{A3}$$

2. When $p_{\min} \neq 0$ ($\bar{\mu} \geq 0$, $0 < \nu$)

A function Z involving the incomplete gamma function of the second type is defined as follows:

$$\begin{aligned} Z_{\nu/2}\left(\bar{\mu};\eta\right) &\equiv \sum_{k=1}^{\infty} \frac{\exp(k\bar{\mu})}{k^{\nu/2}} \Gamma\left(\nu/2, k\vartheta\right) \\ &= \vartheta^{\nu/2} \int_1^{\infty} \frac{t^{\nu/2-1}}{e^{\vartheta t-\bar{\mu}}-1}\,\mathrm{d}t, \end{aligned} \tag{A4}$$

where $\vartheta \equiv \beta p_{\min}^2/(2m) = \bar{\mu} + \eta$. Subsequently, rewriting the integrand $t^{\nu/2-1}/(e^{\vartheta t-\bar{\mu}}-1)$ allows Z to be expressed approximately in the integral form as follows:

$$\begin{aligned} Z_{\nu/2}\left(\bar{\mu};\eta\right) &\approx \vartheta^{\nu/2} \int_1^{\infty} \frac{t^{\nu/2-1}}{e^{\vartheta t}-1}\,\mathrm{d}t + \vartheta^{\nu/2} \int_1^{t_s} \Delta f(t,\bar{\mu})\,\mathrm{d}t \\ &\approx Z_{\nu/2}^{(0)}\left(\bar{\mu};\eta\right) + \vartheta^{\nu/2} \Delta S_{\nu/2}\left(t_s,\bar{\mu}\right), \end{aligned} \tag{A5}$$

where $\Delta f(t,\bar{\mu})$, $Z_{\nu/2}^{(0)}(\bar{\mu};\eta)$, and $\Delta S_{\nu/2}(t_s,\bar{\mu})$ are defined as follows:

$$\Delta f(t,\bar{\mu}) \equiv \frac{t^{\nu/2-1}}{e^{\vartheta t-\bar{\mu}}-1} - \frac{t^{\nu/2-1}}{e^{\vartheta t}-1}, \tag{A6}$$

$$Z_{\nu/2}^{(0)}\left(\bar{\mu};\eta\right) \equiv \sum_{k=1}^{\infty} \frac{1}{k^{\nu/2}} \Gamma\left(\nu/2, k\vartheta\right), \tag{A7}$$

$$\Delta S_{\nu/2}\left(t_s,\bar{\mu}\right) \equiv \frac{1}{2} \sum_{i=1}^{s} \left[\Delta f(t_i,\bar{\mu}) + \Delta f(t_{i-1},\bar{\mu})\right](t_i - t_{i-1}), \tag{A8}$$

respectively. Specifically, the value of t_s should satisfy $0 < \Delta f(t_s,\bar{\mu})/\Delta f(t_0,\bar{\mu}) \ll 1$ ($t_0 = 1$). At $\bar{\mu} = 0$, Eq. (A7) becomes equivalent to Eq. (A4). Based on Eq. (A7), increases in $\bar{\mu}$ decrease the value of $Z_{\nu/2}^{(0)}$ for $\nu = 3$ and $\nu = 5$. The behavior of $Z_{\nu/2}^{(0)}$ is shown also by Eq. (A9).

In Eq. (A6), the second term on the right-hand side decreases with increases in $\bar{\mu}$ at $t = 1$. However, at $t = 1$, the first term is independent of an increase in $\bar{\mu}$ and remains large. Thus, $\Delta f(t,\bar{\mu})$ increases with increases in $\bar{\mu}$. This allows $Z_{\nu/2}$ to increase with increases in $\bar{\mu}$, although $Z_{\nu/2}^{(0)}$ decreases.

In Eq. (A7), the summation is approximated by an integration. An approximation of

$Z^{(0)}$ is then obtained for either $\nu = 3$ or $\nu = 5$ as

$$\begin{aligned} Z^{(0)}_{\nu/2}(\bar{\mu};\eta) &\approx \zeta\left(\nu/2\right)\Gamma(\nu/2) - \gamma(\nu/2,\vartheta) - \int_1^\infty (t+1/2)^{-\nu/2}\gamma(\nu/2,(t+1/2)\vartheta)\,\mathrm{d}t \\ &= \zeta(\nu/2)\Gamma(\nu/2) - \gamma(\nu/2,\vartheta) - \frac{2}{\nu-2}\left(\frac{3}{2}\right)^{-\nu/2+1}\gamma(\nu/2,3\vartheta/2) \\ &\quad - \frac{2}{\nu-2}\vartheta^{\nu/2-1}e^{-3\vartheta/2}, \end{aligned} \tag{A9}$$

where $\gamma(\nu/2,z) = \int_0^z t^{\nu/2-1}e^{-t}\,\mathrm{d}t$ (i.e., the incomplete gamma function of the first type).

Similarly, an approximate expression of $Z^{(0)}$ for $\nu = 1$ is obtained and avoids the divergence of $\zeta(\nu/2)$ as follows:

$$\begin{aligned} Z^{(0)}_{1/2}\left(\bar{\mu};\eta\right) &\approx \Gamma\left(1/2,\vartheta\right) + \int_1^\infty (t+1/2)^{-1/2}\Gamma\left(1/2,(t+1/2)\vartheta\right)\mathrm{d}t \\ &= 2\vartheta^{-1/2}e^{-3\vartheta/2} + \Gamma\left(1/2,\vartheta\right) - 6^{1/2}\Gamma\left(1/2,3\vartheta/2\right)). \end{aligned} \tag{A10}$$

The behavior of $\Gamma(1/2,k\vartheta)$ is exhibited by $\Gamma(1/2,k\vartheta) = (k\vartheta)^{-1/2}e^{-k\vartheta}[1+\sum_{n=1}^\infty (k\vartheta)^{-n}\prod_{i=1}^n (1/2-i)]$. Thus, Eq. (A10) reveals that $Z^{(0)}_{1/2}(\bar{\mu};\eta)$ given by the sum in Eq. (A7) remains extremely large without diverging to infinity, although $\sum_{k=1}^\infty k^{-\nu/2}$ diverges to infinity for $\nu = 1$.

When $\bar{\mu} = 0$, the use of Eq. (A9) allows $Z_{\nu/2}$ to be expressed in the following approximate form:

$$Z_{\nu/2}\left(0;\eta\right) \approx \zeta\left(\nu/2\right)\Gamma\left(\nu/2\right) - \frac{2}{\nu-2}\eta^{(\nu-2)/2} \quad (\text{for } 0 < \eta \ll 1 \text{ and } \nu = 3,\ 5). \tag{A11}$$

3. Estimates of two types of integrals

a. Type I

$$\begin{aligned} &\int_{p_{\min}}^\infty p^\nu \frac{1}{\exp(\beta p^2/(2m) - \bar{\mu}) - 1}\,\mathrm{d}p \\ &\qquad = \begin{cases} \frac{1}{2}(2m/\beta)^{(\nu+1)/2} Z^0_{(\nu+1)/2}\left(\bar{\mu}\right) & (p_{\min} = 0 \text{ and } 0 \le \nu), \\ \frac{1}{2}(2m/\beta)^{(\nu+1)/2} Z_{(\nu+1)/2}\left(\bar{\mu};\eta\right) & (p_{\min} \ne 0 \text{ and } 0 \le \nu). \end{cases} \end{aligned} \tag{A12}$$

b. Type II

$$\int_{p_{\min}}^{\infty} p^2 \ln\left[1-\exp(-\beta p^2/(2m)+\bar{\mu})\right] \mathrm{d}p$$
$$= \begin{cases} -\frac{1}{3}\left(\frac{2m}{\beta}\right)^{3/2} Z^0_{5/2}(\bar{\mu}) & (p_{\min}=0), \\ -\frac{1}{3}\left(\frac{2m}{\beta}\right)^{3/2} \left\{ (\bar{\mu}+\eta)^{3/2} \ln\left(1-e^{-\eta}\right) + Z_{5/2}(\bar{\mu};\eta) \right\} & (p_{\min}\neq 0). \end{cases} \tag{A13}$$

4. Derivatives

$$\frac{\partial}{\partial\bar{\mu}} Z^0_{\nu/2}(\bar{\mu}) = \left(\frac{\nu}{2}-1\right) Z^0_{(\nu-2)/2}(\bar{\mu}) \quad (p_{\min}=0 \text{ and } 3\leq\nu), \tag{A14}$$

$$\frac{\partial}{\partial\bar{\mu}} Z_{\nu/2}(\bar{\mu};\eta) = \left(\frac{\nu}{2}-1\right) Z_{(\nu-2)/2}(\bar{\mu};\eta) \quad (p_{\min}\neq 0 \text{ and } 3\leq\nu), \tag{A15}$$

$$\frac{\partial}{\partial\eta} Z_{\nu/2}(\bar{\mu};\eta) = \frac{-1}{e^{\eta}-1} (\bar{\mu}+\eta)^{(\nu-2)/2} \quad (p_{\min}\neq 0 \text{ and } 3\leq\nu). \tag{A16}$$

Appendix B: Estimations of two quantities $\partial U_r/\partial\rho$ and η

1. Derivative $\partial U_r/\partial\rho$ related to repulsive effects caused by hard cores of particles

Based on the relation $\langle N\rangle = (\partial\beta^{-1}\ln Q^{(\mu)}/\partial\mu)_\beta$, $\langle N\rangle$ for $T_c < T$ is estimated as

$$\langle N\rangle = \frac{2}{\xi_T} Z^0_{3/2}(\bar{\mu}). \tag{B1}$$

The value of $\bar{\mu}$ for $T_c < T$ is estimated from Eq. (B1) when $\langle N\rangle$ is given. At $T = T_c$, it must satisfy $\bar{\mu} = 0$.

At $T = T_c$, Eq. (B1) is modified as $\xi_T = 2\Gamma(3/2)\zeta(3/2)/\langle N\rangle$. If this expression for ξ_T is substituted into Eq. (601), a formula is obtained as

$$V_{\rm eff}^c = \mathcal{A}\beta_c^{3/2}\langle N\rangle, \tag{B2}$$

where $V_{\rm eff}^c \equiv V_{\rm eff}|_{T=T_c}$ and $\mathcal{A} \equiv \sqrt{\pi}(2s)^{-1}(2\pi\hbar^2/m)^{3/2}[\Gamma(3/2)\zeta(3/2)]^{-1}$. Additionally, Eq. (B2) implies that the temperature T_c depends on $V_{\rm eff}^c$ under the condition that $\langle N\rangle$ remains constant.

From Eqs. (589) and (B2), Eq. (590) is obtained, and the differentiation of Eq. (590) with respect to ρ yields the following expression:

$$\frac{\partial U_r}{\partial \rho} = -(\rho\beta_c)^{-1}\left\{1 - \frac{1}{2}e^{-\beta_c U_r} + \left[\frac{3}{2}\left(1 - \frac{1}{2}e^{-\beta_c U_r}\right) + \beta_c U_r\right]\rho\beta_c^{-1}\frac{\partial\beta_c}{\partial\rho}\right\}. \tag{B3}$$

Based on Eq. (C4), $\partial\beta_c/\partial\rho$ is positive. Hence, Eq. (B3) requires $\partial U_r/\partial\rho$ to be negative. This is consistent with Eq. (C6) because $\partial U_r/\partial V = -(\rho/V)\partial U_r/\partial\rho$ is satisfied at constant $\langle N\rangle$. At 20 bar, the transition temperature for liquid ^{4}He is 1.928 K.[99] In this case, $\partial U_r/\partial\rho$ should become negative.

2. Estimation of coefficient η

Based on the relation $\langle N\rangle = (\partial\beta^{-1}\ln Q^{(\mu)}/\partial\mu)_{\beta,p_{\rm min}}$, $\langle N\rangle$ for $T \le T_c$ is estimated as

$$\langle N\rangle = \langle\bar{n}\rangle + \frac{2}{\xi_T}Z_{3/2}\left(\bar{\mu};\eta\right). \tag{B4}$$

Given that $\langle N\rangle$ remains constant, when the temperature increases, $\langle\bar{n}\rangle$ reaches a minimum at $T = T_c$. The value of $(2/\xi_T)Z_{3/2}(\bar{\mu};\eta)$ then attains a maximum. Conversely, decreases in the temperature from T_c increase $\langle\bar{n}\rangle$ because $(2/\xi_T)Z_{3/2}(\bar{\mu};\eta)$ decreases. Then, the value of $\bar{\mu}$ should not significantly increase because an increase in $\bar{\mu}$ increases $Z_{3/2}(\bar{\mu};\eta)$ based on Eq. (A5). Thus, if $\langle N\rangle$ is constant, the condition $0 \le \bar{\mu} \ll 1$ should always be satisfied for $T \le T_c$. This simplifies the estimation of $\langle\bar{n}\rangle$, and $\langle\bar{n}\rangle$ is determined as independent of U_a.

Under the condition that $\langle N\rangle$ remains constant, the value of $\langle N\rangle$ evaluated at $T = T_c$ from Eq. (B4) should be equal to that evaluated at $T = T_c$ from Eq. (B1). This exhibits $\lim_{\delta\to 0}\langle N\rangle|_{T=T_c+\delta} = \lim_{\delta\to 0}\langle N\rangle|_{T=T_c-\delta}$. Re-writing the relation yields the following relation between $\langle\bar{n}\rangle|_{T=T_c}$ and η:

$$0 = \langle\bar{n}\rangle_c - \frac{2}{\sqrt{\pi}}sV_{\rm eff}^c\left(\frac{m}{2\pi\hbar^2\beta_c}\right)^{3/2}\sum_{k=1}^{\infty}\frac{1}{k^{3/2}}\gamma\left(3/2, k\eta\right). \tag{B5}$$

In Eq. (B5), the summation is approximated by an integration and yields the following expression:

$$\sum_{k=1}^{\infty} \frac{1}{k^{3/2}} \gamma\left(3/2, k\eta\right) \approx \gamma\left(3/2, \eta\right) + \int_{1}^{\infty} \left(t + 1/2\right)^{-3/2} \gamma\left(3/2, \eta(t + 1/2)\right) \mathrm{d}t$$
$$= \gamma\left(3/2, \eta\right) + \left(8/3\right)^{1/2} \gamma\left(3/2, 3\eta/2\right) + 2\eta^{1/2} e^{-3\eta/2} \approx 2\eta^{1/2}. \tag{B6}$$

In Eq. (B6), the behavior of the incomplete gamma function for $0 < \delta \ll 1$ is approximated by $\gamma(3/2, \delta) \approx 2\delta^{3/2}/3$. Finally, if Eqs. (B2) and (B6) are considered in Eq. (B5), the value of η is estimated as follows:

$$\eta \approx \frac{\pi}{16} \left[\zeta(3/2) \frac{\langle \bar{n} \rangle_c}{\langle N \rangle}\right]^2, \tag{B7}$$

although the value of $\langle \bar{n} \rangle_c$ is unknown. Additionally, if the value of η is known at constant $\langle N \rangle$, Eq. (B4) exhibits the dependence of $\langle \bar{n} \rangle$ on T.

The derivative $\partial\bar{\mu}/\partial\tau$ is estimated by differentiating Eq. (B4) with respect to a variable τ corresponding to either β or V, and the derivative $\partial\bar{\mu}/\partial\tau$ is expressed as follows:

$$\frac{\partial\bar{\mu}}{\partial\tau} = \frac{\xi_T}{Z_{1/2}(\bar{\mu};\eta)} \left[\frac{\partial\langle N \rangle}{\partial\tau} - \frac{\partial\langle \bar{n} \rangle}{\partial\tau} + \frac{2}{\xi_T^2} Z_{3/2}(\bar{\mu};\eta) \frac{\partial\xi_T}{\partial\tau} + \frac{2}{\xi_T} \frac{\partial\eta}{\partial\tau} \frac{\sqrt{\bar{\mu}+\eta}}{e^{\eta}-1}\right]. \tag{B8}$$

To obtain the derivative $\partial\eta/\partial V$ occurring in Eq. (618), the expression obtained from Eq. (B4) at $T = T_c$ must be differentiated with respect to V. Subsequently, if $\partial\langle \bar{n} \rangle_c/\partial V$ in the derivative thus obtained is substituted by $\partial\langle \bar{n} \rangle_c/\partial V$ obtained by differentiating Eq. (B7) with respect to V, then $\partial\eta/\partial V$ is estimated. When $\langle N \rangle$ is constant, $\partial\eta/\partial V$ is expressed as follows:

$$\frac{\partial\eta}{\partial V} = -\eta^{1/2} Z_{3/2}(0;\eta) \left[\frac{\xi_{T_c}\langle N \rangle}{\sqrt{\pi}\zeta(3/2)} - \frac{\eta}{e^{\eta}-1}\right]^{-1} V_{\mathrm{eff}}^{c} \frac{\partial V_{\mathrm{eff}}^{c}}{\partial V}. \tag{B9}$$

3. Contribution of particles with small momenta in temperature range $T_c < T$

For $T_c < T$, the number $\langle \bar{n} \rangle_I$ of particles with momenta $0 \le p \le p_{\min}$ is given as follows:

$$\langle \bar{n} \rangle_I = \frac{2}{\xi_T} \sum_{k=1}^{\infty} \frac{e^{k\bar{\mu}}}{k^{3/2}} \gamma(3/2, k\eta\beta/\beta_c). \tag{B10}$$

If the number of particles with momenta $p_{\min} < p < \infty$ is denoted as $\langle \bar{n} \rangle_{II}$, Eq. (B1) is rewritten as follows:

$$\langle N \rangle = \langle \bar{n} \rangle_I + \langle \bar{n} \rangle_{II}, \tag{B11}$$

where

$$\langle \bar{n} \rangle_{II} = \frac{2}{\xi_T} \bar{Z}_{3/2}(\bar{\mu}, \eta\beta/\beta_c) \tag{B12}$$

with

$$\bar{Z}_{\nu/2}(\bar{\mu}, \eta\beta/\beta_c) \equiv \sum_{k=1}^{\infty} \frac{e^{k\bar{\mu}}}{k^{\nu/2}} \Gamma(\nu/2, k\eta\beta/\beta_c), \quad (0 < \nu). \tag{B13}$$

When $0 < \eta\beta/\beta_c \ll 1$ is satisfied, an approximate relationship between $\bar{Z}_{\nu/2}(\bar{\mu}, \eta\beta/\beta_c)$ and $Z^0_{\nu/2}(\bar{\mu})$ is given as follows:

$$\bar{Z}_{\nu/2}(\bar{\mu}, \eta\beta/\beta_c) - Z^0_{\nu/2}(\bar{\mu}) \approx -\frac{2}{\nu} \frac{(\eta\beta/\beta_c)^{\nu/2}}{e^{-\bar{\mu}+\eta\beta/\beta_c} - 1}, \quad (0 < \nu). \tag{B14}$$

If the approximation given by Eq. (B14) is considered, the derivative $(\partial \bar{Z}_{\nu/2}/\partial\beta)_V$ is given as follows:

$$\left(\frac{\partial \bar{Z}_{\nu/2}(\bar{\mu}, \eta\beta/\beta_c)}{\partial \beta} \right)_V \approx \left(\frac{\nu}{2} - 1 \right) Z^0_{(\nu-2)/2}(\bar{\mu}) \frac{\partial \bar{\mu}}{\partial \beta} - \frac{1}{\beta} \frac{(\eta\beta/\beta_c)^{\nu/2}}{e^{-\bar{\mu}+\eta\beta/\beta_c} - 1}, \quad (0 < \nu). \tag{B15}$$

Furthermore, Eq. (B14) yields an approximate expression for $\langle \bar{n} \rangle_I$, i.e.,

$$\langle \bar{n} \rangle_I \approx \frac{4\eta^{3/2}}{3\xi_{T_c}} \frac{1}{e^{-\bar{\mu}+\eta\beta/\beta_c} - 1}. \tag{B16}$$

Eq. (B16) allows the differentiation of $\langle \bar{n} \rangle_I$ with respect to β to be approximately given as follows:

$$\left(\frac{\partial \langle \bar{n} \rangle_I}{\partial \beta} \right)_V \approx \frac{\langle \bar{n} \rangle_I}{1 - e^{\bar{\mu}-\eta\beta/\beta_c}} \left(\frac{\partial \bar{\mu}}{\partial \beta} - \frac{\eta}{\beta_c} \right). \tag{B17}$$

If the contribution of the $\langle \bar{n} \rangle_I$ particles to the internal energy E and the contribution of the $\langle \bar{n} \rangle_{II}$ particles to E are denoted as E_I and E_{II}, respectively, then E_I is given as follows:

$$E_I = E - E_{II}. \tag{B18}$$

For $0 < v_f/V_{\rm eff} \ll 1$, Eq. (600) allows E_{II} to be approximately estimated as

$$E_{II} \approx \frac{2}{\beta\xi_T} \bar{Z}_{5/2}(\bar{\mu}, \eta\beta/\beta_c) - \frac{2}{\beta\xi_T} (\beta U_a - \beta U_r) \bar{Z}_{3/2}(\bar{\mu}, \eta\beta/\beta_c). \tag{B19}$$

If Eqs. (604), (B1), and (B15) are considered, Eq.(B19) allows the derivative $(\partial E_{II}/\partial\beta)_V$ to be approximately given as follows:

$$\begin{aligned} \left(\frac{\partial E_{II}}{\partial \beta} \right)_V \approx & -\frac{2}{\beta\xi_T} \left(\frac{5}{2\beta} - \frac{1}{V_{\rm eff}} \frac{\partial V_{\rm eff}}{\partial \beta} \right) \left[\bar{Z}^0_{5/2}(\bar{\mu}) - \frac{3\xi_T}{10} \frac{\eta\beta}{\beta_c} \langle \bar{n} \rangle_I \right] \\ & + \frac{3}{2\beta} \frac{1}{V_{\rm eff}} \frac{\partial V_{\rm eff}}{\partial \beta} (\beta U_a - \beta U_r) \langle \bar{n} \rangle_I \\ & + \frac{3}{2\beta} \left(\langle N \rangle \frac{\partial \bar{\mu}}{\partial \beta} - \frac{\eta}{\beta_c} \langle \bar{n} \rangle_I \right). \end{aligned} \tag{B20}$$

Appendix C: Effective volume $V_{\rm eff}$ caused by hard cores of particles

1. Derivatives $\partial V_{\rm eff}/\partial V$ and $\partial U_r/\partial V$

Differentiating Eq. (589) with respect to V yields $\partial V_{\rm eff}/\partial V$ for $0 < v_f/V \ll 1$ as follows:

$$\left(\frac{\partial V_{\rm eff}}{\partial V}\right)_\beta - \frac{V_{\rm eff}}{V} \approx -\frac{V_{\rm eff}}{V}\left(1+\frac{V_{\rm eff}}{V}\right) V\beta\frac{\partial U_r}{\partial V}. \tag{C1}$$

Differentiating Eq. (589) with respect to β yields $\partial V_{\rm eff}/\partial\beta$ for $0 < v_f/V \ll 1$ as

$$\left(\frac{\partial V_{\rm eff}}{\partial \beta}\right)_V \approx -V_{\rm eff}U_r\left(1+\frac{V_{\rm eff}}{V}\right). \tag{C2}$$

At $T = T_c$, Eq. (589) is expressed as $\beta_c U_r \approx \ln\frac{1}{2}(1+V/V_{\rm eff}^c)$ given that $0 < v_f/V \ll 1$. If the relation is differentiated with respect to V, a relation between $\partial V_{\rm eff}^c/\partial V$ and $\partial U_r/\partial V$ is obtained for constant $\langle N\rangle$ as follows:

$$\frac{\partial V_{\rm eff}^c}{\partial V} \approx \frac{V_{\rm eff}^c}{V}\left(1+\frac{V_{\rm eff}^c}{V}\right)\left(\rho\frac{\partial\beta_c}{\partial\rho}U_r - V\beta_c\frac{\partial U_r}{\partial V}\right). \tag{C3}$$

Subsequently, Eq. (C1) at $T = T_c$ should be equivalent to Eq. (C3) . Hence, $\rho\partial\beta_c/\partial\rho$ must satisfy

$$\rho\frac{\partial\beta_c}{\partial\rho} \approx \frac{1}{U_r}\left(1+\frac{V_{\rm eff}^c}{V}\right)^{-1}. \tag{C4}$$

If Eq. (B2) is differentiated with respect to V at constant $\langle N\rangle$, then the relation given by Eq. (C4) allows $\partial V_{\rm eff}^c/\partial V$ to be expressed as follows:

$$\frac{\partial V_{\rm eff}^c}{\partial V} \approx -\frac{3}{2\beta_c U_r}\frac{V_{\rm eff}^c}{V}\left(1+\frac{V_{\rm eff}^c}{V}\right)^{-1}. \tag{C5}$$

The use of Eq. (C5) allows $\partial V_{\rm eff}^c/\partial V$ to be eliminated from the formula obtained from Eq. (C1) at $T = T_c$, and the following formula is obtained:

$$V\beta_c\frac{\partial U_r}{\partial V} \approx \left(1+\frac{V_{\rm eff}^c}{V}\right)^{-1}\left[\frac{3}{2\beta_c U_r}\left(1+\frac{V_{\rm eff}^c}{V}\right)^{-1}+1\right]. \tag{C6}$$

$\partial^2 U_r/\partial V^2$ is obtained from differentiating Eq. (C6) with respect to V. If Eq. (C5) is considered, then Eq. (614) allows $(\partial\bar\mu/\partial V)Z_{1/2}^0(\bar\mu)\big|_{T=T_c}$ to be estimated as follows:

$$\frac{\partial\bar\mu}{\partial V}Z_{1/2}^0(\bar\mu)\bigg|_{T=T_c} \approx \frac{3Z_{3/2}^0(0)}{V\beta_c U_r}\left(1+\frac{V_{\rm eff}^c}{V}\right)^{-1}. \tag{C7}$$

2. Other volumes

Based on Eq. (589), the ratio v_f/V that is neglected in the above expressions is given as follows:

$$\frac{v_f}{V} = \frac{1}{2}\left(\frac{V_{\rm eff}}{V} - \frac{1}{2e^{\beta U_r}-1}\right)\frac{2e^{\beta U_r}-1}{e^{\beta U_r}-1}. \tag{C8}$$

The ratio $v_{\rm eff}/V$ is given as follows:

$$\frac{v_{\rm eff}}{V} = \frac{3}{2}\left(\frac{V_{\rm eff}}{V} - \frac{1}{2e^{\beta U_r}-1}\right)\frac{1}{e^{\beta U_r}-1}. \tag{C9}$$

Appendix D: Contributions from quasiparticles

1. Estimation of parameter u for free energy caused by rotons and phonons

The contributions from rotons and phonons to the free energy are estimated given a specific phase involving the effect of anisotropy[106], and are expressed by

$$F_\lambda = \frac{1}{\beta}\int_0^{\hat{p}_{\rm max}}\int_0^{\pi}\frac{2\pi V\hat{p}^2\,{\rm d}\hat{p}\,\sin\theta\,{\rm d}\theta}{(2\pi\hbar)^3}\ln\left\{1-\exp\left[-\beta\left(\hat{\varepsilon}_\lambda(\hat{p})-\hat{p}u\cos\theta\right)\right]\right\} \quad (\lambda=1,\ 2), \tag{D1}$$

where

$$\hat{\varepsilon}_\lambda(\hat{p}) = \begin{cases}\hat{\Delta}+\dfrac{1}{2\hat{\mu}}(\hat{p}-p_0)^2 & (\lambda=1\ \text{for rotons}),\\ c\hat{p} & (\lambda=2\ \text{for phonons}).\end{cases} \tag{D2}$$

The two parameters u and $\hat{p}_{\rm max}$ on which F_λ ($\lambda=1,\ 2$) depends are unknown. Four parameters $\hat{\mu}$, p_0, $\hat{\Delta}$, and c are known for liquid helium (^{4}He): $c = 238\,{\rm m/s}$, $\hat{\Delta}/k_B = 8.712\,{\rm K}$, $p_0/\hbar = 1.913\times10^{10}\,{\rm m}^{-1}$, and $\hat{\mu} = 0.1608 m_{\rm He}$ ($m_{\rm He}$ = ^{4}He atomic mass).[111] The parameter u is given as $u = |\mathbf{u}|$ and must satisfy the inequality $0 < u \le v_{\rm max}$ because the expectation value of $\hat{n}_\lambda(\hat{\mathbf{p}})$ of quasiparticles with the momentum $\hat{\mathbf{p}}$ ($\hat{p} = |\hat{\mathbf{p}}|$) is given by $\langle\hat{n}_\lambda(\hat{\mathbf{p}})\rangle = \{\exp[\beta(\hat{\varepsilon}_\lambda(\hat{p}) - \hat{\mathbf{p}}\cdot\mathbf{u})]-1\}^{-1}$ ($\lambda=1,\ 2$), which is always positive. Thus, the quantity $\hat{\varepsilon}_\lambda(\hat{p})$ satisfies the two relations $d\hat{\varepsilon}_\lambda/d\hat{p}|_{\hat{p}=\hat{p}_m} = v_{\rm max}$ and $\hat{\varepsilon}_\lambda(\hat{p}_m) = v_{\rm max}\hat{p}_m$, which require $v_{\rm max}$ to be given for $\lambda=1$ as $v_{\rm max} = (p_0/\hat{\mu})[(1+2\hat{\mu}\hat{\Delta}/p_0^2)^{1/2}-1] \approx \hat{\Delta}/p_0$ (for instance, $\hat{\mu}\hat{\Delta}/(2p_0^2) \approx 0.016$). Therefore, the inequality $0 \le u \le v_{\rm max}$ is equivalent to three inequalities $0 \le p_0 u/\hat{\Delta} \le 1$, $0 \le \hat{\mu}u^2/(2\hat{\Delta}) \le \hat{\mu}\hat{\Delta}/(2p_0^2)$, and $0 \le \hat{\mu}u/p_0 \le \hat{\mu}\hat{\Delta}/p_0^2$ (for example, $\hat{\mu}\hat{\Delta}/p_0^2 \approx 0.031$).

It is reasonable to estimate the value of u without considering the contribution from phonons.[1,106,112] Equation (D1) is expressed as follows:

$$F_\lambda = -\frac{V}{(2\pi)^2\hbar^3\beta^2}\left(\frac{1}{u}\right)\sum_{k=1}^{\infty}\frac{1}{k^2}\int_0^{\hat{p}_{\max}} \mathrm{d}\hat{p}\,\hat{p}e^{-k\beta\hat{\varepsilon}_\lambda(\hat{p})}\left(e^{k\beta u\hat{p}} - e^{-k\beta u\hat{p}}\right) \quad (\lambda = 1,\ 2). \tag{D3}$$

For $\lambda = 1$, $\exp[-k\beta\hat{\varepsilon}_\lambda(\hat{p})]$ is expressed as follows:

$$e^{-k\beta\hat{\varepsilon}_1(\hat{p})} = e^{-k\beta\hat{\Delta}}\exp\left[-\frac{1}{2\sigma_k^2}(\bar{p}-1)^2\right], \tag{D4}$$

where

$$\sigma_k \equiv \sqrt{\frac{\hat{\mu}}{k\beta p_0^2}} = \frac{\sigma_1}{k^{1/2}}, \tag{D5}$$

$$\bar{p} \equiv \hat{p}/p_0. \tag{D6}$$

The inequality $0 < \sigma_k \ll 1$ is then satisfied. For instance, σ_1 satisfies $0 < \sigma_1 \leq 0.088$ at $\beta = 3.34 \times 10^{22}\,\mathrm{J}^{-1}$. In Eq. (D4), the Gaussian function is finite for $|\bar{p}-1| \ll 1$. The inequality $e^{-k\beta\hat{\Delta}} \ll 1$ holds even for $k = 1$. The aforementioned facts allow the exponential functions in Eq. (D3) to be approximated as finite power series in $k\beta u\hat{p}$ when u remains small.

For arbitrary values of β, the first and second derivatives of F_1 exactly satisfy the following expression:

$$-\lim_{u\to 0} u^{-1}V^{-1}\frac{\partial F_1}{\partial u} = -\lim_{u\to 0} V^{-1}\frac{\partial^2 F_1}{\partial u^2}. \tag{D7}$$

The term $-V^{-1}(\partial^2 F_1/\partial u^2)$ contributes as the mass density ρ_m of the fluid,[106] and $-u^{-1}V^{-1}(\partial F_1/\partial u)$ contributes as the mass density of the normal component $\rho_m^{(n)}$ of the fluid.[1,106,112] Hence, if the ratio of the mass density of the non-normal component to the mass density of the fluid is denoted by f_r, then it is estimated as

$$f_r = 1 - \frac{u^{-1}V^{-1}\left(\partial F_1/\partial u\right)}{V^{-1}\left(\partial^2 F_1/\partial u^2\right)}. \tag{D8}$$

Additionally, although the relationship between f_r and T for liquid helium is obtained from experimental data,[109] it can be made to correspond to the ratio $\langle\bar{n}\rangle/\langle N\rangle$ obtained from Eq. (B4).

Approximating the exponential functions in Eq. (D3) as finite power series in $k\beta u\hat{p}$ allows f_r to be estimated as follows:

$$f_r \approx \frac{2}{3}(\beta p_0 u)^2 \sum_{k=1}^{\infty} k^3 \int_0^{\bar{p}_{\max}} \mathrm{d}\bar{p}\, \bar{p}^6 e^{-k\beta\hat{\varepsilon}_1(\hat{p})} \left[\frac{10}{3} \sum_{k=1}^{\infty} k \int_0^{\bar{p}_{\max}} \mathrm{d}\bar{p}\, \bar{p}^4 e^{-k\beta\hat{\varepsilon}_1(\hat{p})} + (\beta p_0 u)^2 \sum_{k=1}^{\infty} k^3 \int_0^{\bar{p}_{\max}} \mathrm{d}\bar{p}\, \bar{p}^6 e^{-k\beta\hat{\varepsilon}_1(\hat{p})} \right]^{-1}. \tag{D9}$$

Equation (D9) gives a simple relation between u and f_r for small u, and it indicates that u decreases when f_r decreases.

Without approximation, the derivatives of F_1 satisfy the following general equation:

$$\nu \frac{\partial^{(\nu-1)} F_1}{\partial u^{(\nu-1)}} + u \frac{\partial^{(\nu)} F_1}{\partial u^{(\nu)}} = (-1)^{\nu} \frac{V p_0^2}{(2\pi)^2 \hbar^3 \beta^2} \sum_{k=1}^{\infty} \frac{(k\beta p_0)^{\nu}}{k^2} \Big\{ \exp[-k\beta(\hat{\Delta} + \tau(u))] I_k^{(\nu+1)}(u, \bar{p}_{\max}; \beta) + (-1)^{\nu+1} \exp[-k\beta(\hat{\Delta} + \tau(-u))] I_k^{(\nu+1)}(-u, \bar{p}_{\max}; \beta) \Big\} \quad (\nu = 1, 2, 3, \dots). \tag{D10}$$

F_1 also satisfies the equation for $\nu = 0$. However, the first term for $\nu = 0$ is equal to zero. In Eq. (D10), $\tau(u)$ and $I_\nu(u, \bar{p}_{\max}; \beta)$ are defined as follows:

$$\tau(u) \equiv p_0 u - \hat{\mu} u^2/2, \tag{D11}$$

$$\begin{aligned} I_k^{(\nu)}(u, \bar{p}_{\max}; \beta) &\equiv \int_0^{\bar{p}_{\max}} \mathrm{d}\bar{p} \bar{p}^{\nu} \exp\left[-\frac{1}{2\sigma_k^2} \left(\bar{p} + q(u) \right)^2 \right] \\ &= \frac{(-1)^{\nu}}{2} (2\sigma_k^2)^{(\nu+1)/2} \sum_{n=0}^{\nu} \frac{\nu!}{(\nu-n)! n!} \left(\frac{q(u)}{\sqrt{2}\sigma_k} \right)^n \left\{ \left[1 - (-1)^{\nu-n+1} \right] \Gamma\left(\frac{\nu-n+1}{2} \right) \right. \\ &\quad \left. - \Gamma\left(\frac{\nu-n+1}{2}, \frac{q(u)^2}{2\sigma_k^2} \right) + (-1)^{\nu-n+1} \Gamma\left(\frac{\nu-n+1}{2}, \frac{(\bar{p}_{\max} + q(u))^2}{2\sigma_k^2} \right) \right\} \\ &\quad (\nu = 1, 2, 3, \dots \quad \text{and} \quad \bar{p}_{\max} \geq -q(u)). \end{aligned} \tag{D12}$$

In the above, $q(u)$ is defined as follows:

$$q(u) \equiv -1 + (\hat{\mu}/p_0) u. \tag{D13}$$

Additionally, the quantity σ_k given by Eq. (D5) is very small. This implies that $1/(2\sigma_k^2)$ is sufficiently large such that $I_k^{(\nu)}(u, \bar{p}_{\max}; \beta)$ is independent of $\bar{p}_{\max}$. Hence, $I_k^{(\nu)}(u, \bar{p}_{\max}; \beta)$ is approximated as $I_k^{(\nu)}(u, \bar{p}_{\max}; \beta) \approx \bar{I}_k^{(\nu)}(u; \beta)$. $\bar{I}_k^{(\nu)}(u; \beta)$ is given by the following expression:

$$\bar{I}_k^{(\nu)}(u; \beta) = \frac{(-1)^{\nu} \sigma_1}{\sqrt{2} k^{1/2}} \sum_{n=0}^{\nu} \frac{\nu!}{(\nu-n)! n!} \Big(q(u) \Big)^n \Big(\sqrt{2}\sigma_k \Big)^{\nu-n} \Big[1 - (-1)^{\nu-n+1} \Big] \Gamma\left(\frac{\nu-n+1}{2} \right). \tag{D14}$$

The use of Eq. (D14) allows Eq. (D10) to be modified as

$$\nu\frac{\partial^{(\nu-1)}F_1}{\partial u^{(\nu-1)}}+u\frac{\partial^{(\nu)}F_1}{\partial u^{(\nu)}}\approx-\frac{Vp_0^2\sigma_1(\beta p_0)^\nu}{\sqrt{2}(2\pi)^2\hbar^3\beta^2}\sum_{n=0}^{\nu+1}\frac{(\nu+1)!}{(\nu+1-n)!n!}\Big[1-(-1)^{\nu-n+2}\Big]\Gamma\left(\frac{\nu-n+2}{2}\right)$$
$$\times\left(\sqrt{2}\sigma_1\right)^{\nu+1-n}\Big\{\big[q(u)\big]^n\mathcal{L}^{(6-\nu-n)}(u,\hat{\Delta};\beta)+(-1)^{\nu+1}\big[q(-u)\big]^n\mathcal{L}^{(6-\nu-n)}(-u,\hat{\Delta};\beta)\Big\}. \tag{D15}$$

where

$$\mathcal{L}^{(6-\nu-n)}(u,\hat{\Delta};\beta)\equiv\sum_{k=1}^{\infty}\frac{e^{-k\beta(\hat{\Delta}+\tau(u))}}{k^{(6-\nu-n)/2}}. \tag{D16}$$

If the relations $-V^{-1}(\partial^2F_1/\partial u^2)=\rho_m$ and $-u^{-1}V^{-1}(\partial F_1/\partial u)=\rho_m^{(n)}$ are considered,[106] two equations that are obtained for $\nu=1$ and $\nu=2$ from Eq. (D15) can form a system of equations to estimate u and $\hat{\Delta}/k_B$ as parameters dependent on T. The two equations are expressed as follows:

$$\mathcal{H}_1(u,\hat{\Delta};\beta)\equiv u^3(1-f_r)+\bar{A}\Big\{\big[q(u)-\sigma_1^2\beta p_0u\big]\mathcal{L}^{(5)}(u,\hat{\Delta};\beta)-\big[q(-u)+\sigma_1^2\beta p_0u\big]\mathcal{L}^{(5)}(-u,\hat{\Delta};\beta)\Big\}$$
$$-\bar{A}\beta p_0u\Big\{\big[q(u)\big]^2\mathcal{L}^{(3)}(u,\hat{\Delta};\beta)+\big[q(-u)\big]^2\mathcal{L}^{(3)}(-u,\hat{\Delta};\beta)\Big\}=0, \tag{D17}$$

$$\mathcal{H}_2(u,\hat{\Delta};\beta)\equiv u(3-2f_r)+\bar{A}(\beta p_0)^2\Big\{3\sigma_1^2\Big[q(u)\mathcal{L}^{(3)}(u,\hat{\Delta};\beta)-q(-u)\mathcal{L}^{(3)}(-u,\hat{\Delta};\beta)\Big]$$
$$+\big[q(u)\big]^3\mathcal{L}^{(1)}(u,\hat{\Delta};\beta)-\big[q(-u)\big]^3\mathcal{L}^{(1)}(-u,\hat{\Delta};\beta)\Big\}=0, \tag{D18}$$

where f_r satisfies $f_r=1-\rho_m^{(n)}/\rho_m$ and $\bar{A}$ is defined by

$$\bar{A}\equiv\frac{\sigma_1p_0^2}{(2\pi)^{3/2}\hbar^3\beta^2\rho_m}. \tag{D19}$$

The derivatives $\partial u/\partial\beta$ and $\partial\hat{\Delta}/k_B/\partial\beta$ are obtained from differentiating Eqs. (D17) and (D18). Despite this, the assumption that $\hat{\Delta}/k_B$ is constant allows $\partial u/\partial\beta$ to be estimated from one of the two derivatives. For example, from the derivative of Eq. (D18),

$$\frac{\partial u}{\partial\beta}=-\frac{\partial\mathcal{H}_2}{\partial\beta}\left(\frac{\partial\mathcal{H}_2}{\partial u}\right)^{-1}, \tag{D20}$$

where

$$\frac{\partial \mathcal{H}_2}{\partial u} \equiv \bar{A}(\beta p_0)^2 \frac{1}{u^2}\Big\{ -3\sigma_1^2\Big[\mathcal{L}^{(3)}(u,\hat{\Delta};\beta) - \mathcal{L}^{(3)}(-u,\hat{\Delta};\beta)\Big]$$
$$+\big[q(u)\big]^2\Big[q(u) - \frac{3\hat{\mu}u}{p_0} - 3\sigma_1^2\beta p_0 u\Big]\mathcal{L}^{(1)}(u,\hat{\Delta};\beta)$$
$$-\big[q(-u)\big]^2\Big[q(-u) + \frac{3\hat{\mu}u}{p_0} + 3\sigma_1^2\beta p_0 u\Big]\mathcal{L}^{(1)}(-u,\hat{\Delta};\beta)$$
$$-\big[q(u)\big]^4\beta p_0 u\mathcal{L}^{(-1)}(u,\hat{\Delta};\beta) - \big[q(-u)\big]^4\beta p_0 u\mathcal{L}^{(-1)}(-u,\hat{\Delta};\beta)\Big\},$$
$$\frac{\partial \mathcal{H}_2}{\partial \beta} \equiv -2\frac{\partial f_r}{\partial \beta} + \frac{\bar{A}\beta p_0^2}{2u}\Big\{ 9\sigma_1^2\Big[q(u)\mathcal{L}^{(3)}(u,\hat{\Delta};\beta) - q(-u)\mathcal{L}^{(3)}(-u,\hat{\Delta};\beta)\Big]$$
$$+\Big[\big[q(u)\big]^3 + 6\sigma_1^2 q(u)\beta\Big(\hat{\Delta}+\tau(u)\Big)\Big]\mathcal{L}^{(3)}(u,\hat{\Delta};\beta)$$
$$-\Big[\big[q(-u)\big]^3 + 6\sigma_1^2 q(-u)\beta\Big(\hat{\Delta}+\tau(-u)\Big)\Big]\mathcal{L}^{(3)}(-u,\hat{\Delta};\beta)$$
$$+2\big[q(u)\big]^3\beta\Big(\hat{\Delta}+\tau(u)\Big)\mathcal{L}^{(-1)}(u,\hat{\Delta};\beta) - 2\big[q(-u)\big]^3\beta\Big(\hat{\Delta}+\tau(-u)\Big)\mathcal{L}^{(-1)}(-u,\hat{\Delta};\beta)\Big\}. \tag{D21}$$

2. Contributions from rotons and phonons to internal energy

The contribution E_λ ($\lambda = 1,\ 2$) from quasiparticles to the internal energy is estimated from the relation $E_\lambda = (\partial(\beta F_\lambda)/\partial\beta)_{u,\bar{p}_{\max}} - u(\partial F_\lambda/\partial u)_{\beta,\bar{p}_{\max}}$. The contribution E_λ depends on at least four parameters — u, β, V, and $\bar{p}_{\max}$ — and should be expressed as $E_\lambda = E_\lambda(u,\beta,V;\bar{p}_{\max})$, which is estimated from the free energy F_λ as follows:

$$E_\lambda(u,\beta,V;\bar{p}_{\max}) = \frac{Vp_0^2}{(2\pi)^2\hbar^3}\left(\frac{1}{\beta u}\right)\sum_{k=1}^{\infty}\frac{1}{k}\int_0^{\bar{p}_{\max}}\hat{\varepsilon}_\lambda(\bar{p})e^{-k\beta\hat{\varepsilon}_\lambda(\bar{p})}\Big[e^{k\beta p_0 u\bar{p}} - e^{-k\beta p_0 u\bar{p}}\Big]\bar{p}\mathrm{d}\bar{p}. \tag{D22}$$

Despite the aforementioned description, the contribution E_1 from rotons should be expressed as $E_1(u,\hat{\Delta},\beta,V;\bar{p}_{\max})$ because the contribution is given without any approximation by

$$E_1(u,\hat{\Delta},\beta,V;\bar{p}_{\max}) = \frac{Vp_0^4}{2(2\pi)^2\hbar^3\hat{\mu}}\left(\frac{1}{\beta u}\right)\sum_{k=1}^{\infty}\frac{1}{k}\Big\{\exp\big[-k\beta(\hat{\Delta}+\tau(-u))\big]\Big[I_k^{(3)}(-u,\bar{p}_{\max};\beta)$$
$$-2I_k^{(2)}(-u,\bar{p}_{\max};\beta) + \left(1+\frac{2\hat{\mu}\hat{\Delta}}{p_0^2}\right)I_k^{(1)}(-u,\bar{p}_{\max};\beta)\Big]$$
$$-\exp\big[-k\beta(\hat{\Delta}+\tau(u))\big]\big[I_k^{(3)}(u,\bar{p}_{\max};\beta) - 2I_k^{(2)}(u,\bar{p}_{\max};\beta)$$
$$+\left(1+\frac{2\hat{\mu}\hat{\Delta}}{p_0^2}\right)I_k^{(1)}(u,\bar{p}_{\max};\beta)\Big]\Big\}. \tag{D23}$$

In the range where $\bar{p}_{\max} > -q(u)$ is satisfied, $E_1(u, \hat{\Delta}, \beta, V; \bar{p}_{\max})$ is approximately independent of $\bar{p}_{\max}$ due to $0 < \sigma_k \ll 1$. The behavior of $E_1(u, \hat{\Delta}, \beta, V; \bar{p}_{\max})$ is expressed as $E_1(u, \hat{\Delta}, \beta, V; \bar{p}_{\max}) \approx \hat{E}_1(u, \hat{\Delta}, \beta, V)$. If Eq. (D14) is considered in Eq. (D23), $\hat{E}_1(u, \hat{\Delta}, \beta, V)$ is given as follows:

$$\begin{aligned}\hat{E}_1(u, \hat{\Delta}, \beta, V) = \frac{\bar{A}\beta p_0^2 V \rho_m}{2\hat{\mu}u}\Big\{&-\big(3q(-u)+2\big)\sigma_1^2\mathcal{L}^{(5)}(-u, \hat{\Delta}; \beta) + \big(3q(u)+2\big)\sigma_1^2\mathcal{L}^{(5)}(u, \hat{\Delta}; \beta) \\ &- \Big[\big[q(-u)\big]^3 + 2\big[q(-u)\big]^2 + \Big(1 + \frac{2\hat{\mu}\hat{\Delta}}{p_0^2}\Big)q(-u)\Big]\mathcal{L}^{(3)}(-u, \hat{\Delta}; \beta) \\ &+ \Big[\big[q(u)\big]^3 + 2\big[q(u)\big]^2 + \Big(1 + \frac{2\hat{\mu}\hat{\Delta}}{p_0^2}\Big)q(u)\Big]\mathcal{L}^{(3)}(u, \hat{\Delta}; \beta)\Big\}. \end{aligned} \tag{D24}$$

Differentiating E_1 with respect to β at constant V and constant $\hat{\Delta}$ yields the following expression:

$$\left(\frac{\partial E_1}{\partial \beta}\right)_V \approx \frac{\partial u}{\partial \beta}\left(\frac{\partial \hat{E}_1}{\partial u}\right)_\beta + \left(\frac{\partial \hat{E}_1}{\partial \beta}\right)_u, \tag{D25}$$

where $\partial u/\partial\beta$ is estimated from Eq. (D20). The other derivatives in Eq. (D25) are obtained from the differentiation of Eq. (D24) as follows:

$$\begin{aligned}\left(\frac{\partial \hat{E}_1}{\partial \beta}\right)_{u,V} = &-\frac{3\hat{E}_1}{2\beta} + \frac{\bar{A}p_0^2 V\rho_m}{2\hat{\mu}u}\Big\{\sigma_1^2\big[3q(-u)+2\big]\mathcal{L}^{(5)}(-u, \hat{\Delta}, \beta) - \sigma_1^2\big[3q(u)+2\big]\mathcal{L}^{(5)}(u, \hat{\Delta}, \beta) \\ &+\sigma_1^2\big[3q(-u)+2\big]\beta\big[\hat{\Delta} + \tau(-u)\big]\mathcal{L}^{(3)}(-u, \hat{\Delta}, \beta) - \sigma_1^2\big[3q(u)+2\big]\beta\big[\hat{\Delta} + \tau(u)\big]\mathcal{L}^{(3)}(u, \hat{\Delta}, \beta) \\ &+\Big[\big[q(-u)\big]^3 + 2\big[q(-u)\big]^2 + \Big(1 + \frac{2\hat{\mu}\hat{\Delta}}{p_0^2}\Big)q(-u)\Big]\beta[\hat{\Delta} + \tau(-u)]\mathcal{L}^{(1)}(-u, \hat{\Delta}, \beta) \\ &-\Big[\big[q(u)\big]^3 + 2\big[q(u)\big]^2 + \Big(1 + \frac{2\hat{\mu}\hat{\Delta}}{p_0^2}\Big)q(u)\Big]\beta[\hat{\Delta} + \tau(u)]\mathcal{L}^{(1)}(u, \hat{\Delta}, \beta)\Big\}, \end{aligned} \tag{D26}$$

$$\begin{aligned}\left(\frac{\partial \hat{E}_1}{\partial u}\right)_{\beta,V} = &-\frac{\hat{E}_1}{u} + \frac{\bar{A}\beta p_0 V\rho_m}{2u}\Big\{3\sigma_1^2\Big[\mathcal{L}^{(5)}(-u, \hat{\Delta}, \beta) + \mathcal{L}^{(5)}(u, \hat{\Delta}, \beta)\Big] \\ &+\Big[\frac{\beta p_0^2}{\hat{\mu}}q(-u)\big[3q(-u)+2\big]\sigma_1^2 + 3\big[q(-u)\big]^2 + 2q(-u) + 1 + \frac{2\hat{\mu}\hat{\Delta}}{p_0^2}\Big]\mathcal{L}^{(3)}(-u, \hat{\Delta}, \beta) \\ &+\Big[\frac{\beta p_0^2}{\hat{\mu}}q(u)\big[3q(u)+2\big]\sigma_1^2 + 3\big[q(u)\big]^2 + 2q(u) + 1 + \frac{2\hat{\mu}\hat{\Delta}}{p_0^2}\Big]\mathcal{L}^{(3)}(u, \hat{\Delta}, \beta) \\ &+\frac{\beta p_0^2}{\hat{\mu}}\Big[\big[q(-u)\big]^3 + 2\big[q(-u)\big]^2 + \Big(1 + \frac{2\hat{\mu}\hat{\Delta}}{p_0^2}\Big)q(-u)\Big]q(-u)\mathcal{L}^{(1)}(-u, \hat{\Delta}, \beta) \\ &+\frac{\beta p_0^2}{\hat{\mu}}\Big[\big[q(u)\big]^3 + 2\big[q(u)\big]^2 + \Big(1 + \frac{2\hat{\mu}\hat{\Delta}}{p_0^2}\Big)q(u)\Big]q(u)\mathcal{L}^{(1)}(u, \hat{\Delta}, \beta)\Big\}. \end{aligned} \tag{D27}$$

Additionally, the phonon contribution $E_2(u,\beta,V;\bar{p}_{\max})$, which is estimated from the free energy F_2 without any approximation, is given as follows:

$$E_2(u,\beta,V;\bar{p}_{\max}) = \frac{Vp_0^3}{(2\pi)^2\hbar^3\beta}\left(\frac{c}{u}\right)\sum_{k=1}^{\infty}\frac{1}{k}\left[J_k^{(2)}(-u,\bar{p}_{\max};\beta) - J_k^{(2)}(u,\bar{p}_{\max};\beta)\right], \tag{D28}$$

where

$$\begin{aligned} J_k^{(\nu)}(u,\bar{p}_{\max};\beta) = & -\exp\left(-k\beta cp_0(1+u/c)\bar{p}_{\max}\right)\sum_{n=0}^{\nu}\frac{\nu!}{(\nu-n)!}\frac{(\bar{p}_{mac})^{\nu-n}}{\left[k\beta cp_0(1+u/c)\right]^{n+1}} \\ & + \frac{\nu!}{\left[k\beta cp_0(1+u/c)\right]^{\nu+1}}. \end{aligned} \tag{D29}$$

For $u/c \ll 1$, the phonon contribution E_2 becomes insensitive to the value of u. This implies that the behavior of E_2 is not governed by the effects of anisotropy.

If the sum $\sum_{\alpha^*}\langle n_{\alpha^*}\rangle\varepsilon_{\alpha^*}$ in Eq. (602) is the contribution from quasiparticles, then it should be given as $\sum_{\alpha^*}\varepsilon_{\alpha^*}\langle n_{\alpha^*}\rangle = E_1(u,\hat{\Delta},\beta,V;\bar{p}_{\max}) + E_2(u,\beta,V;\bar{p}_{\max})$. However, E_2 is ignored because the contribution from phonons is significantly smaller than that from rotons for $0 < (T_c - T)/T \ll 1$.

3. Estimation of the number of rotons in temperature range $T_c < T$

Based on Eq. (B10), the momenta of the $\langle\bar{n}\rangle_I$ particles remains in the range $0 \le p \le p_{\min}$ even for $T_c < T$. The $\langle\bar{n}\rangle_I$ particles can contribute to the generation of quasiparticles, even if the dependence of F_1 on u disappears. Given the aforementioned possibility, the contribution of the $\langle\bar{n}\rangle_I$ particles to the internal energy should be estimated as the contribution E_I from quasiparticles for $u = 0$. The total number $\mathcal{N}_{\text{roton}}(\bar{p}_{\max},\beta)$ of rotons is given for $u = 0$ as follows:

$$\mathcal{N}_{\text{roton}}(\bar{p}_{\max},\beta) = \frac{2Vp_0^3}{(2\pi)^2\hbar^3}\int_0^{\bar{p}_{\max}}\mathrm{d}\bar{p}\bar{p}^2\sum_{k=1}^{\infty}e^{-k\beta\hat{\Delta}}\exp\left[-\frac{1}{2\sigma_k}(\bar{p}-1)^2\right]. \tag{D30}$$

$\mathcal{N}_{\text{roton}}(\bar{p}_{\max},\beta)$ must be limited by the value of $\langle\bar{n}\rangle_I$. If $\langle\bar{n}\rangle_I$ decreases toward zero, $\mathcal{N}_{\text{roton}}(\bar{p}_{\max},\beta)$ should decrease toward zero. This suggests that $\bar{p}_{\max}$ decreases with decreasing $\langle\bar{n}\rangle_I$, and it allows ensuring that the assumption that $0 \le \bar{p}_{\max} \le -q(u)\big|_{u=0}$ is satisfied for $T_c < T$. Furthermore, two assumptions are considered to simplify estimations. The first corresponds to the assumption that $\mathcal{N}_{\text{roton}}(\bar{p}_{\max},\beta) = c_0\langle\bar{n}\rangle_I$ is approximately satisfied with c_0 being the proportionality constant. The other corresponds to the assumption

that $\bar{p}_{\max} - 1 = 0$ is satisfied at $T = T_c$. The aforementioned two assumptions require $c_0 = \mathcal{N}_{\rm roton}(\bar{p}^{(c)}_{\max}, \beta_c)/\langle \bar{n} \rangle^{(c)}_I$ to be satisfied with $\langle \bar{n} \rangle^{(c)}_I \equiv \langle \bar{n} \rangle_I \big|_{T=T_c}$ and $\bar{p}^{(c)}_{\max} \equiv \bar{p}_{\max}|_{T=T_c} = 1$.

Eq. (D30) allows $\mathcal{N}_{\rm roton}(\bar{p}_{\max}, \beta)$ to be approximately given for $u = 0$ and $0 \le \bar{p}_{\max} \le 1$ as

$$\begin{aligned}\mathcal{N}_{\rm roton}(\bar{p}_{\max}, \beta) \approx & \frac{\sqrt{2}\pi V p_0^3 \sigma_1}{(2\pi)^2 \hbar^3} \Big[2\sigma_1^2 \hat{\mathcal{L}}^{(3)}(\hat{\Delta}, \beta, \bar{p}_{\max}) - 2^{3/2} \sigma_1 \hat{\mathcal{L}}^{(2)}(\hat{\Delta}, \beta, \bar{p}_{\max}) \\ & + \hat{\mathcal{L}}^{(1)}(\hat{\Delta}, \beta, \bar{p}_{\max}) \Big], \end{aligned} \tag{D31}$$

where

$$\hat{\mathcal{L}}^{(\nu)}(\hat{\Delta}, \beta, \bar{p}_{\max}) = \sum_{k=1}^{\infty} \frac{e^{-k\beta\hat{\Delta}}}{k^{\nu/2}} \Gamma\left[\frac{\nu}{2}, \frac{(\bar{p}_{\max} - 1)^2}{2\sigma_k^2} \right]. \tag{D32}$$

Therefore, the relation $\mathcal{N}_{\rm roton}(\bar{p}_{\max}, \beta) = c_0 \langle \bar{n} \rangle_I$ allows $\bar{p}_{\max}$ to be estimated. Furthermore, the relation allows the derivative $\partial \bar{p}_{\max}/\partial\beta$ to be estimated as follows:

$$\begin{aligned}\left(\frac{\partial \bar{p}_{\max}}{\partial \beta} \right)_V = & \left[c_0 \left(\frac{\partial \langle \bar{n} \rangle_I}{\partial \beta} \right)_V + \frac{\sigma_1}{2\beta} \left(\frac{\partial \mathcal{N}_{\rm roton}}{\partial \sigma_1} \right)_{\beta \bar{p}_{\max}} - \left(\frac{\partial \mathcal{N}_{\rm roton}}{\partial \beta} \right)_{\sigma_1 \bar{p}_{\max}} \right] \\ & \times \left[\left(\frac{\partial \mathcal{N}_{\rm roton}}{\partial \bar{p}_{\max}} \right)_{\sigma_1 \beta} \right]^{-1}. \end{aligned} \tag{D33}$$

In Eq. (D33), the derivative $\left(\partial \langle \bar{n} \rangle_I / \partial \beta \right)_V$ is given by Eq. (B17).

For $T_c < T$, an approximate contribution $E_1(\hat{\Delta}, \beta, V; \bar{p}_{\max})$ to the internal energy is estimated by considering $0 < \sigma_k \ll 1$, $u = 0$, and $\bar{p}_{\max} \le 1$. Subsequently, the use of Eq. (D22) allows the approximate contribution to be given as follows:

$$\begin{aligned}E_1(\hat{\Delta}, \beta, V; \bar{p}_{\max}) \approx & \frac{\sqrt{2} V p_0^5 \sigma_1}{(2\pi)^2 \hbar^3 \hat{\mu}} \Big\{ 2\sigma_1^4 \hat{\mathcal{L}}^{(5)}(\hat{\Delta}, \beta, \bar{p}_{\max}) - 2\sqrt{2}\sigma_1^3 \hat{\mathcal{L}}^{(4)}(\hat{\Delta}, \beta, \bar{p}_{\max}) \\ & + \sigma_1^2 \Big(1 + \frac{2\hat{\mu}\hat{\Delta}}{p_0^2} \Big) \hat{\mathcal{L}}^{(3)}(\hat{\Delta}, \beta, \bar{p}_{\max}) - 2\sqrt{2}\sigma_1 \frac{\hat{\mu}\hat{\Delta}}{p_0^2} \hat{\mathcal{L}}^{(2)}(\hat{\Delta}, \beta, \bar{p}_{\max}) \\ & + \frac{\hat{\mu}\hat{\Delta}}{p_0^2} \hat{\mathcal{L}}^{(1)}(\hat{\Delta}, \beta, \bar{p}_{\max}) \Big\}. \end{aligned} \tag{D34}$$

The differentiation of $E_1(\hat{\Delta}, \beta, V; \bar{p}_{\max})$ at constant V and constant yield the following expression:

$$\left(\frac{\partial E_1}{\partial \beta} \right)_V = \frac{\partial \bar{p}_{\max}}{\partial \beta} \left(\frac{\partial E_1}{\partial \bar{p}_{\max}} \right)_\beta + \left(\frac{\partial E_1}{\partial \beta} \right)_{\bar{p}_{\max}}. \tag{D35}$$

Therefore, the use of Eqs. (D33) and (D34) allows the derivative $(\partial E_1/\partial\beta)_V$ to be estimated.

REFERENCES

[1]R. P. Feynman, *Statistical Mechanics* (Benjamin, 1972).

[2]T. L. Hill, *Statistical Mechanics* (Dover Publications, Inc., 1987), Chap. 5, pp. 152-164; Chap. 6, pp. 233-251; Chap. 6, pp. 262-268; Appendix 7.

[3]A. Coniglio, U. De Angelis, A. Forlani, and G. Lauro, J. Phys. A: Math. Gen. **10**, 219 (1977); A. Coniglio, U. De Angelis, and A. Forlani, ibid. **10**, 1123 (1977).

[4]Y. C. Chiew and E. D. Glandt, J. Phys. A: Math. Gen. **16**, 2599 (1983).

[5]T. DeSimone, S. Demoulini, and R. M. Stratt, J. Chem. Phys. **85**, 391 (1986); C. S. Netemeyer and E. D. Glandt, J. Chem. Phys. **85**, 6054 (1986); N. A. Seaton and E. D. Glandt, J. Chem. Phys. **86**, 4668 (1987); Y. C. Chiew and Y. H. Wang, J. Chem. Phys. **89**, 6385 (1988); T. Kaneko, Phys. Rev. E **53**, 6134 (1996).

[6]Y. C. Chiew, G. Stell, and E. D. Glandt, J. Chem. Phys. **83**, 761 (1985).

[7]Y. C. Chiew and G. Stell, J. Chem. Phys. **90**, 4956 (1989).

[8]T. Kaneko, Phys. Rev. E **58**, 5808 (1998).

[9]L. E. Reichl, A Modern Course in Statistical Physics (University of Texas, Austin, Texas, 1984), Chap. 11, pp. 373-377; Chap. 11, pp. 377-381.

[10]J. P. Hansen and I. R. McDonald, Theory of Simple Liquids (Academic Press, Tokyo, 1996), Chap. 4, pp. 79-84, PP. 92-96; Chap. 5, pp. 104-128.

[11]N. F. Carnahan and K. E. Starling, J. Chem. Phys. **51**, 635 (1969).

[12]R. D. Mountain, Rev. Mod. Phys. **38**, 205 (1966).

[13]N. H. March and M. P. TOSI, Atomic Dynamics in Liquids (Dover, New York, 1991), Chap. 9, pp. 233-236.

[14]G. N. Sarkisov, J. Chem. Phys. **119**, 373 (2003).

[15]J. Ulander and R. Kjellander, J. Chem. Phys. **114**, 4893 (2001); J. Chem. Phys. **109**, 9508 (1998).

[16]P. Attard, Phys. Rev. E **48**, 3604 (1993).

[17]J. G. Brankov and D. M. Danchev, J. Math. Phys. 32, 2543 (1991).

[18]M. E. Fisher, J. Math. Phys. **5**, 944 (1964).

[19]G. Schönherr, R. W. Schmutzler, and F. Hensel, Phil. Mag. B **40**, 411 (1979).

[20]W. Hefner and F. Hensel, Phys. Rev. Lett. **48**, 1026 (1982).

[21]H. Uchtmann, F. Hensel, and H. Overhof, Philos. Mag. **42**, 583 (1980).

[22]R. F. Berg and M. R. Moldover, J. Chem. Phys. **93**, 1926 (1990).

[23]J. K. Bhattacharjee, R. A. Ferrell, R. S. Basu, and J. V. Sengers, Phys. Rev. A **24**, 1469 (1981).

[24]R. N. Bhatt and T. M. Rice, Phys. Rev. B **20**, 466 (1979).

[25]M. J. Solomon and P. Varadan, Phys. Rev. E **63**, 51402-1 (2001).

[26]E. P. Sakonidou, H. R. van den Berg, C. A. ten Seldam, and J. V. Sengers, J. Chem. Phys. **105**, 10535 (1996).

[27]J. Xu and G. Stell, J. Chem. Phys. **89**, 1101 (1988).

[28]G. Stell, J. Phys. A: Math. Gen. **17**, L855 (1984).

[29]C. Donati, J. F. Douglas, W. Kob, S. J. Plimpton, P. H. Poole, and S. C. Glotzer, Phys. Rev. Lett. **80**, 2338 (1998) ; R. Yamamoto and A. Onuki, ibid. **81**, 4915 (1998).

[30]E. R. Weeks, J. C. Crocker, A. C. Levitt, A. Schofield, and D. A. Weitz, Science **287**, 627 (2000).

[31]W. K. Kegel and A. van Blaaderen, Science **287**, 290 (2000).

[32]A. H. Marcus, J. Schofield, and S. A. Rice, Phys. Rev. E **60**, 5725 (1999).

[33]J. G. Kirkwood and F. P. Buff, J. Chem. Phys. **19**, 774 (1951).

[34]J. N. Glosli and F. H. Ree, Phys. Rev. Lett. **82**, 4659 (1999).

[35]D. W. Brenner, Phys. Rev. B **42**, 9458 (1990).

[36]M. S. Wertheim, Phys. Rev. Letts. **10**, 321 (1963); E. Thiele, J. Chem. Phys. **39**, 474 (1963); L. Blum and J. S. Hϕye, J. Stat. Phys. **19**, 317 (1978); Y. Hu, J. W. Jiang, H. L. Liu and J. M. Prausnitz, J. Chem. Phys. **106**, 2718 (1997); C. Tutschka and G. Kahl, Phys. Rev. E **64**, 31104 (2001).

[37]T. Kaneko, Phys. Rev. E **64**, 31201 (2001).

[38]M. H. J. Hagen and D. Frenkel, J. Chem. Phys. **101**, 4093 (1994).

[39]U. Alon, I. Balberg, and A. Drory, Phys. Rev. Lett. **66**, 2879 (1991).

[40]T. Vicsek, Fractal Growth Phenomena (World Scientific, New Jersey, 1992), Chap. 8, pp. 212-267; Chap. 9, pp. 271-300; Chap. 10, pp. 301-339.

[41]J. K. Bhattacharjee and R. A. Ferrell, Phys. Rev. A **28**, 2363 (1983).

[42]T. Kaneko, J. Phys. Chem. B **113**, 10732 (2009).

[43]R. J. Baxter, J. Chem. Phys. **52**, 4559 (1970).

[44]P. H. Poole, T. Grande, C. A. Angell, P. F. McMillan, Science, 275, 322 (1997).

[45]M. Ginoza, J. Phys.: Condens. Matter **6**, 1439 (1994); L. Blum and J. S. Hϕye, J. Stat.

Phys. **19**, 317 (1978).

[46]J. S. Hϕye and L. Blum, J. Stat. Phys. **16**, 399 (1977); P. T. Cummings and E. R. Smith, Chem. Phys. bf 42, 241 (1979); P. T. Cummings and E. R. Smith, Mol. Phys. **38**, 997 (1979).

[47]T. Kaneko, Phys. Rev. E **70**, 066143 (2004).

[48]T. Kaneko, AIP Advances **12**, 015107 (2022).

[49]T. Kaneko, J. Chem. Phys. **123**, 134509 (2005).

[50]D. M. Zuckerman, M. E. Fisher, and B. P. Lee, Phys. Rev. E **56**, 6569, (1997).

[51]M. E. Fisher, J. Stat. Phys. **75**, 1 (1994); Y. Levin and M. E. Fisher, Physica A **225**, 164 (1996); B. P. Lee and M. E. Fisher, Phys. Rev. Lett. **76**, 2906 (1996); D. M. Zuckerman, M. E. Fisher,and B. P. Lee, Phys. Rev. E **56**, 6569 (1997).

[52]T. Kaneko, Phys. Rev. E **66**, 51502-1 (2002).

[53]P. T. Cummings and E. R. Smith, Chem. Phys. **42**, 241 (1979); Molec. Phys. **38**, 997 (1979).

[54]S. Pittois, B. V. Poie, C. Glorieux, and J. Thoen, J. Chem. Phys. 121, 1866 (2004).

[55]J. A. Barker and D. Henderson, Rev. Mod. Phys. 48, 587 (1976).

[56]E. Lomba and N. G. Almarza, J. Chem. Phys. 100, 8367 (1994)

[57]L. P. Kadanoff, W. Götze, D. Hamblen, R. Hecht, E. A. S. Lewis, V. V. Palciauskas, M. Rayl, J. Swift, D. Aspnes, and J. Kane, Rev. Mod. Phys. 39, 395 (1967).

[58]M. Alexanian, J. Math. Phys. **17**, 528 (1976).

[59]C. A. Cerdeiriña, D. González-Salgado, L. Romani, M. D. C. Delgado, L. A. Torres, and M. Costas, J. Chem. Phys. 120, 6648 (2004).

[60]M. Yao and H. Endo, J. Phys. Soc. Jpn. **51**, 974 (1982).

[61]J. C. Nieuwoudt and J. V. Sengers, J. Chem. Phys. **90**, 457 (1988).

[62]N. G. Almarza and E. Enciso, Phys. Rev. E **59**, 4426 (1999).

[63]P. D. Gallagher, M. L. Kurnaz and J. V. Maher, Phys. Rev. A **46**, 7750 (1992); P. D. Gallagher and J. V. Maher, Phys. Rev. A **46**, 2012 (1992); D. Beysens and D. Estève, Phys. Rev. Lett. **54**, 2123 (1985).

[64]M. E. Fisher and P. G. de Gennes, C. R. Acad. Sci. Ser. B **287**, 207 (1978) ; P. Attard, C. P. Ursenbach, and G. N. Partey, Phys. Rev. A **45**, 7621 (1992) ; T. W. Burkhardt and E. Eisenriegler, Phys. Rev. Lett. **74**, 3189 (1995) ; R. R. Netz, Phys. Rev. Lett. **76**, 3646 (1996) ; M. Krech, Phys. Rev. E **56**, 1642 (1997) ; A. Hanke, F. Schlesener, E.

Eisenriegler, and S. Dietrich, Phys. Rev. Lett. **81**, 1885 (1998).

[65]C.Tutschka, G. Kahl, and G. Pastore, Phys. Rev. E **63**, 61110 (2001).

[66]C. J. Wu, J. N. Glosli, G. Galli, and F. H. Ree, Phys. Rev. Lett. **89**, 135701 (2002).

[67]M. Y. Lin, H. M. Lindsay, D. A. Weitz, R. Kein, R. C. Ball, and P. Meakin, J. Phys.: Condens. Matter **2**, 3093 (1990).

[68]M. Carpineti and M. Giglio, Phys. Rev. Lett. **68**, 3327 (1992); D. Asanaghi, M. Carpineti, M. Giglio, and M. Sozzi, Phys. Rev. A **45**, 1018 (1992); M. Carpineti, F. Ferri, and M. Giglio, Phys. Rev. A **42**, 1018 (1990).

[69]D. A. Weitz, J. S. Huang, M. Y. Lin, and J. Sung, Phys. Rev. Lett. **54**, 1416 (1985); D. A. Weitz and M. oliveria, Phys. Rev. Lett. **52**, 1416 (1984).

[70]S. Manley, L. Cipelletti, V. Trappe, A. E. Bailey, R. J. Christianson, U. Gasser, V. Prasad, P. N. Segre, M. P. Doherty, S. Sankaran, A. L. Jankovsky, B. Shiley, J. Bowen, J. Eggers, C. Kurta, T. Lorik, and D. A. Weitz, Phys. Rev. Lett. **93**, 108302-1 (2004); J. Bibette, T. G. Mason, H. Gang, and D. A. Weitz, Phys. Rev. Lett. **69**, 981 (1992).

[71]L. Belloni, Phys. Rev. Lett. **57**, 2026 (1986).

[72]M. D. Haw, W. C. K. Poon, and P. N. Pusey, Phys. Rev. E **97**, 1918 (1997); M. Lach-hab, A. E. González, and E. Blaisten-Barojas, Phys. Rev. E **57**, 4520 (1998); A. AlSunaidi, M. Lach-hab,E. Blaisten-Barojas, and A. E. González, Phys. Rev. E **57**, 4520 (1998).

[73]M. Lach-hab, A. E. González, and E. Blaisten-Barojas, Phys. Rev. E **54**, 5456 (1996).

[74]D. W. Schaefer, J. E. Martin, P. Wiltzius, and D. S. Cannell, Phys. Rev. Lett. **52**, 2371 (1984); M. Y. Lin, H. M. Lindsay, D. A. Weitz, R. C. Ball, R. Kein, and P. Meakin, Proc. R. Soc. Lond. A **423**, 71 (1989); M. Carpineti and M. Giglio, Phys. Rev. Lett. **70**, 3828 (1993); M. Carpineti, M. Giglio, and V. Degiorgio, Phys. Rev. E **51**, 590 (1995); A. Fernández-Nieves, J. S. van Duijneveldt, A. Fernández-Barbero, B. Vincent, and F. J. de las Nieves, Phys. Rev. E **64**, 051603-1 (2001).

[75]A. Tani and D. Henderson, J. Chem. Phys. **79**, 2390 (1983);M. J. Gillan, Mol. Phys. **49**, 421 (1983); G. Stell, J.Stat. Phys. **78**, 197 (1995).

[76]N. Bjerrum, K. Dan. Vidensk. Selsk. Mat. Fys. Medd. **7**, 1 (1926).

[77]A. Oleinikova and M. Bonetti, J. Chem. Phys. **104**, 3111 (1996).

[78]D. R. Schreiber, M. C. P. de Lima, and K. S. Pitzer, J. Phys. Chem. **91**, 4087 (1987).

[79]J. A. Given and G. Stell, J. Chem. Phys. **106**, 1195 (1997).

[80]T. Kaneko, Phys. Rev. E **60**, 6742 (1999).

[81]T. A. Witten and L. M. Sander, Phys. Rev. Letts. **47**, 1400 (1981); Phys. Rev. B **27**, 5686 (1983); L. Paterson, Phys. Rev. Letts. **52**, 1621 (1984); E. Ben-Jacob, R. Godbey, N. D. Golgenfeld, J. Koplik, H. Levine, T. Mueller, and L. M. Sander, ibid. **55**, 1315 (1985); G. L. M. K. S. Kahanda, X. Zou, R. Farrell, and P. Wong, ibid. **68**, 3741 (1992); P. Keblinski, A. Maritan, F. Toigo, and J. R. Banavar, Phys. Rev. E **49**, R4795 (1994).

[82]M. Ginoza and M. Yasutomi: Phys. Rev. E **59** 2060 (1999).

[83]M. Ginoza, J. Phys.: Condens. Matter **6**, 1439 (1994).

[84]L. Blum and J. S. Hϕye, J. Stat. Phys. **19**, 317 (1978).

[85]D. Beysens and D. Estève, Phys. Rev. Lett. **54**, 2123 (1985); Y. Jayalakssmi and E. W. Kaler, Phys. Rev. Lett. **78**, 1379 (1997).

[86]K. To and H. J. Choi, Phys. Rev. Lett. **80**, 536 (1998).

[87]N. B. Wilding, F. Schmid and P. Nielaba, Phys. Rev. E **58**, 2201 (1998).

[88]I. R. Tsang and I. J. Tsang, Phys. Rev. E **60**, 2684 (1999).

[89]A. AlSunaidi, M. Lach-hab, A. E. Gonzalez and E. Blaisten-Barojas, Phys. Rev. E **61**, 550 (2000).

[90]R. K. Bhaduri and W. van Dijk, Phys. Lett. A **380**, 2480 (2016).

[91]S. Biswas, J. Mitra, and S. Bhattacharyya, J. Stat. Mech. P03013 (2015).

[92]K. Huang, Phys. Rev. Lett. **83**, 3770 (1999).

[93]P. A. Martin and J. Piasecki, Phys. Rev. E **71**, 016109 (2005).

[94]E. J. Mueller and G. Baym, Phys. Rev. A **62**, 053605 (2000).

[95]G. M. Kavoulakis, A. D. Jackson, and G. Baym, Phys. Rev. A **70**, 043603 (2004).

[96]S.-J. Jiang and F. Zhou, Phys. Rev. A **92**, 013619 (2015).

[97]S. Floerchinger and C. Wetterich, Phys. Rev. A **79**, 063602 (2009).

[98]S. Bhattacharyya, T. K. Das, and B. Chakrabarti, Phys. Rev. A **88**, 053614 (2013).

[99]J. V. Pearce, R. T. Aruah, B. Fak, A. R. Sakhel, H. R. Glyde, and W. G. Stirling, J. Phys.: Condens. Matter **13**, 4421 (2001).

[100]S. O. Diallo, R. T. Azuah, D. L. Abernathy, J. Taniguchi, M. Suzuki, J. Bossy, N. Mulders, and H. R. Glyde, Phys. Rev. Lett. **113**, 215302 (2014).

[101]K. H. Andersen and W. G. Stirling, J. Phys.: Condens. Matter **6**, 5805 (1994).

[102]G. Zsigmond, F. Mezei, and M. T. F. Telling, Physica B **388**, 43 (2007).

[103]J. Wilks, *An Introduction to Liquid Helium* (Oxford University Press, 1970).

[104]L. D. Landau and E. M. Lifshitz, *Statistical Mechanics* (Pergamon, 1980).

[105]G. Ahlers, Phys. Rev. A **3**, 696 (1971); J. A. Lipa, D. R. Swanson, J. A. Nissen, T. C. P. Chui, and U. E. Israelsson, Phys. Rev. Lett. **76**, 944 (1996); J. A. Lipa, J. A. Nissen, D. A. Stricker, D. R. Swanson, and T. C. P. Chui, Phys. Rev. B **68**, 174518 (2003).

[106]I. N. Adamenko, K. E. Nemchenko, V. A. Slipko, and A. F. G. Wyatt, Phys. Rev. Lett. **96**, 065301 (2006).

[107]M. Tohyama, Phys. Rev. A **71**, 043613 (2005).

[108]C. J. Pethick and H. Smith, *Bose–Einstein Condensation in Dilute Gases* (Cambridge University Press, 2002).

[109]J. R. Clow and J. D. Reppy, Phys. Rev. A **5**, 424 (1972).

[110]O. W. Dietrich, E. H. Graf, C. H. Huang, and L. Passell, Phys. Rev. A **5**, 1377 (1972).

[111]R. J. Donnelly and P. H. Roberts, J. Low Temp. Phys. **27**, 687 (1977); R. J. Donnelly, J. A. Donnelly, and R. N. Hill, J. Low Temp. Phys. **44**, 471 (1981).

[112]A. L. Fetter and J. D. Walecka, *Quantum Theory of Many-Particle Systems* (McGraw-Hill, 1971).